Characterisation of the hydrological processes and responses to rehabilitation of a headwater wetland of the Sand River, South Africa

by

Edward Sebastian Riddell

Submitted in fulfilment of the academic requirements for the degree of
Doctor of Philosophy in the
School of Bioresources Engineering and Environmental Hydrology,
University of KwaZulu-Natal, Pietermaritzburg

February 2011

As the candidate's supervisor I have approved this thesis for submission.

Signed: _____
Name: Simon Antony Lorentz
Date: 3 June 2010

PREFACE

The experimental work described in this thesis was carried out in the School of Bioresources Engineering & Environmental Hydrology, University of KwaZulu-Natal, Pietermaritzburg, from October 2005 to March 2010, under the supervision of Professor Simon A. Lorentz.

These studies represent original work by the author and have not otherwise been submitted in any form for any degree or diploma to any tertiary institution. Where use has been made of the work of others it is duly acknowledged in the text.

DECLARATION 1 - PLAGIARISM

I, Edward Sebastian Riddell declare that

1. The research reported in this thesis, except where otherwise indicated, is my original research.

2. This thesis has not been submitted for any degree or examination at any other university.

3. This thesis does not contain other persons' data, pictures, graphs or other information, unless specifically acknowledged as being sourced from other persons.

4. This thesis does not contain other persons' writing, unless specifically acknowledged as being sourced from other researchers. Where other written sources have been quoted, then:
   a. Their words have been re-written but the general information attributed to them has been referenced
   b. Where their exact words have been used, then their writing has been placed in italics and inside quotation marks, and referenced.

5. This thesis does not contain text, graphics or tables copied and pasted from the Internet, unless specifically acknowledged, and the source being detailed in the thesis and in the References sections.

Signed: ……

DECLARATION 2 - PUBLICATIONS

DETAILS OF CONTRIBUTION TO PUBLICATIONS that form part and/or include research presented in this thesis (include publications in preparation, submitted, *in press* and published and give details of the contributions of each author to the experimental work and writing of each publication)

Publication 1 - Chapter 4 of this thesis has been published in the scientific journal, Hydrology and Earth Systems Science (August 2010) titled, 'A geophysical analysis of hydro-geomorphic controls within a headwater wetland in a granitic landscape, through ERI and IP' by Riddell ES, Lorentz SA and Kotze DC. The first author developed the field procedure, collected and analysed the field data, and was responsible for compiling the manuscript. The second and third authors commented thoroughly on the manuscript's early drafts.

Publication 2 – Chapter 5 of this thesis is in preparation and will be submitted to a scientific journal. It is entitled, 'The hydrodynamic response of a semi-arid headwater wetland to technical rehabilitation interventions' by Riddell ES, Lorentz SA and Kotze DC. The first author developed the field procedure, collected the field data, and was responsible for its analysis and for compiling the manuscript. The second and third authors commented thoroughly on the manuscript's early drafts.

Publication 3 – Chapter 6 of this thesis has been submitted to the scientific journal, Hydrological Processes (February 2010) titled, 'Hydrologic mechanisms in a granitic hillslope that induce rapid phreatic surface responses in a headwater wetland' by Riddell ES & Lorentz SA. The first author set up and installed the monitoring apparatus, collected the field data, examined hydrological responses, developed and parameterized the hydrological model and was responsible for compiling the manuscript. The second author assisted by guiding in the set up the hydrological model, some parameter development and commented thoroughly on the manuscript's early drafts.

Publication 4 – Chapter 7 of this thesis is in preparation and will be submitted to a scientific journal. It is entitled, 'Examination of wetland streamflow control variables using conceptual hydro-pedological processes on hillslopes and tested in a distributed physically-based catchment model' by Riddell, ES, Lorentz, SA and Le Roux, PAL. The first author developed the field procedure, collected and analysed the field data, and was responsible for compiling the manuscript. The second author assisted by guiding in the set up the hydrological model, advised on parameter development and commented thoroughly on the manuscript's early drafts. The third author provided information collected in the field on the general hydrological behaviours of catchments soil types which was used to develop parameters used in the hydrological model discussed in the paper.

Publication 5 - Chapter 8 of this thesis is in preparation and will be submitted to a scientific journal, and is entitled, ‘Four years of wetland rehabilitation monitoring through process hydrology – what have we learnt?’ by Riddell ES who compiled the manuscript.

Signed: ……
E.S. Riddell

ABSTRACT

Characterisation of the hydrological processes and responses to rehabilitation of a headwater wetland of the Sand River, South Africa

E.S. Riddell
2010

The erosion of headwater wetlands in the Sand River catchment, in the lowveld of north-eastern South Africa has led to a focus on their rehabilitation, both for livelihood security for those that use them for subsistence agriculture, as well as for provision of streamflow regulation services for the Sand River itself. One such wetland, the Craigieburn-Manalana itself undergoing severe erosion was subject to technical rehabilitation using concrete weirs and gabion dams to stabilize the erosion gullies during 2007. Through a series of papers the research discussed in this thesis examined the response of the wetland's hydrodynamics to the implementation of these measures. Through the installation of a network of hydrometric apparatus the research has shown that the wetlands hydrology is largely controlled by the presence of both horizontal and vertical clay aquicludes within a hydraulically conductive sandy matrix. The sequence of these aquicludes had allowed for artesian phreatic surface phenomena identified in a relatively hydrologically intact region of the wetland. The gully erosion had initiated hydraulic drawdown of the wetland's water table leading to the desiccation of the system. The construction of a buttress weir within the erosion gully had restored the wetlands hydrodynamics to that typical of conditions upstream of a clay-plug.

The research also explored the role that clay plays in terms of controlling the wetland's hydro-geomorphic setting through geophysical analysis. A conceptual model was then derived that states that these wetlands are held in place by clay-plugs that form through clay illuviation from the hillslopes at regions of valley confinement. This has important implications for the connectivity of wetland process domains.

The research also determined the inputs of surface and subsurface flows to the wetland and it was found through detailed examination of soil moisture responses and variably saturated soil physics modelling using the HYDRUS model, that the wetland is hydrologically connected to

its contributing hillslope by threshold induced preferential flow pathways, via macropores, that only respond after specific antecedent soil moisture conditions are met.

In addition, the thesis describes novel approaches to use information provided by soil scientists for the development of catchment hydrological models. It was shown that the use of this hydropedology information improved the low flow response function of the catchment model, ACRU. This development has important implications for up-scaling of catchment process domains, or hydrological response units by being able to generalize on hillslope hydrological responses based on configuration of their soil type elements.

The research also undertook to examine the role that the wetlands play in catchment processes. It was found through water budgeting, supported by hydrological time-series, stable isotope analysis and the quantification of vegetation water use within the wetland and contributing catchment, that these wetlands do not augment baseflows during the dry season. Furthermore, it is only early on during the wet season that these systems may attenuate peak flows, thereafter they act as conduits for high storm flows. Similarities emanated from this research with previous hydrological studies of headwater wetland systems in southern Africa and these are discussed.

ACKNOWLEDGEMENTS

The research presented here was funded by the South African Water Research Commission (WRC), and the National Research Foundation (NRF).

The research conducted to fulfil this thesis was jointly supervised by Professor Simon Lorentz of the School of Bioresources Engineering & Environmental Hydrology (SBEEH), Dr Donovan Kotze of the Centre for Environment and Development (CEAD) both of the University of KwaZulu-Natal, and Professor William (Fred) Ellery of the Department of Environmental Science (ES) at Rhodes University. I am grateful to you all for your enthusiastic supervision which has made this thesis a thoroughly enjoyable and rewarding pursuit.

Dr Sharon Pollard provided invaluable mentorship during the research period and provisioned a great introduction to the field of integrated water resource management. A thank you also to all the other members of the Association for Water and Rural Development (AWARD), for all your assistance over the last few years, it has been a pleasure to work with you all.

The community of Craigieburn, thank you all for making me feel welcome in conducting the research in the Manalana catchment, your help and assistance is most appreciated. Mr Difference Thibela, Mr Ronny Maaboi, Mr Rex Mothlabini and others for assistance with various aspects of instrument installation and data collection, thank you very much.

Mr Cobus Pretorius at SBEEH for his help and advice with all technical and logistical matters arising as part of this research, as well as to Mr John Ngeleka and Mr Sean Thornton-Dibb also of SBEEH. Mr Manqoba Dlamini for laboratory analysis of soil samples. Also, to the various students of SBEEH that also helped out on the project.

Thanks also to Working for Wetlands, Eastern Wetland Rehabilitation Ltd, including Mr Anton Bothma, Mr Grenios Sebatane and the late Mr Bill Russell, for various aspects in dealing with the construction of the rehabilitation structures and incorporation of our research requirements.

Thanks also the Ms Sandra McFadyen (SANParks), Mr Ngetar Njoya (UKZN) and Bigboy Mkhabela (AWARD) for assistance with GIS. Mrs Guin Zambatis (SANParks) and Mr John Rushworth for assistance with vegetation identification.

Mr David Lindley, Dr Matthew McCartney, and Dr Constantin von der Heyden for their help, advice and leads with respect to getting into the field of wetland management and conservation.

I am also grateful to Mr Johannes Hachmann for his volunteer time in assisting me with ERI surveys.

Of course, these acknowledgements would not be complete with out saying a big thank you to my parents Mrs Angela Binns and Mr Phil Riddell, my sisters, my step-families, grandparents, and my fiancé, Navashni Govender, you have all always been there for me and without whose constant support and encouragement none of this would have been possible.

CONTENTS

LIST OF FIGURES

LIST OF TABLES

1 INTRODUCTION

1.1 RATIONALE

In recent years increasing attention has been afforded to wetland ecosystems as their value from hydrological, ecological and socio-economic perspectives has developed appreciation (Schuyt & Brander, 2004). To clarify; wetlands are deemed to provide hydrological benefits in terms of river flow processes such as the reduction of flood damage, soil erosion limitation and water resource maintenance and hence wetlands are acknowledged to play a very important role in the global hydrological cycle as well as human well-being in terms of a variety of ecosystem goods and services (Millennium Ecosystem Assessment, 2005). The main ecological value is that of contributing to biodiversity, not only due to there being a considerable variety of wetland types from seeps to coral reefs but also through their function as an ecotone or ecological gradient between terrestrial and aquatic environments. In socio-economic terms wetlands provide a variety of benefits, such as ecologically derived functions of water purification and maintenance of domestic water supplies, as well as the provision of harvestable plants for crafts and medicinal purposes and grazing lands (Dixon *et al.*, 2001).

It has been proposed that, 'Hydrologic conditions are extremely important for the maintenance of a wetland's structure and function' (Mitsch & Gosselink, 2007). Furthermore recent research in South Africa has shown that without the development of an understanding of how wetlands form from both a hydrological and geomorphological perspective, the predicted function and wise management of such systems would prove difficult to ascertain (Ellery *et al.*, 2008). Indeed Mitsch & Gosselink (2007) reiterate this sentiment by stating that only by understanding the structure and function of a natural wetland is one qualified to undertake wetland creation and restoration endeavours. Hence the hydrogeomorphic principles underlying wetland processes should be taken on board when embarking upon any interventions to address or redress any wetland ecosystem concerns.

Hydrogeomorphology itself is the study of the way landforms are created through the action of water (Babar, 2005). The concept of a hydrogeomorphic type means the degree to which hydrological, geomorphological and biological fluxes into, through and within the wetland have facilitated the origin of the wetland in its present state and how it is connected to other systems,

such as surrounding forests and grasslands, but also with modified systems such as urban or agricultural landscapes (Mitsch & Gosselink, 2000). Wetlands themselves can also become a modified component of the landscape as people use them and inevitably modify them in some way. Modifications can take the form of drainage, pollution or conversion to some other land use such as building development or agriculture. Indeed, in areas of high land-use demand, wetland mitigation is becoming increasingly widespread as wetlands are created to compensate for their removal elsewhere (Zedler and Callaway, 1999).

There is a debate in the field of wetland science as to the extent that wetlands play in river catchment processes. A particular argument centres around the role of wetlands in attenuating flood water and in augmenting low flows. Bullock & Acreman (2003) for instance review a plethora of studies for discussion in this respect, of which many acknowledge that wetlands reduce floods, recharge groundwater and augment low flows. Many studies however also show that wetlands (particularly at headwaters) increase floods, act as a barrier to recharge and reduce base flows (through evaporation during dry periods). Furthermore, if situated at the headwaters of a stream, a wetland would function in ways different from those of a wetland located near the stream's mouth (Mitsch & Gosselink, 2000). Indeed similar hydrological responses have been observed in headwater catchments with and without wetlands (McCartney *et al.*, 1998) which suggests that the presence of a wetland in a catchment cannot imply an anticipated hydrological response. Therefore acquiring information on how wetlands of particular hydrogeomorphic settings actually function hydrologically is indeed necessary. The hydrologic signature of various wetland types may then be quantified through the development of a wetland water budget, which is a resulting change in storage emanating from the balance of the inflows and outflows of water to and from the system (Mitsch & Gosselink, 2007).

Particularly pertinent to this thesis is the modification of wetland systems through subsistence cultivation, a relatively common practice in the developing world and of particular importance in terms of food security in sub-Saharan Africa where the FAO recognizes their importance as such (e.g. FAO, 2001). Furthermore, in South Africa the development of wetlands for small-scale agriculture continues extensively with little or no control, whilst the development by large scale commercial agriculture has not continued (Kotze & Silima, 2003). The situation therefore highlights the particular importance that wetlands play in terms of food security for the rural poor of South Africa. However, both the Government and the NGO sector in South Africa recognize that the degradation of the wetland environment seriously needs to be addressed (Whyte, 1995 as cited in Kotze & Silima, 2003). The challenge therefore is to reconcile the

needs of South Africa's rural poor whose primary concern is food security, with the rest of society who are increasingly expecting that their river catchments are maintained. Hence the security of the nation's water resources and environmental integrity are particularly pertinent issues when discussing the values of wetlands in the South African context (DWAF, 2001).

The wetlands of relevance to this research are found at the headwaters of the Sand River, Mpumalanga, South Africa. These wetlands are a prime example of the pattern of dependency on these ecosystems. The Sand River itself is the main tributary of the Sabie River, situated in the Incomati River basin. The Sabie River is also the last of six major rivers flowing through the Kruger National Park into Mozambique to retain its perennial status. The Sand River catchment is itself relatively small at 1910km² but densely populated at 400,000 people, a situation that has arisen in large part due to the political legacy of enforced relocation and settlement. This has placed untold pressures on the natural environment, including the wetlands, as well as groundwater aquifers. This results from the need to derive a livelihood through small-scale agriculture often in a wetland setting, heavily influenced by high unemployment and population pressure. The purpose of the research described in the following thesis is to assess the rehabilitation of a degradationary process that is afflicting the Sand River, namely the eroding away of headwater riparian wetlands in the Sand River catchment.

Degradation of the Sand river system has therefore arisen, it is suggested (by Pollard *et al.*, 2005), through a number of factors derived from the need for food security coupled with substantial population pressures. It is thought that the wetlands which lie at the headwaters of the river, occupying approximately 6% of the foothill zone of the Klein Drakensberg Escarpment, play a particularly important role in the regulation of stream flow and maintenance of low flows in the Sand River. However, through the dependency of the densely populated rural poor on the wetland systems for harvesting and cropping of subsistence crops as well as other land-use practices in the surrounding catchment, it has been noted that the wetlands themselves as well as the rest of the catchment have gone through a period of severe degradation. This follows multidisciplinary research conducted in the Craigieburn-Manalana catchment between 2003-4 (Pollard *et al.*, 2005). Furthermore this degradation is readily acknowledged by the wetland users who have observed increased desiccation and erosion with a corresponding decrease in fertility and hence productivity of the wetland environment (Pollard *et al.*, 2005). Degradation is also noted on the slopes of these headwater catchments, where peri-urban development has increased the area of bare surfaces through roads and housings etc, as

well as the thinning and alteration of the indigenous veld through uncontrolled communal grazing.

Figure 1.1 displays a conceptual model presented by Pollard *et al.*, (2005) suggesting the causes and effects of wetland degradation in these headwater catchments. Here localised mechanical disturbance through hoeing, harvesting and clearance of natural vegetation in the wetlands, through ridge and furrow type agriculture, is assumed to lead to a decrease in on-site vegetation and increases in hydraulic radius, whilst catchment slope (interfluve) vegetation is also reduced for reasons just mentioned. The combination of these factors is thought to then lead to increased volumes and velocity of water entering and exiting the micro-catchments, principally through the reduction in retention time. A longer duration retention time would otherwise have existed through roughness provided by natural vegetation cover and infiltration into and through the catchment soils. The increased velocities of water now flowing through the modified wetland system would also therefore have a corresponding increase in energy for erosion and an inverse propensity for groundwater recharge, due to the reduced retention time. These factors in all likelihood lead to the problems of soil erosion and land desiccation that seem to be afflicting these wetlands. In addition, increased erosion and desiccation are probable contributing forces for the loss of soil fertility through the loss of organic carbon. This fertility decline is in itself exacerbated by present farming practices which limit the replenishment of organic matter in the wetland soils (such as the burning of organic wastes).

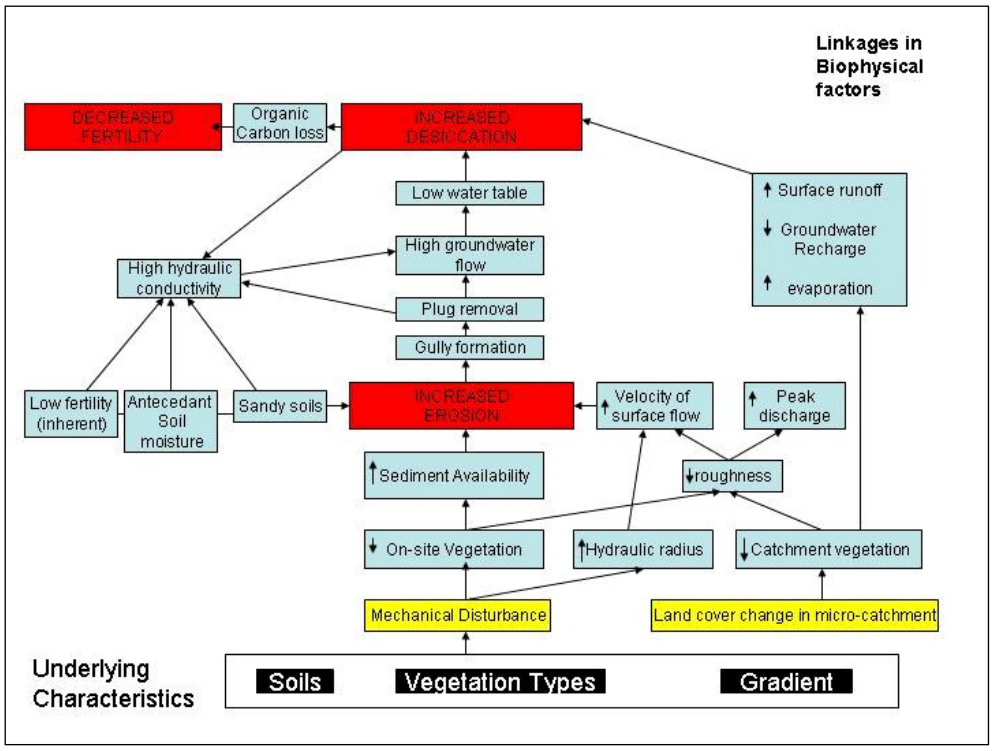

Figure 1.1: Conceptual model illustrating the biophysical factors leading to the degradation of the Craigieburn-Manalana wetlands (adapted from Pollard *et al.*, 2005).

These human-induced changes are likely not to be the sole factors contributing to the degradation observed, this is due to the very nature of the landscape itself. The headwater catchments (where erosional processes will tend to dominate, [Thoms *et al.*, 1990; Naiman *et al.*, 2005]) lie within an area which is geologically derived from a granitic parent material, this in combination with their location at the base of the Klein Drakensberg escarpment, an area of particularly intense rainfall, results in this area being highly prone to landscape scale erosion. The erosion of granitic landscapes is largely attributable to the susceptibility of weathering by moisture of the bedrock material (Campbell, 1997). The headwater catchments of the Sand River lie on Archaean and Proterozoic granite, tonalite and granodiorite, which are sodium-rich granitic rocks. These typically weather to produce catenal sequences that are associated with duplex soils with an excess of sodium, which in semi-arid landscapes are highly erosive (Chappell & Brown, 1993; Pollard *et al.*, 2005). The agricultural activities in the wetland and in the micro-catchment probably exacerbate the natural erosional processes in this landscape, of particular note in this regard are the huge erosion gullies, or, *dongas*, which can be tens of metres long and several meters deep and characterise these headwater catchments of the Sand River. It is thought that these dongas have arisen as a natural consequence of the wetland's steep

longitudinal gradient at the headward end of the valley. These steep gradients arise from the processes of clastic sedimentation. It is believed that, in general, South African wetlands maintain an equilibrium longitudinal gradient close to thresholds that are very sensitive to external perturbations (Ellery *et al.*, 2008). Increasing the volume of clastic sediment input will act to steepen this gradient even further and thus increase the risk of instability, which often arises from activities in the contributing catchment. In the case of the Sand River headwater catchments this may well have occurred through the clearance of indigenous forests and grassland to make way for commercial forestry as well as the degradation of the remaining veld through grazing and settlement, etc. In addition, factors downstream of a wetland which may lead to the lowering of the base level, such as some cultivation practices perhaps, may initiate headward erosion in an existing wetland and potentially drain it (Ellery *et al*., 2008). Hence, the human activities in the Sand River wetlands may very well be perturbations that are sufficient to initiate gully erosion.

Furthermore, Pollard *et al.*, (2005) proposed that since the sediments of the wetlands at the headwaters of the Sand River contain a very high sand content, they generally have a high hydraulic conductivity, and moisture is retained in the wetland by a plug of finer sediment at the wetland toe. The consequent removal of this plug through gully incision as a result causes the hydraulic drawdown of the water table in the wetland leading to the desiccation of the system.

This entire process is proposed schematically in Figure 1.2 where sections 1-3 suggest how the catchment geomorphology has shifted from one where sediment inputs approximately equal outputs over time, under more natural conditions. As a consequence of increased anthropogenic pressures in the catchment, delivery of sediment to the valley bottom wetland increases in proportion to that able to leave the wetland, and as a result, the longitudinal profile of the wetland steepens to such a point that fluvial energy leads to incision and down-cutting of the wetland surface by Figure 1.2 section 4 This results eventually in the loss of the buffering fine sediments plugging the wetland at it's toe (Figure 1.2 section 5) and retained moisture in the system (saturated sediment reflected by the water table) becomes unrestricted and drains from the system.

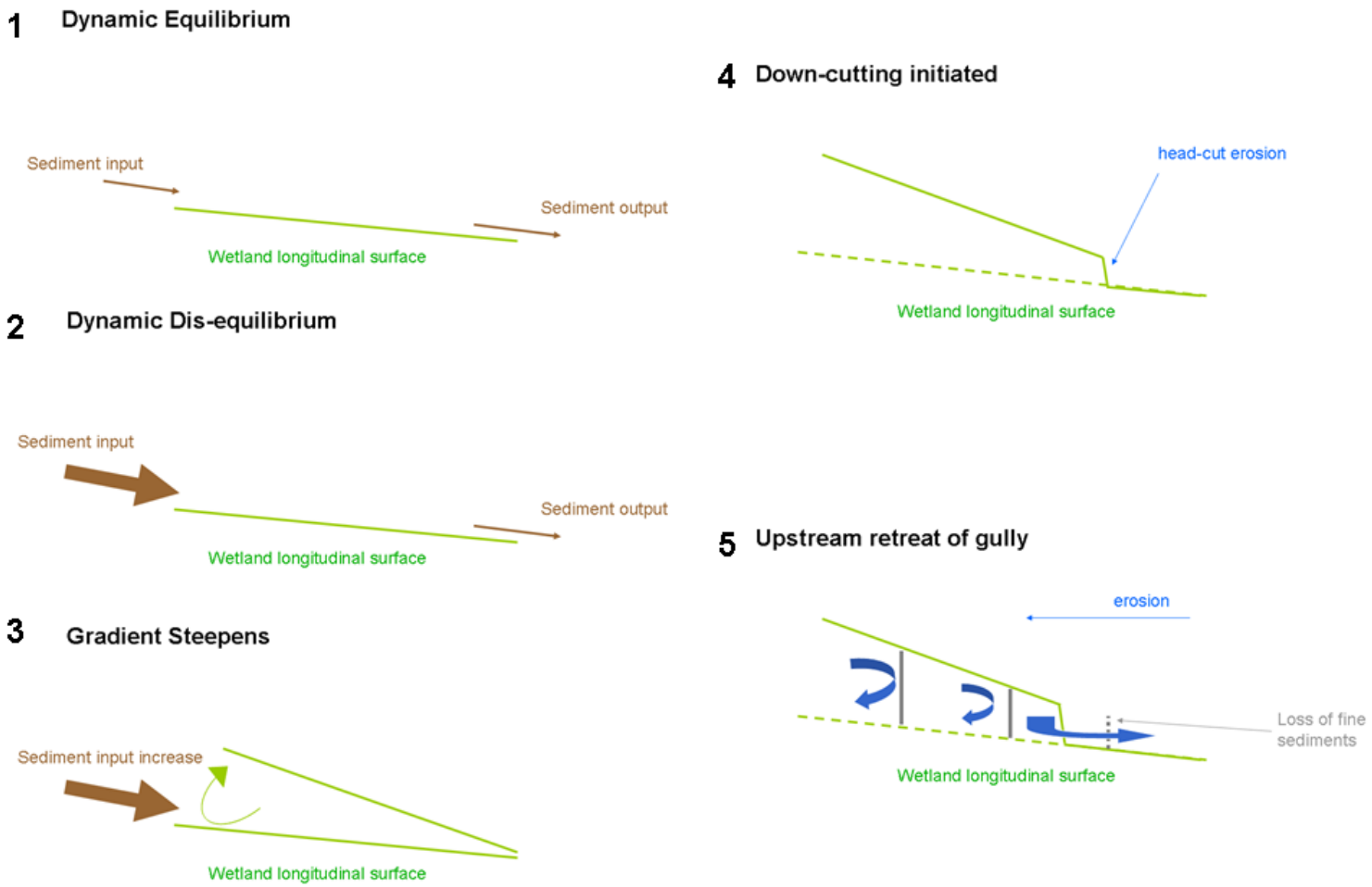

Figure 1.2: Proposed mechanism for wetland erosion in the Manalana catchment and possible cause for loss of moisture (blue arrows in section 5) through the loss of fine sediments.

It is believed that 80% of the streamflow of the Sand River is generated in the upper 20% of the catchment (Pike *et al.*, 1997). This area contains a considerable proportion of riparian wetlands at headwater locations, c. 1200ha (Pollard *et al.*, 2005). As Pollard *et al.* (2005) hypothesize; dramatic reductions in the base flows of the Sand River (up to 70%) over the last 15 years may be due to two principle factors:

- inappropriate forestry and commercial agricultural practices

- degradation of the extensive wetlands through their conversion to agriculture

The importance of these wetlands for the maintenance of base flow was supported through an *ACRU* (Schulze, 1995) based modelling exercise (King, 2005 unpublished MSc Thesis; Pollard *et al.*, 2005) run with the scenarios of catchments with and without wetlands (wetland sub-model). It was found that low flows downstream of wetlands were not as low as those where there were no wetlands. Furthermore, the model results suggested that the wetlands of the Craigieburn-Manalana catchment (of core relevance to this study) and similar catchments are maintained by the flow of water through the surrounding micro-catchment hillslopes rather than up-welling groundwater. The *ACRU* model simulates this by using physically based parameters to determine the partitioning of rainfall based on multi-soil layer properties and land-use type characteristics.

The important factor to note therefore is the underlying susceptibility of this landscape to erode, exacerbated by practices in the wetland and catchment slopes, since this would limit sustained hillslope contributions to the wetland system. However, due to the need to derive a livelihood from the natural environment, with the given population pressure in the headwater region of the Sand River catchment, a progressive solution must be developed to allow for the continual small-scale agronomic use of this landscape. At the same time the solution should also aim to minimize the erosion, desiccation and fertility problems that this population pressure exacerbates. Nevertheless on a broader scale, water and other environmental needs for all catchment users must be met. In order to achieve these goals a methodology of Integrated Catchment Management (ICM) must and is being deployed by a locally based NGO (The Association for Water and Rural Development, AWARD) to facilitate the needs of all stakeholders in the Sand River catchment. ICM is viewed as an important tool for the management of watersheds as it facilitates individual involvement in water resources management at the grass-roots level, an important prerequisite for successful water policy and planning (Zehnder *et al.*, 2003). Moreover the integrated approach to water resource management in South Africa, as enshrined in the National Water Act, 1998 is one governed

by an (eco)-systems approach to resource management. Through this approach there is an integration of links between processes and activities that cause biophysical and ecological changes in the catchment; there is an active and acceptable partnership with all stakeholders in a catchment; and the approach follows the principles of adaptive management i.e. a flexible management framework that can respond to changes in information and knowledge or in other words, learning by doing. These ethics are incorporated in to management by the *Save the Sand* Programme run by AWARD (e.g. Pollard, 2002). As a compliment to this ICM program the research undertaken here is far reaching in terms of providing crucial information on wetland hydrogeomorphic processes, and the relevance of these as a service to the maintenance of the Sand River. In particular the research will describe the flow regulation services of wetland hydrological response units (HRU's) and how this natural capital may (or may not) be important to the Sand River catchment.

Cowan (1999) highlighted the general ignorance by planners of the physical capabilities and properties of the wetlands that are chosen for rehabilitation, particularly in an African context. However since then significant progress has been made in terms of the integrated management and rehabilitation planning for wetlands, for instance the comprehensive suite of guidelines, the 'WET-Series' compiled by Breen *et al.,* (2008). This is of crucial importance to the successful application of the expanded public works program *Working for Wetlands* (WfW) in ensuring wetland sustainability in South Africa. Also, it is anticipated that the findings presented here would contribute significantly to this endeavour, by leading to recommendations on hydrological and geomorphic restoration of wetland processes.

1.2 CONCEPTUAL FRAMEWORK

The conceptual framework for this study is represented in Figure 1.3. The research aims at gaining a comprehensive understanding of the Craigieburn-Manalana wetland and catchment's water budget and the response of this to technical rehabilitation by WfW. This will include identifying how water moves through the wetland and the response of the wetland through-flow processes to the specific rehabilitation interventions deployed at the study site (by WfW on the erosion gullies). For instance is there any buffering of sub-surface water by these rehabilitation structures, as a remedy for the loss of fine sediment plugs? This will therefore provide a critical foundation of knowledge regarding the wetlands in this particular hydrogeomorphic setting. Through this knowledge recommendations will then be

developed for application to rehabilitation of other similarly degraded wetlands of the upper Sand River catchment. This forms the major aim of the proposed research.

Through the determination of the wetland-catchment water budget the research will describe the holistic hydrological function of these headwater systems with respect to broader catchment processes, necessary given the context of the degraded condition of the Sand River as has been discussed. Meanwhile the wetland-catchment water budget describes the component hydrological fluxes into and out of the system (see following section). The research will quantify each of these fluxes, through process descriptions to facilitate the understanding of the role of these wetland systems at the broader scale. The same applies to the geomorphic aspects that have allowed for the origin of the wetland in the first place, including the identification of fine sediment zones and proposed mechanisms for their development, as well as the hydrological feedbacks and controls that any geomorphic structures have had on the wetland hydrology as a whole. In essence therefore the extrapolation of the hydrological processes definition and the geomorphic understanding gleaned from the research sees the feedbacks displayed in Figure 1.2 leading to a precise determination of the wetland hydro-geomorphology. Given that the aim of the research includes examination of the wetland response to rehabilitation through a technical approach it is the imperative of the research to describe the impacts of this on both hydrological and geomorphic aspects governing the system.

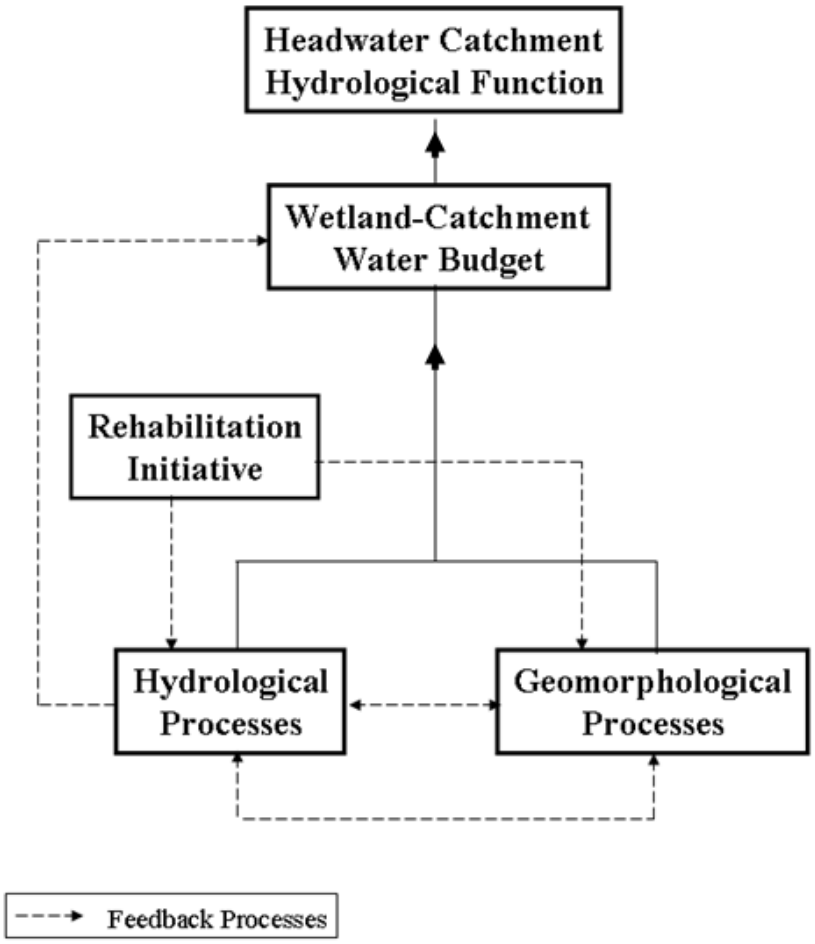

Figure 1.3: Diagrammatic representation of the conceptual framework of the components for the proposed research at the Craigieburn-Manalana wetlands.

The outcomes of the research detailed in the proceeding sections of this introduction contribute to the hydrological and geomorphological state of the art by procurement of the following key products:

- defining in detail the precise hydrological processes that operate in a wetland catchment, particularly in semi-arid river systems (in this case specific to the Sand River headwaters).

- identifying the response to technical rehabilitation on wetland hydrodynamics, and these hydrodynamics have yet to be defined for these systems.

- further refining our understanding of the linkages between hydrological and geomorphic processes that interact to contribute to the form and function of wetland hydrogeomorphic units.

- assessing the impacts of land degradation on these processes. This therefore enables these data to be used for understanding the socio-biophysical interactions in this and other catchments.

Specific objectives relating to the above points are defined in sections 1.3 - 1.5.

1.3 GEOMORPHOLOGY – UNDERSTANDING PROCESSES AND SETTING

1.3.1 Context - Equilibrium, Connectivity and Thresholds

Geomorphology, the study of the landscape from the perspective of interacting energy (by water or wind vectors) and mass (parent material, sediments) and resulting land-forming processes, has a set of underlying principles that facilitate a deeper contextual understanding of the landscape in question. The notion that landforms represent an accommodation between dominant processes and local geology was first put forward by GK Gilbert (cf. Gilbert, 1877), and this underpinning was carried forward to the present day with the concept of *dynamic equilibrium* (cf. Hack, 1960), which in essence describes that landscape elements adjust to processes operating on the geology and thus process and form in that landscape reveal a cause-effect relationship (Ritter *et al.*, 2002). The operating form and processes in a landscape therefore constitute components in a system, for example a drainage basin system with its component slopes, floodplains and channels, and hence processes operate within and between these components and therefore require delineation of spatial scale. Whilst it is apparent that landscapes are somewhat transient in nature it is important to consider the landscape element (in this case headwater micro-catchments containing valley bottom wetlands within the drainage network) and the processes that operate within them, and the thresholds that may switch their present state to another alternative state. Phillips (2006) describes at length the largely *non-linear* nature of geomorphic systems, in which it is stated that, 'a system is nonlinear if the outputs (or responses or outcomes) are not proportional to the inputs (or stimuli, changes, or disturbances)'.

Considering non-linearity in catchment processes, the scenario in Figure 1.5 highlights the connectedness of process domains across scales within a catchment. Particularly in headwater/upland areas drainage forms and evacuates sediment to the streams (or wetlands) and in these instances are deemed to be coupled to the surrounding hillslopes. Meanwhile as

one moves downstream sediment and water in the fluvial system becomes increasingly allochthonous and the river is decoupled from the surrounding land. The shift from a coupled hillslope-channel system to one that is uncoupled is an example of a transition that is a fundamental threshold in the river system (Church, 2002). It is therefore necessary to give context when defining the zone of interest for a particular study. In the case of the communal wetlands at the headwaters of the Sand River one is dealing largely with a coupled upland system.

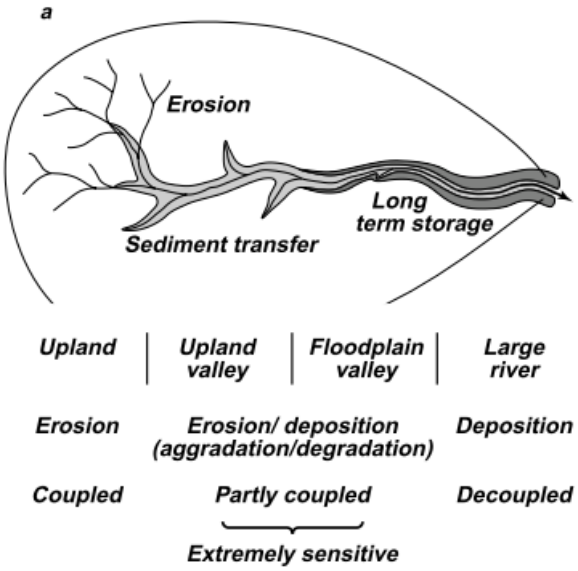

Figure 1.4: Connectivity of processes in a stream network (Taken from Church, 2002).

Furthermore, this (de)coupling or (dis)connectivity comprises three forms: *longitudina*l (water and sediment conveyed along the stream network), *lateral* (slope-channel interaction), and *vertical* (surface-subsurface interaction) and the nature of these relationships varies over time. In addition various buffers (e.g. a tributary fill) or barriers (e.g. bedrock outcrop) exist within a geomorphic system that act to reduce the connectivity (or conveyance) of water and sediment (e.g. Fryirs *et al.*, 2007) and in this case act to keep 'switched-off' the systems conveyance pathways. However, trigger rainfall/geomorphic events can 'switch-on' these conveyance paths and thereby increase or re-couple parts of the system, and the capacity for an event to do this is termed *breaching capacity* (Fryirs *et al.*, 2007). These switches are therefore the thresholds that need to be identified (quantified), for instance how close to these thresholds must a landform exist and what frequency and magnitude of event will trigger it?

Generally a landform close to a threshold condition will require an event of lesser magnitude to trigger it. This concept is best represented schematically in Figure 1.6.

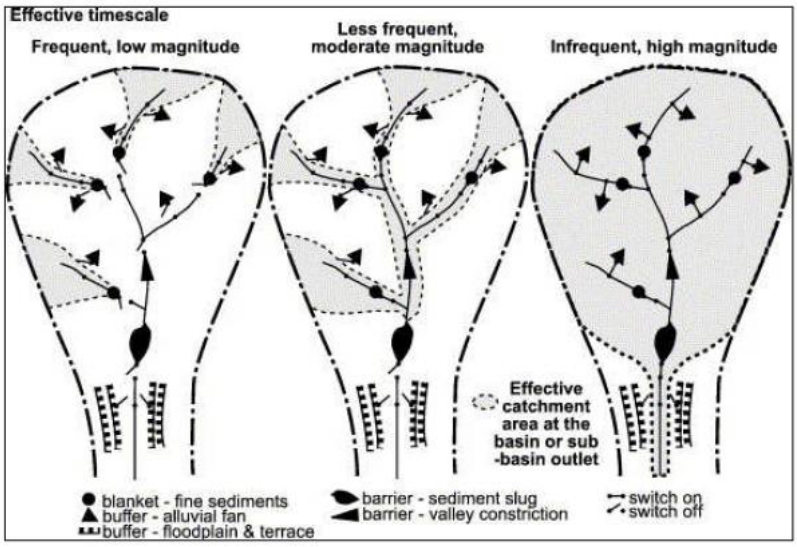

Figure 1.5: Switches in catchment conveyance (Taken from Fryirs *et al.*, 2007)

Phillips (2006) conveniently simplifies what he terms as *deterministic chaos* (a system sensitive to initial conditions and small perturbations) and *dynamic instability* (disproportionate effects of perturbations manifested over different temporal scales) mean for geomorphic systems, in the following way:

'Geography matters and history matters. Geography matters because local variations and disturbances result in increasing divergence over time. History matters because geomorphic systems "remember" initial variations and perturbations. Because geography and history matter, factors and controls specific to place and time (local factors) are irreducibly significant'.

The implications of this statement are that for managing a landscape in terms of rehabilitation or conservation, one needs to examine the system in a broader context, for instance in determining present processes and viewing them in light of past processes and therefore defining the boundary conditions for acceptable variability of these non-linear dynamics.

1.3.2 Wetland setting

The ‘geomorphic setting’ or landscape position of a wetland is a crucial determinant of the wetlands hydrology, as it is this position which will accommodate the flows and storages of water. Water flows and wetland position are therefore inextricably linked (Brinson, 1993). As has just been discussed, we know that riparian ecosystems are functionally connected to upstream and downstream ecosystems and are laterally connected to upslope (upland) and downslope (aquatic) ecosystems. This feature is pertinent to the statement describing the origins of wetlands within the drainage network by Ellery *et al.* (2008):

‘Wetlands generally occur in geomorphic settings where river transport capacity is less than or equal to load. Current velocities and discharges in wetlands are thus usually sufficiently low to limit or prevent erosion, and wetlands occur primarily in settings that overall are non-erosional or are depositional.’

Reiterating the notion of catchment connectivity and the fact the Sand River’s headwater have significant gully erosion i.e. channel initiation, it is probably fitting to briefly describe the associated channelisation that afflicts rivers in dryland environments such as the Sand River and specifically the processes leading to gully erosion such as that which is taking place within the Craigieburn-Manalana catchment. Gully erosion is defined as the process whereby runoff water accumulates and often recurs in narrow channels, which over short periods removes the soil from the narrow area to considerable depths (Peosen *et al.*, 2002). This runoff initiates ‘nick-points’ whereby a threshold level of resistance to detachment and transport of topsoil is overcome by this concentrated flow of water. Once initiated these nick-points often retreat upstream leaving deep channels and the nick-points develop into what are known as ‘head-cuts’, which are near vertical drops on the channel bed elevation. These head-cuts are sites of large scale erosional processes, such as the concentrated overland flow, but also plunge pooling, piping, tension cracking, and the mass failure of the gully bank sediments.

If one is to view headwater wetlands as part of the river continuum as is suggested by the aforementioned processes, then understanding of why a particular river form (in this case a headwater wetland) exists, requires the determination of both the hydrological and geomorphic regimes of that particular reach. This gives rise to the final sub-objective of the proposed study:

O1. The determination of the present and the past sedimentary and depositional processes within the Manalana catchment that have shaped its present hydrological functioning.

.

Factors influencing the rate of soil loss within a basin include the following (after Ritter, 1986): precipitation and vegetation; basin size; elevation and relief; rock type; and human activity. In the small catchment studied here it is deduced that all sediment inputs to the wetland are derived from the surrounding hillslope, as there is no upstream inflow to the wetland. These hillslope sediments are fluvially transported to lower slope positions, generally referred to as *colluvium*. Since hillslope sediments tend to thicken downslope (Daniels and Hammer, 1992) including the wetland at the footslope, it was deemed feasible to determine the sedimentary processes that have occurred within this wetland in the geological past. Moreover, remembering that a major theory emerging from previous studies in these catchments proposes that moisture is retained in these sandy wetland systems by zones of finer sediments, this warrants further study. The following two hypotheses then arise from this discussion as follows.

O1.i There is no discernable evidence that zones of fine sediments exist at longitudinal sections within the Manalana wetland that may retard the wetland throughflows (clay plug theory)

O1.ii There is no discernable evidence that zones of fine sediments exist in horizontal layers (stratified) within the Manalana wetland that may impact wetland throughflows.

1.4 THE WETLAND WATER BUDGET

In understanding the hydrology of a wetland, two key concepts need to be understood:

1. The concept of a 'hydroperiod' is a fundamental one when considering how and why a wetland is formed and maintained. A hydroperiod is simply the seasonal pattern of the water level of a wetland and largely characterises each wetland type by the flux of a wetlands surface and sub-surface water (Mitsch and Gosselink, 1993). Furthermore, the constancy of this flux pattern is particularly important for the stability of a wetland environment.

2. Hydrodynamics refers to the motion of water and the capacity of that water to do work, such as the transport of sediments and nutrients etc (Brinson, 1993). The hydroperiod is a

resulting component of the hydrodynamics of a wetland, as it is the prevailing hydrodynamic conditions that determine the wetlands hydroperiod.

The hydroperiod can be viewed as the sum of the influences of the three following factors (Mitsch and Gosselink, 1993; Mitsch and Gosselink, 2000):

i. The balance between the inflows and outflows of water in the wetland,
ii. Surface contours of the landscape and
iii. Subsurface soil, geology and groundwater conditions.

Point i. can be described as the wetland's water budget (or mass balance) as shown in equation 1.1.

(1.1) $$\frac{\Delta V}{\Delta t} = Pn + Si + Gi - ET - So - Go$$

where: V is the volume of water storage in a wetland; t is time; Pn is gross precipitation (measured + intercepted); Si are the surface inflows via streams or overland flow; Gi are the groundwater inflows; ET is the evapotranspiration; So are the surface outflows; and Go are the groundwater outflows.

A comprehensive understanding of this water budget for any wetland is important for understanding the functioning of the system and particularly so for the rehabilitation of the wetland ecosystem, especially where the restoration of the natural flow regime is required (Ellery *et al.*, 2008). Furthermore, this equation provides insight into how and why wetlands occur where they do, as wetlands are formed where the rates of water movement into, through and out of the system vary, resulting in the change in saturated storage of water. This storage change is expressed over time as a water table close to or above the wetland surface, and the length of time this exists dictates the seasonal or perennial status of the system. Therefore in terms of wetland hydrological science it is these component rates of water movement that need to be quantified, in essence the core endeavour of this study. Furthermore, it is necessary to define the sources and pathways of water flow, since these can be impacted upon by various activities in the contributing catchment.

It is widely accepted that the inputs to a wetland (apart from ombrotrophic wetlands, such as pans) are essentially derived from processes in the contributing catchment or interfluve, as well as direct precipitation, i.e. points ii and iii above. It is therefore essential to understand

the inter-relationships between a wetland and its surrounding catchment, since this enables the quantification of system inputs and outputs to the wetland (McCartney, 1998), and it is summarised in equation 1.2.

(1.2) $$Si = P_{catch} - ET_{catch} - (\Delta Ss + \Delta Sg)_{catch}$$

Where: *Si* is the surface inflow; P_{catch} equals catchment precipitation; ET_{catch} is the actual catchment evapotranspiration; $\triangle Ss$ is the change in soil moisture storage in the catchment; and $\triangle Sg$ is the change in groundwater storage in the catchment.

LeBaugh (1986) reviewed the literature pertaining to wetland hydrology in which it was noted that many of the studies acknowledge the importance of catchment hydrology to wetland ecosystem research. However, few of these studies attempted to quantify this and in conclusion it was suggested that hydrology remained one of the least understood components of wetland ecosystems. Furthermore, where hydrology was studied it appeared that this was not comprehensive and that only component parts of the wetland water budget were investigated, such that residual values were allocated to those parts of the water budget that were not measured. In the twenty years since LeBaugh's (1986) review the study of wetland water budgets has increased but weighted considerably to studies in the boreal and temperate northern hemisphere (e.g. Devito *et al.*, 2005; Bradley, 2002; Riekerk & Korhnak, 2000). Very few studies with a sole focus on wetland hydrology have been conducted in South Africa (Grenfell *et al.*, 2005), and only a further few exist for studies in southern Africa for which much attention focuses on 'dambo' hydrology in Zimbabwe (Bullock, 1992; McCartney, 2000), the foundation of which was instigated by Balek and Perry's (1973) work on Zambian dambo water budgets in the 1960's. Von der Heyden (2004) refers to Dambos as being, 'shallow, seasonally waterlogged depressions forming the headwaters of ephemeral and perennial streams in subtropical and tropical Africa.' Meanwhile McCartney (1998) describes dambos as existing predominantly where the relief is characterised by flat, gently undulating country. However, as the wetland catchment in this proposed study is not a shallow depression, although it is a headwater wetland, and it exists in a more rugged terrain at the foothills of the Klein Drakensberg escarpment, it may not fit the typical definition of a dambo, which have been the hydrologically described headwater wetland systems in Southern Africa to date. Nevertheless it probably still constitutes what may be classed as a dambo, since the true definition actually varies quite subjectively from author to author. Nevertheless, one of the bi-products of this research will allow clarification on how well the Sand River wetlands conform to the dambo model to date.

The distinction between the proposed study here and previous studies on dambo hydrology is the issue of landscape setting and anthropogenic disturbance. The Craigieburn-Manalana catchment is a highly altered, degraded headwater catchment, which lies at a relatively low altitude on the fringe of the South African lowveld, whereas other dambo studies have focused on sites at much higher elevations within the African interior and in a much less altered state.

1.5 HYDROLOGICAL PROCESSES DEFINITION

1.5.1 Inputs to the Water Budget

This thesis required detailed hydrological process studies at a much finer resolution than at the catchment scale, as it is these processes that define how precipitation will be partitioned at the catchment soil surface, infiltrate into the sub-surface and, how it may move through the catchment and eventually reach it's outlet. Furthermore it is important to determine how long water is stored as surface water, soil water and/or groundwater (e.g. Uhlenbrook *et al.*, 2005). The study of hillslope processes enables the determination of the dynamics of surface and sub-surface inputs to the wetland system as well as their quantification. This forms the first objective with regards to the wetland water budget:

O2a. Quantification of surface and sub-surface inputs to the Manalana wetland: which are the most significant contributors to the wetland water budget and do these vary by location and season (time)?

This follows from the principal question of whether the Manalana catchment conforms to the 'Horton Overland Flow Model' of runoff generation, or, whether it satisfies the 'Variable Source-Area (VSA)/Partial Area/Interflow Model'. The former model applies to areas devoid of vegetation and areas impacted by human activity where infiltration rates are less than rainfall rates. The latter applies to catchments that are well vegetated, with well developed soils and with minimal human impacts where infiltration rates are usually greater than most rainfall rates so that rainfall infiltrates and flows through the soil towards a stream (or wetland) as interflow (Ward & Trimble, 2004).

Two definitions are critical to understanding soil water infiltration within a catchment. The first is the *hydraulic conductivity* of the soil, described as the rate at which water is transported away into the profile per unit hydraulic gradient. The second is the *infiltration capacity* which is the maximum rate that water can infiltrate at any point under given conditions, and this is a function of soil type, soil moisture content, organic matter, seasonal vegetation, season and porosity (Lorentz *et al.*, 1995).

Darcy's Law (Darcy, 1856), states that the flow of groundwater is proportional to the slope of the piezometric surface or hydraulic gradient (i) and the hydraulic conductivity (K) of the soil (Mitsch & Gosselink, 1993). Where Darcy's Law has been extended to describe the flow of water through unsaturated porous media, the Green-Ampt equation (Green & Ampt, 1911) was developed directly as an analytical solution to describe the flow of infiltrating water (f), or wetting front, under constant rainfall, this complements the initial Horton Equation (Horton, 1940) describing infiltration at time t. These equations (which the reader can refer to original sources) are the critical basis for understanding the separation of surface and subsurface water and their consequent flow paths.

Furthermore, *redistribution* is the term used to describe movement of water once infiltration has terminated and is defined as the movement of water through the unsaturated soil profile (Schulze, 1995). Redistribution may occur as water movement down to the groundwater store by percolation, primarily due to gravity but influenced by layers in the soil profile. Otherwise it may travel towards the soil surface by soil water evaporation and transpiration induced capillary action. The Richards Equation (Richards, 1931) is a combination of the Darcy equation and the continuity equation (for continual discharge per unit area), and it is a standard equation that will describe infiltration and redistribution (unsaturated flow). The Richards Equation is dealt with in greater detail in chapter 6 of this thesis where is it used within the context of the HYDRUS (Šimúnek *et al.* 1999) model to describe dominant soil physical processes that facilitate hillslope-wetland hydrological connectivity.

In addition to water redistribution with the soil matrix, it is also the case that water that infiltrates the soil may also take one of two principal routes; near surface macro-pore flow (through- or inter-flow); or groundwater perched at the soil-bedrock interface. A third route is deep percolation into an aquifer. Water that does not infiltrate the soil matrix runs off the soil surface as overland flow. Overland flow can be estimated using the laws of *conservation of mass and momentum* which give rise to the equations of continuity and momentum or more simply, the equations of motion (Gerits *et al.*, 1990; after Chow, 1959). Overland flow generation arises due to certain parameters which describe the potential infiltration rate which

in turn influences the rate of runoff on a hillslope. This is due to the unsaturated hydraulic conductivities and related saturated conductivity of a hillslope soil which are a function of the soil pore size distribution and the hysteric properties associated with this. These factors limit the water storage capacity and water retention characteristics of the soil in question. For instance Martinez-Mena *et al* (2001) found that pore size distribution was a critical factor influencing the variability of threshold runoff generation on different hillslopes in semi-arid northern Spain. This effect is described by the hysteric properties of the soil (where small pores fill first during wetting, whilst large pores empty first during drying; a function of soil water potential/tension) and its history of wetting and drying. Meanwhile, Nicolau (2002) found that mechanisms leading to Hortonian overland flow on artificial slopes in the Mediterranean could be attributed to surface sealing on one mine residue substrate, and the degree of vegetation cover on another substrate covered by topsoil. Discussed in Martinez-Mena *et al* (1998) is the spatial non-uniformity of runoff generation on hillslopes, which in humid and semi-arid areas is attributable to spatial variation in soil infiltration capacities. This variation is due to antecedent soil moisture conditions in humid areas, whilst in arid and semi-arid landscapes this is due to rainfall characteristics and the physical and chemical properties of the soil surface. This therefore highlights the need to account for this spatial variation in runoff generation at the hillslope scale.

Studies of hillslope hydrology have largely focused on determining the sources of storm-flow water in catchments, this has generally been through a combination of experimental and validated modelling techniques, where experimental approaches have been used inferentially to form or update the perceptual models of watershed processes (Sivapalan, 2003). Particular attention has focused on the flowpaths of subsurface water, with recent research concentrating on the mechanisms that explain rapid movement of old water into stream channels (Weiler & McDonnell, 2004). Of the four conceptual processes of subsurface stormflow generation summarised by Weiler & McDonnell (2004), two are pertinent to objective O1a in this study: the first, *transmissivity feedback*, is where vertical recharge into the saprolite (geochemically weathered bedrock) must first occur before the water table rises into the transmissive soil zone whereupon lateral flow commences; second *lateral flow at the soil bedrock interface*, where water ponds above the bedrock and induces lateral flow due to the steepening gradient of the ponding water, described by the *saturated-wedge hypothesis* which assumes a threshold gradient from which flow is instigated (McDonnell, 2003). It is the knowledge of the bedrock topography therefore that is important for understanding the runoff generation mechanism at the hillslope scale (Freer *et al.*, 2002). Either of these processes, or a combination of the two, may occur in the steep Manalana catchment and ascertaining the contribution of these to the wetland water budget is crucial to understanding the hydrological dynamics of the Manalana

wetland. Furthermore, determination of whether these groundwater inputs adhere to the *steady-state* hypothesis (no change of head with time, i.e. the magnitude of groundwater flux velocity is constant with time) of groundwater flow will enable the inference of whether the wetland water table and surface flows respond in accordance with or independently of these sub-surface hillslope inputs. For instance, Seibert *et al* (2003) have shown that catchment runoff correlates well with groundwater levels close to the runoff channel, but that upslope groundwater levels were quite independent of this catchment runoff response.

Quantification of the three principal hillslope processes at experimental locations has been described by Lorentz *et al* (2004) where; overland flows have been determined by analysis of runoff plot data; macro-pore flows have been monitored through a combination of runoff plot data and hydrometric observation techniques (automated soil moisture tensiometers); and perched groundwater flows were examined through further hydrometric observations (automated soil moisture tensiometers and groundwater level records). Determination of the underlying hillslope hydrologic processes addresses the following hypothesis with respect to objective 1a:

H_0 – water is not supplied to the Manalana wetland largely as overland surface flow from the contributing catchment (as a consequence of reduced infiltration into the sub-surface within the catchment interfluves).

Since this thesis had a core focus on quantifying the wetland water budget and in essence also aimed to quantify the inputs and outputs to and from the wetland, it was therefore a necessary prerequisite to understand how the water inputs actually flow through the wetland as surface and sub-surface throughflows (interflows). Since these throughflows will flow through the wetland in three domains; horizontally (infiltration), vertically (diffusion), and at the wetland surface (discharge), it is necessary to quantify these processes explicitly as they are integral components of the wetland's hydrodynamics. Furthermore since water within the wetlands subsurface may flow within both a saturated and unsaturated zone (variably saturated) it is necessary to also delineate these processes by the identification of the wetlands water table (or phreatic surface).

Thus the discussion yields a second sub-objective as follows:

O2b. Quantification of the wetland throughflows (in the horizontal sub-surface, vertical sub-surface and surface domains).

By stating this objective at the outset it is therefore rational to continue the discussion here in relation to the proposed rehabilitation intervention taking place at the Craigieburn-Manalana catchment.

Recall that the assumed underlying causes of wetland degradation in the Manalana catchment is erosion (principally gully erosion), with consequent desiccation and loss of fertility, then rehabilitation attempts to reduce runoff velocity and encourage sedimentation (or at least minimise sediment losses) are the main objectives for intervention. These kinds of intervention often make use of specialised structures, or bio-engineering or a combination of both, which control the flow of water and promote sedimentation (Grenfell *et al.*, 2004). Dam and weir type gully *plug* structures have been used in South Africa in an attempt to rehabilitate wetlands affected by gully erosion. These structures are generally impermeable to relatively permeable structures built across channels in order to obstruct the flow of water and raise the upstream water level as well as retard the downstream runoff velocities. As a consequence these structures block the erosion channel and reinstate the original flooding regime and sedimentation processes (Grenfell *et al.*, 2004). These weir type structures are generally placed within the gully at a pre-defined downstream location away from the headcut to follow the natural sedimentation slope (Figure 1.4). This downstream position allows for flooding back to the problem area in order to protect it by ponded (low energy) water and to create a stilling area for sediment deposition to in-fill the gully (Russell, 2008). Although it is generally acknowledged within the engineering fraternity that these types of structures can be used to reinstate the wetland groundwater regime, there appears to be a paucity of precise hydrological information in the scientific literature to support this specific tenet (this is discussed in more detail in the respective paper dealing with this issue, Chapter 5).

The analysis of data from wetland sites, mainly in the form of groundwater level measurements, can yield important insights into the likely response of the sites to changes in their surroundings; furthermore these measurements should therefore provide a means of assessing the hydrological behaviour of a wetland site to both natural and artificial influences (Gilman, 1994). Dixon (2002) has shown how alteration of on-site conditions, through drainage cultivation practices, has deleteriously impacted the wetland groundwater regime through comparative analysis of pristine and cultivated headwater wetlands of the Illubabor region of Ethiopia. Hence it was envisaged to possible that responses of the water table to rehabilitation interventions such as the one at the Manalana catchment could be observable with such measurements. A sub-objective therefore arises from this discussion with a corresponding hypothesis:

O3. Quantification of the responses to the rehabilitation intervention on the wetland hydrological dynamics (to include an inference on the natural hydrological dynamics before headcut erosion in the absence of baseline data).

O3.i. H_0 – The rehabilitation structure (buttress weir) to be installed at the first headcut within the Manalana catchment does not raise the wetland water table (phreatic surface) upstream of it.

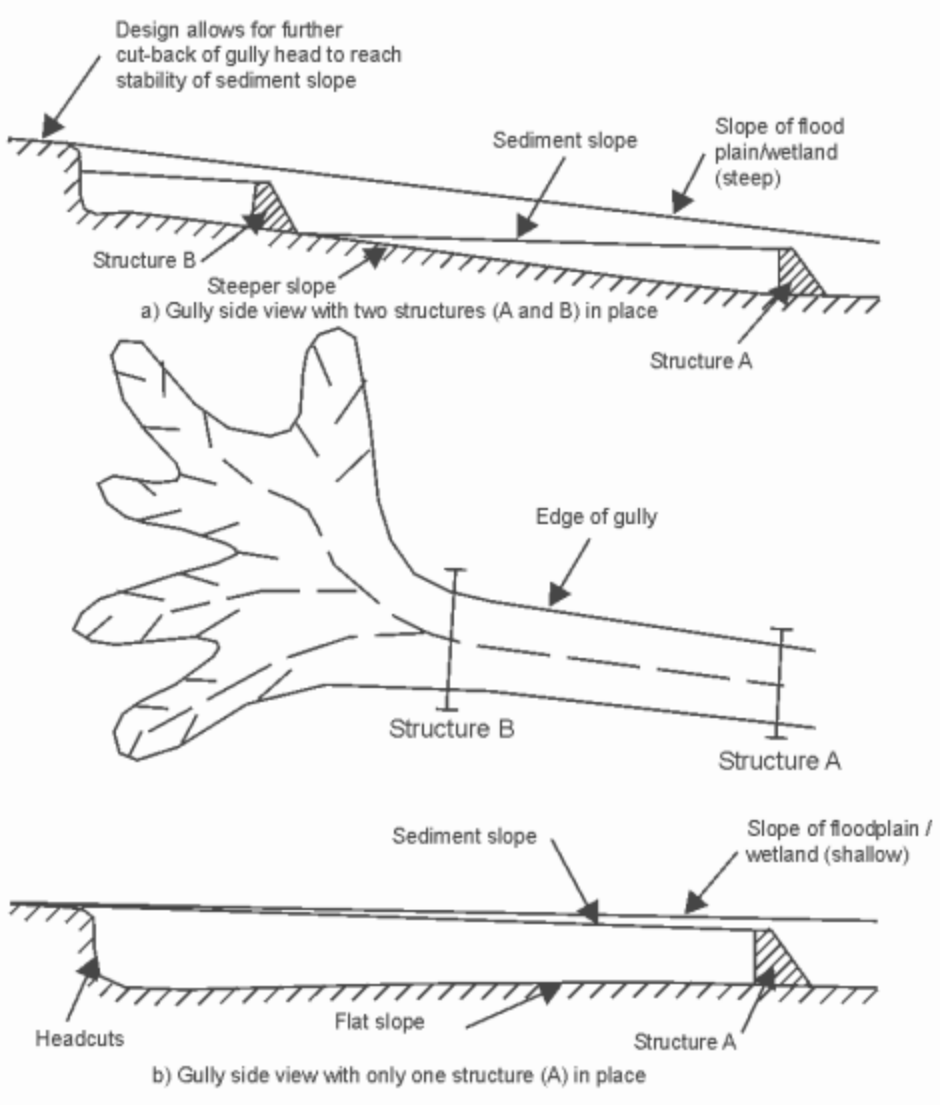

Figure 1.6: Wetland rehabilitation principles using 'plug' weir type structures (From Russell, 2008).

1.5.2 Outputs from the Water Budget

Evapo-transpiration (ET) is another crucial component of the wetland water budget and as such it should not be overlooked as it often comprises a considerable output from the mass balance, particularly in arid and semi-arid settings with high solar radiation and temperature. For instance Bullock and McCartney (1996) found that the evapotranspiration component exceeded that of base-flow (dry season discharge) from dambo catchments during the dry season in Zimbabwe. However when water supply is limited, evapotranspiration is limited as well (Mitsch & Gosselink, 1993), although this is generally a rare occurrence in permanent wetlands it could be a regular feature in temporary and seasonal wetlands located in dry, warm (as well as windy areas) with high solar radiation, such as the Manalana wetland and its contributing catchment. This is due to the meteorological conditions of solar radiation or surface temperature that increase the vapour pressure at the evaporation surface of the wetland, or otherwise, decreased humidity or increased wind speed that decrease the vapour pressure of the surrounding air (Mitsch & Gosselink, 1993).

Evapotranspiration comprises two stages by considering the soil water availability (Jacobs *et al.*, 2002). First stage evapotranspiration/potential evapotranspiration (E_{tp}) describes the rate at which water if available would be removed from soil and plant surfaces, this rate is therefore only limited by available energy. Whilst second stage/actual evapotranspiration (E_t) occurs during drying conditions when water availability becomes limited. As described by Jacobs *et al* (2002); first stage evapotranspiration largely characterises wetlands when they are inundated. Meanwhile when the water table fluctuates below the shallow root zone during drying phases, the wetland vegetation becomes stressed and hence they transpire at less than their potential, hence second stage evapotranspiration occurs. When considering the case of the Manalana catchment which lies in a strongly seasonal region of warm dry winters and wet warm summers, it was anticipated to be highly likely that this two stage scenario of evapotranspiration will occur.

Discharge (Q) which for wetlands, as discussed earlier can be quite variable depending on the type of wetland one is dealing with as well as other factors such as seasonality in climatic conditions. This variable is measured through the provision of flow measuring devices such as weirs or flumes. These are widely used for measuring channel discharge in many circumstances, and in terms of wetlands this is considered as the *surface discharge*. For the purposes of this study a continuous record was of course desirable and was factored in at the point of rehabilitation to double-up as a weir.

If we are to assume that the rehabilitation structure to be installed at nick-point 1 in the Manalana catchment aims to isolate groundwater discharge from the downstream section of the wetland (and hence increase upstream recharge), then stream discharge and evapotranspiration should represent the only outputs from the water budget of the Manalana wetland. Therefore stream discharge may represent an enhanced output from the wetland water budget.

Groundwater can flow into, through, or out of a wetland. The contribution of groundwater flow and/or loss to wetland systems can be hugely variable between some wetland systems that are groundwater dependent and often linked to an underlying or adjacent groundwater aquifer in which case the groundwater discharges to the wetland. Whilst other wetlands are termed groundwater recharge systems, in which case water concentrates within the wetland and then percolates down to a deeper groundwater aquifer. Other wetlands may show spatial variability where they gain groundwater at one location but lose it at another. It is also important to note that individual wetlands may temporally change from one type to another depending on how the surface water levels in the wetland relate to the aquifer water levels, and how these change over time in response to climatic variations and water management in the catchment (McEwan *et al.,* 2006). The flow of groundwater flow to or from a wetland can be quantified by Darcy's Law and the measurement of this in-situ is described in section 3.1.3 of this thesis.

1.6 LAND-USE IMPACTS

This study is cognisant of the pressures derived from anthropogenic land-use and management, because some land-use practices could (and likely are given the earlier discussion) inadvertently have an effect on the hydrological, geomorphological and ecological component processes of the wetland (hydro)ecosystem.

Since wetlands are very fragile systems, severe ecological and environmental deterioration may occur as a result of *wetland alteration* in their conversion to cropland (Tegene and Hunt, 2000). The most common impacts of the conversion of wetland soils to cropland are the severe erosion of wetland soils, disruption of water flow regulation, and loss of water quality, these all inevitably lead to loss of wetland function and biodiversity. In the Illubabor region of Ethiopia poorly managed cultivation within the wetlands there has led to the abandonment of some cultivated areas due to considerably reduced fertility, as a consequence of increased

erosion and desiccation of the wetland soils (Tegene and Hunt, 2000). This in essence is a similar scenario reported by the resident wetland farmers of the Craigieburn-Manalana catchment. Meanwhile Roberts (1998) suggests that the impacts of intensive cultivation and overgrazing on dambo wetlands have led to their deterioration through a lowering of the water table, reduction in surface vegetation cover subsequent exposure of the soil, erosion and gully formation, and reduction in organic matter and desiccation of the soils. The point to be made here is that once a natural system is modified by human impacts whether directly through physical disturbance, or indirectly such as by grazing, then there will be consequent impacts on the inherent processes of that natural system.

The objective of the rehabilitation interventions at the Craigieburn-Manalana catchment are to address the current erosion and desiccation issues, and the focus of the proposed research here is to determine the wetland and catchment's hydrodynamics and the response of this to rehabilitation. As this also has a wider application in terms of integrated catchment management for the Sand River system, then it is the integrated approach to wetland rehabilitation that must be followed in this regard, as the wetland cultivation and other land-uses occurring at Craigieburn are likely to continue for the foreseeable future. Hence, it was deemed necessary to define (quantitatively) the impacts that these agricultural practices have on the wetland hydrological and geomorphological processes, so that these findings are relevant for future management in the broader Sand River catchment. However as the study proceeded and land-uses changed (see study site Chapter) an interaction with the local land-users at this level of investigation was not deemed practical. The thesis instead attempts to qualify the impacts of land-uses based on the hydrological and geomorphological characterisations of the Manalana catchment. A sub-objective then arises from this discussion:

O4. Qualification of the impacts of land-use practices within the Craigieburn-Manalana catchment that impacts on the wetland (and contributing catchment) hydrodynamics.

1.7 STRUCTURE OF THE THESIS

Figure 1.7 provides a road-map for the structure of this thesis and how each of the following chapters addresses the objectives just developed. These objectives and hypothesis testing will be returned to explicitly in the discussion in chapter 9.

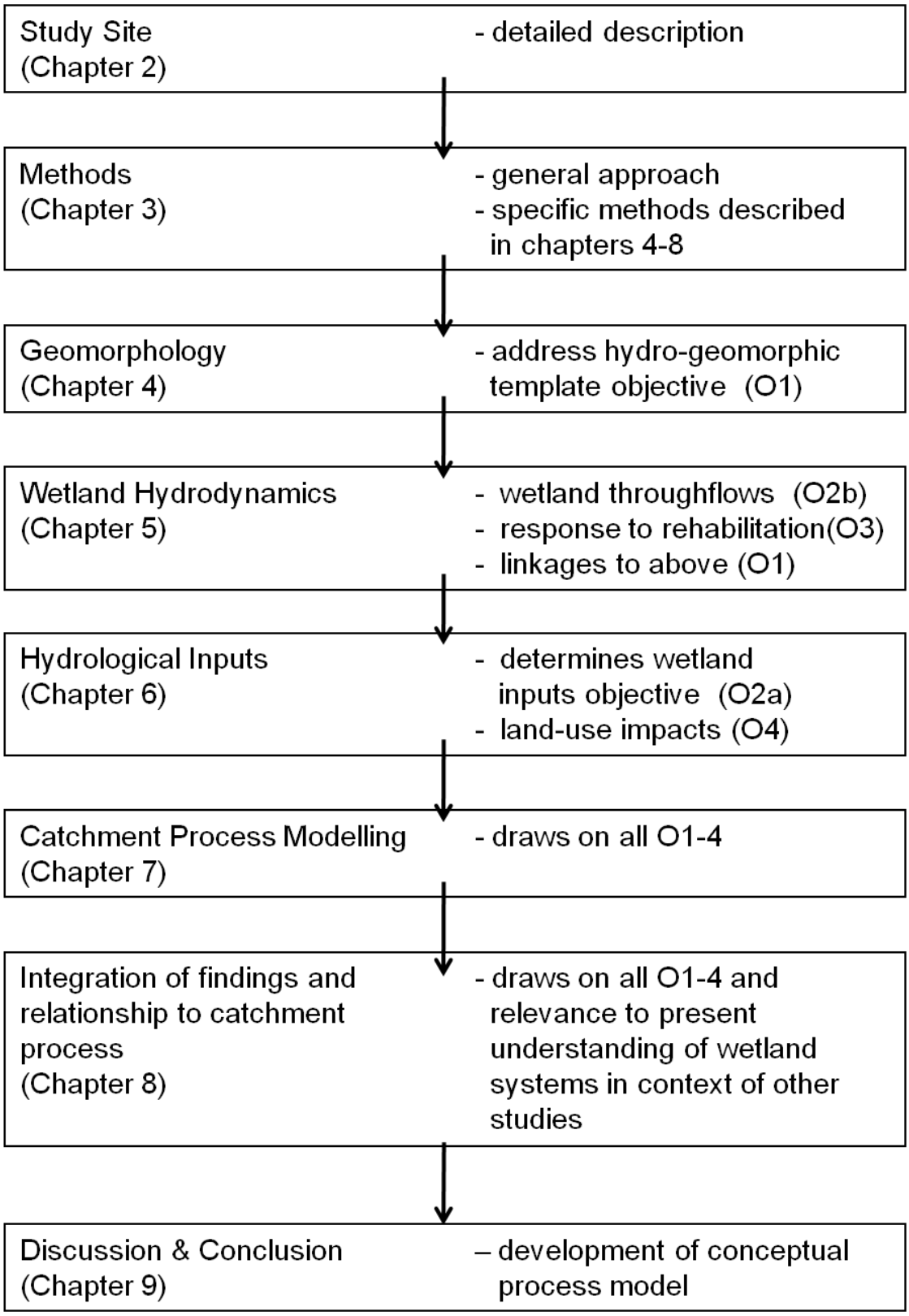

Figure 1.7: Road-map of the thesis structure and the chapter address each of the developed objectives

2 STUDY SITE

2.1 SAND RIVER LOCATION, CLIMATE & SOCIAL SETTING

The Manalana sub-catchment lies at the headwaters of the Sand River (Figure 2.1). This river basin, at 1910 km^2 is the main tributary of the Sabie River and is situated in its entirety within the South African Lowveld (formerly the eastern Transvaal) and was at one stage considered a perennial river (Pollard *et al.*, 2003). However the river is now considered severely degraded and is essentially a seasonal river system.

A key feature of the Sand River catchment is its high degree of variability (Pollard *et al.*, 2005). An distinctive biophysical characteristic is its sharply decreasing altitude from 1800 m.asl in the west at the Klein Drakensberg escarpment (Figure 2.2) to 450 m.asl in the east, within a distance of just 80 km. This relates to the tectonic uplift (over two periods, 20 M and 5 M years ago) of the erosion resistant quartzites, formed by sedimentary infilling of small rifts in the ancient continent of Kaapvaal that now make up the Drakensberg escarpment. The erosion resistant rocks contrast strongly against Archaean granites in the lowveld, themselves the unburied relicts of the basement complex rocks of the ancient Kaapvaal continent (McCarthy & Rubidge, 2005). The impact that this combination of tectonic activity and geology has on present erosion processes dominated by water is suggested in Figure 2.2. Here it is apparent that the steep relief in the west facilitates greater hydraulic energy to erode the landscape. However as one moves further east the lowveld relief becomes a far less steep, planation type landscape where geomorphology becomes increasingly dominated by weathering.

Corresponding to the sharp change in relief there is a sharp decrease in rainfall from 2000 $mm.a^{-1}$ in the humid/lower temperature mountainous region to 550 $mm.a^{-1}$ in the eastern semi-arid/higher temperature savanna region. Precipitation in the lowveld is strongly seasonal with rain falling during the hot summer months (October-March) which is governed by the seasonal shift in the South Indian Anticyclone, part of a subtropical anticyclone belt centred n 30°S, bringing with it moist air from the south-east (Ross *et al.*, 2001). The Sand River catchment is itself prone to periodic droughts with a return interval as frequent as every three and a half years (Save the Sand Project, 2002).

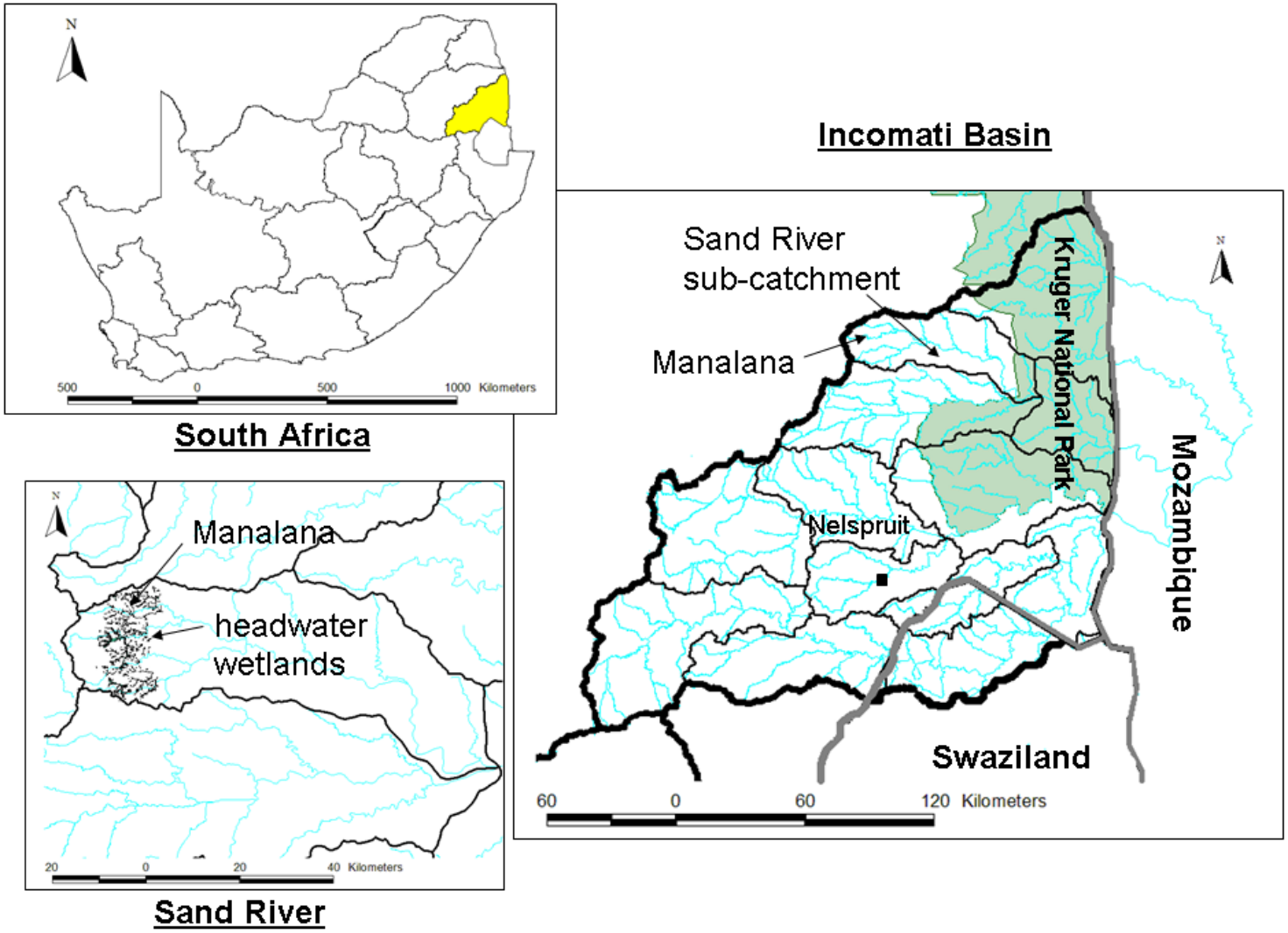

Figure 2.1: Location of the Manalana wetland with respect to the Sand River, Incomati Basin, and north-eastern South Africa.

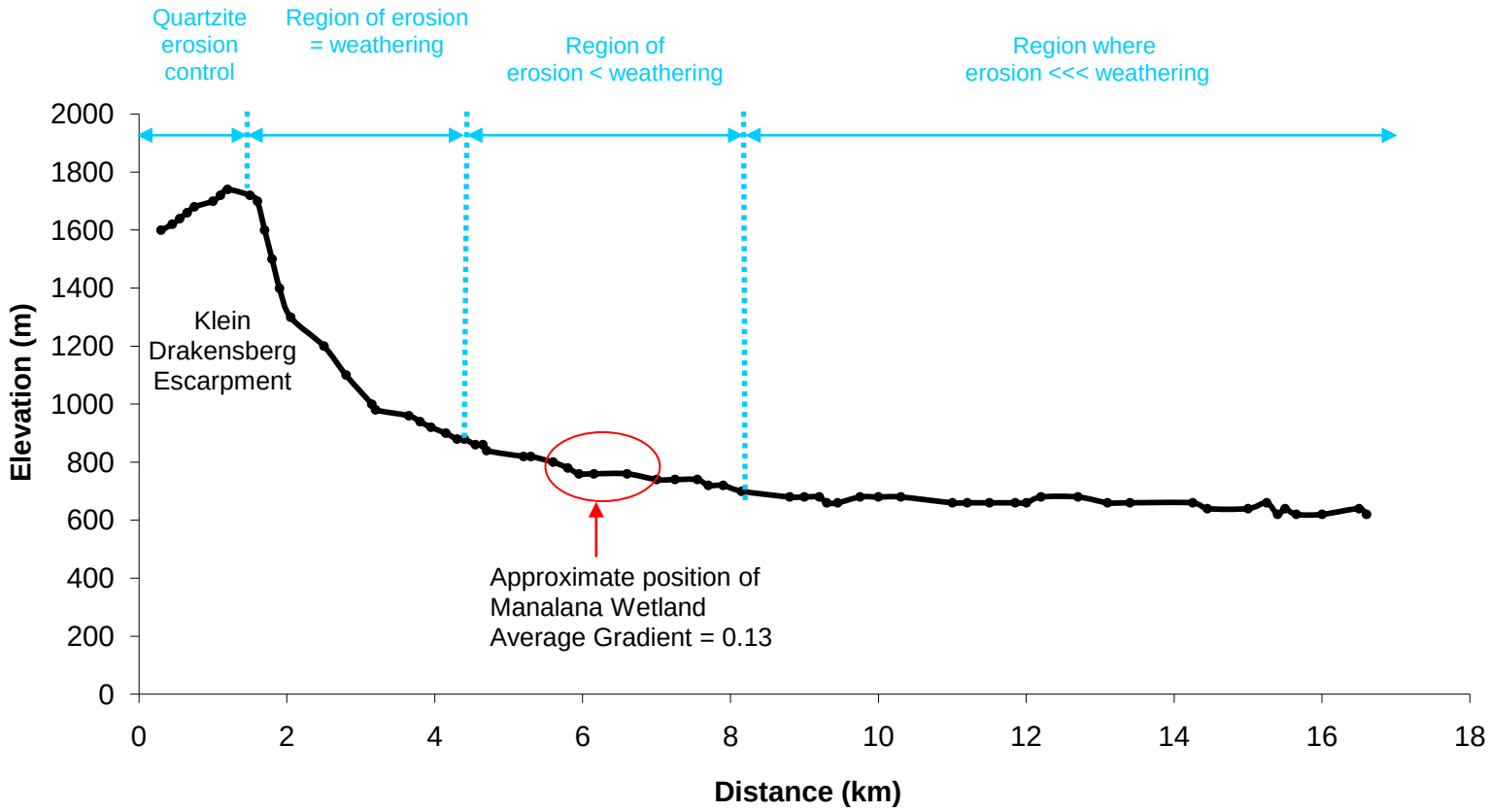

Figure 2.2: Cross-sectional profile of the upper Sand River catchment, position of the Manalana wetland, and general erosion processes (adapted from Pollard *et al.*, 2006).

The main land-uses in the catchment include state-owned exotic forestry in the upper catchment (extreme west on escarpment); the central region consists of rural residential areas in which subsistence cultivation is a major livelihood generator, as well as limited irrigated agriculture, and conservation areas in the east.

In 1972 the central lowveld, in which the majority of the Sand River is situated, was divided under grand apartheid planning into the two former homelands (bantustans) of Gazankulu in the east and Lebowa in the west. The former was established as a self-governing state for the Tsonga 'tribe' and the latter for the Pedi people. After 1994 these were abolished and these areas are now generally referred to as communal lands.

2.2 THE MANALANA SUB-CATCHMENT

The Manalana, a 2.61 km^2 catchment lies within the foot hills of the Klein Drakensberg and has an altitude of 654 m.asl at its confluence with the Motlamogasana stream and a maximum altitude of 744 m.asl at the highest point along the watershed. Whilst the Manalana has experienced a 1000% increase in population since the 1960's (Pollard *et al.,* 2006) as a result of re-settlement programs, the wetland extent has diminished considerably in the same period as noted through aerial photograph analysis (Pollard *et al.,* 2006) and recent delineation by the author and assistants (Figure 2.3). The approximate change in wetland extent during the period 1965-2007 was from 8% to 3% of the total catchment area (Figure 2.4).

Within the catchment there are three major nick-points/headcuts along its 2.5 km stream reach (Figure 2.5). These are instigating the headcut erosion which is leading to the elongation of the erosion dongas and loss of wetland extent. The site of rehabilitation that was scheduled for the 2006-2007 season is located at nick-point 1 situated at 24°40'03" S, 30°58'35" E, at which the wetland is considered to be an unchannelled valley bottom wetland and 1st order tributary. The rehabilitation at the second site at nick-point 2 commenced during 2006, this is situated at 24°40'04" S, 30°58'57" E whereupon the Manalana becomes a second order tributary.

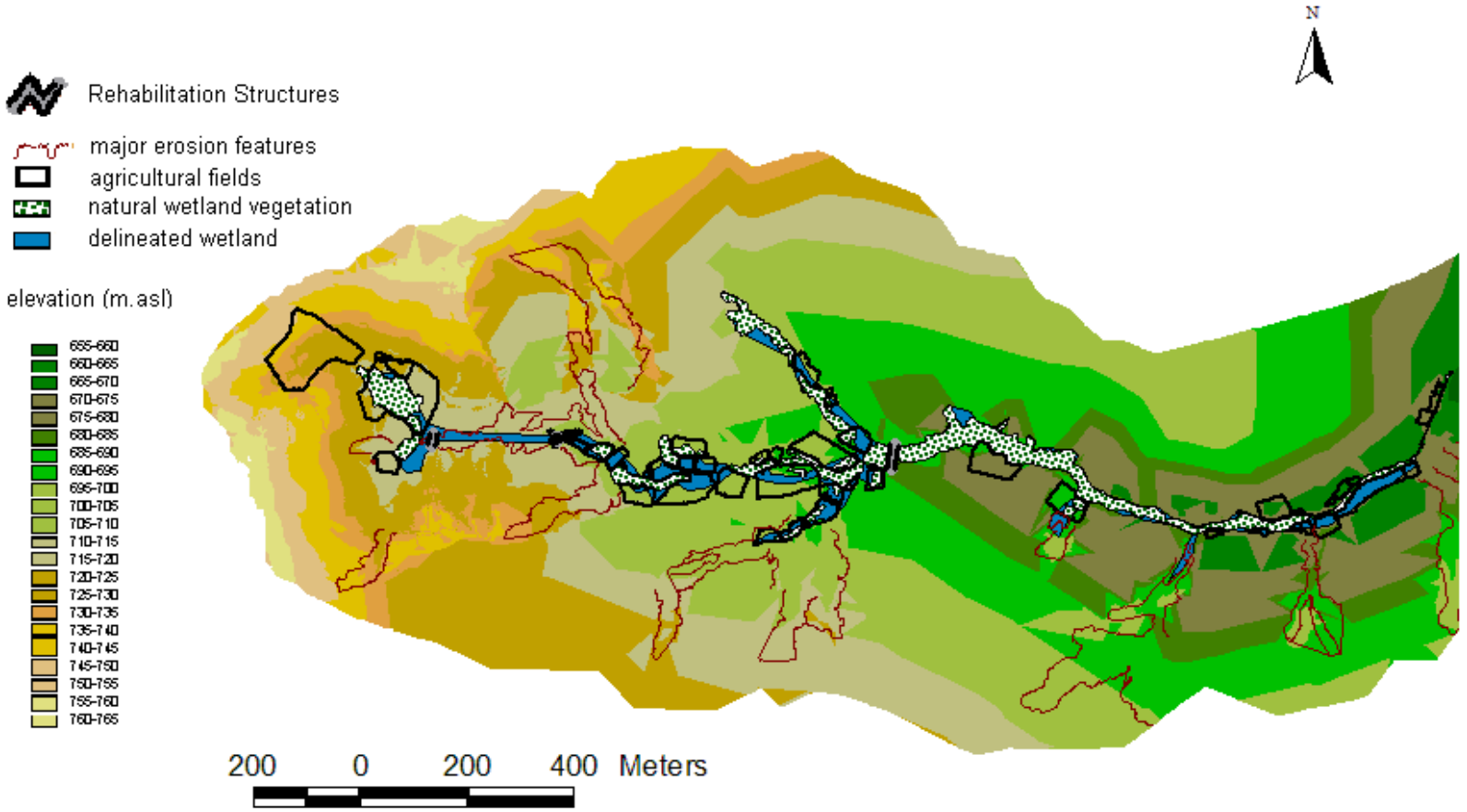

Figure 2.3: Digital Elevation Model and surface area data for the Manalana wetland and catchment (mapped 2007).

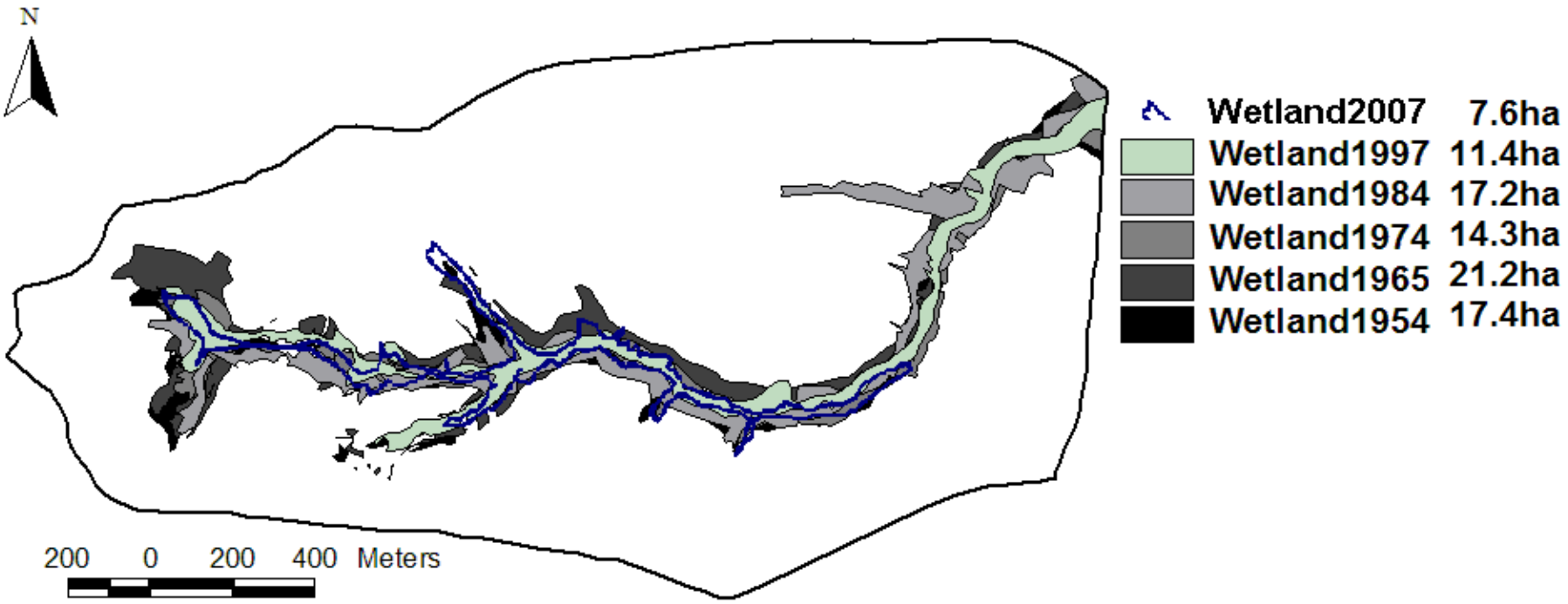

Figure 2.4: Historical extent of the Manalana wetland area (1954-1997 derived from aerial photo analysis described in Pollard *et al.*, 2006; through wetland delineation and GPS mapping 2007).

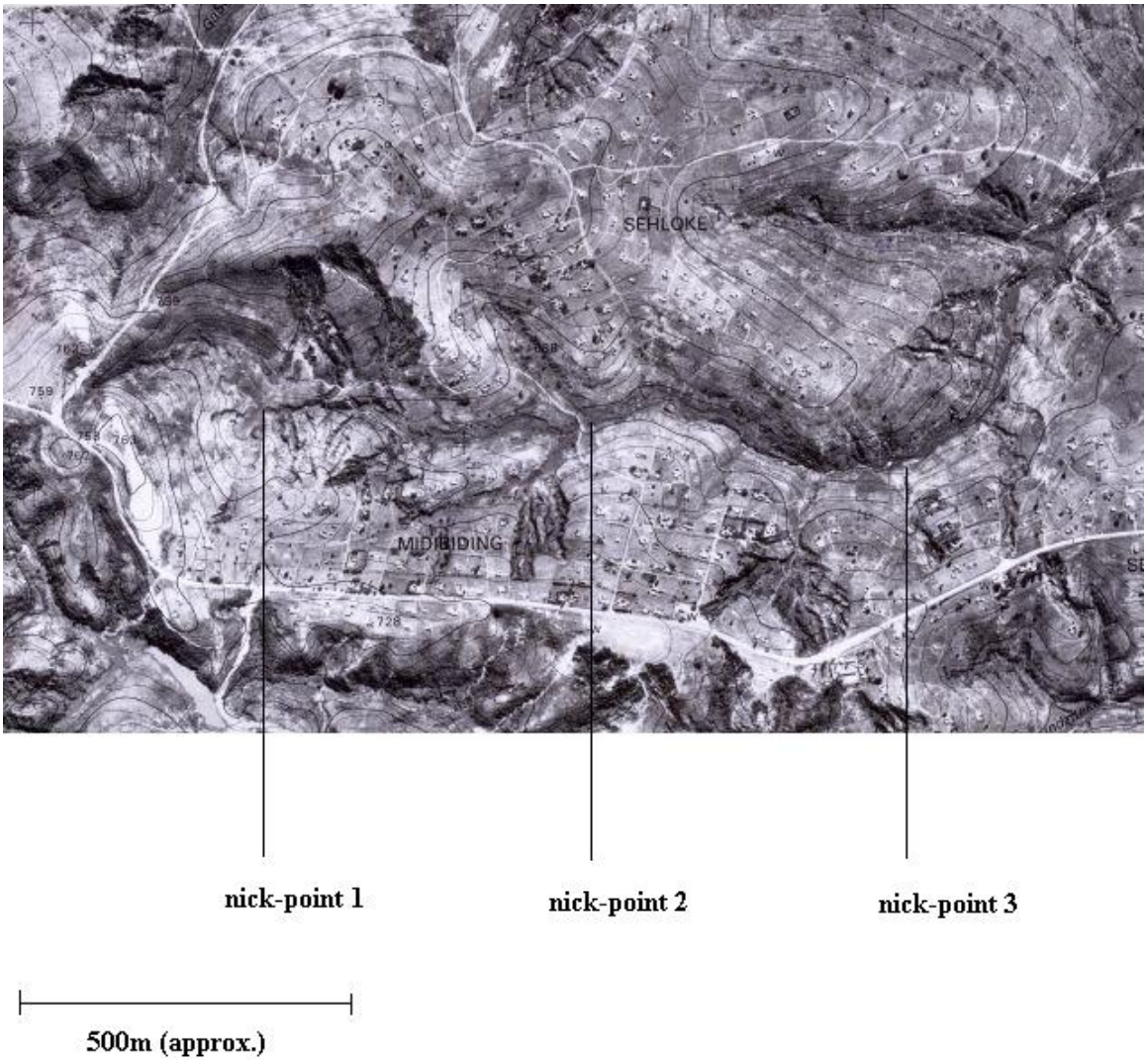

Figure 2.5: Orthophoto and location of nick-points along the Manalana sub-catchment (position 2005).

2.2.1 Climate

The mean annual precipitation for the local area has been derived from the 'Wales' catchment rain gauge (South African Weather Service gauge 0594819W) with a value of 1160 mm a^{-1} (the Craigieburn-Manalana catchment probably receives considerably less than this as it further away from the Klein Drakensberg escarpment, the mean precipitation for three full years of record 2006-2009 was 1024 mm). Historical records for nearby forestry stations (Figure 2.6) show the considerable inter-annual variability in rainfall in this catchment, but also the context over which this study was undertaken. The study commenced at the beginning of October 2005 (Hydrological Year 2005) and this first year had above average

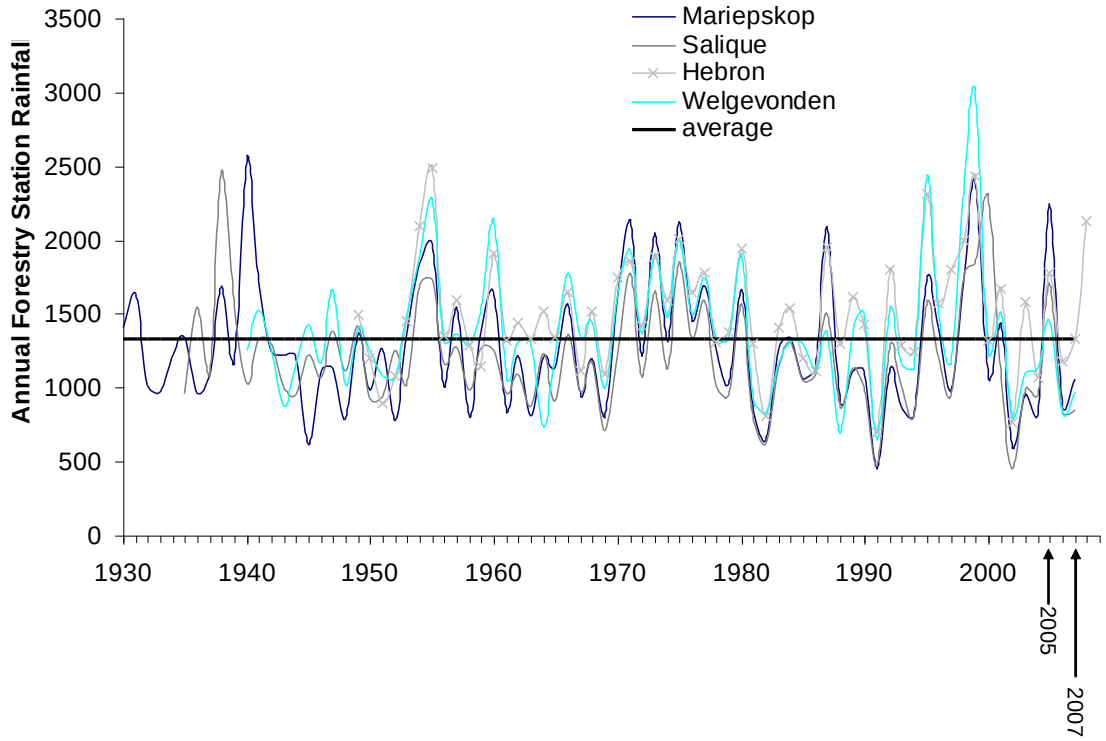

Figure 2.6: Historical rainfall for nearby forestry stations, plotted according to hydrological years (Source: South African Weather Service).

rainfall, whilst 2006 and 2007 where below average, and the final season examined in this study, 2008 was again above the general average.

2.2.2 Geology and Soils

The Manalana catchment lies in the granitic geological zone of the basement complex, underlain by white to pale brown, medium to coarse grained porphyritic biotite granite.

A survey of the Manalana catchment in 2004 described a stretch of the Manalana wetland, from its headward position downstream for approximately 700 m in geomorphological and botanical terms (encompassing the proposed rehabilitation site), (see Pollard *et al.*, 2005). As indicated by soil characteristics this wetland was consistently greater than 40m wide, and at its widest it was greater than 80 m. The regional gradient of the wetland was 1.3%, with the gradient above nick-point 1 at 2.1%. The absence of a considerable increase in aluminium with soil depth and distance downslope suggested that duplex soils are absent, whilst the variable concentrations of aluminium also suggest that clay content is quite variable in the catchment. In addition, low sodium concentrations overall imply that the presence of erodible

soils is unlikely to be due to sodicity, which is otherwise characteristic of the lowveld. Furthermore it was found that soil catenas are not well developed in this catchment as implied from particle size analysis. This being a result of the very dynamic geomorphology arising from the processes attributed to tectonic uplift.

The soils at the most headward reach of the Manalana, where the hydrological investigation was most focused, where classified according to the South African binomial soil classification (Soil Classification Working group, 1991) by a team from the Department of Soil, Crop and Climate Sciences, University of the Free State, Bloemfontein (Le Roux *et al.*, 2009). They identified six soil forms at this area of the catchment (Figure 2.7 and Table 2.1), and through the combination of these soil types, hillslope hydrological response units were identified for use in catchment based modelling, (see Chapter 7). The key aspect of the soil form analysis reveals that all soils in this catchment are overlain by Orthic-A horizons, which are generally regarded as 'normal' and lack organic, humic, vertic (strongly developed structure), or melanic (dark, structured) characteristics, and are widespread across South Africa (Soil Classification Working Group, 1991). Upland areas are dominated by the shallow Mispah soils overlying hard rocks, making them rather responsive hydrologically due to their shallow soil moisture store and hydraulically conductive due to their coarse grained composition. Interestingly the valley bottom areas show signs of fluvial sorting in the form of Dundee sub-surface horizons and heavily illuviated clay G horizons of the Kroonstad and Katspruit soil forms, these soils were also classified as being relatively responsive at the interface between the coarser grained leached A-horizons overlying dense and low hydraulic conductivity G horizons. The Oakleaf soils were described as recharge type soils due to their deep unconsolidated material in the neocutanic horizons, which facilitate the vertical movement of water rather than the predominantly lateral transmission feature of the former soils.

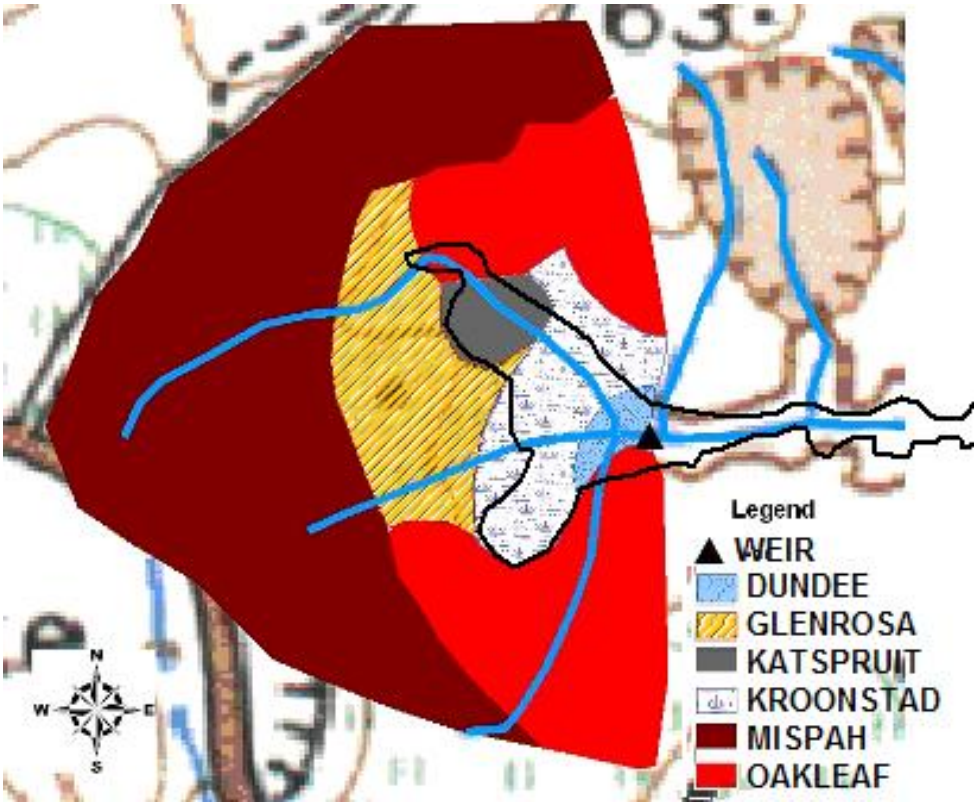

Figure 2.7: Approximate distribution of SA soil forms with respect to the headward end of the Manalana wetland (adapted from UFS, 2009).

Table 2.1: Soil form summary.

Form	**Horizon-1**	**Horizon-2**	**Horizon-3**
Dundee	Orthic A	Stratified Alluvium	
Glenrosa	Orthic A	Lithocutanic B	
Katspruit	Orthic A	G	
Kroonstad	Orthic A	E	G
Mispah	Orthic A	Hard rock	
Oakleaf	Orthic A	Neocutanic B	

2.2.3 Vegetation and Land-use

The results of the vegetation study (in Pollard *et al.,* 2005) revealed through cluster analysis, the presence of 8 plant communities ranging from grassy shrub land communities intolerant of flooding to communities that were tolerant of permanently flooded conditions. In addition the author undertook to describe the vegetation composition adjacent to and in-between hydrology monitoring stations according to the relevé method described by Mueller-Dombois & Ellenberg (1974) during February-March 2007, these descriptions are to be found in Appendix i. The upland areas tended to be dominated by *Parinari curatellifolia* (mabola plum) shrub land and valley bottom by *Phragmites mauritianus* (reed grass).

Land use in the Manalana sub-catchment itself comprises dense peri-urban housing on the catchment slopes with additional subsistence cultivation within smallholder plots. Cultivation of *Colocasia esculenta* (madumbe), spinach, sugar and bananas predominate the use of the wetlands as an agri-resource (Figure 2.8). This in the vast majority of cases takes place on a ridge and furrow system (running parallel to streamflow). There is also some harvesting of indigenous wetland plants for craft production. Whilst the headward end of the Manalana catchment was also used for subsistence cultivation in this way, this region had been abandoned (~ 2005) probably as a result of perceived desiccation of the wetland (by way of gully incision and hydraulic drawdown – Riddell *et al.,* 2007). As a result, for the duration of the study, this region was largely fallow, hence the re-colonisation by reed grass and other hydrophytic vegetation (Figure 2.9 & 2.10), although the ridge and furrow systems still remained.

Communal grazing also characterizes the catchment, which is often unrestricted. In addition there is a dense network of paths and roads crisscrossing the catchment. Table 2.2 summarises the agricultural practices observed within the Craigieburn-Manalana wetland and possible impact on bio-physical function of the wetland, these are described in greater detail in Pollard *et al.,* (2005).

Figure 2.8: Typical wetland agricultural plot in the Manalana

Figure 2.9: Summer/rain season view of the headward end of the Manalana wetland

Figure 2.10: Winter/dry season view of the headward end of the Manalana wetland

Table 2.2: Summary of agricultural practices observed within the Craigieburn-Manalana wetland and potential bio-physical impacts

Agricultural Practice	**Summary of possible bio-physical effects**
Tillage (frequent)	disturbance of soil, decrease soil strength, lack of root binding, increased erosion risk
Vegetation removal	decrease organic matter content, reduced catchment roughness; increase soil temperature volatilisation of nutrients, fertility decline and soil desiccation
Furrow excavation	increase velocity of wetland surface flows - increased erosion risk
Furrow steepness	increase velocity of wetland surface flows - increased erosion risk
Furrows unblocked	increase velocity of wetland surface flows - increased erosion risk
Bed orientation	often parallel to surface flow, hence increase velocity of wetland surface flows, increased erosion risk
Crops (high water demand)	desiccation of the wetland environment
Poor soil protection	by canopy cover (reduced through clearing and grazing), minimal application of surface mulch, increased susceptibility to rainsplash and sheet erosion, volatilisation of soil nutrients
Manure (low application, protection)	volatilisation of nutrients, fertility decline
Burning of residues	volatilisation of nutrients, fertility decline

3 METHODOLOGY

3.1 DEFINITION OF WETLAND AND CATCHMENT HYDROLOGICAL PROCESSES

In order to establish and quantify those mechanisms which sustain this wetland and its interaction with the surrounding catchment, and further to monitor the effects of the proposed rehabilitation structure, monitoring of the in-situ hydrodynamics of the catchment was required. The initial proposed study period was to encompass the two wet-dry season cycles between 2005 and 2007, however due to unforeseen failures in the rehabilitation interventions this was extended for the following two wet-dry cycles up to end of winter, September 2009. The following chapter outlines the general methods used to characterise the hydrology and other aspects of the Craigieburn-Manalana wetland, specific methods and maps of instrument location are described in the respective papers. A general location map is shown in Figure 3.1. (Locations in Chapter 4 differ from those in the rest of the document, Table 3.1 summarises the nomenclature and respective hillslope positions).

3.1.1 Meteorologic data

This data was continually recorded for the duration of the study period from June 2006 with the installation of an in-situ meteorologic weather station. This station recorded the following meteorologic variables in metric SI units:

Rainfall* (mm) – using a Campbell Scientific. Inc TE525MM tipping bucket rain gauge, calibrated to record 0.1 mm rainfall increments on a 15-minute time-step to record ¼ hour rainfall intensities.

Temperature (°C) & Relative Humidity (%) – using a Campbell Scientific. Inc HMP50 sensor providing 15-minute averages.

Wind Speed (m/s) – recorded using a Young Instruments^{TM} 03001 wind sentry, providing 15-minute average values.

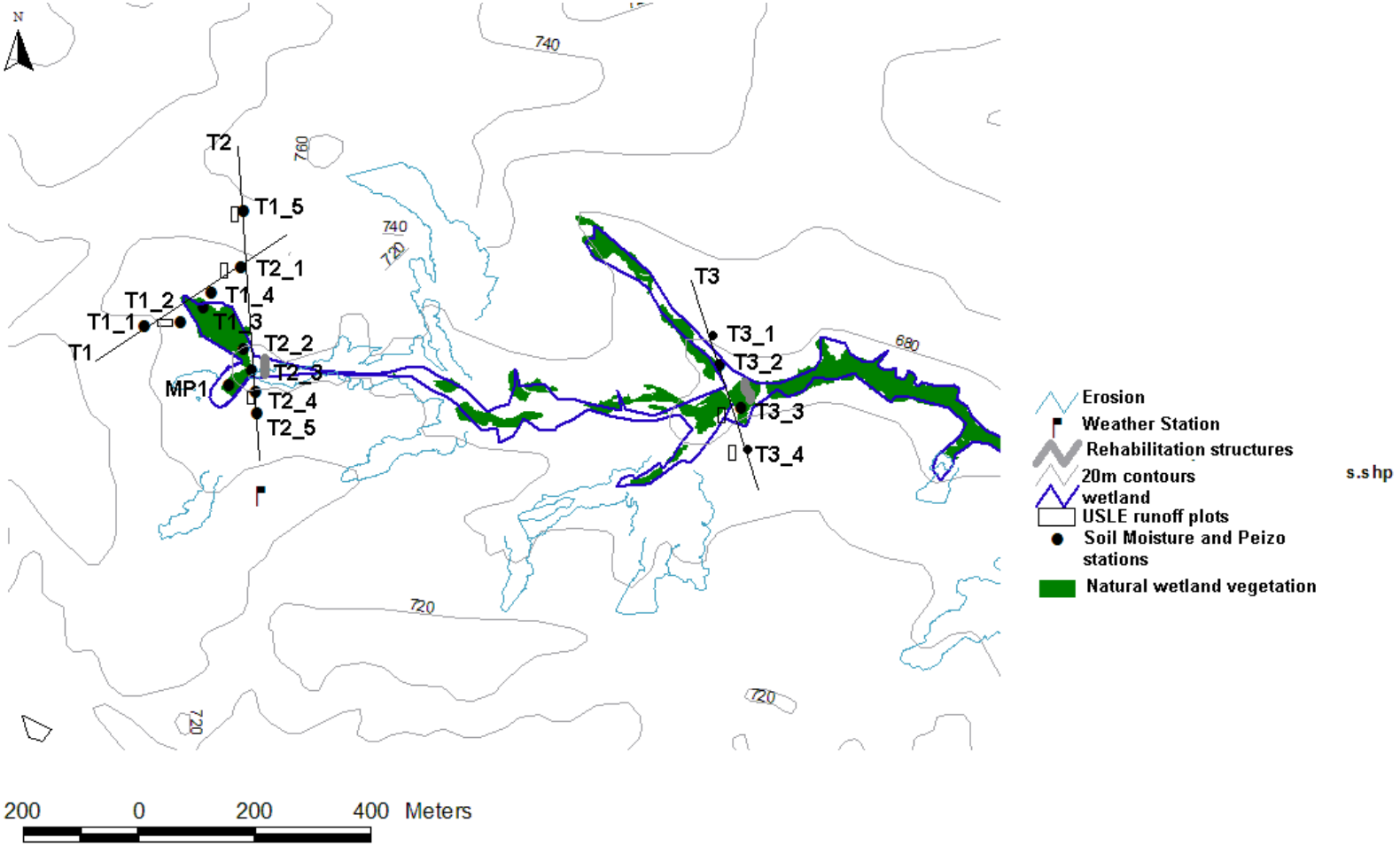

Figure 3.1: Location of hydrological monitoring apparatus in the Manalana catchment (streamflow was determined at the buttress weir rehabilitation structure adjacent to T2_3 on Transect T2, a gabion dam was installed downstream of Transect T3), for names of runoff plots which relate to their positions along the transects see Appendix viii,.

Table 3.1: Site names and their respective hillslope positions in the Craigieburn-Manalana

Site Name	Description	Chapter 4 Name	Hillslope Position
T1_1	Transect 1 Site 1	H1	Mid-slope
T1_2	Transect 1 Site 2	H2	Foot-slope
T1_3	Transect 1 Site 3	H3	Toe-slope (wetland)
T1_4	Transect 1 Site 4	H4	Foot-slope
T1_5	Transect 1 Site 5	H5	Up-slope
T2_1	Transect 2 Site 1	H6	Mid-slope
T2_2	Transect 2 Site 2	H7	Toe-slope (wetland)
T2_3	Transect 2 Site 3	H8	Toe-slope (wetland)
T2_4	Transect 2 Site 4	H9	Foot-slope
T2_5	Transect 2 Site 5	H10	Mid-slope
T3_1	Transect 3 Site 1	-	Foot-slope
T3_2	Transect 3 Site 2	-	Toe-slope (wetland)
T3_3	Transect 3 Site 3	-	Toe-slope (wetland)
T3_4	Transect 3 Site 4	-	Foot-slope
MP1	Manual Piezometer 1	H11	Toe-slope (wetland)

Solar Radiation (W/m^2) - recorded with an Apogee Instruments. Inc PYR pyranometer, these values were then converted to MJ/m^2 using the hourly constant 3.57×10^{-3}.

These sensors were connected to a Campbell Scientific Inc. CR200 data logger and interfaced with a notebook PC using the LoggerNet 3.0 and Device Configuration Utility 1.0 softwares.

Data assimilation prior to June 2006 made use of rainfall and other meteorological data via the South African Weather Service (SAWS) national database.

*Rainfall data was additionally measured on the opposite side of the catchment using a Texas Instruments TE525 tipping bucket rain gauge attached to an Onset HOBO™ Event Logger in order to collect breakpoint rainfall data, facilitating greater resolution in rainfall intensity measurements. In addition a 100 mm manual conical rainfall collector was installed in the wetland centre attached to a piezometer stand and this was recorded during routine site visits.

3.1.2 Catchment discharge and stable isotope sampling

This represents the surface outflow from the wetland and was recorded through the provision of a compound 90° v-notch (low flows) and rectangular section (high flows) weir

incorporated into the rehabilitation structure (buttress weir) placed at the first major erosion gully in the Craigieburn-Manalana catchment.

The design of the flow gauging parts of structure followed the design protocols as described by Van Heerden *et al.,* (1986) and predicted storm-flow peak discharge using desktop analysis Visual SCS-SA based design rainfall-runoff for small South African catchments (Schulze *et al.*, 1993). Meanwhile the entire structure was designed by Land Resources International (LRI) Ltd, and was constructed by Eastern Wetland Rehabilitation Ltd. contractors to the *Working for Wetlands* expanded public works program. A steel v-notch plate (Figure 3.2) was fitted into a rectangular opening in the structure by the University of KwaZulu-Natal.

3.1.2.i Peak discharge determination

The Visual SCS-SA method is a modified method of peak discharge determination using the Soil Conservation Service (SCS) method for small catchments, adjusted for southern African conditions. In order to determine peak discharge control variables in the Craigieburn-Manalana catchment physical and hydrological characteristics were required. The SCS method takes the form of equation 3.1 and 3.2:

(3.1) $$Q = \frac{(P - I_a)^2}{P - I_a + S} \quad for\ P > I_a$$

(3.2) $$S = \frac{25400}{CN} - 254$$

where;

Q = stormflow depth (mm)

P = rainfall depth (mm), usually input as a one-day design rainfall for a given return period

S = potential maximum soil water retention (mm), ≡ index of the wetness of the catchment's soil prior to a rainfall event

I_a = initial losses (abstractions) prior to the commencement of stormflow, comprising depression storage, interception and initial infiltration (mm) ≡ $0.1S$ recommended by Schulze *et al.,* (1993) as empirically derived for South Africa

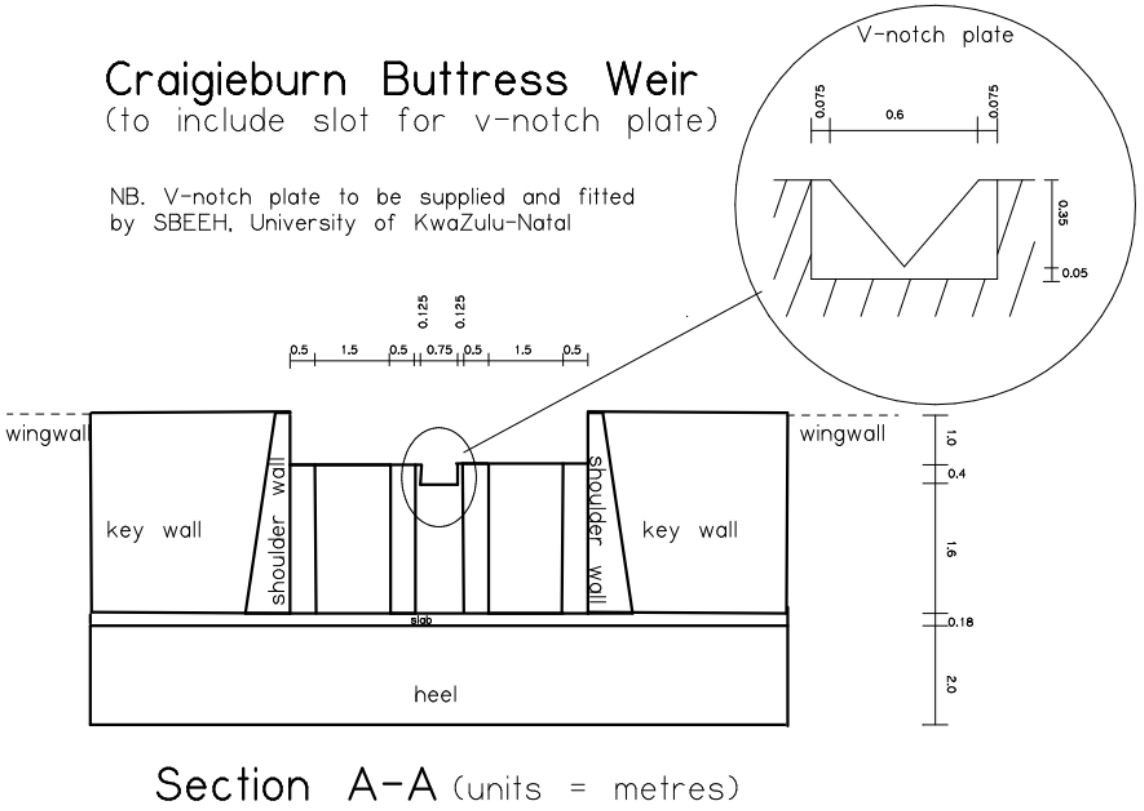

Figure 3.2: Design of the Craigieburn-Manalana rehabilitation buttress weir incorporating v-notch and rectangular flow gauging sections (adapted from design by Russell, B. Land Resources International [LRI], 2006)

CN = curve number ≡ index expressing a catchments stormflow response to a rainfall event, using look up tables considering catchment soil and land cover properties, and antecedent soil moisture status.

Meanwhile peak discharge for an increment of time (ΔD) is governed by equation 3.3, according to the triangular unit hydrograph concept (equation 3.3):

(3.3) $$\Delta q_p = \frac{0.2083 A \Delta Q}{\Delta D / 2 + L}$$

where;

Δq_p = peak discharge of incremental unit hydrograph (m^3/s)
A = catchment area (km^2)
ΔQ = incremental stormflow depth (mm)
ΔD = unit duration of time (h), used with the distribution of daily rainfall to account for rainfall intensity variations
L = catchment lag (hours), an index of the catchments response time to the peak discharge.

Due to the dry winters and limited vegetation cover in the semi-arid Craigieburn-Manalana catchment, *L*, was determined using the SCS lag equation 3.4:

(3.4) $$L = \frac{l^{0.8}(S'+25.4)^{0.7}}{7069\, y^{0.5}}$$

where;

L = catchment lag time (h)
l = hydraulic length of catchment along the main channel (m)
y = average catchment slope (%)
$S' = \frac{25400}{CN - II} - 254$
with

CN-II = retardance factor approximated by the initial Curve Number unadjusted for antecedent soil moisture (empirical look-up tables)

Table 3.2 shows a summary of the conservative input variables for the Visual SCS-SA determination of peak discharge in the Craigieburn-Manalana catchment for the weir design. To account for differences in soil types between the valley bottom wetland and upland, the catchment was disaggregated to two sub-catchments. The results of the simulation and final weir flow ratings (next section) are displayed in Figure 3.3.

Table 3.2: Summary input variables for Visual SCS-SA peak discharge determination

Total area (km^2)	0.292
Rainfall Intensity zone	Type 2
Mean Annual Precipitation (mm)	1198
Altitude (m)	~750
Slope	13%
Soils	deep sandy loams (upslope)
	very deep sandy clay loams (wetland)
SCS soil type	B/C (combined upslope/wetland)
Veld cover	poor (high stormflow potential)
Final CN	73.3 (upland)
	91 (wetland)

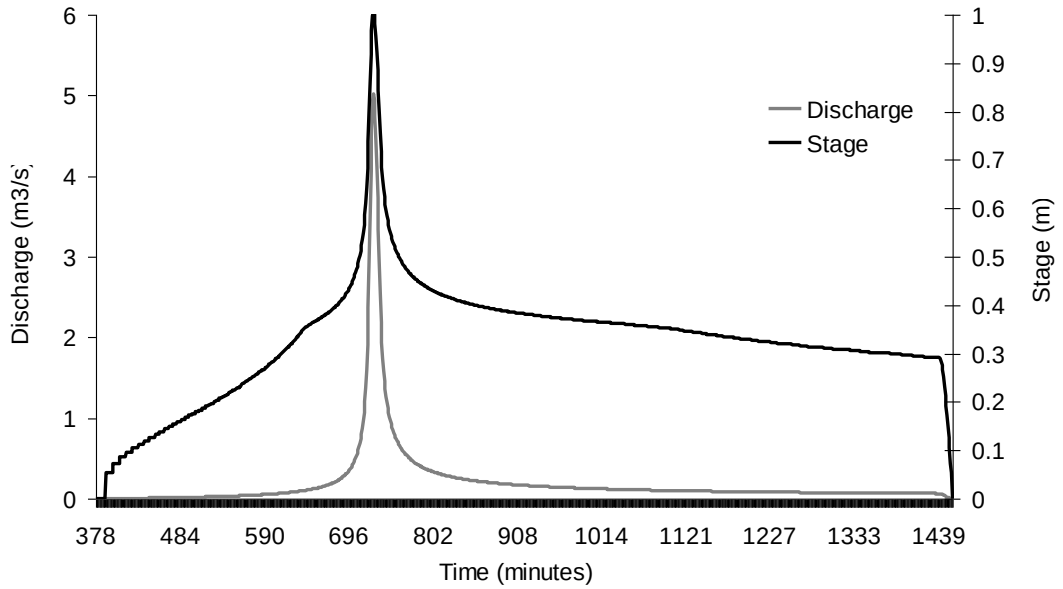

Figure 3.3: Stage-discharge relationship for Visual SCS-SA design rainfall (discharge) simulation of the Craigieburn-Manalana catchment against rated section (stage) of the buttress weir, for a 2-year return interval storm (for rating see section 3.1.2.ii).

3.1.2.ii Weir ratings

The ratings for the two weir sections are shown graphically in Figure 3.4, and were applied using the following empirical stage-discharge relationships of equation 3.5, described in US Department of the Interior (2001).

(3.5a) $$Q = 2.49h_1^{2.48}$$

where: Q is the discharge over the weir in m^3/s; and h is the head (stage) on the weir v-notch section in metres.

(3.5b) $$Q = 3.9h_1^{1.72} - 1.5 + 3.3Lh_2^{1.5}$$

where: Q is the discharge over the weir in m^3/s; h_1 is the head (stage) on the weir v-notch section in metres; L is the combined length of the horizontal portions of the weir in metres; and h_2 is the head (stage) above the horizontal crest on the weir in metres.

3.1.2.iii Stream data and sampling

Time-series records of Q and h were logged using a Campbell Scientific Inc. CR200 datalogger and CS410 Shaft Encoder with float and counter weight mechanism in a stilling well connected to the ponded area behind the weir (Figure 3.5), such that the water in the stilling well remained the same as that flowing over the weir.

In addition, the weir incorporated an ISCO® 24-bottle (500ml) sequential flow water sampler which was housed next to the structure and collected water at predefined flow rates for isotopic end-member analysis, Oxygen (^{18}O) and Deuterium (^{2}H). Since one is interested in both low and high flows, the prescribed incremental volumes for triggering low flow samples were 500 cm^3 and 2000 cm^3 for the high flows. This required compiling a CR200 data logger program that triggered a 12 volt pulse being sent to the ISCO sampler from the CR200 logger at these prescribed flows. This took the form of the relationship that is displayed schematically in Figure 3.6a as follows:

- initialising a time step, deltaT, for interrogating the encoder and determining the depth of flow, H.
- initialise a fixed depth of flow change, deltaHR, for flow recording which was set at 0.005 m

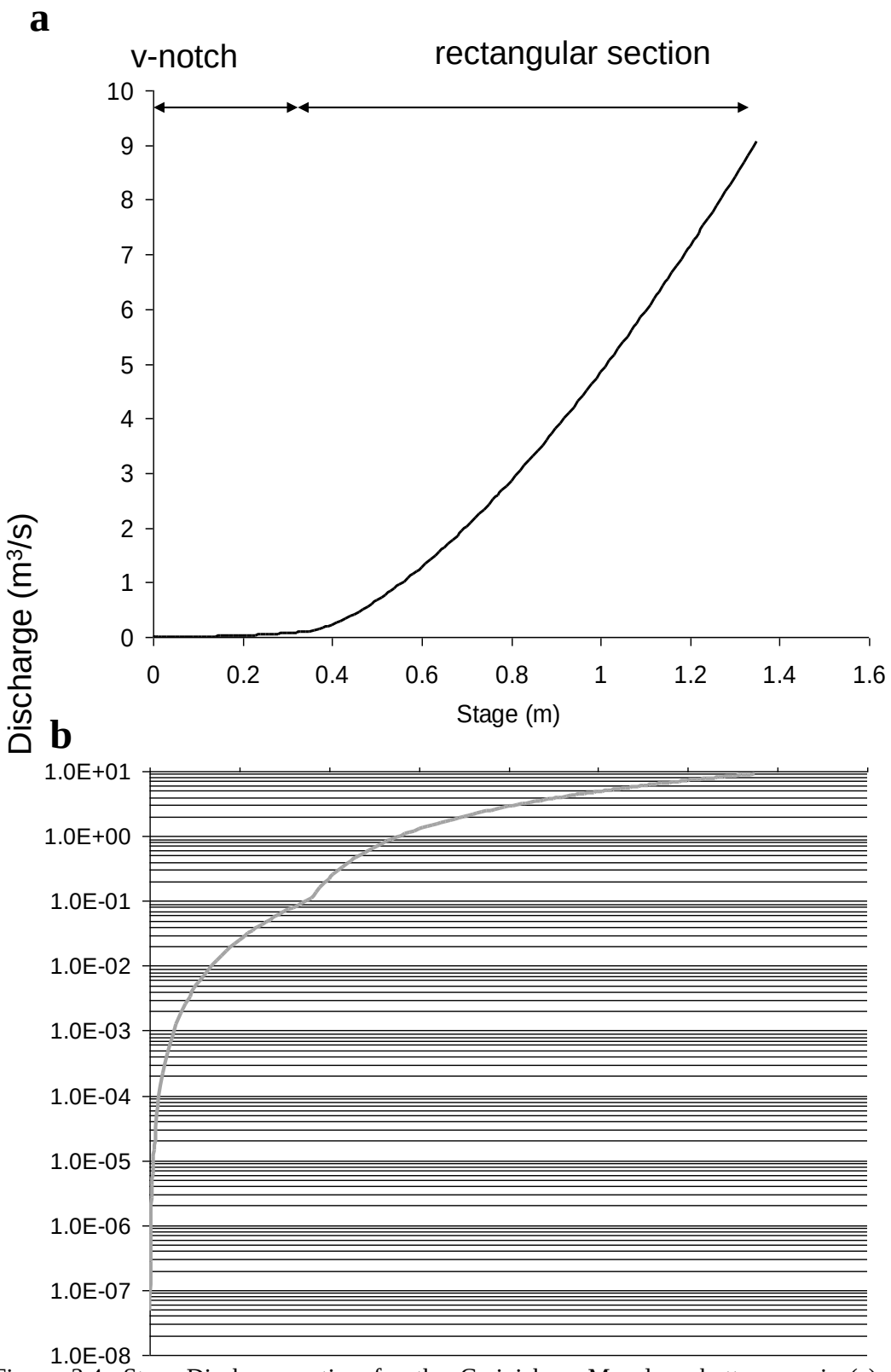

Figure 3.4: Stage-Discharge rating for the Craigieburn-Manalana buttress weir (a), log-Discharge plot (b).

- interrogate the encoder every deltaT minutes (1 minute) and determine H to calculate current flow, using the default Campbell Scientific Inc. program.
- determine the difference between the current flow depth H_i and at the last flow saved to memory H_{i-x}. If the difference equals or exceeds deltaHR, then save the current H_i flow rate Q_i and the time, i, to memory.
- determine whether flow is steady or rapidly varying by comparing sequential flow depths, H_i-H_{i-1}, to a present head difference, deltaHS.
- if H_i-H_{i-1} is less than deltaHS, then low flows are assumed, otherwise rapidly varied (high) flows are assumed.
- integrate the flows by summing the product of flow Q_i and deltaT for each time step to give the cumulative flow volume, V.
- if in a low flow period, check the cumulated flow volume against V_{LF} and in a rapidly varying flow against V_{HF}.
- if the cumulated flow volume is greater than or equal to the appropriate preset volume, then trigger a sample by sending a 12 volt pulse to ISCO sampler terminals.

The use of natural isotope tracers within the Manalana catchment were incorporated within the study to provide valuable insights into the sources, pathways and dynamics of the components of flow from the initial precipitation input to the catchment to the stream outlet. These environmental isotopes are most beneficial in catchment studies due to their relatively stable nature in comparison to alternative chemical tracers. Furthermore, solutes that are derived from atmospheric sources are often isotopically distinct from those that are derived from biologic and geologic sources within a catchment (Kendall & Caldwell, 1998).

In addition isotope water samples collected at the wetland outlet, incremental rainfall samples were collected using the sampler design of Kennedy *et al* (1979), see Figure 3.6b which incorporated a 6 x 250 ml collection bottle sequence. Water samples for isotope analysis were also taken from the installed piezometer network and runoff plots collectors. Since the deeper soils (>2000 mm) within the Craigieburn-Manalana had a very high clay content the bailer extraction of piezometer water and replenishment with new in-flowing aquifer water for sampling was not feasible, instead a 12 volt water pump was used to extract water from the very base of the piezometer to ensure the extraction of ‘new’ piezometer water that would have not undergone evaporative/mixing effects.

Isotope samples were sent to the Soil and Water Laboratory, School of Bioresources Engineering and Environmental Hydrology at the University of KwaZulu-Natal for determination of ^{18}O and ^{2}H concentrations using a Laser Isotope Analyser.

downstream view

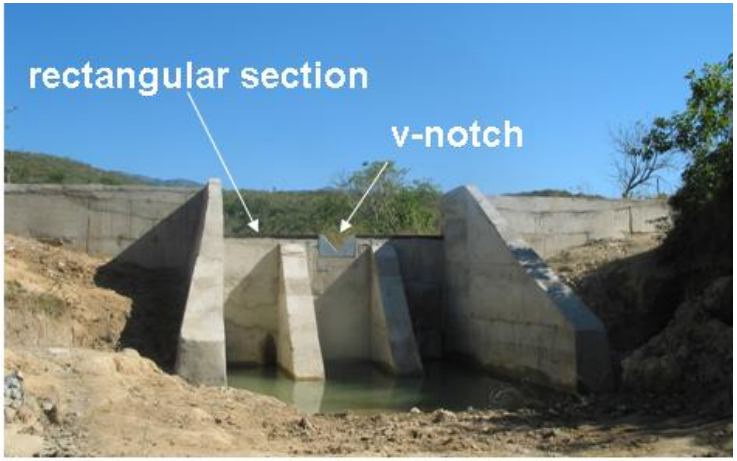

upstream view

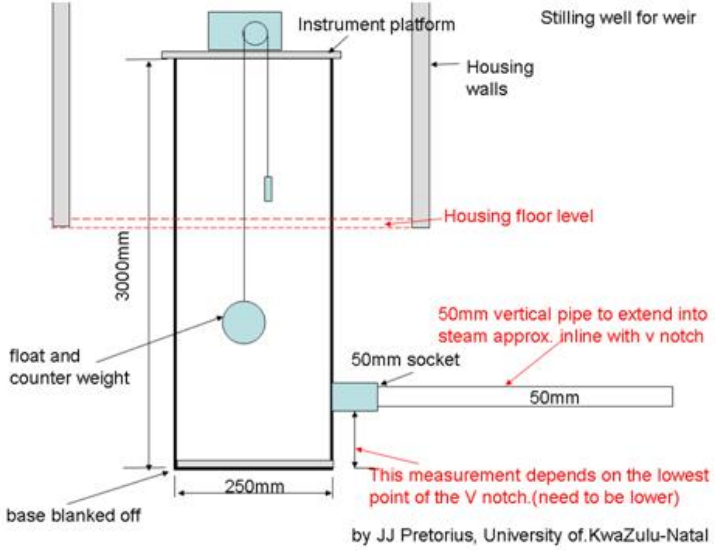

Figure 3.5: Installed buttress weir (top left, top right) with design and location of stilling well (bottom left), gabion dam (bottom right)

a

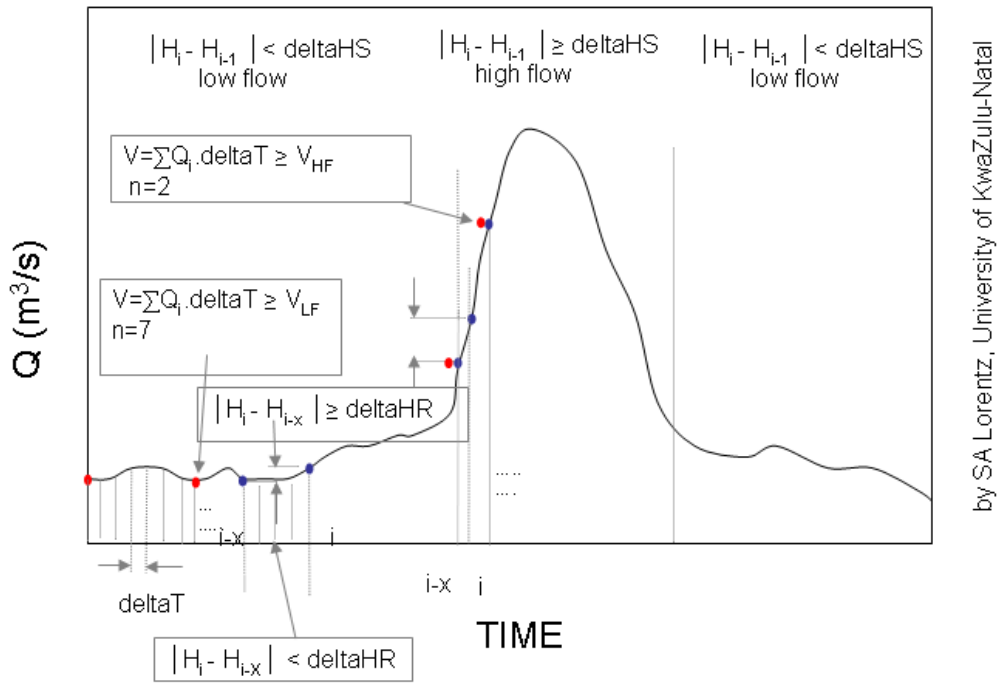

b

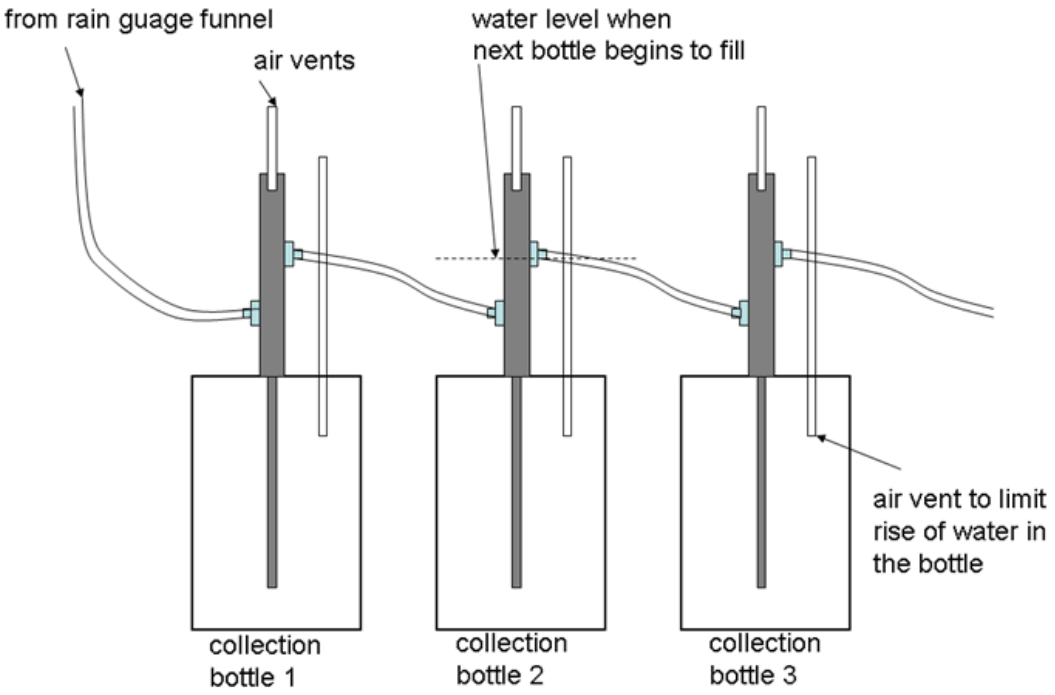

Figure 3.6: Low and high flow streamflow sampling regime (a) and incremental rainfall sampler adapted from Kennedy *et al.*, (1979) (b).

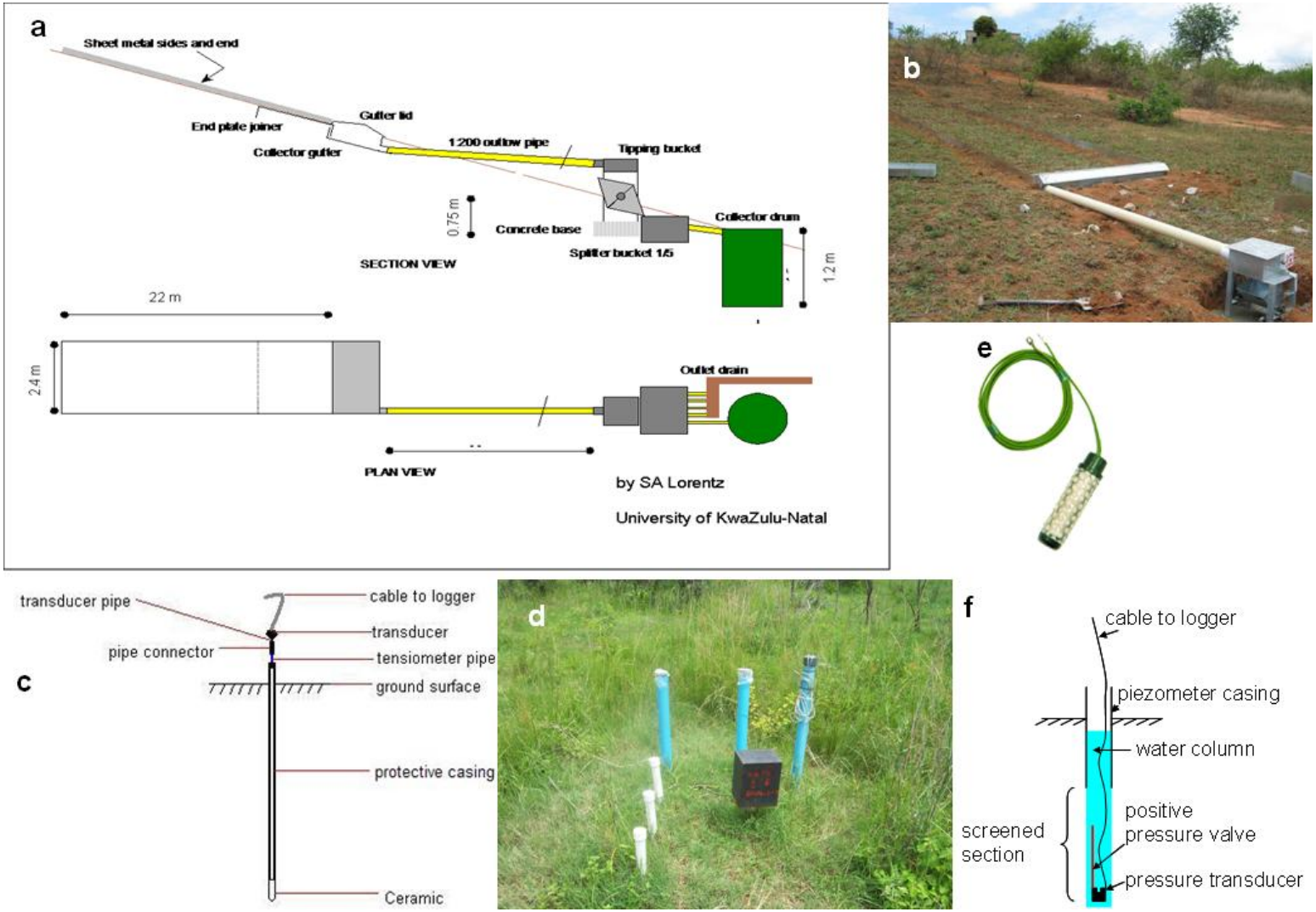

Figure 3.7: Hydrometry apparatus used in the Craigieburn-Manalana research catchment: schematic and installed USLE runoff plots (a and b); schematic of a soil moisture tensiometer (c); installed soil moisture and groundwater (piezometer) observation nest (d); and Irrometer Watermark® sensor (www.irrometer.com, e); schematic of automated piezometer (f).

3.1.3 Soil water monitoring stations

The installation of 14 soil water monitoring stations along three transects running perpendicular to the drainage network provided continuous data on the fluctuation of phreatic surfaces (water table) along the catchment interfluves and longitudinally through the wetland upstream of the rehabilitation structure (Figure 3.1).

This was conducted through the installation of shallow groundwater observation holes on upslope positions and automated piezometers fitted with pressure transducers (Figure 3.7) on downslope and wetland positions. These were installed by way of augering to saprolite/bedrock where possible with holes of approximately 100 mm diameter, in which 75 mm diameter slotted pipe was placed (6 mm spacing between slots to a 0.3 m level above the base). These were then backfilled with coarse sand (slotted/screened section) and removed and repacked earth (unslotted section).

The installation of nested piezometers, recording groundwater pressure heads (and hence the saturated soil water) at several depths within the same location, and also at various locations within the wetland system, allowed for the determination of the dominant hydraulic gradients in the system. The hydraulic gradient, which represents the driving force for groundwater flow (Yolcubal *et al.*, 2004) is defined as the change in hydraulic head with distance at two or more locations, and is governed by equation 3.6:

$$\frac{dh}{dl} = \frac{(\psi_2 + Z_2) - (\psi_1 + Z_1)}{(z_2 - z_1)} = \frac{(h_2 - h_1)}{(z_2 - z_1)} \qquad (3.6)$$

where: h is the total hydraulic head; z is the elevation head; and ψ *is* pressure head.

Hydraulic gradients measured at the same location (nested) enables one to determine the vertical component of groundwater flow, as in Figure 3.8 to derive whether groundwater is dominantly discharging (upward) or recharging (downward) in the system. Determination of the hydraulic gradient (i) between two or more locations then provides a directional measurement of the horizontal component of groundwater flow.

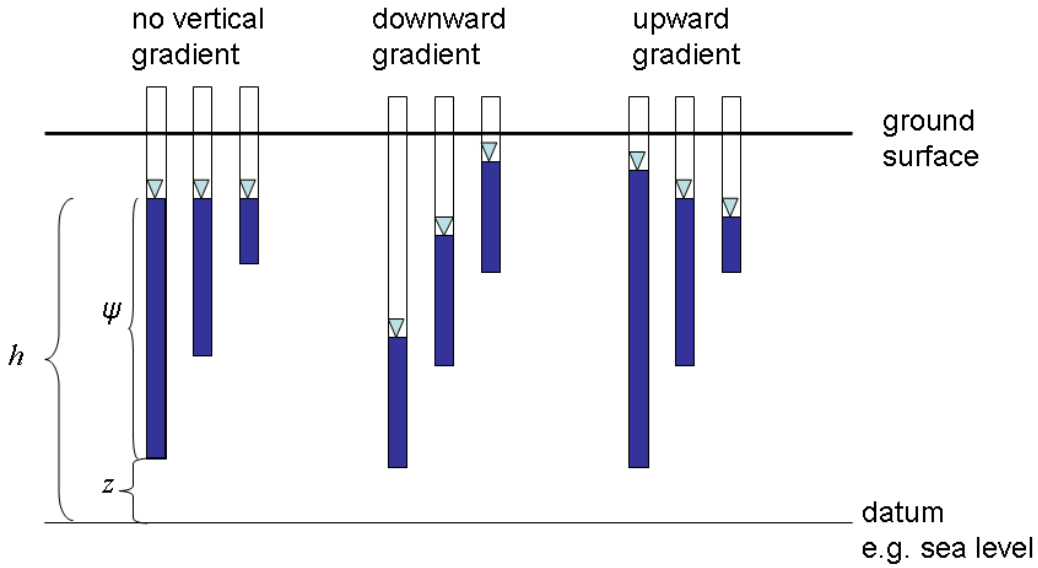

Figure 3.8: Concept of hydraulic head (h), elevation head (z); and pressure head (ψ) with regard to piezometers and determination of dominant direction of groundwater flow over time.

Soil moisture tensiometers were also installed at these locations in order to monitor soil moisture potential (suction) at differing depths (300 mm, 600 mm and 2000 mm), which allowed for the quantification of variably unsaturated and saturated soil water conditions. Tensiometers are water filled tubes with a hollow ceramic cup (porous medium) placed at depth in the soil, with an air tight, fitted pressure transducer (gauge) above the soil surface (Figure 3.7 and Figure 3.9). These apparatus are able to measure soil moisture potential by conversion of the voltage generated by the pressure transducer in response to the variation of suction within the tensiometer cup. With the cup placed in good contact with the surrounding soil (using a diatomaceous earth slurry), water in the tube comes into equilibrium with water in the surrounding soil. As the soil dries out, a partial vacuum is created within the tube as water is in contact with soil water through the porous tip. This reverses as the soil re-wets following a rainfall event. The soil moisture potential can be quantified using tensiometers according to the equation 3.7:

(3.7a) $$\phi_T = \phi_m + \phi_z + \phi_o$$

and

(3.7b) $$\phi_m = \psi_g + \psi_h$$

where: Φ_T is the total soil water potential; Φ_m is the matric potential; Φ_z is the gravitational potential; Φ_o is the osmotic potential (usually omitted except in saline soils); ψ_g is the gauged pressure; and ψ_h is the soil water pressure, in figure 3.9 ψ_t is the head of water in the tube (therefore $\psi_g + \psi_t$ = '0' or '+' if water level is above tensiometer porous cup or '–' if below the porous cup).

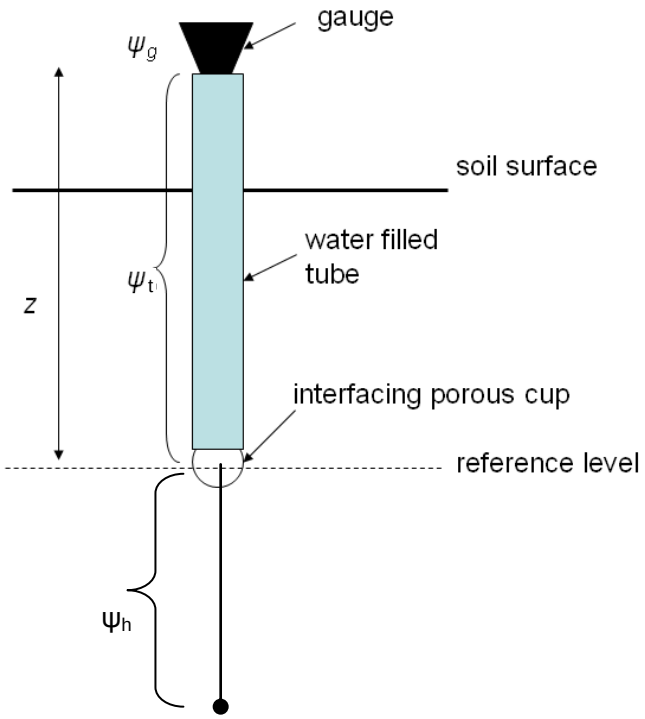

Figure 3.9: Schematic of a soil moisture tensiometer and the components of soil moisture potential in equation 3.7.

Tensiometers have a pressure range of up to 1 bar and are thus most suitable in the wetter positions in the landscape (wetland and lower interfluve positions). Where dryer conditions were anticipated, such as positions on the catchment slopes where tensiometer ranges were thought likely to be exceeded, Irrometer Watermark® sensors were installed instead. Tensiometers (or Watermark®) and automated Piezometer data were recorded at 12 minute intervals using a housed SBEEH-University of KwaZulu-Natal timing board and HOBO® 4-channel data logger. Additional shallow ground water observation holes were installed where

deemed necessary. Manual readings of water table levels were made regularly using an SBEEH constructed dip-meter, at least weekly and following rainfall events.

Both piezometers and tensiometer systems used 1 bar pressure transducer[1] systems, using the positive pressure port for the former and negative pressure valve for the latter, in each case the alternate port of the differential pressure transducer was vented to atmosphere. Each transducer was calibrated according to the methods described in Lorentz, *et al.*, (2001) and Kongo *et al.*, (2007), against 0-100 cm rising and falling mercury pressure column, see Figure 3.10.

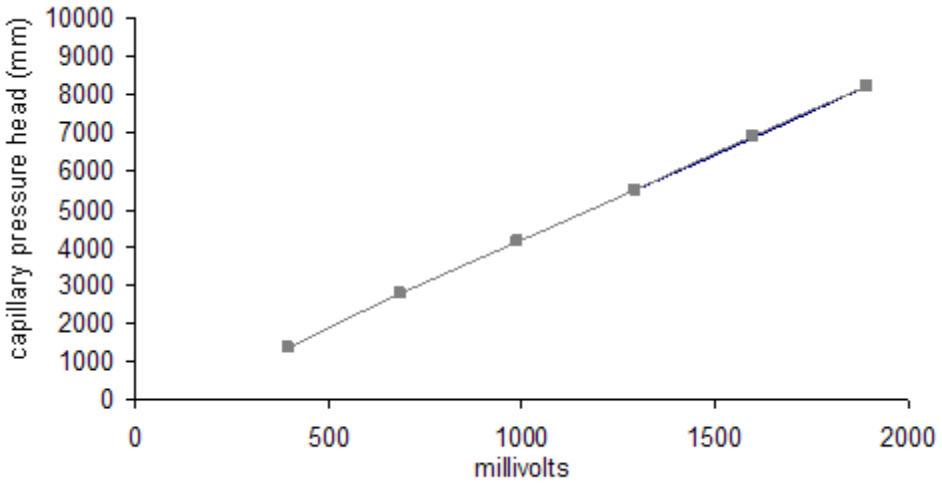

Figure 3.10: Example calibration of pressure transducer versus millivolt signal response.

The use of Watermarks sensors, which measure the electrical resistance (in kilo-ohms, kΩ) of the surrounding porous medium (in this case soil), where there is greater resistance with lower water content of the porous medium and vice-versa, also required calibration to convert millivolt readings to pressure head values. Since each channel has a slightly different millivolt response to the electric resistance measured at the sensor, a 3 channel (of a 4 channel HOBO® data logger) calibration function was derived by pressure pot measurementz (Lorentz & Pretorius, 2008 unpublished, University of KwaZulu-Natal) according to the following equation 3.8:

(3.8a) $\psi_h = 0$ *where* $mV<E$

[1] The Motorola™ MPX5100 pressure transducer has a maximum error of 2.5kPa within the 0-100kPa range, translating to a potential error of +/- 250mm capillary pressure head.

(3.8b) $\psi_h = \frac{A(BmV)}{1-(CmV - DT)}$ *where E<mV<F*

(3.8c) $\psi_h = GmVH$ *where mV>F*

where:

ψ_h = capillary pressure head (mm), tension/suction the positive equivalent of matric potential

mV = millivolts

T = temperature (°C)

and

parameters A:G are constants derived for each logger channel:

	Ch1	Ch2	Ch3
A	-380.0	-760.0	-680.0
B	1900	1900	1700
C	0.37	0.357	0.357
D	0.01205	0.01205	0.01205
E	0.2	0.4	0.4
F	1.85	1.85	1.85
G	2543511.5	2543511.5	2543511.5
H	-4485496	-4633564	-4641163

Where tensiometers have their application in measuring the soil moisture matric potential (capillary pressure head) of a soil, in other words the degree of dryness, Time-Domain Reflectometry (TDR) was used as a complimentary tool to directly measure the actual soil water content. TDR is an apparatus that sends a step pulse of electromagnetic radiation along three probes inserted into the soil. The pulse is ‘reflected’ and returned to the source with a velocity characteristic to a specific dielectric (electrical transmission other than conductance) constant, which can be calibrated to give soil water content based on this constant (Trimble & Ward,

2004). TDR is an advantageous measure of soil water content due to its superior accuracy and excellent spatial and temporal resolution (Jones and Or, 2003). The TDR method is governed by the following equation 3.11:

(3.11) $$\varepsilon_b = \left(\frac{c}{v}\right)^2 = \left(\frac{ct}{2L_p}\right)^2$$

where: ε_b is the soil bulk dielectric constant; c is the speed of light; v is the wave propagation velocity; t is the travel time for the pulse or wave to traverse down and back along the probe; and L_p is the length of the probe. The method to relate soil water content, θ, to ε_b is described by Topp *et al* (1980, in Yolcubal *et al.*, 2004) is by the following regression equation 3.12:

(3.12) $$\theta = -5.3 \times 10^{-2} + 2.92 \times 10^{-2}\varepsilon_b - 5.5 \times 10^{-4}\varepsilon_b^2 + 4.3 \times 10^{-6}\varepsilon_b^3$$

Three TDR probes (Figure 3.11) were inserted at depths corresponding to each of the tensiometer/watermark sensors along transect 1. These were installed on completion of the soil hydraulic properties characterisation as probes were installed horizontally in the soil profile which necessitates digging pits into the soil, which was only completed at the end of soil characterisations during September 2007. The use of a Campbell Scientific® TDR100 device and PCTDR software was also required to trigger electromagnetic waves along the probes in order to derive the volumetric water content readings.

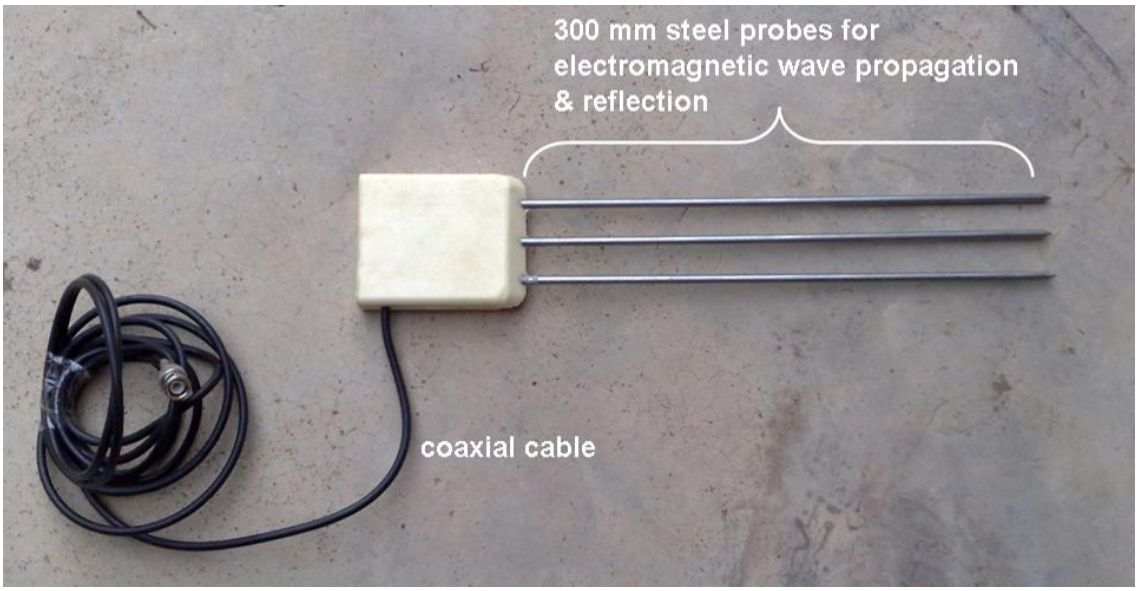

Figure 3.11: Time-Domain Reflectometry probe

3.1.4 Surface run-off

3.1.4.i On interfluve soils

The measurement of overland flow during and after precipitation events was enabled through the installation of USLE surface runoff plots on the catchment slopes (Figure 3.7). This apparatus measured the volume of surface runoff from a confined area. Each runoff plot measured 52.8 m² (22 m x 2.4 m) and this area was enclosed by galvanised steel plates embedded vertically into the ground. Runoff generated within this zone then flowed down-slope into a collection trough, from here it flowed down a 110 mm PVC pipe into a tipping bucket mechanism. These tipping bucket mechanisms were fitted with a reed switch activated HOBO® Event Logger and back-up mechanical counter. This mechanism recorded each tip of the bucket which was pre-calibrated to tip on every 2 litres (or 0.002 m^3) of water which flows into it from the upslope plot. Therefore the runoff depth per tip (RO) is calculated as:

(3.13) $$RO = \frac{0.002}{52.8} = 3.78 \times 10^{-5} mm$$

The timing of tipping events is then correlated with rainfall data in order to give data relating to the run-off generated per precipitation event of known intensity (from break-point rainfall data). These data are then able to give quantification to the mechanisms of soil surface infiltration, and hence any Hortonian or saturated overland flow.

A total of six run-off plots were installed in the Manalana catchment at various locations in order to encompass the variability in soil conditions throughout the catchment. These were placed in close proximity to the soil water monitoring stations so as to understand the sub-surface infiltration processes that influence run-off generation.

3.1.4.ii On wetland soils

Due to the highly modified nature of the wetland surface topography (network of ridge and furrows) the installation of surface run-off plots was anticipated to be problematic. Instead quantification of run-off at these locations was explored by the installation of paired above-below ground automated Piezometers (as previously described) which recorded the stage height

of storm run-off in the furrow channels. The run-off within these furrows was then estimated with the use of the Manning Equation for stream-flow. These apparatus were finally installed at a single location (replicated twice for upstream and downstream stage). The precise method for this required the calculation of the furrows hydraulic radius and cross-sectional area using a theodolite survey, level-line and height staff, as well as precise elevation differences between the two Piezometers. Once this had been determined, the relatively simple Slope-Area (Herschy, 1985) method for small stream discharge was utilised, as follows:

$$Q = \frac{1}{n} A R^{\frac{2}{3}} S^{\frac{1}{2}} \tag{3.14}$$

where: Q is discharge in m^3/s; n is an ascribed Manning's roughness coefficient based on channel bed form and vegetation conditions; R is the ratio of the channel's cross-sectional area to wetted perimeter at any time step; S is the channel bed slope taken as the difference in elevation between two or more points.

3.1.5 Evapotranspiration

Evapotranspiration (ET) was estimated using the widely used empirical estimates derived from meteorologic data. Since all required meteorologic variables were available from the weather station, the Penman-Monteith equation was chosen to drive both daily and hourly data, in order to derive reference potential ET at greater temporal resolution. The FAO56 form of the Penman-Monteith equation (3.15) was used, as described by Allen *et al.*, (1998):

$$daily\, ET_o = \frac{0.408\Delta(R_n - G) + y\dfrac{900}{T+273}u_2(e_s - e_a)}{\Delta + y(1 + 0.34u_2)} \tag{3.15a}$$

and

$$hourly\, ET_o = \frac{0.408\Delta(R_n - G) + y\dfrac{37}{T+273}u_2 \left(^{\circ}(T) - e_a\right)}{\Delta + y\left(+ 0.34u_2\right)} \tag{3.15b}$$

where: ET_o is the reference evapotranspiration (mm/d); R_n net radiation at the vegetation surface (MJ/m^2/d); G is the soil heat flux density; T is the mean air temperature at 2m height (°C); u_2 is the average wind speed at 2m height (m/s); e_s is the mean saturation vapour pressure (kPa); e_a is the mean actual vapour pressure (kPa); $e°$ is the hourly saturation vapour pressure at air temperature; e_s-e_a is the saturation pressure deficit (kPa); Δ slope of the vapour pressure curve (kPa/°C); and y is the psychometric constant (kPa/°C). Readers are referred to Allen *et al.*, (1998) for further derivation of these internal parameters.

In addition, assistance was acquired from the Council for Scientific and Industrial Research (CSIR) to determine actual evapotranspiration (aET) from the wetland vegetation and surrounding grass/shrub land on the surrounding hillsides, to derive accurate fluxes out of the wetland and surrounding catchment interfluves. This was carried out over two periods, one at the end of the dry winter period (September 2008), and mid-summer wet season (January 2009), which allowed for quantification of the vegetative water demands on the wetland and catchment as a function of the seasonal variability of available moisture. The use of Scintillometry, Eddy Co-variance, and Surface Renewal methods for this purpose and detailed results of this monitoring are described by Everson *et al.*, (2009).

3.2 CHARACTERISATION AND SURVEYS

3.2.1 Soil hydraulic properties

The infiltration properties of the soil within the Manalana catchment were characterised in the vicinity of the soil water monitoring stations along transect 1. Here pits were dug to 2000 mm (to coincide with the depth of the deepest tensiometers), where two replicates were taken at successive depths in the soil profile. This follows the methodology described by Lorentz *et al* (2001). These were done by cutting shelves into the pit wall, at which three measures were taken in the following order:

a. Unsaturated Hydraulic Conductivity (K_{unsat}) – this is conducted using an instrument known as a Tension Disc Infiltrometer (Figure 3.12). This method requires maintaining a suction (tension) in the water supply and recording the steady state inflow rate at different tensions.

b. Saturated Hydraulic Conductivity (K_{sat}) – this is a ponded test using a Double Ring Infiltrometer (Figure 3.12), whereby the steady-state infiltration rate from water within a central ring is determined whilst maintaining an outer source of water at the same ponded head (outer ring).

c. Soil water retention and physical characteristics – Undisturbed samples were taken on completion of the above at each location in the profile, using stainless steel rings of known volume (i.e. d = 48 mm, h = 50 mm). The samples were then sent back to the Soil & Water Laboratory of the University of KwaZulu-Natal for analysis of water retention characteristic, bulk density, porosity, texture and organic carbon content.

Slug and Bail tests (Freeze and Cherry, 1979) were used to determine the hydraulic conductivity of deep soils, making use of the groundwater observation holes for this purpose.

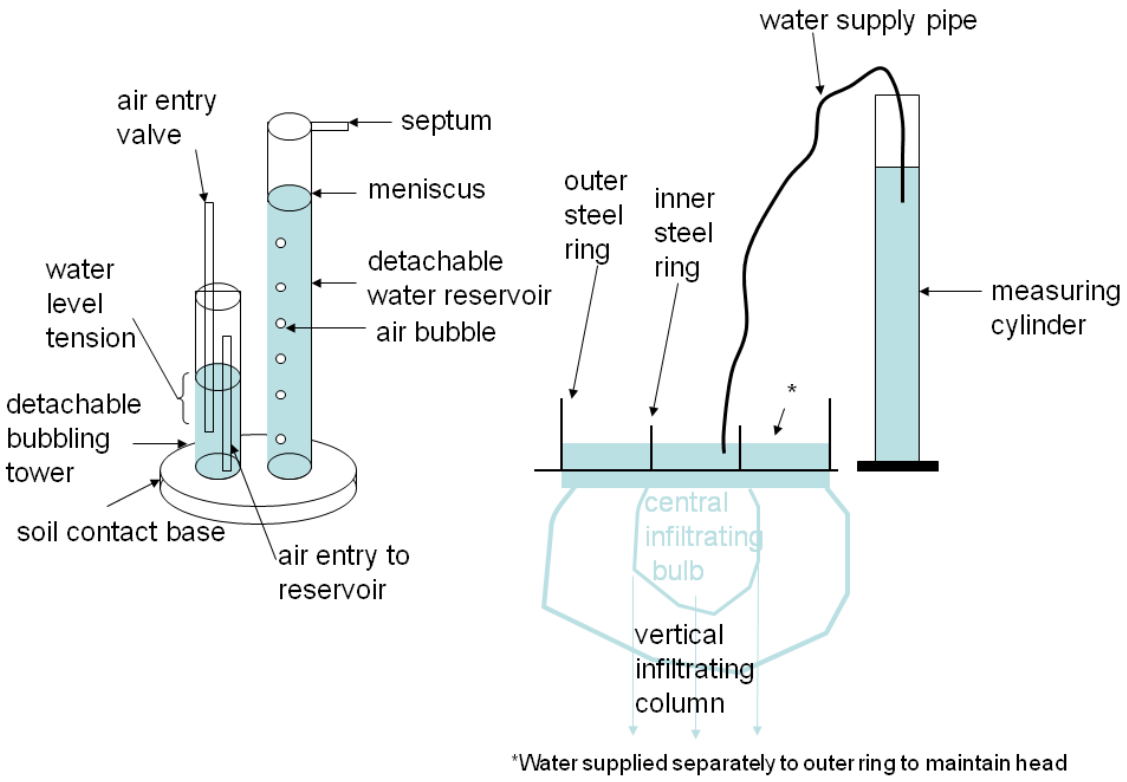

Figure 3.12: Tension Disc Infiltrometer (left) and Double Ring Infiltrometer (Right).

3.2.2 Geomorphology through ERI and IP

The use of the 2D-Resistivity method was used to conduct topographically linked ground surface electrical surveys. These measure the sub-surface resistivity by sending electrical pulses into the ground and recording their distribution. This is based on the electrical resistance of substances encountered by the pulses. These pulses are triggered by an array of probes (current) inserted into the ground and received at other probes (potential) evenly spaced along the resistivity transect cable, this is operated by a pre-programmed transmission protocol in the operating system (Appendix ii). In essence this resistivity is related to various geological parameters, such as the mineral and fluid content in the rock (Loke, 1999). 2D-Resistivity measures this resistance in both a vertical and horizontal direction, enabling the view of a cross-section (pseudosection) of sub-surface lithology and wetness. This technique has rapidly become a well established methodology in hydrologic, mining and geotechnical investigations and is increasingly being used for environmental studies.

The resistivity of a soil or rock type often varies quite widely as a function of the amount and quality of water in pore spaces and fractures. However within a confined geological area this variation may be considerably limited. Hence variations within a certain soil or rock type in such a confined area may reflect differences in their physical properties (ABEM, 2005). Since the 2D–Resistivity method for geophysics is able to distinguish differences in resistivity of subsurface materials, its use as part of the geomorphological crux of this study was invaluable. Todd (1990) notes the apparent resistivities of various sediments and rock types (Figure 3.13), whereby clays and sands seem to have distinct resistivity ranges.

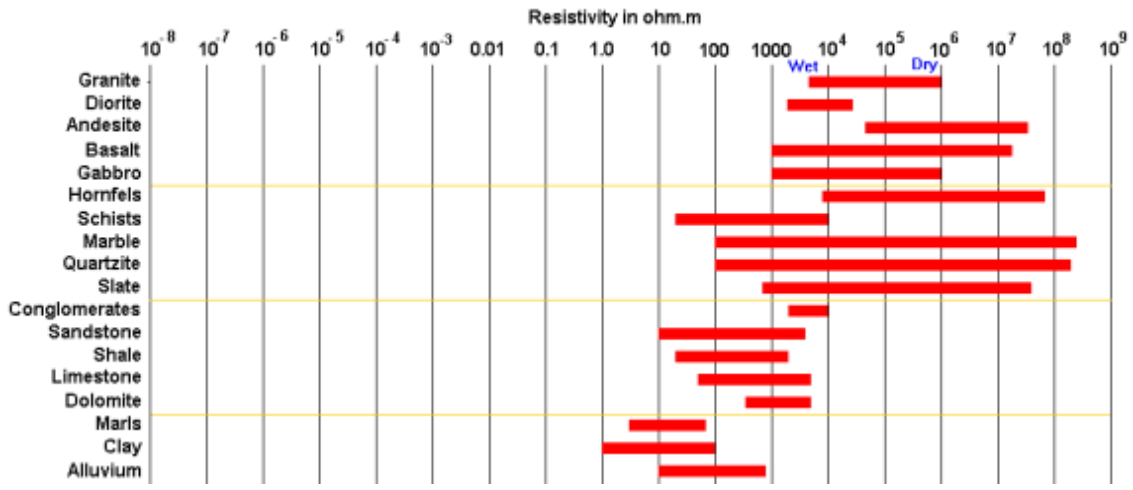

Figure 3.13: Apparent resistivity ranges of various sediment and rock types (after Loke, 2004)

This technique traversed the three transects used for soil water monitoring as well as longitudinal transects along the wetland surface. This analysis was conducted twice per year in order to provide replication and account for changes in the sub-surface water content and movements at the catchment scale.

In addition the complimentary Induced Polarization (IP) technique was used to identify clay zones within the wetland. Further details of the application of this technique can be found in Chapter 6 of this thesis.

The use of the ABEM® Terrameter (2005) will be made for conducting these surveys and the SK4win imaging software and RES2DINV modelling software will also be implemented.

3.2.3 Land typology data

Data were also collected in order to characterise the Manalana catchment, this included detailed land-use mapping and collection of topographic information. In terms of land-use this was determined descriptively and wetland fields were distinguished from in-tact natural vegetation. Whilst for topography this was done by way of differential GPS measurements. This data was

placed into a Geographic Information System (GIS) making use of the ESRI® Arcview software.

Whilst mapping the catchment a wetland delineation was performed for the entire Manalana catchment to assess the change in historical wetland extent (see Chapter 3) using the hydric soils classification system developed by Kotze *et al.*, (1994,1996).

3.3 DATA MANAGEMENT

All hydrological and meteorological data were continually imported into a Microsoft® Access database (Figure 3.14). Here data were converted from raw values to hydrologic units (i.e. millivolts converted to mm tension for tensiometers) and bad data identified. This therefore provided a comprehensive and easily accessible utility for examination of the collated data throughout the study period.

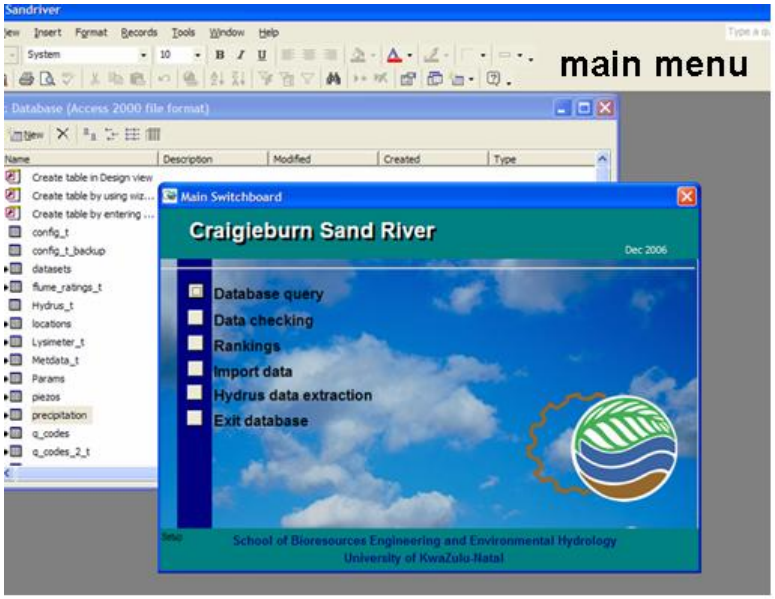

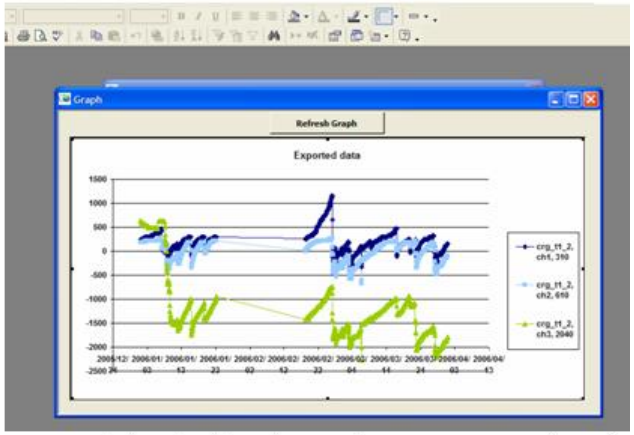

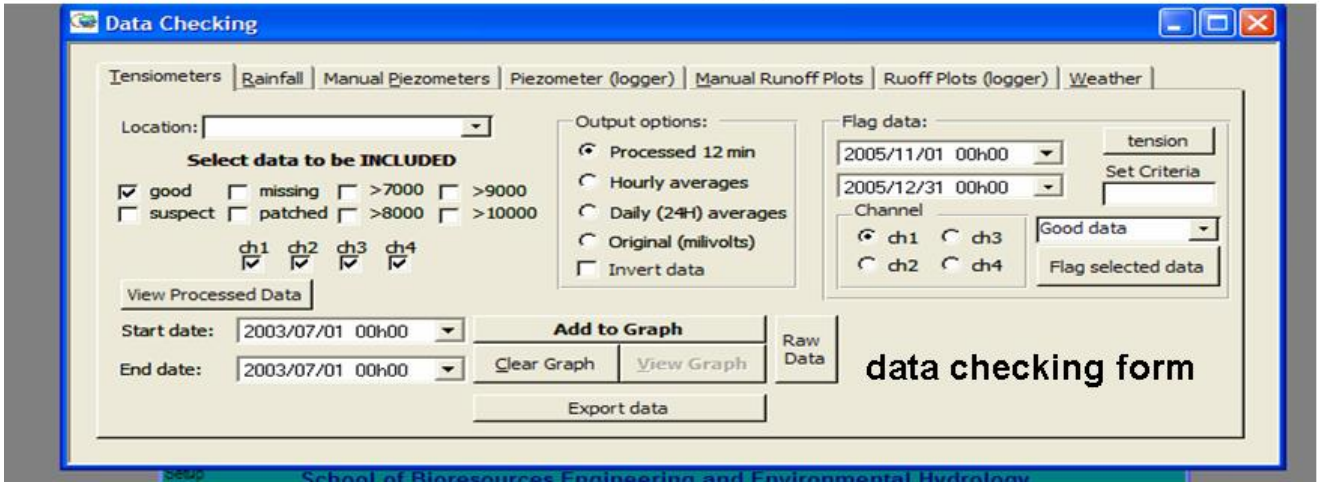

Figure 3.14: Microsoft Access Database configured for hydrometric analysis and data collection (Lorentz *et al.*, 2004).

4 A GEOPHYSICAL ANALYSIS OF HYDRO-GEOMPORPHIC CONTROLS WITHIN A HEADWATER WETLAND IN A GRANITIC LANDSCAPE, THROUGH ERI AND IP

E.S. Riddell[1], S.A. Lorentz[1], D.C. Kotze[2].

[1] School of Bioresources Engineering and Environmental Hydrology, University of KwaZulu-Natal, Private Bag X01, Scottsville, Pietermaritzburg, 3209, South Africa

[2] Centre for Environment and Development, University of KwaZulu-Natal, Private Bag X01, Scottsville, Pietermaritzburg, 3209, South Africa

Paper Published as:

Riddell, ES., Lorentz, SA., Kotze, DC (2010). A geophysical analysis of hydro-geomorphic controls within a headwater wetland in a granitic landscape, through ERI and IP. Hydrology and Earth Systems Science, 14, p1697-1713

doi:10.5194/hess-14-1697-2010

Hydrol. Earth Syst. Sci., 14, 1697–1713, 2010
www.hydrol-earth-syst-sci.net/14/1697/2010/
doi:10.5194/hess-14-1697-2010

Hydrology and Earth System Sciences

A geophysical analysis of hydro-geomorphic controls within a headwater wetland in a granitic landscape, through ERI and IP

E. S. Riddell[1], **S. A. Lorentz**[1], **and D. C. Kotze**[2]

[1]School of Bioresources Engineering and Environmental Hydrology, University of KwaZulu-Natal, Private Bag X01, Scottsville, Pietermaritzburg, 3209, South Africa
[2]Centre for Environment and Development, University of KwaZulu-Natal, Private Bag X01, Scottsville, Pietermaritzburg, 3209, South Africa

Received: 12 March 2010 – Published in Hydrol. Earth Syst. Sci. Discuss.: 22 March 2010
Revised: 13 August 2010 – Accepted: 20 August 2010 – Published: 31 August 2010

Abstract. Wetlands are undergoing considerable degradation in South Africa. As interventions are often technical and costly, there is a requirement to develop conceptual process models for these wetland systems so that rehabilitation attempts will be successful. This paper presents an approach using the geophysical methods of Electrical Resistivity Imaging (ERI) and Induced Polarization (IP) to delineate sub-surface hydro-geomorphic controls that maintain equilibrium disconnectivity of wetland-catchment processes, which through gully erosion are increasing the catchments connectivity through loss of water and sediment. The findings presented here give insight into the geomorphic processes that maintain the wetland in an un-degraded state, this allows for the development of a conceptual model outlining the wetland forming processes. The analysis suggests that sub-surface clay-plugs, within an otherwise sandy substrate are created by illuviation of clays from the surrounding hillslopes particularly at zones of valley confinement.

1 Introduction

Wetlands in southern Africa as in most parts of the world continue to be vulnerable to anthropogenic pressures and climatic shifts which influence the hydrological and geomorphologic processes that otherwise maintain the equilibrium of the wetlands dynamic state. Consequently many wetlands are continually undergoing degradation. In recent years the drive has been to determine the wetlands structure and function within the broader landscape in order for rehabilitation of these degraded systems to be sustainable. In the interests of ecosystem integrity significant emphasis is now placed on understanding a wetlands hydro-geomorphic setting to ensure the success of such intervention, whereby the causes of wetland degradation rather than the symptom are incorporated into the rehabilitation planning (Tooth and McCarthy, 2007). In other words rehabilitation must be sympathetic to and not in conflict with the natural dynamic of the wetland or river system, and hence seek to maintain those processes that govern the systems water balance (Ellery et al., 2008). It is within this context that a detailed hydrological monitoring of a technical rehabilitation effort was undertaken within a headwater wetland catchment of the Sand River in northeastern South Africa, as part of a river rehabilitation program. These headwater sub-catchments are characterized by channeled and un-channeled valley bottom wetlands with a sandy soil matrix derived from the surrounding granitic geology. It was postulated that zones of finer sediment within this matrix controlled the lateral movement of water within these wetlands prior to their degradation, and these fine sediment zones are being removed through extensive gully erosion (Pollard et al., 2005). It is the stabilization of these gullies that are the focus of technical rehabilitation efforts. Descriptions of the hydrodynamic behaviours of the wetland phreatic surfaces prior to rehabilitation interventions revealed stark differences in event driven responses

Correspondence to: E. S. Riddell
(edriddell@gmail.com)

either side of a suspected clay-plug in this wetland (Riddell et al., 2007). Clay-plugs are distinct zones of fine particles in an environment that is otherwise dominated by coarse particles, and due to the lower hydraulic conductivities of this medium, they are thought to exert significant controls on lateral sub-surface flows in the wetlands of the Sand River catchment. It is the identification and examination of these sub-surface structures that are presented here.

This paper presents results of geophysical interpretation of the wetlands hydro-geomorphology using Electrical Resistivity Imaging (ERI) in both 2 dimensional form (2-D) during scoping surveys and a more detailed examination of hydro-geomorphic controls in 3 dimensional form (3-D) using ERI and Induced Polarization (IP) techniques. The 2-D surveys using ERI only were deployed at various times during the hydrological characterization of this catchment (2005–2009) and were used in a reconnaissance fashion to assist in the interpretation of hydrological processes. 2-D readings were conducted as single onetime surveys, however it was preferred to conduct them during the late winter (dry season, March–October/November) period, as soil moisture contents were at their minimum and therefore variability in electrical resistivity measurements were assumed to have been minimally affected.

The 3-D surveys using both ERI and IP were used to examine the clay-plug distribution and develop concepts regarding their geomorphic evolution. The geophysical techniques used here have their roots in the mineral prospecting and other geotechnical investigations (Lowrie, 2007) but are now being increasingly used by the earth science fraternity involved in water resources management and geomorphology studies, whose recognition of their utility has been widely acknowledged (Robinson et al., 2008; Dahlin, 1996). ERI for instance has successfully been used in the interpretation of hillslope flow pathways in research catchments in South Africa (Uhlenbrook et al., 2005), examining permafrost distribution in peri-glacial mountain environments in Europe (Kneisel, 2006) and weathering and erosion processes on lateritic plateaus of south Pacific islands (Beauvais et al., 2007). ERI has been praised as a valuable, cost-effective and non-intrusive tool for conducting reconnaissance surveys in geomorphological investigations (Smith and Sjogren, 2006). Whilst IP has not received as much attention as resistivity methods, it was demonstrated by Slater and Lesmes (2002) to reveal valuable data on clay-free and clay-rich stratifications in 1-D and 2-D field surveys. Meanwhile, IP is now proving important as a complementary tool to resistivity mapping, for instance to delineate sub-surface materials in low resistivity clay rich environments it has shown success such as slope instability studies in Switzerland (Marescot et al., 2008). Interestingly it has also showed promise in mapping the stratigraphy of peatlands in the north-eastern United States, particularly the high chargeability of partially decomposed organic matter found therein (Slater and Reeve, 2002).

The basis of ERI surveying is the induction of an electrical current by an array of *current* electrodes inserted into the ground surface, with a sequence of *potential* electrodes receiving the electrical signal. Hence the measurements of electrical potential at the surface are dependent on the electrical resistance of sub-surface materials, expressed in ohm metres (Ω m), which vary according to sub-surface strata, as a result of their inherent pore size distribution, variations in water content and degree of salinity (Loke, 1999). The collation of this sub-surface resistivity distribution is facilitated by computerized devices known as *switching units* that control the sequence of pairs of current and potential electrodes, known as the quadripole. Variations in the position and sequence of current and potential electrodes along a transect facilitate measurements with different degrees of horizontal and/or vertical resolution, these computer-generated sequences (*protocols*) are known as *arrays*. Inversion algorithms are used to create a model of measured and apparent (calculated) resistivity values. Using Jacobian matrix calculations and forward modeling procedures produces values of the true resistivity, which when plotted in 2-D or 3-D are known as *pseudosections*. The law governing *apparent resistivity* (p_a) is written as follows:

$$p_a = kR \quad \text{and} \tag{1}$$

$$R = V/I \tag{2}$$

where: k is the geometric factor and varies according to the quadripole array, R is the resistance, V is the voltage and I is the current.

These plotted pseudosections are then used to examine sub-surface resistivity heterogeneities based on the differences of equipotential surfaces where they hit the ground surface at potential electrodes; the interpretation of this data is based on known resistivity ranges of geologic materials. Following on from this procedure, IP surveys measure the decay of the electrical pulse from the current electrodes as the sub-surface returns to electrical equilibrium, since particular geologic materials are polarizable, some parts of the sub-surface domain essentially act as capacitors. This is particularly pertinent in the case of clays which have a high propensity for membrane polarization as a result of ion accumulations on the particles surface and hence within pore spaces (Kiberu, 2002). In essence then the IP survey is measuring the *chargeability* (M) of sub-surface materials and this is written in the form:

$$M = \frac{1}{V_0} \int_{t_1}^{t_2} V(t)\,dt \tag{3}$$

Where V_0 is voltage at time (t) 0, where subsequent time-voltage values are an expression of the decay of the steady-state voltage.

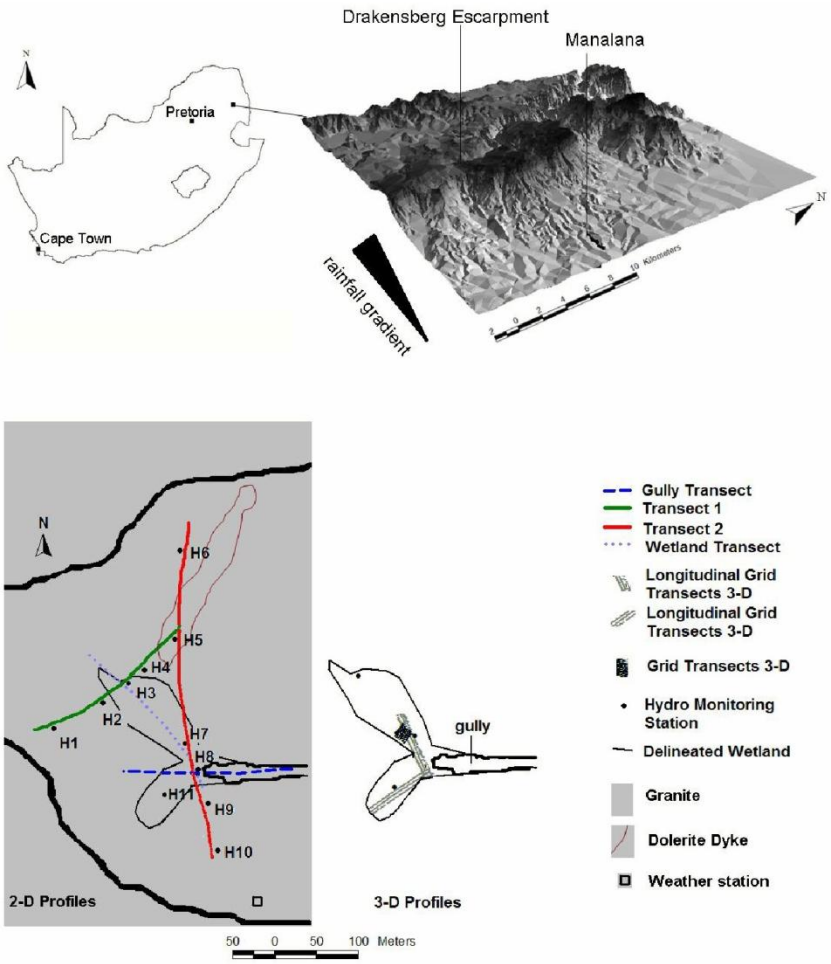

Fig. 1. Map and location of the Manalana sub-catchment within South Africa (above) with delineated wetland with the location of ERI transects and gully head (labels refer to hydrological monitoring stations).

2 Field setting

The study site (Fig. 1) is located within a headwater catchment of the Sand River, Mpumalanga Province, South Africa. This sub-catchment is known as the Manalana in which resides the village of Motlamogatsane (formerly known as Craigieburn). This sub-catchment as with the majority of others at the Sand River headwaters is located within the foothill zone of the northern region of the southern African escarpment. These catchments are underlain by medium to coarse grained porphyritic biotite granite frequented by extrusive dolerite dykes, and the geologies in this region are deeply weathered. The Manalana is situated within a narrow sub-humid belt along the Drakensberg escarpment with stream networks flowing west to east into the semi-arid Lowveld region, a lowland wooded savanna dominated by *Acacia*, *Combretrum* and *Terminalia* species. Mean annual precipitation as determined by the database of South African rainfall stations (Kunz, 2004) is 1075 mm a^{-1} (1904–2000) with a similar evapotranspiration demand. Mean temperature at the study site between October 2006 and October 2009 was 20.9 °C. Rainfalls in this escarpment region are large and intense following the arrival of warm humid air from the south-east during the wet season which occur from October to March (Fig. 1).

Due to the dominant granitic geology, soils within the catchment are medium to coarse grained sands, and significantly, the clay concentration does not increase towards the valley bottom, hence the wetland soils are essentially sandy (Pollard et al., 2005). This description applies certainly to the near surface soils of the catchment and particularly in the valley bottom wetlands, however there are significant clay deposits at depth in the wetland and the surrounding footslopes, which are likely to be due to vertical elluviation of fine material from horizons above. Certainly the presence of certain soil forms in the catchment particularly at the footslopes suggest this to be the case, the delineated soil horizons are summarized in Table 1a and b.

Table 1a. Hydrometry stations in the Manalana catchment with soil form, soil moisture tension and shallow groundwater levels, and soil texture (Soil form and texture data from University of the Free State, unpublished report).

				Sensor Depth (m)					
				0.3	0.6	2	2	4	6
	Slope Element [a]	SA Soil Form [b]	WRB [c]	Soil Moisture Tension (m)			Shallow Groundwater level (m)		
	October 2006								
H5	Backslope	Oakleaf	Regosol	3.39	4.11	3.22			None. obs.
H6	Shoulder	Glenrosa	Leptosol	15.20	87.80	10.31		None. obs.	
H7	Toeslope (wetland)	Katspruit	Gleysol		4.61	0.41	−2.81	−4.40	
H8	Toeslope (wetland)	Kroonstad	Planosol			3.05	−4.52		
H9	Foot-slope	Oakleaf	Regosol			3.92	None. obs.		None. obs.
H10	Backslope	Oakleaf	Regosol	8.72	25.54	18.26			
	November 2006								
H1	Backslope	Glenrosa	Leptosol	3.00	5.50	4.53		None. obs.	
H2	Foot-slope	Kroonstad	Planosol	0.41	0.63	−0.24	None. obs.		None. obs.
H3	Toeslope (wetland)	Katspruit	Gleysol		1.21	0.31	−2.20		
H4	Foot-slope	Kroonstad	Planosol	2.22		2.02	−5.32		
H5	Backslope	Oakleaf	Regosol	1.38	1.17	4.49			None. obs.
H6	Shoulder	Glenrosa	Leptosol	1.60	4.14	9.45		None. obs.	

[a] Slope Element based on classification by Ruhe (1960).
[b] South African Soil Form classification by Soil Classification Working Group (1991).
[c] World Reference Base soil classification, FAO (1998).

Table 1b.

	Horizon	Depth (m)	Texture[a]		Horizon	Depth (m)	Texture[a]
H1	A	0–0.2	sandy loam – sandy clay loam	H6	A	0–0.4	sandy loam
	B	0.2–1.2	sandy clay loam		B	0.4–1.4	sandy clay loam
H2	A	0–0.4	sandy clay loam	H7	A	0-0-.4	sandy loam – sandy clay loam
	G	0.4–1.0	clay		E	0.4–0.9	sandy clay loam
H3	A	0–0.3	sandy loam – sandy clay loam		G	0.9–1.7	clay loam
	G	0.3–0.4	clay loam	H8	A	0–0.2	sandy loam – sandy clay loam
	G	0.4–0.7	clay – clay loam		B	0.2–0.8	sandy loam – sandy clay loam
	G	0.7–1.3	clay – clay loam		B	0.8–1.0	sandy clay loam
	G	1.3–1.5	clay		B	1.0–1.9	sandy clay loam
	G	1.5–2.0	clay – clay loam	H9	A	0–0.1	sandy loam – sandy clay loam
H4	A	0–0.3	sandy loam		B	0.1–0.6	sandy clay loam
	E	0.3–0.6	clay loam		B	0.6–1.0	sandy clay
	E	0.6–1.1	clay – clay loam		B	1.0–1.7	clay loam
	G	1.1–1.7	clay	H10	A	0–0.3	sandy clay loam
H5	A	0–0.2	sandy loam		B	0.3–1.1	sandy clay loam
	B	0.2–0.6	sandy clay loam		C	1.1–1.7	clay loam
	B	0.6–1.4	sandy clay loam				
	B	1.4–2.0	clay – clay loam				

[a] United States Department of Agriculture.

According to the South African vegetation type classification system (Acocks, 1988) this area falls under the lowveld sour bushveld. Land use within the Manalana is essentially densely populated rural housing of the communal land tenure typical of the area including a dense network of roads and pathways. A combination of dry-upland and wetland-valley bottom small holder subsistence cultivation characterizes the area. The Manalana catchment is highly altered in its vegetation composition than would normally be found in more pristine areas of the lowveld sour bushveld. The hillslopes were in part cleared for forestry in the 1960–70 s and never planted, as such the short opportunistic shrub, *Parinari curatellifolia* now dominates. The presence of this shrub, as well as communal grazing of cattle, frequent grassland fires, and harvesting of grass and fuel wood has rendered a catchment with a very low basal cover. In addition, it is extensive wetland cultivation (ridge and furrow systems) that has altered the natural micro-topography of the valley bottom and changed the balance of hydro-geomorphic processes within the wetland system. This may take the form of disaggregating material through tillage practices, as well as increasing the level of channelization within the system by furrowing, amongst several other factors for example. This is believed to be a causative agent facilitating the extensive gullying characterizing the Manalana catchment. The Manalana catchment itself is 2.61 km^2 of which 2.50 km^2 and 0.11 km^2 (or 95.6% and 4.4 %) make up the area of interfluve and wetland respectively. Whilst the wetlands had traditionally been used for subsistence agriculture, the wetland in the study area of the catchment has remained fallow and had since returned to a vegetation community of emergent wetland vegetation dominated by *Phragmites mauritianus*.

3 Methods and techniques

3.1 Overall approach

Since the commencement of the catchment hydrological monitoring program (September 2005) various 2-D ERI surveys were undertaken along transects through the wetland and its contributing catchment. These were followed in July–August 2008 with a detailed 3-D ERI and IP approach to ascertain the distribution of the sub-surface clay-plugs and allow for some speculation on their development. In both cases use was made of an ABEM^{TM} SAS1000 single channel Lund imaging system (Terrameter and switcher unit) with 64 electrode take-out over four cables. Electrode spacing and array types varied with each survey according to information requirements, a summary of these are given in Table 2. In general the Wenner array was used as this is sensitive to vertical changes in the subsurface resistivity distribution and anticipated to be useful for delineating sedimentary layers. Meanwhile, the Schlumberger array was used specifically on transect 1 as this array is sensitive to both vertical and horizontal resistivity distributions and therefore anticipated to be useful for revealing intruding features such as bedrock outcrops, this array was used principally to assist in a complementary study in the catchment on hillslope hydrology. Orientation of these surveys is displayed in Fig. 1. Inversion of 2-D and 3-D datasets were conducted using the RES2DINV and RES3DINV software packages respectively (Loke, 2005a, 2005b). Prior to the final inversion of data, the raw electrical resistivity data was assessed for its quality according to the methods of Loke (2004), where bad data points are removed from a preliminary inversion array that display high RMS error. These bad data points are therefore excluded from the final data inversion process. Inversion data were georeferenced with correct elevations using a Trimble® Pro-XRS differential Global Position System.

3.2 3-D approach

The first part of the 3-D study sought to examine the location and extent of the clay-plugs within the wetland. For this purpose three parallel transects were placed at longitudinal orientation in the two arms of the wetland (as shown in Fig. 1), forming a juncture adjacent to the erosion gully head. Wenner-α arrays were used in each of the parallel transects using a single time interval IP sequence which also records the sub-surface resistivity distribution at the same time, a default setting in the ABEM system.

The second part of the 3-D approach sought to examine the interface between the hillslope and valley bottom (wetland) in order to determine whether these clay-plug zones are contiguous with the hillslope, i.e. at the interface of the wetland with the footslope. Here one location was chosen (Fig. 1) for detailed examination, in which it was hoped that any layered lithographic effects within the wetland substrate could also be discerned. Due to the small localized setting of this particular investigation and due to considerations in terms of the data acquisition time, new protocols were written such that Wenner-β arrays could be deployed using a single cable with a 21 electrode take-out (NB: the system consists of 4 cables, each of 21 take-out positions). This allowed for 3 subsequent transects to be set-up whilst the ABEM system was logging another. Referring to Fig. 2, the survey took the form of a gridded system made up of two orientations of 11 parallel transects, in both X and Y directions, making up a total of 22 parallel lines. Electrodes were spaced at 0.75 m intervals, and thus the total length of each individual transect was 15 m. Correct geometric factors (k) were applied to the raw data in order to recalculate the apparent resistivity, prior to the inversion of the data set since the ABEM system limits the electrode spacing to metre integer values with one decimal place. Hence, the apparent resistivity distributions would be different to those that would otherwise have been calculated automatically by the ABEM system.

In both 3-D approaches the resulting images are quasi-3-D as results are interpolated from 2-D transects, and the one

Table 2. 2-D ERI surveys timing and arrays deployed in the Manalana catchment.

ERT Survey	array type	electrode spacing (m)	date of survey	orientation	purpose
Gully longitudinal transect	Wenner-α (long)	2.5	May 2005	W–E	material and bedrock distribution wetland and gully floor
Transect 1	Schlumberger (short)	5[a]	November 2006	SW–NE	material and bedrock distribution hillslope-wetland-hillslope
Transect 2	Wenner-α (long)	5	October 2006	S–N	material and bedrock distribution hillslope-wetland-hillslope
Wetland transect	Wenner-α (short)	5[a]	October 2006	NW–SE	material and bedrock distribution
Longitudinal Grid Transects 3-D	Wenner-α (long)	2	July 2008	SW–NE & SE–NW	identify clay distribution underlying wetland
Grid Transects 3-D	Wenner-β (21 probe)	0.75	August 2008	SW–SE–NE–NW	identify clay distribution at wetland-footslope interface

[a] used model refinement in inversion to half unit electrode spacing, this allows for dampening of the effect of high resistivity variations that may be encountered in a survey and provides for smoother inversion of resistivity data.

channel SAS1000 ABEM system is limited in this regard. Also parallel transects were placed apart at two times the unit electrode spacing, within the bounds of acceptable error for a quasi-3-D approach (Loke, 1999). A brief explanation of this is warranted: up to this point discussion has focused on the vertical sensitivity of the electrodes to produce a 2-D pseudosection, meanwhile electrodes also exert a radial sensitivity around themselves which becomes important where data is acquired and interpolated through inversion techniques in 3-D. The reader is referred to Loke (1999) for a more detailed explanation. In both 3-D approaches used here, data of 3-D transect "blocks" were defined by the "collate 2-D to 3-D function" within RES2DINV and inverted in RES3DINV. This function takes a series of 2-D surveys (2-D data files) and through an interpolation technique based on known co-ordinates of each electrode produces a 3-D data file. Again, data with high RMS error were removed from the 2-D data arrays prior to final inversion in RES3DINV. 3-D images were plotted using Rockworks® 2006 software for visualizing earth surface and sub-surface data.

The presence of groundwater has an effect on the resistivity range of earth materials (Loke, 2004) and in order to achieve maximum clarity in terms of interpreting these 3-D data, the dry winter period is most appropriate for data collection. Therefore, these surveys were conducted during July–August 2008, during the mid winter period and height of the dry season for this region. Consequently this wetland had undergone a period of desiccation following the cessation of the rains earlier in the year, and as a result, the influence of groundwater on the resistivity and IP soundings was at the minimum possibly achievable for this wetland system. A qualitative ground-truthing was also undertaken of the 3-D transects, using a series of random auger samples where the depth to a change in soil texture was noted, specifically where a change in material dominated by sand fraction switched to that dominated by clay, using a bolus test (Tongway and Hindley, 2004).

3.3 Supporting hydrometry

As part of the hydrological monitoring study undertaken within the Manalana catchment two forms of data are used to assist in the verification and interpretation of ERI and IP data. These are simply shallow groundwater piezometer data, which were measured using regular (bi-/tri-weekly) dip meter readings in nested groundwater piezometers at hydrological monitoring stations within the wetland. The locations of these stations are located in Fig. 1. Moreover, these piezometers were also the subject of in-situ saturated hydraulic conductivity analysis, which took the form of bail tests using the method of Bouwer and Rice (1976), which takes the form:

$$K = \frac{r_c^2 \ln(R_e/r_w)}{2L} \frac{1}{t} \ln \frac{y_0}{y_t} \quad (4)$$

where: K is the hydraulic conductivity of the wetland material, L is the height of the open screen portion of the piezometer at its interface with the wetland matrix (300 mm), y is the vertical distance between water level in the piezometer and that within the wetland material at equilibrium at time 0 and time t. R_e is the effective radius over which y is dissipated

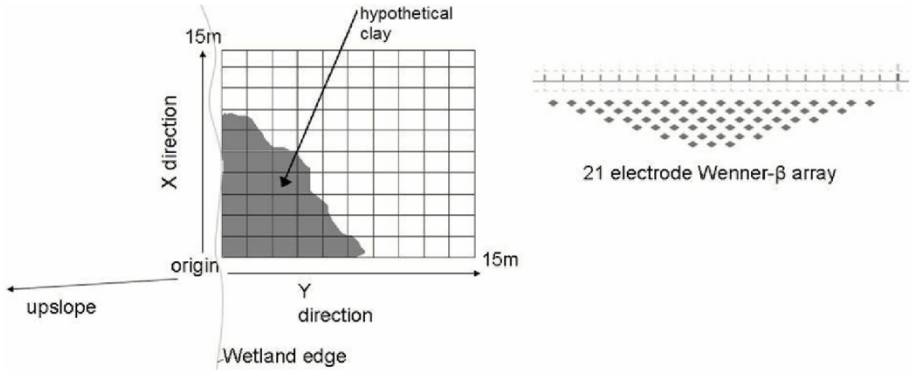

Fig. 2. Grid design and placement of the Wenner-β $\times 21$ transects at the wetland-footslope interface and the data point distribution of the 2-D array (whose series along the grid would be used to interpolate a 3-D profile).

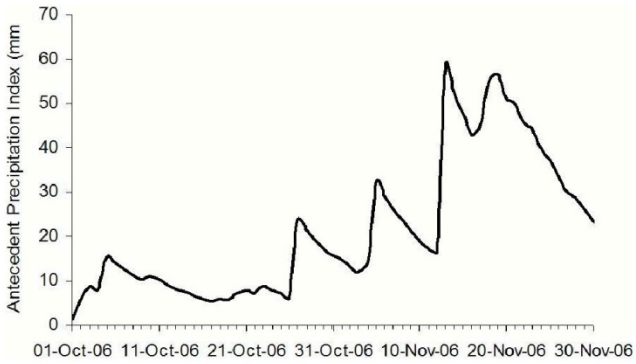

Fig. 3. Antecedent Precipitation Index for the period October–November 2006.

and r_w is the horizontal radius between the centre of the piezometer and the aquifer (plus well casing and interfacing material, 42 mm). r_c is the inside radius of the piezometer casing (27 mm).

In addition, mean soil moisture tension (tensiometers) and shallow groundwater levels for the months of October and November 2006 are displayed in Table 1 to assist in the interpretation of ERI data. Moreover an antecedent precipitation index (API) for these two months is also displayed in Fig. 3, this is based on the method described by Kohler and Linlsey (1951), and commences at the start of the hydrological year in eastern South Africa (October).

4 Results

4.1 2-D surveys

Figure 4 displays the subsurface resistivity distribution where the un-eroded wetland surface descends into the erosion gully at horizontal distance −35 m on the lateral transect. The area between −55 m and −35 m is characterized by emergent wetland vegetation namely *P. mauritianus* and contains a network of drainage furrows, note one such furrow at −50 m. The first point of interest is the shallow resistant overburden (400–1400 Ω m) overlying a conductive horizon (30–150 Ω m) between −45 m and −20 m, underlain by a deeper resistant layer (> 250 Ω m). The second is the vertical protrusions that appear at −15 m and 30 m on the lateral transect. Interpretation of these points reveals the nature of unconsolidated and transported sediments (sands) at the wetland surface and gully floor which overly deep leached fine clay deposits, which are confined by these vertical felsic saprolitic protrusions from the underlying granitic bedrock. Since it is known that the dominant geology of the catchment is granitic, the associated resistivity ranges for this bedrock type are used for ERI interpretation based on geological resistivity ranges provided by Sharma (2008). These vertical protrusions could therefore be interpreted as sub-surface controls intersecting the unconsolidated wetland sediments. This in essence shows that the wetland is characterized by what appears to be a series of semi-confined aquifers with high water retention capacity due to their clay content. This is highlighted by the sharp transitions between the two material types at depths below 2 m (i.e. low resistivity clays versus high resistivity bedrock/saprolite). The significance of this observation is particularly important for the way that the wetland retains water and further hydrochemical analysis will reveal the nature of the groundwater recharge processes that these wetlands facilitate, within the confines of these bedrock controls.

Catchment ERI cross-sections were made perpendicular to the orientation of the wetland along two instrumented transects, transects 1 and 2 (Figs. 5 and 6). In Fig. 5 the region −100 m to −20 m is dominated by the opportunist shrub *P. curatellifolia,* and between −20 m and 20 m by *P. mauritianus* dominated wetland vegetation , and thereafter the hillslopes are again characterised by *P. curatellifolia* shrubland. The same vegetation sequence is observed in Fig. 6 between −200 m to −110 m, -110 m to 30 m, and 30 to 200 m respectively. The valley bottom area in Fig. 5 is an area of wetland that has not been used extensively for subsistence agriculture,

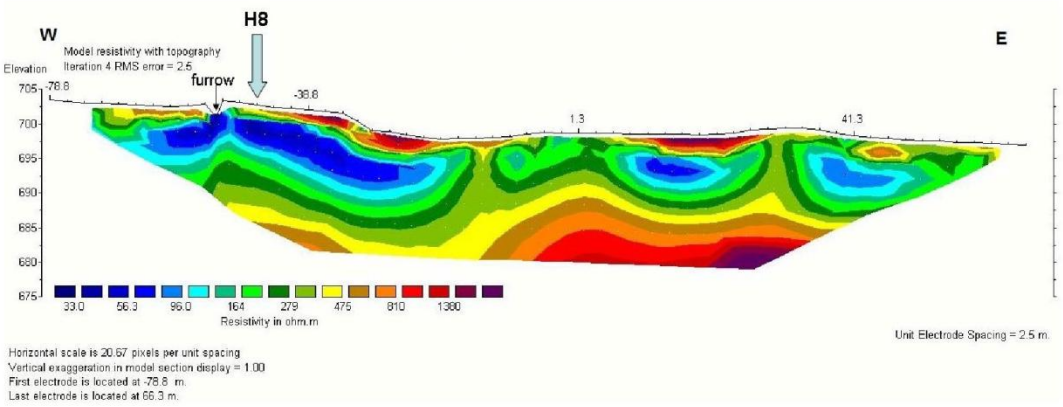

Fig. 4. Longitudinal ERI pseudosection of a transect along erosion gully. (Wenner long). NB. This survey was conducted prior to the installation of hydrometric apparatus.

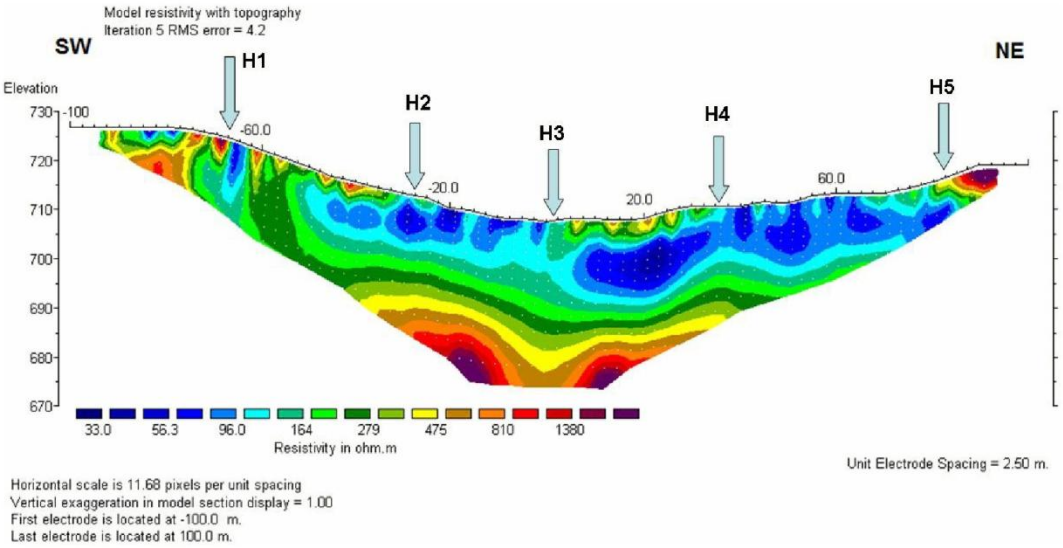

Fig. 5. ERI pseudosection of Transect 1 (hillslope-wetland-hillslope) (Schlumberger short).

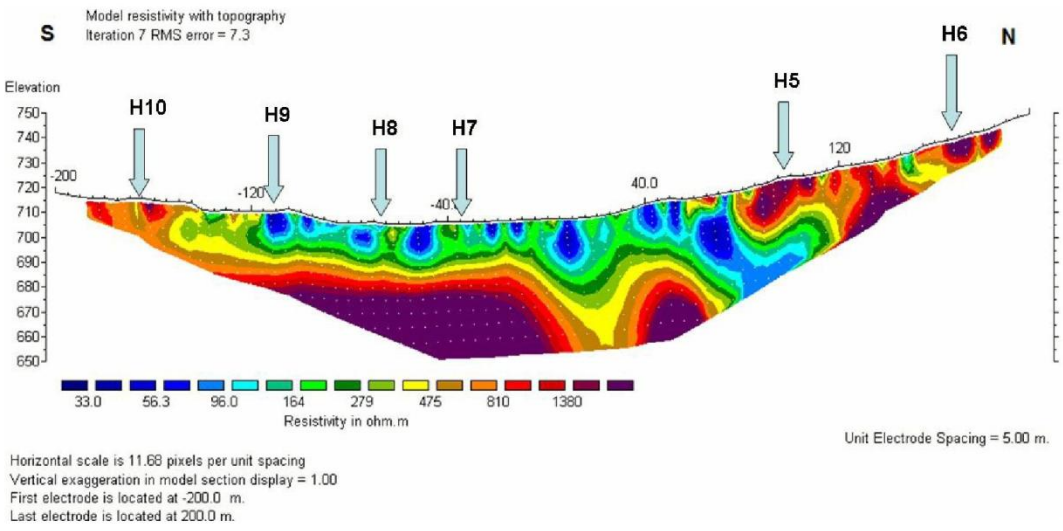

Fig. 6. ERI pseudosection of Transect 2 (Wenner long).

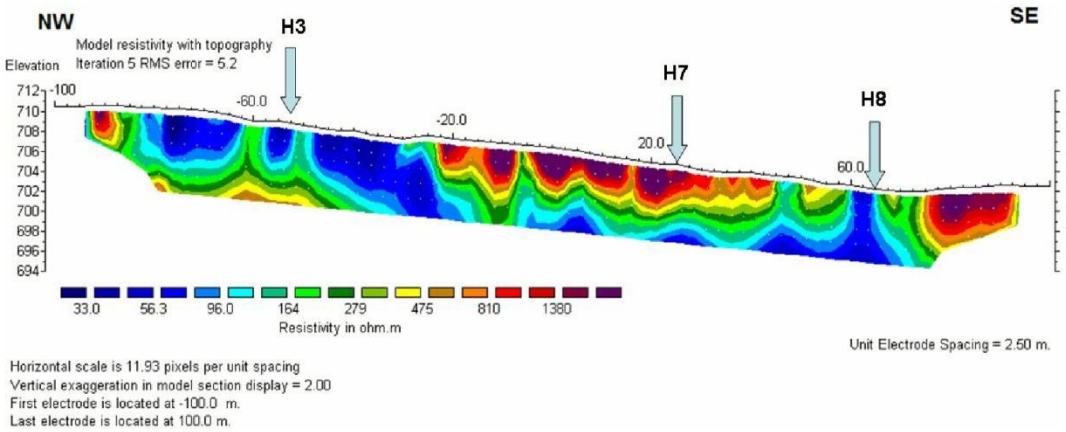

Fig. 7. ERI pseudosection of a transect along the wetland. Wenner short, note 2 × vertical scale exaggeration.

meanwhile the valley bottom area of Fig. 6 has been, and it contains a large network of ridge and furrow systems. In both cases the substrate appears to be increasingly conductive towards the valley bottom and underlain by higher resistant material. The unconsolidated wetland substrates of the valley bottom appear to be some 20–25 m deep and are probably of a more conductive nature due to the higher moisture content of the substrates in this region than on the interfluves. In Fig. 5 it is apparent that the interfluve of the NE side of the transect is more conductive than the SW side. This is due to the intersection of the catchment's northern edge by a doleritic dyke, noted through in-situ observations, whereas the SW is a slope of granitic material. This is seen again in Fig. 6 for the S–N transect, the doleritic dyke is more apparent between 50–100 m with a vertical structure of $< 150\ \Omega$ m extending to the base of the pseudosection. Further to the north of this transect in the upslope region the granitic geology reappears.

These initial 2-D ERI surveys reveal the interplay of bedrock and regolith that characterizes this particular catchment. In particular there is an obvious contrast between the two geological substrates by way of the predominant granitic material and flanking of the catchments by dolerite dykes. This interplay of geologies has important ramifications for the hydrological processes operating within this catchment, particularly since soil hydraulics will be influenced by the different soil textures and porosities yielded from soils on these different geologies. Most notably granites weather to coarse structured soils and dolerites to fine clay rich soils (Schaetzl and Anderson, 2005), and this was reflected by the contrasting conductivities of the materials in Figs. 5 and 6. Hence the lower resistance of the doleritic material is explained by its higher clay content than the opposing granites. The observed hydrological responses reflecting these differing hillslope geologies to precipitation events and antecedent soil moisture conditions, and the consequent variability in the way that water is delivered to the valley bottom wetland have been characterized for this catchment. This has been done through hydrometric observations and hydropedological interpretation of soil form (Riddell et al., 2010).

The entire profile of Fig. 7. has emergent wetland vegetation at the surface, dominated by *P. mauritianus* and subsistence agriculture occurred primarily between −30 m and 70 m. As expected, increasingly conductive material is observed within the longitudinal pseudosection displayed in Fig. 7, in particular the $< 100\ \Omega$ m material on the northern side of the transect which corresponds with the valley bottom material of Fig. 5. This conductive material is seen all along the profile although it is shallower with reduced depth to bedrock at the northern end. However, between −20 m and 40 m a more resistant ($> 1000\ \Omega$ m) layer is seen at the surface. This resistant layer is an area where the wetland topography has been mechanically altered by subsistence agricultural practices. The creation of ridge and furrow systems by digging and re-deposition of material in this way has consequently disaggregated the wetland substrate, reducing its bulk density and hence inducing higher relative apparent resistivity. The furrows themselves are up to approximately 1 m deep, below the top of the raised cultivation beds. It is likely that the traversing of the resistivity probes and cables across both the furrows and raised cultivation beds has allowed for a certain degree of distortion of the observed vertical resistivity distribution in this region of the wetland, allowing for an over exaggerated measurement of resistant material at depth. A significant observation from this pseudosection is the apparent vertical protrusions of high conductivity material at 60 m and a similar possible structure at 45 m (contrasting with the high resistant protrusions of Fig. 5). At the extreme SE of this image a large area of high resistant material occurs and this forms the eroded and deposited sediments of the erosion gully head, corresponding to −40 m in Fig. 4.

The fact that the longitudinal wetland survey (Fig. 7) revealed vertical low resistance structures toward the wetland toe added support to the speculation that sub-surface flows of water through this highly conductive sandy system were buffered by clay-plugs. Furthermore, these were deemed to explain the lateral differences in hydrodynamics of the phreatic surface responses at different longitudinal reaches within the system (Riddell et al., 2007). This was noted because the hydrodynamics of the wetland appeared to be partly de-coupled between longitudinal reaches of these wetlands where these clay-plugs had formed sub-surface hydrodynamic *breaks* in an otherwise sandy and hydraulically conductive system. Similar responses to this were also noted during the 2007–2008 hydrological season where this hydrodynamic break was observed between groundwater levels as recorded at the hydrometry stations. Figure 8 reveals the hydrodynamic responses in paired peizometers (2 m and 4 m deep) to rainfall over this season. It is quite clear that the ground water table has a short lived elevation at the most head-ward reach of the wetland at H3, particularly during the peak of rainfall up to March 2008 as seen in both piezometers. Thereafter, following the cessation of the rains the water table drops below the depth of the 2 m piezometer and there follows a steady decline in water table elevation observed in the 4 m piezometer. Since both piezometers at H3 show similar water table levels this suggests that they both intersect the same aquiferous material in the wetland. Meanwhile moving downstream to H7 the perpetuity of the groundwater level is more sustained. However, whilst water table behaviour between the two piezometers at H7 tallies, there is a discrepancy in their depths of between 0.5–1.0 m over time, suggesting a degree of discontinuity in the aquifer material at depth somewhere between 2–4 m deep. This perpetuity however is to be expected since the contributing area of the catchment and the wetland to this point is considerably greater than at H3. However as one moves downstream this expected perpetuity of groundwater level elevation at H8 is rescinded earlier than at the upstream H7, and in fact the water table in the 2 m piezometer here declines prior to that at H7, furthermore the 4 m piezometer here shows a very dampened response to rainfall and never exceeds −2.5 m. This is attributed to the location of H8 adjacent to the erosion gully head, which facilitates a drawdown of water from the wetland at this location, and this may be noted by the fact that the water levels in both piezometers at H8 are considerably lower than at H7. It would however also be expected that this erosion gully would facilitate a hydraulic drawdown that would also be felt at the nearby H7. Despite this the water table elevations at H7 remain quite close to the surface long after the piezometers at H8 have begun to dry out. This supports the notion that the presence of the clay-plug as seen in Fig. 7, buffers the lateral sub-surface flow of water between H7 and H8.

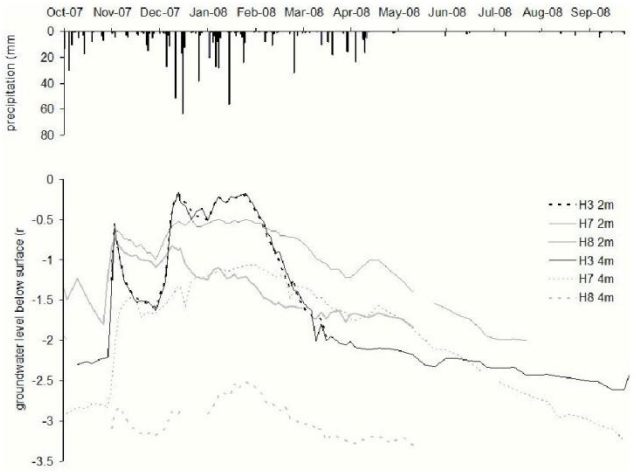

Fig. 8. Hydrometric observations of water table depths within the Manalana wetland October 2007–October 2008 (2 m and 4 m refer to installed piezometer depths).

4.2 3-D surveys

3-D geophysical surveys where used to analyze the distribution of clay bodies within the Manalana wetland and IP surveys were of particular use. 3-D pseudosections are displayed in Fig. 9 for the series of parallel transects orientated SE–NW longitudinally through the wetland. Here one observes the relatively low chargeability of the material within the vicinity of the origin of the pseudosection. However within this material three other factors are apparent. First, the chargeability time increases with distance away from the origin, particularly at a distance beyond ∼ 55 m, and this increases significantly towards the surface of the profile beyond this point. The second observation to consider is the sinuous curve made by the material with a chargeability of between 1–2 ms at around 55 m. The final and rather striking observation is the arch-like appearance of extremely high capacitance (∼ 0.01–0.03 ms) material from the origin to ∼ 50 m. The vertical sections of this arch-like structure correspond to the vertical low resistivity material mentioned in the discussion of Fig. 7. Furthermore, the chargeability distribution does not appear to change within the 4 m breadth of the profile, except for a slightly lower chargeability region (∼ 0.03 ms) at around 20 m at 4 m breadth. Figure 10 displays the same transect except in terms of the subsurface resistivity distribution, and here similarities emerge as would be expected. These being for instance the profile in Fig. 10 which is dominated by conductive material generally no more than 1000 Ω m, which conforms to the high capacitance material of Fig. 9. Meanwhile a band of high resistance material (> 1000 Ω m) is encountered in Fig. 10 in the subsurface below where the high capacitance arch is discernable in Fig. 8, approximately between 5–35 m in Fig. 10. Furthermore, higher resistance material (> 1000 Ω m) is observed

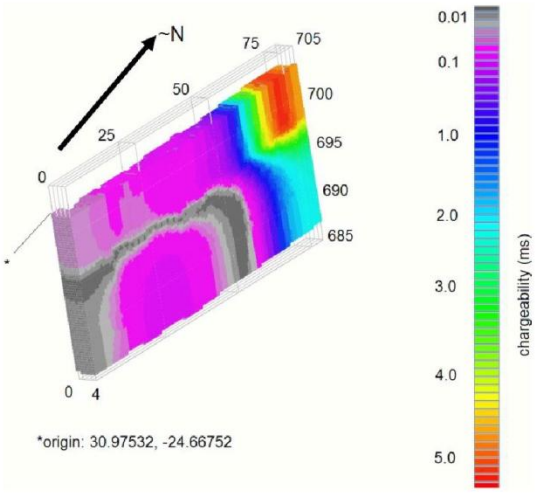

Fig. 9. Pseudo 3-D IP section of the SE–NW parallel transects. Scales are in metres diverging from a geographical origin, vertical scale is altitude a.s.l. (Wenner long, 2 m spacing, 8th iteration, RMS error 8.74%).

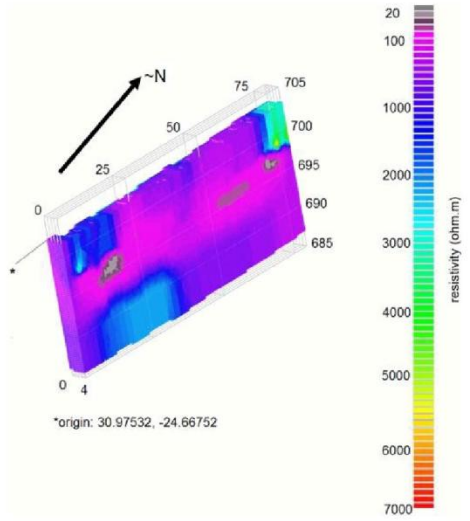

Fig. 10. Pseudo 3-D resistivity section of the SE-NW parallel transects. Scales are in metres diverging from a geographical origin, vertical scale is altitude a.s.l. (Wenner long, 2 m spacing, 8th iteration, RMS error 6.36%).

beyond 70 m near the surface in Fig. 10 when compared to the rest of the pseudosection, corresponding to the lower capacitance material in Fig. 9. However the major difference between the two images relates to the clearer definition of an arch-type distribution of material in Fig. 9, this is not revealed in Fig. 10.

The IP profile of the SW–NE orientated transect (Fig. 11) has a high capacitance material throughout the profile, seldom exceeding 0.1 ms. Hence the inference from this image is that this part of the wetland has a particularly clay rich profile, the full length of the wetland, contrasting with the larger arm of the wetland seen in Figs. 9 and 10. Of particular note in Fig. 10 is the very high capacitance (< 0.01 ms) material seen from the point of origin to ~ 25 m. This material corresponds with the vertical band of material seen near the origin in Fig. 9. Furthermore, one observes a vertical band of high capacitance material (< 0.01 ms) at ~ 30 m extending from the surface to 5 m deep. However, despite the inversion of the data using a robust method with optimized damping factors, the pseudosection was achieved with a relatively high root mean square (RMS) error, and hence this image must be interpreted with caution. Meanwhile, the satisfactory inversion of the corresponding resistivity image for this section aids in the interpretation of this anomalous IP output. This resistivity data is displayed in Fig. 12, where one observes a lateral stratification of the sub-surface media within this profile, particularly a band of material of $< 1000\ \Omega$ m between 693–698 m a.s.l., similarly this banding is also discernable in Fig. 10 for the complementary transect in the alternative orientation. In both cases this low resistivity/high capacitance material overlies a slightly higher resistance material at depth (note the material under-arch in Fig. 10). Moreover, in Fig. 11 one observes the slight reduction in material capacitance below 697 m a.s.l., beyond 30 m. However, Fig. 12 does reveal the anomalous nature of the vertical band of high capacitance material at 30 m seen in Fig. 11, which does not tally with the higher resistant material observed at this location in the resistivity profile. One possible reason for this anomaly, speculatively speaking, may be due to the presence of cracked clay in the profile, which due to the dry winter period at the time of surveying is highly likely. Therefore, although the clays themselves will have high capacitance, if they are cracked and hence have very large inter-pore spaces may engender large resistivity readings due to greater air to pore ratios in the soil medium than under wetter conditions.

The results of IP surveys using the gridded 21 electrode method at the wetland footslope interface revealed the highly variable nature of the material here in terms of its chargeability. Figure 13 displays this data in two orientations around the origin. This variability is reflected in the stratification of chargeability layers and heterogeneities in the near surface. It must be remembered here that due to the short electrode array and short spacing of these electrodes the vertical depth penetration is reduced, and hence the resulting survey provides a resolution to a depth of 3 m. Nevertheless the resulting output reveals the patchy network of low capacitance (> 6 ms) material near the surface and this reflects the disturbed material at the wetland surface that has been mechanically altered to create raised bed and furrow systems used for cultivation purposes. Meanwhile, one is able to discern that this unconsolidated material overlies a deeper layer of rather high capacitance material (< 1 ms), which varies in its depth across the 15 m $\times$ 15 m domain.

Figure 14 displays the same data, except that an IP filter has been applied to display chargeability data only below

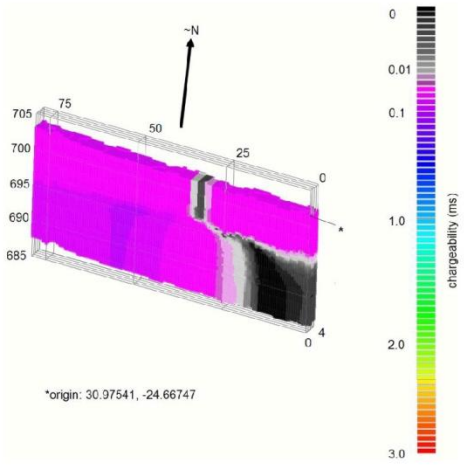

Fig. 11. Pseudo 3-D IP section of the SW–NE parallel transects. Scales are in metres diverging from a geographical origin, vertical scale is altitude a.s.l. (Wenner long, 2 m spacing, 6th iteration, RMS error 13.3%).

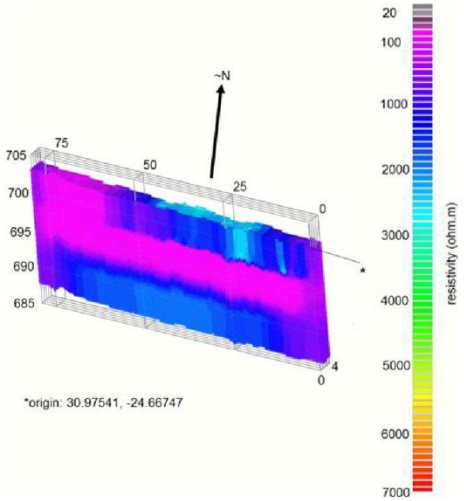

Fig. 12. Pseudo 3-D resistivity section of the SW-NE parallel transects. Scales are in metres diverging from a geographical origin, vertical scale is altitude a.s.l. (Wenner long, 2m spacing, 6th iteration, RMS error 5.92%).

1 ms, which in essence allows for visual representation of only the high capacitance material at the wetland-footslope interface. The resulting pseudosection reveals that although this high capacitance material is somewhat laminar there is an obvious increase in depth to this layer with increasing distance from the point of departure of the grid from the origin. With this origin being at the wetland-footslope interface, one is therefore able to note that this material is protruding from the hillside into the valley bottom, with a descent in the N, NE and E direction.

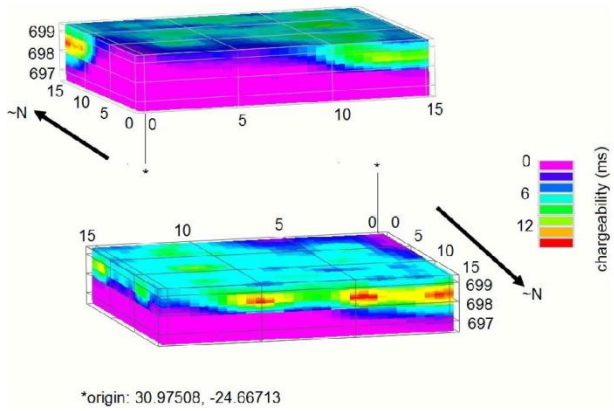

Fig. 13. Pseudo 3-D (with improved XY resolution) IP section of the wetland-footslope interface. Scales are in metres diverging from a geographical origin, vertical scale is altitude a.s.l. (Wenner-β ×21, 4th iteration, RMS error 3.35%)

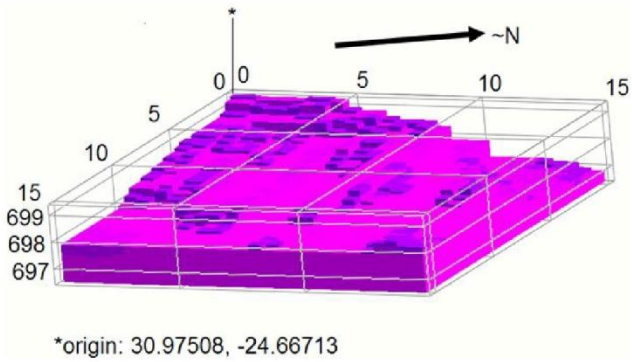

Fig. 14. Pseudo 3-D IP section of the wetland-footslope interface with chargeability values filtered to between 0–1 ms. Scales are in metres diverging from a geographical origin, vertical scale is altitude a.s.l.

4.3 Verification

In order to verify the output of the IP profiles, whose characteristically high capacitance regions suggest the occurrence of clays, a rapid and random series of auger holes were dug to a depth where clay was observed and defined through a bolus test. The locations of the random augered ground truthing points in relation to the parallel transects are displayed in Fig. 15. Furthermore, Fig. 15 also displays an image of the face of the actively eroding gully headcut (wet season March 2006), whereupon the saturation of the soil profile reveals two distinct horizons within the wetland substrate, a shallow sandy loam horizon above a deep fine clay horizon. Since the SE–NW transect (Fig. 9) shows that from the point of origin to approximately 50 m the wetland is made up of a high capacitance material (< 1 ms) and this is relatively consistent from the surface throughout the entire depth of the profile. The fact that clays were encountered within 1 m of

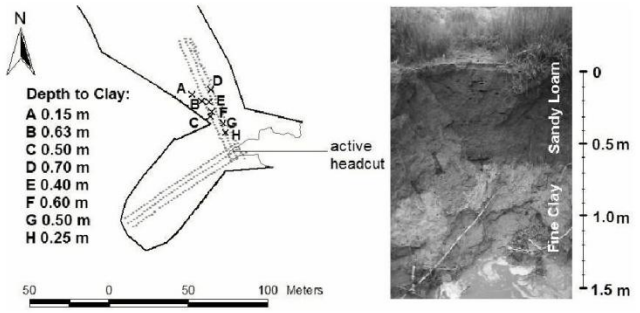

Fig. 15. Locations of auger sample points to clay horizons (L) and discernable shallow sandy loam soils over lying deep fine clays of the Kroonstad (*Planosol*) soil form exposed at the site of active gullying (R).

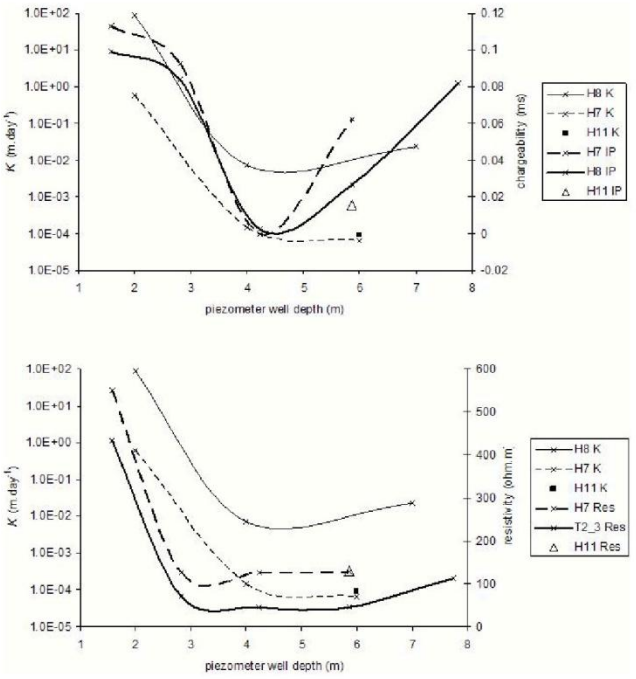

Fig. 16. Plots of log-K vs. IP measurements (above) and resistivity measurements (below).

the wetland surface at these locations support the inferences made about clay distribution from the IP surveys.

An analysis was also undertaken to verify IP interpretations by using measures of saturated conductivity (K) at the hydrometric monitoring stations. This verification is considered semi-quantitative since, as will become apparent, repeated bail tests could not be undertaken due to the extremely slow recoveries of the piezometers. Hence, the displayed K values of Fig. 16 are single measurements and therefore treated as estimates of K at the various piezometer depths. Figure 16 displays the closest measured IP (ms) and apparent resistivity (Ω m) value at each depth corresponding to the depth of the piezometer well at each hydrometric monitoring location (Fig. 2). These values originate from the raw 4 point resitivity measurements rather than from the inverted pseudosections. In cases where K was determined at depths >2m, the K is extremely low, implying that water levels in the wells would take hours if not days to recover to equilibrium levels prior to conducting bail tests.

When resistivity data is plotted against log values of K there appears to be good agreement between the estimated conductivity of the material at the respective piezometer depths and the measured apparent resistivity of the same material for all wells (note there is only one well at H11). However the correlation coefficient for Log K against chargeability at 0.65 is much more agreeable than against resistivity at -0.45. In each case however the plots appear to show a decline in resistance (or increased conductance) with K at depth, which tapers off below a depth of 4 m. The situation with the IP data does not yield the same clear relationship, although trends may be observed. Firstly, there is a general decrease in K of the wetland material whilst capacitance increases (chargeability time decreases), up to 4 m depth. Second, at depths beyond 4 m K increases slightly at piezometer locations H7 and H8, and at H11 capacitance and K tally. Therefore, there is a trend between these two variables of K and chargeability, however the clarity of their relationship is concealed by the very small chargeability range that is plotted on the secondary Y-axis. Obviously, more repeated K tests and precise determination of resistivity and chargeability would be ideal in order to verify the ERI and IP output. However this was negated by conditions in the field i.e. very low conductivities, and output of measured apparent resistivities, where the readings extracted from inversion-model output would not have been in precisely the same location as the piezometer wells.

5 Discussion

The addition of 3-D combined IP and resistivity surveys to the 2-D scoping surveys and supporting hydrometry data have allowed a real insight into the hydro-geomorphic controls within this wetland system and facilitated a proposed model for the development of these controls, particularly in terms of clay-plug formation. The rationale for the proposed model will now be outlined:

Remembering that the SE-NW orientated parallel transects (Figs. 9 and 10) situated in a larger region of the wetland (refer to Fig. 2) show that the chargeability time in the wetlands sub-surface increases with distance NW away from the origin. Meanwhile the SW-NE orientated transects within the smaller wetland region displays an extremely high capacitance all the way along this part of the wetland. This provides for the first point of interest. The suggestion is that the smaller wetland region has a more uniform clay distribution in the sub-surface than the larger region, and the latter

therefore is likely comprised of increasingly coarser (higher resistance, lower capacitance) material away from the juncture of these two regions (tributaries) of the wetland. Furthermore, it was noted that there was a distinct down sloping of higher capacitance material with distance away from the hillslope-wetland interface. These two observations facilitate the notion that finer (clay) particles are removed from the hillslope units through the process of elluviation, which is a common process on these geological terrains in semi-arid settings, particularly in the case of clay enriched sodic sites of the region (e.g. Khomo and Rogers, 2005). This elluviation allows for their deposition (or illuviation) as distinct clay rich horizons at the hillslope toes, which in this catchment have been described according to the South African soil taxonomic system as a *Kroonstad* soil form (Soil Classification Working Group, 1991). Clay rich illuviated horizons are termed "G-horizons" according to the South African definition. These soils translate to the World Reference Base (FAO, 1998) system as *planosols*. This illuviation process has probably been more concentrated within the smaller wetland region due to the higher capacitance and more uniform distribution of this material within this region. This has effectively created a barrier across the confluence with the larger wetland region. Furthermore, the confinement zone or valley pinches that are observed at this confluence has also contributed to this barrier creation, and one observes this process when interpreting Figs. 9 and 11 to their respective positions at this confluence. Indeed the arch-like structure obvious in Fig. 9 suggests an extremely dense clay formation (clay-plug) that could have been created by two (or more) illuvial pathways at this juncture. Effectively what this scenario creates is a zone of infilling by coarser clastic sediments into the larger wetland region from the broader contributing catchment. Indeed the soil types in this larger region of the wetland have been described as hydromorphic soils of the *Katspruit* form, which accordingly translate to *gleysols* (FAO, 1998) which typically develop under wet conditions in unconsolidated materials.

This pedological evidence lends credence to a hypothesis proposed here that valley bottom (wetland) infilling, by unconsolidated colluvial and alluvial material, has occurred behind these clay-plugs. This proposed model therefore implies that there is a lateral as well as vertical removal of finer materials in the slopes of these wetland catchments and their concentration at zones of valley confinement. The proposed model is depicted schematically in Fig. 17 and photographically in Fig. 18.

Based on the observations and measurements presented in this manuscript, it is known that the Manalana wetland is underlain by a deep clay material (> 4 m) with a moderate hydraulic conductivity in relation to an overlying dense clay with extremely low hydraulic conductivity (somewhere between 4 m–2 m). At considerable depth, certainly beyond 6 m the wetland is bounded by bedrock and saprolitic material. It is also known that the clays have a particularly high density at the confluence of the two arms of the wetland, adjacent to the clay-plug. In addition, the near sub-surface of the wetland is largely a sandy horizon with high hydraulic conductivity, and in the smaller arm (SW–NE) of the wetland this horizon is very shallow such that this section is predominantly underlain by clay material, that through lateral illuvial processes, and illuviation of clays from the hillslope at valley constriction (see Fig. 18) has effectively created an illuvial barrier across the confluence with the larger wetland region (SE–NW). Furthermore, as one moves upstream along the larger wetland region, material becomes less consolidated giving way to a deeper sandy matrix.

Understanding of climatically induced evolution of wetlands in southern Africa is outlined in Ellery et al. (2008), as being intimately linked with glacial and interglacial periods of erosion dominated cycles attributed to the warmer and wetter conditions of the latter, and deposition dominated dryer cycles of the former. Furthermore, the clarity of erosion terraces seen within the Manalana catchment reveal that this is indeed the case and the process of cut-and-fill valley evolution in the Manalana has been discussed by Ellery and Kotze (2008), and this reciprocates the findings discussed here, as valley bottom in-filling is noted through our interpretations presented here.

Given the fact that the Manalana represents one of many sub-catchments at the Sand Rivers headwaters which are all in a similar state of degradation the identification of hydro-geomorphic buffers/barriers, such as clay-plugs is crucial. This relates to the concept of catchment connectivity. Whereby, the connectivity of process domains from coupled hillslope-valley bottom wetlands and longitudinal through-wetland processes, as in the case of Manalana catchment and others, are increasing significantly due to degradation process such as erosion gullying. This relates to a concept described by Fryirs et al. (2006) where, the identification and understanding of the hydro-geomorphic processes that buffers/barriers (be they rock outcrops or differential sediment depositions) facilitate in terms of switching on or off these coupled processes within a fluvial network, is important for their successful management. Therefore in light of the already determined hydraulic function that the sub-surface clay-plugs have in terms of ameliorating lateral throughflows in the wetland, and the possible identification of hydro-geomorphic process zones that engender the development of these clay-plug buffers, one should now be able to identify zones within these catchments where they are likely to occur (cryptically). This therefore provides a means to protect these zones, in the absence of access to technical geophysical equipment, one proposes that to reveal and delineate the location of these clay-plugs, identification of regions of valley constriction be made, which may then be analyzed qualitatively through in-situ soil analysis for their clay content.

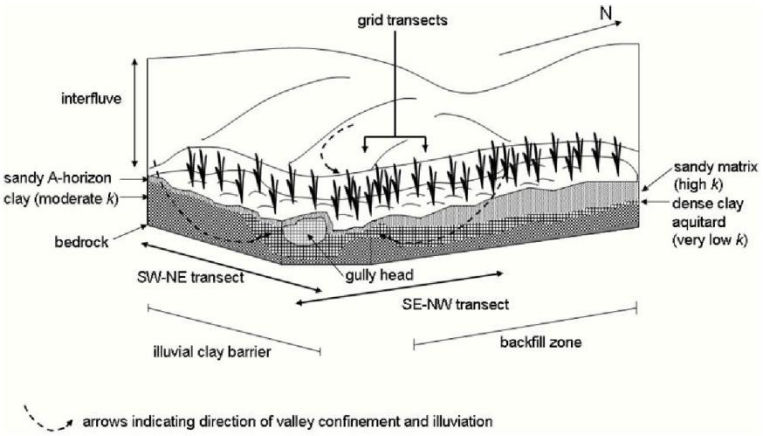

Fig. 17. Schematic of conceptual model for clay-plug development in the Manalana wetland (not to scale).

Fig. 18. South facing view of the Manalana wetland (solid line) with proposed model for clay-plug development highlighting hillslope confinement zones and illuviation pathways (dashed line) and illuvial barrier (dotted line). Inset represent aerial view of hillslope confinement zones.

Beauvais et al. (1999) successfully used ERI to describe hydro-geomorphic processes on other granitic terrains in Senegal by identifying both mechanical and weathering induced drivers of hillslope geomorphology. The ERI approach here using additionally, IP, has similarly assisted in the development of a conceptual model for the evolution of hydrogeomorphic controls in the wetlands of the Sand River system. However it is interesting to note that even in a relatively recent sedimentology study (Baines et al., 2002) making use of similar technology highlighted the lack of a due procedure to be followed when undertaking such geophysical surveys for geomorphic understanding. Given that there are a variety of sources of uncertainty in ERI such as the evenness of electrode spacing (e.g. Oldenborger et al., 2005), not accounting for variations in moisture of the substrate, or even the misappropriation of the correct resitivity range for the geological area in question, highlights the importance of ground truthing of ones geophysical data as far as is possible. Despite these sources of uncertainty Baines et al.(2002) and Loke (1999) advocate the use of qualitative ground truthing to verify geophysical interpretations, and the verification approaches used in this study were highly valuable in this respect. This is an issue that should be developed and refined in the future, particularly where the use of geophysical methods for low cost rapid hydro-geomorphic interpretation (outside of the fields of geological and mineral prospecting for instance) of wetlands and other landscape units is required. It is therefore advocated here that the combined use of ERI and IP be used, were possible, in cases such as wetland rehabilitation planning. This is particularly pertinent to South Africa, a water scarce country, where wetland rehabilitation is common place and where hydrological and geomorphological data relating to the wetland is often lacking. Moreover, it is widely accepted that these geophysical approaches add huge value to understanding hydrological process data in research catchments, in which they aid in the extrapolation of point measurements to the larger scale (Wenninger et al., 2008). Hence the data discussed here will be of real benefit for the development of a hydrological process model of the Manalana wetland and its sister catchments in the future.

6 Conclusions

The use of the geophysical methods of ERI and IP have shown their suitability for describing hydro-geomorphic structures within wetland catchments. In particular these relatively rapid approaches are envisaged to have application in the future for extrapolating hydrological regimes and hydrogeomorphic controls in wetland systems, this has important hydro-ecological and economic implications for the plethora of wetland (and river) rehabilitation projects now underway in South Africa where robust conceptual models of these wetland processes are required to facilitate appropriate and successful rehabilitation measures. In this regard the use of this approach allowed for the identification of crucial geomorphic processes that control catchment connectivity in this region. In particular the surveys allowed for the delineation

of clay-plug sub-surface hydrological buffers and provided information on their modes of formation, albeit by inferring where they will likely occur with respect to longitudinal valley position. The findings will now enable the future protection of these zones from externally derived degradation processes and it is envisaged that this methodology be suitably applied in the future, particularly for wetland rehabilitation planning.

Acknowledgements. The authors are grateful to the South African Water Research Commission (WRC) and National Research Foundation (NRF) for financial support. Professor Fred Ellery (Rhodes University) for assistance with geomorphic concepts and facilitating the initial wetland monitoring project. The kind assistance of the following people for field assistance, data processing and interpretation is duly acknowledged; Johannes Hachman (University of Freiburg), Bertram Koning (University of KwaZulu-Natal). Pieter Le Roux and his team (University of Free State) for assistance in data collection and in interpretation of soil form characteristics. Logistical and administrative support was provided by the Association for Water and Rural Development (AWARD).

Edited by: E. Zehe

References

Acocks, J. P. H.: Veld Types of South Africa, Memoirs of the Botanical Survey of South Africa, Botanical Research Institute, Dept. of Agriculture and Water Supply (South Africa), 57, 146 pp., 1988.

Baines, D., Smith, D. G., Froese, D. G., Bauman, P., and Nimeck, G.: Electrical resistivity ground imaging (ERGI): a new tool for mapping the lithology and geometry of channel-belts and valley-fills, Sedimentology, 49, 441–449, 2002.

Beauvais, A., Ritz, M., Parisot, J. C., Dukhan, M., and Bantsimba, C.: Analysis of poorly stratified lateritic terrains overlying a granitic bedrock in West Africa, using 2-D electrical resistivity tomography, Earth Planet. Sc. Lett., 173, 413–424, 1999.

Beauvais, A., Parisot, J. C., and Savin, C.: Ultramafic rock weathering and slope erosion processes in a South West Pacific tropical environment, Geomorphology, 83, 1–13, 2007.

Bouwer, H. and Rice, R. C.: A slug test for determining hydraulic conductivity of unconfined aquifers with completely or partially penetrating wells, Water Resour. Res., 12(1), 423–428, 1976.

Dahlin, T.: 2-D resistivity surveying for environmental and engineering applications, First Break, 14(7), 275–283, 1996.

Ellery, W. N. and Kotze, D. C.: WET-OutcomeEvaluate, in: WET-Management, The Wetland Management Series, 11 Chapters, edited by: Breen, C., Dini, J., Mitchell, S., and Uys, M., Water Research Commission, Gezina, Pretoria, WRC Report No. TT 343/08, 2008.

Ellery, W. N., Grenfell, M., Grenfell, S., Kotze, D. C., McCarthy, T. S., Tooth, S., Grundling P. L., Beckedahl, H., Le Maitre, D., and Ramsay L.: WET-Origins, Controls on the distribution and dynamics of wetlands in South Africa, in: WET-Management, The Wetland Management Series, 11 Chapters, edited by: Breen, C., Dini, J., Mitchell, S., and Uys, M., Water Research Commission, Gezina, Pretoria, WRC Report No. TT-334, 2008.

FAO 1998.: World Reference Base for Soil Resources, Rome Food and Agriculure Organization of the United Nations FAO, International Society of Soil Science ISSS-AISS-IBG, International Soil Reference Group, available at: http://www.fao.org/ag/agl/agll/wrb/newkey.stm, last access: January 2010.

Fryirs, K. A., Brierley, G. J., Preston, N. J., and Kasai, M.: Buffers, barriers and blankets: The (dis)connectivity of catchment-scale sediment cascades, Catena, 70(1), 49–67, 2006.

Khomo, L. M. and Rogers, K. H.: Proposed mechanism for the origin of sodic patches in Kruger National Park, South Africa, Afr. J. Ecol., 43, 29–34, 2005.

Kiberu, J.: Induced polarization and Resistivity measurements on a suite of near surface soil samples and their empirical relationship to selected measured engineering parameters, Interntional Institute for Geo-information Science and Earth Observation, Enschede, The Netherlands, availabel at: http://www.itc.nl/library/Papers/msc_2002/ereg/kiberu.pdf, (last acces: March 2009), 2002.

Kneisel, C.: Assessment of subsurface lithology in mountain environments using 2-D resistivity imaging, Geomorphology, 80, 32-44, 2006.

Kohler, M. A. and Linsley, R. K.: Predicting the runoff from storm rainfall. Weather Bureau, US Department of Commerce, Washington, Research Paper No. 34, p. 9, 1951.

Kunz, R.: Daily Rainfall Data Extraction Utility, User Manual v. 1.0, Institute for Commercial Forestry Research, Pietermaritzburg, Republic of South Africa, 2004.

Loke, M. H.: Electrical imaging surveys for environmental and engineering studies: A practical guide to 2-D and 3-D surveys, available at: www.terrajp.co.jp/lokenote.pdf, (last acces: August 2008), 1999.

Loke, M. H.: Tutorial: 2-D and 3-D electrical imaging surveys, available at: www.geoelectrical.com, (last acces: August 2008), 2004.

Loke, M. H.: Res2dinv 2-D Resisitivity and IP inversion, Geotomo Software, Malaysia, available at: www.geoelectrical.com, (last access: August 2008), 2005a.

Loke, M. H.: Res3dinv 3-D Resistivity and IP Inversion, Geotomo Software, Malaysia, available at: www.geoelectrical.com, (last access: August 2008), 2005b.

Lowrie, W.: Fundamentals of Geophysics, Second Edition, Cambridge University Press, ISBN-13, 9780521859028, 2007.

Marescot, L., Monnet, R., and Chapellier, D.: Resistivity and induced polarization surveys for slope instability studies in the Swiss Alps, Eng. Geol., 98(1–2), 18–28, 2008.

Oldenborger, G. A., Routh, P. S., and Knoll, M. D.: Sensitivity of electrical resistivity tomography data to electrode position errors, Geophys. J. Int., 163, 1–9, 2005.

Pollard, S., Kotze, D., Ellery, W., Cousins, T., Monareng, J., King, K., and Jewitt, G.: Linking Water and Livelihoods The development of an integrated wetland rehabilitation plan in the communal areas of the Sand River Catchment as a test case, Association for Water and Rural Development Warfsa/Working for Wetlands, AWARD internal report, 2005.

Riddell, E. S., Lorentz, S. A., Ellery, W. N., Kotze, D., Pretorius J. J., and Nketar, S. N.: Water Table Dynamics of a Severely Eroded Wetland System, Prior to Rehabilitation, Sand River Catchment, South Africa, Proceedings of the XXXV IAH Congress on Groundwater and Ecosystems, 17–21 September, Lisbon, Portu-

gal, 2007.

Riddell, E. S and Lorentz, S. A.: Hydrologic mechanisms in a granitic hillslope that induce rapid phreatic surface responses in a headwater wetland, in review, 2010.

Robinson, D. A., Binley, A., Crook, N., Day-Lewis, F. D., Ferré, T. P. A., Grauch, V. J. S., Knight, R., Knoll, M., Lakshmi, V., Miller, R., Nyquist, J., Pellerin, L., Singha, K., and Slater, L.: Advancing process-based watershed hydrological research using near-surface geophysics: a vision for, and review of, electrical and magnetic geophysical methods, Hydrol. Process., 22, 3604–3635, 2008.

Ruhe, R.: Elements of the soil landscape, Trans. 7th Intl. Congr. Soil Sci., Madison, WI, 4, 165–170, 1960.

Schaetzl, R., and Anderson, S. (Eds.): Soils: Genesis and Geomorphology, Cambridge, UK, Cambridge University Press, ISBN-978-0-521-81201-6, 2005.

Sharma, P. V.: Environmental and Engineering Geophysics, Cambridge University Press, ISBN-978-0521576321, 2008.

Slater, L. D. and Lesmes, D.: IP interpretation in environmental investigations, Geophysics, 67(1), 77–88, doi:10.1190/1.1451353, 2002.

Slater, L. D. and Reeve, A.: Investigating peatland stratigraphy and hyderogeology using integrated electrical geophsics., Geophysics, 67(2), 365–378, doi:10.1190/1.1468597, 2002.

Smith, R. C. and Sjorgen, D. B.: An evaluation of electrical resistivity imaging (ERI) in Quaternary sediments, southern Alberta, Canada, Geosphere, 2(6), 287–298, 2006.

Soil Classification Working Group, Soil classification a taxonomic system for South Africa, Memoirs on the Agricultural Natural Resources of South Africa Ed., Memoirs on the Agricultural Natural Resources of South Africa No. 15., SIRI, D.A.T.S., Pretoria, 1991.

Tongway, D. J. and Hindley, N. L. (eds.): Landscape Function Analysis: Procedures for monitoring and assessing landscapes, CSIRO Australia, ISBN-0-9751783-0-X, 2004.

Tooth, S. and McCarthy, T. S.: Wetlands in drylands: geomorphological and sedimentological characteristics, with emphasis on examples from Southern Africa, Prog. Phys. Geog. 31(1), 3–41, 2007.

Uhlenbrook, S., Wenninger, J., and Lorentz, S.: What happens after the catchment caught the storm? Hydrological processes at the small, semi-arid Weatherley catchment, South-Africa, Adv. Geosci., 2, 237–241, doi:10.5194/adgeo-2-237-2005, 2005.

Wenninger, J., Uhlenbrook, S., Lorentz, S., and Leibundgut, C.: Identification of runoff generation processes using combined hydrometric, tracer and geophysical methods in a headwater catchment in South Africa, Hydrolog. Sci. J., 53(1), 65–80, 2008.

5 THE HYDRODYNAMIC RESPONSE OF A SEMI-ARID HEADWATER WETLAND TO TECHNICAL REHABILITATION INTERVENTIONS

E.S. Riddell[1], S.A. Lorentz[1], D.C. Kotze[2].

[1] School of Bioresources Engineering and Environmental Hydrology, University of KwaZulu-Natal, Private Bag X01, Scottsville, Pietermaritzburg, 3209, South Africa

[2] Centre for Environment and Development, University of KwaZulu-Natal, Private Bag X01, Scottsville, Pietermaritzburg, 3209, South Africa

ABSTRACT

Loss of wetland extent continues to be documented as a significant problem and this is true for the headwaters of the Sand River system in the north-east of South Africa. Here wetlands are undergoing severe down-cutting by erosion gullies (dongas) leading to desiccation of the system and loss of viable substrate that is used for subsistence agriculture. The Manalana sub-catchment was the focus of an integrated wetland rehabilitation program between 2004-2009, a major focus of which was the stabilisation of such erosion gullies by large retaining structures. This study presents findings of a hydrological monitoring study of the shallow groundwaters to determine the wetland's hydrodynamic behaviours and the extent to which these had degraded as a result of erosion. Furthermore, whether technical rehabilitation could ameliorate any degradation in the wetland's hydrological condition was also assessed. The findings show that the wetland groundwater hydrology is strongly controlled by the distribution of clays within it, and the loss of these impacts severely on the systems hydrology. The installation of an impermeable buttress weir was able to restore these hydrodynamics as observed through the reversal of the hydraulic gradients between groundwater observation stations, but the precise placement of the structure was shown to be crucial for this effect. A downstream pervious gabion dam was also monitored for its effect on restoring the wetland's hydrology, but observed responses showed little change, and in fact the wetlands hydrology here remained intact, attributed to presence of a clay plug that had was saved from erosion by the placement of this structure.

Keywords: Wetlands, Rehabilitation, Phreatic surface, Piezometer, Aquitard

5.1 INTRODUCTION

Wetland loss through erosion and conversion to alternative land uses in South Africa is extensive, and within several major catchments of the country some 35-60% loss of wetland extent had been experienced (Dada *et al.*, 2008). This loss may have significant implications for streamflow regulation processes given that wetlands are thought to be important for base-flow augmentation and flood peak attenuation, although these are still poorly understood phenomena (e.g. Bullock & Acreman, 2003). Wetlands within the savanna biome of sub-Saharan Africa are well utilised due to the potential, if properly managed, for diverse crop productivity and an array of other direct and indirect benefits. A wetland's economic as well as hydrological value were recognised as key factors that engender the need for their management by integrated means (Scoones, 1991). Nevertheless, wetlands continue to play a crucial role in livelihood security for a large part of the rural South African population and are most often not stringently subject to 'best management practices' and adequate governance systems that facilitate sustainable use of these environmental resources (Kotze & Silima, 2003). Wetland degradation thus poses a serious threat to the country's water and livelihood sustaining resources.

'Wetland Rehabilitation' has recently been put forward, particularly within South Africa, as the process by which one seeks to re-establish ecological driving forces within part or the whole of a degraded wetland to recover former or desired ecosystem structure, function, biotic composition and/or ecosystem services (Grenfell *et al*., 2007). Since it is the hydroperiod, or seasonal pattern of wetland water levels which is the criterion that characterises each wetland type (Mitsch & Gosselink, 1993), it is this that needs to be restored when rehabilitating a wetland whose hydrological regime has been altered. It is the hydrodynamics, or the ability of water to do work, specifically the direction and force of flow (Brinson, 1993) that controls the water storage of the system, as well as allogenic factors such as climate that define the wetlands hydroperiod. Monitoring of a wetland's hydrodynamics, such as water table depths can reveal important insights into the likely response of wetland sites to changes in their contributing area as well as *in-situ* impacts whether they be natural or artificial (Gilman, 1994). Furthermore these approaches are useful for tracking the trajectory of restoration attempts to restore a wetland's hydrology (Moorhead, 2003). Monitoring the hydrodynamics of wetlands is also useful for quantifying the extent of wetland degradation, as has been characterised for communally used wetlands in Ethiopia (Conway & Dixon, 2000).

The study, initiated in 2005, was in response to the technical rehabilitation, on a larger scale, of erosion gullies which were deemed to be threatening the integrity of the wetlands within the headwaters of the Sand River system. The majority of these headwater catchments situated within the foothills of the Klein Drakensberg escarpment, provide considerable livelihood benefits for local communities in terms of wet and dry season agriculture. Un-wise cultivation practices by local land-users, such as the creation of deep drainage furrows, poor tillage, and poor vegetative cover are seen to be contributing in large part to the degradation of these systems. This is exacerbated by the huge demand for wetland agricultural space in this former 'homeland' area that was subject to enforced settlement (1960's onwards). This population pressure compounds the fact that the soils in these wetlands are inherently unstable, predominantly coarse sands, and in a region subject to very intense storm events. These wetlands are also assumed to be crucial for flow regulation (attenuation and augmentation) of the now degraded Sand River, the main tributary of the perennial Sabie River, serving the Kruger National Park (Pollard *et al.*, 2005). Furthermore, the development of the gully networks, or at the very least their continued movement, was deemed (Pollard *et al*., 2005) attributable to these un-wise cultivation practices that may well increase surface water discharges within the wetlands themselves. In addition, certain land-use practices within the contributing catchments such as overgrazing and densely populated housing including a dense network of hardened surfaces in the form of roads and pathways were also a contributing factor. Similar phenomena have been experienced with wetland processes and gully erosion associations in other degraded landscapes (e.g. Whitlow, 1989; McFarlane & Whitlow, 1991; McHugh *et al*, 2007).

Whilst there appears to be scant information in the academic literature surrounding hydrological restoration with respect to technical rehabilitation of eroded wetlands in general, there have been a few specific studies that allow for a certain degree of contextualisation. These have for the most part examined the hydrological response of temperate wetlands with organically rich soils to reversion of management practices such as blocking of drainage ditches. For instance, Patterson & Cooper (2007) showed that fen water tables could successfully be restored by rehabilitation (blocking) of road induced drainage ditches, which in this instance was ascribed to the raising of the mean water table in the fen during the post-rehabilitation period and the concomitant recovery of peatland associated plant species in following seasons. Meanwhile Price *et al* (2003) suggested that degraded mined peatlands do not recover well given the degradation of subsurface *sphagnum*. However blocking of drainage ditches would lead to stabilisation of the peatlands water balance, but it would require several years to allow for the

total recovery of the peatland due to *sphagnum* recolonisation. Nevertheless, Price *et al* (2003) explored the water table drawdown phenomena around drainage ditches through a simple unpublished model relating the rate of drawdown to the conductivity (*K*) and specific yield (*Sy*) of peat, and showed that water table drawdown by drainage ditches was relatively modest based on the values of *K* and *Sy* for their peat system. Similar models have been used such as DITCH to explore the possibility or re-flooding wetland sites in the UK by managing ditch water levels. However limitations were found in the approach due to vertical and horizontal heterogeneities in *K* and *Sy*, which do not necessarily transcribe to successful management of water levels in the centre of drained fields. (Armstrong, 2000; Gavin, 2003).

The attention to specific responses of wetlands to technical rehabilitation by channel control structures has received very little attention, however Debano & Hansen (1989) and Schmidt & Debano (1990) showed through various catchment studies in the south-western United States that the inclusion of gully check dams were not only able to trap sediment but also raise water tables in desiccated riparian channel surroundings, with the effect of re-establishing lost riparian vegetation.

This manuscript presents findings from a monitoring study characterising the hydrological response to technical rehabilitation of one particular wetland which had been severely eroded by gully incisions (dongas). This is necessary since erosion, consequent wetland desiccation, and loss of ecosystem services are considerable problems that need to remedied in the Sand River catchment, as these wetlands support the local population through being a subsistence cultivation resource.

5.2 METHODS

The Manalana catchment (Figure 5.1) comprises densely populated rural housing with wetland and dryland cropping areas, as well as a dense network of roads and pathways. The dominant geology is granite, with doleritic dykes running parallel to the orientation of the catchment drainage. The catchment is also characterised by large erosion scars on its hillsides in addition to those erosion gullies within the wetland itself. The catchment comprises heavily grazed lowveld sour bushveld grassland (Acocks, 1988) and thicket. The natural wetland vegetation is dominated by *Phragmites mauritianus* in areas that are not being cultivated and commonly re-

colonizes abandoned cultivated plots fairly rapidly. The wetland itself is predominantly an unchannelled valley bottom wetland, although a distinct channel is now observed downstream of the central gully head. The wetland itself is generally of a coarse sand matrix, with lower clay content than the surrounding interfluves, although this sand overlies a deep clay horizon below ~2 m deep. The mean annual precipitation for the catchment has been derived from the nearest long term dataset, at the Wales rain gauge (1904-2000) some 2.3 km away, at 1075 mm a^{-1}, which is strongly seasonal, falling mainly between October and March (hence hydrological years, HY, run October-September).

The rehabilitation of the wetlands in the Manalana sub-catchment (Figure 5.2) adjacent to the village of Motlamogatsane (formerly Craigieburn) included the installation of an impervious buttress weir (including a 2 m keyed in heel at the gully floor plus 3 m freeboard to the spillway) and a pervious gabion dam (30 m wide, with 5.3 m deep spillway including 3.3 m of freeboard) during the latter half of 2006, the western and central gully head in Figure 2 respectively. The two stages of installation of the buttress weir are discussed in the results.

Hydrological monitoring of the wetland catchment was undertaken with a network of groundwater piezometers and soil moisture tensiometers with up to three of each installed at various depths. This was initiated at the onset of the rains in October 2005, the location of those monitoring stations relevant to this document are displayed in Figure 5.2. The piezometer plastic tubing (53 mm inside diameter) had a 300 mm slotted interface with the wetland substrate at their installation depths in which 1mm openings were spaced every 6 mm. The annulus between the piezometer tube and augured hole was screened with 10 mm of coarse sand and then the annulus was backfilled with the original wetland substrate.

Piezometers were regularly dip-read and in some cases automated with differential pressure transducers. The automated piezometers are recorded in accordance with soil moisture tensiometers on a 12-minute time step using a University of KwaZulu-Natal (SBEEH-UKZN) and Hobo® timing board and logger system. The use of the Electrical Resistivity Tomography (ERT) technique was used to delineate sub-surface geomorphic features, using an ABEM™ SAS1000 Terrameter.

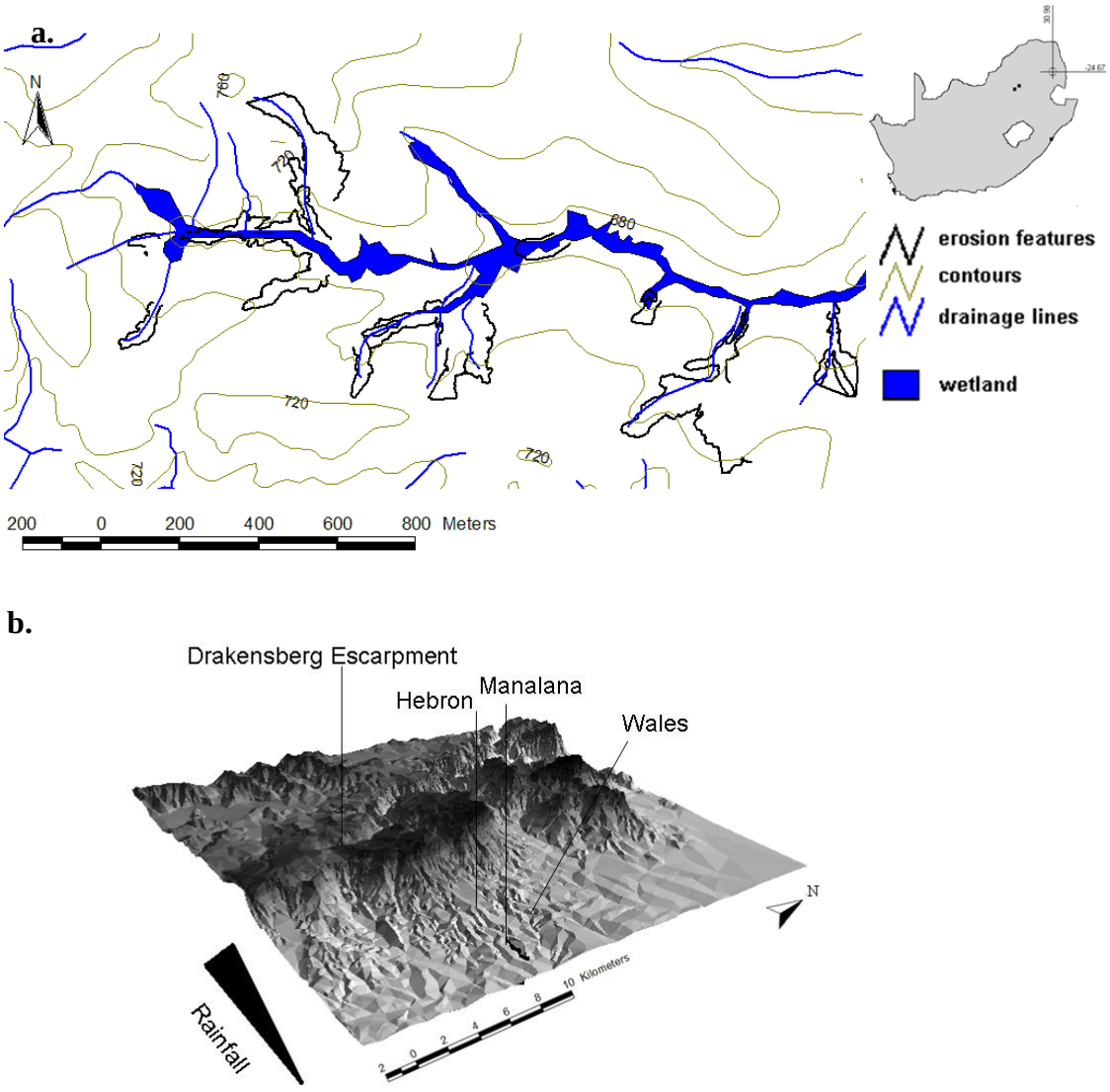

Figure 5.1: The Manalana sub-catchment of the Sand River and its position within South Africa (a), and its location in proximity to the northern Drakensberg Escarpment and rainfall gauging stations (b).

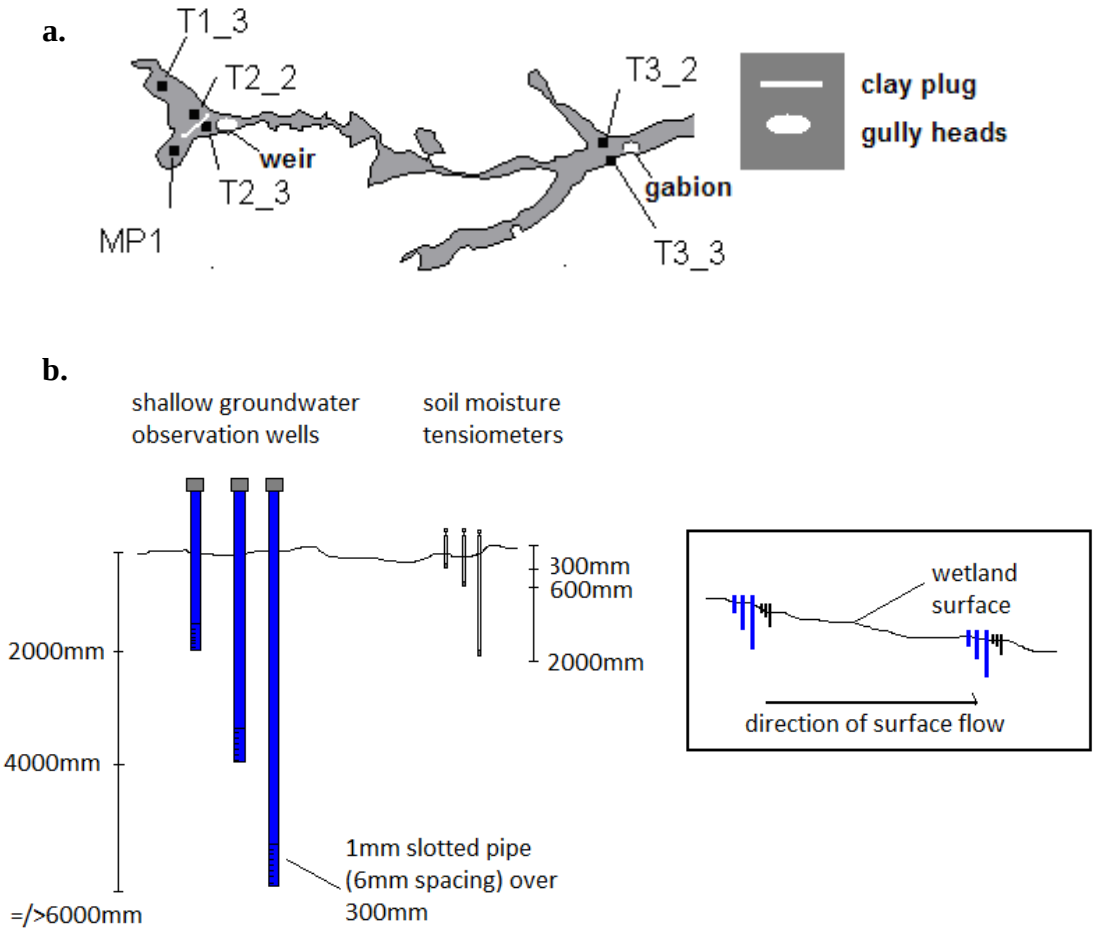

Figure 5.2: Location of monitoring stations at the headward end of the Manalana wetland (a), typical piezometer well nest installation (b).

Hydraulic conductivities of the matrix in which the piezometers were installed were estimated using slug tests, which requires the near instantaneous removal of a known volume of water using a 2 ℓ bailer from the piezometer well and measuring the water table recovery over time. Estimates of conductivity were determined using the method of Bouwer & Rice (1976) in the form:

$$K = \frac{r_c^2 \ln(R_e / r_w)}{2L} \frac{1}{t} \ln \frac{y_0}{y_t} \tag{5.1}$$

where: K is the hydraulic conductivity of the aquifer, L is the height of the open screen portion of the piezometer at its interface with the wetland matrix, y is the vertical distance between

water level in the piezometer at any time *t* and that within the aquifer at equilibrium at time *0*, where *y* can be at any depth below the surface at the time of measurement. R_e is the effective radius over which *y* is dissipated estimated using known values of piezometer depth (H) and depth to the base of an unconfined aquifer (D, assumed to be 15000 mm here) and empirical look up tables for dimensionless coefficients describing the geometry of the aquifer (See Bouwer & Rice, 1976 for further explanation). r_w is the horizontal radius between the centre of the piezometer and the aquifer (plus piezometer casing and screening material). r_c is the inside radius of each of the piezometer casings.

5.3 RESULTS

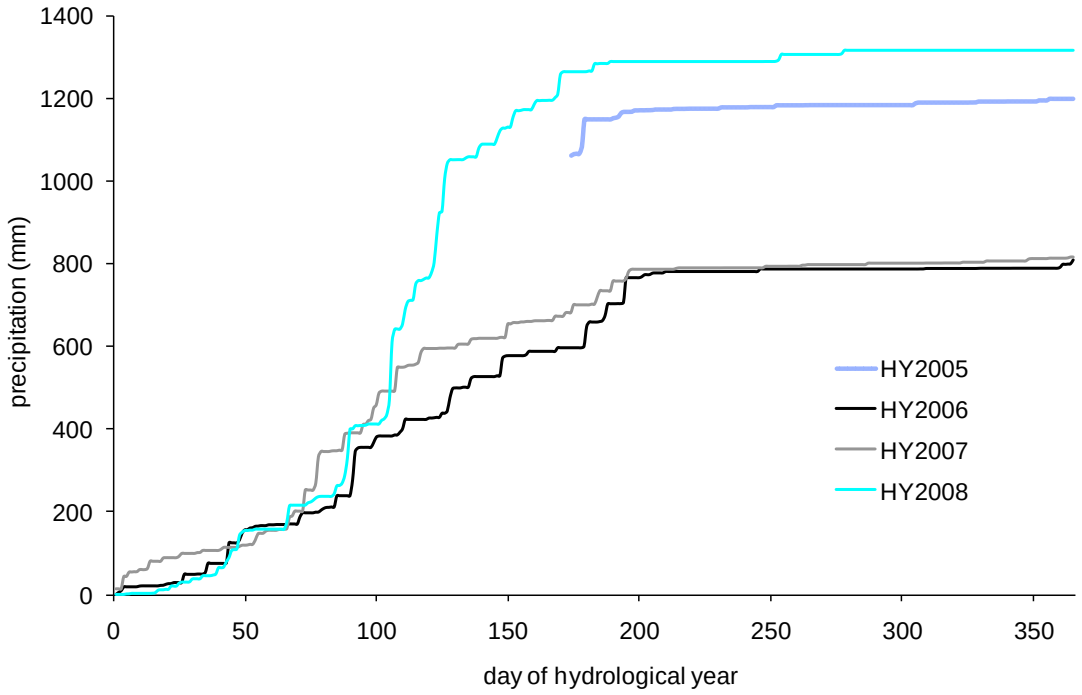

Figure 5.3: Cumulative rainfall plot for four hydrological years of monitoring (HY2005 estimated from on-site manual rain-gauge, following day 174 automated data supplemented the record).

Collection of rainfall data within the Manalana catchment itself commenced at the start of October 2005, and allows for examination of inter-annual differences in rainfall regime over the study period (Figure 3). It is quite apparent that HY2005 and HY2008 were relatively wet, and characterised by intense rainfall events as noted by the sharp increases in accumulative

precipitation. Meanwhile HY2006 and HY2007 were relatively dry with approximately a third less volume of rainfall than HY2005 and HY2008.

5.3.1 Initial hydrodynamic behaviour

The initial observation of the wetland's hydrodynamics during HY2005 came soon after the installation of piezometers at different levels in the wetland substrate and shortly after the onset of heavy rains in early December 2005. Figure 5.4 displays the piezometric heads as observed in three piezometers at location T2_2 between October 2005 and April 2006. After the installation of the three piezometers, shallow groundwater levels declined during early October in the 4000 mm piezometer, whilst the deeper 6000 mm and shallow 2000 mm piezometers remained dry. Thereafter there was a steady recharge leading to elevated piezometric head reflected in the 4000 mm piezometer through to March 2006. Meanwhile, piezometric heads appeared in the remaining piezometers in early January 2006 after significant precipitation events, and these were maintained throughout the rest of the rain season. Three distinct phenomena were therefore highlighted by this observation first the wetland seems to display piezometric head stratification, whereby possible shallow seasonal water tables overlay lower permeability horizons in the subsurface. These in turn overlay deeper recharging water tables. The cause of this phenomenon was revealed during soil characterizations in the winter months of 2006. A vertical series of clay horizons were identified in the wetland profiles. These horizons form clay aquitards amongst the coarse sandy matrix dominating the wetland (Figure 5.5). Second, the wetland also displays an upward recharging effect within deeper piezometers, since the piezometric head observed in the 4000 mm piezometer exceeds the elevation of the piezometric head in the 2000 mm piezometer during March 2006, suggesting that it exists within a (semi-) confined aquifer system and is subject to artesian pressures. Finally, it appears that a threshold condition is required to recharge a deeper groundwater store, as noted by the appearance of a piezometric head in the 6000 mm piezometer following a rapid elevation of the piezometric head in the 4000 mm piezometer in early January 2006 (the discontinuity in data for the 4000 mm piezometer is due to the exceeding of the sensor range), either from the confined aquifer above or from some other mechanism in the catchment.

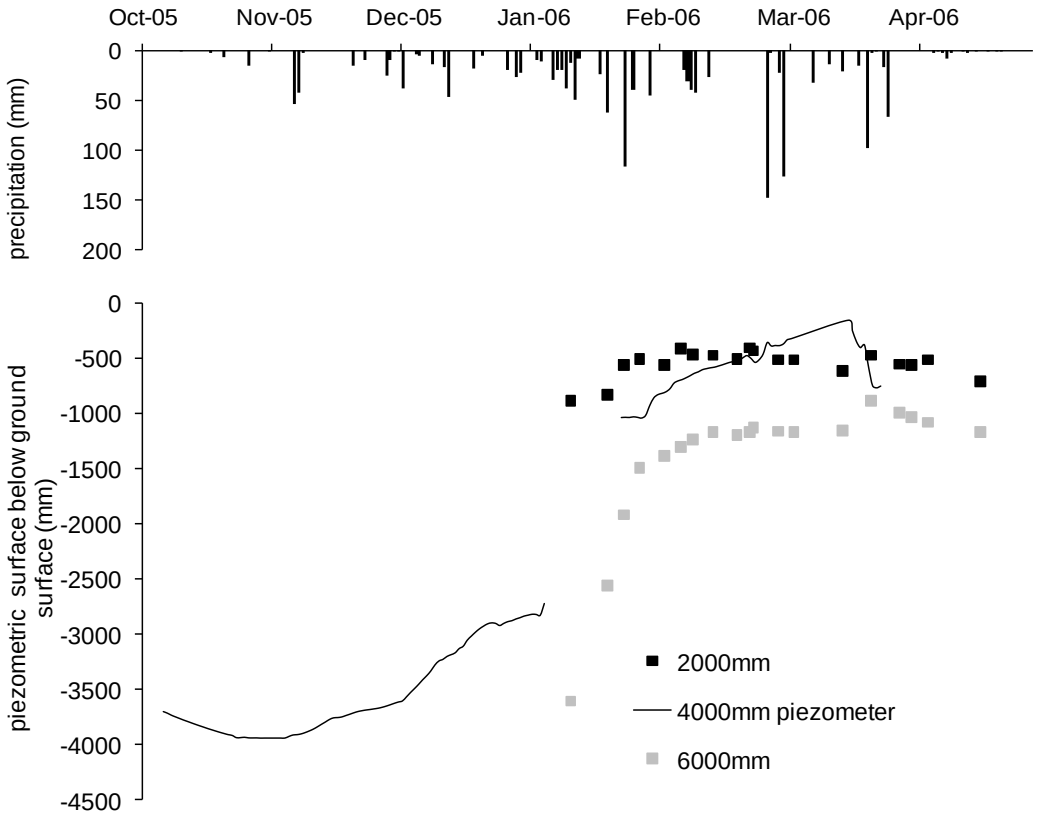

Figure 5.4: Piezometric heads at T2_2 during HY2005

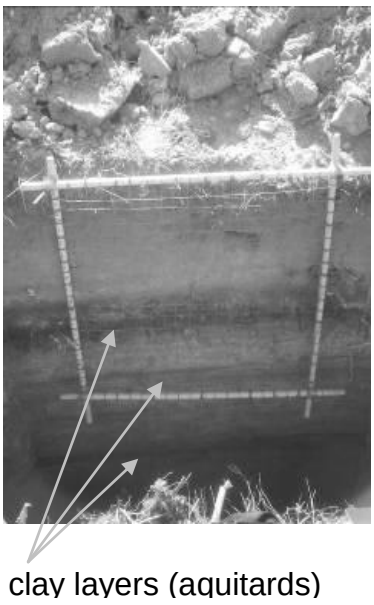

Figure 5.5: Clay aquitards identified in the wetland matrix during soil characterisation.

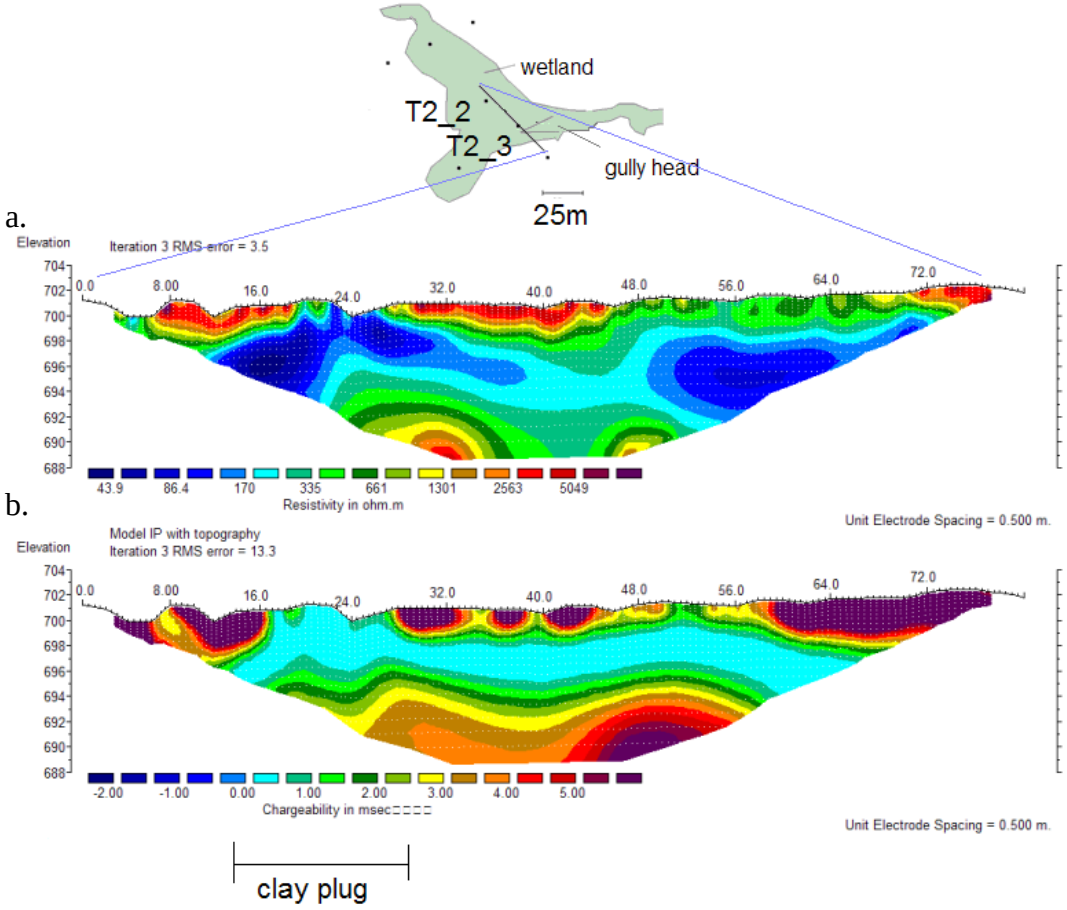

Figure 5.6: ERT (a) and IP (b) survey of longitudinal transect through stations T2_2 and T2_3.

5.3.2 Geophysical characterisations

In addition to the lateral clay deposits in the wetland, it had been postulated by geomorphologists (Ellery & Pollard *pers com*) prior to rehabilitation that moisture is retained within this sandy and rather hydraulically conductive wetland substrate by zones of finer sediment, or in other words vertical clay sub-terrainean barriers termed 'clay plugs'. This has been examined over the course of the study, and Figure 5.6 displays examination of the clay plug that was first identified through geophysical analysis in 2006. The use of the geophysical technique 2-dimensional electrical resistivity (ERT) and induced polarisation (IP) identified one such clay plug that was threatened by any further advance upstream of the erosion gully (the true characterisation and ground truthing of this geomorphic feature is described in a parallel manuscript by Riddell., *et al*, Chapter 7). Here zones of low resistivity material (0-100 ohms) correspond to the resistance range of clays in the absence of groundwater, similarly the high

chargeability bands (chargeability time decreases with increasing capacitance) in the lower diagram correspond to the capacitance range of fine clays. It had been noted during the initial year of monitoring that the hydrodynamic behaviour of the wetland was markedly different upstream and downstream of this clay plug (Riddell *et al.*, 2007). This is demonstrated in Figure 5.7 where it is the apparent large fluctuations seen in the shallow phreatic surfaces at T2_3 which contrast strongly with the lower amplitude fluctuations seen in the corresponding piezometers further upstream (T1_3 and T2_2). This suggests a hydraulic drawdown through free drainage within the vicinity of T2_3 and/or a buffering effect, such as by a clay plug, somewhere between T2_3 and T2_2 (the clay-plug is hypothetically shown in Figure 5.2). Also of note in Figure 5.6 is the distinct horizontal band of high chargeability material along the length of transect between 694-697 m.asl, a significant clay aquitard decoupling surface materials from deeper materials.

Figure 5.8 displays a longitudinal ERT cross section of the erosion gully and the position of the installed buttress weir, the descent into the gully occurs at chainage -35 m along the ERT transect. Using the apparent resistivity ranges for earth materials of Todd (1990) and Sharma (2008), where approximate resistivity values range between 10^0 - 10^2 ohm.m, 10^1 – 10^3 ohm.m and 10^0 – 10^2 ohm.m for clay, sand and saprolitic materials respectively. Firstly, one observes a low resistance material (blue) to the left of the image. This corresponds to clay materials as just described, whilst the materials >100 ohms correspond to sands as well as felsic saprolitic intrusions, which form the vertical bands of high resistivity material at -14 m and 27 m. This effectively reveals that the wetland certainly at the location revealed in the ERT image, overlies a series of semi-confined aquifers at depth (i.e. the disjointed blue zones of Figure 5.8). Of particular note therefore is the positioning of the buttress weir (adjacent to the headcut) in close proximity to the intruding bedrock material.

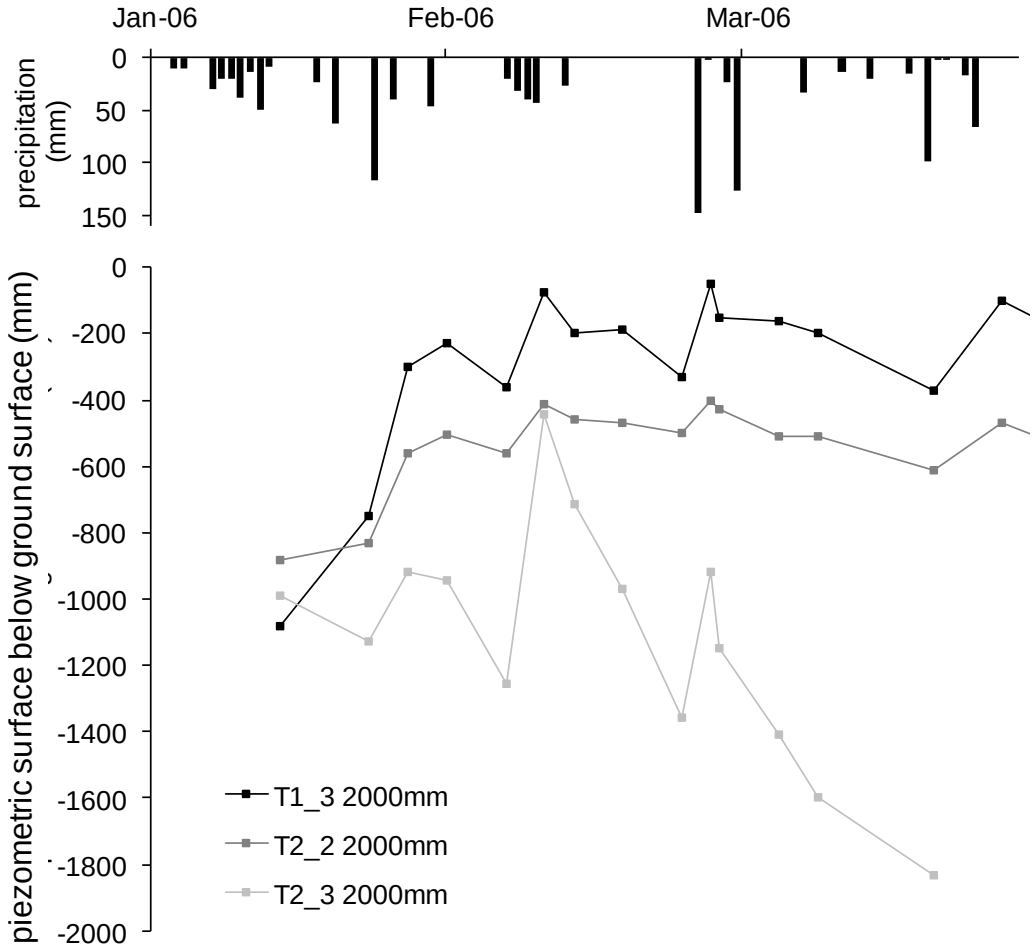

Figure 5.7: Shallow piezometric head behaviours January to April during HY2005.

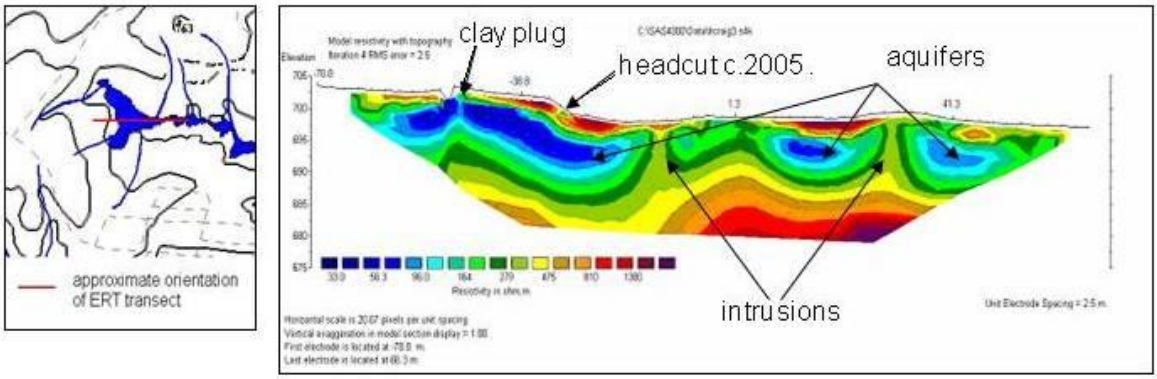

Figure 5.8: ERT longitudinal section through the erosion gully (May 2005).

5.3.3 Hydrodynamic response to rehabilitation

Table 5.1 summarises the accumulative rainfall from the beginning of the hydrological year to dates at which various aspects of the buttress weir installation were implemented during HY2006 and their equivalent dates in pre- and proceeding hydrological years. One notes the relative similarity in rainfall leading up to the completion of the buttress weir heel at day 81 for HY2005, 2006 and 2008, and large difference in cumulative rainfall at the closure of the weirs spillway between HY2005, 2008 and HY2006, 2007.

Table 5.1: Accumulative rainfall in the Manalana catchment for stages of construction of the buttress weir by equivalent day of year for the four hydrological years of monitoring which each start at 1st October (* year structure was actually put in place).

		day of year	HY2005	HY2006*	HY2007	HY2008
heel start	05-Dec	66	162.8	169.3	159.4	175.5
heel complete	20-Dec	81	222.8	210.6	345.8	237.1
slab	05-Feb	128	569.0	475.5	596.6	1050.5
spillway shut	23-Mar	174	1063.0	597.0	682.5	1263.4

Figure 5.9a displays the longitudinal topography of the Manalana wetland with the section of down-cutting by the erosion gully and the relative position of the buttress weir across the erosion gully and keyed in to 2 m below the gully floor. The aim of this structure was first to prevent any further sediment movement out of the wetland by way of the gully channel, by creating an area of ponded back-water behind it. A secondary effect would also possibly lead to a buffering of the seasonal hydraulic drawdown adjacent to the erosion gully. Furthermore it may then facilitate vertical recharge to the deeper groundwater store, and as such it is proposed to lead to a restoration of the hydrodynamic regime of the wetland. The initial season observations, HY2005 effectively provides evidence for a degraded hydrological state from which observations in subsequent years following rehabilitation would allow for the assessment of hydrodynamic response to technical rehabilitation. The HY2006 season

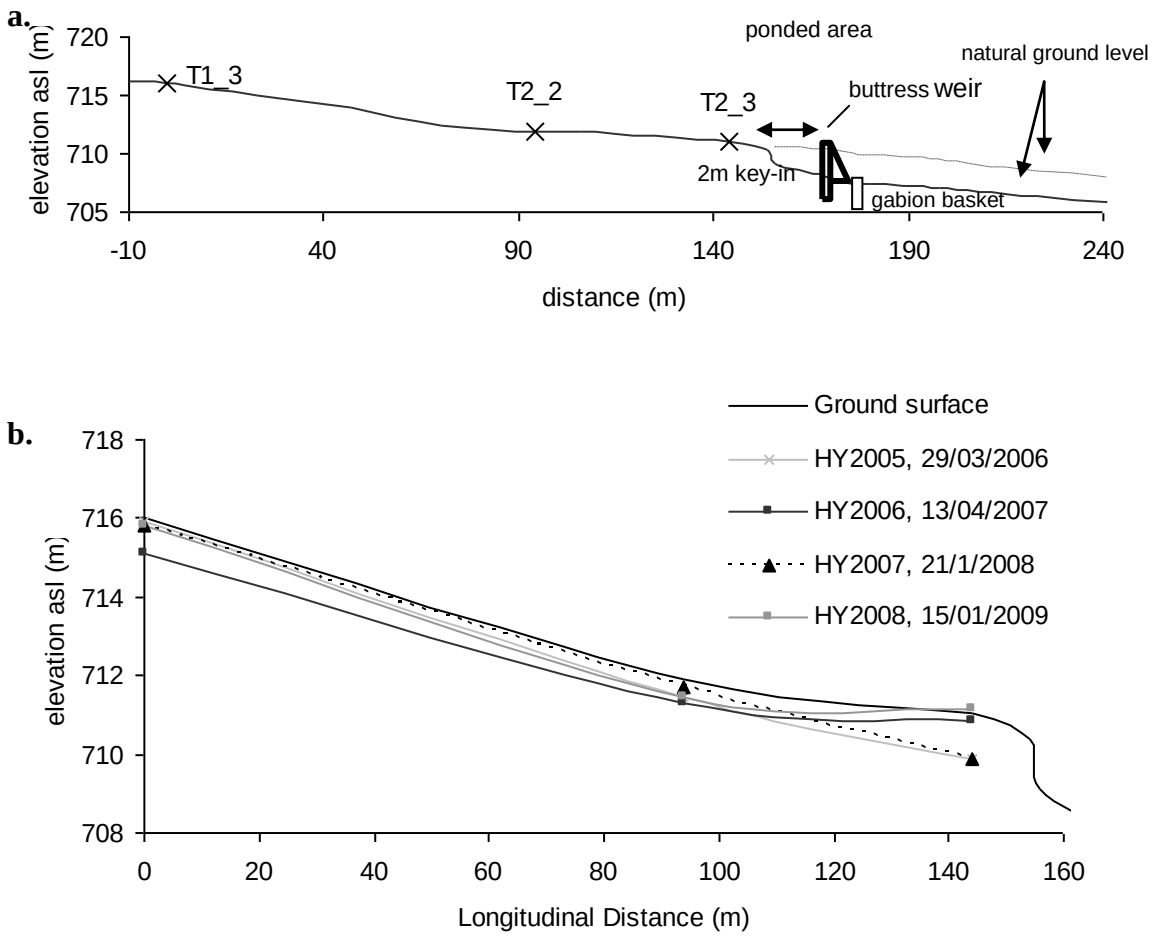

Figure 5.9: Longitudinal topography of the Manalana wetland (a), maximum seasonal (perched) water table elevations (b).

represents data during and immediately following rehabilitation (which was initiated in November 2006). During the HY2007 season erosion processes undermined the structure and prevented the weir from buffering any wetland discharges at the surface and near sub-surface. The HY2008 season represents data where the erosion problems had been remedied and the weir was doing its job as intended, at least geomorphologically speaking, for the duration. Figure 5.9b then displays the initial observed effect of this rehabilitation structure, in which again the longitudinal topography is displayed along with the maximal piezometric head elevations (or minimum depths) experienced during HY2005, HY2006, HY2007 and HY2008

wet seasons. It is important to note here that the HY2006 season was considerably drier than the previous year (recalling Figure 5.3), and during this year where the rehabilitation was implemented the piezometric head rose to a greater elevation than the wetter HY2005. Also in Figure 5.9b the perched (seasonal) piezometric head did not rise as close to the surface in the second year after rehabilitation where erosion had undermined the structure (HY2007). Additionally, in the latest season following successful intervention (HY2008), the perched piezometric head had a similar elevation as the HY2005 season and adjacent to the weir it was dominantly near the ground surface.

Closer examination of the initial response of the wetland hydrodynamics to the buttress weir installation are revealed in Figure 5.10 and 5.11. In both cases the phases of construction are displayed, whereby the 2 m heel was constructed first followed by the weir itself with key and wing walls. The most noticeable aspect in Figure 5.10 is the steady rise and fall of the seasonal piezometric heads in the pre-rehabilitation year in response to precipitation inputs. Meanwhile, following the construction of the weir and in particular its full completion it had appeared to create a rapid seasonal phreatic surface rise which is observed all the way up the wetland up to station T1_3 in response to some 50-60 mm events towards the end of March 2007. Furthermore, the sequence of head differences is a reversal of the previous year's hydrodynamic behaviour in the shallow subsurface (within 2000 mm). For instance the piezometric head at T2_3 is shallower than at T1_3 in the HY2005 hydrological year. More significantly, however, it is the permanency of these two piezometric heads that is also important. The T2_3 piezometric head is short lived in the HY2005 season, observed only between January – April 2006, meanwhile the T1_3 piezometric head resides for a much longer period between December 2005 – May 2006. Since the T2_3 piezometric head is further downstream it would be expected that the phreatic surface would exist for longer due to a greater contributing area of inflow from upstream, however what occurs here is a hydraulic drawdown of the seasonal water adjacent to the active gully head, effectively a 'leakage' from the system. Meanwhile the expected order has been restored in the HY2006 season. The T2_3 piezometric head exists for longer and now in closer proximity to the wetland surface than that at T1_3 due to the 'plugging' of the system at the weir.

Figure 5.11 reveals the process responses of the wetland at the point of T2_3 to the new buttress weir that had been installed during HY2006. Firstly the sharp rise in the piezometric head in the deepest piezometer (7000 mm) and appearance of piezometric heads in the shallower piezometers (2000 and 4000 mm) after the construction of the heel. The fact that the deeper

piezometer expresses a head similar to the shallower piezometers suggests the upward (artesian) movement of water at that region, possibly as a result of a (semi-) confining aquiclude of subsurface material between the 4000 mm and 7000 mm piezometers. This is therefore similar to that observed at T2_2 in Figure 5.4 for HY2005. Thereafter a downward movement of water occurs for the remainder of January 2007 due to lower heads expressed at each successively deeper piezometer. The piezometric head in both the 2000 mm and 4000 mm piezometers had disappeared by the end of February 2007 and then reappeared following large rainfall events at the end of March, in which the 2000 mm piezometer experiences a very rapid rise in head followed by a decline, whilst the 4000 mm piezometer has a steady reappearance and recharge in head. These are then followed by a much slower increase in piezometric head in the 7000 mm piezometer throughout April 2007, although the artesian pressures here are less pronounced than earlier in the season. The behaviours of the two shallow piezometers compared to the deepest at T2_3 suggest that vertical movement of water is not totally disconnected from depths greater >4000 mm, but rather the wetland operates largely as an unconfined aquifer system in the shallow sub-surface overlying semi-confined aquifers at depth.

5.3.4 Hydrodynamics over 4 years

The piezometric head distributions for all the observation piezometers at the headward end of the Manalana wetland over the 4 years of monitoring are displayed in Figure 5.12 Examination of the behaviours at this temporal scale reveals some interesting contrasts amongst different locations in the wetland. For the most headward responses at T1_3 (Figure 5.12a), the elevated piezometric head is short- lived and is unconfined at least up to 4000 mm, as both piezometers show similar elevations. Interestingly the piezometric head here reaches winter (dry period) stable depth of around 2300 mm below the ground surface in most years, except that the dry period of 2008 there was some considerable drawdown of the piezometric head here to around -2900 mm. This

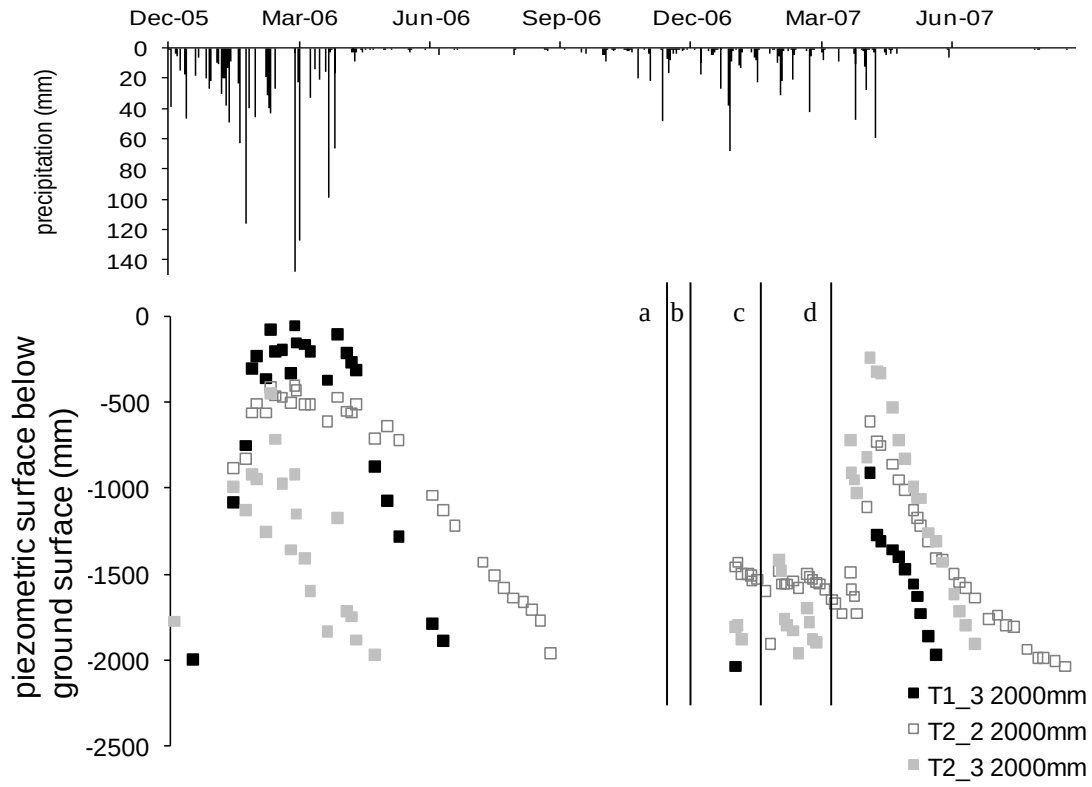

Figure 5.10: Initial responses in the piezometers to placement of heel and closure of structure ([a] commence heel installation, [b] finish heel, [c] lay buttress weir slab, [d] close spillway).

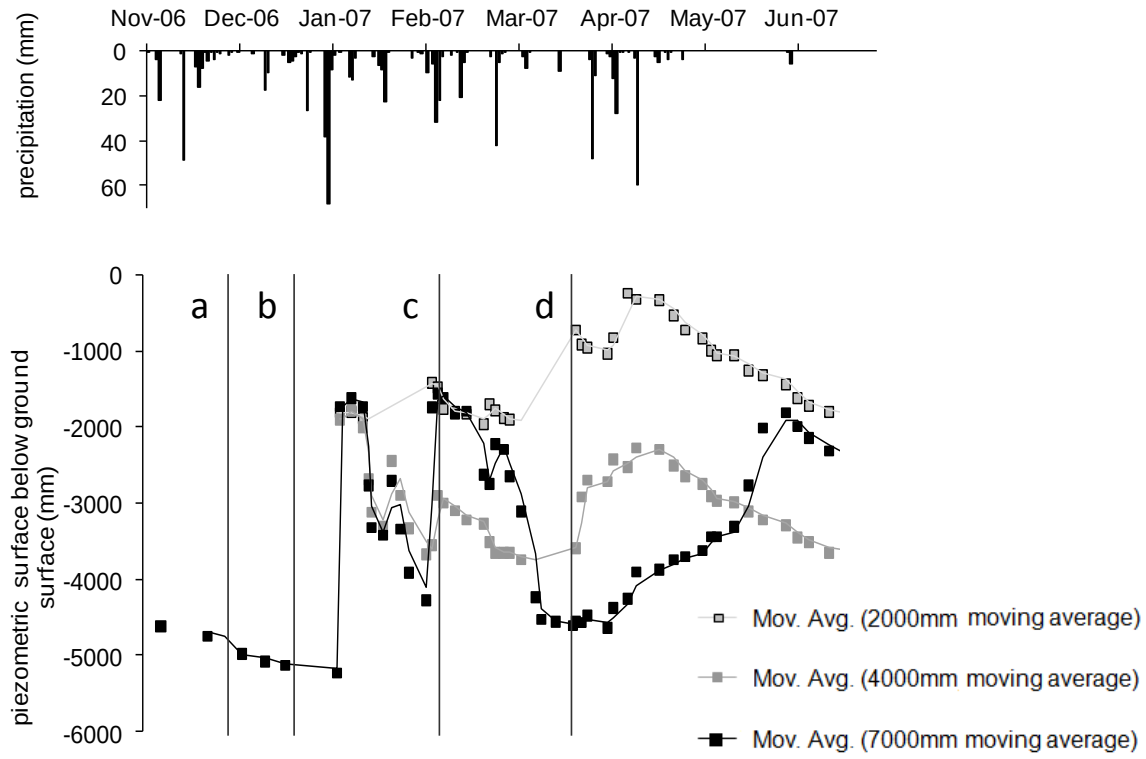

Figure 5.11: Initial response to placing of heel and closure of structure for the three piezometers at T2_3 ([a] commence heel installation, [b] finish heel, [c] lay buttress weir slab, [d] close spillway).

likely represents the effect of consecutive dry periods (i.e. preceding two seasons were relatively dry). Furthermore, this region has a very rapid response to precipitation inputs as the piezometric head elevates rapidly following the onset of rains. Within the core of the wetland at T2_2 (Figure 5.12b), as discussed previously, the groundwater are somewhat disconnected as is evident by their different elevations in piezometric head. Here there is a sharp response in all piezometers to the installation of the weir particularly the large event preceding it in March 2007. Meanwhile the following seasons HY2007 and HY2008 a change in the hydrodynamic behaviour in the 6000 mm piezometer is noted. Here the winter recession is observed during 2007, as in previous seasons, however, there is no recovery of this in the subsequent seasons. Despite this the piezometric heads observed in the shallower piezometers continue to respond as they had previously and in the winter of 2008, the piezometric surface effectively dropped below the 4000 mm depth which had not occurred in previous seasons. Also of interest is the closeness of responses in the 2000 mm and 4000 mm piezometer at this location. Observations

at T2_3 (Figure 5.12c) reveal the nature to which the installation of the weir induces a rapid change in the hydrodynamics of the wetland at this location. During the first season of monitoring, there was a very low head expressed deep within the wetland substrate (7000 mm piezometer), whilst the shallow 2000 mm and 4000 mm piezometers revealed their seasonal nature and possible connectivity as both displayed piezometric surfaces at similar elevations below the ground surface. Subsequently, following the initiation of rehabilitation, artesian pressures are reflected by the 7000 mm piezometer for the remainder of the period (except for the winter of 2008, when water was extracted from this piezometer for analysis), whilst only in HY2008 is there a return to the similarity of piezometric heads seen in the 2000 mm and 4000 mm piezometers. In the preceding two seasons, which, despite similar fluctuations, were of marked difference in terms of their expressed piezometric heads, possibly a reflection of saturation variabilities arising from large differences in seasonal rainfall Artesian pressures were again seen in the HY2008 season in the 7000 mm piezometer following an extraction of water from this well during winter. At MP1 the seasonal trends can quite clearly be seen (Figure 5.12d), with a steady decrease in the piezometric head from the wet HY2005 season to the dry HY2007 season. However, even in the wet HY2008 season, and following the rehabilitation the maximal expressions of head do not reach the same shallow depths as were observed during the HY2005.

Figure 5.13 shows the expressed piezometric heads further downstream adjacent to the other rehabilitation site where a large gabion dam was installed during late winter (June-September) 2006. In the piezometer at T3_2 which was installed to a depth of 2000 mm one observes an initial recovery of the shallow groundwater following its installation, this is repeated in early 2008 when water was abstracted from this piezometer. Particularly noteworthy is the extremely slow recovery of the head in the piezometer following abstraction. Clearly this is not due to rainfall since the expressed piezometric head at this location remains relatively stable throughout the entire monitoring period. Hence a material exists here with extremely low hydraulic conductivity, as explained by the very fine clays throughout the profile observed. Furthermore the piezometric head seems to be relatively stable here even during the dry season, with only a slight decline of some 200 mm during the dry winter of 2007. Meanwhile T3_3 also installed to 2000 mm and in a slightly upslope position than T3_2 again shows a relatively continuous piezometric surface, except for flashy periods during mid-summer coinciding with large rain events, from personal observation this site sits adjacent to a hillslope seep that feeds the wetland, through rapid lateral hillslope transfer (as discussed in complementary manuscript, Riddell & Lorentz *in review*, Chapter 6), which was not apparent during the installation. Both

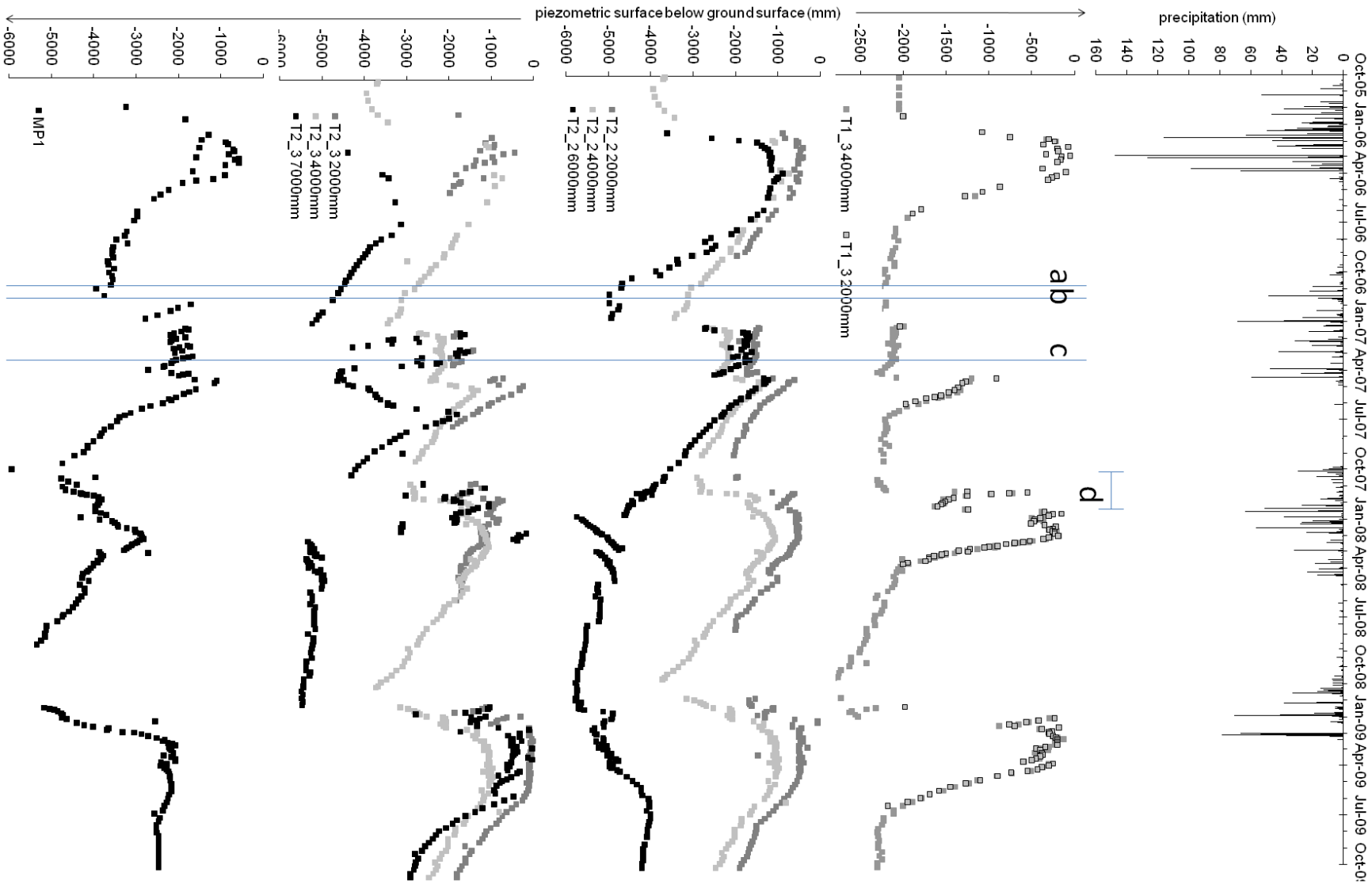

Figure 5.12: Piezometric head distribution over 4 monitoring seasons at all locations above the buttress weir ([a] commence heel installation, [b] finish heel, [c] close spillway, [d] erosion around weir).

sites are located at a position downstream that receives perennial water, whereas the upstream sites are very much in a seasonal zone.

5.3.5 Hydraulic Conductivity

K was determined for each of the piezometer wells upstream of the buttress weir, however since the conductivities in the majority of piezometers and in particular those deeper than 2000 mm were extremely low, repeated measurements were therefore not undertaken. Hence, the estimates derived are for single piezometer recovery readings where the Bouwer & Rice (1976) method was applied to the straight line portions of the recovery curve (Appendix iv). Figure 5.14 displays the final estimates for these piezometers (albeit without T3_3 since the phreatic surface was too low such that a bailer was inadequate to remove known volume of water) and it is quite apparent that the piezometers in the shallowest substrate have the highest conductivities, with the most headward piezometer at T1_3 having the greatest conductivity of all, whilst the shallow piezometer at T2_3 is in a more conductive substrate than the 2000 mm piezometer at T2_2. The exception is of course further downstream at T3_2 where even the shallow material has extremely low conductivity. There is also a trend that may be observed within this plot in that, the conductivity of the wetland substrate decreases considerably with depth to 4000 mm, after which it maintains a very low K of between 0.01 – 0.0001 mm/hr.

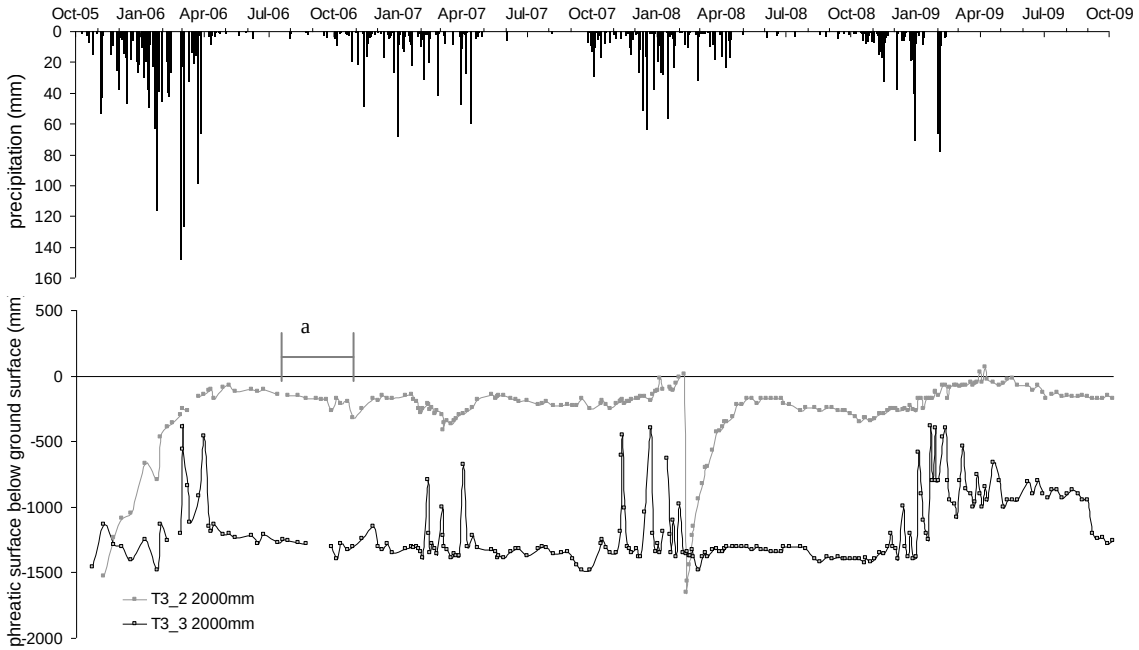

Figure 5.13: Piezometric head distributions over 4 monitoring seasons at the two sites adjacent to the gabion dam ([a] installation and completion of the gabion dam).

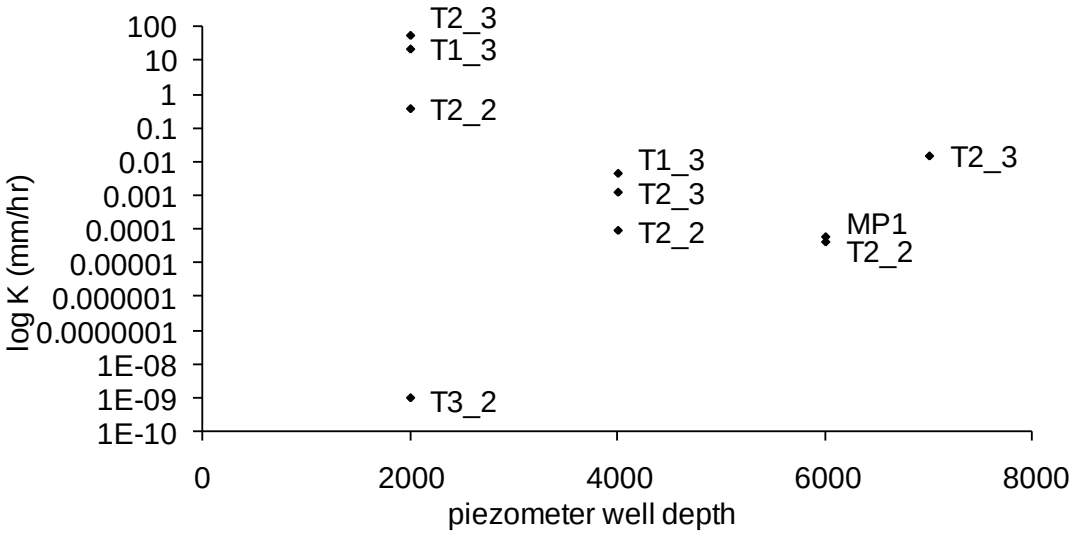

Figure 5.14: K estimates for piezometers within the Manalana wetland.

5.3.6 Hydraulic Gradients

Examination of the hydraulic gradients (*i*) observed between Piezometers at T2_3, in Figure 5.15, reveals how the hydraulics of the wetland switched quite markedly following the installation of the weir during HY2006 and in particular during the latest season HY2008, when the structure was fully functional. It is noticeable from Figure 5.15 that during the first year of monitoring *i* between the 2000 mm and 4000 mm well was virtually 0 and therefore largely static, whilst a positive gradient existed between 2000 mm and 7000 mm, as well as between the 4000 mm and 7000 mm piezometers implying vertical recharge from the shallow layers above. However the following two seasons, HY2005 and HY2006, *i* increased between 2000 mm and 4000 mm wells and *i* between the 4000 mm and 7000 mm wells reduced and became negative at the height of the rains. Most striking is the latter part of the season HY2008 where *i* in all instances became homogenised (i.e. no large fluctuations) and there seems to be a discharging effect in the shallower zone, for instance the positive *i* between the 2000 mm and 4000 mm piezometer, whilst a persistent negative *i* exists between the 4000 mm and 7000 mm piezometer indicating recharge contributions from elsewhere to the 7000mm depth and an upward flux between 7000 mm and 4000 mm at the buttress.

The observed *i* between the deepest piezometers in the system (Figure 5.16) are also noteworthy, although their magnitudes are much lower than those just described, there is a noticeable switching of hydraulic gradients. One may note the gradient of flow from both 6000

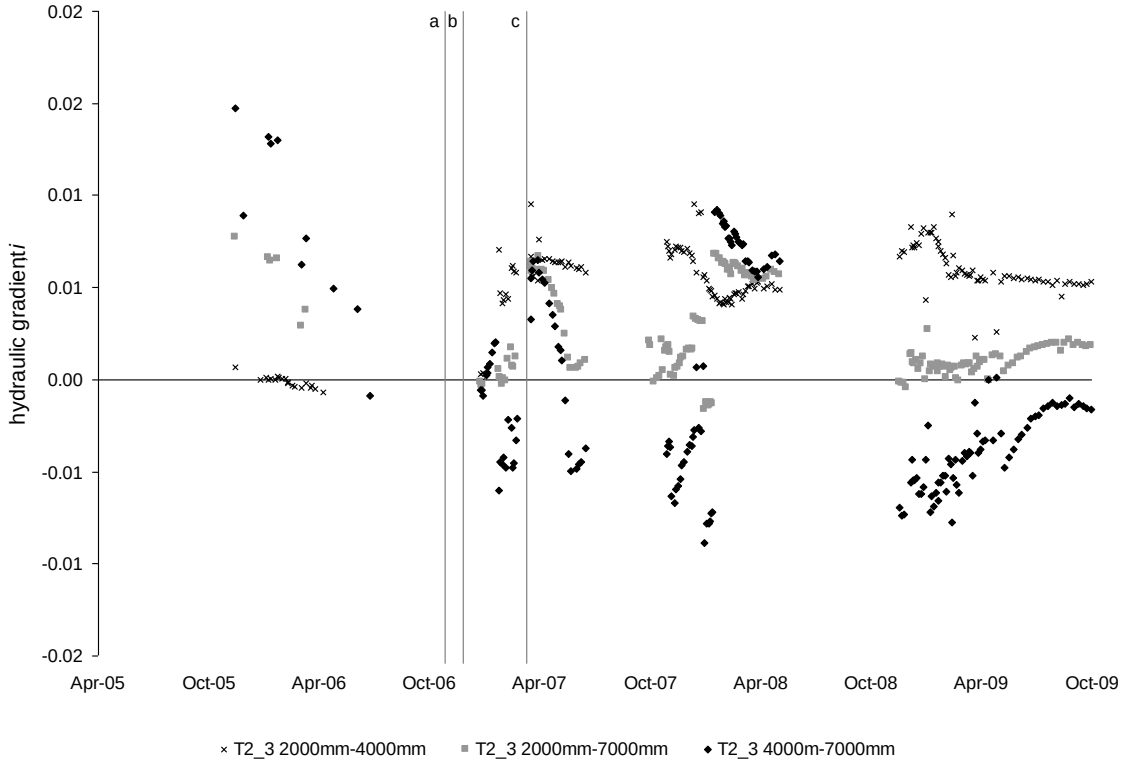

Figure 5.15: Hydraulic gradients as determined at T2_3 ([a] commence heel installation,[b] finish heel, [c] close spillway).

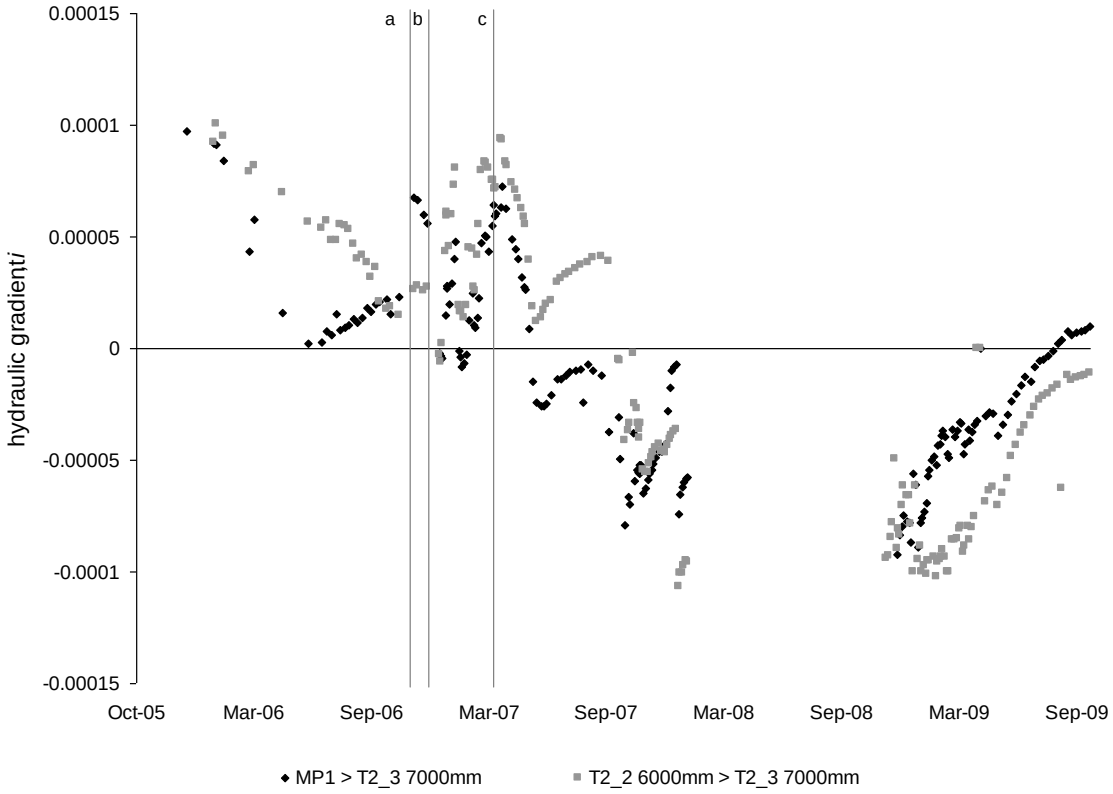

Figure 5.16: Hydraulic gradients as determined between the deepest Piezometers at MP1, T2_2 and T2_3 ([a] commence heel installation, [b] finish heel, [c] close spillway).

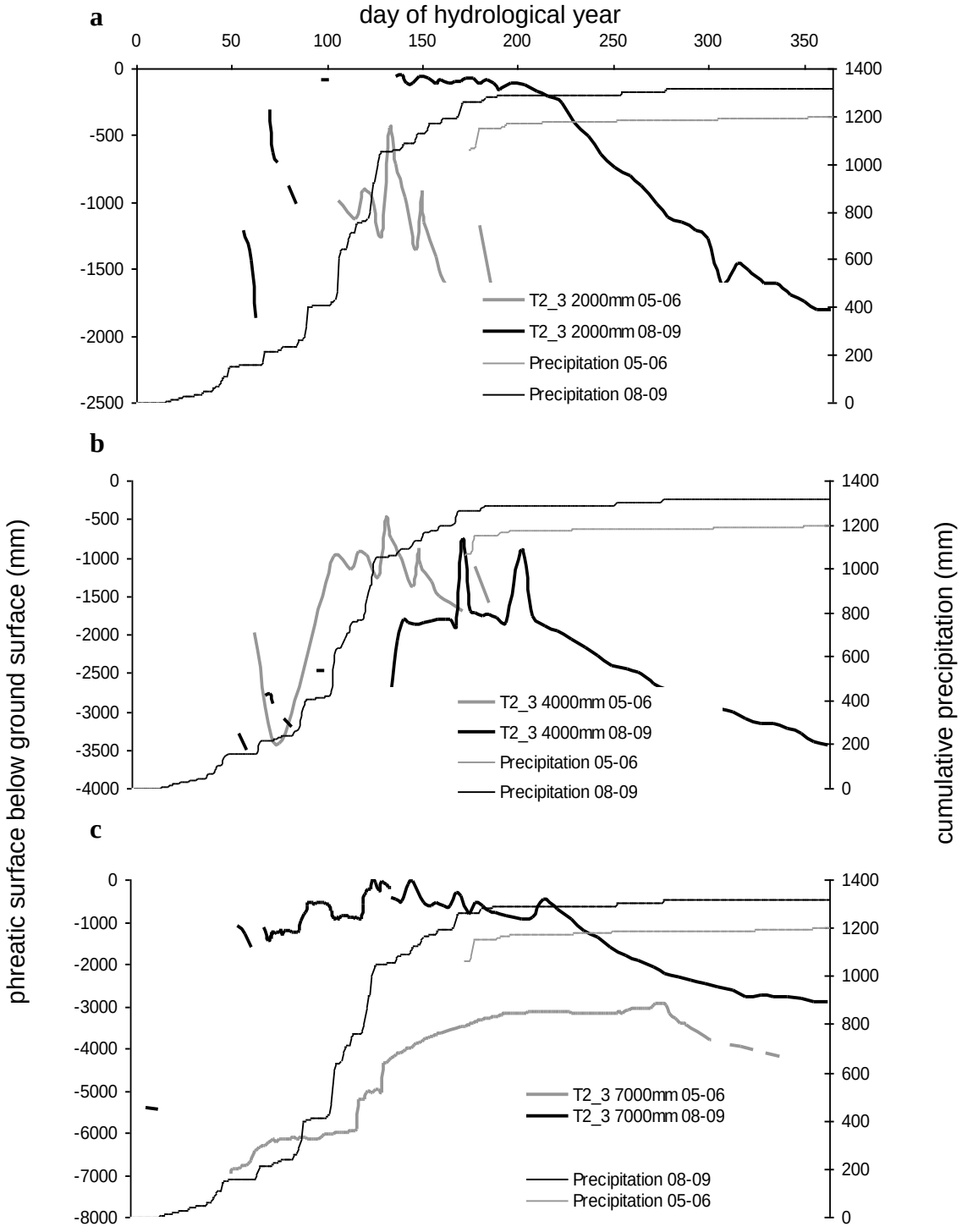

Figure 5.17: Examination of annual piezometric head responses at T2_3 for years with similar rainfall regimes pre- and post rehabilitation.

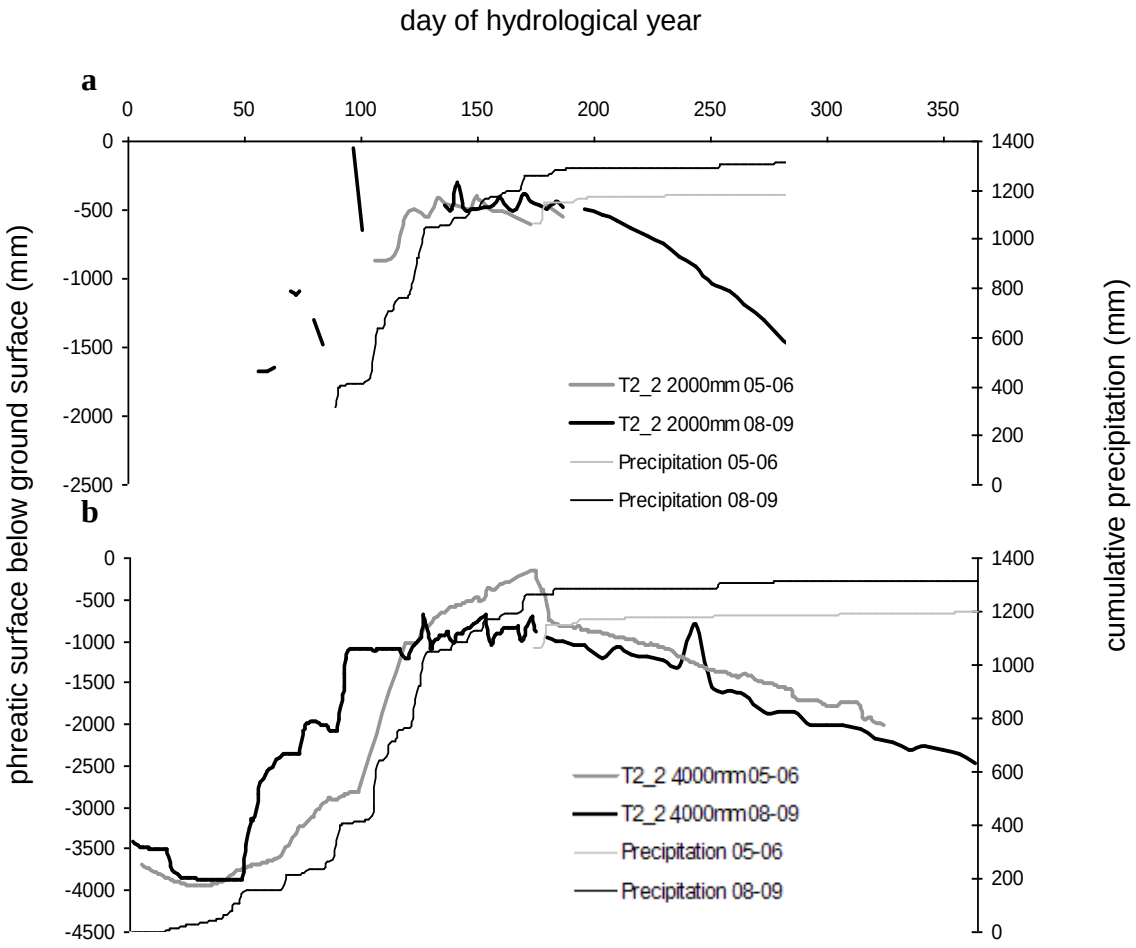

Figure 5.18: Examination of annual piezometric head responses at T2_2 for years with similar rainfall regimes, pre- and post rehabilitation.

mm piezometers at MP1 and T2_2 to T2_3, during the first season, HY2005. The hydraulic gradient in both cases reduced close to 0 during the winter of 2006, suggesting that a hydraulic head and consequent recharge from elsewhere in the catchment was also diminishing. This phenomenon continued into the following season, HY2006, until the installation of the weir between December 2006 and March 2007, following which the hydraulic gradient reversed, this was also a noticeably dryer season than the preceding one. The period between March – September 2008 the data is erroneous due to water abstractions from the piezometer wells and have therefore been excluded. Finally in the most recent season, HY2008 the hydraulic gradient remains in the reversed state with piezometric heads at T2_3 apparently greater at T2_3 than at either MP1 or T2_2.

5.3.7 Antecedent and seasonal effects

Examination of piezometric head behaviour within the Manalana wetland would not be complete without the contextual understanding of conditions within the system at the start of the hydrological year, in addition to a complete hydrological year before and after the rehabilitation intervention (i.e. where there were no failures or modifications to the structure). Figure 5.17 displays the piezometric head hydrodynamics at the T2_3 site adjacent to the erosion gully for two complete hydrological years with similar cumulative rainfall HY2005 and HY2008, the former year being that prior to rehabilitation and the latter where the rehabilitation structure remained intact. It is quite clear from Figure 5.17a that the hydrodynamic behaviour within the heads of the shallow piezometers of T2_3 during HY2005 were very erratic and short-lived, falling below the -2000 mm depth of the well early on into the dry season, beyond day 150. Meanwhile during HY2008 a piezometric head was observed here for short periods early on up to day 140, whereupon it had a relatively stable elevation close to the wetland surface, and, despite a winter drawdown a piezometric head was still recorded within this piezometer up to the start of the following hydrological year. A similar response is also observed for the piezometric head as recorded in the 4000 mm piezometer in Figure 5.17b, although here a piezometric surface appeared early on during HY2005, however it had ceased to be present by day 200, whereas during the HY2008 a piezometric surface was again observed throughout the year and never dropped below the 4000 mm piezometer well. Figure 5.17c reveals the very different nature of response at depth in the 7000 mm piezometer. Here one sees that the piezometric head during HY2008 appears very suddenly soon after day 50 and remains largely within 1000 mm of the wetland surface well into the winter months past day 200. By the end of HY2008, a piezometric head is still expressed here above -3000 mm depth. This contrasts strongly with HY2005 where the piezometric head in the 7000 mm well appears to gradually elevate early on during the season reaching an asymptote at approximately day 275 before receding once more.

Figure 5.18a displays the hydrodynamics of the piezometruc surface at T2_2 for the 2000 mm piezometer. Here one observes a short-lived piezometric surface during HY2005 having disappeared well before day 200 contrasting strongly with an expressed head of greater duration during HY2008 which only falls below the 2000 mm piezometer at approximately day 280. Interestingly, Figure 5.18b for the 4000 mm piezometer shows that the piezometric surfaces at this depth behave with great similarity with a gradual recharge in elevation early on during both hydrological years, there is also a steady decline into winter after the mid-summer asymptote, with both maintaining a presence above -3000 mm beyond day 300.

5.4 DISCUSSION

Initial hydrodynamic behaviours showed that the system has vertical recharge processes and that at depth the presence of semi-confined aquifers deeper within the wetland at times these yield artesian conditions. Recharge processes occur through the shallow subsurface via direct precipitation and localized infiltrating runoff. However, in deeper regions of the wetland below 4000 mm water is likely to also be percolating from shallower horizons but that also the behaviour of the piezometric surfaces at these depths suggests another mechanism in the form of recharge to the wetland at a larger scale, from the surrounding catchment or regional water table for example. Indications for this are the late appearance of a deep piezometric surface at T2_2 during the first year of monitoring and the permanent occurrence of water in the deepest piezometer at T1_3. Furthermore the artesian forces observed at T2_2 in the 4000 mm piezometer during this same season suggest that such large scale recharge processes also occur in shallower regions below 2000 mm. In essence therefore the vertical recharge processes suggest coupling to surface waters at shallow depth, whilst this becomes increasingly decoupled with depth in favour of coupling to broader groundwater sources in the catchment. The observations here imply a connection of the wetland to a dual aquifer system, similar to that identified for a dambo wetland system in Zambia (von der Heyden & New, 2003). Hence a shallow aquifer from the catchment soils and saprolites maintained the shallowest piezometric responses and the deeper and more permanent (perennial) piezometric surface was connected to underlying bedrock or in this case perhaps deeper saprolites, which are quite evident in exposed surfaces of deeply eroded areas within the surrounding interfluve. This of course has warranted further investigation using tracer techniques in the case of the Manalana wetland.

The ERT analysis also supports this notion of a shallow surface hydrology decoupled from a system at depth, as the results quite clearly portray a horizontal aquiclude. The *K* estimates possibly confirm this as we see a slight increase in the conductivity of the wetland material at piezometer depths below 4000 mm, whilst the 4000 mm material itself has an extremely low hydraulic conductivity. This warrants further assessment of the hydraulic conductivity of this wetland at such depths with a greater spatial sampling intensity. Whether this aquiclude system would have continued downstream in the same decoupled manner remains uncertain. However, the vertical intrusions observed downstream of the headcut in Figure 5.6 suggests that this would not have been the case. What does this say about the consequent impacts of the rehabilitation structures?

Figure 5.6 suggests also that the actual site selection of a rehabilitation structure and indeed the type of structure will certainly have an influence on the hydrologic regime of a wetland. This could for instance be due to introducing foreign materials (rehabilitation) coming into contact with materials that shape the hydrology of the system, such as an impermeable material adjacent to permeable materials and thus inducing preferential flow processes. The proximity of this structure to the vertical intrusion implies a sealing off of the wetland at the toe of the upstream portion (refer to Figures 5.1 & 5.2 noting the large erosion gully between the regions monitored) from the stream channel and stream bed that now exists where the wetland has been eroded due to gullying. Whereupon a deep groundwater discharge zone which likely seeped further downstream is now inducing recharge to the wetland from below. This would then explain the artesian phenomena observed at T2_3 following rehabilitation. Moreover this would reiterate the similar artesian phenomena observed at T2_2 prior to rehabilitation. There is no doubt that the placement of a deep 2 m heel plus 3 m freeboard on the buttress weir has had an effect in terms of changing the hydrology of the system from its eroded state, as shown by the shift in hydraulic gradients over the season and stark contrast between HY2005 and HY2008. Whether these hydraulic gradient shifts would have occurred had the structure been placed in an alternate location leads to speculation. However, the precise positioning of rehabilitation structures certainly needs to be considered when rehabilitating large systems where managing these systems for hydrology is deemed important. This should also be considered in catchments where many rehabilitation interventions are likely to take place where cumulative hydrological effects are most likely to be felt downstream. As Owen (1995) as well as Preston & Bedford (1988) proposes, evaluating the cumulative effects of wetland loss or modification on the landscape and catchment processes should be based on wetlands with various fluxes contributing to different types of water budget and their altered/unaltered role on stream flow processes. Although the precise role of differing wetland types in the hydrological cycle is still uncertain (e.g. Bullock & Acreman, 2003), the fact that the hydrology of wetland systems undoubtedly changes through erosion processes means that there are certain fundamental requirements for catchment rehabilitation through wetland rehabilitation. In cases such as the Sand River wetlands where there are a plethora of potential rehabilitation interventions, it necessitates the most appropriate method and precise deployment of the intervention in order to revert to wetland hydrological processes as close to the unaltered state as possible

Aside from the cumulative effects just discussed, there is also the issue of within-wetland variability. This study has quite clearly shown that different regions even within this comparatively small system yield differing hydrodynamic responses to rainfall inputs and throughflows, and this adds another layer of complexity to the two usually exclusive issues of

wise-use of and rehabilitation of wetlands suggesting the moniker ‘wise-rehabilitation’ of these heavily degraded systems. Dixon (2002) showed a similar scenario in the wetlands of the Illubabor Zone of Ethiopia, which were also used for subsistence agriculture derived from both natural and enforced re-settlement. Here different hydrological ‘micro-regions’ were also noted to exist within the systems in question, and these had different responses to the impacts of drainage and cultivation. However, Dixon (2002) concludes that despite the agronomic pressures on these wetlands, for the most part these practices are hydrologically sustainable, and attributed this to indigenous knowledge of these systems. This unfortunately is lacking in the wetlands of the Sand River, where there was no history of wetland cultivation particularly in this setting by the resettled population. Nevertheless, this study reveals that sustainable utilisation of these wetlands may be achieved through the careful identification of hydrologically sustainable micro-regions within the Sand Rivers wetlands, married with suitable rehabilitation of degraded regions; however it may be that the considerable demands on these catchments may negate this.

Nevertheless, guiding principles emerge from the evidence outlined in this paper that can be used for successful rehabilitation of wetlands in the Sand River catchment and possibly elsewhere, and this will be achieved when detailed ground truthing is carried out prior to any construction of structures. First, based on the soil (soil water processes) and geological (obvious controls, bedrock controls for example) composition of the wetland will allow for the development of some form of conceptual hydrological model of the wetland and the impact that differing types of rehabilitation interventions may have on the conceptual wetland hydrology. In the case presented here it is certainly the presence of layered and plugged clays that control the hydrology in the natural state and the positioning of bedrock outcrops can play an important role in restoring the hydrodynamics if the rehabilitation structures are keyed into a satisfactory depth to effectively seal the wetland. The type of monitoring discussed here (i.e. piezometer networks and geophysical surveys) can be done at relatively little cost especially when compared to significant capital expenditure of installing and maintaining such rehabilitation structures, in order to develop conceptual hydrological models, and the merit of this approach has been shown here.

Very few studies have addressed the wetland rehabilitation issue directly from the hydrodynamic or hydroperiod perspective, and those that do often entail the use of a reference undisturbed system from which to rate the achievement of the rehabilitation. For instance, Bruland *et al* (2003), showed that the restoration of Carolina Bay wetland in the USA, where filling-in drainage ditches was shown to have relatively rapid responses and to be successful

when the water table elevations were seen to closely resemble the depth and duration when compared to a similar natural wetland. Meanwhile Dixon & Wood (2003) used cluster analysis to show the clear differences in the hydrodynamics of several comparable wetlands undergoing differing degrees of anthropogenic impact in eastern Africa. These direct comparisons with 'pristine' systems are obviously the optimal scenario for tracking rehabilitation success, however this is negated by the extensive alteration of the wetland environments in the Sand River system, where there are very few if any truly pristine systems left, compounded by variation in their topographical, geological, climatic and ecological settings. Despite the short term examination of the wetlands response to rehabilitation in this study, there has clearly been noticeable positive responses within small regions of the wetland, seemingly controlled by the clay plug and aquicludes. Recalling the artesian pressures observed upstream of the clay plug at T2_2 in the year prior to rehabilitation, contrasting with the hydraulic drawdown of piezometric surfaces in the shallow as well as deep zones at T2_3 downstream of the clay plug, then the fact that artesian pressures are then observed at T2_3 following rehabilitation would suggests a level of success in restoring the system's hydrology to a certain extent. Of course, longer term monitoring is required, especially if use can be made of vegetative indicators of hydrologic regime, whereupon it would be expected that the system will return to hydrophytic vegetation just upstream of the weir.

In terms of the wetland's ability to sustain agricultural practices, this is likely on the proviso that the rehabilitation structures remain in place and sediment in-filling is allowed in the ponded-area behind them. However key controls on the wetlands hydrology are obviously the distribution of clays within the sandy wetland substrate and these, particularly those that plug the system should remained untouched from any anthropogenic/mechanical alteration where they still exist. In addition, as a horizontal aquiclude controls the vertical distribution of water in the wetland, conservation tillage practices should ideally be incorporated that may alter the bulk density of the sandy material but leave these clay horizons intact.

5.5 CONCLUSION

This paper has shown that the wetlands of the Sand River headwaters have a variable hydrodynamic behaviour governed by the distribution of clays within an otherwise sandy matrix. These clays form shallow horizontal aquicludes that separate seasonal shallow ground water from deeper perennial groundwater stores. The underlying of this wetland by a deep

aquiclude as well as a vertical clay plug facilitates the artesian pressures in the perennial groundwater. The gullying of the wetlands had quite clearly created a desiccating environment through hydraulic drawdown adjacent to the gully heads, whilst upstream of sub-surface clay plugs the wetland remained hydrologically intact, as revealed by hydraulic gradients within and between shallow groundwater monitoring stations. The loss of these plugs, it was shown, could be ameliorated by the installation of rehabilitation controls structures, but as became apparent as the study progressed the exact positioning of the structures had a considerable influence on the resulting restored hydrodynamic response of the system, and this response could be coincidental, highlighting the need for comprehensive ground-truthing of wetland systems when costly rehabilitation measures are planned.

ACKNOWLEDGEMENTS

The authors are grateful to the South African Water Research Commission (WRC) and National Research Foundation (NRF) for financial support. Working for Wetlands and Eastern Wetland Rehabilitation Ltd for the rehabilitation of the wetland. The kind assistance of the following people for field assistance, data processing and interpretation is duly acknowledged; Mr Ronny Maaboi and Mr Difference Thibela for field assistance. Mr Cobus Pretorius (University of KwaZulu-Natal) and Mr Sean Thornton-Dibb (University of KwaZulu-Natal) for technical assistance. Logistical and administrative support was provided by the Association for Water and Rural Development (AWARD).

REFERENCES

Acocks, JPH. (1988) Veld Types of South Africa. Mem. Bot. Surv. S. Afr No. 57

Armstrong, A. (2000) DITCH a model to simulate field conditions in response to ditch levels managed for environmental aims. Agriculture, Ecosystems and Environment 77 179-192.

Dada, R., Kotze, D., Ellery, W., Uys, M (2007). WET-RoadMap. A Guide to the Wetland Management Water Research Commission. Pretoria. Report TT 321/07

Bouwer, H. Rice, RC. (1976) A Slug Test for Determining Hydraulic Conductivity of Unconfined Aquifers With Completely or Partially Penetrating Wells. Water Resources Research 12.3 423-428.

Brinson, MM (1993). Hydrogeomorphic classification of wetlands. U.S. Army Corps of Engineers Waterways Experiment Station. Vicksburg, MS. Report WRP-DE-4

Bruland, GL., Hanchey, MF., Richardson, CJ. (2003) Effects of agriculture and wetland restoration on hydrology, soils, and water quality of a Carolina bay complex. Wetlands Ecology and Management 11 141-156.

Bullock, A. Acreman, M. (2003) The role of wetlands in the hydrological cycle. Hydrology & Earth Systems Sciences 7.3 358-389.

Conway, D. Dixon, AB. (2000) The hydrology of wetlands in Illubabor Zone. Report 1 for Objective 3.. EWRP and University of Huddersfield. Metu and Huddersfield,

Debano, LF., Hansen, WR. (1989) Rehabilitating Depleted Riparian Areas Using Channel Structures .Practical Approaches to Riparian Resource Management. An Educational Workshop. American Fisheries Society. Bethesda MD. 141-148

Dixon, AB. (2002) The hydrological impacts and sustainability of wetland drainage cultivation in Illubabor, Ethiopia. Land Degradation & Development 13 17-31.

Dixon, AB. Wood, AP. (2003) Wetland Cultivation and hydrological management in eastern Africa: Matching community and hydrological needs through sustainable wetland use. Natural Resources Forum 27 117-129.

Kotze, D. & Silima, V. (2003) Wetland cultivation reconciling the conflicting needs of the rural poor and society at large through wetland wise use. Int. J. Ecol. Env. Sci. 29 65-71.

Gavin, H. (2003) Impact of ditch management on the water levels of a wet grassland in Southeast England. Agriculture, Ecosystems and Environment 99 51-60.

Gilman, K. (1994) Hydrology and Wetland Conservation. John Wiley & Sons, Chichester.

Grenfell, M.C. Ellery, W.N. Garden, S.E. Dini, J. van der Valk, A.G. (2007) The language of intervention A review of concepts and terminology in wetland ecosystem repair. Water SA 33.1 (2007) 43-50.

McFarlane, MJ. Whitlow, R. (1991) Key factors affecting the initiation and progress of gullying in dambos in parts of Zimbabwe and Malawi. Land Degradation & Development 2.3 215-235.

McHugh, OV., McHugh, AN., Eloundou-Enyegue, PM., Steehuis, TS. (2007) Integrated Qualitative Assessment of Wetland Hydrological and Land Cover Changes in a Data Scarce Dry Ethiopian Highland Watershed. Land Degradation & Development 18 1-16.

Mitsch, W.J. & Gosselink, J.G. (1993) Wetlands. John Wiley & Sons.

Moorhead, KK. (2003) Effects of drought on the water-table dynamics of a southern Appalachian mountain floodplain and associated fen. Wetlands 23.4 792-799.

Owen, CR. (1995) Water Budget and flow patterns in an urban wetland. Journal of Hydrology 169 171-187.

Patterson, L., Cooper, DJ. (2007) The Use of Hydrologic and Ecological Indicators for the Restoration of Drainage Ditches and Water Diversions in a Mountain Fen, Cascade Range, California. Wetlands 27.2 290-304.

Pollard, S. Kotze, D., Ellery, W., Cousins, T., Monareng, J., King, K., Jewitt, G. *et al* (2005) Linking Water and Livelihoods The development of an integrated wetland rehabilitation plan in the communal areas of the Sand River Catchment as a test case. Association for Water and Rural Development. URL http//www.award.org.za/wetlandsoct04.pdf

Preston, EM., Bedford, BL. (1988) Evaluating cumulative effects on wetland functions A conceptual overview and generic framework. Environmental Management 12 565-583.

Price, JS., Heathwaite, AL., Baird, AJ. (2003) Hydrological processes in abandoned and restored peatlands An overview of management approaches. Wetlands Ecology and Management 11 65-83.

Riddell, ES., Lorentz, SA., Ellery, WN., Kotze, D., Pretorius JJ., Nketar, SN. (2007) Water Table Dynamics of a Severely Eroded Wetland System, Prior to Rehabilitation, Sand River Catchment, South Africa.. XXXV IAH Congress Groundwater and Ecosystems Ed. Ribeiro, L., Chambel, A. Condesso de Melo, MT. Lisbon, Portugal.

Schmidt, LJ., Debano, LF. (1990) Potential for Enhancing Riparian Habitats in the Southwestern United States with Watershed Practices. Forest Ecology and Management 33/3.1/4 385-403.

Scoones, I. (1991) Wetlands in Drylands Key Resources for Agricultural and Pastoral Production in Africa. Ambio 20.8 366-371.

von der Heyden, CJ. New, MG. (2003) The role of dambo hydrology of a catchment and the river network downstream. Hydrology and Earth System Sciences 7.3 339-357.

Whitlow, R. (1989) A review of dambo gullying in south-central Africa. Zambezia XVI.ii (1989) 123-148

6 HYDROLOGIC MECHANISMS IN A GRANITIC HILLSLOPE THAT INDUCE RAPID PHREATIC SURFACE RESPONSES IN A HEADWATER WETLAND

Riddell, ES. Lorentz, SA.

[1] School of Bioresources Engineering and Environmental Hydrology, University of KwaZulu-Natal, Private Bag X01, Scottsville, Pietermaritzburg, 3209, South Africa

ABSTRACT

Hydrometric observations revealed an interesting mechanism inducing rapid near surface recharge processes into a headwater wetland in a sub-humid setting along a granite fringe of the great escarpment of Southern Africa. These findings have consequences for the way that the catchment should be managed in the future given the present pressures from extensive and intense subsistence agricultural practices in the wetlands of this region, as well as the manner in which these practices combine with hillslope and valley water delivery to cause loss of viable wetland sediments. During the monitoring period it was noted that, following steady soil moisture recharge during the early rain season threshold-exceeding precipitation events induce a significant rise in matric pressure head at the clay rich hillslope toe soils and near instantaneous elevation of groundwater levels within the valley bottom wetland. This paper outlines these observed responses with respect to antecedent soil moisture conditions and event driven lateral sub-surface flows at the hillslope toe. Unsaturated zone modelling of a hillslope in this catchment was undertaken using the software package HYDRUS-2D which solves the Richard's equation. This model used detailed soil hydraulic parameters and effective infiltration rates derived from modelled USLE runoff plot data using a kinematic overland flow mass balance function. The results suggest that this rapid phreatic response mechanism is induced by a steady increase in the degree of saturation of deep clay rich horizons within the catchment following the onset of seasonal rains. The rapid phreatic response in the wetland is then driven by significant macro-pore dominated preferential flow pathways throughout the soil profile from upslope.

Keywords: Hydrus-2D, unsaturated zone modelling, macropores, recharge, wetlands, South Africa

6.1 INTRODUCTION

The general framework that process hydrologists have utilised is to garner knowledge of water flow pathways and residence times and this is essential for predicting a catchments response to rainfall (Uhlenbrook *et al.,* 2005). In aiming to determine the hydrological process function of catchments, three basic issues need to be addressed: what happens to water once precipitation occurs? What path does this water take to the stream? And how long does this water reside in the catchment? (McDonnell, 2003). Indeed, determining flow pathways into and through wetlands is also a necessary prerequisite for understanding the role of wetlands in catchments (e.g. McCartney & Neal, 1999). It is these hydrological processes that are receiving increasing attention in recent years, and the particular role of groundwater-surface water interactions and wetland-hillslope connectivity are common themes in the emerging science of wetland hydrology. However most studies to date have focused on wetland catchments in the humid temperate regions of the world where, for instance, the volume of groundwater inputs to wetlands were identified as being proportional to the depth of upslope till deposits on the Canadian shield landscape (Devito *et al.*, 1996) and more recently by sub-surface cobble channel piping (Frisbee *et al.*, 2007), and by lateral transfers through organic transmission (humic-litter) layers above the soil in grasslands of South Island, New Zealand (Bowden *et al.*, 2001). There have been a limited number of studies in recent years that explore wetland-hillslope relationships in semi-arid settings in general (e.g. Reuters & Bell, 2003), whilst fair attention was paid to dambo catchment processes in southern Africa during the last two decades (e.g. McFarlane, 1992; McCartney, 2000; and von der Heyden & New, 2003). However this dearth in knowledge of key process zones between wetlands and their catchments for semi-arid regions of the southern hemisphere represents a key information gap given that there is a significant and continued loss and/or modification of wetland environments, particularly to subsistence agriculture in southern Africa (Kotze & Silima, 2003).

The study of hillslope hydrological processes is becoming a well documented science, where most research has focused on rainfall partitioning and runoff processes in the surface and sub-surface on natural slopes (e.g. Weiler & McDonnell, 2004, Martinez-Mena, 2001) as well as on the artificial slopes of reclamation sites (e.g. Nicolau, 2002). However hillslope hydrology is a complex suite of interacting processes, governed by process thresholds and connectivity of process domains. These interacting processes operate differently at varying scales and are confounded by multi-scale heterogeneities, within the hillslope medium and the biotic state

above ground. Some of these complex processes were highlighted by Ridolfi *et al.,* (2003), and included: the spatial heterogeneity of soil properties; climatic variability, which although generally uniform at the hillslope scale may trigger mechanisms within the hillslope to alter its spatial dynamics; lateral redistribution of water along a hillslope due to the formation of a saturated zone within the soil; lateral sub-surface flow in the unsaturated zone; the longitudinal hillslope profile and form; and boundary conditions at the bottom of the hillslope. With all this complexity, it is suggested best practice to isolate some mechanisms when seeking to understand hillslope processes and examine them independently using simplified assumptions on their behaviour (Ridolfi *et al.,* 2003). Furthermore, it is the field based approach to describing these hillslope processes that facilitates a 'bottom-up' conceptualisation from which to understand how the complexity of hillslope processes integrates to the relative simplicity of watershed response in deterministic physically based modelling approaches (Sivapalan, 2003). Moreover, this notion is receiving attention in recent years where traditionally lumped-catchment based models seek a homogenous hydrological response, or hydrological response unit (HRU). However this concept belies the true dominant units of hydrological response, the hillslopes and the stream network (Lorentz *et al.*, 2008). Critically, whilst there has been considerable development in defining hillslope hydrological processes, there is a need to upscale the hydrological processes on hillslope drainage networks, where non-linear threshold type responses often exist and it is necessary to conceptualise these non-linear effects at the catchment scale, for differing geographic areas with varying climates and geologies (Tetzlaff *et al.*, 2008). If we are to view wetlands as part of the hydrological continuum, then this concept similarly applies to the first-order controls operating at the coupling of hillslope-wetland units which then manifest to hydrological processes at the catchment scale.

Threshold hillslope hydrological processes are known to occur under different conditions and through a variety of mechanisms, most notably in the case of runoff initiation, there is marked contrast between semi-arid and humid areas. In the case of the former, surface runoff initiation is controlled by a one-dimensional vertical soil water balance, whilst the latter is often dominated by lateral sub-surface flow through topographic coupling in a catchment (Kirkby *et al.*, 2002). Meanwhile various forms of sub-surface threshold responses have been described as delivering water from the hillslope to the valley bottom or stream channel and these more often than not are controlled by a complex suite of factors dominated by antecedent soil moisture conditions and rainfall intensity. Examples of these thresholds include: the reaching of conditions suitable for preferential flow through macropores upon exceeding a volumetric water content of 33% in a sandy-loam A-horizon overlying a clay-rich B-horizon in a forested

catchment of New Mexico (Newman, *et al.*, 1998). Sidle *et al*., (2000) developed a conceptual model of threshold induced preferential flow in a headwater catchment dominated by volcanic ash soils in Japan. Using tracers of discharge in soil pits and catchment outlets, it was suggested that thresholds leading to increased stormwater discharges were directly proportional to the depth of the soil in the surrounding hillslopes. Tromp van Meerveld & McDonnell (2006a) proposed, based on their observations at the Panola Mountain Research Watershed (PMRW), USA, that sub-surface stormflow on the hillslope results from ponding of water at the soil bedrock interface, through a fill-and-spill process whereby the sub-surface bedrock depressions intermittently overtop relinquishing water to further down the hillslope.

There are therefore a multitude of threshold hillslope hydrological mechanisms that have been described to deliver water to downslope regions. This paper describes the application of a deterministic variably saturated flow model used to assist in the interpretation of observed key threshold hydrological processes on a granitic hillslope that provide considerable in-flux to a valley bottom wetland. Based on the above, the manuscript aims to address the following objectives:

- descriptions of observed hillslope hydrometric responses within a semi-arid wetland.
- propose mechanisms for any hydrological responses of the hillslope to antecedent soil moisture and rainfall conditions.
- develop a deterministic hillslope soil physics model to examine these proposed mechanisms.

Based on these results the possible consequences of changing land-uses in this wetland catchment through intensive cultivation practices by subsistence farming activities will be discussed.

6.2 STUDY SITE

The focus of this paper is one of the headwater sub-catchments of the Sand River, Mpumalanga Province, NE South Africa. The Manalana is one of many sub-catchments at the foothills of the northern range of the Great Southern African Escarpment. These catchments are underlain by porphyritic biotite granite with intersecting doleritic dykes. This region forms part of the

Archaean granite and gneiss suite of NE South Africa (Johnson *et al.*, 2006). The soils of the catchment are predominantly sandy due to the underlying geology, and so the catchment is characterised by a long and narrow un-channelled valley bottom wetland (Figure 6.1), which is also of a sandy material.

Soils in this catchment have been described according to their taxonomic form using the South African system (Soil Classification Working Group, 1991) and were further described according to hydro-pedological processes by the UVS (unpublished 2008). Soils on the granitic hillslopes are generally shallow and sandy, classed as leptosols internationally (FAO, 1998) or Glenrosa's in South Africa (Soil Classification Working Group, 1991). Meanwhile considerable deep clay G-horizons (South African definition) have formed at the hillslope toes due to illuviation processes, overlain by coarser grained A and E horizons. These soil types would be classed as planosols (FAO, 1998) or Kroonstad soil forms (Soil Classification Working Group, 1991).

Rainfall is strongly seasonal, falling between October-March as warm humid air arrives from the southern Indian Ocean in a south easterly direction. Mean annual precipitation (MAP) for the site derived from the nearest long term record at the Wales Forestry Station rain gauge is $1075mm^{-1}$ (1904-2000), which is 2.3km away. Rainfall intensities are very high, with storms in excess of 100mm being not uncommon. Hydrological years (HY) run from the start of rainfall in October through September for this region, such that HY2005 runs from October 2005 to the end of September 2006.

Land use in the Manalana catchment comprises densely populated rural housing, free ranging communal grazing, as well upland and wetland subsistence agriculture. The wetland itself represents a valuable livelihood security resource for the poorest of the poor, in terms of both wet and dry season agriculture, despite the soils in the wetland being nutritionally poor due to their dominance by granitic sands (Adey & Kotze, unpublished 2008). Due to the population pressures in this region of South Africa, which comprises a former homeland of a resettled populace, the Manalana wetland, as with the majority of the others at the headwaters of the Sand River, are almost fully subscribed in terms of available agricultural space. This agronomic pressure conflated with often un-wise and mis-informed agricultural practices, and combined with local geology and climate, makes the soils of the area relatively vulnerable to disturbance and is likely be leading to a significant loss of wetland extent through gully erosion (Pollard *et al.*, 2005). Meanwhile, the authors note that the significant conversion of the hillslope toes

(wetland-hillslope interface) from a natural to agricultural (mechanically altered through tillage practices) state is typical within these rather marginal lands.

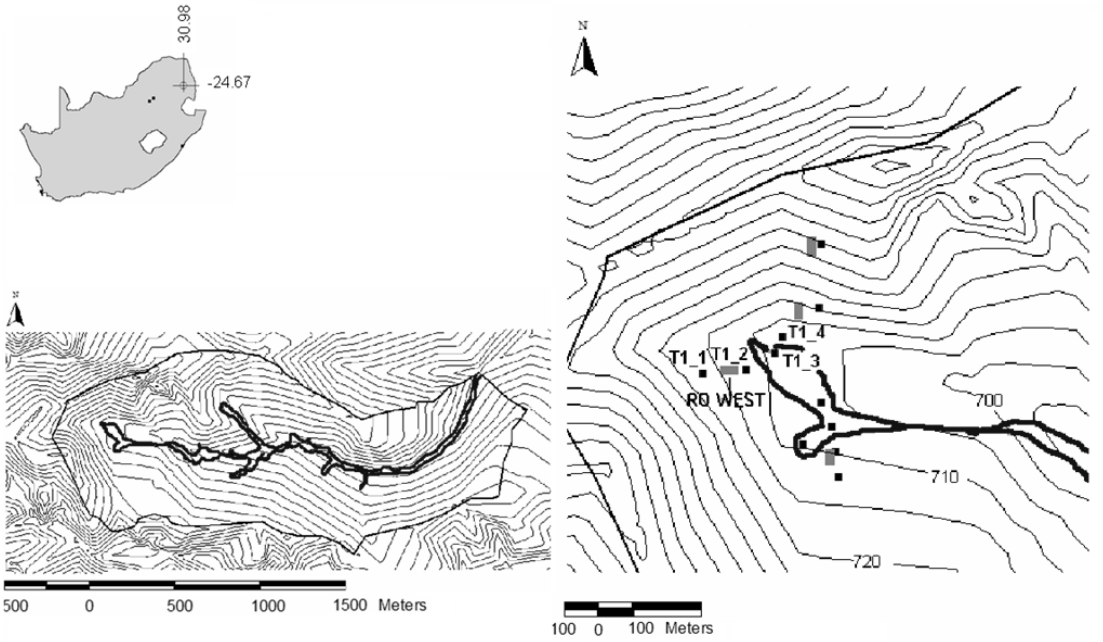

Figure 6.1: Location of the Manalana catchment within South Africa (above), the Manalana watershed and wetland in its entirety (left) and location of monitoring stations (right).

6.3 METHOD

The establishment of a hydrological monitoring network in the Manalana was initiated in response to the planned rehabilitation of the Manalana wetland through gully stabilisation measures constructed between 2005 and 2007. This network included hydrometric observation stations and a wetland outflow gauging weir. Sites relevant to this manuscript are shown in Figure 6.1. These installations were made prior to the onset of the rain season during August to October 2005. The installed apparatus included: University of KwaZulu-Natal (UKZN-SBEEH) constructed soil moisture tensiometers (T1_2 and T1_3); shallow groundwater piezometers (equipped with pressure transducers), and USLE runoff plots (24m x 2.4m) along three transects traversing the hillslopes and valley bottom. These automated hydrometry stations recorded soil moisture and groundwater levels using a UKZN-SBEEH timing board system and 4-channel HOBO® data logger based on an on-the-hour 12 minute time-step. Mid-slope (T1_1 in Figure

6.1) hydrometric observation stations were fitted with Watermark™ sensors prior to the second monitoring season in August 2006. In addition, piezometric water levels were manually read on a regular basis during the period of study. Runoff plots recorded overland flows routed through a calibrated 2 litre tipping bucket mechanism, so that overland flows could be recorded in real-time, using a HOBO® event logger and back-up mechanical counter. Rainfall data were collected using two Texas Instruments™ rain gauges, one being standalone and the other adjacent to an automatic weather station using a CR200 Campbell Scientific Inc. data logger recording wind speed, solar radiation, relative humidity and temperature. Additional rainfall data were collated from a nearby forestry station at Hebron some 3.7km to the west.

Following the methods described in Lorentz *et al.,* (2001) detailed soil hydraulic conductivity determination was conducted in-situ during the dry winter period of 2006 (May-August) adjacent to each of the hydrometry stations (see Figure 6.1). These used an 84mm diameter pressure head disc infiltrometer (TDI) and the unsaturated soil hydraulic conductivity (K_{unsat}) for each soil horizon to a depth of 2000mm was determined where possible at four pressure heads (5, 30, 90 and 160mm) using the method of Ankeny *et al.,* (1991) to determine a soil hydraulic conductivity characteristic. Following the K_{unsat} determination at each successive soil horizon saturated soil hydraulic conductivities (K_s) were determined using a double ring infiltrometer (DRI) with inner ring diameter of 110mm. Despite the slopes of the catchment being some 13% on average, it was felt that the use of TDI and DRI's on the surfaces of these hillslopes required no additional corrective measures, since these hillslopes fall within the acceptable 20% slope range (Bodhinayake *et al.,* 2004) for use of this type of apparatus. An undisturbed soil core of 94.8 cm^3 was then taken for laboratory determination of the water retention characteristic and bulk density using the multi-step controlled outflow method as reported by Lorentz *et al.,* (2001). These cores were taken at each soil horizon at each location where K characteristics were determined. All of the above data may be viewed in Appendix iii. Transect elevation profiles were collected using a Trimble™ Pro-XRS differential global positioning system.

6.3.1 Model Description

The HYDRUS-2D model (Šimùnek *et al.,* 1999) numerically solves for the Richard's (1931) equation to simulate variably saturated flow in two dimensions using a finite element grid flow domain. It is particularly useful for simulating flow in natural heterogeneous environments where soil type distributions are non-uniform and subject to anisotropic processes, and may

incorporate various boundary conditions such as atmospheric (root and soil surface fluxes), free drainage, seepage faces and prescribed variable pressure head boundaries. A simple form of the Richards equation may be written as follows:

$$\frac{\partial \theta}{\partial t} = \frac{\partial}{\partial z}\left[K(\theta)\left(\frac{\partial \psi}{\partial z} \right) + 1 \right] \quad (6.\ 1)$$

Where: K is the hydraulic conductivity [L T^{-1}]; θ is the volumetric water content [L^3L^{-3}]; t is time [T]; ψ is the pressure head [L]; and z is the gravitational head [L].

6.3.2 Domain design

A domain section was developed from a midslope position adjacent to hydrometry station T1_1 through the toeslope area adjacent to T1_2 before descending to the valley bottom wetland area at T1_3, which correspond to three soil horizon domains (Figure 6.2). The model domain was given a total depth of 4000mm and incorporated 9 soil types described for their hydraulic conductivity and water retention characteristics. The hillslope domains of mid-slope and toe, each had four soil horizons represented on the model, whilst the wetland itself was represented by one homogenous material. The three soil horizon domains had their vertical boundaries blended with increasing mesh densities to facilitate greater model stability. The mesh was generated with MESHGEN2D within the HYDRUS-2D graphical user interface and consists of a total of 5667 nodes and 10833 triangular elements. Nodes below 2000mm were assumed to have the same hydraulic and retention characteristics as that measured for the horizon at 2000mm. Four boundary conditions were stipulated for the domain as depicted in Figure 6.2. The atmospheric boundary condition comprised a 4:1 partition of estimated reference evapotranspiration (ET_o) for soil surface evaporation to root transpiration respectively. The basis of this partition was the very low basal cover of vegetation observed on these hillslopes as a result of overgrazing (this was based on the approximately <20% vegetation cover on this hillslope at and between sites T1_1, T1_2 and T1_3, for determinations see Appendix i). ET_o was estimated using the Penman-Monteith method for a grass reference crop only, based on the method used by Allen *et al*., (1998). The variable pressure head boundary at the right of the domain incorporated positive pressure head data recorded from an automated piezometer at T1_3. Free drainage was applied as a boundary condition above the variable pressure head boundary. No flow boundary conditions were applied at the base of the domain as fluxes to and

from bedrock were assumed to be negligible. A no-flux upslope boundary was also applied to the left of the domain[2]. A root distribution of 1 (dimensionless), equating to a low root-length density as implied by the poor vegetative cover, was applied to the first 1000mm of the midslope and toe domains, whilst the same distribution was applied to the first 2000mm of the wetland domain, this specifies the water uptake zone at these nodes.

6.3.3 Simulation

The simulation of the wetland rapid phreatic surface elevation was run for the period 00:00 hrs 25/12/2006 to 00:00 hrs 08/01/2007, which incorporated a large frontal rainfall event of the period 30/12/2006-01/01/2007. The simulation domain incorporated 9 observation nodes corresponding with the locations and depths of 3 soil moisture tensiometers each at T1_3, T1_2 and 3 Watermark^{TM} sensors at T1_1 (Figure 6.2). Starting conditions were based on measured pressure head values at T1_3 (variable pressure head at t=0, 1800mm) with a linear distribution of pressure head for the rest of the domain from this lowest located nodal point, up to the highest located nodal point. A matric pressure head tolerance of 100mm was applied to the domain with 70 iterations invoked as the maximum allowable for mathematical convergence. Maximum allowable soil suction at the surface was given as 2 x 10^6mm throughout the simulation recommended for a clay-silt soil. Furthermore, a series of paired observation nodes were incorporated vertically at the toe-wetland interface (see sub-region 1 and 2 in Figure 6.2) in the domain to develop a hydraulic gradient based mass balance determination for water leaving the hillslope towards the wetland, in essence therefore the paired nodes act as a seepage face.

[2] Initially a variable pressure head boundary was also specified at the upslope boundary, but this led to mathematical model instabilities and it was eventually excluded.

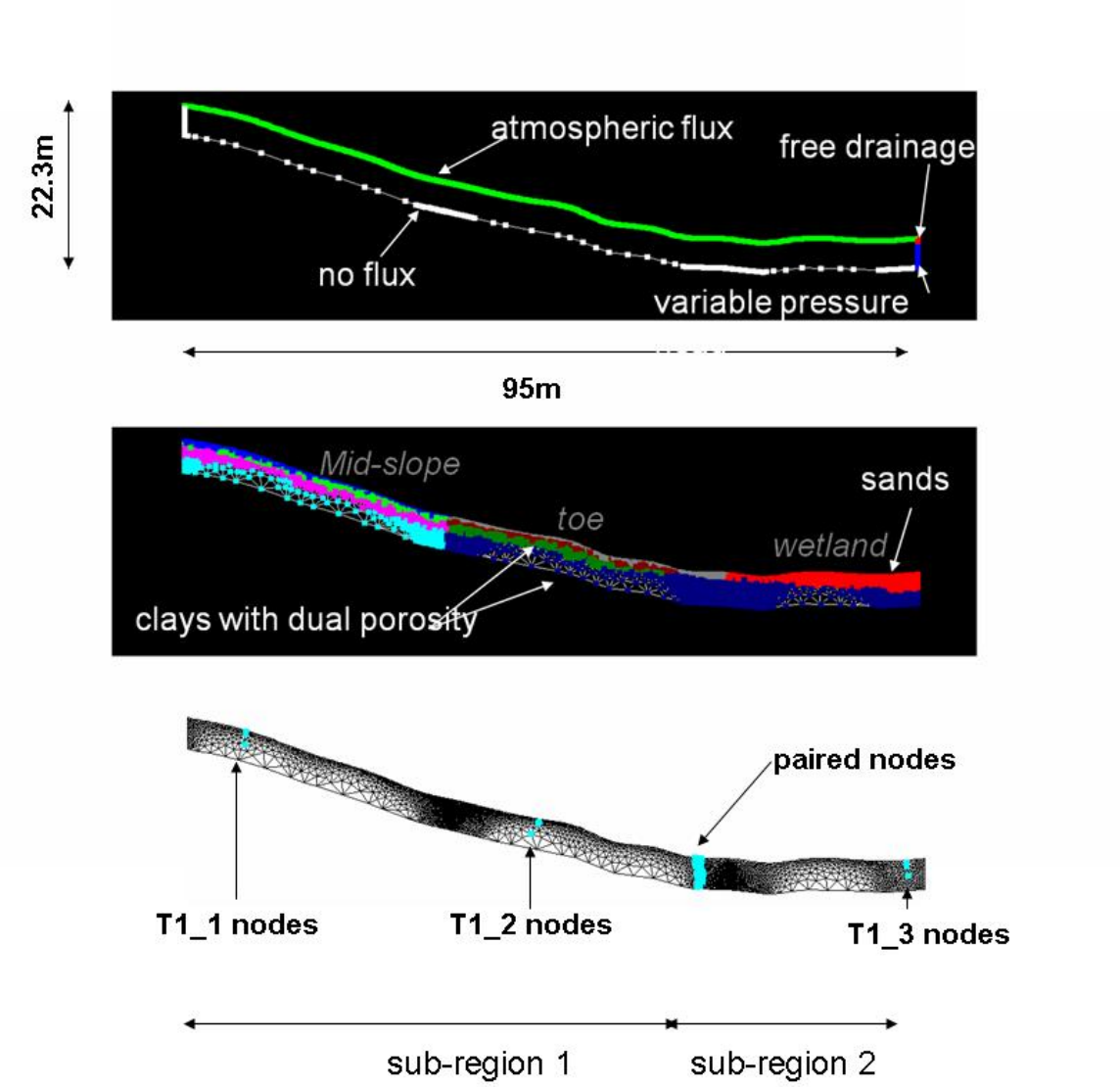

Figure 6.2: Hillslope domain with boundary conditions (above), soil type stratification within the hillslope domain (middle) with increased mesh density at element boundaries and location of observation nodes (lower). NB. Clays with dual porosity represent the G-horizon described in the text.

The soil hydraulic characteristics within HYDRUS-2D follow the predictive water retention function of van Genuchten (1980) and incorporates the statistical pore-size distribution function of Mualem (1976) for known hydraulic conductivities. The van Genuchten (1980) equation may be written for water content (θ), and hydraulic conductivity (K), at pressure heads (h) as follows:

(6.2a) $$\theta(h) = \begin{cases} \theta_r + \dfrac{\theta_s - \theta_r}{\left[1 + |\alpha h|^n\right]^m} & h < 0; \\ \theta(h) = \theta_s & h \geq 0 \end{cases}$$

(6.2b) $$K(h) = K_s S_e^l \left[1 - \left(1 - S_e^{\frac{1}{m}}\right)^m\right]^2$$

(6.2c) $$m = 1 - \frac{1}{n}, n \geq 1$$

Where: θ_r is the residual water content [L^3L^{-3}], θ_s saturated water content [L^3L^{-3}], α is the air entry value [L^{-1}], S_e effective water content $(\theta-\theta_r)/(\theta_S-\theta_r)$ and m, n and l are parameters related to the pore size distribution and structure.

The five independent parameters have to be estimated for use in the HYDRUS simulation by curve fitting to known $\theta(h)$ and $K(h)$ values. The RETC code (van Genuchten *et al*., 1991) was used to optimise these parameters for each measured $\theta(h)$ and $K(h)$ dataset for the soil types in the domain.

Since observations in the Manalana catchment led to the speculation of macropore dominated preferential flow, the option to invoke dual-porosity within HYDRUS-2D was selected. This modified form of the van Genuchten (1980) equation incorporates the dual-porosity function of Vogel and Císlerová (1988) which is displayed in Figure 6.3 and may be written as follows for $\theta(h)$ and $K(h)$:

(6.3a) $$\theta(h) = \theta_a + \frac{\theta_m - \theta_a}{(1 + |\alpha h|^n)^m} \qquad h \leq h_k$$

(6.3b) $\theta_a \qquad h \geq 0$

and

(6.3c) $K(h) = K_s K_r(h) \qquad h \leq h_k$

(6.3d) $K(h) = K_k - \frac{h - h_k}{h_k}(K_s K_k) \qquad h_k < h < 0$

(6.3e) $K(h) = K_s \qquad h \geq 0$

where

(6.3f) $$K_r = \frac{K_k}{K_s}\left(\frac{S_e}{S_{ek}}\right)^{\frac{1}{2}}\left[\frac{F(\theta_r) - F(\theta)}{F(\theta_r) - F(\theta_k)}\right]^2$$

(6.3g) $$F(\theta) = \left[1 - \left(\frac{\theta - \theta_a}{\theta_m - \theta_a}\right)^{\frac{1}{m}}\right]^m$$

(6.3h) $$S_{ek} = \frac{\theta_k - \theta_r}{\theta_s - \theta_r}$$

Where: K_r is the relative hydraulic conductivity [L T^{-1}]; K_k is the predicted hydraulic conductivity close to but less than K_s where dual-porosity is enabled [L T^{-1}]; h_k is the predicted head corresponding to K_k [L]; θ_a is a fictitious/extrapolated parameter slightly smaller than θ_r ; and θ_m is a fictitious/extrapolated parameter slightly larger than θ_s

Hence the measured values of *θ(h)* and *K(h)* were plotted in a similar manner to that in Figure 6.3 and extrapolated values of θ_m and K_s were estimated (data used in the model are plotted in Appendix iii).

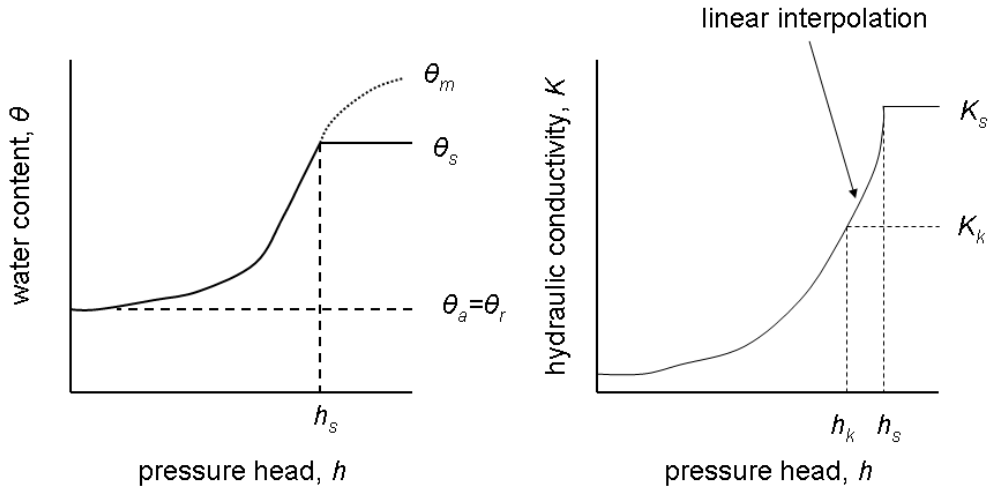

Figure 6.3: Relationship of water retention (left) and hydraulic conductivity (right) for given matric pressure heads, according the modified form of the Mualem-van Genuchten equation, by Vogel Císlerová (1988).

Following initial simulations where model instability was observed during the intense precipitation event of 30-31/12/2006 an *effective rainfall* depth was estimated using data recorded at the USLE runoff plot for that slope (RO WEST in Fig. 6.1), and this allowed the deployment of surrogate precipitation values for that period. The method for this approach follows that of Moore & Foster (1990) as cited by Lorentz *et al.,* (2003), whereupon a model of discharge is developed for a 10 element runoff plot to derive a kinematic overland flow mass balance scheme using a Green-Ampt/Horton infiltration mechanism. First the time to ponding (t_p) is derived as follows:

(6.4)
$$t_p \frac{K_s(\theta_s - \theta_i)H}{i(i - K_s)}$$

Where: θ_i is the initial water content [L^3L^{-3}]; i is the rainfall intensity (mm/hr); and h is the pressure head at the Green-Ampt wetting front.

The infiltration rate f at any segment at any time interval Δt is given by:

(6.5a) $$f = K_s + \frac{1}{k\Delta t}(i_p - K_s)\left(e^{k\Delta t} - 1\right)e^{-k(t-t_p)} \qquad t > t_p$$

(6.5b) $$f = i \qquad t < t_p$$

Where: $k = 8Ks/((\theta_s-\theta_i)H)$ [L^{-1}]; and i_p is the rainfall intensity at ponding time. hydraulic head (H) at the wetting front is given by Brooks-Corey (1964) water retention characteristic parameters for a given soil as (where in this instance macropore flow at the soil surface was assumed to be negligible):

(6.6) $$H = \frac{(2+3\lambda)}{(1+3\lambda)}\frac{h_b}{2}$$

Where: λ is a dimensionless pore size distribution index [0.5]; and h_b is the inverse air-entry pressure head [L^{-1}]. (These values were derived for the surface soil types using RETC).

A Newton-Raphson iterative function is then applied to each of the 10 finite elements of the (see Figure 6.4) USLE runoff plots for each time increment, where the most upstream and all initial downstream cross-sectional areas are taken to be 0, as follows:

(6.7) $$\frac{A_{n+1;t+1}}{2} + Q_{n+1;t+1}\frac{\Delta t}{\Delta x_e} = \frac{\left(A_{n;t} + A_{n+1;t} - A_{n;t+1}\right)}{2} + Q_{n;t+1}\frac{\Delta t}{\Delta x_e} + i_e A_e \frac{\Delta t}{\Delta x_e}$$

Where: i_e is the rainfall excess (taken as the difference between rainfall intensity i and infiltration f); A_e is the surface area of the flow element (4.8 m); Δt is the time increment (1-minute); Δx_e is the space increment (2.2 m). Suffixes n and t denote the upstream and previous time-step respectively, whilst suffixes $n+1$ and $t+1$ refer to the downstream node and current timestep. The Manning's equation for broad sheet flow on a slope is used to calculate discharge (Q), as:

(6.8) $$Q = \alpha A^{\frac{5}{3}} \quad \textit{where} \quad \alpha = \frac{1}{n} w^{-\frac{2}{3}} s^{\frac{1}{2}}$$

Where: n is a prescribed Manning's roughness coefficient [dimensionless]; s is the slope (%); and w is the width of the surface element (2.4 m).

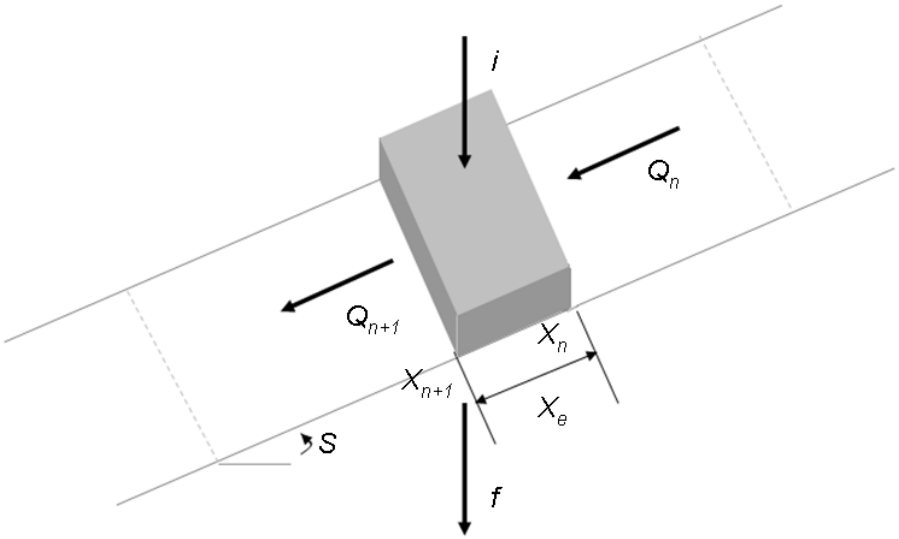

Figure 6.4: Schematic of finite element kinematic overland flow model (adapted from Lorentz *et al.*, 2003).

The effective rainfall intensity (i_t) is then derived as the total rainfall for the time increment minus the rainfall excess such that it equals the total infiltration (f) to the model domain:

(6.9) $$i_t = i - i_e = f$$

6.4 RESULTS

6.4.1 Hydrometric observations

Hydrometric monitoring revealed that the soil moisture regime is influenced by the seasonal rains in this catchment, as would be expected, such that matric pressure heads are generally high (i.e. approach 0 mm) during the wet summer months and low (i.e. increasingly < 0 mm) during the dry winter months (not reported here). It was however noted during the first two years of hydrometric monitoring of the Manalana catchment that, following steady wetting up of the catchment after the start of seasonal summer rains, the shallow soil horizons (0-600 mm) of the mid-slopes and hillslope toe wet-up and dry-out very rapidly during and after a rainfall event,

respectively, whilst the deeper soils (>600 mm) have different responses according to their hillslope position. In the case of the mid-slope soils, the deeper horizons remained rather dry throughout the seasonal rains, with only slight changes to matric pressure head ranges in response to large events, meanwhile the deep horizons at the hillslope toe had a comparatively high matric pressure head range throughout the year, but during the height of the rains these switched to being dominated by positive matric pressures (i.e. >0 mm) indicative of matrix saturation, that were then followed by slow drying throughout the dry winter. In addition, the valley bottom/wetland was in a very dry state up to 2000 mm deep, and following successive rains this then soon compromised a largely saturated profile as the water table within the wetland elevates.

The nature of the peak-wet summer profiles is depicted in Figures 6.5 and 6.6 for 2005-06 and 2006-07 respectively. For the former period (prior to installation of mid-slope watermark sensors) the wet profile seen at T1_2, with both shallow tensiometers (310 mm and 610 mm) showing similar pressure head responses in the range close to saturation (matric pressure head close to 0), whilst the deeper tensiometer (2040 mm) although still showing matric conditions close to saturation is not in the same range as the shallower soils above. Meanwhile the tensiometers at T1_3 in the wetland show that the shallower soils (320 mm) are still showing relatively large matric pressure head responses in the unsaturated state, whilst the deeper tensiometers at 620 mm and 1990 mm are very close to saturation. Figure 6.5 also displays the responses for the toe of the hillslope on the opposite side of the wetland at T1_4, where the shallow 305 mm and 620 mm sensors show similar responses to those corresponding sensors at T1_2, whilst the deeper 2000 mm sensor has lower pressure head of some 1000 mm lower than that observed for the corresponding sensor at T1_2.

During the latter season, (Figure 6.6) annual precipitation was considerably lower than the preceding year (nearby Hebron Forestry estate HY2006 1772 mm, HY2007 1177 mm), but the tensiometer responses showed a similar regime, albeit in this example that the deeper 2040 mm tensiometer at T1_2 was already closer to saturation than the overlying shallow soils, and that even the 620 mm tensiometer at T1_3 was in a largely unsaturated profile at that depth. Figure 6.6 also displays matric pressure head values for the 2006-07 season at T1_1 and here it may be observed that the deeper watermark sensors show a very dry condition with low matric pressure head at the deep soils of the 2000 mm sensor despite this being the height of the rain season, whilst the shallower soils have a rapid wetting-drying response as seen with the 300 mm and 600 mm sensor.

Both Figures 6.5 and 6.6 reveal an interesting phenomenon that could reveal threshold connectivity and/or vertically driven processes from the hillslope toe to the valley bottom wetland, in the case of the former this may be observed on the 08/01/2006 and the latter on the 31/12/2006. In both cases it is evident that there is a significant transition of matric pressure head of the deep 2040 mm tensiometer at T1_2 from unsaturated to ponded conditions, following a large rainfall event and the hillslope response is likely triggered by some threshold antecedent soil moisture condition. The shallower soil at this location also comes close to saturation. For the similar event during the 2006-07 season in Figure 6.6 a piezometer corresponding to the deep tensiometer also reveals the appearance of a water table at this depth.

Meanwhile a similar response is yielded on the opposite hillslope is shown for the response at T1_4 in Figure 6.5, where there is a significant rise in pressure head and is observed first for the 2000 mm sensor here, where pressure head rises to positive pressure heads also on the 08/01/2006.

Interestingly it is the water table elevation response of the wetland (T1_3 piezometer) that is near instantaneous in the 2005-06 season and in fact occurs over a number of hours causing a rapid saturation of the wetland profile at T1_3. Following the event of the 2006-07 there is also a near instantaneous response within the wetland, the water table elevation in fact rises more steadily over two days.

6.4.2 Model simulations

The results of the hydraulic conductivity and water retention characteristics, along with van Genuchten curve (fitted) parameters (using the RETC code) of the soils along the modelled hillslope are displayed in Table 6.1. Also incorporated in Table 6.1 are parameters derived for the soil types using RETC and extrapolated parameters for the dual-porosity function of Vogel & and Císlerová (1988), where the deep soils of the hillslope toe comprise artificially high K_s values (NB. an extrapolated value above actual K_s, which were chosen to be an order of magnitude greater than the real values that were placed for K_k).

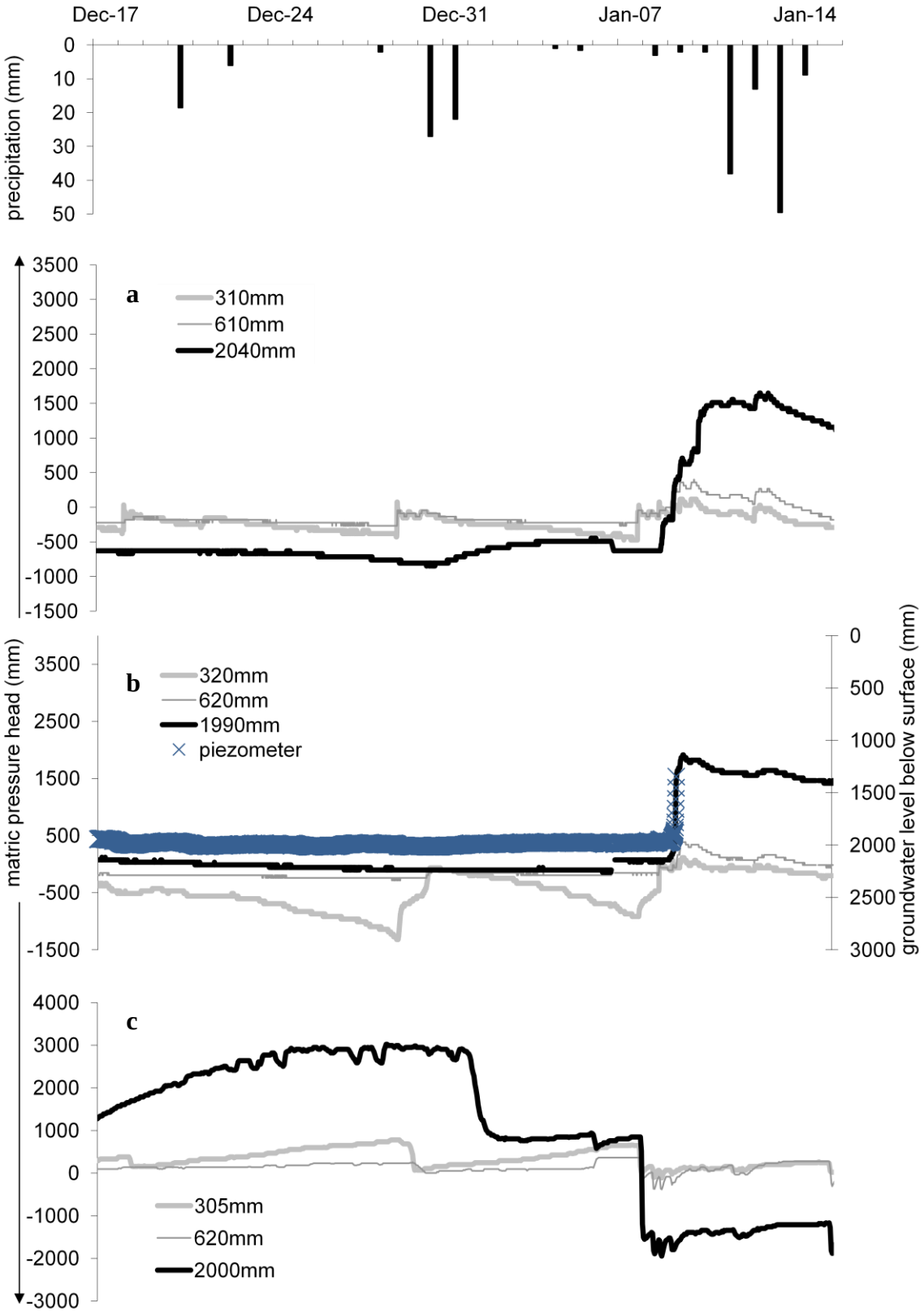

Figure 6.5: Pressure head responses for site T1_2 (a), T1_3 (b), and T1_4 (c) for the period 17/12/2005-15/01/2006 (precipitation data – Hebron Forestry estate).

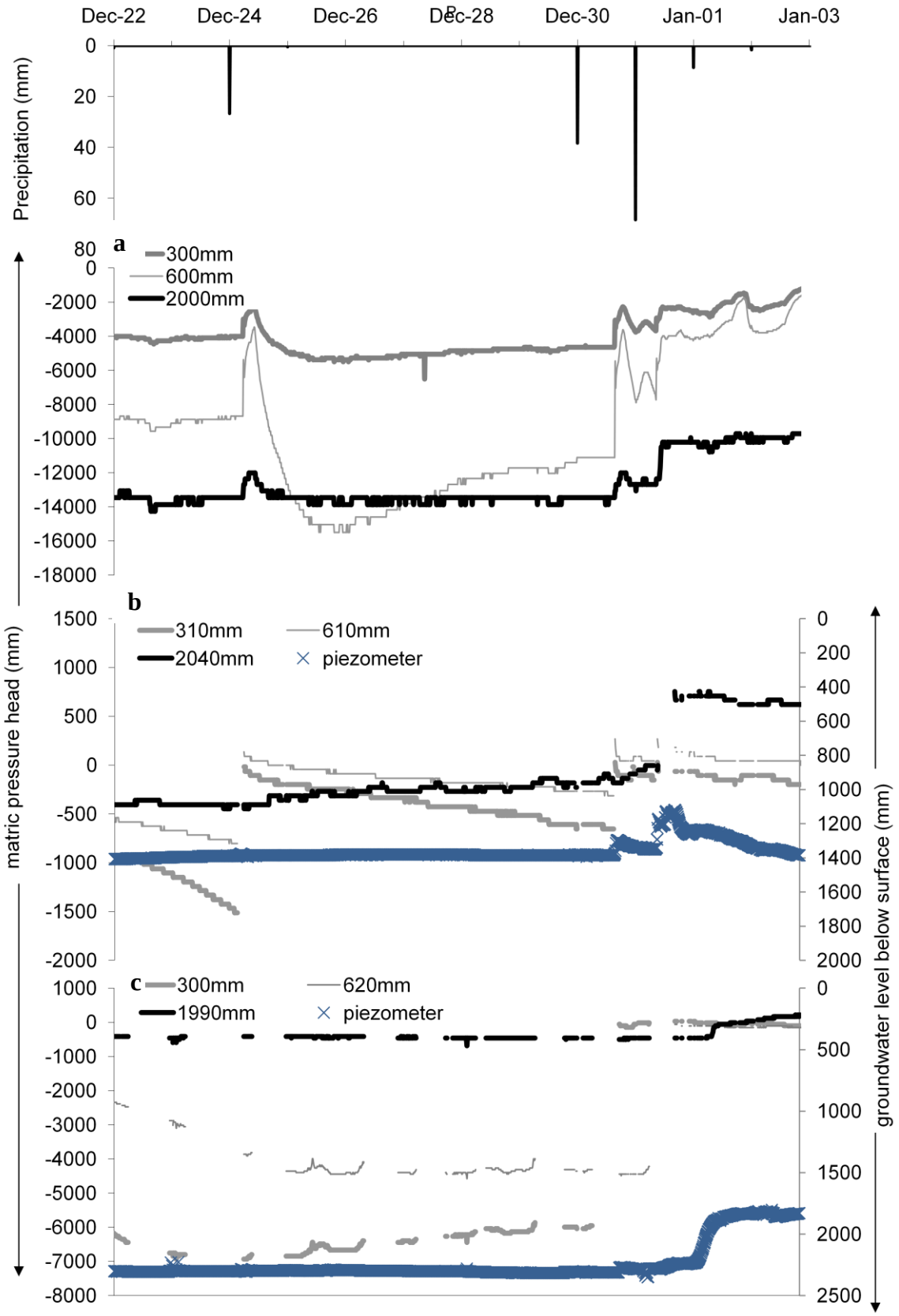

Figure 6.6: Pressure head responses for site T1_1 (a), T1_2 (b) and T1_3 (c) for the period 22/12/2006-03/01/2007 (precipitation data – onsite).

Figure 6.7 Displays how the kinematic overland flow model was applied to the overland flow intensity data from the USLE runoff plot for the events of 30-31/12/2006. Effectively the event of the 30/12/2006 was of a fairly short duration (1.5 hrs), but was relatively intense (given the limits of tipping bucket rain gauges high intensities have propensity for error[3]), with peak intensities approaching 120 mm/hr and 180 mm/hr in two successive periods within that time. This was reflected by the measured runoff plot data and resulting OFM. The second event, on the 31/12/2006 had an initial intense period, approaching 120 mm/hr, thereafter the event had a significantly prolonged duration over 24 hrs but with a steady precipitation. The resulting difference in actual rainfall and infiltration excess (overland flow) is applied as effective rainfall (total infiltration) to the model domain for that period.

Figure 6.8a-d displays the outputs of the simulations with respect to the matric pressure heads estimated at the nodes in the domain that correspond with actual installed soil moisture sensors at each location on the hillslope, along with input precipitation and evaporation-transpiration partitioning.

With respect to Figure 6.8b for the midslope representation at T1_1 we see that the model performs reasonably well at all depths, whereby both the 300 mm and 600 mm modelled nodes reveal a rise in pressure head following the on-set of rains at hour 145. This comes close to saturation at the 300 mm depth and close to -2000 mm pressure head at 600 mm. However, the modelled responses are not as instantaneous as the observed data, furthermore, the observed responses at 300 mm and 600 mm show an initial decrease in pressure head following the first precipitation input, which is followed by a steady rise in pressure head until conditions close to saturation are noted some 50 hours after the first rainfall, in response to the consistent steady precipitation during that period. These saturated conditions are realized much sooner in the modelled data. At the same time, the deeper 2000 mm observed response remains dry with a very low pressure head, however there is a rise in pressure head of some 4000 mm at the onset of the intense precipitation period, but this still stabilizes at a dry -10000 mm pressure head.

[3] Stated error range for Texas TE525M tipping bucket rain gauges are 1% upto 25mm/hr, therefore higher intensities could present larger error ranges due to spillages in the tipping bucket mechanism (for e.g. http://www.campbellsci.ca/App_Rainfall_India.html)

Table 6.1: Fitted parameters and hydraulic conductivity and water retention characteristic values for soil horizons used in model simulations (Hydraulic Conductivity and Water Retention curves plus supporting data may be found in Appendix iii).

Location	**Soil**	θ_r	θ_s	α (mm^{-1})	n	K_s (mm/hr)	l	θ_m	θ_a	θ_k	K_k (mm/hr)
wetland 0-4000mm	1	0.426	0.538	0.104	1.127	6.942	0.5	0.538	0.426	0.538	6.942
midslope 0-300mm	2	0.168	0.385	0.106	1.316	1.106	0.5	0.385	0.168	0.385	1.106
midslope 30-600mm	3	0.270	0.480	0.037	1.313	1.458	0.5	0.480	0.270	0.480	1.458
midslope 60-2000mm	4	0.335	0.537	0.019	1.638	0.478	0.5	0.537	0.335	0.537	0.478
midslope >2000mm	5	0.223	0.450	0.019	1.594	0.171	0.5	0.450	0.223	0.450	0.171
toe 0-300mm	6	0.122	0.434	0.265	1.263	7.766	0.5	0.434	0.122	0.434	7.766
toe 30-600mm	7	0.266	0.373	0.080	1.294	0.939	0.5	0.373	0.266	0.373	0.939
toe 60-2000mm	8	0.090	0.308	0.014	1.119	0.900	0.5	0.408	0.090	0.300	0.543
toe >2000mm	9	0.090	0.308	0.014	1.119	0.400	0.5	0.408	0.090	0.300	0.155

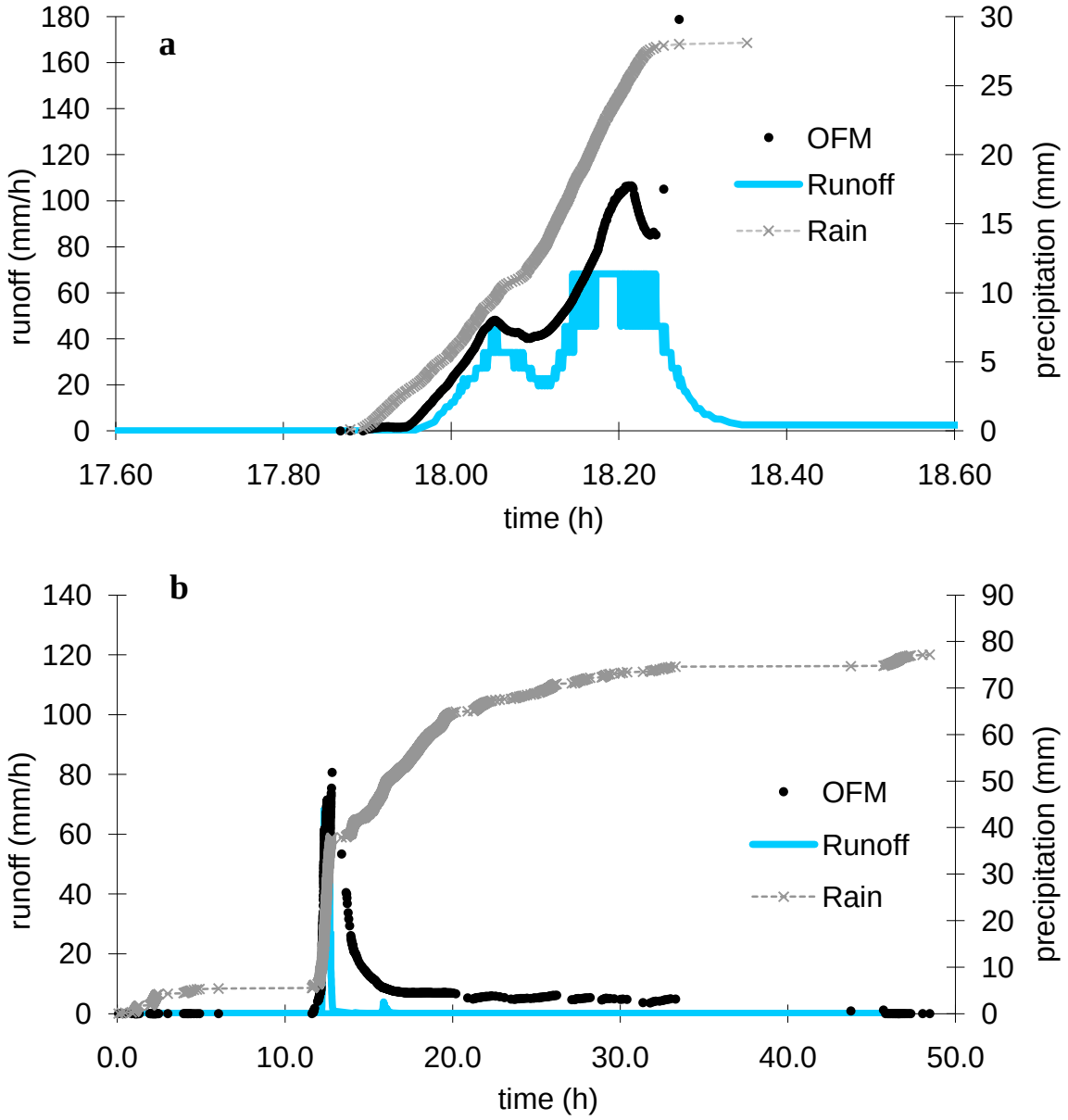

Figure 6.7: Kinematic overland flow model (OFM) as applied to rainfall intensity and overland flow intensity from 0000 hrs for event of 30/12/2006 (a) and 31/12/2006 (b). (NB. Flat-lining of the runoff plot is due to maximum volumetric capacity of the tipping mechanism being reached)

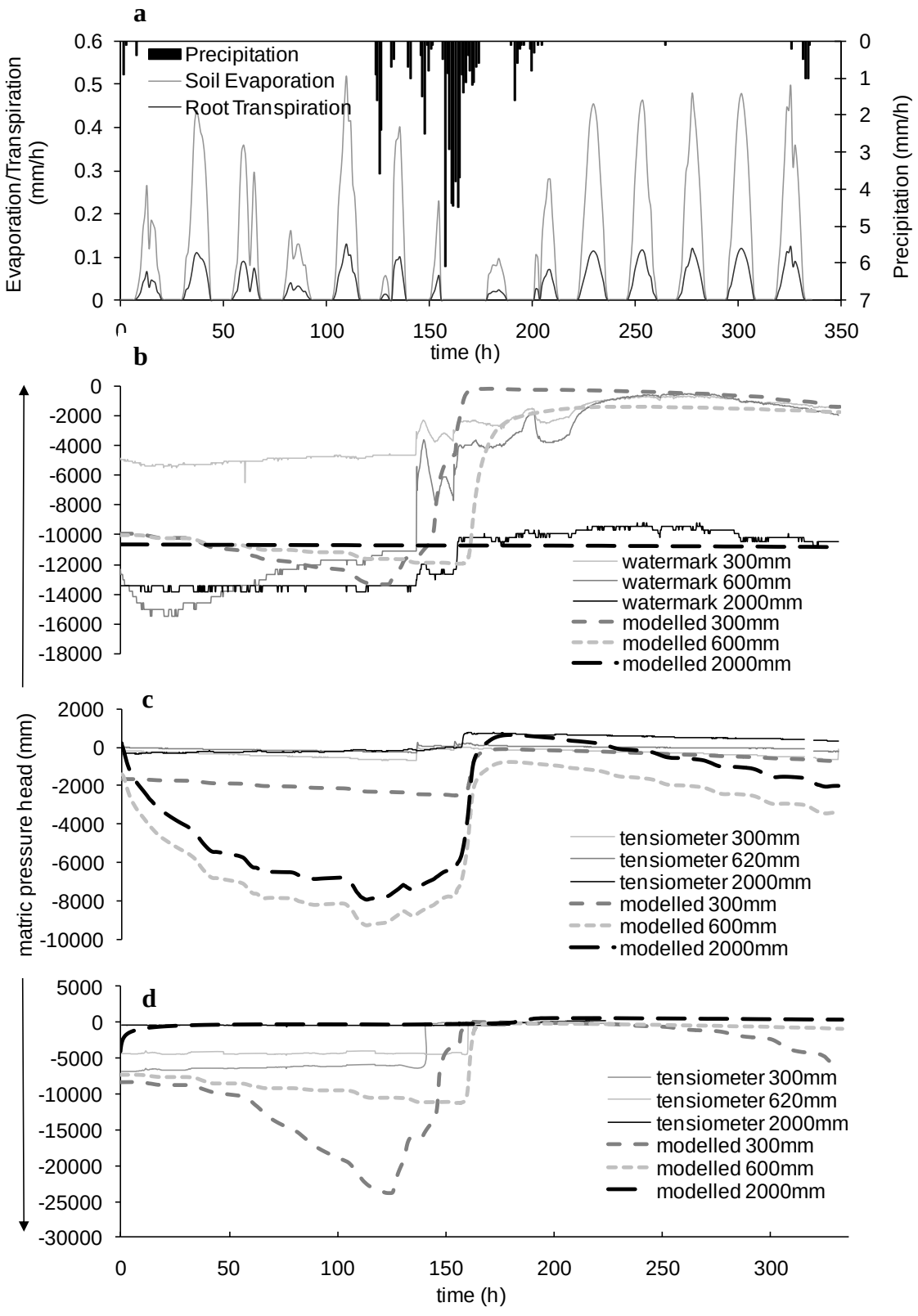

Figure 6.8: Comparison of observed and modelled responses. Input rainfall and evapotranspiration (a); T1_1 observed vs modelled (b); T1_2 observed vs modelled (c); and T1_3 observed vs modelled (d).

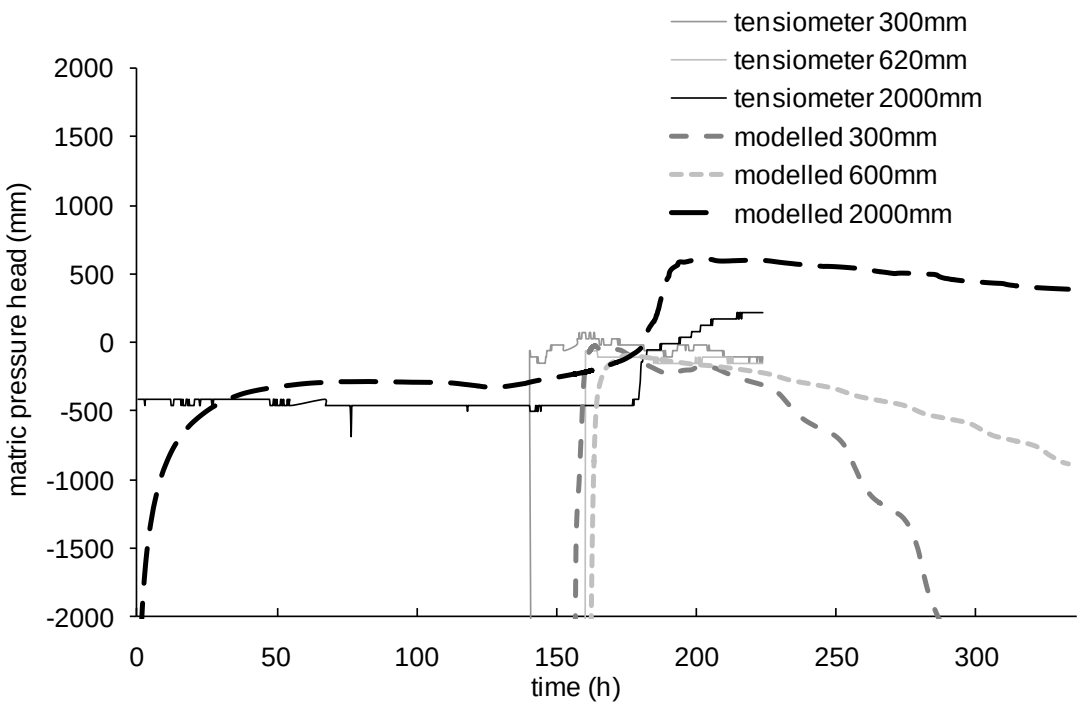

Figure 6.8e: Comparison of observed and modelled responses at and T1_3 with reduced matric pressure head range.

Meanwhile the simulated response at this depth 2000 mm remains static throughout the duration at approximately -10500 mm of pressure head.

Figure 6.8c reveals the nature of the responses at the toe-slope position. Here it is noted that all the observed locations have conditions close to saturation, which at the point of initiation of precipitation positive pressures are noted at all depths but this is particularly so for the 2000 mm tensiometer which yields a positive pressure of 1000 mm, in this case these positive pressures begin to fall after the precipitation events until the end of the simulation at 336 hours. Meanwhile, the modelled responses follow the same trend, except that despite these nodes commencing at similar high pressure heads as the observed data, in all cases the pressure heads decline markedly during the first 140 hours. This is most noticeable for the modelled responses at 600 mm and 2000 mm. However, following the initiation of precipitation the pressure heads rise very rapidly in accordance with the observed responses, except that the maximum pressure head is reached some 10 or so hours after the observed data. Importantly, the modelled 2000 mm response also yields a positive head in accordance with the observed data at the height of the rains. Similarly the modelled responses show deccreased pressure heads following the cessation of the rains. This signifies that the observed and modelled soils at this point on the hillslope are able to relinquish soil water rather rapidly after a precipitation event.

In the case of the responses observed and modelled within the wetland region (Figure 6.8d)we see that the surface soils indicated by the 300 mm and 600 mm tensiometers remain relatively dry until the onset of significant rains at hour 145, whereupon the pressure head at these positions rises considerably upon reaching conditions close to saturation. Meanwhile in terms of the corresponding modelled responses at these depths we see an initial drying out, particularly for the shallowest 300 mm node and a moderate decrease in pressure head at the 600 mm node, until the onset of rains. At hour 123, where there is an initial moderate precipitation event the response in the 300 mm modelled node is almost instantaneous with a steady rise in pressure head until saturated conditions are reached around hour 160. The 600 mm modelled node does not respond to rainfall until well after the commencement of rains, responding only at hour 160. This matches closely the observed response at the same depth, whilst the shallow node at 300 mm responds prior to the observed response. With regard to the deeper responses at 2000 mm, it may be noted that the observed and modelled data match fairly well, except that there is an initial rise in pressure head at this depth for the modelled node. Significantly however there is a rise to a positive pressure head which commences at hour 174 and 179 for the modelled and observed responses respectively. This response is more clearly revealed with a reduced y-axis matric pressure head range in Figure 6.8e. The maximum positive pressures are reached at hour 197 and 219, with pressure heads of 587 mm and 214 mm for the modelled and observed responses respectively. In both cases the move to positive pressure heads at 2000mm occurs some 30 hours after the onset of the significant rains.

In order to check the model performance and estimate the volume of water that passed out of the hillslope and into the wetland a mass balance was calculated for the hillslope, to include the mid-slope and toe-slope sections. The results of this calculation are summarised in Table 6.2. Here one observes that the product of cumulative atmospheric fluxes (soil and root evaporation) plus cumulative seepage (derived from discharge across paired nodes, recall Figure 6.2) out of the region correspond closely with the Hydrus-2D, with a 3.7% margin of error.

Table 6.2: Model mass balance information for sub-region 1 (mid-slope and toe-slope positions); where Q_a is cumulative actual evaporation flux from soil; Q_r is the cumulative actual root uptake flux; S is the seepage out of sub-region 1; and In is cumulative inflow into the model domain (summarised within Hydrus-2D).

Q_a	2.31 x 10^7mm^3
Q_r	4.96 x 10^6mm^3
S	2.67 x 10^6mm^3
$\Sigma_{(Qa:Qr:S)}$	1.55 x 10^7mm^3
In	-1.49 x 10^7mm3
Error	3.7%

6.5 DISCUSSION

The observed hydrometric data revealed that a mechanism exists through which hillslopes likely relinquish water to the valley bottom wetlands in this granitic landscape. In particular it was the noted rapid rise in soil matric pressure head to positive pressures observed at the hillslope toe soils at T1_2 that was swiftly followed by a rapid water table elevation within the wetland profile at T1_3. The soil hydraulic characteristics that were deemed to be responsible for this functionality are revealed in Appendix iii, which include actual K_{unsat}, retention data as well as the theoretical dual-porosity curves.

The results presented here reveal that this phenomenon occurred during hydrological years 2005 and 2006, although not reported here, similar observations were made during early November in HY2007 and late December during HY2008. Examination of Figure 6.6 facilitates the development of a conceptual model for this process. This follows the observed flashy nature of responses at the mid-slope region (T1_1) whereby the shallow 300 mm and 600 mm sensors reveal a rapid wetting and drying response between 24/12/06-26/12/06 and a marginal response in the deeper sensor at 2000 mm. This response implies and is supported by hydro-pedological interpretation of the catchment soils (UVS, unpublished 2008), that these soils are coarse grained and shallow, such that these slopes respond by lateral flow at the soil bedrock interface. The bedrock itself is partially fractured through weathering process, which under certain wet conditions where sufficient ponding has occurred, enables percolation into these fractures and hence rises in matric pressure head in this material on occasion, whilst in a dry state retains very

high negative matric pressure. The shallow soils on these mid-slopes are then hydraulically controlled by a vertical water balance yielding saturation excess overland flow in addition to the down-slope sub-surface lateral contributions, hence the observed and modelled data of the OFM in Figure 6.7. Meanwhile the high pressure head observed for the deep 2000 mm sensor, which increases very slowly over time at T1_2 in Figure 6.5 in conjunction with the dynamic responses of the shallower 300 mm and 600 mm sensors also suggests a hydraulically decoupled profile, initially. By this it is meant that the deeper soils at this location are consistently wet during the rain season, whilst the shallower soils have a more transient soil moisture regime. It is therefore, most likely that the deeper soils at T1_2, i.e. the G-horizon, have been recharged by soil water either from upslope contributions for instance that which moves laterally at the soil bedrock interface until reaching this clay rich material at the hillslope toe. Alternatively, these G-horizons as proposed by UVS (unpublished 2008) have been recharged by a phreatic water table surface from below. However this alternative is unlikely for two reasons; first at T1_2 there is also a 6000 mm piezometer which has remained dry throughout the monitoring period; second the 1000 mm piezometer at the same location shows a stable ponded surface at this depth with a spike in water level following the peak rainfall 30-31/12/2006 suggesting rapid water delivery from above rather than a steady delivery from below. Planned tracer analysis of stable isotopes will reveal more insight into this. It is therefore quite likely that lateral contributions from upslope render a perched region above this now saturated G-horizon and this may feasibly contribute in part to the rapid groundwater elevation as observed at the valley bottom in the wetland. However the rise in matric pressure head, to positive pressures at T1_2 in addition to the observed spike in the 1000 mm piezometer at this location at the same time suggests that this water may be moving through this G-horizon in a preferential manner. This is the reason why this region of the hillslope was modelled with a dual-porosity function.

This preferential flow through an otherwise low conductivity material of the hillslope toe at T1_2 may allow for a rapid delivery of sub-surface water into the high conductivity sandy material of the wetland at T1_3. However, whilst the model presented here represents the processes of one half of a valley i.e. one hillslope and partial cross-section of the valley bottom wetland, the true behaviour of the sensors at T1_3 merely reflects the contributing hydrological behaviour of the hillslopes either side of the wetland. Remembering the responses of T1_4 in Figure 6.5, it is known that a similar process to that modelled occurs on the opposite hillslope. Acknowledging this is imperative in the modelling process since a variable pressure head boundary was incorporated in the model domain, which comprised observed positive pressures as recorded by the piezometer at T1_3. Whilst the incorporation of this observed data at this

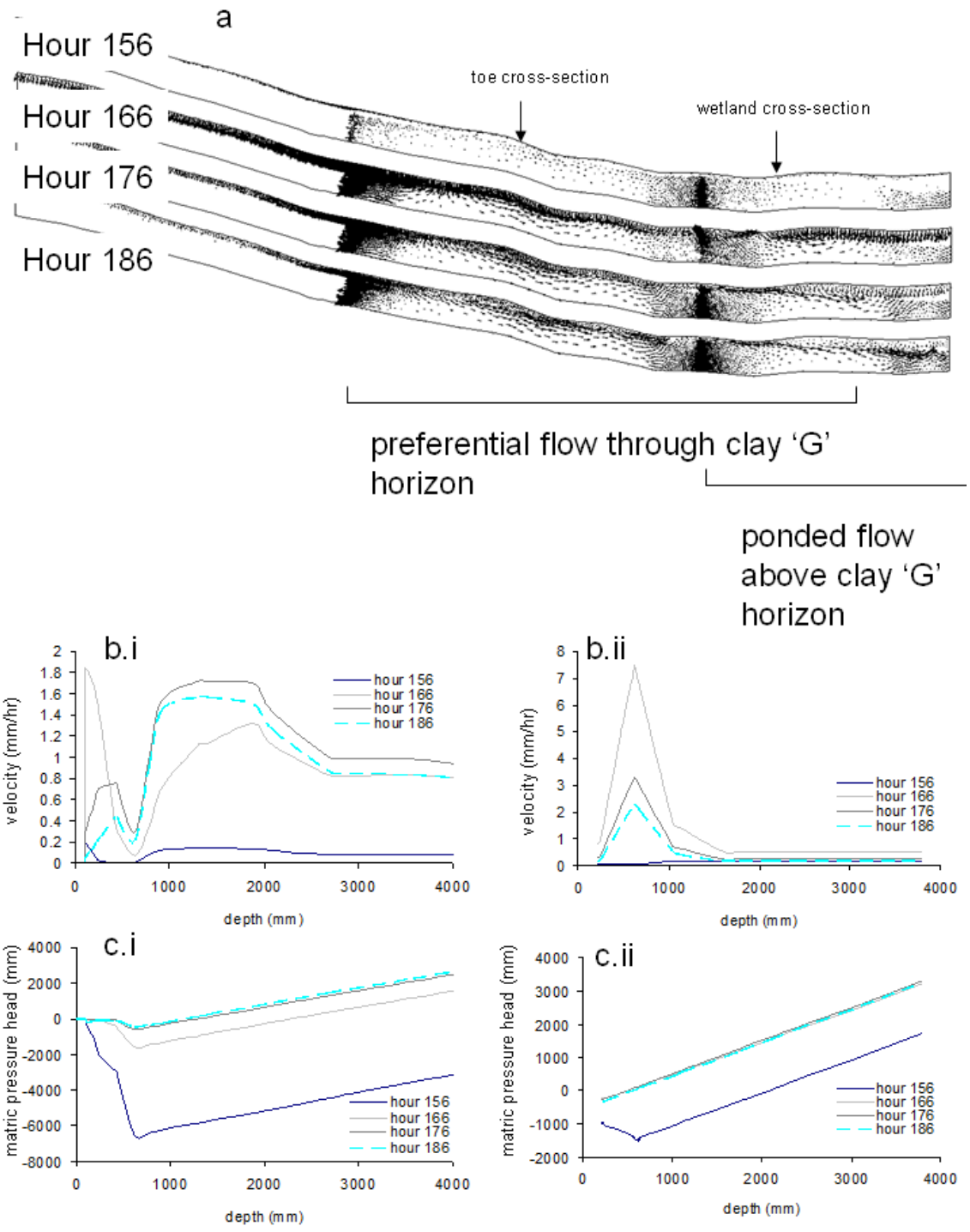

Figure 6.9: Velocity vectors in the model domain between hours 156-186 showing regions of preferential and ponded flow (a)*; velocity cross-section through profile at hillslope toe (b.i) and at wetland (b.ii); pressure head cross-section through profile at hillslope toe (c.i) and at wetland (c.ii). (*darker areas are due to increased mesh density in order to blend between soil types and facilitate model stability). NB. Recall G-horizon from Figure 6.2.

downslope boundary may imply forcing of the model outcome, model instability was reached early on during the simulation period with a no-flux boundary at this location. Meanwhile, the alternative of incorporating a free drainage boundary at this location yielded unrealistic results whereby water drained out of the hillslope domain rapidly. Hence, this was not a true reflection of the axis-symmetric water distribution of the opposite hillslope where T1_4 resides. To ensure that this variable pressure head boundary condition was not forcing the model to capitulate a move to positive matric pressure heads at the hillslope toe of T1_2 from downslope matric pressure head conditions, but rather transfer of water to the toe-slope from upslope, examination of the unsaturated flow velocities was required. Furthermore, the precise timing of responses to positive matric pressure head at T1_2 and T1_3 is also necessary.

Figure 6.9a shows the velocity vectors for the model domain just prior to the on-set of heavy rains at hour 156, with variably saturated flows proceeding the rains at hours 166, 176 and 186, whereupon the arrows indicate the direction of flow (larger arrows signify greater velocity, and more dense signifies greater volume). Meanwhile Figure 6.9b.i and b.ii show the cross-section of water flow velocity at the hillslope toe and wetland respectively, and Figure 6.9c.i and c.ii shows the equivalent matric pressure head distribution for the same cross-section. It is quite apparent from this schematic that flow is moderate in the domain prior to rains, as implied by the low density and size (related to speed, L/T) of the arrows at hour 156. Meanwhile, 10 hours after the on-set of rains at hour 166, it may be observed that whilst rain is still entering the hillslope domain through infiltration processes, as indicated by the high density of arrows at the surface, significant preferential flow via macropores is simulated through the clay rich horizon at depth. This velocity distribution is depicted graphically as shown in Figure 6.9b.i where there are greater velocities between 1000 and 2500 mm deep in the profile. This continues through to hours 176 and 186. Furthermore, it is also evident that ponded lateral flow commences between hours 166 and 176 above this clay rich horizon, as noted by the increase in arrow density mid-level in the wetland region. This is apparent in the graphical depiction of Figure 6.9b.ii, where greater flow velocities are revealed between 0-1000 mm deep. There is an observed influence to the prescribed increase in variable pressure head (at this boundary, recall Figure 6.2) which is observed at the extreme right of the section for hour 186 (arrows reversed to the left and upwelling). This is a significant amount of time after the drop in matric pressure head modelled and observed at the deep 2000 mm sensor at T1_2, which responds markedly between hours 157-169. Meanwhile the stipulated variable pressure head response at the right hand-side boundary was initiated at hour 161 and reaches its maximum at hour 193, the model responses as observed at the nodes corresponding to the stations at T1_3 were shown not to yield a response until hour 180 through to hour 191. There is therefore a lag in the model response here which cannot be attributed to forcing by implementing a greater positive pressure at the variable

pressure head boundary, this is in addition to the upslope lateral and preferential macropore contributions which occur prior to this.

The rapid water table rise in streams has been purported to result from a process known as ‘matric fringe conversion’ (Jayatilaka & Gillham, 1996) particularly in humid regions, whereupon the pressure head saturated near-stream water is converted to a phreatic state by the displacement of pre-event water during rainfall events. Although the observed rapid water table rise in the wetland and observed rise in pressure head of the toe-slope soils, which at depth were already close to saturation, could easily imply this phenomenon, the model simulation and interpretation of it’s output would render the processes more in tune with McDonnell & Buttle’s (1998) rebut that macro-pore dominated preferential flows yield this type of rapid phreatic response at a stream (or wetland). The first point of non-conformity with Jayatilaka & Gillham’s (1996) theory and model is that the Manalana, although being situated within a sub-humid fringe of the semi-arid lowveld savanna, is not characterised by very shallow water tables as one would find in humid systems. Second, as McDonnell & Buttle (1998) note, soil physics is the major limitation on the matric fringe conversion process, through which the pressure head saturated zone is controlled by the water retention, itself being a function of the texture of the soil, ranging from centimetres in the case of coarse sand through to tens of metres for fine clays. Should the Manalana hillslopes be derived of coarse sand then this matric fringe phenomenon would be a possibility, however only the valley bottom wetland is dominated by coarse sand underlain by clays at depth (>2 m). Moreover, the hillslopes toes are dominantly clay with shallow coarse sand horizons near the surface. Whilst it is likely that some matric fringe conversion does occur within these clays, which we know to be close to saturation when this rapid phreatic surface elevation process takes place, the fact that the wetland material itself is sand, and the distance between these materials and the hillslope toe materials is actually quite far (~20 m), would preclude this to be the sole driving process. It is likely that this is a minor contributing process at best. The model presented here has demonstrated that it is highly likely that it is the dominance of the preferential flow path system that controls this rapid water induction process to the wetland. Indeed, the author’s themselves have noted during particularly wet occasions, the occurrence of small pipe-flow springs along eroded surfaces of the hillslope toe where the clay rich G-horizon has been exposed.

Despite the satisfactory outcome of this deterministic model in confirming the dominance of a preferential flow system and ponded flows at the hillslope toe in these catchments, certain model outcomes remain questionable. First is the significant decrease in matric pressure heads for most modelled nodes at the outset of the simulation, which is seen for the T1_1 300 mm and 600 mm model nodes. But particularly noticeable drying out was observed at the 600 mm and

2000 mm nodes of the hillslope toe at T1_2 and 300 mm and 600 mm nodes in the wetland at T1_3, up to the onset of major rains at hour 156. Since this is not seen in the observed responses, it would suggest that the model configuration relinquishes a certain amount of free drainage or exacerbated anisotropy than would occur naturally. Besides this, it would also be expected that these deep nodes in the low conductivity clay material at T1_2 would not yield such a significant rise in pressure head (some 8000 mm). This implies that because the starting conditions at this location were close to saturation, similar to the observed situation, the dual porosity function had already been invoked in this material at the start of the simulation causing unhindered drainage. The outcome of the model responses in this region of the domain following the intense rains proceeding hour 156 therefore represent a threshold induced response to rainfall input rather than a threshold antecedent soil moisture condition per se, which would not be unfounded and has indeed been noted elsewhere e.g. Tromp van Meerveld & McDonnell (2006b). This response is noteworthy and represents an added issue of complexity that constantly evades the process hydrologist when trying to simulate macropore dominated flow. Furthermore, since macropore-facilitated preferential flow is not a static process spatially, as it is known that macropore conduits may change in size and state of connectivity as a result of varying soil moisture conditions (Sidle *et al.*, 2001), and as has been shown just trying to simulate the correct antecedent response in two dimensions is a challenge enough.

The second shortcoming of the models performance relates to the magnitude of the difference in pressure heads between those modelled and those observed. It is most likely that this relates to a combination of the prescribed starting condition, which used a linear distribution of pressure head from the lowest located nodal point. In addition the soil heterogeneity of the model domain and lack of scaling factors deployed in the model may well have contributed to this. Meanwhile, it may also be possible that an increase in mesh density, to greatly increase in the number of connected nodes may also help solve this problem, which would be limited however by computer processing power.

All this being said, the incorporation of the soil heterogeneities in the model developed here reveals that a relatively robust performance of the hillslope simulation was achieved and this exercise rather highlights the areas were future deterministic hillslope model development can focus its attentions, particularly in terms of the antecedent preferential flow controls.

6.6 A NOTE ON THE POTENTIAL IMPACTS OF LAND-USE

Whilst this paper has determined the mechanisms through which wetland recharge is facilitated in the Manalana catchment and it is most probable that other wetlands within the particular geological template at the headwaters of the Sand River operate in a similar fashion, the context under which it operates must be discussed. It needs to be remembered that these wetlands, including the hillslope toe-wetland interfaces, are used extensively for subsistence agriculture. The interface zone is most often mechanically altered to form small tillage plots for the cultivation of staple crops. Schaetzel & Anderson (2005) state that soil disturbance of this nature, *anthroturbation*, causes the development of an *agric* soil horizon immediately below the newly mixed (tilled) zone of the soil. The result is an enriched agric horizon composed of illuviated clays, silts and organic matter, which may significantly affect the macroporosity properties of the underlying soil horizons. It is is these macropore-preferential flow paths, such as cracks or worm holes, that will quickly fill up with sediment. The implications of which is a reduction in *Ks* of the soil medium. Similar processes have been reported for the interfluves of agricultural wetlands (bas-fonds) in Benin where a stark decrease in *Ks* was reported between the natural savanna and that converted to agriculture surrounding these wetlands (Giertz & Diekkrüger, 2003). This was also noted for the toe-slope plinthosols which are similar to planosols in that they have two high permeability horizons above a low permeability lower horizon, a plinthic crust for the former and illuviated clays in the case of the latter (G horizon in this case). Therefore not only is it highly likely that the preferential flow properties of the hillslope toe soils of the Manalana catchment will be impacted, particularly if tillage occurs to depth, but that the ponded-lateral flow mechanism above the low permeable horizon will also be impacted, likely in favour of a significant reduction of transmissivity. Speculation on the effects of this to threshold inducement of rapid wetland recharge is now certainly warranted and should lead to research objectives to understand these impacts further. Although it would seem likely that there would be a reduced propensity for the hillslopes to transmit water under threshold precipitation events, and under certain antecedent conditions, resulting in more water being stored in the hillslope in time and space. This would possibly lead to exacerbated saturation overland flows, as an initial hypothesis. What this means for hydrodynamic variability within the wetland and ultimately to broader catchment streamflow processes one can only guess at this stage, but this is certainly a realm of enquiry that the hydrologists and hydropedologists should think about in the future.

6.7 CONCLUSION

The use of a deterministic physically based model to aid in the interpretation of observed hydrometric responses has shown the versatility of this finite-element modelling framework for hillslope process simulations. Furthermore it has proved extremely useful to develop our process understanding at the scale of the hillslope within these heavily utilised wetland catchments. The uncovering of a threshold controlled dual-porosity and perched water table dynamic that yields rapid wetland hydrological responses has revealed that this process based understanding at the small scale if the hillslope has important ramifications for the way that these catchments should be utilised in the future. This being in terms of minimising further conversion of the wetland-hillslope toe soils (Kroonstad) and indeed ameliorating degradationary processes afflicting these wetlands and their contributing catchments, by now revealing which hillslope units are important for certain hydrological processes and examining ways in which any degraded hillslope units may also be rehabilitated in terms of their hydrology and soil genesis.

ACKNOWLEDGEMENTS

The authors are grateful to the South African Water Research Commission (WRC) and National Research Foundation (NRF) for financial support. The kind assistance of the following people for field assistance, data processing and interpretation is duly acknowledged; Mr Ronny Maaboi, Mr Rex Mothlabini, Professor Pieter Le Roux (University of Free State), Mr Cobus Pretorius (University of KwaZulu-Natal), Mr Sean Thornton-Dibb (University of KwaZulu-Natal). Logistical and administrative support was provided by the Association for Water and Rural Development (AWARD).

REFERENCES

Allen RG, Pereira LS, Raes D, Smith M. 1998. Crop evapotranspiration - Guidelines for computing crop water requirements. FAO Irrigation and drainage Volume paper 56. FAO - Food and Agriculture Organization of the United Nations, Rome

Ankeny MD, Ahmed M, Kaspar TC, Horton R. 1991. Simple Field Method for Determining Unsaturated Hydraulic Conductivity. Soil Science Society of America Journal 55 : 467-470.

Bodhinayake, W, Si BC, Noborio K. 2004. Determination of Hydraulic Properties in Sloping Landscapes from Tension and Double-Ring Infiltrometers. Vadose Zone Journal 3 : 964-970.

Bowden WB, Fahey BD, Ekanayake J, Murray DL. 2001. Hillslope and wetland hydrodynamics in a tussock grassland, South Island, New Zealand. Hydrological Processes 15 :1707-1730.

Brooks RH, Corey AJ. 1964. Hydraulic properties of porous media. Hydrology Paper 3, Colorado State University, Fort Collins, CO.

Devito KJ, Hill AR, Roulet, N. 1996. Groundwater-surface water interactions in headwater forested wetlands of the Canadian Shield. Journal of Hydrology 181 : 127-147.

FAO 1998. World Reference Base for Soil Resources. Rome Food and Agriculure Organization of the United Nations FAO, International Society of Soil Science ISSS-AISS-IBG, International Soil Reference Group.

Frisbee MD, Allan CJ, Thomasson MJ, Mackereth R. 2007. Hillslope hydrology and wetland response of two small zero-order boreal catchments on the Precambrian Shield. Hydrological Processes 21 : 2979 2997

Giertz S, Diekkruger B. 2003. Analysis of the hydrological processes in a small headwater catchment in Benin West Africa. Physics and Chemistry of the Earth 28 : 1333-1341.

Jayatilaka CJ, Gillham RW. 1996. A deterministic-empirical model of the effect of the capillary fringe on near-stream area runoff 1. Description of the model. Journal of Hydrology 184 : 299-315.

Johnson MR, Anhausser CR, Thomas RJ.Eds. 2006 The Geology of South Africa. Geological Society of South Africa, Johannesburg/Council for Geoscience, Pretoria,.-691.

Kirkby M, Bracken L, Reaney S. 2002. The influence of land use, soils and topography on the delivery of hillslope runoff to channels in SE Spain. Earth Surface Processes and Landforms 27 : 1459-1473.

Kotze D, Silima V. 2003. Wetland cultivation reconciling the conflicting needs of the rural poor and society at large through wetland wise use. International Journal of Ecology and Environmental Science 29 : 65-71.

Lorentz SA, Goba P, Pretorius J. 2001. Hydrological Processes Research: experiments and measurements of soil hydraulic characteristics. Water Research Commission, Pretoria, South Africa. WRC Report K5/774

Lorentz S, Thornton-Dibb S, Pretorius JJ, Goba P. 2003. Hydrological Systems Modelling Research Programme Hydrological Processes, Phase II Quantification of Hillslope, Riparian and Wetland Processes, Report to the Water Research Commission on the Project A Field Study of Two and Three Dimensional Processes Water Research Commission, Pretoria, South Africa WRC Report K5/1061

Lorentz SA, Bursey K, Idowu O, Pretorius C, Ngeleka K. 2008. Definition and Upscaling of Key Hydrological Processes for Application in Models. Water Research Commission, Pretoria. South Africa. WRC Report K5/1320/1/08

Martinez-Mena M, Castillo V, Albaladejo J. 2001. Hydrological and erosional response to natural rainfall in a semi-arid area of south-east Spain. Hydrological Processes 15 : 557-571.

McCartney MP, Neal C. 1999. Water flow pathways and the water balance within a headwater catchment containing a dambo inferences drawn from hydrochemical investigations. Hydrology and Earth Systems Sciences 3(4) : 581-591.

McCartney MP, 2000. The Water Budget of a Headwater Catchment containing a Dambo. Physics and Chemistry of the Earth B 25(7-8) : 611-616.

McDonnell JJ, Buttle JM. 1998. Comment on A deterministic-empirical model of the effect of the capillary-fringe on near-stream area runoff. 1. Description of the model by Jayatilaka, CJ. and Gillham, RW. Journal of Hydrology Vol. 184 1996 299-315. Journal of Hydrology 207 : 208-285.

McDonnell JJ. 2003. Where does water go when it rains? Moving beyond the variable source area concept of rainfall-runoff response. Hydrological Processes 17 : 1869-1875.

McFarlane MJ. 1992. Groundwater movement and water chemistry associated with weathering profiles of the African surface in parts of Malawi. In (eds) Wright EP, Burgess WG. Hydrogeology of Crystalline Basement Aquifers in Africa. Geological Society, London, Special Publications v66 101-129

Mualem Y. 1976. A New Model for Predicting the Hydraulic Conductivity of Unsaturated Porous Media. Water Resources Research 12(3) : 513-522.

Newman BD, Campbell AR, Wilcox BP. 1998. Lateral sub-surface flow pathways in a semiarid ponderosa pine hillslope. Water Resources Research 34(12) : 3485-3496.

Nicolau JM. 2002. Runoff generation and routing on artificial slopes in a Mediterranean-continental environment the Teruel coalfield, Spain. Hydrological Processes 16 : 631-647.

Pollard S, Kotze D, Ellery W, Cousins T, Monareng J, King K, Jewitt G.. et al, 2005. Linking Water and Livelihoods The development of an integrated wetland rehabilitation plan in the communal areas of the Sand River Catchment as a test case
Association for Water and Rural Development URL http//www.award.org.za/wetlandsoct04.pdf (January 2010)

Reuter RJ, Bell JC. 2003. Hillslope hydrology and soil morphology for a wetland basin in South-Central Minnesota. Soil Science Society of America Journal 67 : 365-372.

Ridolfi L, D'Odorico P, Porporto A, Rodriguez-Iturbe I. 2003. Stochastic soil moisture dynamics along a hillslope. Journal of Hydrology 272 : 264-275.

Schaetzl R, Anderson S. 2005. Soils Genesis and Geomorphology. Cambridge University Press. Cambridge, UK. p817.

Sidle RC, Tsuboyama Y, Noguchi S, Hosoda I, Fujieda M, Shimizu T. 2000. Stormflow generation in steep forested headwaters a linked hydrogeomorphic paradigm. Hydrological Processes 14 : 369-385.

Šimúnek J, Šejna M, van Genuchten M.Th., 1999. The HYDRUS-2D software package for simulating water flow and solute transport in two-dimensional variably saturated media. U.S. Salinity Laboratory. Riverside, California

Sivapalan M. 2003. Process complexity at the hillslope scale, process simplicity at the watershed scale is there a connection? Hydrological Processes 17 : 1037-1041.

SOIL CLASSIFICATION WORKING GROUP, 1991. Soil classification a taxonomic system for South Africa.. Memoirs on the Agricultural Natural Resources of South Africa Ed. Memoirs on the Agricultural Natural Resources of South Africa No. 15. SIRI, D.A.T.S., Pretoria.

Tetzlaff D, McDonnell JJ, Uhlenbrook S, McGuire KJ, Bogaart PW, Naef F, Baird AJ, Dunn SM, Soulsby C. 2008. Conceptualizing catchment processes simply too complex?. Hydrological Processes 22 : 1727-1730.

Tromp-van Meerveld HJ, McDonnell JJ. 2006. Threshold relations in sub-surface stormflow 1. A 147-storm analysis of the Panola hillslope. Water Resources Research 42 doi:10.1029/2004WR003778

Tromp-van Meerveld HJ, McDonnell JJ. 2006. Threshold relations in sub-surface stormflow 2. The fill and spill hypothesis. Water Resources Research 42 doi:10.1029/2004WR003800

Uhlenbrook S. Wenninger J. Lorentz S. 2005. What happens after the catchment caught the storm? Hydrological processes at the small, semi-arid Weatherley catchment, South Africa. Advances in Geosciences 2 : 237-241.

van Genuchten M.Th. 1980. A Closed-form Equation for Predicting the Hydraulic Conductivity of Unsaturated Soils. Soil Science Society of America Journal 44 : 892-898.

van Genuchten M.Th, Leij FJ, Yates SR. 1991. The RETC Code for Quantifying the Hydraulic Functions of Unsaturated Soils. U.S. Salinity Laboratory, USDA, ARS, Riverside, California.

Vogel T, Cislerova M. 1988. On the reliability of unsaturated hydraulic conductivity calculated from the moisture retention curve. Transport in Porous Media 3(1) : 1-15.

von der Heyden CJ, New MG. 2003. The role of dambo hydrology of a catchment and the river network downstream. Hydrology and Earth Systems Sciences 7(3) : 339-357.

Weiler M, McDonnell J. 2004. Virtual experiments a new approach for improving process conceptualization in hillslope hydrology. Journal of Hydrology 285 : 3-18.

7 EXAMINATION OF WETLAND STREAMFLOW CONTROL VARIABLES USING CONCEPTUAL HYDRO-PEDOLOGICAL PROCESSES ON HILLSLOPES AND TESTED IN A DISTRIBUTED PHYSICALLY-BASED CATCHMENT MODEL

Riddell, E.S.[1], Lorentz, S.A.[1], Le Roux, P.A.L.[2]

[1] School of Bioresources Engineering and Environmental Hydrology, University of KwaZulu-Natal, Private Bag X01, Scottsville, Pietermaritzburg, 3209, South Africa

[2] Department of Soil-, Crop- and Climate Sciences, Faculty of Natural and Agricultural Sciences University of the Free State, PO Box 339, Bloemfontein , 9300, South Africa

ABSTRACT

The addition of new soil hydrology sub-routines to a distributed hydrological model, the ACRU agrohydrological modelling system, a commonly applied model in southern Africa, were applied to a headwater wetland catchment of the Sand River, South Africa. The inclusion of non-linear advection dispersion functions (ADFs) to inferred hydrological processes at the hillslope scale, through the incorporation of hydro-pedological principles was applied at the scale of delineated hillslope response units in the catchment. These functions have the potential to enhance the traditional linear fill-and-spill type soil compartment responses of previous versions of ACRU. The new ACRU_Int model as it is now known was, through the application of hydro-pedological principles able to simulate with a very reasonable accuracy the low-flow inter-rainfall periods for the period of simulation. This assessment was made in the context of inter-comparison with the traditional ACRU2000 model, which failed to yield satisfactory low-flow responses. However ACRU_Int did fail to respond to low intensity threshold triggers of peak flow and possible reasons for this are discussed. Overall the potential for the integration of hydro-pedological interpretations of hillslope hydrological processes within distributed hydrological applications has shown significant promise with this research.

Keywords: Hydro-pedology, Advection-Dispersion Functions, ACRU, hillslopes, streamflow

7.1 INTRODUCTION

The vast majority of hydrological processes-orientated research has focused on the temperate climate zone, whilst tropical and sub-tropical areas have had only a very limited exposure to this field of research (Giertz & Diekkrüger, 2003). Semi-arid and dry sub-humid savannas of the globe are currently experiencing extensive population and agricultural water resource pressure (Falkenmark & Rockström, 2004). Since we are now moving into an era of adaptive management of ecosystems where information on state change thresholds are a prerequisite for their sustained management, it is necessary to invest in understanding the biophysical processes which maintain these systems and the anthropogenic pressure that they can withstand. In other words, an ecosystem approach to the management of water resources should allow society to harness the functioning of ecosystems and therefore ensure the sustainable use of resources, services and goods that they provide (Jewitt, 2002). Included in the biophysical template of a system is, of course, the hydrological process regimen that largely controls the distribution of water and other resources in the landscape, and given that landscapes, for the most part, are highly heterogeneous, then there is a requirement for a degree of understanding regarding the dominant processes operating at a variety of scales within them. Pertinent to this understanding is the acknowledgement of a continuum of processes throughout scales within the landscape which are often compound effects of non-linear relationships and threshold-triggered responses. Given this complexity, it has been proposed that novel interdisciplinary approaches be sought to understand hydrological processes in a heterogeneous landscape (Troch *et al*., 2008). Moreover, defining these processes in an interdisciplinary context is becoming increasingly valuable for successful landscape management given the emphasis on connectivity within a landscape (Michaelides & Chappell, 2009).

Concurrent interest in the management of low-flows particularly in semi-arid regions of the world, such as South Africa, has spurned a plethora of applied scientific endeavour into this field. This has been the subject of an extensive review by Smakhtin (2001) which, at the outset, highlighted the importance of catchment geology in governing the mechanism by which storage and transmission of water takes place, particularly during dry periods when the importance of low-flows for river health may be elevated. Determining these functions is crucial in terms of predictability and natural flow estimation of rivers.

Nevertheless, despite the seemingly chaotic organisational properties of the geological landscape, there is structure and organization across spatial and temporal scales, and when the how's and why's are understood this should facilitate improved hydrologic predictability in models (e.g. McDonnell *et al.,* 2007). For this reason hydro-pedology has been suggested as a vital interdisciplinary science for contributions to the earth's critical zone (Lin, 2009) which may be defined as the earth's outer layer including vegetation canopy and the surface and groundwaters in a watershed. Whilst the fields of pedology and hydrology have traditionally been mutually exclusive, there is a need for the soil scientist to benefit from flow theory when transcribing qualitative descriptions into quantitative expressions, a prerequisite for modern policy formulation, and in *vice-versa* for the hydrologist for developing representative pedo-transfer functions in hydrological modelling (Bouma, 2006). Increasingly, the marrying of these two disciplines is proving most valuable for conceptualisation and quantification of hillslope and catchment hydrological processes. For instance, Ticehurst *et al* (2007) found that soil morphological characteristics, most notably soil colour and presence of redox concretions were useful for indicating locations and depths where saturation and lateral flow occur on hillslopes in New South Wales, Australia. Testing their conceptual flow path model against hillslope networks of piezometers and flumes yielded satisfactory agreement, but they warned that further catchment information should be sought to reduce model uncertainty, such as the geomorphic context of the region in question as well as insights from land users in the area.

Taking this approach to the next level has been the domain of the hydropedologist, as well as the theoretical hydrologist in recent years, most notably by translating catchment soils information in the form of hydrological processes and responses to effective parameter development in catchment modelling frameworks. Whilst there is of course the acknowledgment amongst hydrologists that catchment modelling requires accounting for the great heterogeneity of the catchment subsurface in addition to the traditional use of controlling surface topography, there have been a variety of modelling and theoretical approaches to account for controls within the sub-surface.

Attention has been placed on issues such as equifinality and site uniqueness in catchment based modelling (Beven, 2000), particularly in emphasising that reproduction of catchment runoff alone is not necessarily a satisfactory outcome of the modelling exercise. This is due to the significant likelihood that physical processes at the small scale are not encapsulated within the larger scale of the model grid or framework, and hence it may be that a satisfactory outcome is achieved in modelling simply by an accident of over-parameterization. It has been advocated

that the use of perceptual hydrological models, whilst being largely qualitative conceptualisations, offer the potential for model development based on process understanding of key zones or 'reservoirs', and that this 'soft' data can be married to the 'hard' hydrological observations (streamflow, soil water content) to facilitate the reduction in parameter uncertainty (Seibert & McDonnell, 2002; Lorentz *et al.*, 2003). Moreover, Seibert & McDonnell (2002) went so far as to suggest, through their use of a 3-box catchment model, that it may indeed be valid to accept lower efficiencies in modelling runoff if one is able to derive a more accurate representation of the real world processes within the catchment. For instance, Seibert *et al.* (2003) then tested their modelled process perceptions against observed isotope data with satisfactory results.

Sivapalan (2003) asked why watershed hydrological responses were seemingly simple and hillslopes comparatively complex, but suggested that by aggregating these hillslope complexities into dominant processes we could parameterise the hillslope as the basic unit within the catchment model. This suggestion was soon followed by novel approaches such as the derivation of hillslope similarity through the hillslope Peclét number (Berne *et al.*, 2005) which is a dimensionless representation of the dominant hillslope process, or the characteristic response function (CRF). Moreover, Lyon & Troch (2007) took this a stage further by testing this on real world hillslopes and found that estimating the Peclét number for a given hillslope does not require explicit determination of parameters such as conductivity and porosity, but more simply requires information on average hillslope storage, based on geomorphological controls of hillslope elevation and soil depth. This conforms with the recommendations of Kampf and Burges (2007) who note that when considering which processes to represent in a model, it is necessary to seek balance between a comprehensive representation of dominant flow processes whilst having a minimum number of parameters, and more specifically with attention given the importance (or dominance) of process. Furthermore, these should be manifested at the appropriate scale, and in this case the hillslope response type unit is probably the most appropriate. What is more, Pachepsky *et al*.,(2006) suggest that whilst hydrological modelling can learn a lot from the field of pedology, this opens the door to further pedological development in terms organizing or classifying soil (and hillslope) behaviours that are useful to the hydrologist.

The ACRU Agrohydrological Modelling System (Schulze, 1995) is a daily, multi-layer soil water budgeting total evaporation model, and has been used extensively in southern Africa and internationally, and is versatile in that it has been tested on a wide variety of water resource

applications. These include, for instance, afforestation streamflow reduction assessments (Jewitt & Schulze, 1999), montane grassland water budgeting (Everson, 2001) and climate and land-use change scenario modelling (Schulze, 2000). Whilst the ACRU model has proved worthy of simulating streamflow at the catchment scale by the inclusion of linear storage reservoirs, it has been suggested that the contributions of surface and subsurface flow that are now quantified at the scale of the hillslope catena may be better represented within the ACRU model by the means of non-linear advection-dispersion function (ADF) routines in order to capture for instance threshold induced, event based lateral discharge, macropore and/or groundwater recharge of sub-surface water (Lorentz *et al*., 2003, 2008). By reducing the number of hydrological parameters, in the aspirant spirit of reducing the likelihood of problems associated with equifinality in catchment based models (Beven, 1996) a research version of the ACRU model has been developed in recent years that represents these well observed ADF functions in research catchments in South Africa. This model builds upon the presently used java version of the ACRU model (ACRU2000) by incorporating a third 'intermediate' soil layer below the traditional A and B soil horizons and above the groundwater store, which in its developmental form is referred to as the ACRU Intermediate Zone model (ACRU_Int). The routing of soil water is in ACRU_Int is shown schematically in Figure7.1.

Specifically, the ACRU_Int model incorporates time dependant unit response functions applied to different components of flow in these 4 compartment land segments, which are convoluted with an excitation function (related to excess rainfall) to initiate runoff response by lateral, preferential (macropore) and groundwater means. Essentially what this means is an introduction of non-linear transfer functions into the ACRU model to potentially replace the linear functions of fluxes between storage-boxes that govern soil compartment hydrological processes in the traditional ACRU2000 model. These take the form of the convolution integral in equation 1.

(7.1) $$q_{out} = \int_0^{\infty} g(\delta(t - t').dt'$$

Where:

$\delta(t)$ = the excitation function, (e.g. the time series of excess rainfall, i_e) dependant on time, t,

$g(t)$ = the unit response function

q_{out} = the runoff response.

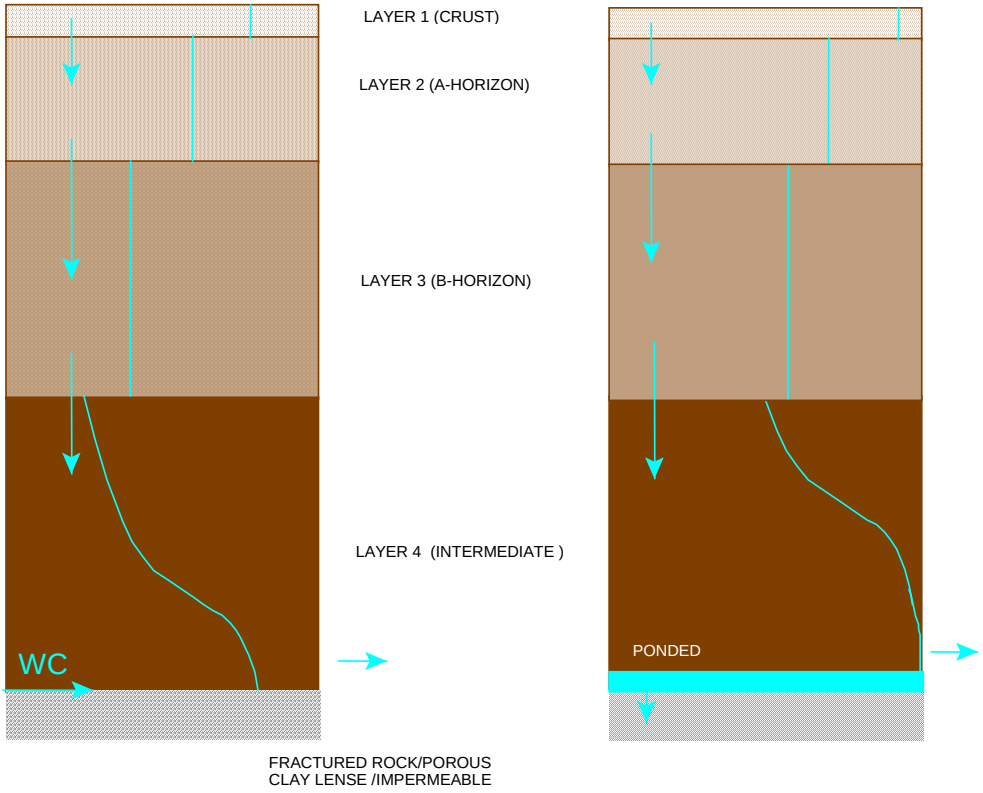

Figure 7.1: Schematic representation of an intermediate layer showing the progressive accumulation of water at the base of the layer, prior to the onset of lateral and vertical discharge. The water volume is distributed within the layer as an equilibrium retention characteristic (Lorentz *et al.*, 2008)

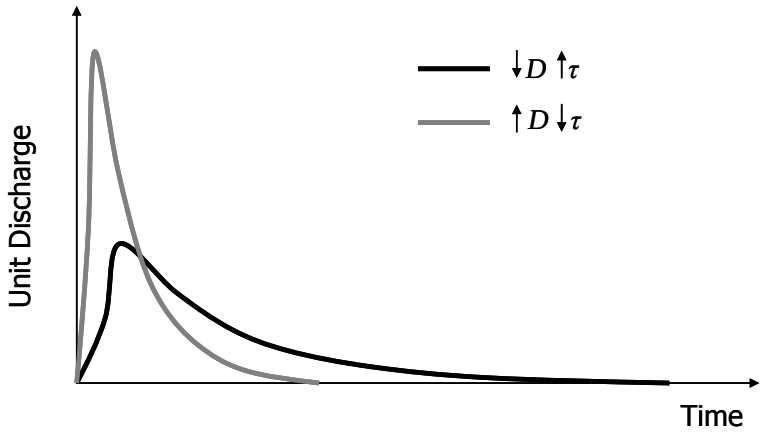

Figure 7.2: Example of varying parameters for D and t in the convolution integral for soil compartment discharge.

Whilst, a typical unit response time distribution would be represented by the exponential advection-dispersion of equation 7.2.

(7.2) $$g(t) = \left(\frac{4\pi D\tau}{\tau} \right)^{-1/2} t^{-1} e^{(-1(1-t/\tau)^2 \tau/(4/Dt))}$$

D = the dispersion coefficient, describing the spread of travel times

τ = response time.

These functions are represented schematically in Figure 7.2 for hypothetical values of D and τ, whereby decreasing the dispersion coefficient and increasing the response time of unit discharge from a soil compartment within a land segment results in a lower unit response and longer recession time for discharge, as a result of the convolution integral, and vice-versa if one increases the dispersion coefficient and decreases the response time.

7.2 METHODS

The catchment in discussion is the Craigieburn-Manalana, one of many small micro-catchments at the headwaters of the Sand River (within the Incomati Basin) in Mpumalanga, South Africa. This area is characterized by strongly seasonal rainfall occurring primarily between October-March, leading to very dry winters. This catchment, as well as the vast majority of others in the vicinity of the Sand Rivers headwaters, is experiencing severe wetland degradation through gullying and consequent desiccation due to extensive resettlement programs of a bygone era. This erosion gullying is due to excessive land-use pressure through ungoverned, largely subsistence, agriculture compounded by an easily erodible geology (granite) and steep catchments, and being in a region that experiences intense rainfall events at the foothills of the Klein Drakensberg escarpment. This site has been the focus of on-going integrated wetland rehabilitation monitoring since 2005 (Pollard *et al*., 2006, Riddell *et al*., 2007), and for this purpose was instrumented with a comprehensive suite of hydrological apparatus for hillslope and wetland mass balance determination, of which the following were utilized for this study:

Rainfall: These data were recorded using a 0.1 mm Texas Electronics^{TM} TE525 tipping bucket rain gauge, adjacent to an automatic weather station using a CR200 Campbell Scientific Inc. data logger. Intra-catchment spatial variability in rainfall was assumed negligible for the purpose of this study due to the very small catchment area (0.197 km^2).

Evaporation: the automatic weather station recorded wind speed (RM Young. Co. 03001 Wind Sentry); solar radiation (apogee instruments PYR pyranometer); and relative humidity with temperature (Campbell Scientific, Inc. HMP50 sensor). These variables allowed for the derivation of hourly Penman-Monteith potential evapotranspiration, pET (Allen *et al.*, 1998), this being tallied up to a daily total pET.

Due to loss of sensitivity of the solar radiation and humidity sensors by the 2008-09 season the pET data showed an annual incremental decrease in hourly pET values. Thus the data was patched using the nearest available RH record from the SAWS Hoedspruit station (35.9 km at 10.36° north of the site). Since there was no available pyranometer nearby a simple correction was made (assuming a linear decline in sensitivity overtime) to this data by deriving the slope of the hourly decline over the annual data set and adding the inverse of this value to actual hourly recorded solar radiation data (example see Figure 7.3).

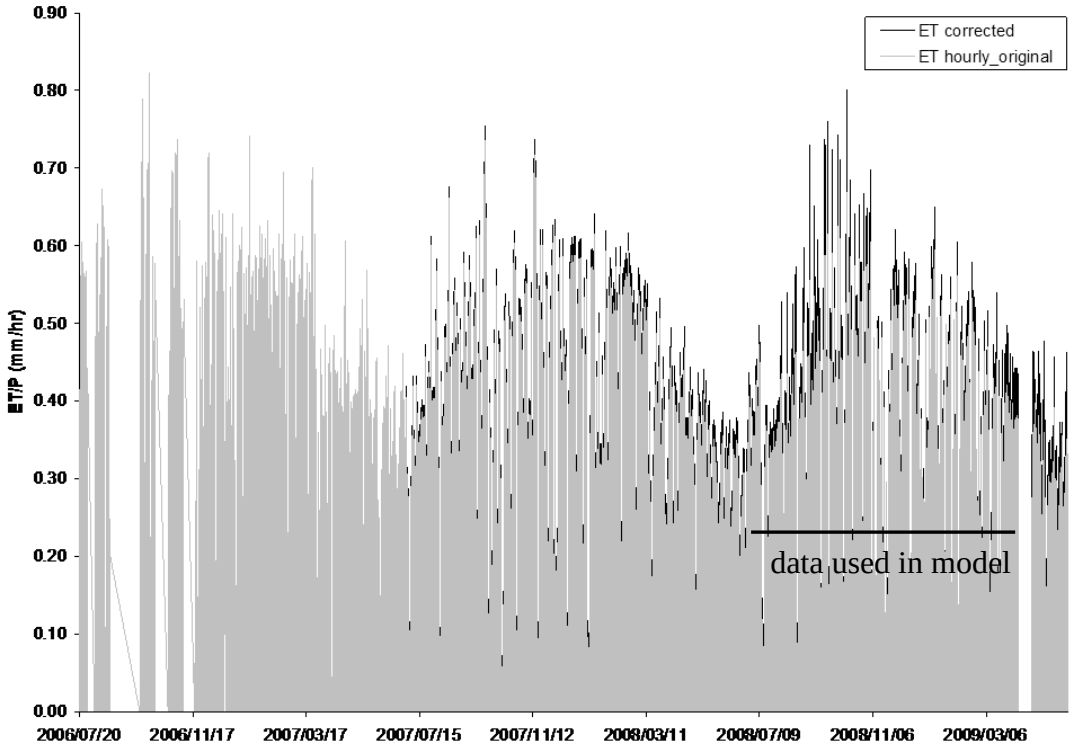

Figure 7.3: Hourly pET data with correction accounting for sensor sensitivity loss.

These meteorological variables were incorporated into a composite data file to drive the ACRU model such that pET as expressed is daily A-Pan equivalent evaporation (mm), minimum and maximum temperature (°C), incoming radiation flux density (MJ $m^2.d^{-1}$), relative humidity (%) and wind run ($km.d^{-1}$).

Streamflow: Discharges leaving the wetland were recorded at a concrete buttress weir that served the dual purpose of being the wetland rehabilitation structure. Flows were observed over a compound weir with 90º v-notch and rectangular notch sections for which a metric units equivalent rating was derived from the methods described by US. Dept of Interior (2001). Flows were recorded by way of a Campbell Scientific, Inc. float and CS410 Shaft Encoder with a CR200 data logger. Observed streamflow was expressed as depth of flow in mm as a function of catchment area for comparison with ACRU outputs.

Soil water content readings were taken at regular intervals during the 2008-09 season using Time Domain Reflectometry (TDR) with in-house manufactured 300 mm three pronged stainless probes and 3 m coaxial cable. Dielectric pulses were made using a Campbell Scientific, Inc. TDR100.

The ACRU basic model structure was set up and populated for the headward end of the Craigieburn-Manalana research catchment using the ACRU331 menubuilder. The input files were then converted to java from FORTRAN using the AcruMenuConverter.jar for use in the ACRU2000 and ACRU_Int zone modelling system. Input menu files were then populated using a text editor. The model was then run for inter-comparison between the regular ACRU2000 and the ACRU_Int zone which incorporates the ADF sub-routines. In addition to driving meteorological variables, all instance of the ACRU model simulations incorporated soil physical hydraulic information determined via the controlled outflow cell method (Lorentz *et al*., 2003) and textural information (van Tol *et al*., 2007).

In addition to comparison of the two versions of ACRU a semi-quantitative hydro-pedological description of hillslope soil forms was made and on this basis conceptual hillslope hydrological models were developed incorporating relative contributions of hillslope recharge, interflow and responsiveness that were made by Le Roux *et al.* 2009. As a result two hillslope type configurations were then deployed. This took the form of a simple two hillslope type configuration routed through the valley bottom wetland (Figure 7.4) based on initial

(hydrologists) interpretation of the catchment as two hillslope types, one dominated by granite derived soils and the other on doleritic soils, with their compartmentalization into upslope (recharge), footslope (interflow) and wetland (responsive). Recharge soils are those have a dominantly vertical infiltration and facilitate recharge into permeable bedrock, whilst interflow soils are those that facilitate sub-surface lateral flow either by ponding on bedrock or on soil horizon with a lower hydraulic conductivity. Responsive soils are those that have a low water holding capacity or are shallow such that they have limited infiltration potential and saturate very quickly generating overland flows.

This compartmentalization was followed by a more detailed configuration incorporating three hillslope types described in terms of their hydro-pedological (soil scientist and hydrologist) configuration by Le Roux *et al*. (2009) (Figure 7.4) in order to assess the validity of including greater hillslope heterogeneity at the catchment scale. As a result of the difference between the initial interpretation of the Craigieburn-Manalana catchment and the proceeding hydropedology interpretation, the ratios of recharge: interflow: responsive soil varied between the two model configurations.

The ACRU model was run in distributed mode for the period 01 October 2008 to 08 April 2009, a period for which an unbroken meteorological and streamflow record was available. This distribution allowed for the invoking of discrete soil hydrological units based on their position within the hillslope catena. The delineated catchment areas of Le Roux *et al*. (2009) were then overlain in GIS (ArcView 3.2) for determination of areal extent of distributed (hillslope) sub-catchment areas.

Figures 7.4 and 7.5 display how the sub-catchments and soil water storage horizons at the hillslope scale were routed in the model set-ups, along with the conceptual hillslope hydrology. Note that the hillslope configuration of Le Roux *et al*. (2009) incorporates detailed representation of contributions of hillslope recharge, interflow (interflow between A & B horizons and soil-bedrock interfaces were lumped in these simulations) and responsive zones, as shown in Figures 4 and 5.

The ACRU_Int control variables governing the ADF processes are summarized in Table 7.1.

7.3 RESULTS

7.3.1 Simple Configuration

The Craigieburn catchment was modelled using both the ACRU2000 model and the developmental ACRU_Int model, using the distributed catchment and soil configuration as shown in Figure 7.4. Initial soil horizon depths were taken from Le Roux *et al.* (2008) detailed soil form characterizations adjacent to instrumented hydrological monitoring stations in the catchment. Since the ACRU2000 and ACRU_Int modelling systems express soil water contents (SMAINI, SMBINI and SMIINI) at the start of simulation as a percentage of plant available water (PAW) as well as being a function of depth, in the form of equation 7.3, it was necessary to derive these values from TDR volumetric water content readings. Since early simulations yielded modelled water contents (STO) inconsistent with observed values, the model was therefore calibrated in order to find the optimum soil horizon depths at which modelled water contents approximated those observed in the field, prior to any calibration of the intermediate zone parameters. In the majority of cases soils were close to wilting point and thus the catchment was very dry at the start of the simulation and the catchment was in water deficit. The final modelled and input soil horizon depths may be observed in Figure 7.6 (since ACRU2000 does not include a deeper soil horizon 2000mm water contents were not simulated) and Table 7.2 respectively. It is shown therefore that ACRU in both instances of the model was able to simulate the soil water contents in the catchment to a reasonable representation of reality as water contents and their temporal variability were similar, particularly with the inclusion of an intermediate soil layer, represented by the 2000 mm TDR and modelled readings.

(7. 3a) If $$\theta_{PAW} = \theta_{FC} - \theta_{WP}$$

(7. 3b) and $$\%\theta_{PAW} = \frac{\theta - \theta_{WP}}{\theta_{PAW}}.100$$

(7. 3c) then $$\frac{\delta \%\theta_{PAW}}{\delta d} = \left(\theta_{FC} D\right).\%\theta_{PAW} + \left(\theta_{WP} D\right)$$

where*:* θ_{PAW} is plant available water; θ_{WP} is wilting point; θ_{FC} is field capacity; and d is soil horizon depth.

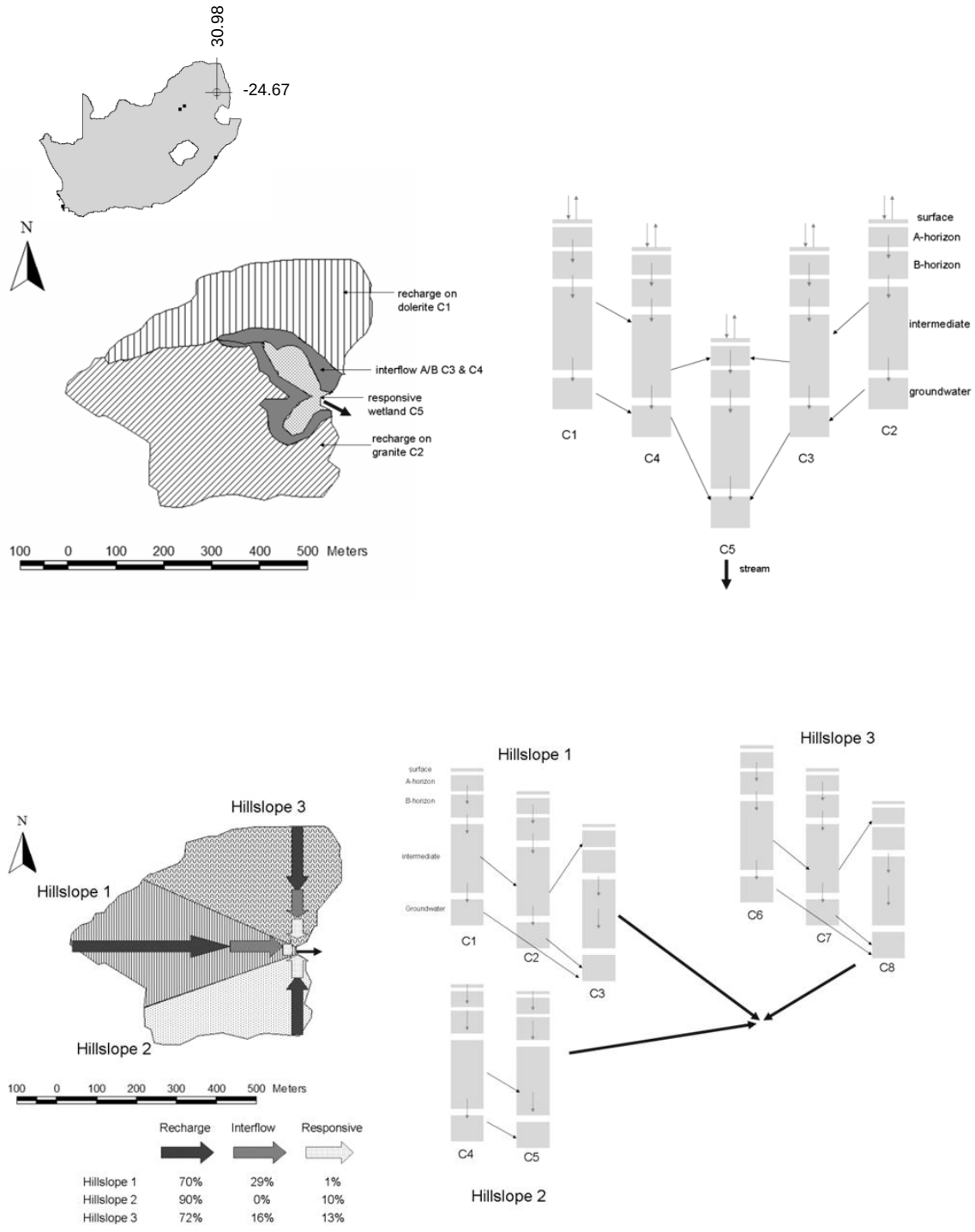

Figure 7.4: Location of the Craigieburn catchment and simple hillslope 2 sub-catchment configuration and soil compartment configuration (above) and more detailed (Le Roux *et al.* 2009) 3 sub-catchment and soil compartment configuration (below). NB. Hillslope 1 and 3 differ with respect to their material types and water storage capacities.

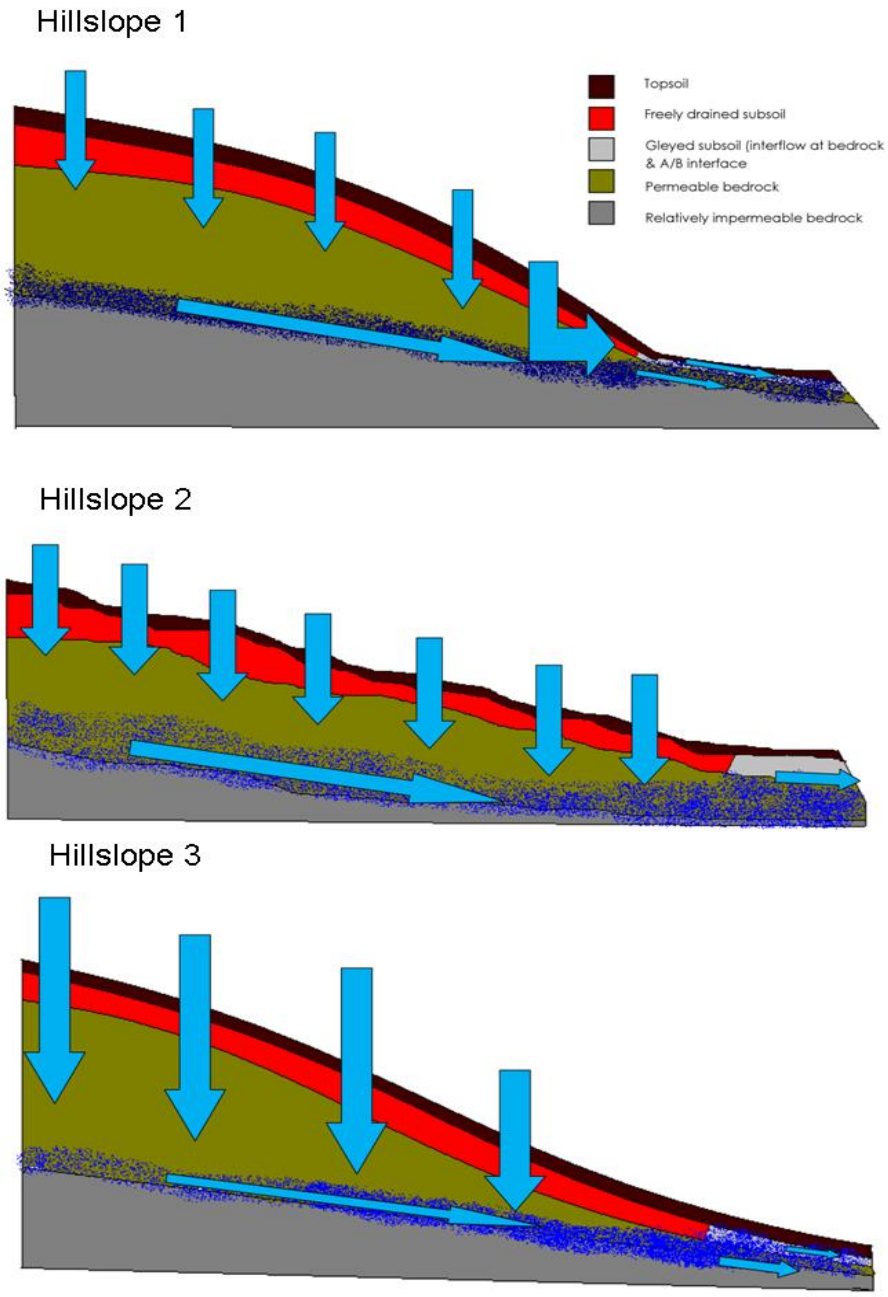

Figure 7.5: Dominant hillslope processes according to hydro-pedology in the Craigieburn catchment (Le Roux *et al.*, 2009)

Table 7.1: ACRU_Int intermediate zone control variables summary

QFRESP	Stormflow response fraction for the sub-catchment (daily)
DEPAHO, DEPBHO, DEPINTZ	Depth of the A-, B- and Intermediate soil horizons respectively (m)
ABRESP	Fraction of the saturated soil water to be distributed daily from the topsoil into the subsoil when the topsoil is above its drained upper limit
BFRESP	Fraction of the saturated water to be distributed daily from the subsoil into the intermediate/groundwater store when the subsoil is above its drained upper limit.
WP1, WP2, WPINTZ	Wilting point of the A-, B- and Intermediate soil horizons respectively
FC1, FC2, FCINTZ	Field capacity of the A-, B- and Intermediate soil horizons respectively
PO1, PO2, POINTZ	Porosity of the A-, B- and Intermediate soil horizons respectively
SMAINI, SMBINI, SMIINI	Soil water content of the A-, B- and Intermediate soil horizons at the start of the simulation respectively as a percentage of plant available water (m)
INTZRESP	Intermediate zone response factor (dimensionless)
RESDISPL	Response dispersion for the lateral response function (dimensionless)

RESTIMEL	Mean response time for the lateral response function (days)
NDAYSMAXI	Max duration of unit response for the lateral response function (days)
RESDISPGW	Response dispersion for the groundwater response function (dimensionless)
RESTIMEGW	Mean response time for the groundwater response function (days)
NDAYSMAXGW	Max duration of unit response for the groundwater response function (days)
RESDISPMP	Response dispersion for the macropore response function (dimensionless)
RESDIMEMP	Mean response time for the macropore response function (days)
NDAYSMAXMP	Max duration of unit response for the macropore response function (days)
MPRESP	Macropore response factor (dimensionless)

Based on empirical information, it is known that the Craigieburn catchment has a very flashy rainfall-runoff regime, due to its situation within an area prone to intense rainfall distribution, particularly when, at the height of the rainy season, valley bottom areas in the form of riparian wetlands are saturated. For this reason, as well as the catchment being much smaller than those typically modelled with ACRU, the quickflow response factor (QFRESP) was kept relatively high, such that for the ACRU2000 model this was found to be optimum at a value of 0.9. It was found that even with lower values for QFRESP ACRU2000 over predicted peakflows and that the higher values allowed for better simulation of low flows. Meanwhile, the ACRU_Int model, which is able to facilitate quickflow through ADFs via macropore responses, it was found that 0.7 proved to be optimum for its purpose. In all cases except for the quickflow response factor, corresponding parameter values remained equal between the ACRU2000 and ACRU_Int models, except of course for the inclusion of intermediate zone control variables in the latter. Values for saturated soil water redistribution, ABRESP and BFRESP were based on soil textural information reported by van Tol *et al* (2007) for each soil horizon and using a Rawls soil texture table (Rawls, 1983) to derive the appropriate parameter value for that soil textural class in the ACRU user manual v4.00 (Smithers & Schulze, 2004). Whilst both instances of the ACRU model showed good correlation with observed peak flows, as may be seen in Figure 7.7, these were significantly overestimated by the ACRU2000 model and modelled with greater satisfaction by the ACRU_Int model such that the mean difference in streamflow between the two models when compared with observed data was 2.3 mm and 0.3 mm respectively (with SE of 0.57 and 0.17). This is most clearly represented in Figure 7.8 with a cumulative plot of modelled streamflow, showing the consistent overestimation of streamflow during intense rainfall periods, where the slope of the curves increase drastically in accordance with the precipitation curves. As a function of total flow, the total difference of the two models to observed streamflow was 444.3 mm and 42.7 mm for ACRU2000 and ACRU_Int respectively. This difference is attributed in large part to the inclusion of an intermediate water store below the A- and B-horizons in ACRU_Int where water infiltrates from above and is relinquished based on a specified hydraulic conductivity/retention characteristics and advection-dispersion coefficients, this additional store is lacking in ACRU2000.

Whilst there certainly is an over-estimation, of peakflows by the ACRU2000 model this does not explain the total over-estimation of streamflow. Figure 7.9 shows a plot of cumulative departure from the observed streamflow, here greater clarity is revealed between the two models during low-flow periods. It is quite apparent that the ACRU2000 model also over simulated the low-flows of the Craigieburn catchment as noted by the steeper slopes of this departure during

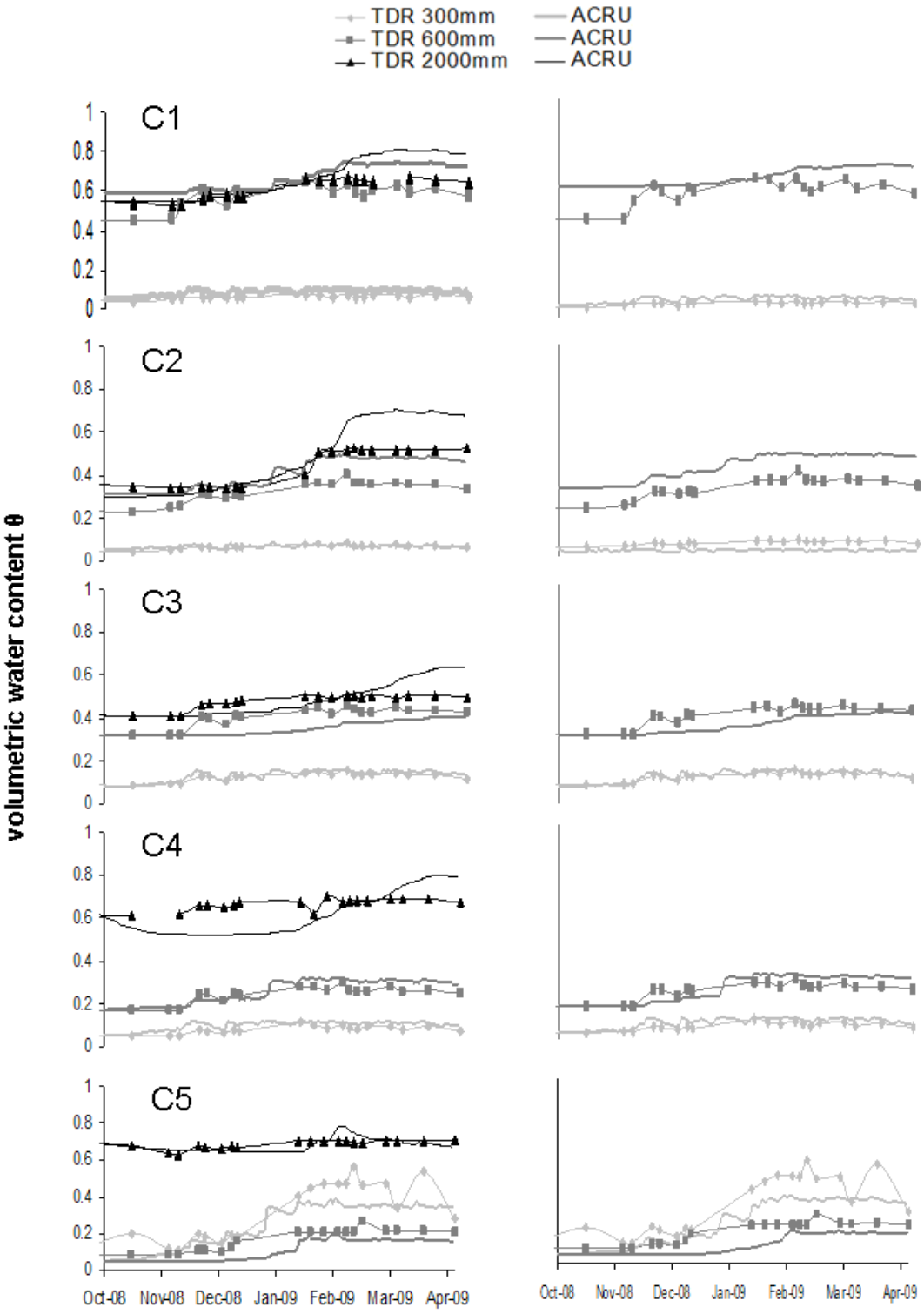

Figure 7.6: Modelled (STO) versus observed volumetric water contents (TDR) for ACRU_Int (Left) and ACRU2000 (Right), for subcatchments C1-C5. (Water content units are in metres of storage per profile i.e. water content multiplied by the depth of the soil horizon).

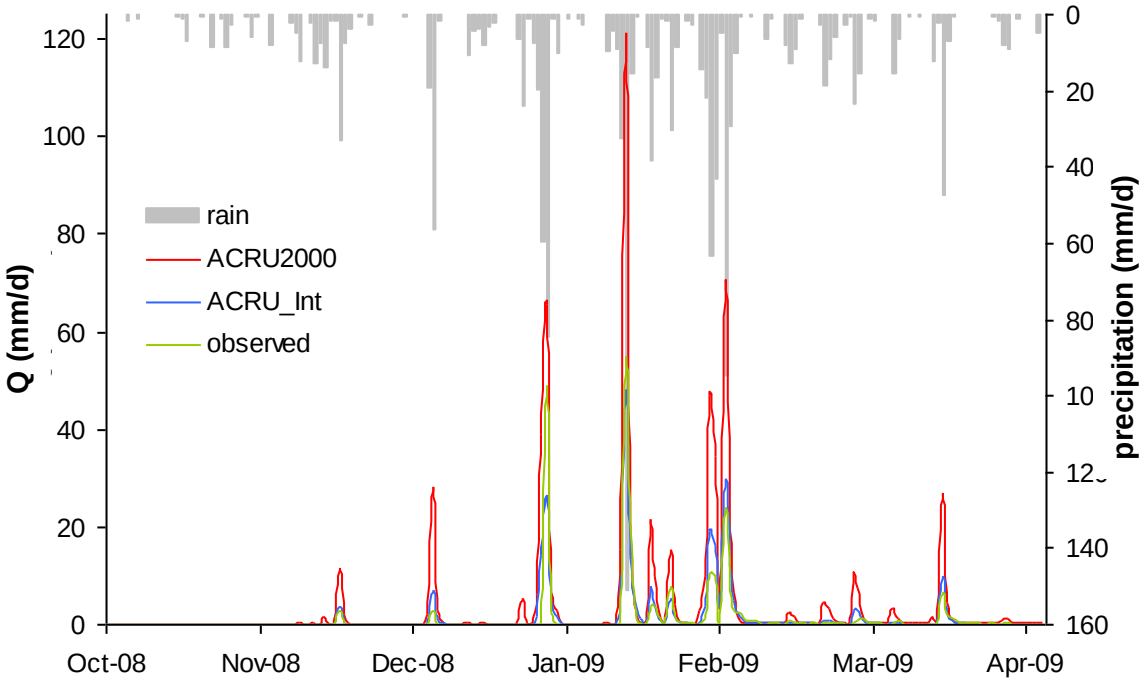

Figure 7.7: Plot of modelled (CHOUTF) and observed streamflow for the simple configuration.

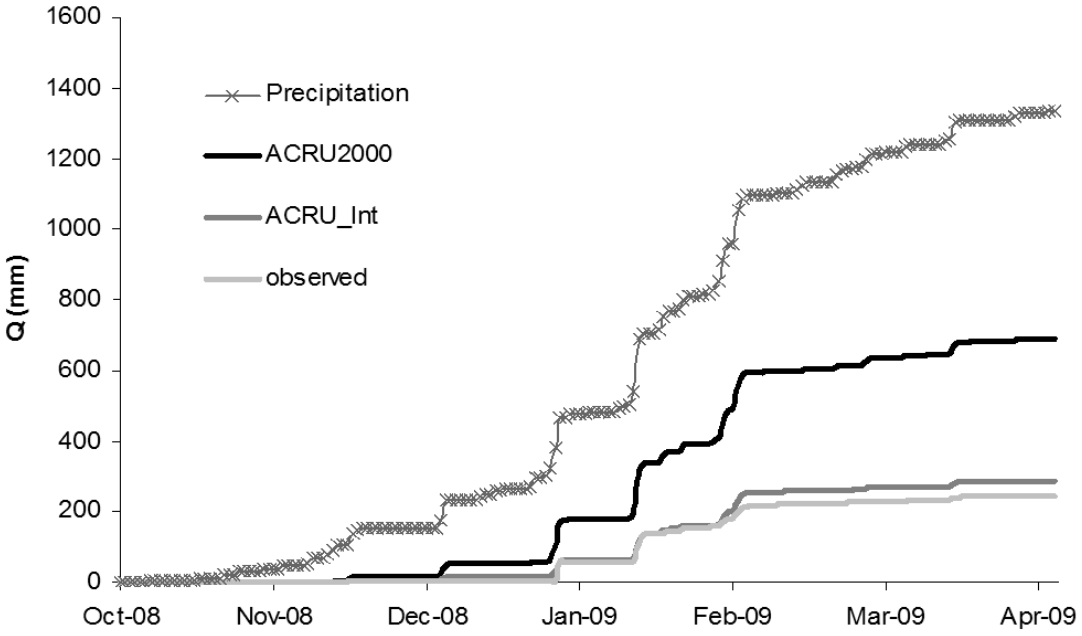

Figure 7.8: Cumulative plot of modelled (CHOUTF) and observed streamflow for the simple configuration.

the inter-rainfall periods. Remembering that parameter values remained equal between the two models, closer inspection of the period at the height and towards the end of the rains reveal how the inclusion of intermediate zone control variables in the ACRU_Int model allowed for a more suitable simulation of the low-flow recession periods. This is displayed by way of a Log plot of discharge in Figure 7.10 and divulges how the introduction of ADFs, through the use of a convolution integral algorithm are able to capture the falling limb of the streamflow curve more adequately. At this juncture it should be noted that the ACRU2000 models fails to adequately represent this recession limb, but rather yields an un-dynamic baseflow response during inter-rainfall periods, this is most noticeable for the lower intensity rainfall days between February and April 2009. The improvement of the streamflow response in ACRU_Int has been facilitated by the inclusion of variations in water transfer, vertically and laterally, within the hillslope compartments, that has emanated from the hydropedological interpretation of the catchment. Specifically it is the inclusion of responsive areas at the valley bottom that contribute to peak flows, and interflow soils at the footslope that contribute to discharge during periods of streamflow recession. The diminishing flows seen in ACRU_Int (rather than static in ACRU2000) are fostered by the convolution integral applied to the intermediate zone within the footslope and valley bottom, and to a lesser extent the recharge soils of upslope positions during the low-flow periods.

These results were achieved using the ACRU_Int model (Table 7.2) with varying values for D and τ for the intermediate zone response factor and within the lateral dispersion and macropore dispersion factors whilst assuming that groundwater had no influence at the scale of the catchment investigated. Thus the groundwater parameters remained uniform across all five sub-catchments in the distribution. In this instance, it was noted that the recharge hillslopes, sub-catchments C1 and C2 had a low influence and long lateral response time on daily streamflow, in which case values for INTZRESP = 0.01 and had a longer duration lateral response to downslope (proceeding sub-catchments). Meanwhile, macropores were suggested to have a role in these recharge areas but over a significantly longer duration than footslope and valley bottom areas (MPRESP = 0.5, NDAYSMAXMP = 50 days). The interflow areas at the footslope within the catchment were represented by having a rather transmissive response (INTZRESP = 0.05) and a lateral response dispersion of short duration (RESDISPL = 5, RESTIMEL = 1 day) allowing for high a degree of lateral transfers between soil compartments preventing sustained transfers that would attenuate the hydrograph. There was also a significant macropore response provided within the intermediate zone of significantly shorter duration than upslope, or preceding sub-catchments (MPRESP = 0.5, NDAYSMAXMP = 1). The responsive valley

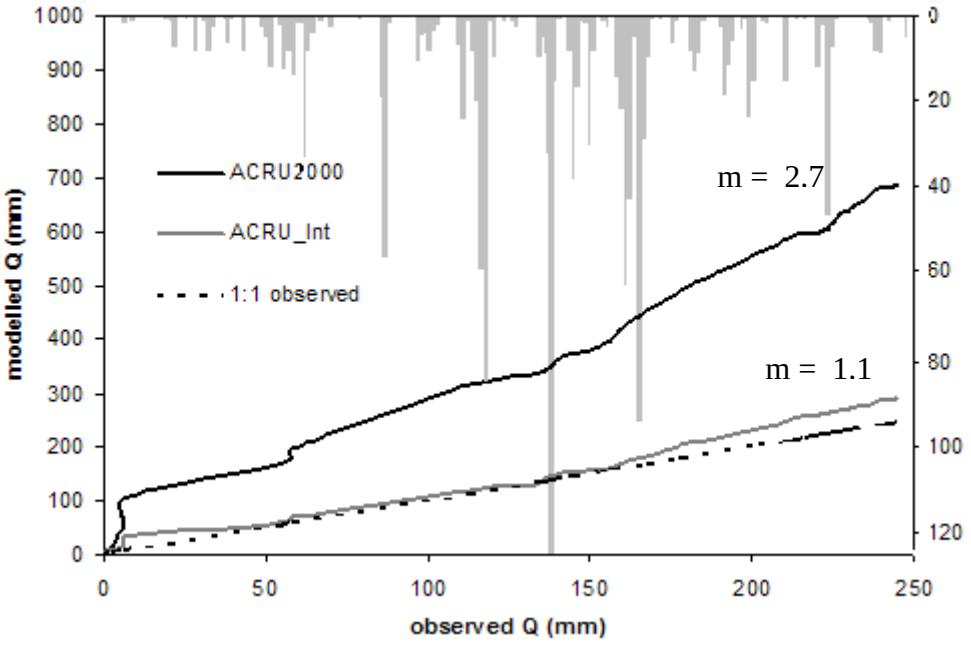

Figure 7.9: Plot of cumulative departure of two modelled scenarios against observed streamflow for the entire simulation period (m = slope of best fit trend line) simple configuration.

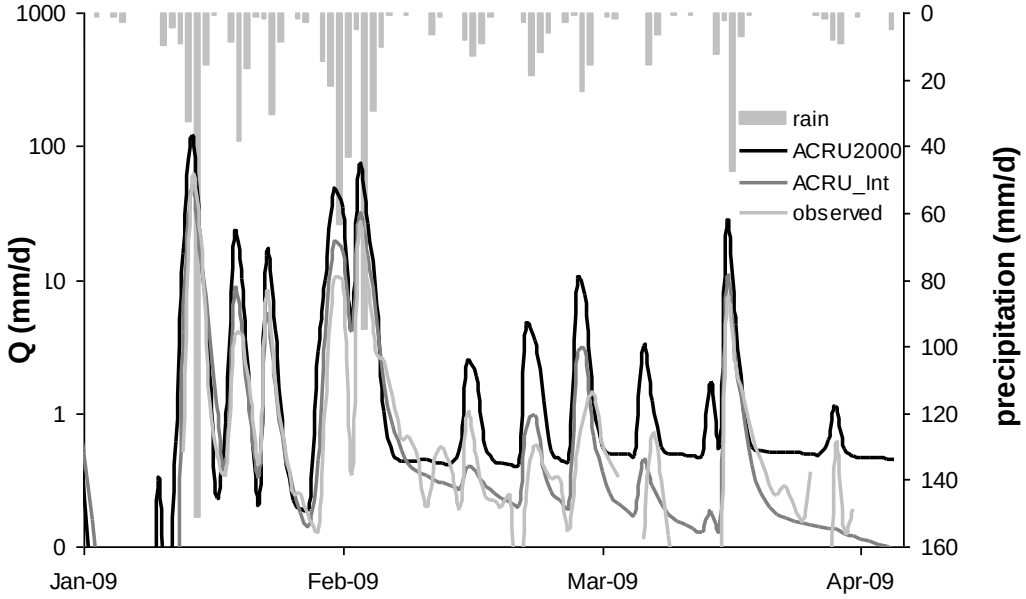

Figure 7.10: Log-normal plot of modelled (CHOUTF) and observed streamflow for the simple configuration between 2009/01/01 and 2009/04/08.

bottom areas were best represented by also having a high interflow response factor compared to the surrounding hillslopes (INTZRESP = 0.05) and also with a high lateral transmission (RESDISPL = 5), macropores were also deemed to be present but at significantly lower influence than in the intermediate zone of the contributing catchment (MPRESP = 0.1).

In order to quantify any improvement in the performance of the ACRU_Int model over ACRU2000, the daily streamflows were subjected to efficiency analysis in three forms as revealed in Table 7.3 where values approaching unity signify a perfect match and smaller values represent poorer results. The R^2, or coefficient of determination, is a simple relation of best fit by linear regression. The Nash-Sutcliffe (NS) efficiency is a measure of the mean square error to the observed variance, if NS = 1 then the model is a perfect fit, else closer to 0 then the model error comes into parity with the variance in the observed data, poor performance of the model will then be noted if the value of NS becomes increasingly negative. The Willmott (W) efficiency is similar to the NS where a value of 1 represents a perfect fit except that a value of 0 represents a total failure for the model to fit observed

Table 7.2: Soil water control variables (A&B Horizons) and intermediate zone (I Horizon) control variables for sub-catchments within the ACRU2000 & ACRU_Int simulations in a simple configuration.

	C1	***C2***	***C3***	***C4***	***C5***
ACRU2000					
QFRESP	0.9	0.9	0.9	0.9	0.7
DEPAHO	0.2	0.1	0.4	0.3	1.1
DEPBHO	1.8	1.0	1.3	0.8	0.6
ABRESP	0.4	0.65	0.5	0.65	0.5
BFRESP	0.4	0.5	0.15	0.15	0.5
WP1	0.27	0.253	0.191	0.166	0.048
WP2	0.332	0.315	0.243	0.213	0.077
FC1	0.47	0.338	0.38	0.38	0.319
FC2	0.41	0.48	0.372	0.372	0.277
PO1	0.517	0.419	0.397	0.397	0.411
PO2	0.534	0.537	0.4	0.4	0.402
SMAINI	0.054	0.051	0.076	0.05	0.053

SMBINI	0.598	0.315	0.316	0.17	0.046

ACRU_Int

QFRESP	0.7	0.7	0.7	0.7	0.7
DEPAHO	0.2	0.1	0.4	0.3	1.1
DEPBHO	1.8	1.0	1.3	0.8	0.6
ABRESP	0.4	0.65	0.5	0.65	0.5
BFRESP	0.4	0.5	0.15	0.15	0.5
WP1	0.27	0.253	0.191	0.166	0.048
WP2	0.332	0.315	0.243	0.213	0.077
FC1	0.47	0.338	0.38	0.38	0.319
FC2	0.41	0.48	0.372	0.372	0.277
PO1	0.517	0.419	0.397	0.397	0.411
PO2	0.534	0.537	0.4	0.4	0.402
SMAINI	0.054	0.051	0.076	0.05	0.053
SMBINI	0.598	0.315	0.316	0.17	0.046
DEPINTZ	2	1.5	1.5	1.5	1.5
WPINTZ	0.274	0.199	0.273	0.233	0.131
FCINTZ	0.395	0.45	0.451	0.521	0.406
POINTZ	0.412	0.461	0.475	0.532	0.48
INTZRESP	0.01	0.01	0.05	0.05	0.05
SMIINI	0.548	0.299	0.41	0.614	0.698
INTZRESP	0.01	0.01	0.05	0.05	0.05
RESDISPL	1	1	5	5	5
RESTIMEL	10	10	1	1	1
NDAYSMAXI	365	365	365	365	365
RESDISPGW	1	1	1	1	1
RESTIMEGW	1	1	1	1	5
NDAYSMAXGW	365	365	365	365	365
RESDISPMP	5	5	5	5	5
RESDIMEMP	1	1	1	1	1
NDAYSMAXMP	50	50	1	1	1
MPRESP	0.5	0.5	0.5	0.5	0.1

Table 7.3: Modelled (CHOUTF) efficiencies against observed daily streamflow for the simple configuration (R^2, coefficient of determination; *NS*, Nash-Sutcliffe; *W*, Willmott).

Efficiency	R^2	*NS*	*W*
ACRU2000	0.805	-0.961	0.798
ACRU_Int	0.836	0.834	0.952

data. Here it is quite apparent that the ACRU_Int simulations yielded consistently better outcomes than the ACRU2000 in all cases, and this improvement by ACRU_Int is attributed to the inclusion of discrete hillslope units that have differences in the way that they store and transmit water by way of variations in D and τ that was estimated from the hydropedological interpretations of Le Roux *et al* (2009). Particularly noteworthy from Table 7.3 is the negative value for the Nash-Sutcliffe efficiency with regard to ACRU2000, which represents an error in the model greater than the variance in model output (Wainwright & Mulligan, 2004), in this case observed flows. This is a rather poor representation of observed streamflow, despite the maintaining of equal parameter values (albeit except QFRESP) between the two models, without an intermediate layer functionality in ACRU2000. Since the values of the coefficient of determination in both cases are comparable, it suggests that consistent proportional errors are associated in both models. This is likely, in the case of ACRU2000, to be due to consistent over-representation of peakflows and the rather homogenous representation of low-flows where there is no apparent recession in the hydrograph between peak flows. Speculation arises that since both models fail to allow for intermittent cessation of streamflow, as observed in Figure 7.10 this may account to some extent for their relative similarity under the scrutiny of R^2. It must be remembered that the application of ACRU in a small catchment such as the Craigieburn-Manalana is an exploratory undertaking as ACRU is most usually applied in catchments between 5-50 km², and so this observation may reveal the shortcomings of ACRUs application at this scale.

7.3.2 Detailed configuration

The second model configuration which allowed for a greater degree of hillslope heterogeneity has parameters summarized in Table 7.4. For these simulations the quickflow response fraction (QFRESP) was maintained at 0.9 for ACRU2000 runs but found to be optimum at 0.5 for the

ACRU_Int. Again both instances of the model showed agreement with peakflows as shown in Figure 7.11, and this was again significantly overestimated by ACRU2000 and the margin by which ACRU_Int overestimated quickflows was reduced. The mean difference between observed and modelled values was 1.3 mm and 0.4 mm (with a SE of 0.46 and 0.18) for the ACRU2000 and ACRU_Int models respectively. Thus at the scale of the daily time-step, the ACRU2000 model had seemingly improved by a considerable margin from the simpler configuration, whilst the ACRU_Int showed marginal decline in performance, nevertheless ACRU_Int still performed better than ACRU2000. The cumulative plot for streamflow (CHOUTF) is shown in Figure 7.12 and underlines the fact that the ACRU_Int model was able overall to simulate total streamflow with better representation than the ACRU2000 model, however since the total difference using a greater degree of hillslope heterogeneity in the ACRU2000 model was reduced quite considerably to 251.8 mm, and the total difference increased to 74.2 mm for the ACRU_Int model this then contrasts somewhat with the simpler configuration.

Figure 7.13 shows the cumulative departure plot for the two models under a more detailed configuration, and here the average slopes of the lines reveal the nature of the differences in model performance compared to the simple configuration. First, the ACRU2000 model has a much lower slope of m = 2.0, which is most notable (than when compared to Figure 7.9) for the low intensity rainfall periods. Meanwhile the ACRU_Int model has slightly increased slope of m = 1.3 and clearly it was unable to capture the low-flows in quite a satisfactory a fashion as the simpler configuration. Whilst it may be suggested that the departure of the modelled cumulative discharge from the observed may be due to inadequate removal of water from the catchment via evapotranspiration, it is most obvious from Figure 7.13 the slope of the modelled curves increases in tandem with the precipitation events. Therefore it is rather an inefficiency in modelling peak flows that explains the steepening of the cumulative curves over time.

If one cross references Figures 7.10 and 7.14 of the log plots for the simple and more detailed simulations respectively, it may be observed that despite the lower quickflow response in the ACRU_Int detailed configuration there is quite clearly a more adequate representation of peak flows particularly for the period between February and March 2009. Interestingly, whilst quickflow was maintained at the same value in the more detailed configuration, it too simulated peakflows more adequately. Comparison of these two Figures also reveals that the ACRU2000 model, despite its apparent improvement in predicting peakflows, still fails to yield a

Table 7.4: Soil water control variables (A&B Horizons) and intermediate zone (I Horizon) control variables for sub-catchments within the ACRU2000 & ACRU_Int simulations in a detailed configuration.

	C1	***C2***	***C3***	***C4***	***C5***	***C6***	***C7***	***C8***
ACRU2000								
QFRESP	0.9	0.9	0.9	0.9	0.9	0.9	0.9	0.9
DEPAHO	0.2	0.2	0.4	0.2	0.3	0.2	0.2	0.4
DEPBHO	1	1.2	0.6	1.6	1	1	1.6	0.6
ABRESP	0.5	0.65	0.5	0.5	0.5	0.5	0.5	0.5
BFRESP	0.5	0.5	0.15	0.5	0.5	0.5	0.5	0.15
WP1	0.183	0.253	0.191	0.27	0.048	0.183	0.27	0.191
WP2	0.252	0.315	0.243	0.332	0.077	0.252	0.332	0.243
FC1	0.385	0.338	0.38	0.47	0.319	0.385	0.47	0.38
FC2	0.432	0.48	0.372	0.41	0.277	0.432	0.41	0.372
PO1	0.43	0.419	0.397	0.517	0.411	0.43	0.517	0.397
PO2	0.48	0.461	0.4	0.534	0.402	0.48	0.534	0.4
SMAINI	0.04	0.051	0.076	0.054	0.014	0.04	0.054	0.5
SMBINI	0.25	0.378	0.146	0.531	0.077	0.25	0.531	0.15
ACRU_Int								
QFRESP	0.5	0.5	0.5	0.5	0.5	0.5	0.5	0.5
DEPAHO	0.2	0.2	0.4	0.2	0.3	0.2	0.2	0.4
DEPBHO	1	1.2	0.6	1.6	1	1	1.6	0.6
ABRESP	0.5	0.65	0.5	0.5	0.5	0.5	0.5	0.5
BFRESP	0.5	0.5	0.15	0.5	0.5	0.5	0.5	0.15
WP1	0.183	0.253	0.191	0.27	0.048	0.183	0.27	0.191
WP2	0.252	0.315	0.243	0.332	0.077	0.252	0.332	0.243
FC1	0.385	0.338	0.38	0.47	0.319	0.385	0.47	0.38
FC2	0.432	0.48	0.372	0.41	0.277	0.432	0.41	0.372
PO1	0.43	0.419	0.397	0.517	0.411	0.43	0.517	0.397
PO2	0.48	0.461	0.4	0.534	0.402	0.48	0.534	0.4
SMAINI	0.04	0.051	0.076	0.054	0.014	0.04	0.054	0.076
SMBINI	0.25	0.378	0.146	0.531	0.077	0.25	0.531	0.146

DEPINTZ	1	1.7	2.5	1	0.7	1	1	3.5
WPINTZ	0.299	0.199	0.273	0.274	0.131	0.199	0.274	0.273
FCINTZ	0.45	0.45	0.451	0.395	0.406	0.45	0.395	0.451
POINTZ	0.461	0.461	0.475	0.412	0.48	0.461	0.412	0.475
INTZRESP	0.01	0.05	0.05	0.01	0.05	0.01	0.05	0.05
SMIINI	0.2	0.338	0.683	0.274	0.326	0.2	0.274	0.956
RESDISPL	1	10	10	1	10	1	10	10
RESTIMEL	10	1	1	10	1	10	1	1
NDAYSMAXL	365	365	365	365	365	365	365	365
RESDISPGW	1	1	1	1	1	1	1	1
RESTIMEGW	1	1	1	1	1	1	1	1
NDAYSMAXGW	365	365	365	365	365	365	365	365
RESDISPMP	5	5	5	5	5	5	5	5
RESTIMEMP	1	1	1	1	1	1	1	1
NDAYSMAXMP	50	1	1	50	1	50	1	1
MPRESP	0.5	0.7	0.1	0.4	0.1	0.5	0.7	0.1

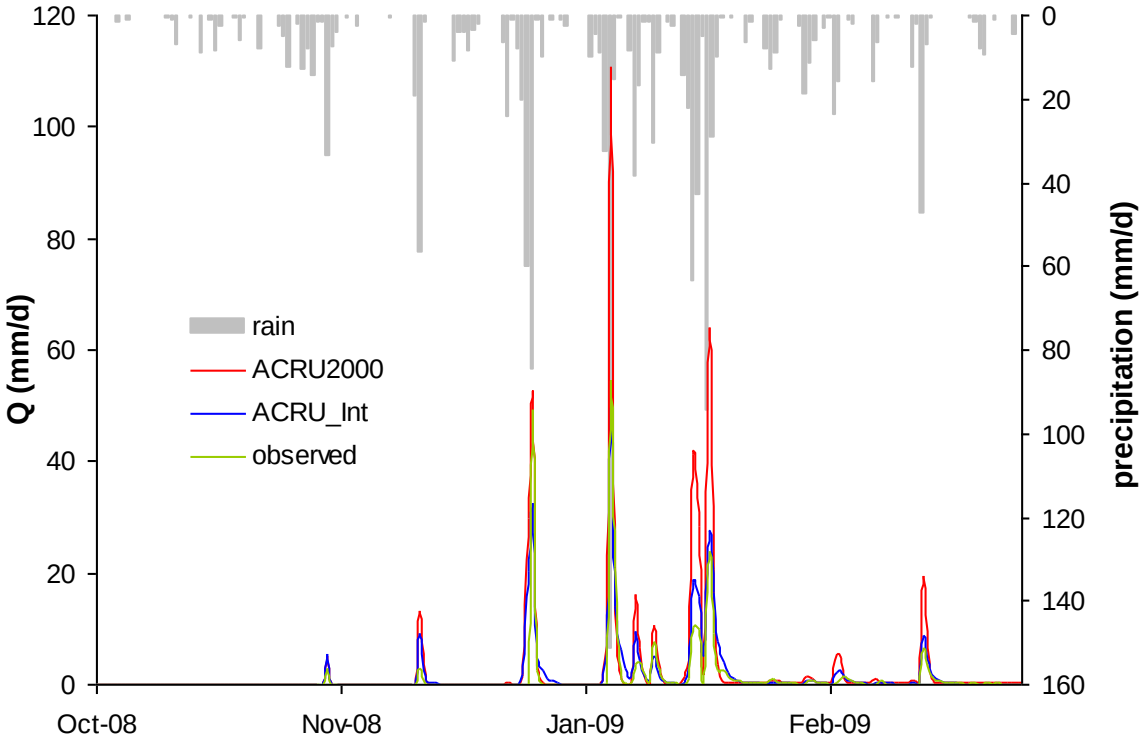

Figure 7.11: Plot of modelled (CHOUTF) and observed streamflow for the detailed configuration.

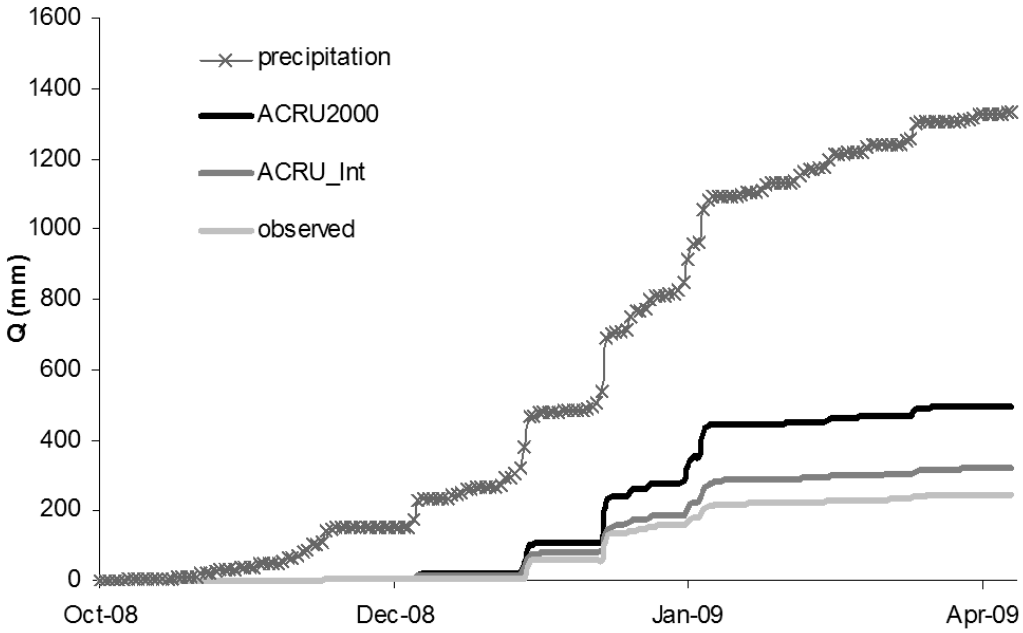

Figure 7.12: Cumulative plot of modelled (CHOUTF) and observed streamflow for the detailed configuration.

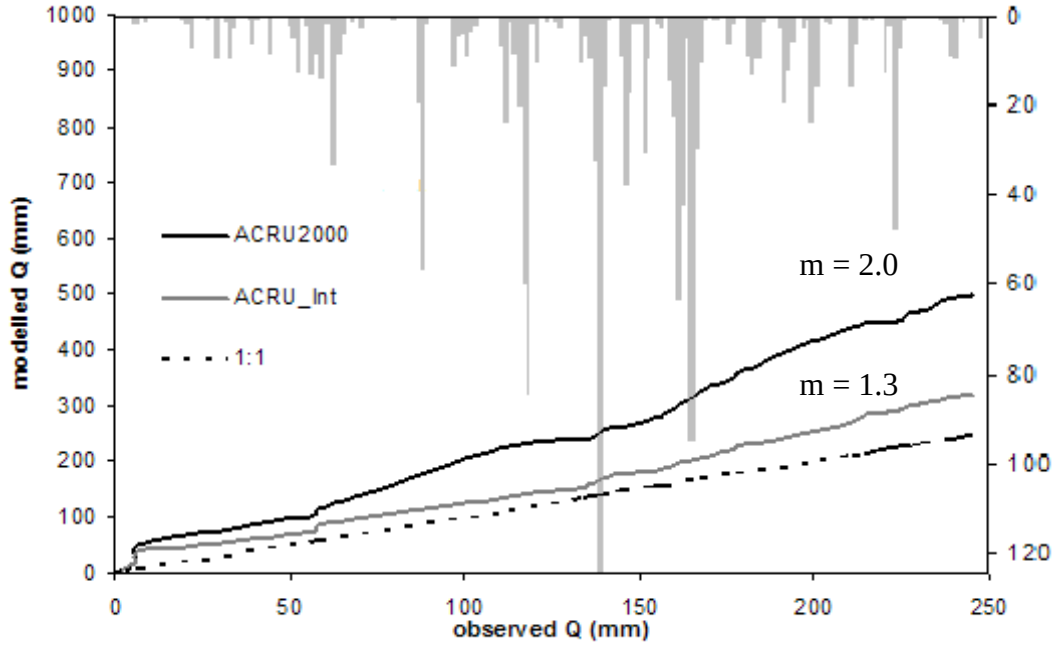

Figure 7.13: Plot of cumulative departure of the two models against observed streamflow for the entire simulation period (m = slope of best fit trend line) detailed configuration.

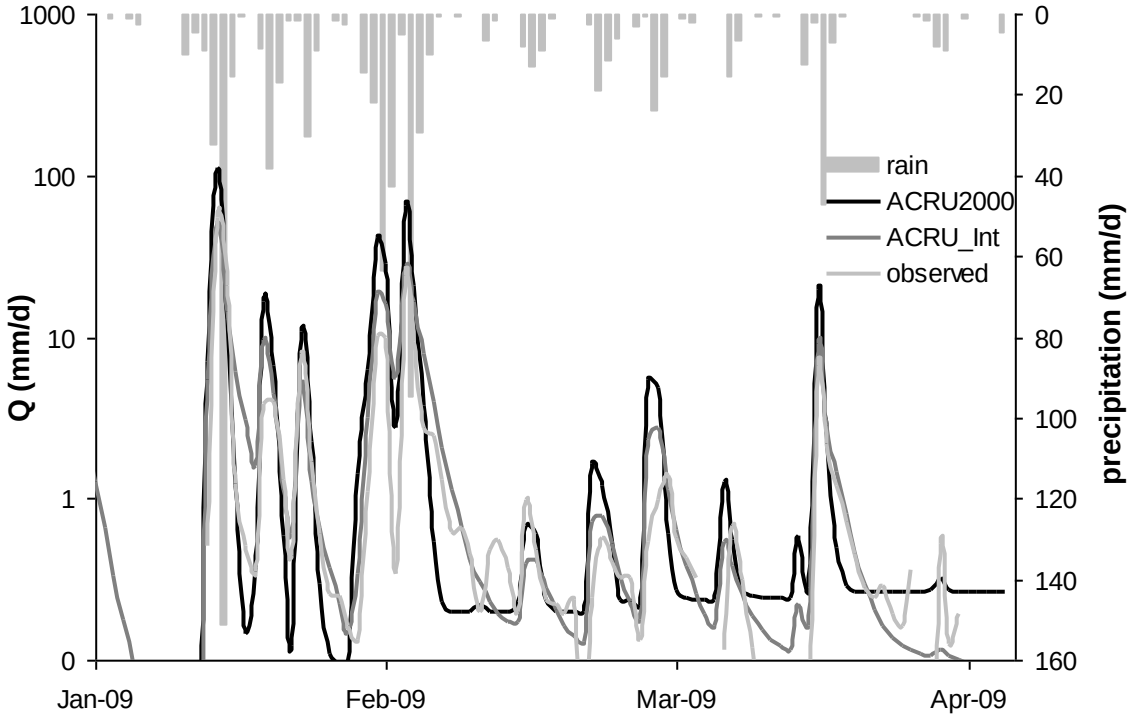

Figure 7.14: Log-normal plot of modelled (CHOUTF) and observed streamflow for the detailed configuration between 2009/01/01 and 2009/04/08.

satisfactory response on the low-flow domain, whilst the ACRU_Int seems to represent these periods with more reasonable responses than ACRU2000. The difference in behaviours of the two models is therefore due to the convolution integral function of the intermediate zone in ACRU_Int which allows for a diminishing discharge over time (daily i.e. RESTIMEL = 1) from the intermediate soil water store particularly at the footslopes to the stream, but also over longer time scales from the recharge areas of the hillslopes (several days i.e. RESTIMEL = 10), this functionality is lacking in the traditional ACRU2000.

Again the groundwater parameters remained uniform across all eight sub-catchments in the distribution. In this instance the results were achieved by applying similar values of D and τ as was the case for hillslopes in the simple configuration. In this instance, it was noted that the recharge hillslopes, sub-catchments C1, C4 and C6 had a low influence and long lateral response time on daily streamflow, where INTZRESP = 0.01. Again, macropores were suggested to have a relatively large but longer duration response mechanism in the upslope domains when compared to footslope and valley bottom areas (MPRESP = 0.5, NDAYSMAXMP = 50 days), whilst the footslopes had the largest and most rapid macropore response mechanism (MPRESP = 0.7, NDAYSMAXMP = 1 day). The interflow areas, C2 and C7 (remembering that hillslope 2 had no significant interflow area) at the footslope within the catchment were represented by having a greater volumetric response (INTZRESP = 0.05) whose manner was lateral and rapid (RESDISPL = 10, RESTIMEL = 1 day), which in this case was greater than required in the simpler configuration. Interflow soils also had a significant macropore response within the intermediate zone of significantly shorter duration than the upslope preceding sub-catchments. This also required the macropore response to be increased (MPRESP = 0.7, NDAYSMAXMP = 1). The responsive valley bottoms, again, were well represented by a high volumetric response factor (INTZRESP = 0.05) compared to the surrounding hillslopes and also with a high lateral transmission (RESDISPL = 5), macropores were also deemed to be present but of significantly lower influence than in the intermediate zone of the contributing catchment (MPRESP = 0.1).

Examination of the efficiency analysis for this detailed model configuration (Table 7.5) shows that under all constraints the ACRU2000 model showed an increase in performance as compared to the simple configuration (Table 7.3) and only a very minor decline in the performance of the ACRU_Int model.

Table 7.5: Modelled (CHOUTF) efficiencies against observed daily streamflow for the detailed configuration (R^2, coefficient of determination; *NS*, Nash-Sutcliffe; *W*, Willmott).

Efficiency	***R²***	***NS***	***W***
ACRU2000	0.811	-0.184	0.851
ACRU_Int	0.828	0.824	0.951

7.4 DISCUSSION

The exercise in distributed hydrological modelling using the proposed ADF parameters has given insights into the new ACRU_Int model's performance particularly with respect to low-flows. However, these findings must be discussed given the constraints in overall model performance with particular reference to the benchmark of the ACRU2000 model. It would have been apparent to the reader that despite the relatively high R^2 values generated by the ACRU2000 model in both simulations, it significantly under performed as was noticeable under the cumulative plots, and this may have been attributed to the non-effective parameterization of the model in which land segments failed to relinquish soil moisture to the atmosphere. However as is revealed in Table 7.6, for both

Table 7.6: Total potential and actual (modelled) evapotranspiration for the period October 2008-April 2009.

	pET	**ACRU_Int**	**ACRU2000**
	584 mm		
Total aET simple		392.13 mm	373.37 mm
Total aET detailed		365.02 mm	389.49 mm

versions of ACRU and under both the simple and detailed configurations, the difference in evapotranspiration between the two models is no greater than 25 mm, the shortfall from the far greater potential evapotranspiration compared to modelled cumulative evapotranspiration being attributable to the significant soil moisture deficit at the start of the simulation restricting vegetation transpiration. Certainly, the quickflow response fraction may have also been inadequately addressed in the ACRU2000, the reason that the quickflow response in ACRU2000 was not fixed at a certain value is that in early simulations its performance improved by increasing the value of QFRESP, and the higher value of 0.9 was logical given the small size of the catchment. Interestingly there was improved representation of streamflow by this model in the detailed configuration which maintained the same value for QFRESP and was able to simulate both lower peak and low-flows, suggesting that better representation of soil types in the catchment was a significant contributor to this improved model behaviour. Since it was only the soil type distribution that was better represented here than compared to the simple configuration it suggests that accounting for a greater representation of soil types goes someway to improving catchment runoff. This may be expected through correct routing of dominant hydrological processes through the hillslope catena, founded by the hydropedological interpretations of the hillslopes. In this way the general over- and/or under-estimations of hillslope streamflow generating processes traditionally used to overcome complexity in catchment models have been reduced to higher resolution hillslope compartments, that are still able to avoid otherwise complex hydrological process understanding. Meanwhile, the need to reduce QFRESP in the detailed configuration for sufficient peak flow performance by ACRU_Int is most likely attributable to the greater proportion of interflow and responsive hillslope units in this configuration. This is because the simple configuration had 9% and 5% of the catchment under interflow and responsive land segments respectively, whilst the detailed configuration had proportions of 17% and 6%. Of course this reduced QFRESP in the detailed ACRU_Int would also have been offset by the increased response function (INTZRESP) and macropore responses (MPRESP) of the interflow regions. Indeed, a sensitivity analysis was performed on those intermediate zone parameters that had variable values in the detailed model configuration, this was assessed based on the modelled values for daily streamflow (CHOUTF). The analysis deployed the sensitivity index (SI) of Hoffman & Gardner (1983, as cited in Hamby, 1994), which assesses the effect of varying an input parameter through its range of possible values on the modelled output. The index has a unitless value between 0 and 1, such that values closer to 1 reveal a models greater sensitivity to a particular parameter. In varying the final input values for parameters: INTZRESP, RESDISPL, RESTIMEL and MPRESP by -99 to +99% revealed that daily streamflow had an SI of 0.22, 0.23, 0.07 and 0.56 for each of

these respectively. This suggests that the use of ACRU_Int model at least in this study is most sensitive to the effective parameterisation of the macropore response function.

Whilst ACRU2000 seemingly improved through the incorporation of greater heterogeneity in hillslope units, ACRU_Int's performance may have been negligibly worse than the simpler configuration, but still represented the low-flows and peak flows reasonably well as revealed through the efficiency analysis where the differences between the simple and detailed configurations of ACRU_Int are only a factor of 0.01 for R^2 and NS, and 0.001 for W. Despite this the question of why the ACRU_Int model did not at least improve in the same way as the ACRU2000 model remains, however this is most likely due to the large increase in saturated drainage to lower soil horizons (from A to B; B to intermediate store; and intermediate to groundwater storage) across the modelled catchment. When taken as an average for the whole catchment and across all horizons, for the entire period the ACRU2000 showed an increase in average saturated drainage from 0.13 mm to 0.28 mm from the simple to the detailed configuration. Meanwhile the increase for ACRU_Int was only from 0.20 mm to 0.25 mm. Since improvement of the ACRU2000 model was achieved through the inclusion of greater heterogeneity in the A and B soil horizon domains, the fact that the ACRU_Int zone which had the same detailed configuration, albeit with the inclusion of a third 'intermediate' soil horizon suggests that this is where the problem of un-improved model performance may reside. This may simply be due to inappropriate configuration of the soil compartment distribution, specifically the distribution of valley bottom wetland sub-catchments, which in the simple configuration was represented as one lumped sub-catchment (C5).

A distinct limitation of the application of the ACRU_Int zone algorithm to the Craigieburn catchment is of course with respect to the true low-flow or base flow periods, by this it is meant the long dry winter period, rather than the low-flow inter-rain periods of the summer wet season. Since the monitored headward region of the Craigieburn catchment is essentially a seasonal wetland catchment albeit with a very flashy streamflow response, the fact that streamflow cessation occurred soon after the end of the rains and the limited streamflow data set available for the catchment negates a true assessment of ACRU_Int's performance at the scale of the individual sub-catchment. Nevertheless, what the ACRU_Int model did achieve was an adequate representation of seasonal streamflow cessation under both model configurations and in this respect it represented ephemeral reaches of this semi-arid river system quite well, which through the correct incorporation of ADFs by way of hydropedological analysis shows promise for upscaling to the entire headwaters of the Sand River. Such upscaling would certainly

provide a useful understanding of the hillslope (soil) type contributions to catchment processes and particularly whether baseflows arise as a cumulative reflection of these hillslope types and their ADFs. One also wonders whether the nature of the wetland intermediate zone soils, which are clays with a very high water retention capacity, may augment baseflows at increasing stream orders cumulatively downstream. This should be a necessary determination given the apparent net-use of water by wetland vegetation in these systems during the dry winter months (Riddell & Lorentz, 2009), one needs to determine if there is any excess available for baseflow augmentation, although since there is no stream discharge out of this wetland during winter it may be unlikely at the local single catchment scale. Thus a next step would possibly be to incorporate this quantified wetland water use into the ACRU_Int algorithms.

A point must also be made about where the ACRU_Int model showed poor performance, and this relates particularly to low rainfall days. Regarding Figures 7.10 and 7.14 there are periods, for instance the 12/02/2009 and 27/03/2009 where there were minor increases in flow, for which there was no response by ACRU2000 or ACRU_Int. Or, 16/02/2009 and 10/03/2009 where ACRU2000 showed a flow response, but ACRU_Int's response fell far short of the observed. This is quite clearly a reflection of the models failure, at least within the restraints of the parameters that were set to account for low threshold triggers to flow. Furthermore, the fact that on occasion both models failed to generate peak flows in response to low order events is likely to have arisen due to complexities on the ground that were not captured in the model, namely small cultivation drainage channels which will aggregate towards the wetlands outlet. These are assumed to increase the discharges out of the wetland, and are believed to be one of the main anthropogenic forces facilitating wetland degradation (e.g. Pollard *et al*., 2006). Whilst this is an apparently obvious omission from the model's construct, the scale at which these drainage channels have been applied (several within a 100 m² area) would necessitate a whole new exercise in parameterisation beyond the objectives of this manuscript, or preferably in the interests of catchment based modelling to derive a unit response function for this type of land-use. Nevertheless, it should not be ignored in further studies of this kind where they are applied in a complex socio-biophysical landscape. It is issues such as these that have recently been discussed by Zehe & Sivapalan (2009) in relation to closely coupled 'human-geoecosystems' and how to model these interactions from the process to the meso-(catchment) scale. This is pertinent given the acknowledged degradation of certain soil types in the Sand River wetland catchments, namely of the Kroonstad (Planosols) which up to this point have been termed interflow hillslope units, which tend to interface the responsive wetland soils with upslope recharge areas. Whilst these soils have been the subject of detailed process based modelling,

Riddell & Lorentz (in review, Chapter 4) conclude that not only do these interflow soils yield quick lateral flows they also relinquish upslope water to threshold induced macropore flow. This has similarly been modelled in the ACRU_Int zone here, by applying high values of D and low values of τ for the lateral and macropore response. Whilst in the same manuscript (Riddell & Lorentz, in review) through hydrometric observation and modelling at the hillslope scale reveal the recharge phenomenon of upslope hillslope units and responsive valley bottom wetland units and these were represented well in ACRU_Int by applying low D and high τ values to recharge regions and high D and low τ to responsive regions. Speculation therefore arises as to what the implications are of altering the extent and distribution of the interflow soils, which are slowly being modified through the impacts of subsistence farming on marginal lands. In the spirit of Zehe & Sivapalan's (2009) discussion, this poses the question of how these threshold type behaviours may be altered at the hillslope scale and how this will be reflected at the scale of the catchment.

Despite some limitations to the modelling as has just been described, it has been shown that the introduction of non-linear transfer functions between soil compartments on hillslope units, using hydro-pedological inferences of dominant hillslope processes has yielded a much improved representation of the wetland-catchment hydrology, particularly in the low-flow domain. The use of hydro-pedological knowledge in this form of distributed hydrological modelling has clearly allowed for the simplification of process to a few parameters, that would otherwise have required parameterisation of soil physical laws governing variably saturated flow in heterogeneous media, which at the scale of the catchment would be replete with complexities exacerbating the notions of equifinality and uncertainty in model performance. The promising interdisciplinary understanding held within the field of hydropedology seems to have already begun with the successful collusion of hydrologists and soil scientists in South Africa as has been demonstrated here.

7.5 CONCLUSION

Whilst the use of ACRU_Int failed to provide absolute values of D and τ to reflect complete agreement with the streamflow observed in the Craigieburn-Manalana catchment, the potential for capturing low-flow periods, particularly through the use of conceptual hydro-pedological process zones on hillslopes has clearly been demonstrated through the analysis presented here.

Furthermore, since these non-linear processes have been encapsulated through ADF functions within the hillslope the catchment model has been alleviated of parameter uncertainty, which will more likely increase should parameter development occur at the scale of the soil horizon. What this exercise has also demonstrated is that in development of the distributed catchment model, the wetland itself may as easily be represented as an element of the hillslope rather than as a separately modelled entity within the model. However this does need to be explored further, given the possible problems with valley bottom configuration and routing. This work has shown the beneficial interaction of soil scientists and hydrologists in applying hydro-pedological information, at a low cost, to potentially costly hydrological investigations.

ACKNOWLEDGEMENTS

This research was funded by the South African Water Research Commission (WRC). The authors acknowledge the kind contributions of Mr Ronny Maaboi, Mr Rex Mothlabini, and Mr Difference Thibela for fieldwork assistance. Mr Johan van Tol, Mr Bataung Kunene, and Mr Conrad Freankel for their hydro-pedological interpretation and laboratory analysis. Mr Sean Thornton-Dibb for his advice and assistance with the development of the new ACRU model, Mr Cobus Pretorius for technical assistance. Logistical and administrative support was provided by the Association for Water and Rural Development (AWARD).

REFERENCES

Berne, A., Uijenhoet, R., Troch, PA. (2005). Similarity analysis of subsurface flow response of hillslopes with complex geometry. Water Resources Research, 41, W09410; doi: 10.1029/2004WR003629

Beven, KJ. (1996) A Discussion of distributed hydrological modelling. Distributed Hydrological Modelling Ed. Abbott, MB., Refsgaard, JC. The Netherlands: Kluwer Academic Publishers, p 255-278.

Beven, KJ. (2000). Uniqueness of place and process representations in hydrological modelling. Hydrology and Earth Systems Sciences, 4(2), 203-213.

Bouma, J. (2006). Hydropedology as powerful tool for environmental policy research. Geoderma, 131, 275-286.

Everson, C.S. (2001). The water balance of a first order catchment in the montane grasslands of South Africa. Journal of Hydrology, 241, 110-123.

Falkenmark, M. Rockstrom, J. (2004). Balancing Water for Humans and Nature: The New Approach in Ecohydrology. London: Earthscan.

Giertz, S. Diekkruger, B. (2003). Analysis of the hydrological processes in a small headwater catchment in Benin (West Africa). Physics and Chemistry of the Earth, 28, 1333-1341.

Hamby, DM. (1994). A review of techniques for parameter sensitivity analysis of environmental models. Environmental Monitoring and Assessment 32, 135-154.

Jewitt, GPW,. Schulze, RE. (1999). Verification of the ACRU model for forest hydrology applications. Water SA, 25(4), 483-489.

Jewitt, G. (2002). Can Integrated Water Resources Management sustain the provision of ecosystem goods and services?. Physics and Chemistry of the Earth, 27, 887-895.

Kampf, SK., Burges, SJ. (2007) A framework for classifying and comparing distributed hillslope and catchment hydrologic models. Water Resources Research 43: W05423, doi:10.1029/

Le Roux, PAL et al., (2009) Soil data for hydrologists (Weatherley & Craigieburn) Unpublished report, University of the Free State, South Africa.

Lin, HS. (2009). Earth's Critical Zone and hydropedology: concepts, characteristics, and advances. Hydrology and Earth Systems Science Discussions, 6, 3417-3481.

Lorentz, S. Thornton-Dibb, S. Pretorius, JJ. Goba, P. (2003) Hydrological Systems Modelling Research Programme: Hydrological Processes, Phase II: Quantification of Hillslope, Riparian and Wetland Processes, Report to the Water Research Commission on the Project: A Field Study of Two and Three Dimensional Processes. Water Research Commission. Pretoria, South Africa. WRC Report K5/1061

Lorentz, SA., Bursey, K., Idowu, O., Pretorius, C., Ngeleka, K. (2008) Definition and Upscaling of Key Hydrological Processes for Application in Models. Water Research Commission, Pretoria, South Africa. Report K5/1320/1/08

Lyon, SW., Troch, PA. (2007). Hillslope subsurface flow similarity: Real-world tests of the hillslope Peclet number." Water Resources Research 43: W07450, doi:10.1029/2006WR005323

McDonnell, JJ., Sivapalan, M., Vaché, K., Dunn, S., Grant, G., Haggerty, R., Hinz, C., Hooper, R., Kirchner, J., Roderick, ML., Selker, J., Weiler, M. (2007) Moving beyond heterogeneity and process complexity: A new vision for watershed hydrology. Water Resources Research, 43. doi:10.1029/2006WR005467

Michaelides, K., Chappell, A. (2009). Connectivity as a concept for characterising hydrological behaviour. HYDROLOGICAL PROCESSES, 23, 517-522.

Pachepsky, YA., Rawls, WJ., Lin, HS. (2006) Hydropedology and pedotransfer functions. Geoderma 131: 308-316.

Pollard, S. Kotze, D., Ellery, W., Cousins, T., Monareng, J., King, K., Jewitt, G. et al. (2006) Linking Water and Livelihoods: The development of an integrated wetland rehabilitation plan in the communal areas of the Sand River Catchment as a test case. Association for Water and Rural Development. http://www.award.org.za/wetlandsoct04.pdf

Rawls, WJ. (1983). Estimating bulk density from particle size analysis and organic matter content. Soil Sci. 135: 123-125

Riddell, ES., Lorentz, SA., Ellery, WN., Kotze, D., Pretorius JJ., Nketar, SN. (2007) Water Table Dynamics of a Severely Eroded Wetland System, Prior to Rehabilitation, Sand River

Catchment, South Africa. XXXV IAH Congress Groundwater and Ecosystems Ed. Ribeiro, L., Chambel, A. Condesso de Melo, MT. Lisbon, Portugal: 2007.

Riddell, ES. & Lorentz, SA. (2009) Four years of wetland rehabilitation monitoring through process hydrology – what have we learnt? 14th SANCIAHS Symposium, 21-23 September 2009, Pietermaritzburg, South Africa

Schulze, RE (1995) Hydrology and Agrohydrology: A Text to accompany the ACRU 3.00 Agrohydrological Modelling System. Water Research Commission, Pretoria, South Africa. Report TT 69/95

Schulze, RE., (2000). Modelling Hydrolgical Responses to Land Use and Climate Change: A Southern African Perspective. Ambio, 29(1), 12-22.

Seibert, J., McDonnell, JJ. (2002). On the dialog between experimentalist and modeler in catchment hydrology: Use of soft data for multicriteria model calibration. Water Resources Research, 38(11), 1241-1255.

Seibert, J., Bishop, K., Rodhe, A., McDonnell, J.J. (2003). Groundwater dynamics along a hillslope: A test of the steady state hypothesis. Water Resources Research, 39(1)

Sivapalan, M (2003). Process complexity at the hillslope scale, process simplicity at the watershed scale: is ther a connection?. Hydrological Processes, 17, 1037-1041.

Smakhtin, VU. (2001). Low-flow hydrology: a review. Journal of Hydrology, 240, 147-186.

Smithers, J., Schulze, R (2004) ACRU Agrohydrological Modelling System User Manual version 4.00. School of Bioresources Engineering and Environmental Hydrology. University of KwaZulu-Natal, Pietermaritzburg, South Africa.

Ticehurst, JL., Cresswell, HP., McKenzie, NJ., Glover, MR. (2007). Interpreting soil and topographic properties to conceptualise hillslope hydrology. Geoderma, 137, 279-292.

Troch, AP., Carillo, GA., Hiedbuchel, I., Rajgopal, S., Switanek, M., Volkmann, THM., Yaeger, M. (2008). Dealing wth Landscape Heterogeneity in Watershed Hydrology: A Review of Recent Progress toward New Hydrological Theory. Geography Compass, 2, 1749-8198

U.S. Department of the Interior. Bureau of Reclamation (2001) Water Measurement Manual. Water Resources Research Laboratory. http://www.usbr.gov/pmts/hydraulics_lab/pubs/wmm

van Tol, JJ. Kunene, BT., Freakelm CH., Le Roux, PAL., Riddell, ES. (2007) Hydropedological survey report on the Craigieburn-Manalana Research Catchment. Unpublished report, University of the Free State, South Africa

Wainwright, J. Mulligan, M. (2004) Environmental Modelling: Finding Simplicity in Complexity. Chichester: John Wiley & Sons. pp 408.

Zehe, E., Sivapalan, M. (2009) Threshold behaviour in hydrological systems as (human) geo-ecosystems: manifestations, controls, implications. Hydrology and Earth Systems Science 13: 1273-1297.

8 FOUR YEARS OF WETLAND MONITORING THROUGH PROCESS HYDROLOGY – WHAT HAVE WE LEARNT?

ES Riddell[1]

[1]School of Bioresources Engineering and Environmental Hydrology, University of KwaZulu-Natal, P/Bag X01, Scottsville, Pietermaritzburg, 3209.

ABSTRACT

This paper presents a synopsis of the findings of a monitoring and hydrological process definition of a valley bottom wetland under going technical rehabilitation at the headwaters of the Sand River in the Mpumalanga lowveld.

Findings include the identification of a rapid delivery mechanism of water from the surrounding hillslopes to the wetland following a threshold exceeding precipitation event. The reintroduction of artesian groundwater phenomena has also been determined as a result of the rehabilitation structure installed in the wetland. There is an evaluation of short and long term impacts of such rehabilitation measures. Hydro-geomorphic controls in the form of *clay plugs* have also been revealed and their role within these catchments is explored. A summary of the water budget and associated fluxes of the wetland is developed and it is revealed that this wetland does not necessarily confirm to the typical assumptions that wetlands augment low flows and attenuate peak flows. Rather it is that these functions are expressed differently at different periods within the hydrological season in relation to catchments soil moisture defecit.

The potential for extrapolation of results to other headwater catchments of the Sand River, which are also similarly degraded is discussed as well as the integration of these findings for catchment management in a complex socio-biophysical landscape. Recommendations are made, based on our findings for future sustainable use of and future restoration efforts for these catchments and their wetlands.

Keywords: Erosion, Hillslope Processes, Hydro-geomorphology, Rehabilitation, Wetlands.

8.1 INTRODUCTION

It is the case that wetlands are generally seen as important ecologically rich areas within the broader landscape. For the water resources fraternity wetlands may, but are not always, seen to be valuable hydrological units within river networks, where different wetland types have various hydrological functions within different parts of the catchment (Mitsch & Gosselink, 2000). In recent years as the commoditization of natural resources has become an important mechanism through which to gauge the value of preserving natural ecosystems and their status in terms of facilitating human well-being, wetlands for the most part score highly for provision of ecosystem goods and services both intrinsically and extrinsically (e.g. Millennium Ecosystem Assessment, 2005). This is certainly true for sub-Saharan Africa where their use for subsistence activities through for example hunting, harvesting and, increasingly, cultivation continues. Moreover, it is expected that conversion of natural savanna landscapes, which make a significant portion of the African continent, to agricultural production is likely to increase in the future (Falkenmark and Rockström, 2004), due to increasing demographic pressures. This is in all likelihood going to lead to the modification of the wetland systems within this biome. Hence understanding the hydrological processes of these wetland systems in the savannas is critical to ensure the sustainable utilization of these landscapes in the future.

There is a general dearth in the knowledge of the hydrology of wetland systems in Africa, and this has duly been noted for Southern Africa also (Grenfell *et al*., 2005). Where hydrological studies have been undertaken on wetlands in the region, they are constrained by the heterogeneous geomorphic templates of the landscape that cause each wetland to seemingly operate in different ways, this precludes the development of a unifying wetland hydrological process framework. The fact that the geological and climatic template of southern Africa is vastly different from the temperate northern continents also means that general underscoring principles of wetland management gathered now quite comprehensively in that region are unlikely to be suitably applied to the wetlands of southern Africa (e.g. Ellery et al, 2008). Nevertheless the more the systems of southern Africa are studied in detail, it is hoped that a sphere of overarching principles will emerge through which the sustainable management of their processes and resources may be secured in the future. This issue is of tantamount importance given that great emphasis is put on wetland rehabilitation particularly in South Africa through poverty relief strategies. This of course is a laudable undertaking for political, social and environmental reasons, however the environmental component of this objective may well be

undermined by unsatisfactory understanding of the hydro-geomorphic controls and fluxes that would otherwise characterise these wetlands in a natural state, possibly leading to inappropriate rehabilitation measures (Tooth & McCarthy, 2007).

This paper summarises the hydrology of a riparian headwater wetland in the semi-arid north east of South Africa, whose degradation through significant gully erosion is similarly experienced in other wetlands in the area. This degradation is assumed to be a compound effect of firstly, the local geological and climatic conditions, steep granitic geology and intense rainfall due to their position close to the northern Drakensberg Escarpment. Second, historical political legacies have asserted a significant anthropogenic pressure on this landscape through forced resettlement and consequent expansion of population pressure on this sensitive region of the South African lowveld. A major pressure of which is the extensive use of the valley bottom wetlands for subsistence agriculture. An extensive assessment of the causal mechanisms for the wetland degradation in the Sand River headwaters is provided by Pollard *et al.,* (2006) and the assumption outlined that this degradation, along with streamflow reduction by commercial forestry, has contributed to the loss of baseflow in the Sand River system. Essentially these conditions have fostered a switch in the Sand River from being a major perennial tributary of the Sabie River to one that is now dominated largely by a seasonal flow regime. In the same report an exploratory modelling exercise using the ACRU model (Schulze, 1995) at a variety of scales supported the notion that loss of wetland extent in the headwaters of the Sand River catchment has significant effects on streamflow processes at the broader catchment scale.

8.1.1 Headwater wetland hydrology

To date, in the subcontinent, most attention has been paid to the process definition of a certain type of wetland which lie at the headwaters of large river systems and usually termed *vlei* (South Africa), *dambo* (Zimbabwe/Zambia), or *mbuga* (East Africa), with various names in other parts of the continent. Early works generated the belief that these systems are important for streamflow regulation processes in terms of flood attenuation and low flow augmentation, in essence by acting as ‘sponges’ absorbing water during the rains and releasing slowly during the dry season (e.g. Balek & Perry, 1972). Recent works have however challenged this assumption (von der Heyden & New, 2003, McCartney, 2000, Bullock, 1992). Meanwhile these systems retain the potential and often are used as an agricultural and grazing resource within the region

and the continent for that matter, due to their moisture holding properties particularly in the dry season.

Von der Heyden (2004) produced a comprehensive review based on these works and others, extrapolating the common hydrological processes that were experienced in different headwater wetland studies and critiquing them against various proposed models of dambo hydrological and hydrogeological function from the literature. It was however acknowledged that due to their widespread distribution and hence high variability in geo- and meteorological characteristics, no unifying model could be prescribed for estimating the hydrological responses of dambos. Nevertheless an attempt was made to link estimated hydrological response to a set of catchment characteristics, based on:

1. the size of the catchment (m^2)
2. the size of the dambo (m^2)
3. the vegetation of the catchment
4. the catchment rainfall regime
5. the sand to silt and clay fraction of the interfluve soil.

Which yielded von der Heyden's (2004) hypothesis of dambo wetland hydrological processes:

1. The dominant source of water to the dambo i.e. the ratio of wetland water derived from direct rainfall compared with that from groundwater discharge is inversely proportional to the catchment: dambo surface area ratio.

2. The interfluve vegetation characteristics are the primary determinants of the relationship between dambo and interfluve evapotranspiration (ET) losses.

3a. The duration of dry season flow from dambos is directly proportional to the catchment: dambo surface area ratio, and inversely proportional to the interfluve woodland: grassland surface area ratio when the ratio of direct rainfall to groundwater input to the dambo is less than a certain threshold value.

3b. This duration of dry season flow is also directly proportional to the ratio of the sand fraction to the clay-silt fraction within the interfluve soils, when soil depth is greater than a certain threshold value.

4. The volume of dry season flow from dambos, normalized for rainfall, is directly proportional to the catchment: dambo surface area ratio (and hence, as expected, is directly proportional to the duration of dry season flow.

5a. The attenuation and retardation of stormflow is a function of the intensity of the rainfall event

5b. The attenuation and retardation of stormflow is a function of the product of the sum of current seasonal precipitation and the inverse of the time since the last rainfall event greater than a certain threshold value.

5c. The attenuation and retardation of stormflow is a function of the catchment: dambo surface-area ratio.

5d. The attenuation and retardation of stormflow is a function of the ratio of the sand fraction to the clay-silt fraction within the interfluve soils.

Furthermore, three models were presented from the literature describing the hydrogeological controls on these systems. All of which acknowledge the presence of a low permeability layer close to the dambo surface that impedes the vertical flow of water into the dambo, and these had evident consequences on the hydrological processes within the dambos.

8.1.2 Sand River wetlands: typically Dambos? Consequences for rehabilitation?

This paper outlines the discernible hydrological fluxes that have been described so far for the Craigieburn-Manalana wetland sub-catchment of the Sand River. The main objective for instrumenting this catchment for hydrological processes definition was to examine the response of the wetlands hydrology to technical rehabilitation of large erosion gullies and determining the broader hydrological context of the system. The findings presented here are discussed in relation to components of the wetland water budget and reflected upon the understanding above of the dambo hydrology to date, as well as the effects of wetland rehabilitation.

8.2 METHODS

8.2.1 Study site information

The Craigieburn-Manalana research catchment lies on the granitic geology of the basement complex and is intersected by doleritic dykes, consequently the catchment is dominated by sandy soils, particularly in the valley bottom, except for doleritic areas which yield fine clays. It lies in the sub-humid fringe of the semi-arid lowveld and has a mean annual precipitation of 1075 mm per annum (1904-2000) and a similar rate of potential evapotranspiration. Land use in the catchment is dominated by peri-urban rural settlement, free roaming grazing and extensive use of the valley bottom wetlands used particularly for the cultivation of madumbes. Typically wetland plots consist of steep raised beds and deep drainage furrows which run parallel to the direction of catchment runoff. There is also extensive gully erosion in with the wetland itself as well as on the catchment interfluves.

8.2.2 Hydrology

The catchment was instrumented with hydrometric apparatus during the latter half of winter of 2005 (August-October), along three transects perpendicular to the catchment (two of which are shown in Figure 8.1). Along these transects hydrometric stations fitted with 3-channel soil moisture sensors, typically at 300, 600 and 2000 mm depths alongside nested groundwater level piezometers, which in some instances were fitted with pressure transducers. This data collected using HOBO data loggers using an SBEEH-UKZN timing board system allowed continuous, 12-minute time-step recording of soil moisture tension and groundwater levels along hillslope-wetland and longitudinal wetland transects. Piezometers were also manually read with a dip-meter to record groundwater levels. In addition stations on hillslopes were paired with standard dimension (22 m x 2.4 m) USLE runoff plots with tipping bucket recording mechanism to record runoff volumes.

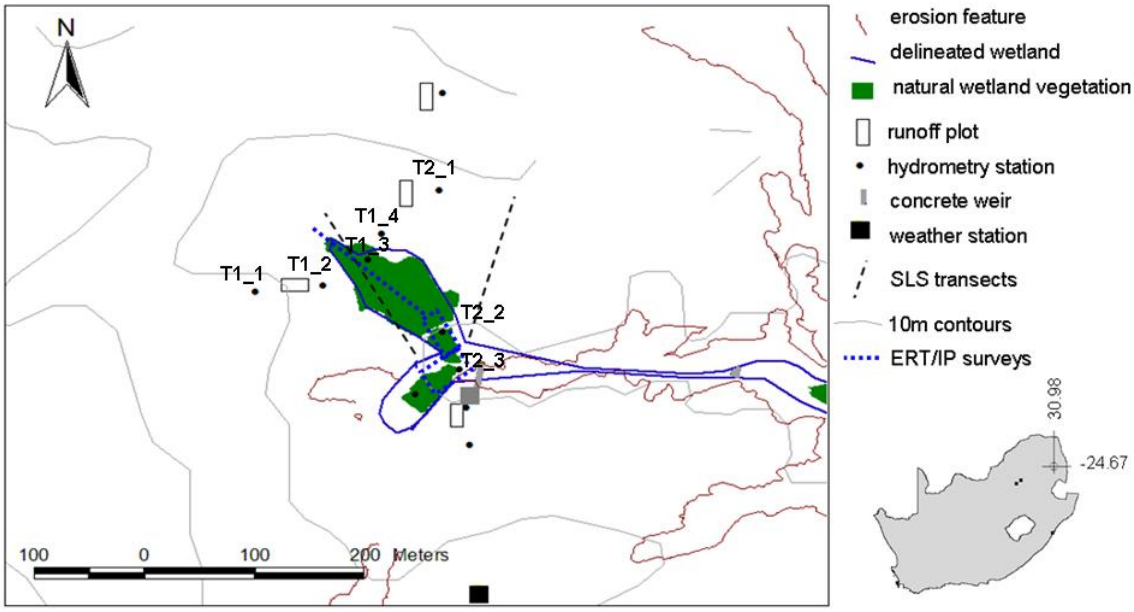

Figure 8.1: The Craigieburn-Manalana wetland with locations of hydrometric instrumentation and measurements (T1 and T2 denote transects 1 and 2 respectively).

The catchment was also fitted with a full meteorological Campbell Scientific weather station for estimation of potential evapotranspiration (pET) using the Penman-Monteith equation (Allen *et al*., 1998). This station was also fitted with a Texas Instruments rain gauge, in addition to a standalone rain gauge on the opposite side of the catchment.

Streamflows were recorded at the outlet of the intact portion of the wetland after the completion and integration with a concrete buttress weir for the 2008-09 wet season. This used a submersible float gauge with Campbell Scientific shaft encoder. An ISCO sampler was also integrated with this logging system to collect in-stream isotope species (O^{18} – Oxygen-18 and H^2 - Deuterium) at prescribed flow depths. Two component hydrograph separation was achieved using the method described by Ulhenbrook & Hoeg (2003) in the form of equation 8.1:

(8.1) $$Q_E = Q_T \frac{c_T^{18}O - c_P^{18}O}{c_E^{18}O - c_P^{18}O}$$

Where: Q_E is the total contribution of event (rainfall) water to stream discharge; Q_T is the total volume of discharge; c_T is the total isotopic composition of discharge water; c_P is the isotopic

composition of pre-event water; c_E is the isotopic composition of event water; ^{18}O reflects the stable isotope used in this case Oxygen-18.

The weir structure was initially installed between December 2006 and March 2007, however due to unforeseen erosion problems it only became effective following remedial actions prior to the 2008-09 season.

Isotope samples were also taken from piezometers and runoff plots at regular intervals during the 2008-09 season using a hand held electronic pumping system, and grab samples were taken at points downstream of the wetland as well as nearby DWAF boreholes.

Furthermore the use of the geophysical method of Electrical Resistivity Imaging (ERI) was undertaken at various parts of the catchment throughout the study, with an intensive use of this method alongside the complementary Induced Polarisation (IP) technique during July-August 2008.

In addition, the 2008-09 season saw the actual quantification of evapotranspiration losses from vegetation types in the Craigieburn-Manalana catchment using a suite of energy balance methods including surface layer scintillometry (SLS), eddy co-variance, and surface renewal by the CSIR (Everson *et al*., 2009) the key findings of which are summarised in Appendix viii. At this juncture it should be noted that the wetland itself is dominated by reed beds (*Phragmites mauritianus*) and that the interfluve by mixed seasonal grassland and Mabola plum (*Parinari curatellifolia*). The wetland and interfluve represent 4% and 96% of the catchment area respectively.

8.3 RESULTS

This results section provides summaries relating to various components of the wetland water budget and hydrogeomorphic findings.

8.3.1 Inflow mechanisms

The Craigieburn-Manalana catchment is characterized by rainfall that can often be quite intense as well as having a relatively high inter-annual variability, this is summarized for the period of monitoring between 2005-2009 in Table 8.1.

Table 8.1: Summary precipitation information for the Craigieburn-Manalana catchment

2005-06*	1771.9 mm	
2006-07	809.6 mm	Mean (2006-09) 15-min rainfall intensity 2.59 mm/hr
2007-08	817.0 mm	ST. Dev 1.4
2008-09	1444.9 mm	Peak 85.2 mm/hr

* Full record from nearby (4.6km) Hebron Forestry Estate

During the course of the soil moisture and shallow groundwater monitoring it was noted that the soil moisture regime of the catchment follows as would be expected, the distribution of seasonal rainfall, such that they are dry during winter and wet during summer. However noticeable differences were observed on the soils of the two dominant geologies of the catchment. Firstly, the shallow but coarse grained hillslope soils on granite (glenrosa soil form – UFS, 2008) were characterized by rapid fluctuations in soil moisture tension in the shallow soils (0 - 600 mm) due to infiltrating rain water, whilst deeper soils remained largely dry except under exceptional rainfall conditions where saturated vertical flow filled cracks and voids in these weathering horizons. Second the deep fine grained soils (oakleaf soil form UFS, 2008) of the doleritic hillslopes were characterized by more moderate wet-drying cycles and were freely drained, noted by the more apparent changes in soil moisture tension in the deeper horizons, thus contrasting with the granitic soils. The differences in the water holding properties of these soils and contrasting hydraulic behaviours are shown in Figure 8.2a.

Whilst the two different dominant geologies showed different hydrological responses, it has been recorded in each of the four successive years of monitoring that following a large rainfall event usually when the catchment was close to saturation, that a threshold exceeding soil moisture response is initiated at the hillslope toe soils (Kroonstad soil form). This mechanism which follows the reaching of a certain antecedent soil moisture status and trigger rainfall event

induces a rapid delivery of water to the valley bottom wetland with a near instantaneous elevation in the wetland phreatic surface. This behaviour is shown for an event during early January 2006 in Figure 8.2b, whereupon there is significant drop in capillary pressure head in the deep 2000mm tensiometer which sits in the clay rich G-horizon of these soils. Consequently one then observes a similar response in the 2000mm tensiometer in the wetland soils, and rapid elevation of the groundwater level as recorded with corresponding piezometer. The precise mechanism for this phenomenon has been attributed to dual-porosity (macro-pore) properties of these hillslope toe soils (Riddell & Lorentz, *in review*, Chapter 4).

During the first year of monitoring of the wetland hydrodynamics (piezometric surface fluctuations), it was noted that there existed a sequence vertical recharge processes from the surface to the shallow subsurface overlying deep recharging piezometric surfaces in the wetland, this is exemplified in Figure 8.3a.i where three different piezometric heads are recorded in each of the three piezometers at T2_2. There is some stratification in the vertical recharge processes in the shallow sub-surface which is attributed to the occurrence of narrow clay aquicludes in an otherwise sandy soil matrix (Riddell *et al*., *in prep*, Chapter 5). Furthermore, it became apparent that certain artesian conditions may also be manifested in this system, particularly at the height of the rains, this is reflected by the shallower groundwater observed in the 4000 mm than the 2000 mm piezometer during March 2006. Whilst this reflected the hydrodynamics for intact regions of the wetland, this was not so for areas in close proximity to erosion headcuts. Note that Figure 8.3a.ii for site T2_3 adjacent to the erosion gully (Figure 8.1) also shows the occurrence of seasonally shallow and a deep recharging piezometric surface, however no artesian pressures are experienced at this region. Furthermore, it had been observed that water table fluctuations at this location contrasted strongly with other regions of this wetland and that there also appeared to be a discernable hydraulic drawdown at this location due to the unimpeded drainage through the erosion gully (Riddell *et al*., 2007). Following the initial installation of the buttress weir, 2006-07 season, the reintroduction of an artesian piezometric surface was revealed at T2_3, this is shown in Figure 8.3b, where the piezometric head in the 7000mm piezometer comes close the heads recorded in the shallower piezometers. This implied a positive response to the system, given that it would have been expected that this type of artesian hydrodynamic behaviour would exist throughout this wetland. However the fact that the deep recharging water table (recorded in 7000mm piezometer) contrasts with that observed at T2_2 where it was the 4000mm piezometer that exhibited this artesian phenomena, suggests a possible different mechanism is occurring.

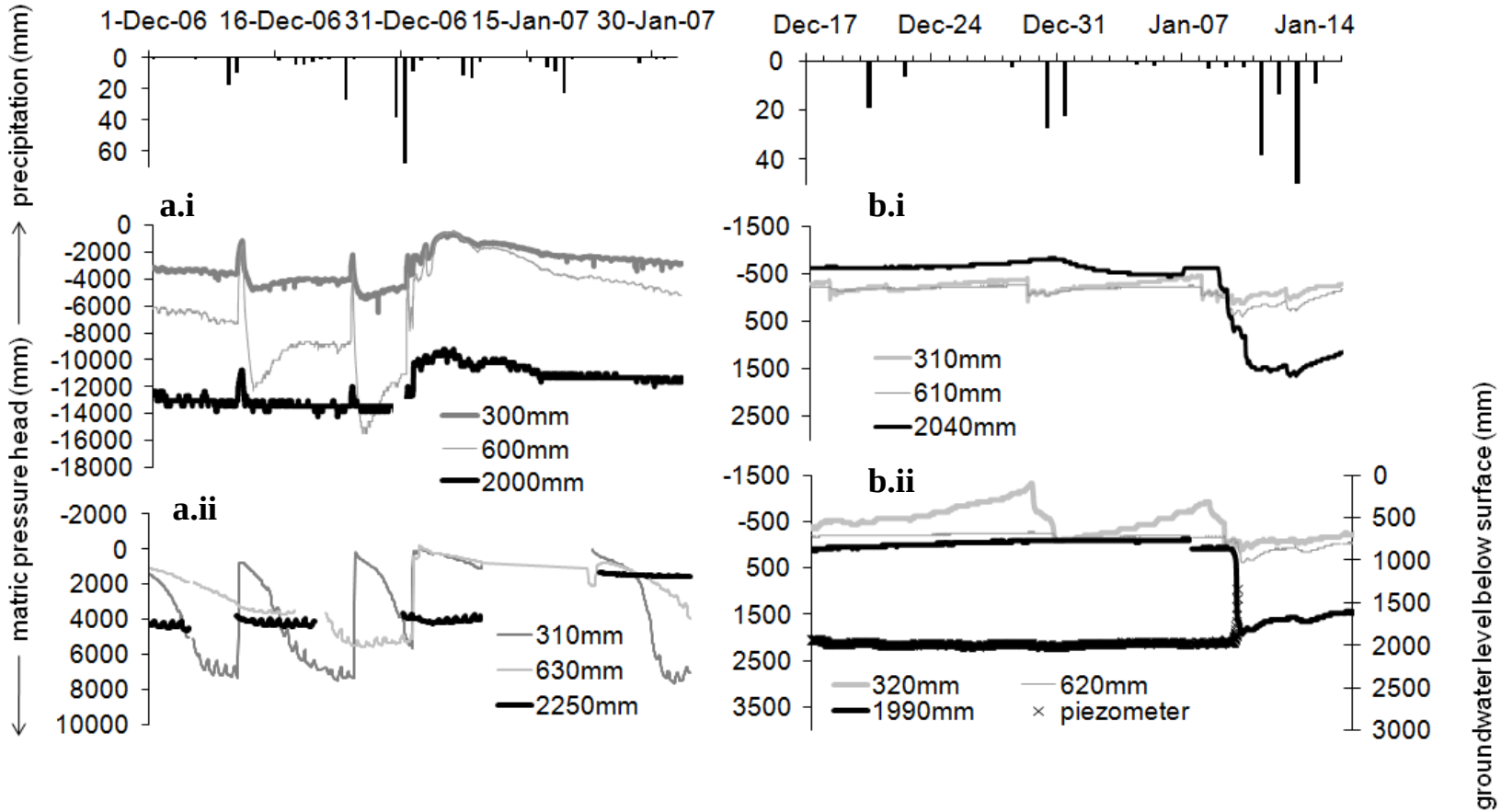

Figure 8.2: typical flashy granite hillslope soil moisture response observed at T1_1 (a.i); typical moderate soil moisture response on doleritic hillslope observed at T2_1 (a.ii); rapid drop in soil moisture tension at 2000mm in G-horizon of hillslope toe (Kroonstad) soils observed at T1_2 (b.i); consequent drop in soil moisture tension at 2000mm in the wetland and rapid elevation of wetland water table observed at T1_3 (b.ii).

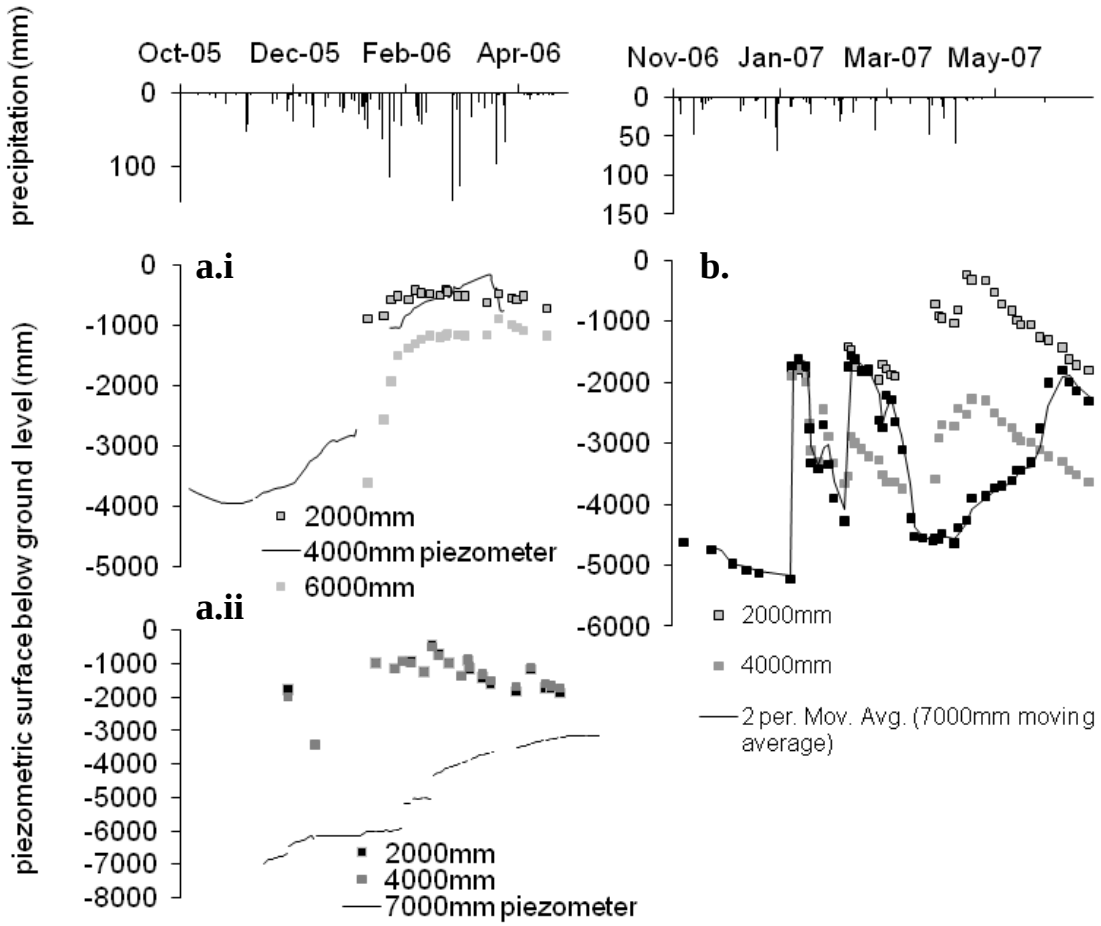

Figure 8.3: Groundwater levels observed at T2_2 during the 2005-06 season (a.i); groundwater levels observed at T2_3 during the 2005-06 season (a.ii); groundwater levels observed at T2_3 during the first rehabilitation year (2006-07).

8.3.2 Hydro-geomorphology

In addition to the horizontal clay lithology previously discussed with regard to the stratification of water tables in the wetland, it was postulated prior to rehabilitation (2004-5) that moisture is retained within this sandy and rather conductive wetland substrate by zones of finer sediment, or in other words vertical clay sub-terrainean walls, which have informally been termed *clay plugs*.

This potential hydro-geomorphic structure was originally identified during the first season of monitoring through Electrical Resistivity Imaging (ERI) and was thought to exert a considerable control on the sub-surface hydraulic processes, by essentially buffering sub-surface throughflows, due to its expected lower hydraulic conductivity than the surrounding sandy wetland substrate (Riddell *et al.*, 2007).

Figure 8.4 shows a more recent determination of this hydrogeomorphic control that is discussed at length by Riddell *et al* (*in review*, Chapter 6). Here the use of the geophysical technique 2-dimensional electrical resistivity (ERI) and induced polarisation (IP) revealed the clay plug which was now threatened by any further retreat upstream of the erosion gully, and hence loss of sub-surface control exerting hydrodynamic protection of the wetland upstream of it. Here zones of low resistivity material (0-100 ohms) correspond to the resistance range of clays in the absence of groundwater, similarly the low chargeability bands in the lower diagram correspond to the capacitance range of fine clays. This survey also revealed that the wetland is underlain at depth by clays and the overburden is dominated by coarse sands.

8.3.3 Outflows and Water Budget

Since the technical rehabilitation of the Craigieburn-Manalana wetland was only fully implemented during the 2008-09 season, as a result of unanticipated failures of the rehabilitation structure, discharges out of the wetland could only be measured during this latest season. The component fluxes of incoming and outgoing water to the catchment mass balance up to the time of writing are depicted in Figure 8.5, assuming at this stage that groundwater fluxes are a minor component. Here the highly seasonal precipitation (P) and runoff (Q) may be observed, resulting in high precipitation and runoff during summer i.e. November to March and in no flows with minimal precipitation in winter (May onwards). Consequently we note that potential evapotranspiration (pET) represents a net loss of water from the system in winter, assuming of

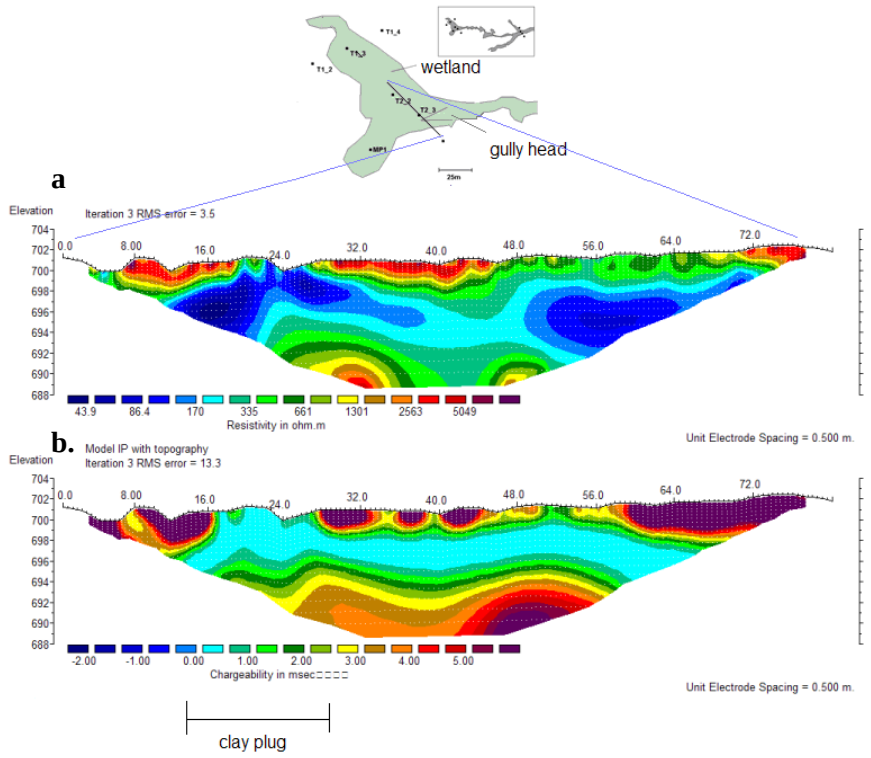

Figure 8.4: 2 Dimensional Electrical Resistivity (a) and Induced Polarisation (b) examination of a clay plug near to the gully head in the Craigieburn-Manalana wetland (August 2008).

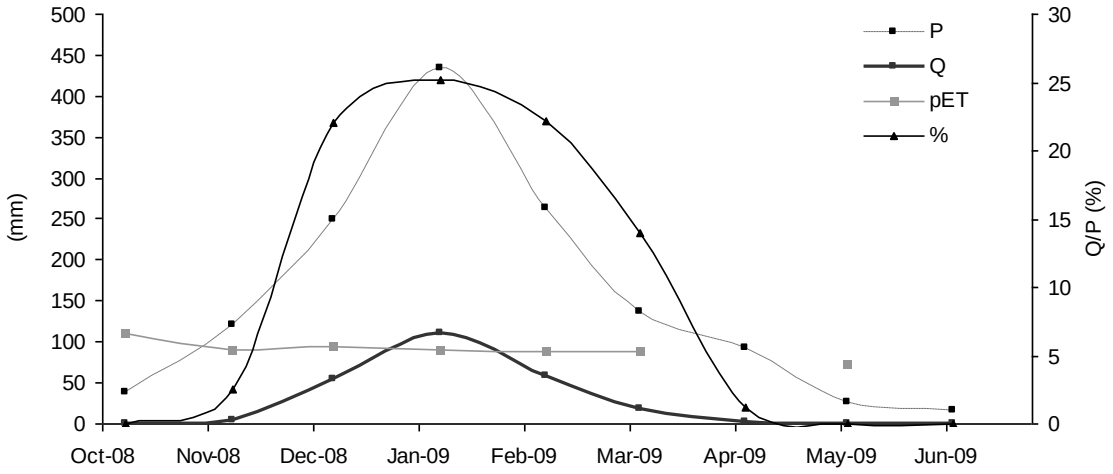

Figure 8.5: Catchment scale water budget components for the 2008-09 hydrological season (groundwater excluded)

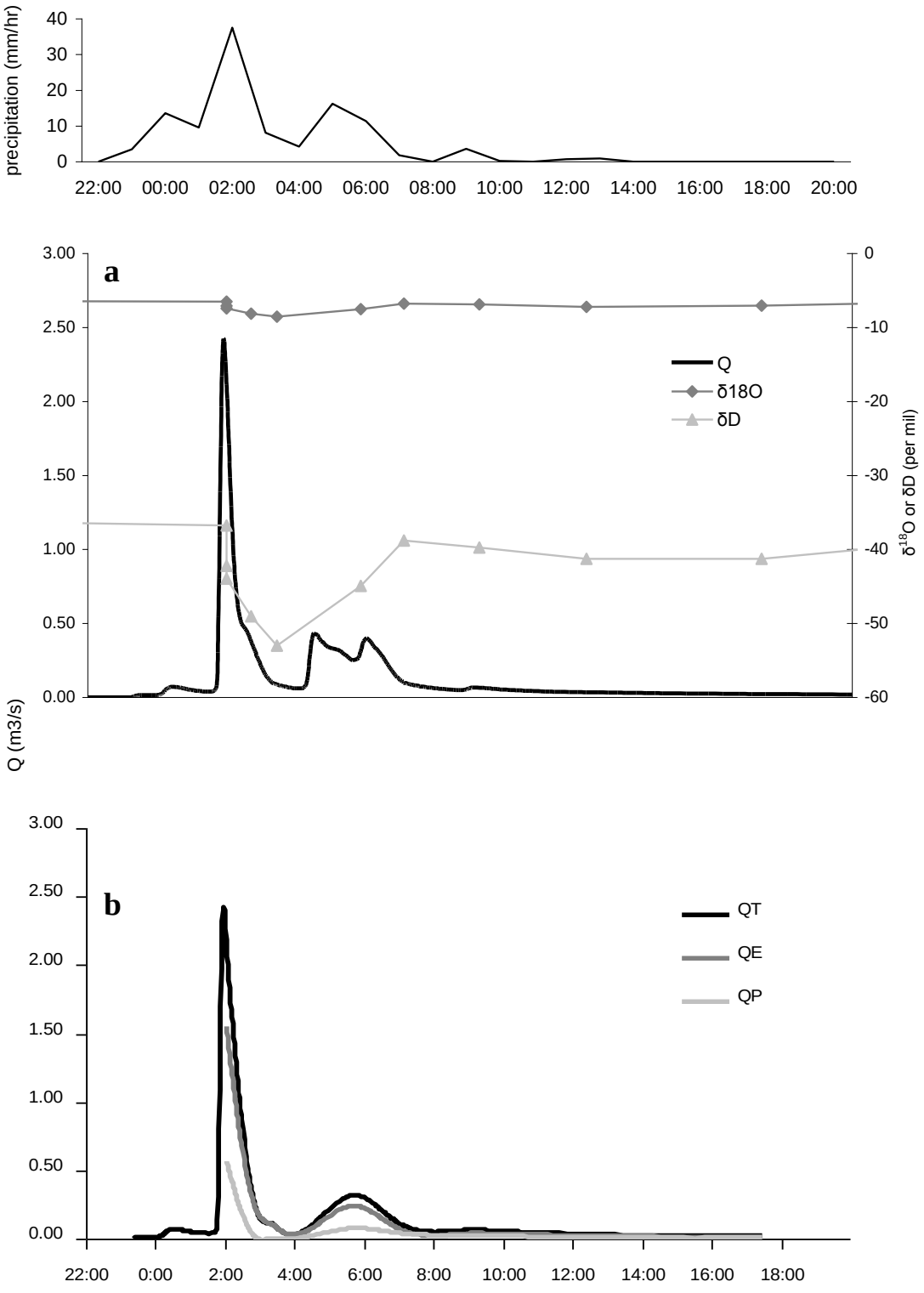

Figure 8.6: a. streamflow concentrations of ^{18}O and ^{2}H (D) and; b. Two component hydrograph separation of ^{18}O for a storm of 28-29 December 2008 (QT is total event discharge; QE is event water discharge; and QP is pre-event water discharge).

course that actual ET approaches or is equal to pET, and conversely there is a net gain in water in summer due to precipitation. However Figure 8.5 reveals an interesting hydrological effect of the catchment when the outgoing runoff is expressed as a percentage of the incoming precipitation, wherein the percentage of rainfall that becomes runoff is minor during October and November at <5%, to be expected as the catchment begins to saturate. Meanwhile during December to February the percentage of runoff generated ranges between 20% and 25%, despite the very heavy rains of January this is not seen to yield a significant conversion to runoff. This may well be attributable to an increase in catchment hydraulic roughness resulting from heightened biomass production of emergent wetland (and upland) vegetation at the height of summer, which in itself will enhance the actual evapotranspiration component of the catchment water budget.

Meanwhile, Figure 8.6 reveals a two component hydrograph separation for an event of late December 2008. Using stable isotopes of oxygen-18 revealed that a significant proportion of the storm water runoff comprises event (i.e. rainfall collected during the event of 28-29 December 2008) water rather than pre-event water (1 sample taken in a ponded area adjacent to a furrow stream inlet upstream of the weir on 12 December 2008) stored in the wetland or catchment prior to the storm. At the peak of the storm runoff, event water comprised 73% of the total, rising to 93% at the lowest point along the storm recession, thereafter remaining at between approximately 60-70%. Furthermore this relationship closely follows the rainfall intensity distribution for the storm event, revealing the exceedingly small lag response for this catchment.

A daily water budget for the Craigieburn-Manalana wetland is revealed in Table 8.2 for the period when surface energy balance techniques (Everson *et al*., 2009) were used to quantify the actual vegetation water use in the wetland and its contributing catchment. This being for 1 week winter/dry season and 1 week summer/wet season periods during the 2008-09 hydrological year. Groundwater movement into and out of the wetland was assumed to be a negligible component of the water budget based on the estimate obtained from piezometer well readings with the deeper clays underlying the wetland (see Appendix vi), estimates for the dry winter period were ~ 0.7×10^{-4} $mm.d^{-1}$ and during the wet summer 1.8×10^{-4} mm/d With respect to the dry season it is noted that the water budget dynamic is a largely intrinsic affair, whereupon there is no or extremely little input by rain as well as no surface water discharge. Rather there is a net flux of water exiting the system through evapotranspiration processes, particularly in the wetland. Since the mean reference evapotranspiration for the winter period was 3.6 mm, these findings reveal that the wetland system loses water to the atmosphere at close to the potential rate, suggesting

that water is still not limited, despite this August-September window tending toward the latter part of the dry season. Meanwhile the interfluve area does not lose water close to the potential rate suggesting that water is limited in this area of the catchment. During the wet season however whose mean reference evapotranspiration was 3.4 mm, the observed water use on the interfluve and the wetland occurs at or above the potential rate. Significantly, therefore, the seasonal balance in water use at the catchment scale is dominated by activation of water use by vegetation on the interfluve which represents a far greater proportion of the catchment surface area. The summer season also sees the far greater role of rainfall and surface discharge on controlling the water balance, facilitating a significantly large change in storage, which is generally recharging, contrasting sharply with the depleting storage of the dry season.

8.4 DISCUSSION

8.4.1 In the context of headwater wetland hydrology

Given the key findings outlined from the Craigieburn-Manalana catchment, and given the context of headwater wetland hydrology in the southern Africa region, are there any parallels to be drawn between this and other studies? In addition what may this tell us about the effects of technical rehabilitation in the wetlands of the Sand River both for intrinsic impacts and/or downstream?

Using the Craigieburn-Manalana wetland as an example of the typical wetland setting in the Sand Rivers headwaters some striking insights and similarities may be gleaned from the literature. In the first instance, it is the underlying geology and concomitant hydrological processes that are particularly interesting. In addition to the strongly seasonal rainfall regime it is the permeable nature of the granitic regolith that typifies the hydrology of interfluves, at least on dambo catchments, which seems to contrast with the low conductivity valley bottom substrates (Bullock, 1992). Whilst our own insights at Craigieburn-Manalana illustrate a permeable interfluve regime being also due to the dominant granitic hillslope, the less dominant doleritic hillslope would seem however to present a contrast to this. However given the dominance of the granite in this landscape we can safely assume that the hydrological processes at the catchment scale reflect the geological influence. Whilst initial dissimilarity with Bullock's (1992) description may be assumed with the typical composition of the valley bottom wetland

Table 8.2: Daily water budget for the Craigieburn-Manalana wetland for days where evapotranspiration was quantified using energy balance techniques.

Winter 2008	**Aug-29**	**Aug-30**	**Aug-31**	**Sept-01**	**Sept-02**	**Sept-03**
ET* interfluve (mm)	1.3	2.2		0.9	1.7	1.3
ET* wetland (mm)	2.3	2.9	3.5	2.5	3.4	2.8
rain interfluve (mm)	0	0	0	0	0	0
rain wetland (mm)	0	0	0	0	0	0
discharge (mm)	0	0	0	0	0	0
ΔS (mm) interfluve	-1.30	-2.20		-0.90	-1.70	-1.30
ΔS (mm) wetland	-2.30	-2.90	-3.50	-2.50	-3.40	-2.80

Summer 2009	**Jan-28**	**Jan-29**	**Jan-30**	**Jan-31**	**Feb-01**	**Feb-02**	**Feb-03**
ET* interfluve (mm)	1.1	3.3	3.8		1.7	4.9	4.8
ET* wetland (mm)	1.2	3.9	4.4	2.7	2.2	5.1	5.1
rain interfluve (mm)	0.2	8.4	27.7	62.3	43.8	4.9	80.3
rain wetland (mm)	0.2	8.4	27.7	62.3	43.8	4.9	80.3
discharge (mm)	0.16	0.13	1.08	10.26	9.89	0.34	24.06
ΔS (mm) interfluve	-0.74	5.23	24.94		51.62	0.33	98.67
ΔS (mm) wetland	-0.99	4.50	23.34	59.98	41.97	-0.19	76.09

*Evapotranspiration quantified using Surface Layer Scintillometer (Everson *et al*., 2009)

ΔS change in storage

material of the Sand River headwaters, who as the names suggests reflects that they are dominated by coarse sands and retain a high hydraulic conductivity. However it has been shown through hydrodynamic observation and geophysical surveys and has now become quite apparent given the water budgeting previously discussed that there is indeed an increase in the content of finer particles at depth in these valley bottom zones, at least in the lower horizons acting as a significant aquitard to groundwater flow. The only major contrast with Bullock's (1992) description of dambos is rather that the Sand River wetland soils are very deep (several metres) rather than shallow.

Whilst dambo systems have also been acknowledged to experience rapid water table rise, for instance by Balek & Perry (1973), the precise duration of this mechanism contrasts with the findings presented here, since their study at the Luano catchments in Zambia, the water table rise occurred over the period of approximately half the month of December 1969 and rose by less than 500 mm. Rather the situation in the wetland of the Craigieburn-Manalana was over 500 mm in a matter of hours. Meanwhile Acres et al., (1985), report variations in water table response according to dambo soil type, in which predominantly sandy soils are saturated earlier in the wet season and are more liable to rapid water level rise and fluctuations than are predominantly clay soils. This therefore exemplifies that a universal response is not apparent in all dambo systems. However the superficially sandy material of the Craigieburn-Manalana wetland suggests it conforms to the rapid water table rise mechanism. Although the precise mechanism for its occurrence at the Craigieburn-Manalana is being ascribed to a dual-porosity function of the interfluve-wetland interfacing soils (Riddell & Lorentz *in review*, Chapter 4) a model for similar mechanisms have been described for dambo catchments in Malawi by McFarlane (1992). The McFarlane model suggests rapid displacement of upwelling groundwater through the clay of dambo floor via the underlying saprolite, this remains a possibility at the Craigieburn-Manalana as a contributory mechanism and needs to be determined. Since there is undoubtedly a substantial clay lens at depth in the Craigieburn-Manalana, it is more likely that no discharge into the wetland occurs via the underlying regolith as was reported by McCartney and Neal (1999) for the Grasslands Research Station dambo in Zimbabwe. Rudimentary stable isotope analysis sampled from piezometers outlined in appendix v suggests that this also may be the case when compared to local groundwater borehole water samples. This was based on qualitative interpretation of the samples proximity to one another on a $^{18}O/^{2}H$ scatter plot. However this evidence is not conclusive and needs to be more thoroughly determined. Moreover the McCartney and Neal (1999) model suggests that runoff within the

dambo was derived from shallow sources and when the water table dropped below the clay lens underlying the dambo consequently discharge out of the dambo ceased. Whilst the evidence of wetland hydrodynamic responses (Riddell *et al.*, in prep, Chapter 5) also shows that wetland through-flows are dominantly shallow in nature, the responses of the Manalana wetland may be similar given the observed responses as shown in Figure 8.7, where soon after the cessation of summer rains during mid-April 2009 streamflow stops by 26th April completely and the shallow water tables adjacent to the to the wetland outlet then begin to decline, however they are still reasonably shallow and have probably just dropped into the clay aquitard but not through it at this time (recall the very shallow clays, or high capacitance material between 16-28 m in Figure 8.4).

The catchment scale water budget components illustrated in Figure 5 showed that the proportion of precipitation that is converted to runoff is generally 20-25% at the height of the rain season. The slight disparity seen for the month of January 2009, where the proportion of rainfall converted to runoff is lower than expected may be a combination of reduced rainfall intensity for this period and problems associated with missing data due to equipment failure. Nevertheless, the hydrograph separation suggests that the dominant component of flow in this wetland system comes from event water and this has interesting implications in terms if downstream processes and contrasts with the common perception that wetlands attenuate flows.

Rather it may appear that these wetlands actually convey storm water to downstream areas most likely due to the emergence of a saturated area in the valley bottom, particularly later in the season which prevents downward infiltration of storm water into the wetland substrate. This transition from an early season storage system when there is a soil moisture deficit (SMD) to one that becomes saturated and acts as a conduit of water after depletion of the SMD has similar been shown by McCartney (1998) and hence this is true similarity with the dambo hydrological model. This of course is influenced by the intensity of the rainfall event and soil hydraulic properties. Nevertheless it does seem to suggest that these wetlands may increase a rivers response to rainfall, as was shown in the majority of headwater wetland studies reviewed by Bullock & Acreman (2003). However, whilst this may be the case in the present situation in the Craigieburn-Manalana, it must also be remembered that certain factors, such as the network of drainage furrows in these wetlands may also act to supply a significant proportion of event water contributing to the wetlands discharge as opportunities for storm water detention have been significantly reduced. Meanwhile due to over three years of abandonment of these plots, emergent hydrophytic vegetation has recolonised the area (personal non-quantified observation)

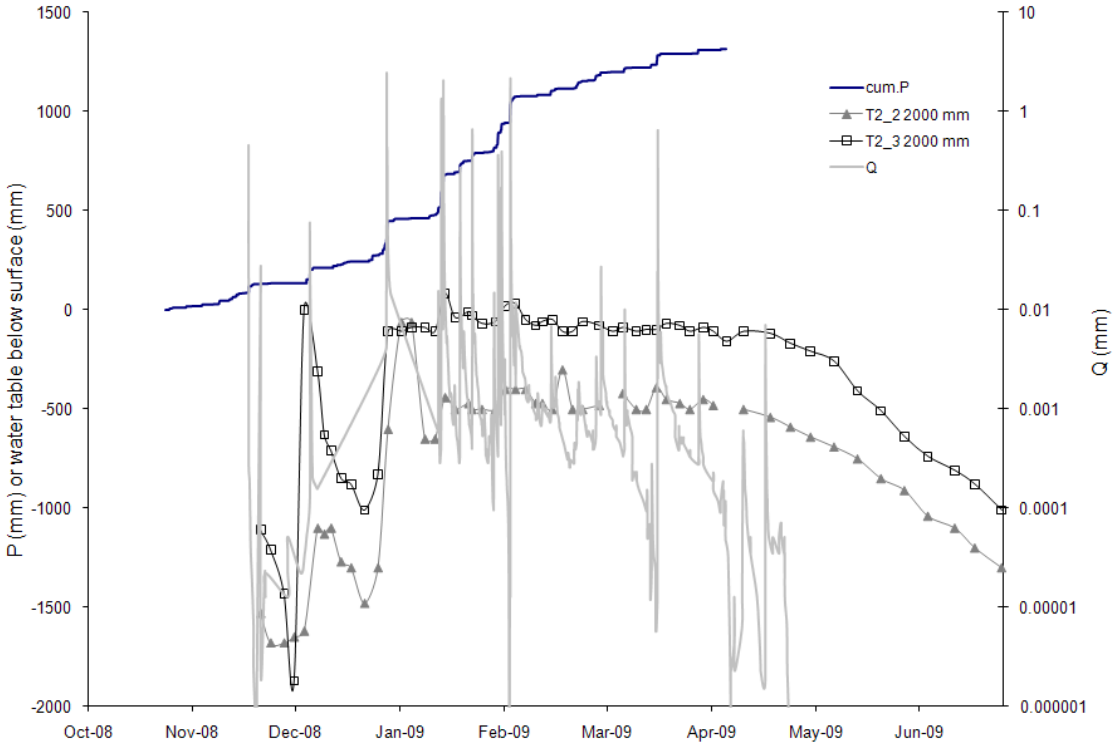

Figure 8.7: Plot of stream discharge (Q) for the 2008-09 hydrological year, against cumulative rain (P) and shallow piezometer reading at T2_2 and T2_3.

and hence the hydraulic roughness portrayed by this vegetation will also now be close to maximum and may go some way to mitigate against the occurrence of these artificial channels.

Since there is now a semblance of the effects of these wetlands on summer peak flows in terms of addressing the flood attenuation hypotheses of wetlands. It is also necessary to consider the effects of dry season effects of wetlands to stream flows in terms of the commonly held perception of low flow augmentation. Bullock & Acreman (2003) in their review of wetland hydrology suggested that the majority of studies implied both the greater net use of water by wetlands when compared with their contributing catchments as well as the effect of wetlands reducing dry season flows downstream through evapotranspiration. The findings as presented here would almost certainly adhere to both of these notions, whereupon a consistent reduction in the wetland storage was observed daily during the ET quantification campaign, attributed fully to the water use of hydrophytic vegetation, when at the same time there was no discharge occurring out of the wetland (at the surface at least and negligibly to groundwater). The findings presented here however merely reflect the water balance at the most headward end of the catchment where distinct seasonality is observed in the streamflow response. As one moves

downstream within the Craigieburn-Manalana catchment the wetland becomes perennial and free flowing water is observed throughout the year. This does however occur at a point where minor tributaries join the main stem of the wetland. Whether this lower part of the wetland intersects the regional water table or receives more sustained augmented low flows from some other hydrological processes in these tributaries remains to be characterized and it is recommended that this be done so in the future (supplementary evidence presented in Appendix v suggests that there could indeed be an intersection of the regional water table). This is particularly necessary for upscaling and extrapolation of findings at the Craigieburn-Manalana to the broader headwaters of the Sand River catchment.

8.4.2 Implications of findings for rehabilitation and future management

Given the context of the hydrological process definition to date of this wetland system a few general principles can be outlined at this stage. The first relates to the impacts of the technical rehabilitation which suggests that the installation of the buttress weir has gone some way to mimic the effects of the otherwise natural clay plugs that would have characterised these systems. This in part seems successful and it certainly is in terms of preventing the removal of any further wetland sediment by erosion, which is crucially important to subsistence agriculture. It is therefore likely that this type of rehabilitation produces meaningful impacts in term of the hydrological consequences of rehabilitation at the wetland scale. Most certainly in the wet season, but the rehabilitation also has prevented the hydraulic drawdown of water too early by the erosion gullies and allows for a more reasonable perpetuity of the shallow water tables into the early half of the dry season, by effectively plugging the system hydrologically. Furthermore a question remains as to whether or not this rehabilitation may lead to enhanced water use by the wetland vegetation given that subsurface flows may now be retained in the system rather than as buffered through flows. Based on the findings (Riddell *et al*, *in review*, Chapter 6) useful insights have been made into the development of the clay plugs in zones of valley confinement. It is suggested, that based on this knowledge, future technical rehabilitation endeavours in the Sand River's wetlands use this information to define optimum sites for rehabilitation, where they will have both greatest hydrological and geomorphological effect.

It is probably safe to assume, given the relatively uniform geology of the Sand River's headwater, that this mechanism occurs in most, if not all of these headwater catchments, although further exploratory analysis of catchment soil forms should ideally be sought in the

other headwater catchments. Moreover, it was not explicitly stated in this manuscript, but it has been observed that these hillslope toe soils in these catchments contain deep clay rich G-horizons and have a high specific water retention, thus they stay moist well into the dry season (e.g. Appendix vii). These two reasons suggest that these parts are particularly important for catchment processes. Given this, and the author's acknowledgment that these areas are often attractive regions of the catchment to develop for agricultural purposes mean that either these regions should be protected from further alteration, or further research is required to determine the optimum depth and type of mechanical alteration acceptable to prevent deterioration of the important processes that they provide to wetland-catchment processes (see discussion in Chapter 4).

Following this review and knowing the context of the land-use that already exits in these wetland catchments, the emerging perception would be that sustainable wetland agriculture in these systems can be achieved by using inherent water that would otherwise be lost to evaporation with little impact on dry season flows. This conclusion has similarly been reached in dambo systems of Zimbabwe (McCartney, 2000). However, the findings presented here still need to be assessed by longer term monitoring within the context of sustained rehabilitation success, but there is promise that suitable biophysical principles and solutions can be developed for the future sustainable use of these systems, but this is within the constraints of a fundamentally more complex socio-biophysical template that has been described in detail by Pollard *et al* (2006), there are signs however that the wise-use of headwater wetlands can be achieved for example in Ethiopia as has been described by Dixon & Wood (2003).

8.5 CONCLUSION

This paper has outlined the findings of hydrological processes definition and effects of technical rehabilitation on a small headwater wetland, and it has done this in the context of current understanding of headwater wetland hydrology in southern Africa, namely dambo systems. For the most part the Sand River wetlands show conformity with processes previously determined in dambo systems and certainly lends support, although not conclusively at this stage, to the recent view that headwater wetlands do not actually attenuate flood water and augment base flows. Moreover it is likely that suitable agronomic methodologies could be developed for the continued use of these systems with little or no impact on catchment scale processes.

ACKNOWLEDGEMENTS

This research was funded by the South African Water Research Commission (WRC). The author acknowledges the kind contributions of Mr Ronny Maaboi, Mr Rex Mothlabini, and Mr Difference Thibela for fieldwork assistance. Logistical and administrative support was provided by the Association for Water and Rural Development (AWARD). Mr Cobus Pretorius for technical assistance. Thanks also to Dr Colin Everson, Mr Alistar Clulow and Dr Michael Mengistu of the Council for Scientific and Industrial Research (CSIR) for their time in quantifying surface energy fluxes.

REFERENCES

Acres *et al.,* (1985) cited in Von Der Heyden, CJ. (2004). The hydrology and hydrogeology of dambos: a review. Progress in Physical Geography, 28(4), 544 - 564.

Allen, R. G., Pereira, L. S., Raes, D., Leuven, K. U., Smith, M., Service, M., et al. (1998). Crop evapotranspiration - Guidelines for computing crop water requirements - FAO Irrigation and drainage paper 56. FAO - Food and Agriculture Organization of the United Nations. Rome.

Balek, J., Perry, JE. (1972) Hydrology of seasonally inundated African headwater swamps. Journal of Hydrology 19: 227-249.

Bullock, A. (1992) Dambo hydrology in southern Africa - review and reassessment. Journal of Hydrology 134: 373-396.

Bullock, A., & Acreman, M. (2003). The role of wetlands in the hydrological cycle. Hydrology and Earth System Sciences, 7(3).

Dixon, A. B., & Wood, A. P. (2003). Wetland cultivation and hydrological management in eastern Africa: Matching community and hydrological needs through sustainable wetland use. Natural Resources Forum, 27, 117-129.

Ellery, WN. *et al.*, (2008). WET-Origins: Controls on the distribution and dynamics of wetlands in South Africa.. Pretoria: Water Research Commission, WRC Report No TT 334

Everson, C., Clulow, A., Mengistu, M. (2009). Quantification of Evapotranspiration from a South African Rehabilitated Headwater Wetland. Water Research Commission, Pretoria. Project No. K8/826

Falkenmark, M. Rockstrom, J. (2004) Balancing Water for Humans and Nature: The New Approach in Ecohydrology. London: Earthscan, p247.

Grenfell, M.C., Ellery, W.N. Preston-Whyte, R.A. (2005). Wetlands as early warning (eco)systems for water resource management. Water SA 31(4) 465-471.

Millenium Ecosystem Assessment (2005). Ecosystems and Human Well-Being: Wetlands and Water Synthesis. World Resources Institute. Washington DC.

Mitsch, W. J., & Gosselink, J. G. (2000). The value of wetlands: importance of scale and landscape setting. Ecological Economics, 35 (200), 25 - 33.

McCartney, M. P. (2000). The Water Budget of a Headwater Catchment Containing a Dambo. Physics and Chemistry of the Earth (B), 25(7-8), 611-616.

McCartney, M.P. (1998) The hydrology of a headwater catchment containing a dambo. PhD Thesis. The University of Reading: Department of Soil Science, 266pp.

McCartney, M. P., & Neal, C. (1999). Water flow pathways and the water balance within a headwater catchment containing a dambo: inferences drawn from hydrochemical investigations. Hydrology and Earth System Sciences, 3(4), 581-591.

McFarlane, M. J. (1992). Groundwater movement and water chemistry associated with weathering profiles of the African surface in parts of Malawi. Geological Society Special Publication, (66), 101-129.

Pollard, S. *et al*., (2006) Linking Water and Livelihoods: The development of an integrated wetland rehabilitation plan in the communal areas of the Sand River Catchment as a test case. Association for Water and Rural Development. http://www.award.org.za/wetlandsoct04.pdf

Riddell, E. S., *et al.*, (2007). Water Table Dynamics of a Severely Eroded Wetland System, Prior to Rehabilitation, Sand River Catchment, South Africa. In M. Ribeiro, L., Chambel, A. Condesso De Melo, XXXV IAH Congress Groundwater and Ecosystems Lisbon, Portugal.

Schulze, RE. Hydrology and Agrohydrology: A Text to accompany the ACRU 3.00 Agrohydrological Modelling System. South Africa: Water Research Commission, 1995.

Tooth, S. McCarthy, TS. (2007). Wetlands in drylands: geomorphological and sedimentological characteristics, with emphasis on examples from Southern Africa. Progress in Physical Geography 31.1: 3-41.

Uhlenbrook, S. & Hoeg, S. (2003). Quantifying uncertainties in tracer-based hydrograph separations: a case study for two-, three- and five-component hydrograph separations in a mountainous catchment. Hydrological Processes. 17: 431-453

UFS (2008). Internal report by the University of the Free State

von der Heyden, C. J., & New, M. G. (2003). The role of a dambo in the hydrology of a catchment and the river network downstream. Hydrology and Earth System Sciences, 7(3), 339-357.

von der Heyden, C. J. (2004). The hydrology and hydrogeology of dambos: a review. Progress in Physical Geography, 28(4), 544 - 564.

9 GENERAL DISCUSSION AND CONCLUSIONS

9.1 OVERVIEW

This chapter brings together the results of the research and discusses the outcomes of the respective results chapters in an integrated manner. This being in general terms with respect to the objectives posed in the introduction and what has been achieved through these findings. It will also allow for some speculation on wetland hydrological and geomorphic function in the context of wetland land-uses for subsistence agriculture, as well as identifying future research needs based on questions that have arisen from this research.

The integrated approach to the re-instatement of wetland function in headwater catchments in Africa is advocated by authors such as Wood (2006). This author specifically calls for the holistic approach to rehabilitation of wetlands, including their contributing catchments, with respect to both the biophysical aspects that are governed by land-management as well as the socio-economic aspects that enable or constrain livelihood security for those that use the wetland systems.

Given that this research emanated from a plan for the integrated rehabilitation of degraded wetlands (erosion, desiccation and loss of fertility), in relation to broader issues surrounding integrated catchment management within the larger Sand River (alteration of the flow regime) following the work done by Pollard *et al.,* (2005). The research presented here has sought to quantify and qualify the hydrology of one particular wetland and it's contributing catchment at this river's headwaters. It is within the context of continuing expansion into wetland systems for agricultural purposes, particularly in sub-Saharan Africa, that ways should be found to facilitate agricultural development in wetlands that do not compromise a wetlands ability to provide ecosystem goods and services to those that use them and also for various streamflow regulation processes required downstream (Rebelo *et al.,* 2009). This is pertinent in the case of the Craigieburn-Manalana where Pollard *et al.,* (2008) identified through cost-benefit analysis that the effect alone of installing rehabilitation structures in the wetland on people's livelihood security, through direct and indirect wetland uses, would pre-empt an anticipated 75% decline in gross wetland derived income (from R149,256 to R38,196 per annum) for the Craigieburn residents. If the wetland was allowed to continually erode then this critical safety net would be

lost. It is anticipated that the findings presented in this thesis may then be constructed to management recommendations used in future and expanded rehabilitation interventions here and elsewhere.

Furthermore, since Chapter 8 describes the relative fitting of the Craigieburn-Manalana's hydrology to conceptual models of wetland hydrology in southern Africa, then these recommendations will be discussed in relation to unifying hydrological themes or those functions otherwise uncovered to-date in the region. This is necessary since the sacrosanct functions that have broadly been ascribed to wetlands, such as deeming them crucial for various streamflow functions have generally no empirical basis in the field of African wetland hydrology as discussed by Bullock *et al* (1998). Therefore the context under which each wetland is examined, needs to be discussed and is done so in the following sections.

9.2 OUTCOMES OF THE OBJECTIVES AND HYDPOTHESES ANALYSIS

Whilst specific findings have been presented in the preceding chapters, these have not been discussed with respect to the overall objectives outlined in Chapter 1. This section is an attempt to do so, based on the evidence acquired during the study and this commences with objective O1:

O1. The determination of the present and the past sedimentary and depositional processes within the Manalana catchment that have shaped its present hydrological functioning.

O1.i There is no discernable evidence that zones of fine sediments exist at longitudinal sections within the Manalana wetland that may retard the wetland throughflows (clay plug theory)

O1.ii There is no discernable evidence that zones of fine sediments exist in horizontal layers (stratified) within the Manalana wetland that may impact wetland throughflows.

As will be elaborated on further, the Manalana wetland displays a variety of geomorphic processes that have an interesting effect on the way the wetland functions hydrodynamically. The spatial movement of colluvium is also variable as demsonstrated with runoff plots sediment yields (Appendix ix). Of course, the alluvial processes that have facilitated the horizontal

zonation of the wetland substrates and partition vertically infiltrating water are but one aspect. Chapter 4 reveals how sorting of sediments from the surrounding hillslopes through illuvial processes has created at least one zone of fine sediment (clays) that effectively buffers throughflows from upstream, with important consequences for moisture retention, as shown in Chapter 5. Since the wetland has experienced severe gully erosion it is proposed that a series of these *plugs* have been removed from areas where the longitudinal orientation of the Manalana catchment is confined. Significantly, this may explain at least in part the apparent non-modification of the hydrodynamic regime of the wetland at the lower headcut where two additional wetland tributaries join the main-stem, and the authors own observations have noted the significantly high clay content of the wetland here, contrasting with the increasingly sandy wetland sediments further upstream.

The results therefore support both hypotheses that the wetland hydrology is controlled by both horizontal and vertical banding of fine sediments (clays) within an otherwise sandy and hydraulically conductive matrix.

O2a. Quantification of surface and sub-surface inputs to the Manalana wetland: which are the most significant contributors to the wetland water budget and do these vary by location and season (time)?

H_0 – water is not supplied to the Manalana wetland largely as overland surface flow from the contributing catchment (as a consequence of reduced infiltration into the sub-surface within the catchment interfluves).

At the outset it was assumed that there was no significant channelized inflow into the Manalana wetland and this held true throughout the study, albeit apart from occasional flows from upstream wetland agricultural plots.

Meanwhile four successive years of monitoring revealed the same threshold induced lateral transfer of water from the hillslope sub-surface to the valley bottom wetland. This mechanism described in Chapter 6 induced significant amounts of water to the wetland domain from upslope through both preferential macro-pore flow initiation in lower clay rich horizons at the hillslope toe and lateral ponded flows above this horizon. It is assumed that this high water flow mechanism is a natural response that would have characterised these catchments, however, presently other hillslope toe regions have already been converted to agricultural use and the

structure of their soils altered, whilst in the specific study area these horizons remained intact. As a consequence of this it may be concluded that water is delivered to the wetland largely as sub-surface flow. In areas where agricultural expansion has moved to the wetland-hillslope interface then reduced infiltration into the subsurface agricultural soils will in all likelihood have occurred to the detriment of wetland hydrological function. In this case the hypothesis for sub-surface flow maintained wetland hydrology is supported, certainly where agriculture has not taken place.

However not all hillslopes in the Manalana catchment responded in this fashion, some for instance showed signs of free drainage at conditions close to but not quite at saturation (compared with those that otherwise yielded the lateral ponded and preferential flow responses) and these were pointed out in Chapter 8.

Whilst it was the sub-surface delivery of water from the hillslopes to the wetland that was shown to be the major contributor, the significant spatial variation in surface runoff generation was also noted. This finding was not made explicit in the results Chapters, but a summary of responses from USLE runoff plots are revealed in appendix ix. Here one will note the significantly higher runoff generation on the shallower soils of the interfluve (on Glenrosa soil type), than on the deeper recharge type soils (Oakleaf soils) associated with dolerite dykes. Thus one would expect, during significant rainfall events that the wetland may be supplemented locally by overland flows on hillsides dominated by the Glenrosa soil form when it's shallow soil moisture storage capacity is exceeded, and saturated overland flows are initiated.

It has also been revealed, although preliminarily, that the stable isotopic signatures of the wetland near surface waters seem to be derived from very recent rainfall processes in the surrounding hillside as these waters have a similar isotopic ratios to event rainfall (Appendix v). These isotopic signatures contrast with the deeper waters of the wetland within the clays (and perhaps below a clay aquiclude) that show similar stable isotope ratios to waters collected in boreholes in the surrounding headwaters of the Sand River (Appendix v). Whilst the deeper permanent groundwater flow rates were not fully quantified (see estimate in Chapter 8) as part of this study we can assume that this is most probably significantly slower than the other near surface inputs of water. Although at times seen in the deep piezometers, it was indicated by the artesian phenomena during peak rainfall periods that this groundwater contribution could be relatively rapid, in general the clays underlying the wetland act as a significant aquitard, restricting groundwater movement into or out of the wetlands surface, at noted in Chapter 8.

One speculates that fissures in the piedmonts of the nearby Klein Drakensberg escarpment may be driving the artesian processes observed on occasion, although the distance of the Manalana to the escarpment of several kilometres may mean that this is not feasible – this needs to be examined in future research.

In summary, water is delivered to the Craigieburn-Manalana wetland via sub-surface flows which are voluminous and rapid from granite derived hillslopes and prolonged and sustained from those hillslopes that contain dolerites. Degradation of these interfluves will promote the generation of overland flows from these hillslopes to the wetland.

O2b. Quantification of the wetland throughflows (in the horizontal sub-surface, vertical sub-surface and surface domains).

Chapter 5 revealed through hydrodynamic observation the nature of the wetland hydroperiod and how a series of shallow water tables seemed to be separated by aquicludes resulting from alluvial sorting. This had implications for the way that water moves through the wetland, and it appeared highly likely that early on during the rain season water ponded above these aquicludes, followed thereafter by vertical recharge to deeper horizons in the wetland soil matrix, such that most of the wetland became saturated. This has implications for the way that the wetland was able to transmit water at the surface. The impact of this was revealed in Chapter 8 where we saw that the wetland converted a greater proportion of rainfall to runoff mid-way through the HY2008 season. The connection is then made that the Manalana wetland was able to take up incoming rainfall early on during the rain season to satisfy its soil moisture deficit which is buffered by shallow aquicludes, and transmitted laterally downstream as interflows. Saturated overland flows then dominate the streamflow generally from mid-rain season onwards when the soil moisture deficit is reduced to 0.

O3. Quantification of the responses to the rehabilitation intervention on the wetland hydrological dynamics (to include an inference on the natural hydrological dynamics before headcut erosion in the absence of baseline data).

O3.i. H_0 – The rehabilitation structure (buttress weir) to be installed at the first headcut within the Manalana catchment does not raise the wetland water table (phreatic surface) upstream of it.

It was quite clear from Chapter 5 that the installation of the buttress weir was able to raise the wetland water table, or certainly the piezometric surface, and therefore the hypothesis that this would not be the case is rejected. Furthermore, it seemed highly likely that there were upstream areas of the wetland that showed intact or natural hydrodynamic behaviour, inferred from piezometer data, that the rehabilitation intervention was able to restore. Due to the hydro-geomorphic understanding of the wetland gleaned from the research the mechanism by which this was deemed possible seemed sensible as a result of the presence of clay aquicludes in the system. Despite this no similar conclusions could be drawn on the response, hydrologically of the lower headcut to rehabilitation as there seemed to be no discernable change in the hydrodynamic regime of the wetland a this location. This was attributed to the very high clay content of the wetland at this location. One speculates that this lower wetland region is also maintained in perpetuity by regional groundwater that intersects the land-surface at the confluence of the wetland tributaries here (Appendix v). The conclusion therefore is that one can expect significant intra-wetland variability in processes as a result of geomorphic processes that vary the partitioning and reconnection of sub-surface water in the wetland domain.

O4. Qualification of the impacts of land-use practices within the Craigieburn-Manalana catchment on the wetland (and contributing catchment) hydrodynamics.

As had been noted in the introductory chapter, wetland agricultural use is now extensive in this catchment and we can speculate that the modification of top-soil horizons at the hillslope toe will prevent the infiltration and consequent replenishment of seasonal moisture in the lower clay rich horizons (where there is a threshold water delivery mechanism). As a result the propensity for the wetland to transmit surface water via quickflows, rather than detain it from threshold sub-surface sources upslope will be significantly increased if these hillslope toe soils are altered in anyway.

In addition, should the shallow aquicludes within the wetland be deconstructed through ploughing for example then the effect of water table stratification and buffered vertical recharge will be lost. As the season progresses and the wetland moves from one of soil moisture deficit to equilibrium and then surplus, the wetland effectively becomes a conduit for quick storm flows as revealed through hydrograph separation (Chapter 8). This has consequences for flow variability during the inter-rainfall periods in the wet season, whereupon low flows (in-between rainfall events) may be augmented to some extent by the shallow ponding of water above these aquicludes. The incorporation of interflow response soils in the wetland allowed for successful

modelling of streamflow against the observed record for the catchment low flow modelling using ACRU in Chapter 7. However should this interflow mechanism be removed then there is an increased propensity for water to move vertically in the wetland, which could perhaps contribute to longer duration low flows and even base flows through the season, rather than quickly as interflow. However, since we also see that the wetland vegetation transpires at close to the potential rates during the hot summer rainfall months then it will relinquish water to the atmosphere, this may have otherwise been better served as part of the stream flow variability continuum downstream.

Whilst not examined explicitly in this study, the modification of the valley bottom wetland in agricultural areas to ridge and furrow agriculture is likely to have contributed to increased stormflow transmission in the wetland, as alluded to in Chapter 8 and by Pollard *et al.,* (2005).

Pollard *et al.,* (2005) suggested that the loss of top-soil horizons in the Manalana interfluves was a contributing factor to increasing catchment quickflows (and consequent erosive potential in the valley bottom wetland and low propensity for vertical recharge). The findings here support this, since it is seen that runoff initiation on Mispah/Glenrosa soil types is very high when compared with that for Oakleaf soil areas. This has implications for the way that the surrounding catchment should be used. If upland agriculture and veld clearing is to continue, then the conversion of soils of the Oakleaf form (on dolerites) should be encouraged over Glenrosa soils, where the former soils will generally have a greater (and deeper) soil moisture deficit than the latter. Indeed, in instances of rehabilitation of the interfluve, it is suggested that the degraded Glenrosa areas should be remedied first, perhaps through contour bunding in order to allow for re-sedimentation and facilitate redevelopment (pedogenesis) of a new A-horizon.

9.3 CONCEPTUAL MODEL DEVELOPMENT

Various findings of this research were discussed in the context of other wetland studies in southern Africa in Chapter 8. This section collates the findings described in to a coherent conceptual model of how the headwater catchments of the Sand River, specifically those containing wetlands, actually function both hydrologically and geomorphologically. This model is represented by means of a flow chart in Figure 9.1. Here the two types of processes, hydrologic and geomorphic are represented through interlinking feedback mechanisms. This

hydro-geomorphic feedback mechanism is known to be most likely caused by the illuviation via sub-surface action of water transporting fine material from upslope via the hillslope toes to constricted areas within the valley bottom. These constricting areas have likely impeded upstream sediment transport, and allowed for an area of backfilling where water is retained for seasonal periods to allow for saturated conditions ideal for wetland formation.

The build up of finer material to develop throughflow buffering *plugs* may also be controlled, fully or in part, by bedrock controls that set a base level for sedimentation. This was alluded to in Chapter 6 and also suggested by Pollard *et al.,* (2005). Concurrently, alluvial processes at the wetland surface allow for some sorting of fine material from coarser material creating the horizontal stratifications that explain some of the shallow throughflow phenomena.

Meanwhile the transport of finer sediments from upslope has also led to the deposition at the hillslope toes by way of deep clay rich horizons which show macro-porosity structure and relinquish water to the wetland only after significant antecedent soil moisture conditions have been met. These clay rich soils also have a high specific water retention that likely augment some subsurface flow to the wetland well into the dry season.

It is also most likely that the geomorphic processes that have created the clay aquiclude may well keep shallow wetland water disconnected from a possible deeper groundwater source external to the wetland. Whilst the rehabilitation initiative deployed in the Craigieburn-Manalana catchment raises the water table it arises most certainly from recent rainfall derived water. It may further have allowed for the reintroduction of deeper water under artesian pressures from below the aquiclude, or simply caused a connection of the two water domains (longer term isotopic analysis is recommended). In this case the rehabilitation structure seems to have successfully *re-plugged* the system, and one can only assume at this stage that re-sedimentation will occur in the gully head upstream of the structure.

Considering the processes depicted in Figure 9.1 and including other knowledge of the hydrogeomorphic construct of the Craigieburn-Manalana, allows one to depict the wetland dimensionally, for clarities sake, to provide a feel for the impacts of wetland modification on process domains within the wetland and its contributing catchment. This is shown in Figure 9.2 where one observes the disparity in hillslope processes on different geologies, where the shallow soils of granitic derived hillslopes which dominate in the catchment tend to have a relatively low vertical infiltration capacity when compared with the deep clay rich doleritic

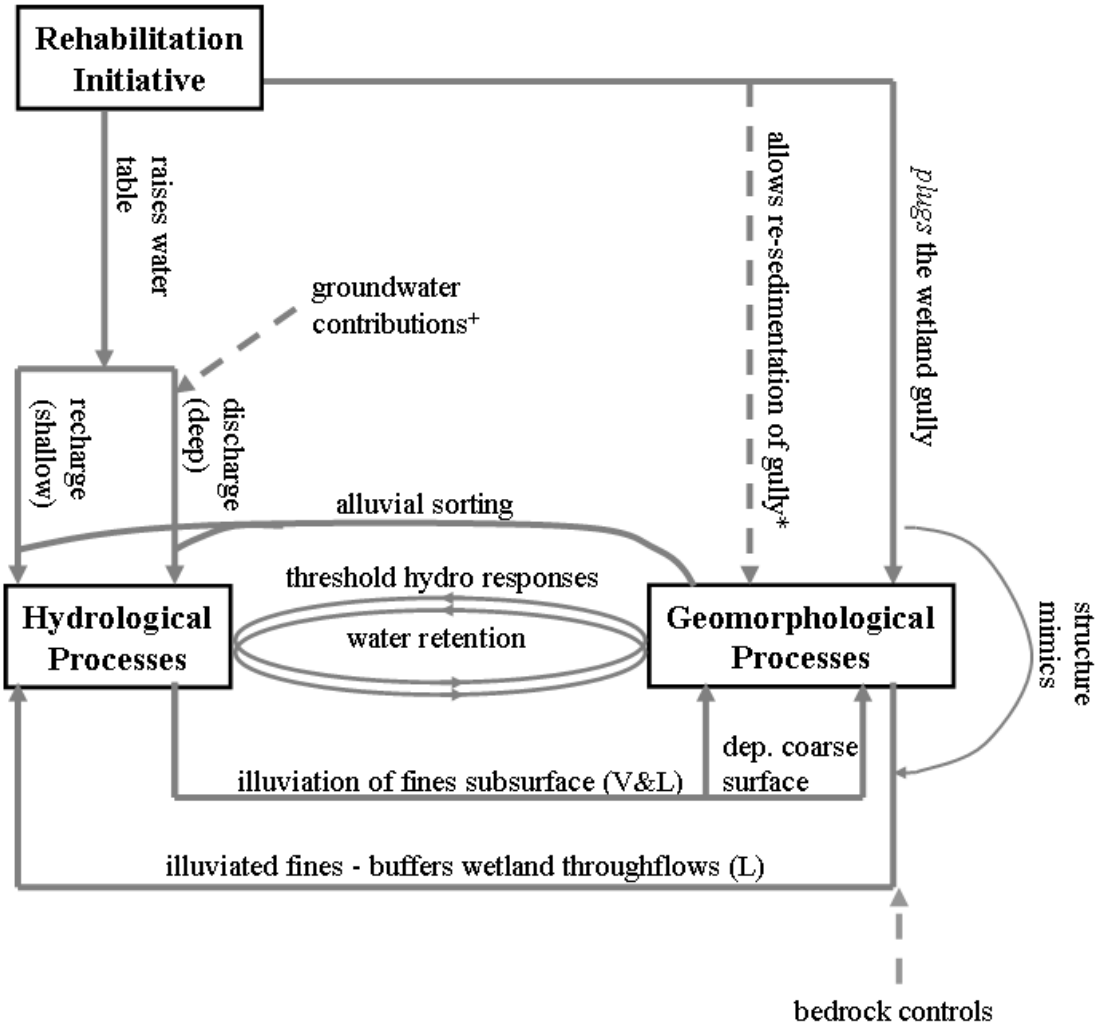

Figure 9.1: Flow diagram of the conceptual hydrological-geomorphological model for the Sand River wetlands based on empirical evidence (where: V is vertical movement; L is lateral movement; and *relates to anticipated effects beyond the time frames of this study, + this becomes increasingly important downstream).

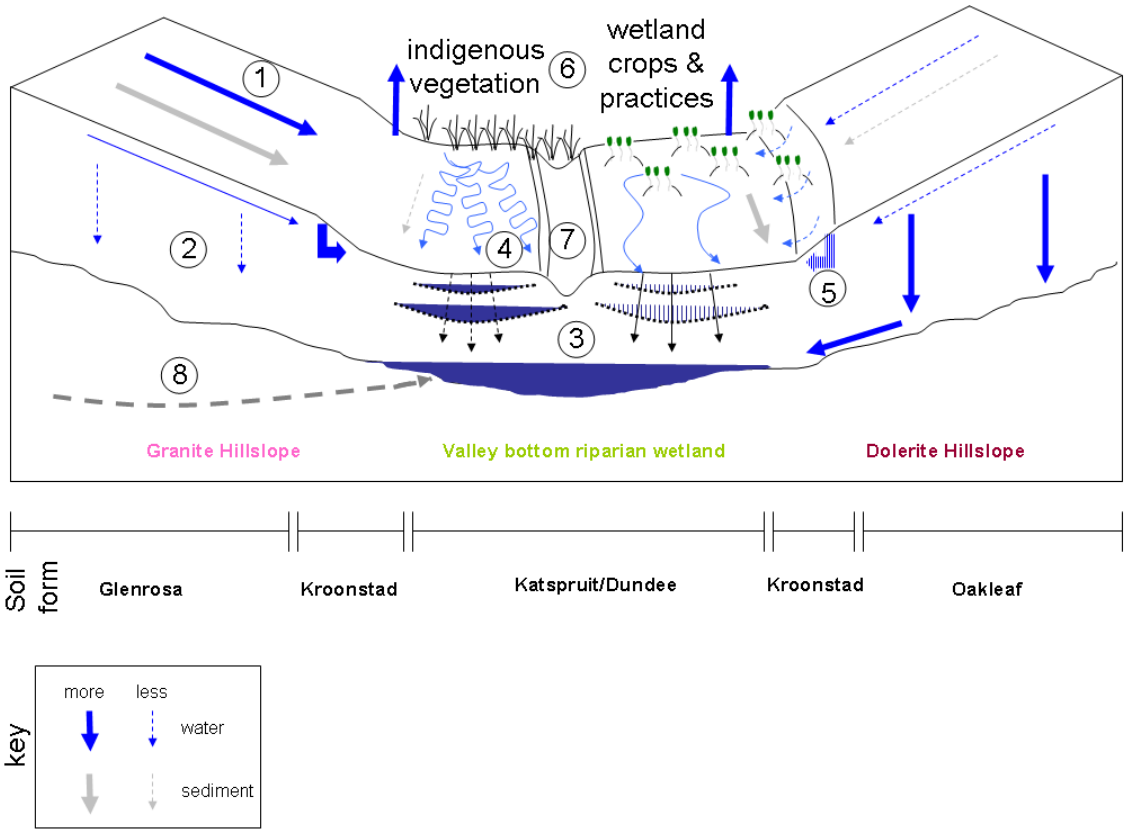

Figure 9.2: Schematic of the conceptual hydrological-geomorphological model of the Sand River headwater wetland catchments.

hillsides (2) and generate more overland flow and sediment transport (1). Meanwhile the hillslope toes are maintained by recharge from upslope, and this mechanism could be lost through their agricultural/erosion alteration (5). The wetland sub-surface itself facilitates vertical recharge into the wetland at a slow rate but has ponded water that flows laterally as throughflows, and the situation would likely be reversed if these soils are disaggregated (3). Wetland flows at the surface are likely to be diffuse in the natural condition but become increasingly rapid as the wetland surface topography is modified by agriculture (4) and main conduits created in the thalweg (7). It is known from our findings (Chapter 8) that indigenous wetland vegetation transpires at close to potential rates even during the dry winter months, likely off-setting any subsequent water that may arrive in the valley bottom from the clay hillslope toes (5). It is likely that water use by agricultural crops would also transpire close to potential rates but their relative rates may in fact be less than the natural vegetation, due to shallower root structures and different physiological requirements.

9.4 FURTHER RESEARCH

There were a number of issues the author uncovered during the course of the study as the level of investigation assessed various complexities of the system. However, in the interests of succinctness key issues will be mentioned relating to outstanding questions from the data and anticipated future requirements from this type of wetland study.

Firstly, the issue of whether groundwater had any interaction with the wetland hydrology was only discovered towards the end of the study, this discovery led one to believe in a de-coupled shallow-to-deep hydrological system. Hence, longer term stable isotopic analysis should be undertaken in this catchment to examine the extent to which groundwater-surface water interactions occur within the wetland and whether or not the rehabilitation interventions have had any contribution to this. It would also be pertinent to use the stable isotope signatures to assess over several seasons, to incorporate a range of wet-dry cycles, the relative contribution of groundwaters to the wetland, as well as the wetland to stream flows downstream. In particular the extent to which the wetland may in fact contribute to downstream baseflows, this aspect certainly needs to be examined with respect to other wetlands in sister catchments. It cannot be ruled out that the Manalana catchment may be an anomaly in the Sand River system, simply because no streamflow emanated from the wetland during winter, that there are no baseflow contributions from this wetland that emerge further downstream. It would also be useful to know through isotope analysis whether the clay rich toe soils relinquish water to the wetland during the dryer periods, and to quantify this. The justification for this being that these soils have such high water retention it would be interesting to determine how much of this water is effectively immobile, and how much, if any, is able to drain freely to supplement wetland moisture during low flow periods.

This thesis also confirmed the strong force of geomorphology at play within these wetlands, influencing their hydrological processes. The major indication being that illuviation of fines from upslope is a key contributor to this process. It would therefore be of utmost importance to typify and quantify the true sources, pathways and timing of this sediment transport. This may then have ramifications for the ways that soil and water are managed on the surrounding hillsides in an integrative rehabilitation framework. Use of geochemical finger printing of sediments for this purpose may be an obvious means, and would fit well with the long term water tracing analysis of stable isotopes just mentioned.

Due to instrumentation problems during the study, the actual wetland surface throughflows within drainage furrows were never fully quantified, and therefore unfortunately could not be expressed as part of the overall water balance. Appendix x shows evidence from an 86 mm/hr precipitation event that was captured during January 2008 and here one estimated that the each drainage furrow close to the wetland outlet transmitted up to 10% of the discharge leaving the wetland. Furtherwork on this would also allow for a quantification of one of the additional rehabilitation mechanisms proposed by Pollard *et al.,* (2005) to slow down water by re-orientation of raised cultivation beds. This should be examined through the use of a hydraulics model, where the impact of wetland terracing as a remedial action to also slow down water transport in these systems could be assessed as an alternative management strategy. Future research in the Manalana wetland should therefore quantify this in greater detail. In accordance with aspects of the wetland water balance that may be modified through wetland agriculture it would also be worthwhile to quantify through energy balance techniques, the wetland crop water use and derive crop coefficients for them. Allen *et al.,* (1998) suggest that sweet potato (the closest proxy to the madumbe cultivated in the Manalana) has a crop factor of 1.15, whilst reed beds have a crop factor of 1.2. It would therefore be worthwhile to determine whether these wetland crops transpire above the potential rate and if so, do they exceed the indigenous wetland vegetation. This would allow for greater understanding of the potentials of converting natural wetland areas to agricultural use, given that these wetlands seem to be net users of water.

It was mentioned in Chapter 5 that cumulative effects of wetland rehabilitation on catchment processes should be taken into account in the future. This is still advocated. Since exploratory analysis of wetland effects in streamflow processes was discussed by Pollard *et al.,* (2005) during the rehabilitation planning phase, it would pay to revisit this analysis given the greater understanding we now have of actual wetland processes and the impacts that rehabilitation impoundments have on these and apply these at the scale of the entire Sand river catchment. In this respect, one would seek to re-visit and update the parameters that govern wetland sub-routines in catchment based modelling. Moreover, this could certainly contribute from greater understanding of wetland low flow parameterisation as uncovered in Chapter 7. Whilst continuing to explore the role of wetlands in catchment based models, which may still rely on some non-empirical parameters. It would pay to install flow gauging structures at all sites of rehabilitation (as had been done at the upper head-cut in the Manalana) in order to carry out crude water balances using this data along with remotely sensed data for evapotranspiration for example (Bastiaanssen *et al.,* 2005; Su, 2002). These flow gauging methods can be done quite inexpensively, relative to the cost of the actual rehabilitation structures, using pressure

transducer gauges at rated sections of channel for example. Thus local water authorities should be encouraged to facilitate this process and view the wetlands as part of the water resource in the same way they would a constructed dam. This is critical, as we now move into an era of near-real time modelling of catchment processes for integrated water resource management, as is presently underway in the Incomati Basin. Through these new modelling approaches, dams are for instance used in part to manage for rivers environmental water requirements (read *ecological reserve* in South Africa) in the low flow (in both wet and dry periods) part of the flow regime. Hence it may be time to start viewing the catchments natural capital in a more strategic manner for this purpose.

In keeping with the catchment modelling and cumulative aspects, it would also be necessary to explore the wetlands as partial contributing areas, and how different wetlands in the Sand River impact the flow regime of the catchment. Despite the relatively uniform geology and climatic conditions of the catchment, the size and orientation of each wetland can be quite different. Since Balek (1983) reports that with general increase in the proportion of catchment area that is wetland, there is an almost proportional decrease in runoff generation, and this should be assessed at the Sand River's headwaters. This was beyond the scope of the thesis, but the results of the general water budgeting and hydrograph separations in Chapter 8 suggests that this avenue of investigation is warranted, and may help determine where and when to focus any future wetland rehabilitation efforts.

Specific issues that should be examined in the short to medium term at the Manalana wetland are to use biophysical indicators of rehabilitation that are not so conspicuously related to the hydrological impacts. The first of these would be to examine the rate of re-sedimentation of the erosion gullies behind the rehabilitation structures, and to determine whether the hydrological regime at these locations may allow for a return to agricultural uses. The second and related matter is to use vegetation indicators to track the rate of rehabilitation success, such as the rate of return of obligate hydrophytic species to the eroded and desiccated areas that are now within the reach of restored water table regimes.

9.5 OTHER COMMENTS

Whilst it was noted by Pollard *et al* (2005) through an older version of the ACRU model that wetlands augment baseflows and attenuate floodwaters, the findings described in this thesis (principally Chapter 8) contrasts with their model findings and the often traditionally held beliefs of wetland functions. However, this is not to say that these wetlands do not provide important streamflow regulation processes, and this needs to be given some context. The first point to note is that the wetland gullying prior to rehabilitation did indeed lead to the desiccation of the system, even during the peak of the summer rains, and therefore the wetlands propensity to augment low flows between rain events (rather than dry season baseflows) will have been severely diminished, and this is an important streamflow regulating mechanism in itself that would be lost at the scale of the Sand River catchment. Meanwhile, since these wetlands not only contain erosion gullies but are also channelled by way of agricultural practices, this will certainly speed up the transmission of surface water throughflows (quickflows). The implications of this being that the threshold at which the wetlands throughflow becomes concentrated in these systems following any given rainfall event is reduced, i.e. the required rainfall intensity and antecedent moisture condition will be less than would occur naturally.

Since intra-wetland and hillslope-wetland hydrological connectivity (and threshold shifts) have increased as a result of anthropogenic modification of the system, it is advocated in the same way that is was by Pollard *et al* (2005) to reduce the velocity of stormflow discharges in the system (that gully erosion was attributed to), perhaps by infilling any disused drainage furrows as well as re-orientating them away from their present parallel-to-streamflow orientation. Similarly the technical rehabilitation interventions are recommended to continue based on the findings presented in Chapter 5, since they buffer the wetlands longitudinal sub-surface throughflow in the same way as the clay plugs do by acting to reduce the connectivity of the wetland subsurface to the channelled flow domains. In addition, the hillslope toe soils must also be protected since their clay rich horizons also effectively plug (and retain) the hydrology of the hillslope surrounding the wetland, despite their interflow and macroporosity properties at the height of the rain season.

It has also been a conclusion within this thesis that the Craigieburn-Manalana wetland shows many similarities to the hydrological processes described in other headwater wetland hydrology studies in the region. However it must be noted that most of those, particularly dealing with

dambo systems, do so on basement granite geologies, in which case the geological template is similar to that described in this study. It is therefore worthwhile to point out that whilst the traditional assumptions of wetland streamflow regulation services may have been challenged here and elsewhere, it is important that wetland hydrology is characterised where they occur in headwater settings on other geologies in the region, since it is highly likely that differing geologies will contribute to different hydrogeomorphic feedback mechanisms leading to wetland formation and possible variations in wetland hydrological function.

9.6 CONCLUSION

The work presented in this thesis has quantified the component fluxes within a headwater wetland, and derived how these fluxes are controlled in large part by geomorphic processes in a landscape setting of considerable anthropogenic pressure. The research also uncovered certain process zones that may be considered hydrologically sensitive in that they are important for the way that the wetland functions. The results though revealed some striking similarities with recent works by predecessors working in the field of African headwater wetland hydrology adding to a growing body of empirical evidence that challenges the conventional wisdom of headwater wetland hydrology in general. Furthermore, the results gleaned from the technical rehabilitation show promise that these activities can restore wetland hydrodynamic function, all this despite the lack of any historical supporting evidence and without any baseline data to benchmark the observed changes against. Fortunately, the hydrological research revealed that some parts of the wetland remained hydrologically intact for the most part and this provided the benchmark for gauging the rehabilitations success. However, this thesis was collated over a short 4 year window and longer term monitoring of the rehabilitations success is warranted both hydrologically, ecologically and in terms of other biophysical aspects. The end goal of which being to ensure that wetland rehabilitation is able to restore wetland function for catchment processes and for those that use them in order to support livelihoods in the long term. It is hoped that these findings may be disseminated to meaningful information that any wetland practitioner, be they land-user or restoration specialist, can use successfully to ensure preservation of nature’s capital for it’s and our continued well-being.

REFERENCES

ABEM (2005). Instruction Manual: Terrameter SAS 4000 / SAS 1000.

Allen, RG., Pereira, LS., Raes, D., Smith, M. (1998) Crop evapotranspiration - Guidelines for computing crop water requirements. FAO Irrigation and drainage paper 56 FAO - Food and Agriculture Organization of the United Nations. Rome

Babar, Md. (2005). Hydrogeomorphology: Fundamentals, Applications and Techniques. New India Publishing Agency. New Delhi. pp272

Balek, J. and Perry, J.E. (1972). Hydrology of seasonally inundated African headwater swamps. Journal of Hydrology 19: 227-249.

Balek, J. (1983) Hydrology and Water Resources in Tropical Regions. Elsevier. Amsterdam

Bastiaanssen, WGM. Noordman, EJM., Pelgrum, H. Davids, G. Thoreson, BP., Allen, RG. (2005) SEBAL Model with Remotely Sense Data to Improve Water-Resources Management under Actual Field Conditions. Journal of Irrigation and Drainage Engineering 131.1 p85-93.

Bradley, C. (2002). Simulation of the annual water table dynamics of a floodplain wetland, Narborough Bog, UK. Journal of Hydrology 261: 150-172.

Breen, C., Dini, J., Mitchell, S., Uys, M. (2008) WET-Management. The Wetland Management Series. 11 Chapters. Water Research Commission. Gezina, Pretoria

Brinson, M.M., Swift, B.L., Plantico, R.C. and Barclay, J.S. (1981). Riparian Ecosystems: Their Ecology and Status. Washington: U.S. Fish and Wildlife Service, Biol.Serv.Prog., FWS/OBS-81/17. as cited in Mitsch and Gosselink, 1993

Brinson, M.M. (1993). Hydrogeomorphic classification of wetlands. Vicksburg, MS: U.S. Army of Engineer Waterways Experiment Station.

Bullock, A. (1992). Dambo hydrology in southern Africa - review and reassessment. Journal of Hydrology 134: 373-396.

Bullock, A., Gilman, K., McCartney, M., Waughray, D., Blyth, K., Andrews, A. (1998) Hydrological strategy to develop and manage African wetland resources for sustainable agricultural use. Wetland characterisation and classification for sustainable agricultural development. FAO/SAFR. Rome (Part II) www.fao.org/DOCREP/003/X6611E/x6611e03b.htm

Bullock, A. and McCartney, M.P. (1996). Wetland and river flow interactions in Zimbabwe. International Association of Hydrological Sciences, Publication no.238: 305-321.
Bullock, A. and Acreman, M. (2003). The role of wetlands in the hydrological cycle. Hydrology & Earth Systems Sciences 7(3): 358-389.

Chappell, CA., Brown, MA. (1993) The use of remote sensing in quantifying rates of soil erosion. Koedoe 36.1: 1-14.

Campbell, E.M. (1997). Granite Landforms. Journal of the Royal Society of Western Australia 80: 101-112.

Cowan, G.I. (1999). Rehabilitation of Wetlands: An African Perspective. Netherlands: Kluwer Academic Publishers.

Church, M. (2002) Geomorphic thresholds in riverine landscapes. Freshwater Biology 47: 541-557.

Daniels, R.B. And Hammer, R.D. (1992). Soil Geomorphology: John Wiley & Sons.
Devito, K.J., Creed, I.F. and Fraser, C.J.D (2005). Controls on runoff from a partially harvested aspen-forested headwater catchment, Boreal Plain, Canada. Hydrological Processes 19(1): 3-25.

Darcy, H (1856) Les Fontaines Publiques de la Ville de Dijon, Dalmont, Paris.

Dixon, A.B., Hailu, A. and Wood, A.P. (2001). Proceedings of the Wetland Awareness Creation and Activity Identification Workshop in Amhara National Regional State. Bahar Dar, Ethiopia

Dixon, A.B (2002). The hydrological impacts and sustainability of wetland drainage cultivation in Illubabor, Ethiopia. Land Degradation & Development 13: 17-31.

Dolman, H. (2003). Ecohydrology: Patterns and variability in vegetation soil atmosphere interaction. Position Paper for the Royal Netherlands Academy of Arts and Sciences working group on hydrology, 6/2/03.

DWAF (2001). Wetland/Riparian Habitats - A practical field procedure for identification and delineation (version 3.00). Department of Water Affairs and Forestry. South Africa.

Ellery, W.N., Kotze, D.C., McCarthy, T.S., Tooth, S., Grenfell, M., Beckedahl, H., Quinn, N. and Ramsay, L. (2005). The Origin and Evolution of Wetlands: Water Research Commission. Pretoria, South Africa – make 2008.

Everson, C., Clulow, A., Mengistu, M. (2009). Quantification of Evapotranspiration from a South African Rehabilitated Headwater Wetland. Water Research Commission, Pretoria. Project No. K8/826

FAO (2001) Wetland Development and Management in SADC Countries. (Eds) Frenken, K., Mharapara, I. Proceedings of an FAO sub-regional workshop in Harare, Zimbabwe 19-23 November 2001. Food and Agriculture Organization of the United Nations (FAO). Harare, Zimbabwe

Freer, J. McDonnell, J.J. Beven, K.J. Peters, N.E. Burns, D.A. Hooper, R.P. Aulenbach, B. and Kendall, C. (2002). The role of bedrock topography on subsurface storm flow. Water Resources Research 38(12): 1269

Freeze, R. A. & Cherry, J. A. (1979) Groundwater. Prentice-Hall, USA.

Fryirs, KA., Brierley, GJ., Preston, NJ., Kasai, M. (2006) Buffers, barriers and blankets: The (dis)connectivity of xatchment-scale sediment cascades. CATENA 70.1 : 49-67.

Gerits, J.J.P. de Lima, J.L.M.P. van den Broek, T.M.W. (1990). Overland flow and erosion. In: Anderson, M.G. and Burt, T.P. (eds). Process Studies in Hillslope Hydrology. New York: John Wiley & Sons.

Gilman, K. (1994). Hydrology and Wetland Conservation. Chichester: John Wiley & Sons.

Grenfell, M.C., Ellery, W.N. and Preston-Whyte, R.A. (2005). Wetlands as early warning (eco)systems for water resource management. Water SA 31(4): 465-471.

Green, W.H., Ampt, G. (1911). Studies of soil physics and the flow of air and water through soils. Journal of Agricultural Science, 4, 1-24.

Grenfell, M.C., Quinn, N.W., Ellery, W.N., Kotze, D.C. and Russell, W. (2004). Trends in Wetland Rehabilitation Methods: A South African Perspective: Water Research Commission Wetlands Research Programme: Wetland Rehabilitation.

Herschy, RW. (1985) Streamflow Measurement. Elsevier pp240

Horton, RE. (1940) An approach toward a physical interpretation of infiltration capacity. Trans. Amer. Geophys. Un. 20, Part IV, 693-711.

Jacobs, J.M., Mergelsberg, S.L., Lopera, A.F. and Myers, D.A. (2002). Evapotranspiration from a wet prairie wetland under dought conditions: Paynes Prairie Reserve, Florida, USA. Wetlands 22(2): 374-385.

Jones, S.B. and Or, D. (2003). Modelled effects on permittivity measurements of water content in high surface area porous media. Physica B 338: 284-290.

Kendall, C. Caldwell, EA. (1998) Fundamentals of Isotope Geochemistry. In Isotope Tracers in Catchment Hydrology Elsevier Science. Amsterdam p51-88

Kennedy, VC., Zellweger, GW., Avanzino, RJ. (1979). Variation of Rain Chemistry During Storms at Two Sites in Northern California. Water Resources Research 15 (3) p687-702

Kongo, VM., Kosgei, JR., Jewitt, GPW, Lorentz, SA.(2007)Establishment of a catchment monitoring network through a participatory approach in a small rural catchment in South Africa. Hydrol. Earth Syst.Sci. Discuss. 4 p3793-3837.

Kotze, D.C., Hughes, J.C., Breen, C.M. and Klug, J.R. (1994). The development of a wetland soils classification system for KwaZulu/Natal. Water Research Commission, WRC Report No 501/4/94.

Kotze, D.C., Klug, J.R., Hughes, J.C. and Breen, C.M. (1996). Improved criteria for classifying hydric soils in South Africa. South African Journal of Plant and Soil 13: 67-73.

Kotze, D. & Silima, V. (2003). Wetland cultivation: reconciling the conflicting needs of the rural poor and society at large through wetland wise use. Int. J. Ecol. Env. Sci. 29: 65-71.

LaBaugh, J.W. (1986). Wetland ecosystem studies from a hydrologic perspective. Water Resources Bulletin 22(1): 1-10.

Loke, M.H. (1999). Electrical imaging surveys for environmental and engineering studies: A practical guide to 2-D and 3-D surveys.

Lorentz, S.A. Hemme, S.W., Buitendag, I and Schulze, R.E. (1995).Physically based infiltration andredistribution of soil water for application at field scale. In: Schulze, R. E. Hydrology and Agrohydrology: A Text to Accompany the ACRU 3.00 Agrohydrological Modelling System. Water Research Commission,Pretoria, Report TT69/95. pp AT9-1 to AT9-26

Lorentz, S.A. and Schulze, R.E. (1995). Sediment Yield. In: Schulze, R. E. Hydrology and Agrohydrology: A Text to Accompany the ACRU 3.00 Agrohydrological Modelling System. Water Research Commission,Pretoria, Report TT69/95. pp AT9-1 to AT9-26

Lorentz, S.A. Goba, P. and Pretorius, J. (2001). Hydrological Processes Research: experiments and measurements of soil hydraulic characteristics. Pretoria, South Africa: Water Research Commission.

Lorentz, S., Thornton-Dibb, S. Pretorius, J.J. and Goba, P. (2004). Hydrological Systems Modelling Research Programme: Hydrological Processes, Phase II: Quantification of Hillslope, Riparian and Wetland Processes, Report to the Water Research Commission on the Project: A Field Study of Two and Three Dimensional Processes. Pretoria, South Africa: Water Research Commission.

Martinez-Mena, M., Albaladejo, J. and Castillo, V.M. (1998). Factors influencing surface runoff generation in a Mediterranean semi-arid environment: Chicamo watershed, SE Spain. Hydrological Processes 12: 741-754.

Martinez-Mena, M. Castillo, V. Albaladejo, J. (2001). Hydrological and erosional response to natural rainfall in a semi-arid area of south-east Spain. Hydrological Processes 15: 557-571.
McCarthy, T. Rubidge, B. (2005) The Story of Earth & Life: A southern African perspective on a 4.6-billion-year journey. Struik, Cape Town pp333

McCartney, M.P. (1998). The hydrology of a headwater catchment containing a dambo. PhD Thesis. The University of Reading: Department of Soil Science.

McCartney, M.P. (2000). The Water Budget of a Headwater Catchment containing a Dambo. Phys. Chem. Earth (B) 25(7-8): 611-616.

McDonnell, J.J (2003). Where does water go when it rains? Moving beyond the variable source area concept of rainfall-runoff response. Hydrological Processes 17: 1869-1875.

McEwan, K., Jolly, I., Holland, K. (2006). Groundwater – surface water interactions in arid/semi-arid wetlands and the consequences of salinity for wetland ecology. CSIRO Land and Water Science Report 53/06

Millennium Ecosystem Assessment (2005). Ecosystems and Human Well-being: Wetlands and Water, Synthesis. Washington D.C.: World Resources Institute.
Mitsch, W.J. and Gosselink, J.G. (1993). Wetlands.: John Wiley & Sons.

Mitsch, W.J. & Gosselink, J.G. (2000). The value of wetlands: Importance of scale and lansdcape setting. Ecological Economics 35(200): 25-33.

Mitsch, WJ., Gosselink, JG. (2007) Wetlands. Fourth Edition Wiley 600pp

Mueller-Dombois, D. and Ellenberg, H. (1974). Aims and Methods of Vegetation Ecology. John Wiley & Sons, Inc.

Naiman, R.J., Decamps, H. and McClain, M.E. (2005). Riparia: Ecology, Conservation, and Management of Streamside Communities.: Elsevier Academic Press.

Nicolau, J.M. (2002). Runoff generation and routing on artificial slopes in a Mediterranean-continental environment: the Teruel coalfield, Spain. Hydrological Processes 16: 631-647.

Phillips, JD. (2006) Evolutionary geomorphology: thresholds and nonlinearity in landform response to environmental change. Hydrol. Earth Syst. Sci. 10 : 731-742.

Pike, A., Schulze, R., Lorentz, S., Ballim, F., Taylor, V., and Howe, B. (1997). Simulation of streamflows and sediment yields in the Sand and Sabie catchments: Initial Results. Pietermaritzburg: Department of Agricultural Engineering, University of Natal.

Poesen, J. Vandekerckhove, L. Nachtergaele, J. *et al* (2002). Gully Erosion in Dryland Environments. In Dryland Rivers: Hydrology and Geomorphology of Semi-arid Channels*;* Bull, L.J. and Kirkby, M.J., (eds); John Wiley & Sons, Ltd. p 229.

Pollard, S. (2002) Operationalising the new Water Act: contributions from the Save the Sand Project - an integrated catchment management initiative. Physics and Chemistry of the Earth 27 941-948.

Pollard, S.R. Shackleton, C. Carruthers, J. (2003). Beyond the fence: People and the Lowveld landscape. In: The Kruger Experience – Ecology and Management of Savanna Heterogeneity. Du Toit, Rogers, K. and Biggs, H. Island Press.

Pollard, S. Kotze, D., Ellery, W., Cousins, T., Monareng, J., King, K., Jewitt, G. et al
(2005) Linking Water and Livelihoods: The development of an integrated wetland rehabilitation plan in the communal areas of the Sand River Catchment as a test case. Association for Water and Rural Development
URL: http://www.award.org.za/wetlandsoct04.pdf

Pollard SR, D Kotze, W Ellery, T Cousins and G. Jewitt (2006) Towards wetland and livelihood improvements: An integrated socio-ecological approach to the rehabilitation of a communal wetland in north-eastern region of South Africa. Association for Water and Rural Development (AWARD)
http://www.award.org.za/File_uploads/File/Towards%20wetland%20Pollard%20et%20al%202006%20WI%20final.pdf

Pollard, S., Kotze, DC., Ferrari, G. (2008) Valuation of the livelihood benefits of structural rehabilitation interventions in the Manalana Wetland. In (Eds) Ellery, W. & Kotze, D.WET-

OutcomeEvaluate. An evaluation of the rehabilitation outcomes at six wetland sites in South Africa Water Research Commission Gezina, Pretoria. WRC Report TT343/08

Rebelo, LM., McCartney, MP.,Finlayson, CM. (2009) Wetlands of Sub-Saharan Africa: distribution and contribution of agriculture to livelihoods. Wetlands Ecology & Management DOI 10.1007/s11273-0

Richards, L.A. (1931). Capillary conduction through porous mediums. Physics, 1, 318-333.

Riddell, ES., Lorentz, SA., Ellery, WN., Kotze, D., Pretorius JJ., Nketar, SN. (2007). Water Table Dynamics of a Severely Eroded Wetland System, Prior to Rehabilitation, Sand River Catchment, South Africa. Proceedings XXXV IAH Congress Groundwater and Ecosystems 17-21 September 2007. Lisbon, Portugal

Riekerk, H. Korhnak, L.V. (2000). The hydrology of cypress wetlands in Florida pine flatwoods. Wetlands 20(3): 448-460.
Roberts, N. (1988). Dambos in development: Management of a fragile ecological resource. Journal of Biogeography 15: 141-148.

Ritter, DF., Kochel, RC., Miller, JR. (2002) Process Geomorphology. Waveland Press, Inc. Long Grove, Illinois

Russell, W. (2008) WET-RehabMethods National Guidelines and methods for wetland rehabilitation. Water Research Commission. Gezina, Pretoria. WRC Report TT341/08

Save the Sand Project (2002). Saving the Sand Series: Professional Portfolio. South Africa: Association for Water and Rural Development.

Schulze, R.E. (1995). Hydrology and Agrohydrology: A Text to accompany the ACRU 3.00 Agrohydrological Modelling System. South Africa: Water Research Commission.

Schulze, R.E., Schmidt, E.J. and Smithers, J.C. (1993). SCS-SA User Manual: University of Natal, Pietermaritzburg, Department of Agricultural Engineering.

Schuyt, K. and Brander, L. (2004). Living Waters: The Economic Value of the World's Wetlands. Gland/Amsterdam: WWF.

Seibert, J., Bishop, K., Rohde, A. and McDonnell, J.J. (2003). Groundwater dynamics along a hillslope: A test of the steady-state hypothesis. Water Resources Research, 39(1), 1014

Sivapalan, M. (2003). Process complexity at the hillslope scale, process simplicity at the watershed scale: is ther a connection? Hydrological Processes 17: 1037-1041.

SOIL CLASSIFICATION WORKING GROUP (1991). Soil classification: a taxonomic system for South Africa. Memoirs on the Agricultural Natural Resources of South Africa No. 15. SIRI, D.A.T.S., Pretoria.

Su. Z. (2002) The Surface Energy Balance System (SEBS) for estimation of turbulent heat fluxes. Hydrology and Earth Systems Sciences 6.1 p85-99.

Tegene, B. and Hunt, C. (2000). The characteristics and management of wetland soils of Metu Wereda, Illubabor zone of Oromia region. Report for objective 2. EWRP and University of Huddersfield.; Metu and Huddersfield.

Thoms, M.C., James, C.S., Moon, B.P. and Rogers, K.H. (1990). Environmental problems in South African Rivers: The need for expertise in fluvial geomorphology. Contract Report, Water Expertise in Fluvial Geomorphology. Contract Report, Water Research Commission, Pretoria 19pp.

Todd, KD (1990). Groundwater Hydrology. New York.: John Wiley and Sons. *As cited by Koning, B (2005) in an unpublished seminar presentation, 'Ecohydrology: A Groundwater Study' at the School of Bioresources Engineering and Environmental Hydrology, University of KwaZulu-Natal*

Uhlenbrook, S., Wenninger, J. and Lorentz, S. (2005). What happens after the catchment caught the storm? Hydrological processes at the small, semi-arid Weatherley catchment, South Africa. Advances in Geosciences 2: 237-241.

U.S. Department of the Interior. Bureau of Reclamation (2001). Water Measurement Manual

Water Resources Research Laboratory. http://www.usbr.gov/pmts/hydraulics_lab/pubs/wmm

Van Heerden, J.J., Van der Spuy, D. and Le Roux, P.J. (1986). Manual for the planning, design and operation of river gauging stations. South Africa: Department of Water Affairs and Forestry.

von der Heyden, C.J. and New, M.G. (2003). The role of dambo hydrology of a catchment and the river network downstream. Hydrology and Earth System Sciences 7(3): 339-357.

Ward, A.D. and Trimble, S.W. (2004). Environmental Hydrology. Boca Raton, Florida, USA: Lewis Publishers, CRC Press

Weiler, M. McDonnell, J. (2004). Virtual experiments: a new approach for improving process conceptualization in hillslope hydrology. Journal of Hydrology 285: 3-18.

Wischmeier, W.H. and Smith, DD. (1978). Predicting rainfall erosion losses - a guide to conservation planning..Washington DC: USDA, Agricultural Handbook. As cited in Lorentz and Schulze (1995)

Wood, A. (2006) Headwater wetlands in eastern and southern Africa The evolving debate (Eds) Krecek, J. & Haigh, M. Environmental Role of Wetlands in Headwaters. Nato Science Series Volume 63 p211-220 Springer Netherlands

Yolcubal, I., Brusseau, ML., Artiola, JF., Wierenga, P., Wilson, LG. (2004). Environmental Physical Properties and Processes. (Eds) Artiola, JF., Pepper, IL., Brusseau, M. Environmental Monitoring and Characterization p207-241 Elsevier, London

Zedler, J.B. and Callaway, J.C. (1999). Tracking wetland restoration: Do mitigation sites follow desired trajectories? Restoration Ecology 7(1): 69-73.

Zenhder, A.J.B., Yang, H. And Schertenleib, R. (2003). Water Issues: The need for action at different levels. Aquatic Science 65: 1-20

APPENDIX i - VEGETATION SURVEYS

The following appendix lists the vegetation species encountered within a 3m Relevé adjacent to the hydrological monitoring stations with the Craigieburn-Manalana catchment and their relative abundances.

KEY:

Releve Diameter	6m (r=3m)

Cover Class (CC)	Range %
1	75-100
2	50-74.9
3	25-49.9
4	5-24.9
5	1-4.9
+	0.5-0.9
R	observed, rare

Sociability Class (SC)	Criteria
1	occuring in large nearly pure stands
2	occuring in large aggregates, coppice or in carpets
3	occuring in small aggregates, clusters or cushions
4	occuring in clumps or bunches
5	occuring singly

Sample Site ID	1		Latitude (S)	24,40,05.7	Date	13/02/2007		
	up from T2_5		Longitude (E)	030,58,31.6				
Taxon	CC	Cover estimate %	SC		Taxon	CC	Cover estimate %	SC
Parinari curatellifolia	4	10	3		Eragrostis capensis	plus	0.5	5
Psidium guajava	5	2	5					
cf. Helichrysum spp 2	R	0.1	5					
Dicoma spp	plus	0.5	5					
Cyperus obtusiflorus	plus	0.8	4					
Eragrostis Racemosa	5	1	4					
Louditia simplex	5	3	4					
Agathisanthenum bojeri subspp bojeri	5	0.5	4					
Ageratum houstonianum	plus	0.2	4					
cf. Helichrysum spp	R	0.1	5					
Cyperacae spp	plus	0.5	4					
Sporobolus africanus	R	0.1	5					
Helichrysum krausii	plus	0.6	4					
cf. Helichrysum athrixifolium	plus	0.6	4					
Paspalum scrobiculatum	5	2	3					
Perotis patens	R	0.2	5					
Aristida congesta sub. barbicollis								
Sporobolus pyramidalus	R	0.2	5					
Triumfetta welwitschii var hirsuta	plus	0.5	4					
Heteropogon contortus	R	0.2	5					
Hyperthelia dissoluta	5	2	4					
Other Taxa Present								
Site Factor Notes heavily grazed, close to settlement, north facing slope, extensive bare surfaces i.e >50%								
General Notes								

Sample Site ID	2		Latitude (S)	24,40,05.0	Date	16/02/2007		
	T2_5		Longitude (E)	030,58,31.6				
Taxon	CC	Cover estimate %	SC		Taxon	CC	Cover estimate %	SC
Parinari curatellifolia	4	10	3		Geigeria burkei subspp burkei var elata	R	0.1	4
Dichrostachys cinerea	5	3	4		Helichrysum pallidum	R	0.1	5
cf. Helichrysum spp 2	plus	0.9	4		Aloe saponaria	R	0.1	5
Rubiaceae spp	5	3	4		Themeda trianda	5	1	4
Louditia simplex	5	2	4		Setaria sphacelata sub. Sphacelata	R	0.1	5
Cyperus obtusiflorus	plus	0.5	4		Trachypogon spicatus	plus	0.8	4
Eragrostis Racemosa	plus	0.5	4					
cf. Helichrysum spp	R	0.1	5					
Agathisanthenum bojeri subspp bojeri	R	0.1	5					
Hyperthelia dissoluta	5	2	4					
Hyparrhenia hirta	plus	0.5	4					
Aristida congesta sub. barbicollis	R	0.1	5					
Schizachyrium sanguineum	5	2	4					
Helichrysum krausii	5	3	3					
Dicoma zeyheri zeyheri	R	0.1	5					
Pearsonia sessilifolia subspp marginata	R	0.1	5					
Decorsea galpinii	R	0.1	4					
Cyperacae spp	plus	0.9	4					
Ageratum houstonianum	plus	0.5	4					
Sporobolus pyramidalis	R	0.1	5					
Paspalum scrobiculatum	5	4	4					
Other Taxa Present								
Site Factor Notes Heavily grazed, extensive bare surface >50%, north facing slope								
General Notes								

Sample Site ID	3		Latitude (S)	24,40,04.2	Date	16/02/2007		
	up from T2_4		Longitude (E)	030,58,31.6				
Taxon	CC	Cover estimate %	SC		Taxon	CC	Cover estimate %	SC
Louditia simplex	4	7	3		Agathisanthenum bojeri subspp bojeri	plus	0.5	4
Parinari curatellifolia	4	7	3		Bricharia brithantha	5	1	4
Sporobolus pyramidalus	4	7	3		Rhoicissus tridentata	plus	0.5	5
Setaria sphacelata sub. Sphacelata	4	7	3		Berkheya zeheri	R	0.1	5
Dichrostachys cinerea	5	2	4		Maerua cafra	R	0.3	5
Helichrysum krausii	plus	0.7	5		Elaeodendron croceum	plus	0.5	5
cf. Helichrysum athrixifolium	plus	0.5	5		Scabiosa columbaria	R	0.1	5
Schizachyrium sanguineum	5	3	4		Canthium mundianum	plus	0.5	5
Hyperthelia dissoluta	4	7	3		Tephrosia spp	R	0.1	5
Andropogon schirensis	4	7	3					
Cyperacae spp	5	3	4					
Themeda trianda	plus	0.5	5					
Agathisanthenum bojeri subspp bojer	R	0.5	5					
Eragrostis Racemosa	plus	0.5	4					
Agathisanthenum bojeri subspp bojer	plus	0.8	4					
Sporobolus africanus	plus	0.5	4					
Euphorbiaceae phyllanthus spp	plus	0.5	5					
119	R	0.2	5					
Zornia cf. capensis	5	0.5	4					
Kohautia spp	plus	0.5	5					
Scadoxus puniceus	5	2	5					
Other Taxa Present								
Site Factor Notes Bare surfaces but not as sparse as sites 1 and 2 , approx 60%, up slope, seems to be a bit of a gully (sparse) on eastern side. North facing slope								
General Notes								

Sample Site ID	4		Latitude (S)	24,40,03.7	Date	28/02/2006		
	T2_4		Longitude (E)	030,58,31.6				
Taxon	CC	Cover Estimate %	SC		Taxon	CC	Cover Estimate %	SC
Parinari curatellifolia	4	7	4		Setaria sphacelata sub. Sericea	plus	0.5	5
Annona senegalensis	4	5	5		Endostemon obtusifolium	plus	0.5	5
Antidesma venosum	5	4	5		119	plus	0.8	5
Rhoicissus tridentata	5	1	5		Hermanna quartiniana subspp stellulata	plus	0.5	5
Maerua cafra	5	4	4		Acanthospernum hispidum	5	3	4
Canthium mundianum	5	3	4					
Dichrostachys cinerea	4	5	4					
Louditia simplex	4	15	2					
Hyperthelia dissoluta	5	2	4					
Helichrysum krausii	5	2	4					
Andropogon schirensis	5	1	4					
Schizachyrium sanguineum	plus	0.5	5					
Sporobolus pyramidalus	plus	0.5	5					
cf. Helichrysum athrixifolium	plus	0.5	5					
Setaria sphacelata sub. Sphacelata	plus	0.8	5					
Kohautia spp	plus	0.8	5					
Berkheya zeheri	plus	0.5	5					
Agathisanthenum bojeri subspp bojeri	plus	0.5	5					
Eragrostis Racemosa	R	0.1	5					
Hyparrhenia hirta	plus	0.9	5					
Cymbopogon excavatus	5	3	3					
Other Taxa Present								
Site Factor Notes - Cover reasonable, at toe of slope, pathway skirts releve on southern side, good woody cover								
General Notes								

Sample Site ID	6		Latitude (S)	24,40,02.7	Date	28/02/2007		
	T2_3		Longitude (E)	030,58,31.1				
Taxon	CC	Cover Estimate %	SC		Taxon	Cover Estimate %	CC	SC
Phragmites Mauritianus	5	4	4					
Sporobolus africanus	4	15	4					
Sporobolus pyramidalus	5	2	4					
Hemarthria altissima	5	2	2					
Cynodon dactylon	3	35	2					
Digetaria longiflora	5	2	4					
Digiteria erientha	5	1	4					
cf. Conyza bonariensis	5	1	5					
Ageratum houstonianum	4	6	3					
Melinis repens	5	3	4					
Veratotheca triloba	5	1	5					
Black Jack	5	1	4					
Helichrysum krausii	5	1	5					
Other Taxa Present								
Site Factor Notes - Highly utilised site, area near construction of weir, cover reasonably good although v short i.e heavily grazed								
General Notes								

Sample Site ID	7		Latitude (S)	24,40,02.0	Date	28/02/2007		
			Longitude (E)	030,58,30.8				
Taxon	CC	Cover Estimate %	SC		Taxon	CC	Cover Estimate %	SC
Phragmites mauritianus	4	7	3		Cynodon dactylon	5	1	2
Hemarthria altissima	3	25	2					
Sporobolus pyramidalus	1	2	4					
Sporobolus africanus	plus	0.5	5					
Digiteria erientha	plus	0.5	5					
Paspalum distichum	plus	0.5	5					
Cyperus latifolius	R	0.1	5					
Paspalum scrobiculatum	plus	0.5	5					
Black Jack	plus	0.9	5					
Digiteria erientha	plus	0.5	5					
Leersia hexandria	5	3	4					
Cyperus longus var. tanuiflorus	plus	0.5	5					
Persicaria spp	plus	0.5	5					
cf. Conyza bonariensis	5	2	4					
Conyza spp (maybe young Conyza bonarien	5	1	4					
Sida cordifolia	5	1	4					
Bidens biternata	5	1	4					
Centella asiatica	5	2	4					
Bidens biternata	5	1	5					
Sida cordifolia	plus	0.5	4					
Cyperus distans	5	1	4					
Other Taxa Present								
Site Factor Notes - In wetland zone, raised bed and furrows, very sandy soil, heavily grazed and pathways, poor cover								
General Notes								

Sample Site ID	8		Latitude (S)	24,40,01.4	Date	28/02/2007		
	T2_2		Longitude (E)	030,58,30.8				
Taxon	CC	Cover Estimate %	SC		Taxon	Cover Estimate %	CC	SC
Phragmites mauritianus	3	30	3					
Bidens biternata	5	2	4					
Cyperus distans	5	3	4					
Cyperus longus var. tanuiflorus	5	2	4					
Leersia Hexandra	5	3	4					
cf. Conyza bonariensis	4	5	4					
Digiteria erientha	5	1	4					
Sporobolus pyramidalus	plus	0.5	5					
Cynodon dactylon	4	10	2					
Sida cordifolia	5	3	4					
Centella asiatica	5	1	4					
clover spp	plus	0.5	5					
Frimbistilys complanata	R	0.4	5					
Kylinga melanosperma	plus	0.5	5					
Conyza spp (maybe young Conyza bonarien	5	2	4					
Helichrysum krausii	plus	0.5	5					
Paspalum distichum	plus	0.5	4					
Helichrysum stenopteruus	5	1	4					
Panicum maximum	5	2	4					
Sida cordifolia	plus	0.6	5					
Other Taxa Present								
Site Factor Notes - raise bed and furrow - cover is better than last site, sandy soils								
General Notes								

Sample Site ID	9		Latitude (S)	24'40'00.7	Date	12/03/2007		
			Longitude (E)	030'58'30.9				
Taxon	CC	Cover Estimate %	SC		Taxon	Cover Estimate %	CC	SC
Phragmites mauritianus	4	20	3					
Hyparrhenia hirta	4	12	4					
Panicum maximum	5	2	4					
Hyperhenia Dissoluta	5	1	5					
Cynodon dactylon	4	5	2					
Hermarthria altissima	4	5	3					
Paspalum distichum	4	5	4					
Sorghum versicolor	5	3	4					
Eragrostis chloromelas	5	4	4					
Sporobolus pyramidalus	4	5	4					
Setaria sphacelata sub. Sericea	5	2	4					
Antidesma venosum	4	10	5					
Hibiscus cannibinus spp	5	4	4					
Sida cordifolia	4	5	4					
cf. Conyza bonariensis	5	1	5					
Sida alba	5	1	5					
Sida rhombifolia	5	1	5					
Other Taxa Present								
Site Factor Notes - in wetland but prob temp zone, v good cover								
General Notes								

Sample Site ID	10		Latitude (S)	24'40'00.7	Date	1/3/2007		
			Longitude (E)	030'58'30.8				
Taxon	CC	Cover Estimate %	SC		Taxon	Cover Estimate %	CC	SC
Phragmites mauritianus	4	15	4		Bidens biternata	plus	0.5	5
Psidium guajava	5	7	4		Agathisanthenum bojeri subspp bojeri	5	2	4
Setaria sphacelata sub. Sphacelata	5	4	4		Dicrostachys cineria	5	1	5
Setaria sphacelata sub. Sericea	5	2	4					
Sporobolus pyramidalus	5	4	4					
Sporobolus africanus	5	4	4					
Hyperhenia hirta	5	4	4					
Hyperhenia dissoluta	5	3	4					
Louditia simplex	5	1	4					
Panicum maximum	5	1	4					
Hermarthria altissima	5	3	4					
Themeda trianda	plus	0.5	5					
Bricharia brithantha	plus	0.5	5					
Paspalum distichum	5	2	4					
Melinis repens	5	1	4					
Cyperus latifolius	5	1	5					
Eragrostis capensis	plus	0.5	5					
Andropogon schirensis	plus	0.5	5					
Sida cordifolia	5	3	4					
Frimbistilys complanata	plus	0.5						
Eragrostis inamoena	R	0.1	5					
Other Taxa Present								
Site Factor Notes - edge of wetland close to saprolite exposure area at edge, good cover, but quite utilised by grazing								
General Notes								

Sample Site ID		11	Latitude (S)	24'39'58.6	Date	1/3/2007		
			Longitude (E)	030'58'30.6				
Taxon	CC	Cover Estimate %	SC		Taxon	Cover Estimate %	CC	SC
Hyperhenia hirta	3	35	3					
Melinis repens	4	6	3					
Mabola plum	5	2	5					
Sporobolus pyramidalus	5	1	5					
Dichrostachys cineria	R	0.1	5					
Hyperhenia dissoluta	5	1	5					
Ageratum houstonianum	4	5	4					
Acalypha villicaulis	5	1	4					
Other Taxa Present								
Site Factor Notes - at toe of slope, sparse cover and species poor, heavily grazed								
General Notes								

Sample Site ID	12	12	Latitude (S)	24'39'57.1	Date	1/3/2007		
			Longitude (E)	030'58'30.6				
Taxon	CC	Cover Estimate %	SC		Taxon	Cover Estimate %	CC	SC
Hyperhenia dissoluta	5	1	4					
Melinis repens	4	15	3					
Helichrysum krausii	plus	0.5	5					
Psidium guajava	plus	0.5	5					
Thelypteris spp	4	6	4					
Paspalum distichum	4	5	4					
Sporobolus africanus	3	40	2					
Tarchonanthus camphoratus	4	10	4					
Acalypha glabrata	plus	0.5	5					
Smilax anceps	plus	0.5	5					
Senna didymobotrya	5	2	5					
Ageratum houstonianum	4	7	4					
Other Taxa Present								
Site Factor Notes - cover good, on red hatton soils, can see S.africanus grazed but is very dense, steep slope								
General Notes								

Sample Site ID	13		Latitude (S)	24'39'56.2	Date	1/3/2007		
			Longitude (E)	030'58'30.4				
Taxon	CC	Cover Estimate %	SC		Taxon	Cover Estimate %	CC	SC
Parinari curatellifolia	4	7	4					
Louditia simplex	4	7	2					
Hyperhenia dissoluta	5	3	4					
Andropogon schirensis	5	4	3					
Helichrysum krausii	5	2	4					
Helichrysum krausii	5	4	4					
Bricharia brithantha	5	2	4					
Dichrostachys cineria	5	3	4					
Rhoicissus tridentata	plus	0.5	5					
Scabiosa columbaria	5	1	4					
119	5	2	4					
cf. Gnidia??	4	6	4					
Eragrostis Racemosa	plus	0.7	4					
Tristchya leucothrix	plus	0.5	4					
Diospyros spp proabably lycioides	5	3	4					
Faurea rochetiana	4	7	4					
Themeda trianda	plus	0.5	5					
Other Taxa Present								
Site Factor Notes - steep, fairly sparse, edge of dolorite, mostly granite soils								
General Notes								

Sample Site ID	14		Latitude (S)	24'39'54.9	Date	1/3/2007		
			Longitude (E)	030'58'30.6				
Taxon	CC	Cover Estimate %	SC		Taxon	Cover Estimate %	CC	SC
Parinari curatellifolia	4	6	4					
Hyperhenia dissoluta	3	35	3					
Dichrostachys cineria	5	4	4					
Paspalum distichum	4	10	2					
Eragrostis Racemosa	5	3	4					
Themeda trianda	plus	0.5	5					
Helichrysum krausii	5	2	4					
Melinis repens	plus	0.5	5					
Eragrostis rigidor	5	4	4					
Rubiaceae spp	plus	0.9	5					
Cyperus obtusiflorus	R	0.1	5					
family - Verbenaceae	plus	0.5	5					
Elaeodendron croceum	5	1	5					
Other Taxa Present								
Site Factor Notes								
General Notes								

Sample Site ID	15		Latitude (S)	24'39'53.9	Date	2007/03/07		
	T1_5		Longitude (E)	030'58'30.9				
Taxon	CC	Cover Estimate %	SC		Taxon	Cover Estimate %	CC	SC
Parinari curatellifolia	4	6	4					
Helichrysum krausii	5	4	4					
Louditia simplex	3	35	2					
Themeda trianda	5	2	4					
Sporobolus pyramidalus	5	2	4					
Hyperhenia hirta	3	25	2					
Hyperhenia dissoluta	5	1	4					
Andropogon schirensis	5	3	4					
Eragrostis Racemosa	5	3	4					
family - Verbenaceae	4	10						
Paspalum distichum	5	3	4					
Helichrysum pallidum	plus	0.5	5					
119	plus	0.5	5					
Hyperhenia filipendula	5	1	4					
Other Taxa Present								
Site Factor Notes - Fairly steep but not as steep as T2_1, relatively ungrazed, high up on slope, good cover								
General Notes								

Sample Site ID	16		Latitude (S)	24,39,58.4	Date	7/3/2007		
	T1_4		Longitude (E)	030,58,29.2				
Taxon	CC	Cover Estimate %	SC		Taxon	Cover Estimate %	CC	SC
Sporobolus Pyramidalus	5	3	4					
Sporobolus africanus	5	1	5					
Thelypteris spp	5	4	4					
Dicrostachya cineria	5	3	4					
Ageratum houstonianum	4	15	3					
Sida cordifolia	5	3	4					
Veratotheca triloba	5	1	5					
Hyperhenia hirta	5	3	4					
Hyperhenia dissoluta	5	1	5					
Paspalum Distichum	4	20	4					
Cynodon dactylon	4	5	2					
Hemarthria altissima	5	1	2					
Panicum maximum	5	3	4					
Setaria sphacelata sub. Sphacelata	5	3	4					
Eragrostis curvula	R	0.5	5					
Antidesma venosum	5	4	5					
Psidium guajava	4	7	4					
Scadoxus puniceus	5	1	5					
Senna didymobotrya	5	4	4					
Grewia monticola	5	2	5					
Tristchya leucothrix	5	3	5					
Other Taxa Present								
Site Factor Notes - at hillslope toe next to wetland, grazed								
General Notes								

Sample Site ID		17	Latitude (S)	24'39'59.3	Date	2007/03/07		
		T1_3	Longitude (E)	030'58'28.7				
Taxon	CC	Cover Estimate %	SC		Taxon	Cover Estimate %	CC	SC
Phragmites mauritianus	3	40	2					
Hemarthria altissima	5	20	2					
Psidium guajava	5	3	4					
Sporobolus pyramidalus	5	1	5					
Setaria sephacelata sericia	5	3	4					
Syzygium cordatum	5	2	4					
Panicum maximum	5	1	5					
Knipholia spp	5	1	5					
Grewia monticola	5	2	5					
Hibiscus cannibinus spp	5	1	5					
cf. Pseudarthria	3	20	3					
Pennisetum macrourum	plus	0.5	5					
Leersia hexandra	5	2	4					
Sida cordifolia	5	1	5					
Rhynchosia spp	5	1	5					
Sida cordifolia	5	2	5					
Frimbistilys complanata	5	3	4					
Helichrysum stenopteruus	5	1	4					
Iridaceae spp	plus	0.5	5					
Cyperus longus var. tanuiflorus	plus	0.5	5					
Other Taxa Present								
Site Factor Notes - in wetland, not permanent zone though grazed, v sandy soil, good cover almost 100%								
General Notes								

Sample Site ID	18		Latitude (S)	24'39'59.5	Date	2007/03/07		
			Longitude (E)	030'58'27.9				
Taxon	CC	Cover Estimate %	SC		Taxon	Cover Estimate %	CC	SC
Sporobolus pyramidalus	4	10	3		Maerua cafra	5	2	5
Setaria sephacelata sericia	4	10	3		Geigeria burkei subspp burkei var elata	5	1	4
Hyperhenia hirta	4	7	3		Bricharia brithantha	5	1	5
Hyperhenia dissoluta	4	7	3		Spermacoce (spp senensis?)	5	1	5
Panicum maximum	5	4	4					
Ageratum houstonianum	4	10	3					
Paspalum distichum	4	10	4					
Parinari curatellifolia	5	2	4					
Antidesma venosum	5	2	5					
Melinis repens	5	2	4					
Louditia simplex	5	3	4					
Setaria sphacelata sub. Sphacelata	5	2	4					
Scabiosa columbaria	5	2	4					
Sporobolus africanus	5	1	4					
cf. Conyza bonariensis	5	1	5					
Helichrysum pallidum	5	1	5					
Dichrostachys cineria	5	1	4					
Sida cordifolia	5	1	4					
Sorghum versicolor	5	2	4					
Cynodon dactylon	5	2	4					
Eragrostis Racemosa	5	1	5					
Other Taxa Present								
Site Factor Notes - edge of wetland, reasonable cover grazed								
General Notes								

Sample Site ID	19		Latitude (S)	24'40'00.0	Date	7/3/2007		
	T1_2		Longitude (E)	030'58.27.0				
Taxon	CC	Cover Estimate %	SC		Taxon	Cover Estimate %	CC	SC
Spermacoce (spp senensis?)	5	4	4					
Parinari curatellifolia	4	8	4					
Hyperhenia dissoluta	5	3	4					
Hyperhenia hirta	5	3	4					
Hyperhenia filipendula	5	3	4					
Helichrysum krausii	5	3	5					
Eragrostis Racemosa	4	6	3					
Paspalum distichum	4	8	3					
Sporobolus pyramidalus	5	2	4					
Andropogon schirensis	4	6	3					
Schizachyrium sanguineum	5	2	4					
Cyperacae spp	5	4	4					
Melinis repens	5	1	4					
155	5	1	5					
Iridaceae spp	5	1	5					
Helichrysum spp2	5	1	5					
Indigofera spp	5	1	5					
Other Taxa Present								
Site Factor Notes - grazed heavily, granite slope, not too steep, pretty bare but more than 50%								
General Notes								

Sample Site ID	20		Latitude (S)	24'40'00.4	Date	8/03/2007		
	T1_1		Longitude (E)	030'58'25.8				
Taxon	CC	Cover Estimate %	SC		Taxon	Cover Estimate %	CC	SC
Parinari curatellifolia	4	8	4					
Sporobolus pyramidalus	5	3	4					
Hyperhenia dissoluta	5	4	4					
Helichrysum krausii	5	4	4					
Eragrostis Racemosa	5	4	3					
Hyperhenia hirta	5	2	4					
Setaria sphacelata sub. Sphacelata	5	1	5					
Brecharia britantha	5	3	4					
Iridaceae spp	plus	0.5	5					
Agathisanthenum bojeri subspp bojeri	plus	0.5	5					
Paspalum Distichum	5	3	4					
Cyperacae spp	5	1	4					
Geigeria burkei subspp burkei var elata	plus	0.5	5					
Polygala (spp hottentotta?)	R	0.1	5					
Heteropogon contortus	plus	0.5	5					
Desmodium barbatum var. dimorphus	plus	0.8	5					
Andropogon schirensis	5	2	4					
Other Taxa Present								
Site Factor Notes - Relatively steep, coarse granite soil, heavily grazed, poor cover								
General Notes								

Sample Site ID	21		Latitude (S)	24'40'00.8	Date	8/03/2007		
			Longitude (E)	030'58'25.8				
Taxon	CC	Cover Estimate %	SC		Taxon	Cover Estimate %	CC	SC
Parinari curatellifolia	5	4	4					
Helichrysum krausii	4	10	4					
Hyperhenia dissoluta	5	3	4					
Sporobolus pyramidalus	5	2	4					
Setaria sphacelata sub. Sphacelata	5	3	4					
Themeda trianda	5	1	4					
Heteropogon contortus	5	2	4					
Melinis repens	plus	0.5	5					
Setaria sephacelata sericia	plus	0.5	5					
Eragrostis Racemosa	5	2	4					
Ageratum houstonianum	5	1	5					
Agathisanthenum bojeri subspp bojeri	5	2	4					
Diospyros spp prob lycoides	5	2	5					
Indigofera spp	5	1	5					
Ficus spp	5	1	5					
Psidium guajava	5	2	5					
Iridaceae spp	5	1	5					
Schizachyrium sanguineum	5	1	4					
Other Taxa Present								
Site Factor Notes - at plateau on slope, bare, granite soils								
General Notes								

Sample Site ID	22		Latitude (S)	24'40'01.4	Date	8/3/2007		
			Longitude (E)	030'58'23.9				
Taxon	CC	Cover Estimate %	SC		Taxon	Cover Estimate %	CC	SC
Parinari curatellifolia	4	5	4					
Sporobolus pyramidalus	5	3	4					
Hyperhenia dissoluta	4	10	3					
Helichrysum krausii	5	4	4					
Eragrostis Racemosa	5	4	3					
Agathisanthenum bojeri subspp bojeri	4	5	4					
Aristida congesta sub. barbicollis	5	3	4					
cf. Helichrysum spp 2	5	1	5					
Helichrysum pallidum	5	2	5					
Heteropogon contortus	5	1	4					
Cyperacae spp 2	plus	0.5	5					
Hermanna quartiniana subspp stellulata?	plus	0.5	5					
Hyperhenia hirta	5	2	4					
Other Taxa Present								
Site Factor Notes - Still on plateau, dry sandy soils, grazed								
General Notes								

Sample Site ID	T3_1		Latitude (S)		Date	13/03/2007		
			Longitude (E)					
Taxon	CC	Cover Estimate %	SC		Taxon	Cover Estimate %	CC	SC
Dichrostachys cineria	5	3	5					
Agathisanthenum bojeri subspp bojeri	5	2	4					
Sporobolus pyramidalus	5	1	5					
Ageratum houstonianum	5	2	4					
Sporobolus africanus	+	0.5	5					
Paspalum distichum	5	3	4					
Eragrostis racemosa	5	4	4					
Setaria sephacelata	5	1	4					
Hyparrhenia filipendula	5	2	4					
Schizachyrium sanguineum	5	1	4					
Parinari curatellifolia	+	0.5	5					
119	5	1	5					
cf. Helichrysum athrixifolium	+	0.5	5					
Hyperhenia dissoluta	+	0.5	5					
Tragus berteronianus	+	0.5	5					
Other Taxa Present								
Site Factor Notes - cover terrible, highly grazed, highly utilized								
General Notes								

Sample Site ID	T3_2		Latitude (S)		13/03/2007			
			Longitude (E)					
Taxon	CC	Cover Estimate %	SC		Taxon	Cover Estimate %	CC	SC
Phragmites mauritianus	1	80	1					
Hemarthria altissima	5	3	3					
Paspalum dilatatum	5	2	4					
Cyperus latifolius	5	2	4					
Cyperacae spp 3	4	5	3					
Leersia hexandra	5	1	5					
Persicaria spp	5	1	5					
Panicum spp	5	2	5					
Asteracae spp	5	1	5					
Centella asiatica	5	1	4					
Ocimum gratissimum	5	1	5					
Other Taxa Present								
Site Factor Notes - wetland proper, good cover								
General Notes								

Sample Site ID	T3_3		Latitude (S)		Date	13/03/2007		
			Longitude (E)					
Taxon	CC	Cover Estimate %	SC		Taxon	Cover Estimate %	CC	SC
Phragmites mauritianus	4	6	3					
Sporobolus pyramidalus	5	2	5					
Cynodon dactylon	2	65	1					
Digiteria erientha	5	2	4					
Tricalysia spp	5	1	5					
Paspalum distichum	5	4	4					
Bidens biternata	5	2	4					
Hyparrhenia filipendula	5	1	4					
Sporobolus africanus	5	1	5					
Centella asiatica	5	4	3					
Panicum maximum	5	1	5					
Hemarthria altissima	5	1	4					
Leersia hexandra	5	2	4					
Senna occidentalis	5	3	4					
Ipomoea (spp obscura?)	5	1	4					
Spermacoce (spp senensis?)	5	1	5					
Other Taxa Present								
Site Factor Notes - heavily grazed, within previously cultivated field, edge of wetland, good cover								
General Notes								

Sample Site ID	T3_4		Latitude (S)		Date	13/03/2007		
			Longitude (E)					
Taxon	CC	Cover Estimate %	SC		Taxon	Cover Estimate %	CC	SC
Sporobolus africanus	4	7	2					
Hyparrhenia filipendula	5	2	3					
Sporobolus pyramidalus	5	2	3					
Ageratum houstonianum	5	3	3					
Melinis repens	5	1	5					
Digiteria erientha	5	1	5					
Setaria sphacelata sub. Sphacelata	5	2	5					
Paspalum distichum	5	4	3					
Dichrostachys cineria	+	0.5	5					
Eragrostis racemosa	+	0.5	5					
Cucumi africanus	R	0.1	5					
Heteropogon contortus	+	0.5	5					
Tricalysia spp	+	0.5	5					
Psidium guajava	+	0.5	5					
Parinari curatellifolia	R	0.5	5					
Other Taxa Present								
Site Factor Notes - very heavily grazed within village, sandy soil, sparse								
General Notes								

APPENDIX ii - ERI protocols and additional data

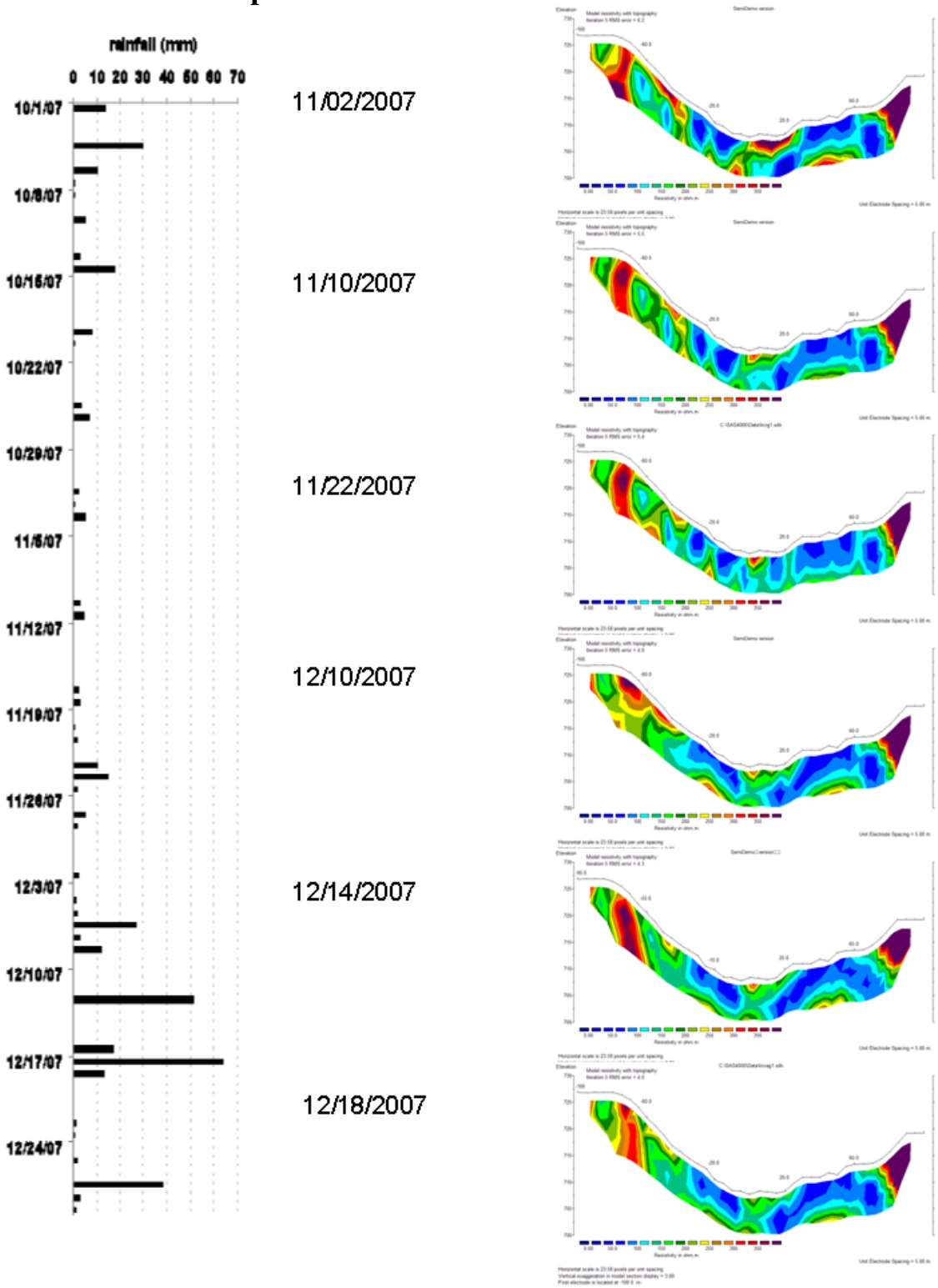

Figure ii.a: Time-series of ERT along transect T1 during November-December 2007 to examine wetting fronts. ERT probes remained in place throughout, therefore there is no variation in geology, the only variations in electrical resisitivity therefore attributed to changes in water content (Left – SW to Right NE or Transect 1).

Example of the address file (.adr) that was written for the 21 take-out Wenner-β array with ABEM Terrameter used in the 3D surveys described in Chapter 6.

1 21 1	number of electrode cables, total number of take-outs per cable
1 0 0	active electrode skip factor, lengths for x-move, lengths for y-move
21	total number of active take-outs, number of take-outs in x-direction
1 1 1-1	number, internal address and physical position of 1st take-out
2 2 1-2	number, internal address and physical position of 2nd take-out
3 3 1-3	“
4 4 1-4	“
5 5 1-5	“
6 6 1-6	“
7 7 1-7	“
8 8 1-8	“
9 9 1-9	“
10 10 1-10	“
11 11 1-11	“
12 12 1-12	“
13 13 1-13	“
14 14 1-14	“
15 15 1-15	“
16 16 1-16	“
17 17 1-17	“
18 18 1-18	“
19 19 1-19	“
20 20 1-20	“
21 21 1-21	“

Example of the protocol file (.org) that was written for the 21 take-out Wenner-β array with ABEM Terrameter used in the 3D surveys described in Chapter 6.

1				code
PD21	//Address File			address file
1	19	7	13	1st measurement position along take-out of A,B,M, & N electrodes*
2	20	8	14	2nd measurement position along take-out of A,B,M, & N electrodes
3	21	9	15	“
1	16	6	11	“
2	17	7	12	“
3	18	8	13	“
4	19	9	14	“
5	20	10	15	“
6	21	11	16	“
1	13	5	9	“
2	14	6	10	“
3	15	7	11	“
4	16	8	12	“
5	17	9	13	“
6	18	10	14	“
7	19	11	15	“
8	20	12	16	“
9	21	13	17	“
1	10	4	7	“
2	11	5	8	“
3	12	6	9	“
4	13	7	10	“
5	14	8	11	“
6	15	9	12	“
7	16	10	13	“
8	17	11	14	“
9	18	12	15	“
10	19	13	16	“
11	20	14	17	“
12	21	15	18	“
1	7	3	5	“
2	8	4	6	“
3	9	5	7	“
4	10	6	8	“
5	11	7	9	“
6	12	8	10	“
7	13	9	11	“
8	14	10	12	“
9	15	11	13	“
10	16	12	14	“
11	17	13	15	“
12	18	14	16	“
13	19	15	17	“
14	20	16	18	“
15	21	17	19	“
1	4	2	3	“
2	5	3	4	“
3	6	4	5	“
4	7	5	6	“
5	8	6	7	“
6	9	7	8	“
7	10	8	9	“
8	11	9	10	“
9	12	10	11	“
10	13	11	12	“
11	14	12	13	“
12	15	13	14	“
13	16	14	15	“
14	17	15	16	“
15	18	16	17	“
16	19	17	18	“
17	20	18	19	“
18	21	19	20	“

*A,B,M & N (current, current, potential, potential respectively)

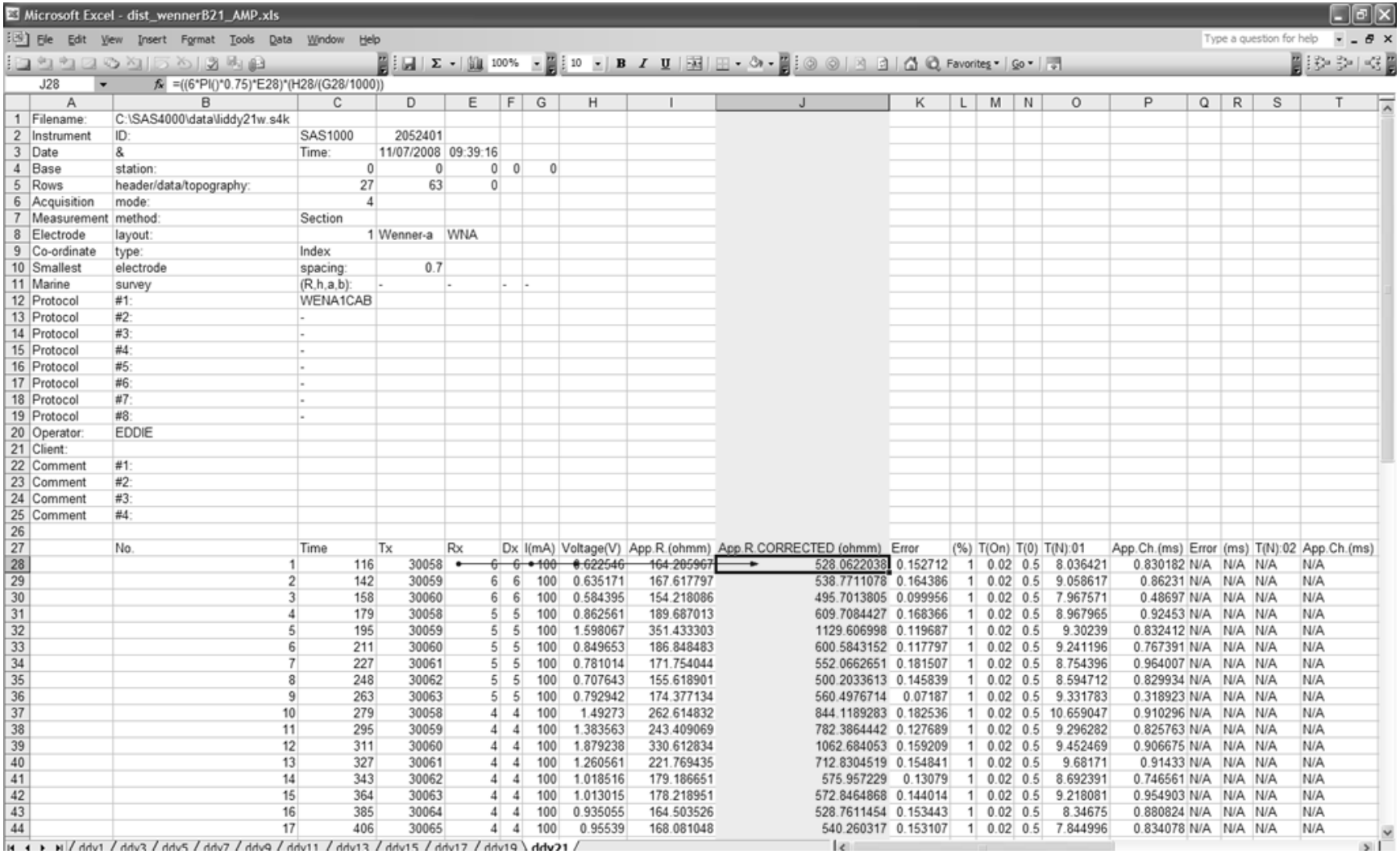

	A	B	C	D	E	F	G	H	I	J	K	L	M	N	O	P	Q	R	S	T
1	Filename:	C:\SAS4000\data\liddy21w.s4k																		
2	Instrument	ID:	SAS1000	2052401																
3	Date	&	Time:	11/07/2008	09:39:16															
4	Base	station:	0	0	0	0	0													
5	Rows	header/data/topography:	27	63	0															
6	Acquisition	mode:	4																	
7	Measurement	method:	Section																	
8	Electrode	layout:	1	Wenner-a	WNA															
9	Co-ordinate	type:	Index																	
10	Smallest	electrode	spacing:	0.7																
11	Marine	survey	(R,h,a,b):	-	-	-	-													
12	Protocol	#1:	WENA1CAB																	
13	Protocol	#2:	-																	
14	Protocol	#3:	-																	
15	Protocol	#4:	-																	
16	Protocol	#5:	-																	
17	Protocol	#6:	-																	
18	Protocol	#7:	-																	
19	Protocol	#8:	-																	
20	Operator:	EDDIE																		
21	Client:																			
22	Comment	#1:																		
23	Comment	#2:																		
24	Comment	#3:																		
25	Comment	#4:																		
26																				
27		No.	Time	Tx	Rx	Dx	I(mA)	Voltage(V)	App.R (ohmm)	App.R CORRECTED (ohmm)	Error	(%)	T(On)	T(0)	T(N):01	App.Ch.(ms)	Error	(ms)	T(N):02	App.Ch.(ms)
28		1	116	30058	6	6	100	0.622546	164.205967	528.0622038	0.152712	1	0.02	0.5	8.036421	0.830182	N/A	N/A	N/A	N/A
29		2	142	30059	6	6	100	0.635171	167.617797	538.7711078	0.164386	1	0.02	0.5	9.058617	0.86231	N/A	N/A	N/A	N/A
30		3	158	30060	6	6	100	0.584395	154.218086	495.7013805	0.099956	1	0.02	0.5	7.967571	0.48697	N/A	N/A	N/A	N/A
31		4	179	30058	5	5	100	0.862561	189.687013	609.7084427	0.168366	1	0.02	0.5	8.967965	0.92453	N/A	N/A	N/A	N/A
32		5	195	30059	5	5	100	1.598067	351.433303	1129.606998	0.119687	1	0.02	0.5	9.30239	0.832412	N/A	N/A	N/A	N/A
33		6	211	30060	5	5	100	0.849653	186.848483	600.5843152	0.117797	1	0.02	0.5	9.241196	0.767391	N/A	N/A	N/A	N/A
34		7	227	30061	5	5	100	0.781014	171.754044	552.0662651	0.181507	1	0.02	0.5	8.754396	0.964007	N/A	N/A	N/A	N/A
35		8	248	30062	5	5	100	0.707643	155.618901	500.2033613	0.145839	1	0.02	0.5	8.594712	0.829934	N/A	N/A	N/A	N/A
36		9	263	30063	5	5	100	0.792942	174.377134	560.4976714	0.07187	1	0.02	0.5	9.331783	0.318923	N/A	N/A	N/A	N/A
37		10	279	30058	4	4	100	1.49273	262.614832	844.1189283	0.182536	1	0.02	0.5	10.659047	0.910296	N/A	N/A	N/A	N/A
38		11	295	30059	4	4	100	1.383563	243.409069	782.3864442	0.127689	1	0.02	0.5	9.296282	0.825763	N/A	N/A	N/A	N/A
39		12	311	30060	4	4	100	1.879238	330.612834	1062.684053	0.159209	1	0.02	0.5	9.452469	0.906675	N/A	N/A	N/A	N/A
40		13	327	30061	4	4	100	1.260561	221.769435	712.8304519	0.154841	1	0.02	0.5	9.68171	0.91433	N/A	N/A	N/A	N/A
41		14	343	30062	4	4	100	1.018516	179.186651	575.957229	0.13079	1	0.02	0.5	8.692391	0.746561	N/A	N/A	N/A	N/A
42		15	364	30063	4	4	100	1.013015	178.218951	572.8464868	0.144014	1	0.02	0.5	9.218081	0.954903	N/A	N/A	N/A	N/A
43		16	385	30064	4	4	100	0.935055	164.503526	528.7611454	0.153443	1	0.02	0.5	8.34675	0.880824	N/A	N/A	N/A	N/A
44		17	406	30065	4	4	100	0.95539	168.081048	540.260317	0.153107	1	0.02	0.5	7.844996	0.834078	N/A	N/A	N/A	N/A

Figure ii.b: Example of the geometric factor correction applied to correct the apparent resistivity (App. R) for a unit electrode spacing from 0.7m to 0.75

APPENDIX iii – Soil Hydraulic Properties

This appendix includes the soil hydraulic properties and van Genuchten curve fitting for hydrometric observation stations, T1_1, T1_2, and T1_3 whose data was incorporated into the HYDRUS modelling of Chapter 4. The appendix also contains tables of in-situ field determined saturated (K_{sat}) and unsaturated (K_{unsat}) soil hydraulic conductivities and laboratory water retention characteristics.

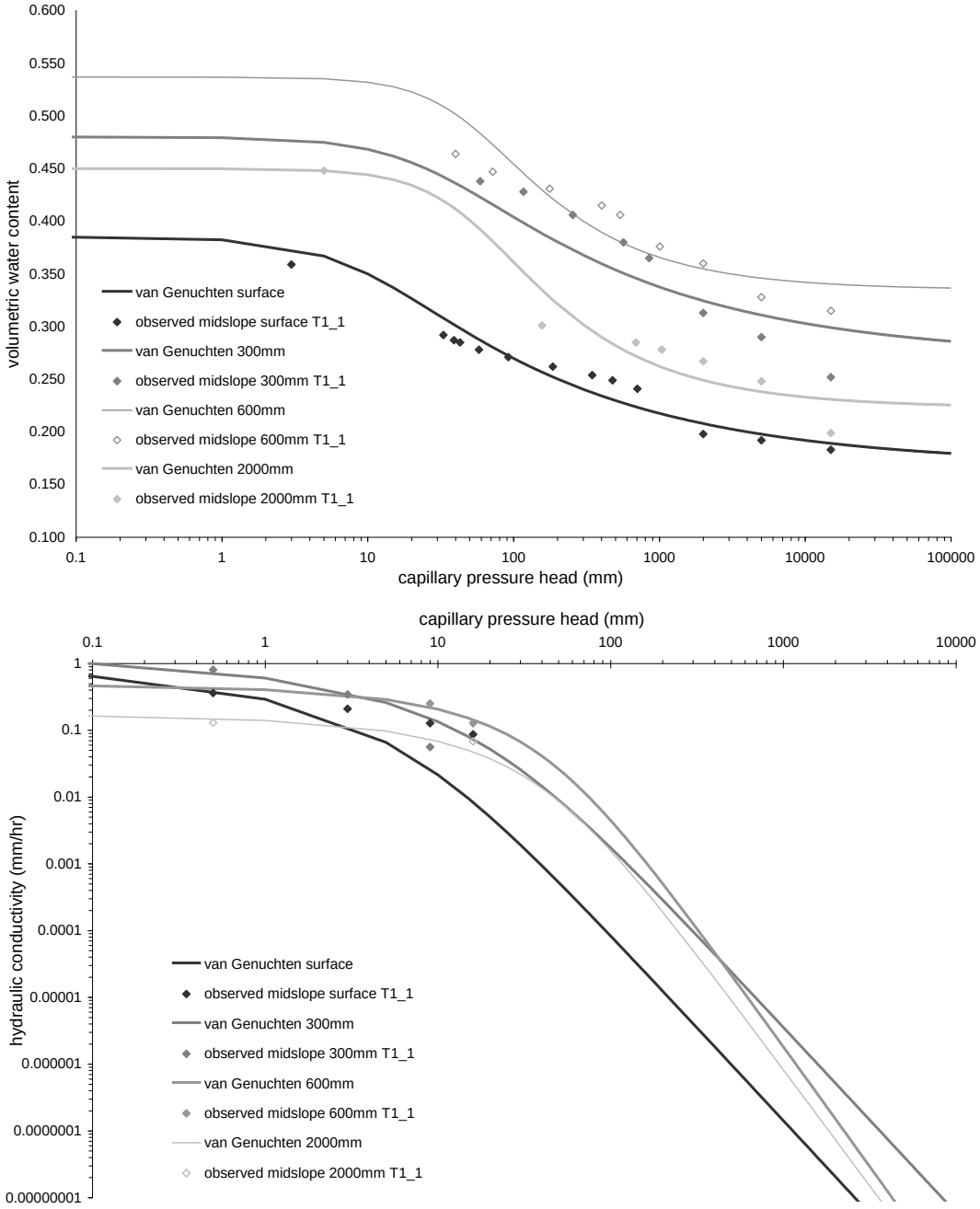

Figure iii.a: Water retention characteristics (above) and hydraulic conductivity characteristics (below) for site T1_1 used in Chapter 4.

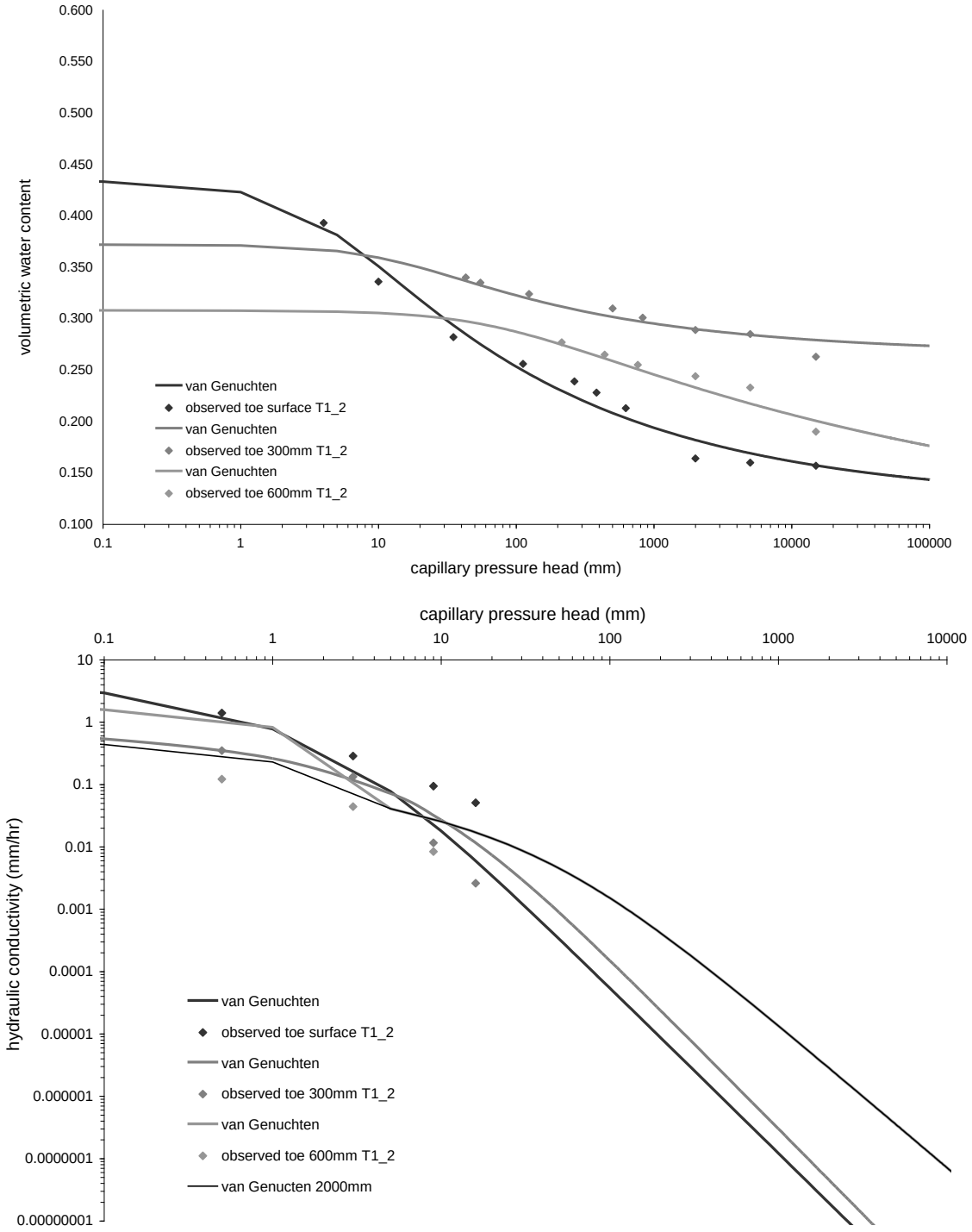

Figure iii.b: Water retention characteristics (above) and hydraulic conductivity characteristics (below) for site T1_2 used in Chapter 4 (NB double curvurture close to saturation for 600 mm and 2000 mm invoking dual porosity of Vogel & Cislerova, 1988).

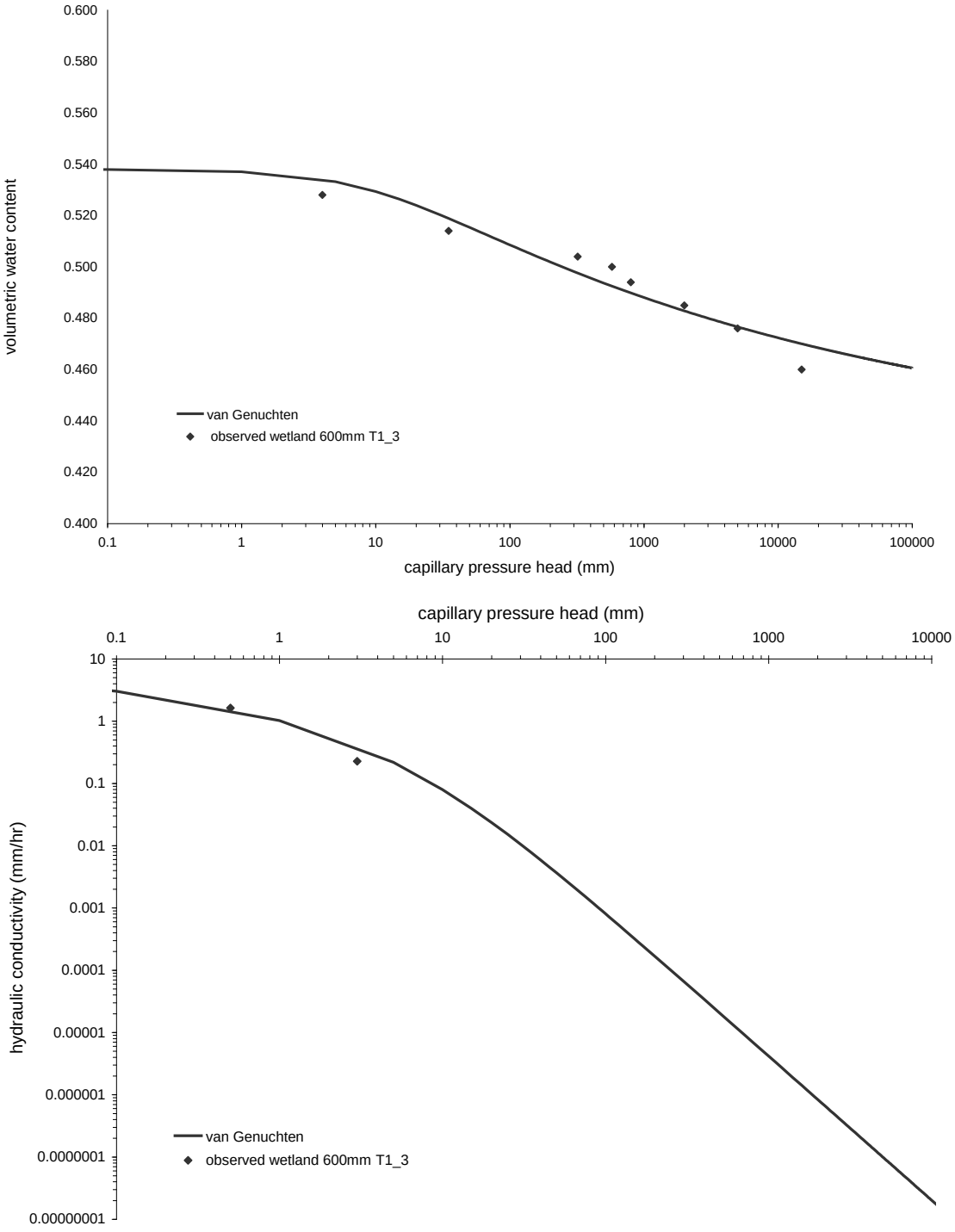

Figure iii.c: Water retention characteristics (above) and hydraulic conductivity characteristics (below) for site T1_3 used in Chapter 4.

Table iii.d

T1_1 Determination of K_{unsat} using Tension Disc Infiltrometer Based on Ankeny *et al* (1991) method

INFILTRATION RADIU 4.200 cm

3D Flux | 1D Flux

3D Flux | 1D Flux

Depth **Surface**
Replicate 1

	TENSION	STEADY STATE FLUX	A	INITIAL HYDRAULIC CONDUCTIVITY K_{i-1}	K_i	FINAL HYDRAULIC CONDUCTIVITY
	(cm) (mm/h)		(cm3/min)	(cm-1)	(cm/min)	(cm/s)
0.5	1.7E+00		8.2E-03		1.4E-04	4.9E+00
3.0	1.3E+00	1.1E-01	2.7E-03	6.2E-03	7.4E-05	2.7E+00
9.0	9.8E-01	4.1E-02	1.6E-03	2.1E-03	3.1E-05	1.1E+00
16.0	7.9E-01	3.0E-02	1.3E-03		2.2E-05	7.8E-01

Depth **Surface**
Replicate 2

	TENSION	STEADY STATE FLUX	A	INITIAL HYDRAULIC CONDUCTIVITY K_{i-1}	K_i	FINAL HYDRAULIC CONDUCTIVITY
	(cm)		(cm3/min)	(cm-1)	(cm/min)	(cm/s) (mm/h)
0.5	1.2E+00		6.0E-03		1.0E-04	3.6E+00
3.0	9.4E-01	1.1E-01	2.4E-03	4.5E-03	5.8E-05	2.1E+00
9.0	6.9E-01	5.0E-02	2.5E-03	1.8E-03	3.5E-05	1.3E+00
16.0	4.1E-01	7.4E-02	1.4E-03		2.4E-05	8.6E-01

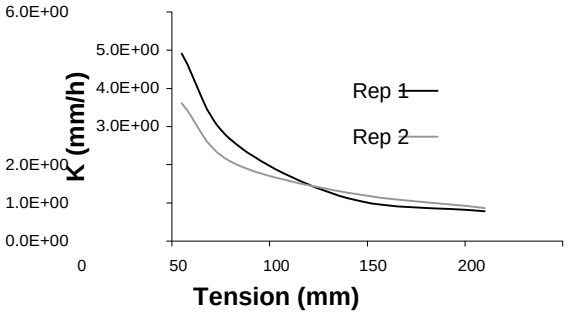

Depth **10cm**
Replicate 1

	TENSION	STEADY STATE FLUX	A	INITIAL HYDRAULIC CONDUCTIVITY K_{i-1}	K_i	FINAL HYDRAULIC CONDUCTIVITY
	(cm)	(cm3/min)	(cm-1)	(cm/min)		(cm/s) (mm/h)
0.5	2.5E+00		2.1E-02		3.4E-04	1.2E+01
3.0	1.3E+00	2.6E-01	6.0E-03	1.0E-02	1.4E-04	4.9E+00
	9.0	6.3E-01	1.1E-01	1.9E-03	3.0E-03	4.1E-05 1.5E+00
	16.0	4.1E-01	6.2E-02	1.2E-03		2.1E-05 7.4E-01

Depth **10cm**
Replicate 2

	TENSION	STEADY STATE FLUX	A	INITIAL HYDRAULIC CONDUCTIVITY K_{i-1}	K_i	FINAL HYDRAULIC CONDUCTIVITY
	(cm)	(cm3/min)	(cm-1)	(cm/min)		(cm/s) (mm/h)
0.5	3.2E+00		2.3E-02		3.9E-04	1.4E+01
3.0	1.9E+00	2.0E-01	1.5E-02	1.4E-02	2.4E-04	8.6E+00
	9.0	3.6E-01	2.3E-01		2.8E-03	

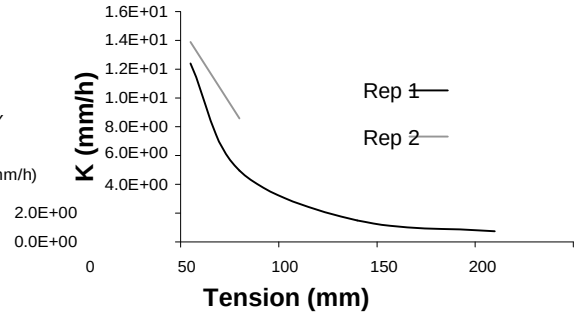

3D Flux | 1D Flux

Depth **30cm**
Replicate 1

TENSION	STEADY STATE FLUX	A	INITIAL HYDRAULIC CONDUCTIVITY K_{i-1}	K_i	FINAL HYDRAULIC CONDUCTIVITY	
(cm)	(cm3/min)	(cm-1)	(cm/min)		(cm/s)	(mm/h)
0.5	1.2E+00		6.1E-03		1.0E-04	3.6E+00
3.0	8.5E-01	1.2E-01	5.3E-03	4.5E-03	8.1E-05	2.9E+00
9.0	3.0E-01	1.6E-01	5.2E-04	1.9E-03	2.0E-05	7.1E-01
16.0	2.4E-01	3.2E-02	4.1E-04		6.9E-06	2.5E-01

3D Flux | 1D Flux

Depth **30cm**
Replicate 2

TENSION	STEADY STATE FLUX	A	INITIAL HYDRAULIC CONDUCTIVITY K_{i-1}	K_i	FINAL STATE HYDRAULIC CONDUCTIVITY	
(cm)	(cm3/min)	(cm-1)	(cm/min)		(cm/s)	(mm/h)
0.5	1.6E+00		1.3E-02		2.2E-04	8.0E+00
3.0	8.1E-01	2.6E-01	4.7E-03	6.8E-03	9.6E-05	3.4E+00
9.0	3.2E-01	1.4E-01		1.9E-03		

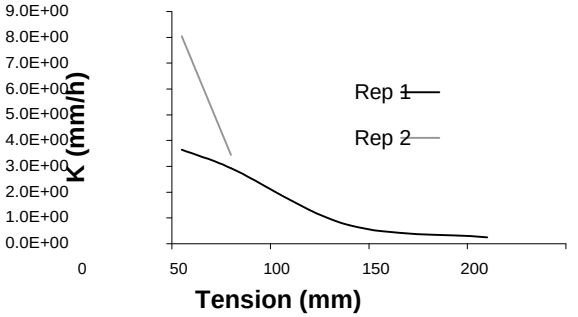

Depth **60cm**
Replicate 1

TENSION	STEADY STATE FLUX	A	INITIAL HYDRAULIC CONDUCTIVITY K_{i-1}	K_i	FINAL HYDRAULIC CONDUCTIVITY	
(cm)	(cm3/min)	(cm-1)	(cm/min)		(cm/s)	(mm/h)
0.5	7.3E-01		5.2E-02		8.6E-04	3.1E+01
3.0	2.3E+00	-4.1E-01	1.0E-02	1.6E-01	1.4E-03	5.1E+01
9.0	1.2E+00	1.0E-01	3.0E-03	5.4E-03	7.0E-05	2.5E+00
16.0	8.7E-01	4.7E-02	2.1E-03		3.5E-05	1.3E+00

Depth **60cm**
Replicate 2

TENSION	STEADY STATE FLUX	A	INITIAL HYDRAULIC CONDUCTIVITY K_{i-1}	K_i	FINAL HYDRAULIC CONDUCTIVITY	
(cm)	(cm3/min)	(cm-1)	(cm/min)		(cm/s)	(mm/h)
0.5	2.2E+00		1.5E-02		2.5E-04	9.1E+00
3.0	1.4E+00	1.8E-01	3.9E-03	9.5E-03	1.1E-04	4.0E+00
9.0	1.0E+00	5.5E-02	4.1E-03	2.8E-03	5.7E-05	2.1E+00
16.0	5.3E-01	8.8E-02	2.1E-03		3.6E-05	1.3E+00

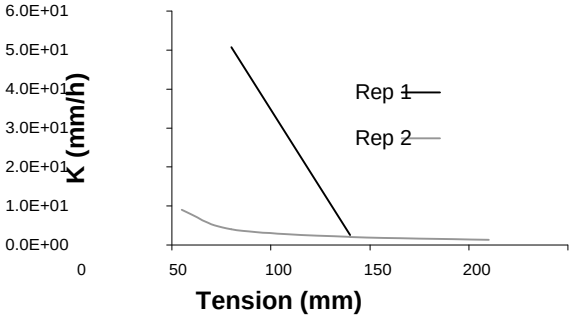

3D Flux | 1D Flux

Depth **200cm**
Replicate 1

TENSION (cm)	STEADY FLUX (cm3/min)	A (cm-1)	INITIAL HYDRAULIC CONDUCTIVITY K_{i-1} (cm/min)	INITIAL HYDRAULIC CONDUCTIVITY K_i (cm/min)	FINAL HYDRAULIC CONDUCTIVITY (cm/s)	FINAL HYDRAULIC CONDUCTIVITY (mm/h)
0.5	1.4E+00		9.8E-03		1.6E-04	5.9E+00
3.0	8.7E-01	1.9E-01	2.2E-03	6.0E-03	6.8E-05	2.5E+00
9.0	6.5E-01	4.9E-02	1.6E-03	1.6E-03	2.7E-05	9.7E-01
16.0	4.6E-01	4.9E-02	1.1E-03		1.9E-05	6.9E-01

3D Flux | 1D Flux

Depth **200cm**
Replicate 2

TENSION (cm)	STEADY STATE FLUX (cm3/min)	A (cm-1)	INITIAL HYDRAULIC CONDUCTIVITY K_{i-1} (cm/min)	INITIAL HYDRAULIC CONDUCTIVITY K_i (cm/min)	FINAL STATE HYDRAULIC CONDUCTIVITY (cm/s)	FINAL STATE HYDRAULIC CONDUCTIVITY (mm/h)
0.5	1.2E+00		2.2E-03		3.6E-05	1.3E+00
3.0	1.1E+00	3.3E-02	4.9E-03	2.0E-03	5.7E-05	2.1E+00
9.0	6.1E-01	9.8E-02	1.7E-03	2.7E-03	3.6E-05	1.3E+00
16.0	4.1E-01	5.5E-02	1.1E-03		1.9E-05	6.8E-01

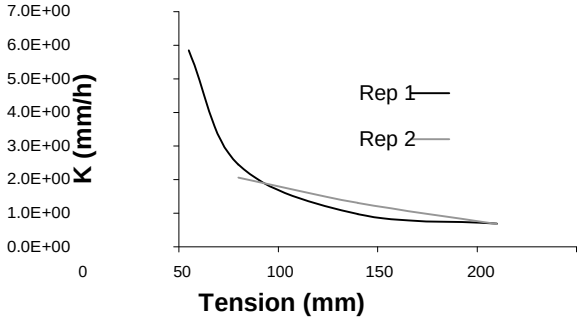

T1 2 Determination of K_{unsat} using Tension Disc Infiltrometer Based on Ankeny *et al* (1991) method

INFILTRATION RADIUS 4.200 cm

3D Flux | 1D Flux

3D Flux | 1D Flux

Depth **Surface**
Replicate 1

TENSION (cm)	STEADY STATE FLUX (cm3/min)	A (cm-1)	INITIAL HYDRAULIC CONDUCTIVITY K_{i-1} (cm/min)	K_i	FINAL HYDRAULIC CONDUCTIVITY (cm/s)	(mm/h)
0.5	2.2E+00		2.3E-02		3.9E-04	1.4E+01
3	6.6E-01	4.3E-01	2.6E-03	7.0E-03	8.0E-05	2.9E+00
9	4.0E-01	8.2E-02	1.6E-03	1.5E-03	2.6E-05	9.4E-01
16	2.1E-01	8.7E-02	8.6E-04		1.4E-05	5.1E-01

Depth **Surface**
Replicate 2

TENSION (cm)	STEADY STATE FLUX (cm3/min)	A (cm-1)	INITIAL HYDRAULIC CONDUCTIVITY K_{i-1} (cm/min)	K_i	FINAL HYDRAULIC CONDUCTIVITY (cm/s)	(mm/h)
0.5	1.7E+00		1.6E-02		2.7E-04	9.7E+00
3	7.4E-01	3.2E-01	2.0E-03	6.9E-03	7.4E-05	2.7E+00
9	5.3E-01	5.4E-02	3.1E-03	1.5E-03	3.8E-05	1.4E+00
16	1.7E-01	1.5E-01	1.0E-03		1.7E-05	6.0E-01

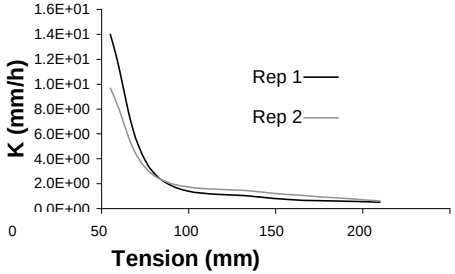

Depth **10cm**
Replicate 1

TENSION (cm)	STEADY STATE FLUX (cm3/min)	A (cm-1)	INITIAL HYDRAULIC CONDUCTIVITY K_{i-1} (cm/min)	K_i	FINAL HYDRAULIC CONDUCTIVITY (cm/s)	(mm/h)
0.5	2.2E+00		2.0E-02		3.3E-04	1.2E+01
3	9.9E-01	3.0E-01	5.1E-03	8.9E-03	1.2E-04	4.2E+00
9	4.6E-01	1.2E-01	1.7E-03	2.4E-03	3.4E-05	1.2E+00
16	2.6E-01	8.1E-02	9.7E-04		1.6E-05	5.8E-01

Depth **10cm**
Replicate 2

TENSION (cm)	STEADY STATE FLUX (cm3/min)	A (cm-1)	INITIAL HYDRAULIC CONDUCTIVITY K_{i-1} (cm/min)	K_i	FINAL HYDRAULIC CONDUCTIVITY (cm/s)	(mm/h)
0.5	6.6E-01		4.9E-03		8.1E-05	2.9E+00
3	3.8E-01	2.1E-01	5.7E-04	2.8E-03	2.8E-05	1.0E+00
9	3.2E-01	2.7E-02	1.6E-03	4.8E-04	1.7E-05	6.1E-01
16	1.4E-01	1.1E-01	6.9E-04		1.1E-05	4.1E-01

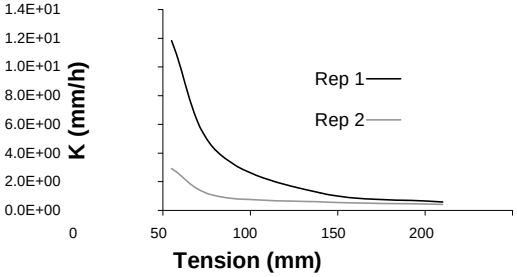

3D Flux | 1D Flux

Depth **30cm**
Replicate 1

TENSION	STEADY STATE FLUX	A	INITIAL HYDRAULIC CONDUCTIVITY		FINAL HYDRAULIC CONDUCTIVITY	
(cm)	(cm3/min)	(cm-1)	(cm/min)		(cm/s)	(mm/h)
0.5	6.3E-01		5.8E-03		9.7E-05	3.5E+00
3	2.7E-01	3.2E-01	2.0E-03	2.5E-03	3.7E-05	1.3E+00
9	5.7E-02	2.2E-01	-4.0E-05	4.3E-04	3.2E-06	1.2E-01
16	6.2E-02	-1.1E-02	-4.3E-05		-7.2E-07	-2.6E-02

3D Flux | 1D Flux

Depth **30cm**
Replicate 2

TENSION	STEADY STATE FLUX	A	INITIAL HYDRAULIC CONDUCTIVITY		FINAL STATE HYDRAULIC CONDUCTIVITY	
(cm)	(cm3/min)	(cm-1)	(cm/min)		(cm/s)	(mm/h)
0.5	7.4E-01		0.0176523		0.0002942	10.591403
3	1.1E+00	0.1730195	0.0085465	0.0273949	0.0001571	5.6545076
9	2.5E-01	0.2148718		0.0018468		

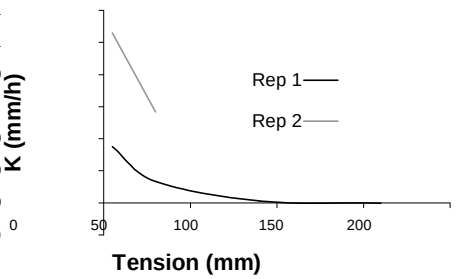

Depth **60cm**
Replicate 1

TENSION	STEADY STATE FLUX	A	INITIAL HYDRAULIC CONDUCTIVITY		FINAL HYDRAULIC CONDUCTIVITY	
		K_{i-1}	K_i			
(cm)	(cm3/min)	(cm-1)	(cm/min)		(cm/s)	(mm/h)
0.5	2.4E-01		2.0E-03		3.4E-05	1.2E+00
3	1.2E-01	2.6E-01	4.5E-04	1.0E-03	1.2E-05	4.4E-01
9	7.6E-02	7.8E-02	0.0E+00	2.8E-04	2.3E-06	8.4E-02
16						

Depth **60cm**
Replicate 2

TENSION	STEADY STATE FLUX	A	INITIAL HYDRAULIC CONDUCTIVITY		FINAL HYDRAULIC CONDUCTIVITY	
		K_{i-1}	K_i			
(cm)	(cm3/min)	(cm-1)	(cm/min)		(cm/s)	(mm/h)
0.5	4.5E-01		3.8E-03		6.4E-05	2.3E+00
3	2.2E-01	2.7E-01	7.8E-04	1.9E-03	2.2E-05	8.0E-01
9	1.4E-01	7.4E-02	3.9E-04	5.0E-04	7.4E-06	2.7E-01
16	9.6E-02	5.4E-02	2.6E-04		4.4E-06	1.6E-01

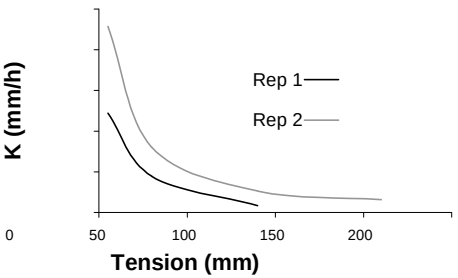

3D Flux | 1D Flux

Depth	200cm					
Replicate	1					
TENSION	STEADY FLUX	A	INITIAL HYDRAULIC CONDUCTIVITY K_{i-1}	FINAL HYDRAULIC CONDUCTIVITY K_i		
(cm)	(cm3/min)	(cm-1)	(cm/min)	(cm/s)	(mm/h)	
0.5	4.4E-01		4.0E-03	6.7E-05	2.4E+00	
3	2.0E-01	3.1E-01	1.4E-03	1.8E-03	2.6E-05	9.5E-01
9	5.3E-02	1.9E-01	0.0E+00	3.7E-04	3.1E-06	1.1E-01
16						

3D Flux | 1D Flux

Depth	200cm					
Replicate	2					
TENSION	STEADY STATE FLUX	A	INITIAL HYDRAULIC CONDUCTIVITY K_{i-1}	FINAL STATE HYDRAULIC CONDUCTIVITY K_i		
(cm)	(cm3/min)	(cm-1)	(cm/min)	(cm/s)	(mm/h)	
0.5	1.4E+00		1.4E-02	2.3E-04	8.3E+00	
3	4.8E-01	3.8E-01	4.0E-03	4.9E-03	7.4E-05	2.7E+00
9	6.0E-02	2.6E-01	0.0E+00	5.0E-04	4.1E-06	1.5E-01
16						

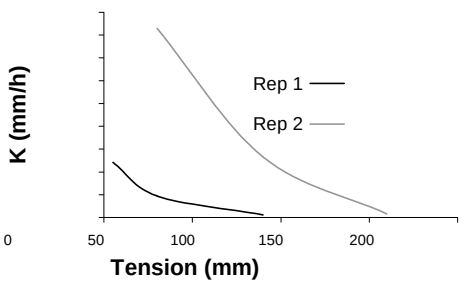

T1_3 Determination of K_{unsat} using Tension Disc Infiltrometer Based on Ankeny *et al* (1991) method

INFILTRATION RADIUS 4.200 cm

3D Flux | 1D Flux

Depth **Surface**
Replicate 1

TENSION (cm)	STEADY STATE FLUX (cm3/min)	A (cm-1)	INITIAL HYDRAULIC CONDUCTIVITY K_{i-1} (cm/min)	K_i	FINAL HYDRAULIC CONDUCTIVITY (cm/s)	(mm/h)
0.5	5.3E-01		0.0037347		6.225E-05	2.2E+00
3	6.5E-01	0.0856978	0.0031401	0.0046309	1.242E-05	4.5E-01
9	3.3E-01	0.1105559	6.74E-05	0.001576	1.257E-05	4.5E-01
16	3.3E-01	0.0034257	6.904E-05		1.15E+06	4.1E-02

3D Flux | 1D Flux

Depth **Surface**
Replicate 2

TENSION (cm)	STEADY STATE FLUX (cm3/min)	A (cm-1)	INITIAL HYDRAULIC CONDUCTIVITY K_{i-1} (cm/min)	K_i	FINAL STATE HYDRAULIC CONDUCTIVITY (cm/s)	(mm/h)
0.5	2.5E+00		1.7E-02		2.8E-04	1.0E+01
3	1.6E+00	1.8E-01	6.8E-03	1.1E-02	1.5E-04	5.3E+00
9	8.7E-01	9.6E-02	4.2E-03	3.8E-03	6.7E-05	2.4E+00
16	3.9E-01	1.1E-01	1.9E-03		3.1E-05	1.1E+00

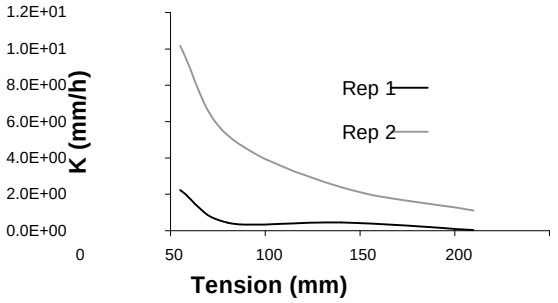

Depth **10cm**
Replicate 1

TENSION (cm)	STEADY STATE FLUX (cm3/min)	A (cm-1)	INITIAL HYDRAULIC CONDUCTIVITY K_{i-1} (cm/min)	K_i	FINAL HYDRAULIC CONDUCTIVITY (cm/s)	(mm/h)
0.5	1.7E+01		1.4E-01		2.3E-03	8.2E+01
3	8.5E+00	2.6E-01	6.8E-02	7.1E-02	1.2E-03	4.2E+01
9	1.4E+00	2.4E-01	9.9E-03	1.1E-02	1.8E-04	6.3E+00
16	2.6E-01	2.0E-01	1.9E-03		3.1E-05	1.1E+00

Depth **10cm**
Replicate 2

TENSION (cm)	STEADY STATE FLUX (cm3/min)	A (cm-1)	INITIAL HYDRAULIC CONDUCTIVITY K_{i-1} (cm/min)	K_i	FINAL HYDRAULIC CONDUCTIVITY (cm/s)	(mm/h)
0.5	1.0E+01		9.2E-02		1.5E-03	5.5E+01
3	4.3E+00	3.2E-01	3.4E-02	4.0E-02	6.2E-04	2.2E+01
9	7.0E-01	2.4E-01	4.7E-03	5.6E-03	8.6E-05	3.1E+00
16	1.6E-01	1.8E-01	1.1E-03		1.8E-05	6.3E-01

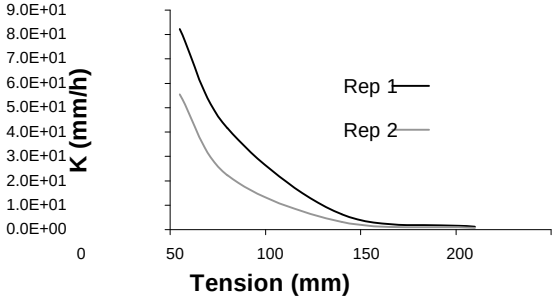

3D Flux | 1D Flux

Depth **30cm**
Replicate 1

TENSION (cm)	STEADY FLUX (cm3/min)	A (cm-1)	INITIAL HYDRAULIC CONDUCTIVITY K_{i-1} (cm/min)	K_i	FINAL HYDRAULIC CONDUCTIVITY (cm/s)	(mm/h)
0.5	2.0E+01		2.2E-01		3.7E-03	1.3E+02
3	5.5E+00	4.6E-01	3.8E-02	6.0E-02	8.1E-04	2.9E+01
9	1.5E+00	1.9E-01	8.7E-03	1.1E-02	1.6E-04	5.8E+00
16	5.4E-01	1.4E-01	3.1E-03		5.1E-05	1.8E+00

3D Flux | 1D Flux

Depth **30cm**
Replicate 2

TENSION (cm)	STEADY STATE FLUX (cm3/min)	A (cm-1)	INITIAL HYDRAULIC CONDUCTIVITY K_{i-1} (cm/min)	K_i	FINAL STATE HYDRAULIC CONDUCTIVITY (cm/s)	(mm/h)
0.5	5.0E+00		4.9E-02		8.2E-04	2.9E+01
3	1.9E+00	3.6E-01	1.2E-02	1.9E-02	2.6E-04	9.2E+00
9	7.0E-01	1.6E-01	3.6E-03	4.3E-03	6.6E-05	2.4E+00
16	2.9E-01	1.2E-01	1.5E-03		2.5E-05	8.8E-01

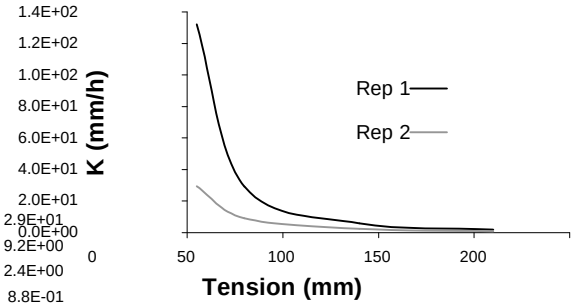

Depth **50cm**
Replicate 1

TENSION (cm)	STEADY FLUX (cm3/min)	A (cm-1)	INITIAL HYDRAULIC CONDUCTIVITY K_{i-1} (cm/min)	K_i	FINAL HYDRAULIC CONDUCTIVITY (cm/s)	(mm/h)
0.5	8.3E+00		2.5E-02		4.2E-04	1.5E+01
3	7.1E+00	6.2E-02	4.5E-02	2.2E-02	5.6E-04	2.0E+01
9	2.4E+00	1.7E-01	1.6E-02	1.5E-02	2.6E-04	9.5E+00
16	4.7E-01	1.9E-01	3.3E-03		5.4E-05	2.0E+00

Depth **60cm**
Replicate 1

TENSION (cm)	STEADY STATE FLUX (cm3/min)	A (cm-1)	INITIAL HYDRAULIC CONDUCTIVITY K_{i-1} (cm/min)	K_i	FINAL STATE HYDRAULIC CONDUCTIVITY (cm/s)	(mm/h)
0.5	2.5E+00		2.7E-02		4.5E-04	1.6E+01
3	7.0E-01	4.5E-01	0.0E+00	7.5E-03	6.3E-05	2.3E+00
9						
16						

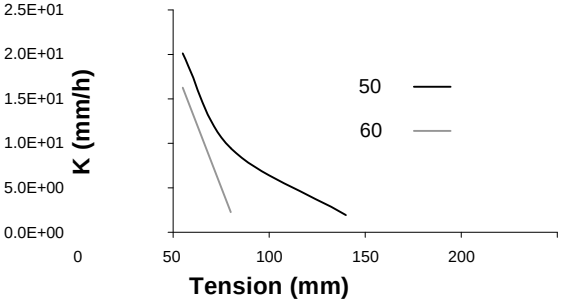

3D Flux | 1D Flux

Depth **85cm**
Replicate 1

TENSION (cm)	STEADY FLUX (cm3/min)	A (cm-1)	INITIAL HYDRAULIC CONDUCTIVITY K_{i-1} (cm/min)	K_i	FINAL HYDRAULIC CONDUCTIVITY (cm/s)	(mm/h)
0.5	3.4E+00		3.2E-02		5.3E-04	1.9E+01
3	1.4E+00	3.3E-01	9.7E-03	1.3E-02	1.9E-04	6.9E+00
9	4.0E-01	1.9E-01	0.0E+00	2.8E-03	2.3E-05	8.3E-01
16						

3D Flux | 1D Flux

Depth **100cm**
Replicate 1

TENSION (cm)	STEADY STATE FLUX (cm3/min)	A (cm-1)	INITIAL HYDRAULIC CONDUCTIVITY K_{i-1} (cm/min)	K_i	FINAL STATE HYDRAULIC CONDUCTIVITY (cm/s)	(mm/h)
0.5	1.6E+01		1.5E-01		2.6E-03	9.3E+01
3	6.6E+00	3.4E-01	4.9E-02	6.3E-02	9.3E-04	3.3E+01
9	1.5E+00	2.1E-01	1.2E-02	1.1E-02	1.9E-04	6.8E+00
16	1.7E-01	2.3E-01	1.3E-03		2.2E-05	7.9E-01

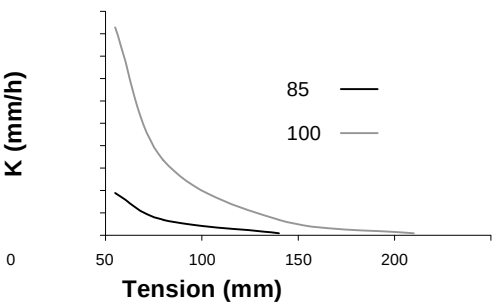

Depth **135cm**
Replicate 1

TENSION (cm)	STEADY FLUX (cm3/min)	A (cm-1)	INITIAL HYDRAULIC CONDUCTIVITY K_{i-1} (cm/min)	K_i	FINAL HYDRAULIC CONDUCTIVITY (cm/s)	(mm/h)
0.5	3.8E-01		7.3E-02		1.2E-03	4.4E+01
3	9.3E-01	-3.3E-01	7.7E-03	1.8E-01	1.5E-03	5.6E+01
9	1.1E-01	2.6E-01	0.0E+00	9.5E-04	7.9E-06	2.9E-01
16						

Depth **200cm**
Replicate 1

TENSION (cm)	STEADY STATE FLUX (cm3/min)	A (cm-1)	INITIAL HYDRAULIC CONDUCTIVITY K_{i-1} (cm/min)	K_i	FINAL STATE HYDRAULIC CONDUCTIVITY (cm/s)	(mm/h)
0.5	7.3E+00		5.5E-02		9.1E-04	3.3E+01
3	4.2E+00	2.2E-01	1.7E-02	3.1E-02	4.1E-04	1.5E+01
9	2.4E+00	9.0E-02	1.6E-02	1.0E-02	2.1E-04	7.7E+00
16	6.1E-01	1.7E-01	4.0E-03		6.6E-05	2.4E+00

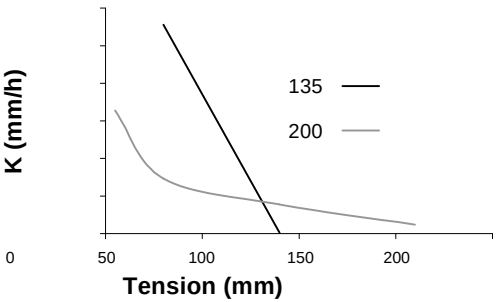

T1_4 Determination of K_{unsat} using Tension Disc Infiltrometer Based on Ankeny *et al* (1991) method

INFILTRATION RADIUS 4.200 cm

3D Flux | 1D Flux

Depth **Surface**
Replicate 1

TENSION (cm)	STEADY FLUX (cm3/min)	A (cm-1)	INITIAL HYDRAULIC CONDUCTIVITY Ki-1 (cm/min)	Ki	FINAL HYDRAULIC CONDUCTIVITY (cm/s)	(mm/h)
0.5	4.4E+00		3.8E-02		6.4E-04	2.3E+01
3	2.1E+00	2.8E-01	1.4E-02	1.8E-02	2.7E-04	9.8E+00
9	6.7E-01	1.7E-01	1.6E-03	4.4E-03	5.0E-05	1.8E+00
16	4.8E-01	4.6E-02	1.2E-03		1.9E-05	6.9E-01

Depth **Surface**
Replicate 2

TENSION (cm)	STEADY STATE FLUX (cm3/min)	A (cm-1)	INITIAL HYDRAULIC CONDUCTIVITY Ki-1 (cm/min)	Ki	FINAL STATE HYDRAULIC CONDUCTIVITY (cm/s)	(mm/h)
0.5	6.5E+00		6.0E-02		1.0E-03	3.6E+01
3	2.8E+00	3.2E-01	2.1E-02	2.6E-02	3.9E-04	1.4E+01
9	6.5E-01	2.1E-01	3.0E-03	4.8E-03	6.5E-05	2.3E+00
16	3.1E-01	1.0E-01	1.4E-03		2.3E-05	8.4E-01

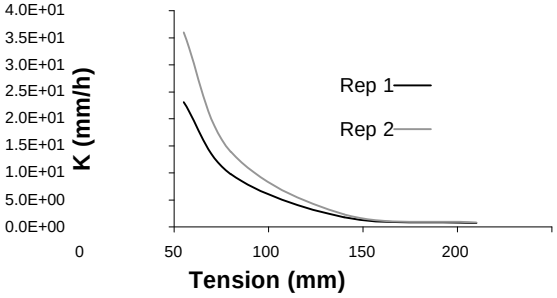

Depth **10cm**
Replicate 1

TENSION (cm)	STEADY FLUX (cm3/min)	A (cm-1)	INITIAL HYDRAULIC CONDUCTIVITY Ki-1 (cm/min)	Ki	FINAL HYDRAULIC CONDUCTIVITY (cm/s)	(mm/h)
0.5	3.7E+00		3.9E-02		6.4E-04	2.3E+01
3	1.1E+00	4.3E-01	7.8E-03	1.2E-02	1.6E-04	5.8E+00
9	2.9E-01	1.9E-01	0.0E+00	2.1E-03	1.7E-05	6.2E-01
16						

Depth **10cm**
Replicate 2

TENSION (cm)	STEADY STATE FLUX (cm3/min)	A (cm-1)	INITIAL HYDRAULIC CONDUCTIVITY Ki-1 (cm/min)	Ki	FINAL STATE HYDRAULIC CONDUCTIVITY (cm/s)	(mm/h)
0.5	2.7E-01		1.9E-03		3.2E-05	1.2E+00
3	1.6E-01	2.0E-01	4.9E-04	1.2E-03	1.4E-05	4.9E-01
9	1.1E-01	6.2E-02	0.0E+00	3.3E-04	2.8E-06	1.0E-01
16						

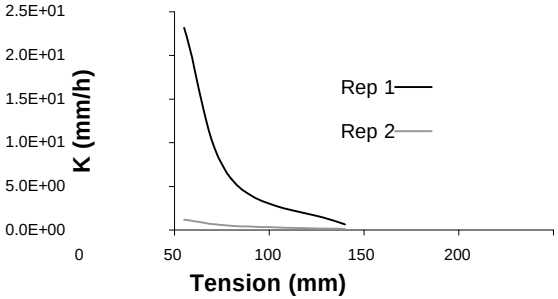

3D Flux | 1D Flux

Depth **30cm**
Replicate 1

TENSION (cm)	STEADY STATE FLUX (cm3/min)	A (cm-1)	INITIAL HYDRAULIC CONDUCTIVITY Ki-1 (cm/min)	Ki (cm/s)	FINAL HYDRAULIC CONDUCTIVITY (mm/h)
0.5	1.1E+00		7.6E-03	1.3E-04	4.6E+00
3	2.5E-01	2.8E-01	4.1E-03	4.6E-03	7.3E-05	2.6E+00
9	2.6E-01	2.3E-01	1.6E-03	1.4E-03	2.5E-05	9.0E-01
16	1.7E-02	1.9E-02	3.2E-04		5.4E-06	1.9E-01

Depth **30cm**
Replicate 2

TENSION (cm)	STEADY STATE FLUX (cm3/min)	A (cm-1)	INITIAL HYDRAULIC CONDUCTIVITY Ki-1 (cm/min)	Ki (cm/s)	FINAL HYDRAULIC CONDUCTIVITY (mm/h)
0.5	6.5E-01		5.6E-03	9.3E-05	3.4E+00
3	3.1E-01	2.8E-01	2.1E-03	2.7E-03	4.0E-05	1.4E+00
9	8.9E-02	1.9E-01	0.0E+00	6.1E-04	5.1E-06	1.8E-01
16						

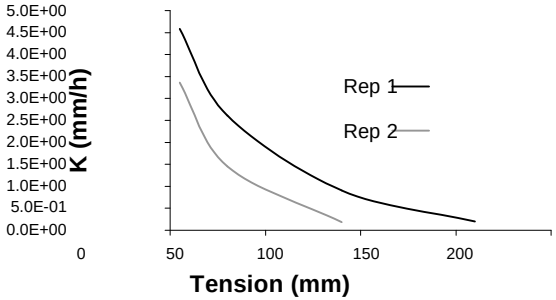

Depth **60cm**
Replicate 1

TENSION (cm)	STEADY STATE FLUX (cm3/min)	A (cm-1)	INITIAL HYDRAULIC CONDUCTIVITY Ki-1 (cm/min)	Ki (cm/s)	FINAL HYDRAULIC CONDUCTIVITY (mm/h)
0.5	2.4E+00		2.0E-02	3.3E-04	1.2E+01
3	1.3E+00	2.5E-01	9.9E-03	1.0E-02	1.7E-04	6.1E+00
9	2.6E-01	2.2E-01	1.7E-03	2.0E-03	3.1E-05	1.1E+00
16	6.1E-02	1.8E-01	4.1E-04		6.8E-06	2.4E-01

Depth **60cm**
Replicate 2

TENSION (cm)	STEADY STATE FLUX (cm3/min)	A (cm-1)	INITIAL HYDRAULIC CONDUCTIVITY Ki-1 (cm/min)	Ki (cm/s)	FINAL HYDRAULIC CONDUCTIVITY (mm/h)
0.5	2.6E+00		2.4E-02	4.0E-04	1.5E+01
3	1.1E+00	3.3E-01	8.7E-03	1.0E-02	1.6E-04	5.6E+00
9	1.5E-01	2.5E-01	0.0E+00	1.2E-03	1.0E-05	3.7E-01
16						

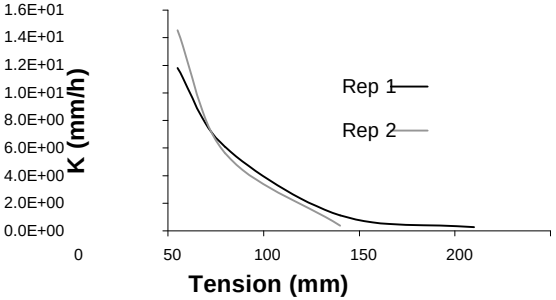

3D Flux	1D Flux

Depth **100cm**
Replicate 1

TENSION	STEADY STATE FLUX	A	INITIAL HYDRAULIC CONDUCTIVITY		FINAL HYDRAULIC CONDUCTIVITY
		Ki-1	Ki		
(cm)	(cm3/min)	(cm-1)	(cm/min)	(cm/s)	(mm/h)
0.5	1.3E+00		1.1E-02	1.9E-04	6.7E+00
3	6.1E-01	2.8E-01	4.8E-03	5.3E-03	8.4E-05	3.0E+00
9	1.1E-01	2.3E-01	0.0E+00	8.8E-04	7.3E-06	2.6E-01
16						

3D Flux	1D Flux

Depth **100cm**
Replicate 2

TENSION	STEADY STATE FLUX	A	INITIAL HYDRAULIC CONDUCTIVITY		FINAL HYDRAULIC CONDUCTIVITY
		Ki-1	Ki		
(cm)	(cm3/min)	(cm-1)	(cm/min)	(cm/s)	(mm/h)
0.5	3.1E-01		2.9E-03	4.8E-05	1.7E+00
3	1.3E-01	3.2E-01	0.0E+00	1.2E-03	1.0E-05	3.7E-01
9						
16						

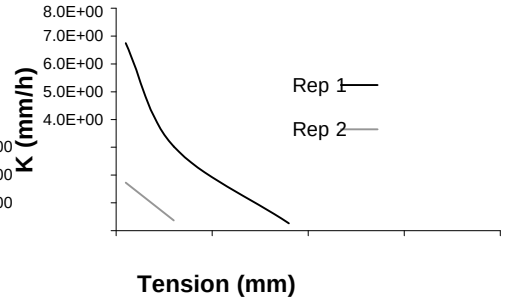

T2_1 Determination of K_{unsat} using Tension Disc Infiltrometer Based on Ankeny *et al* (1991) method

INFILTRATION RADIUS 4.200 cm

3D Flux | 1D Flux

Depth **Surface**
Replicate 1

TENSION (cm)	STEADY STATE FLUX (cm3/min)	A (cm-1)	INITIAL HYDRAULIC CONDUCTIVITY Ki-1 (cm/min)	INITIAL HYDRAULIC CONDUCTIVITY Ki (cm/s)	FINAL HYDRAULIC CONDUCTIVITY (cm/s)	FINAL HYDRAULIC CONDUCTIVITY (mm/h)
0.5	5.5E+00		5.5E-02		9.1E-04	3.3E+01
3	2.1E+00	3.6E-01	1.3E-02	2.0E-02	2.8E-04	1.0E+01
9	7.0E-01	1.6E-01	2.9E-03	4.5E-03	6.1E-05	2.2E+00
16	3.7E-01	9.0E-02	1.5E-03		2.5E-05	9.1E-01

Depth **Surface**
Replicate 2

TENSION (cm)	STEADY STATE FLUX (cm3/min)	A (cm-1)	INITIAL HYDRAULIC CONDUCTIVITY Ki-1 (cm/min)	INITIAL HYDRAULIC CONDUCTIVITY Ki (cm/s)	FINAL HYDRAULIC CONDUCTIVITY (cm/s)	FINAL HYDRAULIC CONDUCTIVITY (mm/h)
0.5	8.8E+00		8.7E-02		1.4E-03	5.2E+01
3	3.3E+00	3.6E-01	1.9E-02	3.2E-02	4.3E-04	1.6E+01
9	1.3E+00	1.5E-01	7.0E-03	7.5E-03	1.2E-04	4.4E+00
16	4.6E-01	1.3E-01	2.6E-03		4.3E-05	1.5E+00

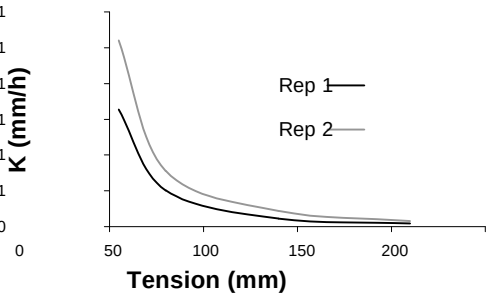

Depth **10cm**
Replicate 1

TENSION (cm)	STEADY FLUX (cm3/min)	A (cm-1)	INITIAL HYDRAULIC CONDUCTIVITY Ki-1 (cm/min)	INITIAL HYDRAULIC CONDUCTIVITY Ki (cm/s)	FINAL HYDRAULIC CONDUCTIVITY (cm/s)	FINAL HYDRAULIC CONDUCTIVITY (mm/h)
0.5	1.0E+01		9.7E-02		1.6E-03	5.8E+01
3	4.0E+00	3.5E-01	2.9E-02	3.8E-02	5.6E-04	2.0E+01
9	9.7E-01	2.0E-01	6.8E-03	7.0E-03	1.1E-04	4.1E+00
16	1.9E-01	1.9E-01	1.3E-03		2.2E-05	7.9E-01

Depth **10cm**
Replicate 2

TENSION (cm)	STEADY STATE FLUX (cm3/min)	A (cm-1)	INITIAL HYDRAULIC CONDUCTIVITY Ki-1 (cm/min)	INITIAL HYDRAULIC CONDUCTIVITY Ki (cm/s)	FINAL STATE HYDRAULIC CONDUCTIVITY (cm/s)	FINAL STATE HYDRAULIC CONDUCTIVITY (mm/h)
0.5	3.7E+00		3.1E-02		5.1E-04	1.9E+01
3	1.9E+00	2.6E-01	1.0E-02	1.6E-02	2.2E-04	7.8E+00
9	8.8E-01	1.2E-01	4.4E-03	4.6E-03	7.5E-05	2.7E+00
16	3.7E-01	1.2E-01	1.9E-03		3.1E-05	1.1E+00

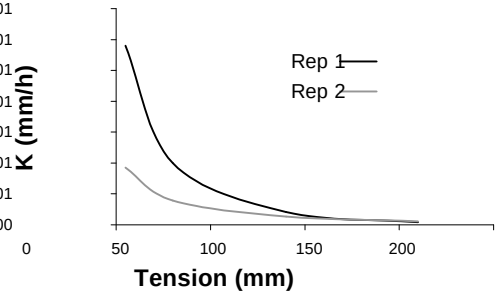

3D Flux | 1D Flux

Depth **30cm**
Replicate 1

TENSION (cm)	STEADY FLUX (cm3/min)	A (cm-1)	INITIAL HYDRAULIC CONDUCTIVITY Ki-1 (cm/min)	Ki	FINAL HYDRAULIC CONDUCTIVITY (cm/s)	(mm/h)
0.5	2.3E+00		1.3E-02		2.1E-04	7.7E+00
3	1.7E+00	1.3E-01	7.0E-03	9.1E-03	1.3E-04	4.8E+00
9	9.3E-01	9.3E-02	5.2E-03	3.9E-03	7.7E-05	2.8E+00
16	3.2E-01	1.4E-01	1.8E-03		3.0E-05	1.1E+00

3D Flux | 1D Flux

Depth **30cm**
Replicate 2

TENSION (cm)	STEADY STATE FLUX (cm3/min)	A (cm-1)	INITIAL HYDRAULIC CONDUCTIVITY Ki-1 (cm/min)	Ki	FINAL STATE HYDRAULIC CONDUCTIVITY (cm/s)	(mm/h)
0.5	2.6E+00		1.6E-02		2.6E-04	9.3E+00
3	1.7E+00	1.5E-01	6.3E-03	1.1E-02	1.4E-04	5.0E+00
9	1.1E+00	7.6E-02	7.6E-03	4.0E-03	9.7E-05	3.5E+00
16	2.1E-01	1.9E-01	1.5E-03		2.5E-05	8.9E-01

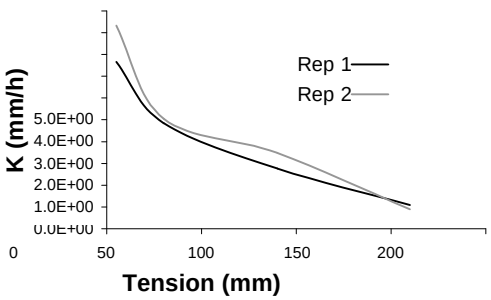

Depth **60cm**
Replicate 1

TENSION (cm)	STEADY FLUX (cm3/min)	A (cm-1)	INITIAL HYDRAULIC CONDUCTIVITY Ki-1 (cm/min)	Ki	FINAL HYDRAULIC CONDUCTIVITY (cm/s)	(mm/h)
0.5	1.8E+00		7.6E-03		1.3E-04	4.6E+00
3	1.4E+00	9.4E-02	4.2E-03	6.0E-03	8.6E-05	3.1E+00
9	9.8E-01	6.1E-02	2.1E-03	2.9E-03	4.2E-05	1.5E+00
16	7.3E-01	4.1E-02	1.6E-03		2.6E-05	9.5E-01

Depth **60cm**
Replicate 2

TENSION (cm)	STEADY STATE FLUX (cm3/min)	A (cm-1)	INITIAL HYDRAULIC CONDUCTIVITY Ki-1 (cm/min)	Ki	FINAL STATE HYDRAULIC CONDUCTIVITY (cm/s)	(mm/h)
0.5	1.6E+00		7.9E-03		1.3E-04	4.8E+00
3	1.2E+00	1.1E-01	3.7E-03	6.0E-03	8.0E-05	2.9E+00
9	8.5E-01	6.1E-02	1.8E-03	2.5E-03	3.6E-05	1.3E+00
16	6.4E-01	3.9E-02	1.3E-03		2.2E-05	8.0E-01

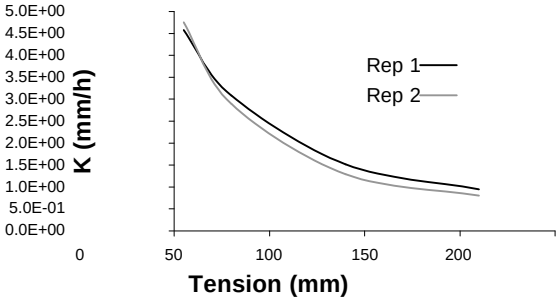

	3D Flux		1D Flux			
Depth	**200cm**					
Replicate	1					
TENSION	STEADY STATE FLUX	A	INITIAL HYDRAULIC CONDUCTIVITY Ki-1	Ki	FINAL HYDRAULIC CONDUCTIVITY	
(cm)	(cm3/min)	(cm-1)	(cm/min)		(cm/s)	(mm/h)
0.5	2.4E+00		2.1E-02		3.4E-04	1.2E+01
3	1.1E+00	2.8E-01	1.8E-03	1.0E-02	9.8E-05	3.5E+00
9	9.6E-01	2.9E-02	5.5E-03	1.5E-03	5.8E-05	2.1E+00
16	3.3E-01	1.4E-01	1.9E-03		3.1E-05	1.1E+00

	3D Flux		1D Flux			
Depth	**200cm**					
Replicate	2					
TENSION	STEADY STATE FLUX	A	INITIAL HYDRAULIC CONDUCTIVITY Ki-1	Ki	FINAL HYDRAULIC CONDUCTIVITY	
(cm)	(cm3/min)	(cm-1)	(cm/min)		(cm/s)	(mm/h)
0.5	1.7E+01		1.7E-01		2.9E-03	1.0E+02
3	6.2E+00	3.8E-01	3.1E-02	6.2E-02	7.7E-04	2.8E+01
9	3.0E+00	1.2E-01	1.9E-02	1.5E-02	2.9E-04	1.0E+01
16	7.3E-01	1.7E-01	4.8E-03		8.0E-05	2.9E+00

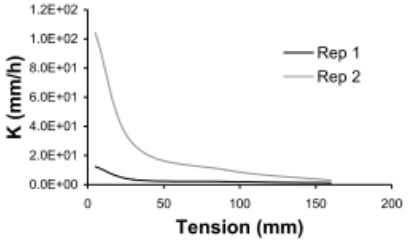

Table iii.e: K_{sat} determined using double-ring infiltrometers (mm/hr)

T1_1			**T1_4**		
Replicate	**1**	**2**	**Replicate**	**1**	**2**
Surface	10.47	11.10	Surface	27.00	269.98
10cm	6.12	5.71	10cm	132.45	148.17
30cm	2.01	14.42	30cm	4.05	30.14
60cm	4.69	2.84	60cm	17.35	13.51
200cm	1.01	1.83	200cm	0.36	2.97
T1_2			**T2_1**		
Replicate	**1**	**2**	**Replicate**	**1**	**2**
Surface	77.57	25.65	Surface	113.56	83.91
10cm	5.62	12.03	10cm	111.03	329.40
30cm	1.95	6.05	30cm	9.56	5.98
60cm	5.42	3.49	60cm	17.11	9.23
200cm	1.55	0.52	200cm	33.37	56.15
T1_3					
Replicate	**1**	**2**			
Surface	562.57	305.00			
10cm	166.59	235.80			
30cm	1237.76	144.73			
50cm	67.07				
60cm	156.21	52.70			
85cm	18.40				
100cm	75.78				
135cm	157.66				
200cm	69.42				

Table iii.f: Water Retention Characteristics

weight after 1bar pressure is actually final outflow cell pressure so do not include in WRC

CRG_T1_1(surface):14/06/06	Volume(cm3)		90.48 ring		73.59
Bur. (ml)	Air/H2O P(cm)		Equil.Transd(cm)	Final Cap.	Water content
48.8	0		-21	0	0.385
46.4	24.1		-18	3	0.359
40.4	74.8		12	33	0.292
39.9	99.5		18	39	0.287
39.7	134		22	43	0.285
39.1	22		37	58	0.278
38.5	30.4		71	92	0.271
37.7	41.1		165	186	0.262
36.9	51.6		325	346	0.254
36.5	61.3		456	477	0.249
35.8	72.4		685	706	0.241
	ring&core (g)	core			
Weight after 1bar pressure:	232.22		158.63	1000	0.241
Weight after 2bar pressure:	228.31		154.72	2000	0.198
Weight after 5bar pressure:	227.7		154.11	5000	0.192
Weight after 15bar pressure:	226.94		153.35	15000	0.183
Weight after Oven dry:	210.37		136.78		
Density (g/cm3)		Porosity		Final WC	
1.512		0.430		0.183	

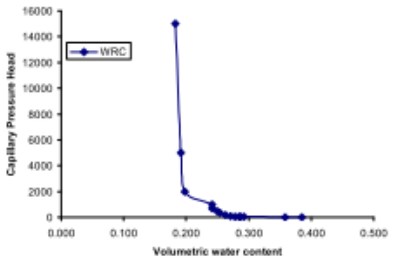

CRG_T1_1(10cm):22/06/06	Volume(cm3)		85.05 ring		74.21
Bur. (ml)	Air/H2O P(cm)		Equil.Transd(cm)	Final Cap.	Water content
46.8	0		-3	0	0.338
46.6	113.7		-2	1	0.336
45.3	13.2		-1	2	0.321
44.2	21.8		5	8	0.308
43.3	39.8		9	12	0.297
42.7	50.1		17	20	0.290
41.6	57.9		66	69	0.277
41.3	75.5		88	91	0.274
	ring&core (g)	core			
Weight after 1bar pressure:	228.53		154.32	1000	0.274
Weight after 2bar pressure:	227.36		153.15	2000	0.260
Weight after 5bar pressure:	227.17		152.96	5000	0.258
Weight after 15bar pressure:	226.79		152.58	15000	0.253
Weight after Oven dry:	205.26		131.05		
Density (g/cm3)		Porosity		Final WC	
1.541		0.419		0.253	

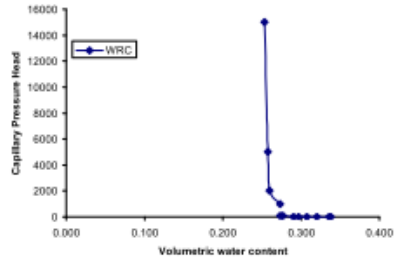

CRG_T1_1(30cm):23/06/06	Volume(cm3)		90.5 ring		70.77
Bur. (ml)	Air/H2O P(cm)		Equil.Transd(cm)	Final Cap.	Water content
48.1	0		-22	0	0.480
44.3	86.9		37	59	0.438
43.4	131.8		95	117	0.428
41.4	20.9		233	255	0.406
39	43.1		545	567	0.380
37.7	62.2		829	851	0.365
	ring&core (g)	core			
Weight after 1bar pressure:	240.02		169.25	1000	0.365
Weight after 2bar pressure:	235.28		164.51	2000	0.313
Weight after 5bar pressure:	233.17		162.4	5000	0.290
Weight after 15bar pressure:	229.78		159.01	15000	0.252
Weight after Oven dry:	206.95		136.18		
Density (g/cm3)		Porosity		Final WC	
1.505		0.432		0.252	

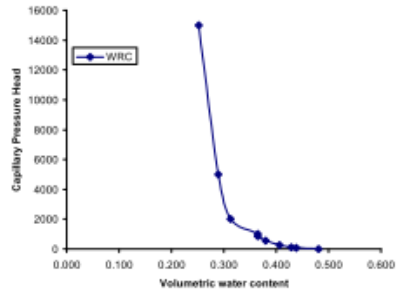

CRG_T1_1(60cm):11/07/06	Volume(cm3)		88.67 ring		95.67
Bur. (ml)	Air/H2O P(cm)		Equil.Transd(cm)	Final Cap.	Water content
47	0		-39	0	0.537
40.5	46.5		1	40	0.464
39	119.5		33	72	0.447
37.6	20.5		138	177	0.431
36.2	41.3		364	403	0.415
35.4	60.1		499	538	0.406
32.7	76.6		967	1006	0.376
	ring&core (g)	core			
Weight after 1bar pressure:	273.44		177.77	1000	0.376
Weight after 2bar pressure:	272.05		176.38	2000	0.360
Weight after 5bar pressure:	269.2		173.53	5000	0.328
Weight after 15bar pressure:	267.99		172.32	15000	0.315
Weight after Oven dry:	240.1		144.43		
Density (g/cm3)		Porosity		Final WC	
1.629		0.385		0.315	

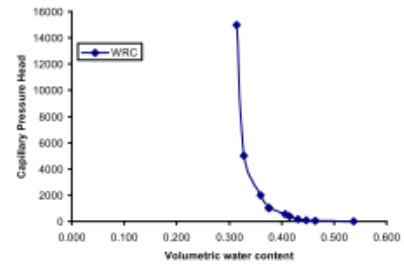

CRG_T1_1(200cm):13/07/06	Volume(cm3)		86.86 ring		70.83
Bur. (ml)	Air/H2O P(cm)		Equil.Transd(cm)	Final Cap.	Water content
47.3	0		-38	0	0.450
47.1	59.9		-33	5	0.448
45.9	120.3		-32	6	0.434
34.4	36.3		119	157	0.301
33	60.4		652	690	0.285
32.4	75.5		1002	1040	0.278
	ring&core (g)	core			
Weight after 1bar pressure:	219.03		148.2	1000	0.278
Weight after 2bar pressure:	218.04		147.21	2000	0.267
Weight after 5bar pressure:	216.39		145.56	5000	0.248
Weight after 15bar pressure:	212.13		141.3	15000	0.199
Weight after Oven dry:	194.85		124.02		
Density (g/cm3)		Porosity			Final WC
1.428			0.461		0.199

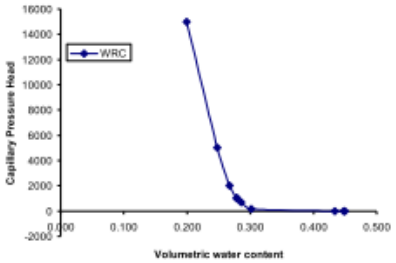

CRG_T1_2(surface):17/07/06	Volume(cm3)		90.48 ring		71.58
Bur. (ml)	Air/H2O P(cm)		Equil.Transd(cm)	Final Cap.	Water content
45.7	0		-23	0	0.434
45.3	25.1		-21	2	0.430
43.3	59.5		-21	2	0.408
42	118.7		-19	4	0.393
41.3	147.6		-20	3	0.386
36.8	22.5		-13	10	0.336
31.9	33.1		12	35	0.282
29.6	41.4		89	112	0.256
28	52.7		242	265	0.239
27	61.8		360	383	0.228
25.7	74		602	625	0.213
	ring&core (g)	core			
Weight after 1bar pressure:	237.52		165.94	1000	0.213
Weight after 2bar pressure:	233.04		161.46	2000	0.164
Weight after 5bar pressure:	232.74		161.16	5000	0.160
Weight after 15bar pressure:	232.46		160.88	15000	0.157
Weight after Oven dry:	218.22		146.64		
Density (g/cm3)		Porosity			Final WC
1.621			0.388		0.157

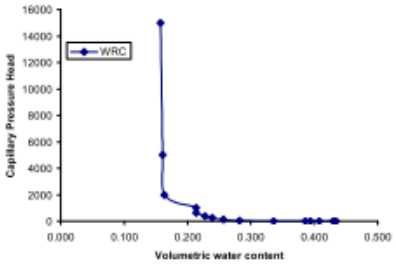

CRG_T1_2(10cm):19/07/06	Volume(cm3)		90.5 ring		70.73
Bur. (ml)	Air/H2O P(cm)		Equil.Transd(cm)	Final Cap.	Water content
46.6	0		-22	0	0.397
45.6	66.8		-20	2	0.386
44.5	124.3		-15	7	0.373
42.4	13.3		-6	16	0.350
40	21.5		25	47	0.324
38.5	40.6		108	130	0.307
36.3	59.8		302	324	0.283
	ring&core (g)	core			
Weight after 1bar pressure:	245.06		174.33	1000	0.283
Weight after 2bar pressure:	239.97		169.24	2000	0.227
Weight after 5bar pressure:	236.81		166.08	5000	0.192
Weight after 15bar pressure:	236.77		166.04	15000	0.191
Weight after Oven dry:	219.47		148.74		
Density (g/cm3)		Porosity			Final WC
1.644			0.380		0.191

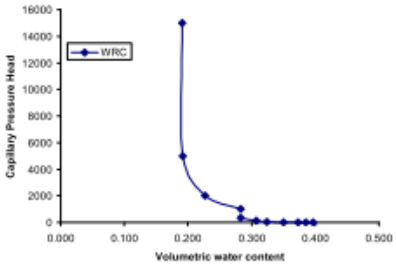

CRG_T1_2(30cm):21/07/06	Volume(cm3)		86.86 ring		70.69
Bur. (ml)	Air/H2O P(cm)		Equil.Transd(cm)	Final Cap.	Water content
48.8	0		-25	0	0.372
46	92.5		18	43	0.340
45.6	130.6		30	55	0.335
44.6	22.6		99	124	0.324
43.4	42.3		476	501	0.310
42.6	61.3		803	828	0.301
	ring&core (g)	core			
Weight after 1bar pressure:	248.94		178.25	1000	0.301
Weight after 2bar pressure:	247.89		177.2	2000	0.289
Weight after 5bar pressure:	247.57		176.88	5000	0.285
Weight after 15bar pressure:	245.67		174.98	15000	0.263
Weight after Oven dry:	222.83		152.14		
Density (g/cm3)		Porosity		Final WC	
1.752		0.339		0.263	

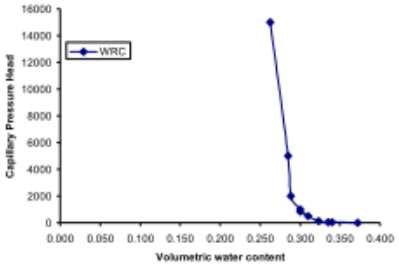

CRG_T1_2(60cm):26/07/06	Volume(cm3)		90.48 ring		97.81
Bur. (ml)	Air/H2O P(cm)		Equil.Transd(cm)	Final Cap.	Water content
48.9	0		-4	0	0.308
46.1	15.5		210	214	0.277
45	40.8		435	439	0.265
44.1	63		761	765	0.255
	ring&core (g)	core			
Weight after 1bar pressure:	294.71		196.9	1000	0.255
Weight after 2bar pressure:	293.71		195.9	2000	0.244
Weight after 5bar pressure:	292.72		194.91	5000	0.233
Weight after 15bar pressure:	288.85		191.04	15000	0.190
Weight after Oven dry:	271.63		173.82		
Density (g/cm3)		Porosity		Final WC	
1.921		0.275		0.190	

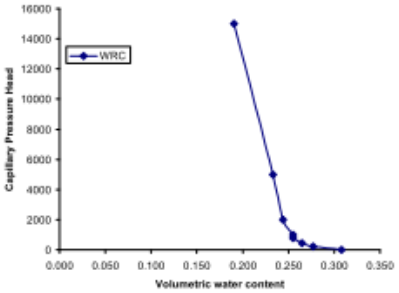

CRG_T1_2 200cm	Volume(cm3)		90.480 ring		72.250
Bur. (ml)	Air/H2O P(cm)		Equil.Transd(cm)	Final Cap.	Water content
43.0				0	0.451
42.0					0.440
34.0					0.352
31.1					0.320
30.7					0.315
27.9					0.284
	ring&core (g)	core			
Weight after 1bar pressure:	241.340		169.090	1000	0.284
Weight after 2bar pressure:	240.860		168.610	2000	0.279
Weight after 15bar pressure:	240.340		168.090	15000	0.273
Weight after Oven dry:	215.610		143.360		
Density (g/cm3)		Porosity		Final WC	
1.584		0.402		0.273	

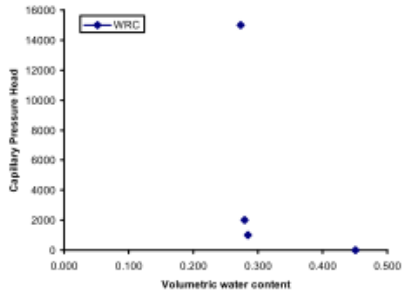

CRG_T1_3(surface):11/08/06	Volume(cm3)		90.48 ring		70.63
Bur. (ml)	Air/H2O P(cm)		Equil.Transd(cm)	Final Cap.	Water content
46	0		-36	0	0.430
45.8	35.7		-32	4	0.428
43.6	68.7		-28	8	0.404
42.2	83.2		-24	12	0.388
41.5	108.7		-24	12	0.380
34.5	20.9		-19	17	0.303
23.4	29.6		19	55	0.180
20.6	41		206	242	0.149
19.6	48.7		394	430	0.138
19	58.1		575	611	0.132
18.5	74.8		778	814	0.126
	ring&core (g)	core			
Weight after 1bar pressure:	210.68		140.05	1000	0.126
Weight after 2bar pressure:	208.12		137.49	2000	0.098
Weight after 5bar pressure:	207.28		136.65	5000	0.089
Weight after 15bar pressure:	207.26		136.63	15000	0.088
Weight after Oven dry:	199.26		128.63		
Density (g/cm3)		Porosity		Final WC	
1.422		0.464		0.088	

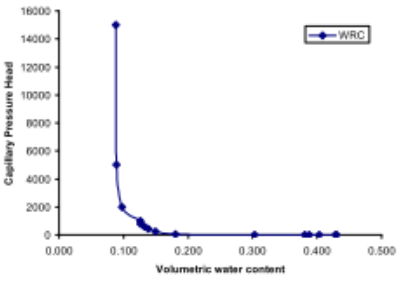

CRG_T1_3(10cm):14/08/06	Volume(cm3)		90.5 ring		71.93
Bur. (ml)	Air/H2O P(cm)	Equil.Transd(cm)	Final Cap.		Water content
47.2	0	-32	#REF!		#REF!
45.3	125.8	-25	#REF!		#REF!
35.4	12.5	-22	#REF!		#REF!
33.3	16.6	-6	#REF!		#REF!
31.2	39.5	6	#REF!		#REF!
31.1	51.2	28	#REF!		0.126
	ring&core (g)	core			
Weight after 1bar pressure:	219.69	147.76	1000		#REF!
Weight after 2bar pressure:	219.4	147.47	2000		#REF!
Weight after 5bar pressure:	219.13	147.2	5000		#REF!
Weight after 15bar pressure:	219.01	147.08	15000		0.118
Weight after Oven dry:	208.31	136.38			
Density (g/cm3)		Porosity			Final WC
1.507		0.431			0.118

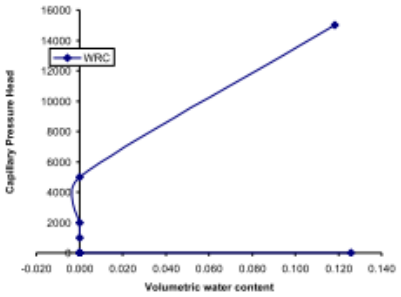

CRG_T1_3(30cm):15/08/06	Volume(cm3)		87.36 ring		70.57
Bur. (ml)	Air/H2O P(cm)	Equil.Transd(cm)	Final Cap.		Water content
49.2	0	-12	0		0.319
37.4	102.5	-11	1		0.184
33.8	17.9	16	28		0.143
29.9	40.3	259	271		0.098
28	60.4	729	741		0.077
27.8	74.8	971	983		0.074
	ring&core (g)	core			
Weight after 1bar pressure:	213.51	142.94	1000		0.074
Weight after 2bar pressure:	212.12	141.55	2000		0.058
Weight after 5bar pressure:	211.18	140.61	5000		0.048
Weight after Oven dry:	207.01	136.44			
Density (g/cm3)		Porosity			Final WC
1.562		0.411			0.048

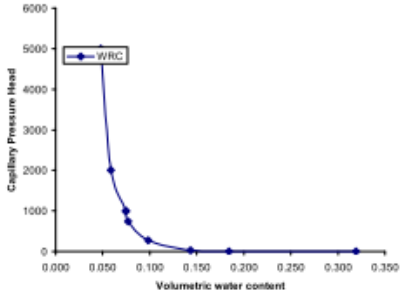

CRG_T1_3(50cm):16/08/06	Volume(cm3)		92.24 ring		71.96
Bur. (ml)	Air/H2O P(cm)	Equil.Transd(cm)	Final Cap.		Water content
49.2	0	0	0		0.411
48.7	55	1	1		0.406
47	112	8	8		0.387
45.7	13.5	11	11		0.373
43.5	22.8	27	27		0.350
41.4	39.9	46	46		0.327
38.9	60	86	86		0.300
36.3	74.2	238	238		0.271
	ring&core (g)	core			
Weight after 1bar pressure:	223.63	151.67	1000		0.271
Weight after 2bar pressure:	219.38	147.42	2000		0.225
Weight after 5bar pressure:	216.46	144.5	5000		0.194
Weight after Oven dry:	198.59	126.63			
Density (g/cm3)		Porosity			Final WC
1.373		0.482			0.194

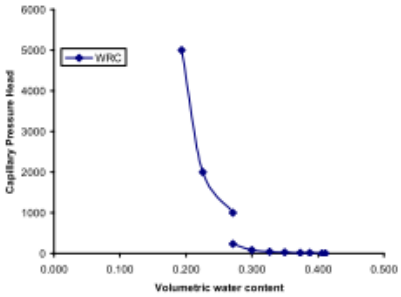

CRG_T1_3(80cm):16/08/06	Volume(cm3)		90.43 ring		70.5
Bur. (ml)	Air/H2O P(cm)	Equil.Transd(cm)	Final Cap.		Water content
47.3	0	-33	0		0.538
46.4	88.9	-29	4		0.528
45.1	144	2	35		0.514
44.2	18.9	288	321		0.504
43.8	41.2	545	578		0.500
43.3	59.3	765	798		0.494
43	76.6	985	1018		
	ring&core (g)	core			
Weight after 1bar pressure:	229.24	158.74	1000		0.494
Weight after 2bar pressure:	228.43	157.93	2000		0.485
Weight after 5bar pressure:	227.56	157.06	5000		0.476
Weight after 15bar pressure:	226.14	155.64	15000		0.460
Weight after Oven dry:	184.56	114.06			
Density (g/cm3)		Porosity			Final WC
1.261		0.524			0.460

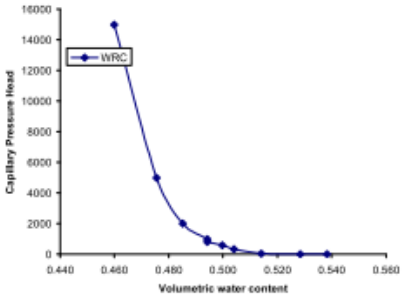

CRG_T1_3(80cm):17/08/06	Volume(cm3)		90.48 ring		71.68
Bur. (ml)	Air/H2O P(cm)		Equil.Transd(cm)	Final Cap.	Water content
47.8	0		-29	0	0.388
47.6	11		-17	12	0.386
46.8	17.6		-7	22	0.377
44.9	29.5		169	198	0.356
40.8	39.6		530	559	0.311
40.4	62.2		745	774	0.307
39.7	85.3		915	944	0.299
	ring&core (g)	core			
Weight after 1bar pressure:	234.97		163.29	1000	0.299
Weight after 2bar pressure:	229.81		158.13	2000	0.242
Weight after 5bar pressure:	227.83		156.15	5000	0.220
Weight after 15bar pressure:	227.65		155.97	15000	0.218
Weight after Oven dry:	207.93		136.25		
Density (g/cm3)		Porosity		Final WC	
1.506		0.432		0.218	

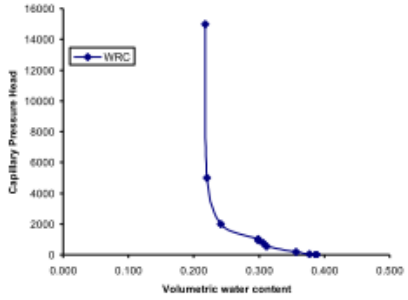

CRG_T1_3(100cm):18/08/06	Volume(cm3)		88.63 ring		71.38
Bur. (ml)	Air/H2O P(cm)		Equil.Transd(cm)	Final Cap.	Water content
49.5	0		-9	0	0.287
49	30.4		-2	7	0.281
43.3	17.9		14	23	0.217
41.1	40.9		28	37	0.192
39.1	58.2		56	65	0.169
37.2	73.3		121	130	0.148
	ring&core (g)	core			
Weight after 1bar pressure:	225.01		153.63	1000	0.148
Weight after 2bar pressure:	220.67		149.29	2000	0.099
Weight after 5bar pressure:	218.75		147.37	5000	0.077
Weight after Oven dry:	211.91		140.53		
Density (g/cm3)		Porosity		Final WC	
1.586		0.402		0.077	

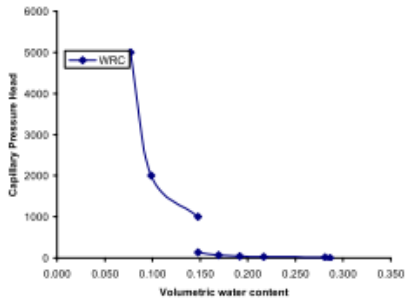

CRG_T1_3(135cm):21/08/06	Volume(cm3)		85.05 ring		72.21
Bur. (ml)	Air/H2O P(cm)		Equil.Transd(cm)	Final Cap.	Water content
49.5	0		-53	0	0.518
44.7	83		2	55	0.463
43.6	85.9		27	80	0.450
40.9	18.1		92	145	0.419
39	39.4		311	364	0.397
37.8	61.6		782	835	0.383
	ring&core (g)	core			
Weight after 1bar pressure:	234.04		161.83	1000	0.383
Weight after 2bar pressure:	233.91		161.7	2000	0.382
Weight after 5bar pressure:	231.63		159.42	5000	0.355
Weight after 15bar pressure:	226.98		154.77	15000	0.302
Weight after Oven dry:	201.31		129.1		
Density (g/cm3)		Porosity		Final WC	
1.518		0.427		0.302	

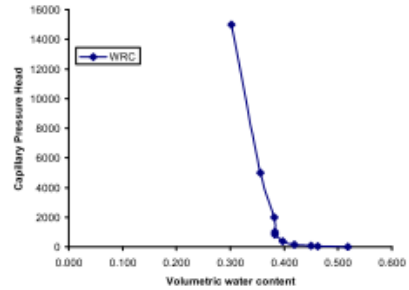

CRG_T1_3 200cm	Volume(cm3)	90.480	ring	94.570
Bur. (ml)	Air/H2O P(cm)	Equil.Transd(cm)	Final Cap.	Water content
47.2			0	0.406
40.5				0.332
40.2				0.329
39.8				0.325
37.5				0.299
35.5				0.277

	ring&core (g)	core		
Weight after 1bar pressure:	242.060	147.490	1000	0.277
Weight after 2bar pressure:	241.140	146.570	2000	0.262
Weight after 15bar pressure:	240.700	146.130	15000	0.131
Weight after Oven dry:	228.840	134.270		

Density (g/cm3)	Porosity	Final WC
1.484	0.440	0.131

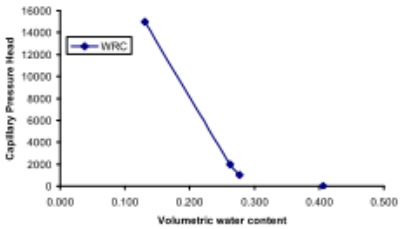

CRG_T1_4(surface):28/07/06	Volume(cm3)	90.48	ring	70.93
Bur. (ml)	Air/H2O P(cm)	Equil.Transd(cm)	Final Cap.	Water content
49.9	0	-20	0	0.467
46.2	39.2	-17	3	0.426
43.1	68.9	-5	15	0.392
41.8	108.5	3	23	0.378
40.5	9.7	11	31	0.363
39.5	21	20	40	0.352
38.4	40.6	46	66	0.340
37.6	59.2	98	118	0.331
36.8	74.2	164	184	0.322

	ring&core (g)	core		
Weight after 1bar pressure:	230.4	159.47	1000	0.322
Weight after 2bar pressure:	225.26	154.33	2000	0.265
Weight after 5bar pressure:	222.05	151.12	5000	0.230
Weight after 15bar pressure:	221.87	150.94	15000	0.228
Weight after Oven dry:	201.24	130.31		

Density (g/cm3)	Porosity	Final WC
1.440	0.457	0.228

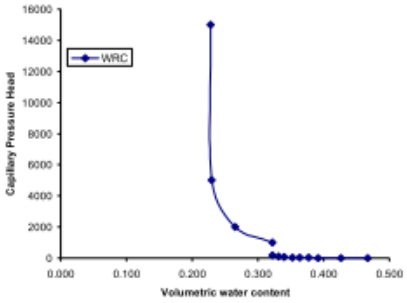

CRG_T1_4(10cm):01/08/06	Volume(cm3)	90.5	ring	75.12
Bur. (ml)	Air/H2O P(cm)	Equil.Transd(cm)	Final Cap.	Water content
48.5	0	-23	0	0.475
47	40.2	-17	6	0.458
44.4	58.9	3	26	0.429
42.1	105.5	3	26	0.404
40.5	7.8	11	34	0.386
39.5	18.9	28	51	0.375
38.6	41.1	270	293	0.365
37	60.7	568	591	0.348
34	74.8	869	892	0.314

	ring&core (g)	core		
Weight after 1bar pressure:	225.1	149.98	1000	0.314
Weight after 2bar pressure:	222.16	147.04	2000	0.282
Weight after 5bar pressure:	219.22	144.1	5000	0.250
Weight after 15bar pressure:	219.14	144.02	15000	0.249
Weight after Oven dry:	196.64	121.52		

Density (g/cm3)	Porosity	Final WC
1.343	0.493	0.249

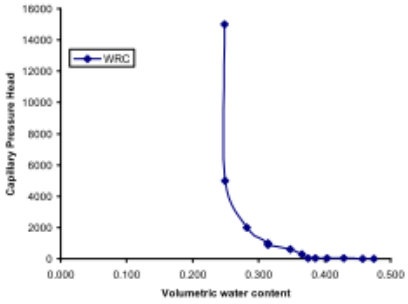

CRG_T1_4 30cm	Volume(cm3)		90.480 ring		72.240
Bur. (ml)	Air/H2O P(cm)	Equil.Transd(cm)		Final Cap.	Water content
48.5				0	0.396
42.8					0.333
42.5					0.330
41.6					0.320
40.0					0.302
38.5					0.285
	ring&core (g)	core			
Weight after 1bar pressure:	242.010		169.770	1000	0.285
Weight after 2bar pressure:	241.260		169.020	2000	0.277
Weight after 15bar pressure:	240.770		168.530	15000	0.272
Weight after Oven dry:	216.190		143.950		
Density (g/cm3)		Porosity			Final WC
1.591			0.400		0.272

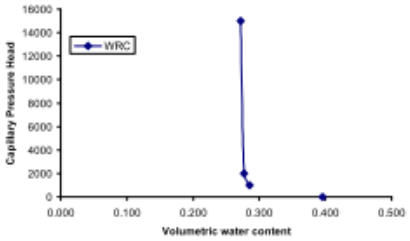

CRG_T1_4(60cm):03/08/06	Volume(cm3)		96.22 ring		96.58
Bur. (ml)	Air/H2O P(cm)	Equil.Transd(cm)		Final Cap.	Water content
49.2	0		-17	0	0.361
47.5	29.6		-14	3	0.343
45.8	76.1		2	19	0.326
44.9	14.7		16	33	0.316
44.4	45.9		80	97	0.311
43.5	59.9		212	229	0.302
42.8	75.7		459	476	0.294
	ring&core (g)	core			
Weight after 1bar pressure:	276.29		179.71	1000	0.294
Weight after 2bar pressure:	274.67		178.09	2000	0.278
Weight after 5bar pressure:	273.17		176.59	5000	0.262
Weight after 15bar pressure:	270.17		173.59	15000	0.231
Weight after Oven dry:	247.96		151.38		
Density (g/cm3)		Porosity			Final WC
1.573			0.406		0.231

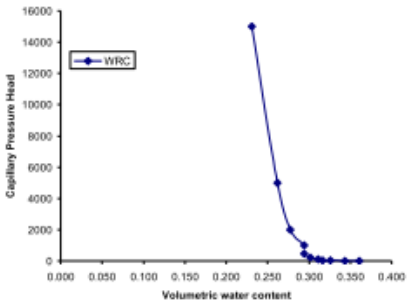

CRG_T1_4(100cm):04/08/06	Volume(cm3)		91.74 ring		70.43
Bur. (ml)	Air/H2O P(cm)	Equil.Transd(cm)		Final Cap.	Water content
51	0		-23	0	0.346
48.1	19		-20	3	0.314
46.5	17.1		40	63	0.296
45.8	39.7		244	267	0.289
44.8	56.3		553	576	0.278
44.2	75		873	896	0.271
	ring&core (g)	core			
Weight after 1bar pressure:	248.25		177.82	1000	0.271
Weight after 2bar pressure:	247.25		176.82	2000	0.261
Weight after 5bar pressure:	246.01		175.58	5000	0.247
Weight after 15bar pressure:	243.77		173.34	15000	0.223
Weight after Oven dry:	223.35		152.92		
Density (g/cm3)		Porosity			Final WC
1.667			0.371		0.223

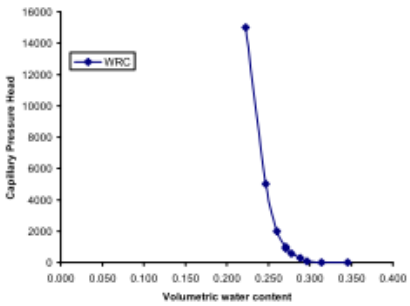

CRG_T1_4 200cm	Volume(cm3)		90.480 ring		73.000
Bur. (ml)	Air/H2O P(cm)	Equil.Transd(cm)		Final Cap.	Water content
47.1				0	0.532
44.3					0.501
43.8					0.495
43.6					0.493
43.0					0.487
42.2					0.478
	ring&core (g)	core			
Weight after 1bar pressure:	249.860		176.860	1000	0.478
Weight after 2bar pressure:	248.740		175.740	2000	0.465
Weight after 15bar pressure:	248.200		175.200	15000	0.233
Weight after Oven dry:	227.150		154.150		
Density (g/cm3)		Porosity			Final WC
1.704			0.357		0.233

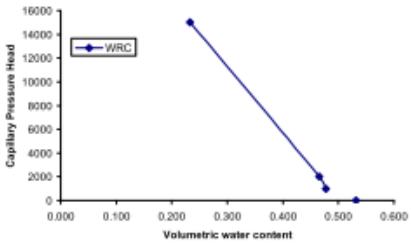

CRG_T2_1(Surface):01/08/06	Volume(cm3)	90.48	ring	69.97
Bur. (ml)	Air/H2O P(cm)	Equil.Transd(cm)	Final Cap. Press. Head	Water content
47.3	0	-40	0	0.470
46.8	77.6	-37	3	0.465
44.1	98	-29	11	0.435
37.7	19.3	58	98	0.364
36.3	28.5	200	240	0.349
35.4	41.5	325	365	0.339
35	51.9	442	482	0.335
34.5	58.3	596	636	0.329
34.2	72.5	715	755	0.326
	ring&core (g)	core		
Weight after 1bar pressure:	215.27	145.3	1000	0.326
Weight after 2bar pressure:	211.72	141.75	2000	0.286
Weight after 5bar pressure:	210.37	140.4	5000	0.272
Weight after 15bar pressure:	210.23	140.26	15000	0.270
Weight after Oven dry:	185.8	115.83		
Density (g/cm3)	Porosity			Final WC
1.280		0.517		0.270

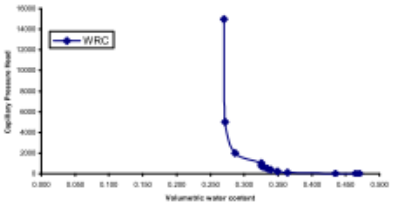

CRG_T2_1(60cm):09/08/06	Volume(cm3)	89.57	ring	70.85
Bur. (ml)	Air/H2O P(cm)	Equil.Transd(cm)	Final Cap. Press. Head	Water content
49.4	0	-24	0	0.410
49.3	26.1	-20	4	0.408
48.9	80.5	-18	6	0.404
47.4	18.6	73	97	0.387
46.6	40.9	249	273	0.378
46.1	59.8	578	602	0.373
45.5	76.2	987	1011	0.366
	ring&core (g)	core		
Weight after 1bar pressure:	214.15	143.3	1000	0.366
Weight after 2bar pressure:	213.6	142.75	2000	0.360
Weight after 5bar pressure:	213.5	142.65	5000	0.359
Weight after 15bar pressure:	211.15	140.3	15000	0.332
Weight after Oven dry:	181.37	110.52		
Density (g/cm3)	Porosity			Final WC
1.234		0.534		0.332

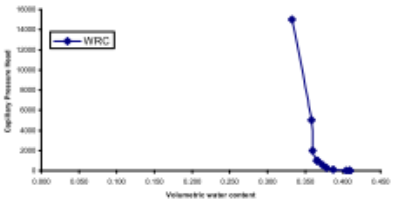

CRG_T2_1(200cm):10/08/06	Volume(cm3)	90.48	ring	70.21
Bur. (ml)	Air/H2O P(cm)	Equil.Transd(cm)	Final Cap. Press. Head	Water content
49.4	0	8	0	0.395
44.6	16.3	12	4	0.342
42.1	10.9	122	114	0.314
41.5	19.5	337	329	0.307
41.3	27.9	442	434	0.305
41.2	42.5	554	546	0.304
41	60.5	782	774	0.302
40.8	75	997	989	0.300
	ring&core (g)	core		
Weight after 1bar pressure:	238.21	168	1000	0.300
Weight after 2bar pressure:	236.96	166.75	2000	0.286
Weight after 5bar pressure:	235.91	165.7	5000	0.274
Weight after Oven dry:	211.11	140.9		
Density (g/cm3)	Porosity			Final WC
1.557		0.412		0.274

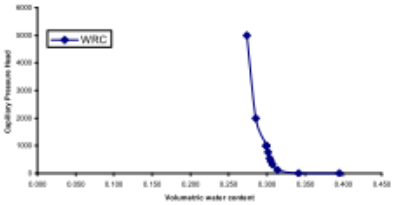

APPENDIX iv – K_{sat} Piezometer Tests

Key:

		2r	r	
r_c	internal radius (mm)	53	27	
r_w	internal radius of pipe plus pipe and interface zone with matrix (mm)	83	42	
	thickness of pipe/casing (mm)	5		
Re	effective radius (mm)	30		
L	height of perforated zone (mm)	300		
D	depth of water table to impermeable layer (mm)	15000		based on ERI images
L/r_w		7.2289		
A	dimensionless coefficient for partially penetrating well where D>H			
B	dimensionless coefficient for partially penetrating well where D>H			
C	dimensionless coefficient for partially penetrating well where D>H			

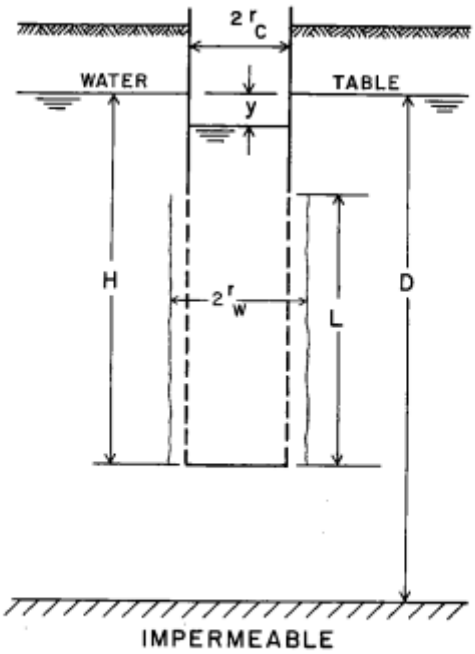

Fig. 1. Geometry and symbols of a partially penetrating, partially perforated well in unconfined aquifer with gravel pack or developed zone around perforated section.

Figure iv.a: Geometry of well in unconfined aquifer (after Bouwer & Rice, 1976)

Table iv.a: Parameter and final saturated conductivity values (K) for piezometers within the Craigieburn-Manalana

Peizometers		**T2_3**			**T2_2**			**T1_3**		**MP1**	**T3_2**
PIPE DEPTHS (mm)	2000	4000	7000	2000	4000	6000	2000	4000	6000	2000
r_c^2	5.30E+01	5.30E+01	5.30E+01	5.30E+01	5.30E+01	5.30E+01	5.30E+01	5.30E+01	5.30E+01	5.30E+01
H	6.90E+02	2.22E+03	1.85E+03	1.46E+03	2.95E+03	1.87E+03	1.65E+03	3.27E+03	1.59E+03	1.00E-01
D	1.50E+04	1.50E+04	1.50E+04	1.50E+04	1.50E+04	1.50E+04	1.50E+04	1.50E+04	1.50E+04	8.00E+03
A	1.79E+00	1.79E+00	1.79E+00	1.79E+00	1.79E+00	1.79E+00	1.79E+00	1.79E+00	1.79E+00	1.79E+00
B	2.83E-01	2.83E-01	2.83E-01	2.83E-01	2.83E-01	2.83E-01	2.83E-01	2.83E-01	2.83E-01	2.83E-01
C	8.89E-01	8.89E-01	8.89E-01	8.89E-01	8.89E-01	8.89E-01	8.89E-01	8.89E-01	8.89E-01	8.89E-01
$ln(R_e/r_w)$	8.86E-01	7.72E-01	7.85E-01	8.04E-01	7.55E-01	7.85E-01	7.94E-01	7.49E-01	7.97E-01	3.18E-01
R_e	1.01E+02	8.98E+01	9.10E+01	9.28E+01	8.83E+01	9.10E+01	9.18E+01	8.77E+01	9.21E+01	5.70E+01
2L	6.00E+02	6.00E+02	6.00E+02	6.00E+02	6.00E+02	6.00E+02	6.00E+02	6.00E+02	6.00E+02	6.00E+02
$ln(y_0/y_t)$	1.87E+03	8.16E+00	3.05E+01	1.38E+02	8.46E-01	2.26E-01	1.92E+03	3.83E+00	1.96E-01	5.43E-04
t	1.62E-03	7.78E-02	8.99E-02	1.63E-02	3.91E-01	2.39E-01	3.78E-03	1.29E-01	1.48E-01	1.00E+01
K (mm/day)	9.05E+04	7.16E+00	2.36E+01	6.00E+02	1.44E-01	6.58E-02	3.56E+04	1.97E+00	9.33E-02	1.52E-06
K (mm/hr)	5.80E+01	4.59E-03	1.51E-02	3.85E-01	9.25E-05	4.22E-05	2.28E+01	1.26E-03	5.98E-05	9.77E-10
K (mm/sec)	1.07E+00	8.46E-05	2.79E-04	7.10E-03	1.71E-06	7.78E-07	4.20E-01	2.33E-05	1.10E-06	1.80E-11
K (m/day)	9.05E+01	7.16E-03	2.36E-02	6.00E-01	1.44E-04	6.58E-05	3.56E+01	1.97E-03	9.33E-05	1.52E-09

APPENDIX v – Stable Isotope Analysis

Key:

GMWL – Global Meteorologic Water Line
LMWL – Local Meteorologic Water Line (from local rainfall samples)

Figure v.a: Adapted Google™ earth image of the local catchment area downstream of the Craigieburn-Manalana with location of stream water sampling locations.

In addition to gauged streamflow isotope samples described in Chapters 3 and 8, rainfall was sampled within the Craigieburn-Manalana with an incremental rainfall sampler since September 2007 to September 2009. Frequent extraction of groundwaters were taken from the piezometer network in Craigieburn during this period, however since the sub-surface material of the wetland had such a low conductivity it was not practical to purge these wells, instead a 12 volt pump was used that extracted water from the very base of each well. Due to the lack of well purging the data are treated as non-definitive.

During the same period grab samples of streamflow were made at 11 sites up to 13 km downstream of the Craigieburn-Manalana wetland and rainfall was collected at two homesteads (Fredman Monareng and Lidya Chilwane) using simple bottle collection – since evaporation could not be controlled here these samples are also treated with speculation. During February 2008 the surrounding Department of Water Affairs (DWA) boreholes were sampled of water, but again it was not feasible to purge these aquifers at that time.

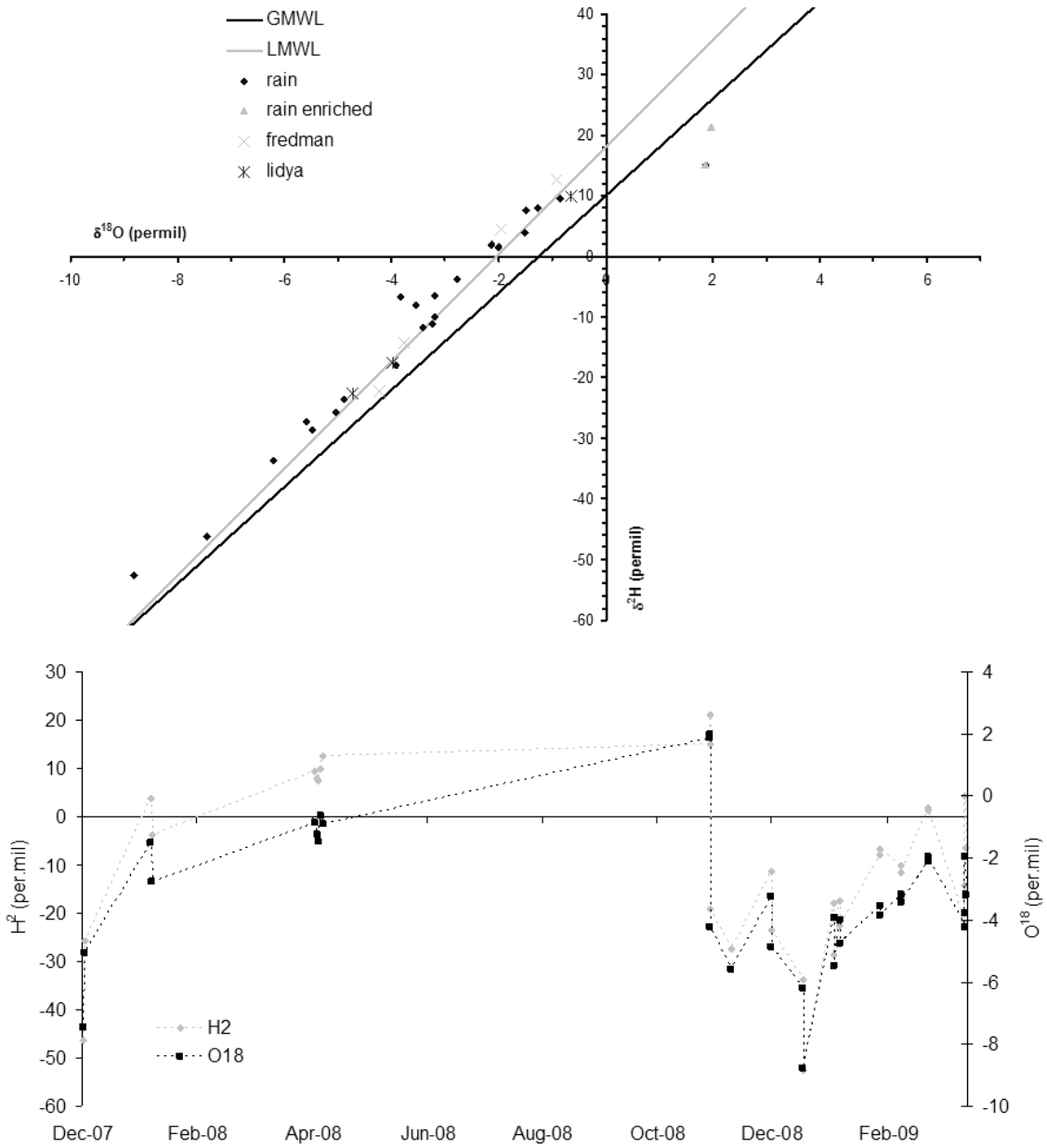

Figure v.b: Stable Isotope ($\delta^{18}O/\delta^{2}H$) ratios of rainfall in the Craigieburn-Manalana 2008-2009 and development of the local meteorologic water line (LMWL); ratio (above) and time series (below).

From Figure v.b it is clear that at the peak of summer rain (Dec-Jan) the isotopic ratio of rainfall suggests highly depleted concentrations of incoming oceanic frontal rainfall, either side of this period, the rainfall ratio shows a more enriched signature of local patchy evaporation storms particularly following February as one moves into the dry season.

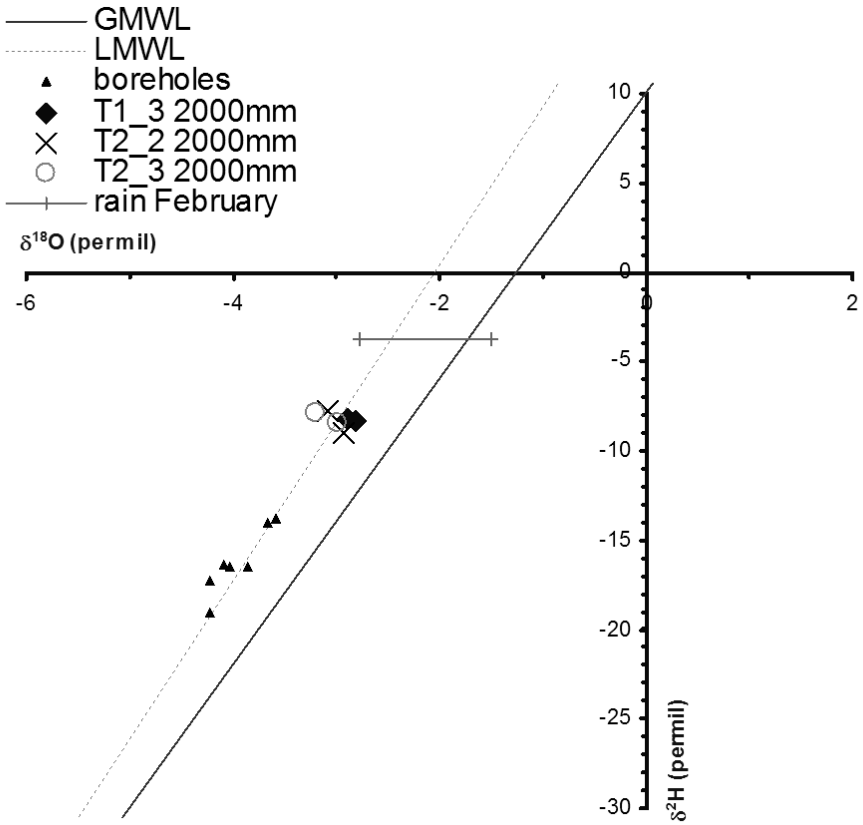

Figure v.c: Stable Isotope ($\delta^{18}O/\delta^{2}H$) ratios for shallow piezometers in the Manalana against local groundwater boreholes during February 2008.

Figure v.c shows the difference in isotopic ratio of shallow piezometers in the Craigieburn-Manalana when compared to local groundwater boreholes during February 2008. One notes the large difference in signatures between the groundwater cluster and that of the shallow piezometers, suggesting (not conclusively) that these waters are not connected.

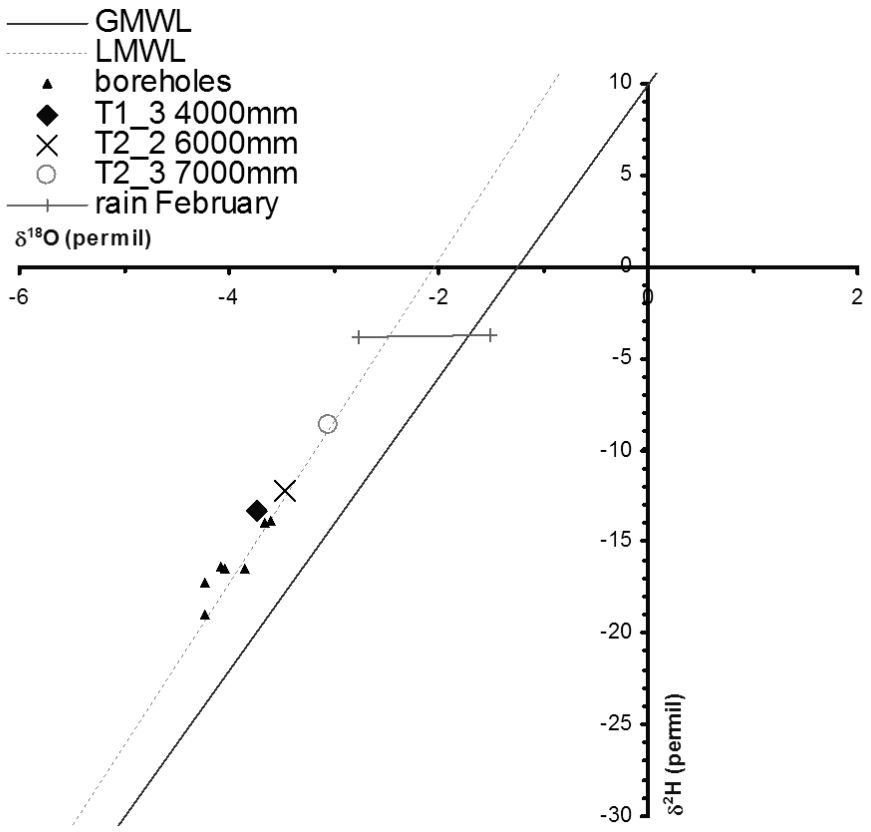

Figure v.d: Stable Isotope ($\delta^{18}O/\delta^{2}H$) ratios for deep piezometers in the Manalana against local groundwater boreholes during February 2008.

Figure v.d shows the difference in isotopic ratio of deep piezometers in the Craigieburn-Manalana when compared to local groundwater boreholes during February 2008. One notes closer association in signatures between two borehole samples and that of two deep piezometers (T1_3 and T2_2), suggesting (not conclusively) that these waters are in contact. This suggests that the wetland sub-surface underlying the clay aquiclude maybe in contact with the regional groundwater table but not the shallow waters above the clay aquiclude. Meanwhile the deep piezometer at T2_3 has a similar isotope ratio to the shallower piezometers suggesting that the installed weir may enabled a connection of shallow to deeper waters (downstream of the clay plug). These isotope data need to be supporting by longer term monitoring of the Craigieburn-Manalana's isotope hydrology, which is on-going.

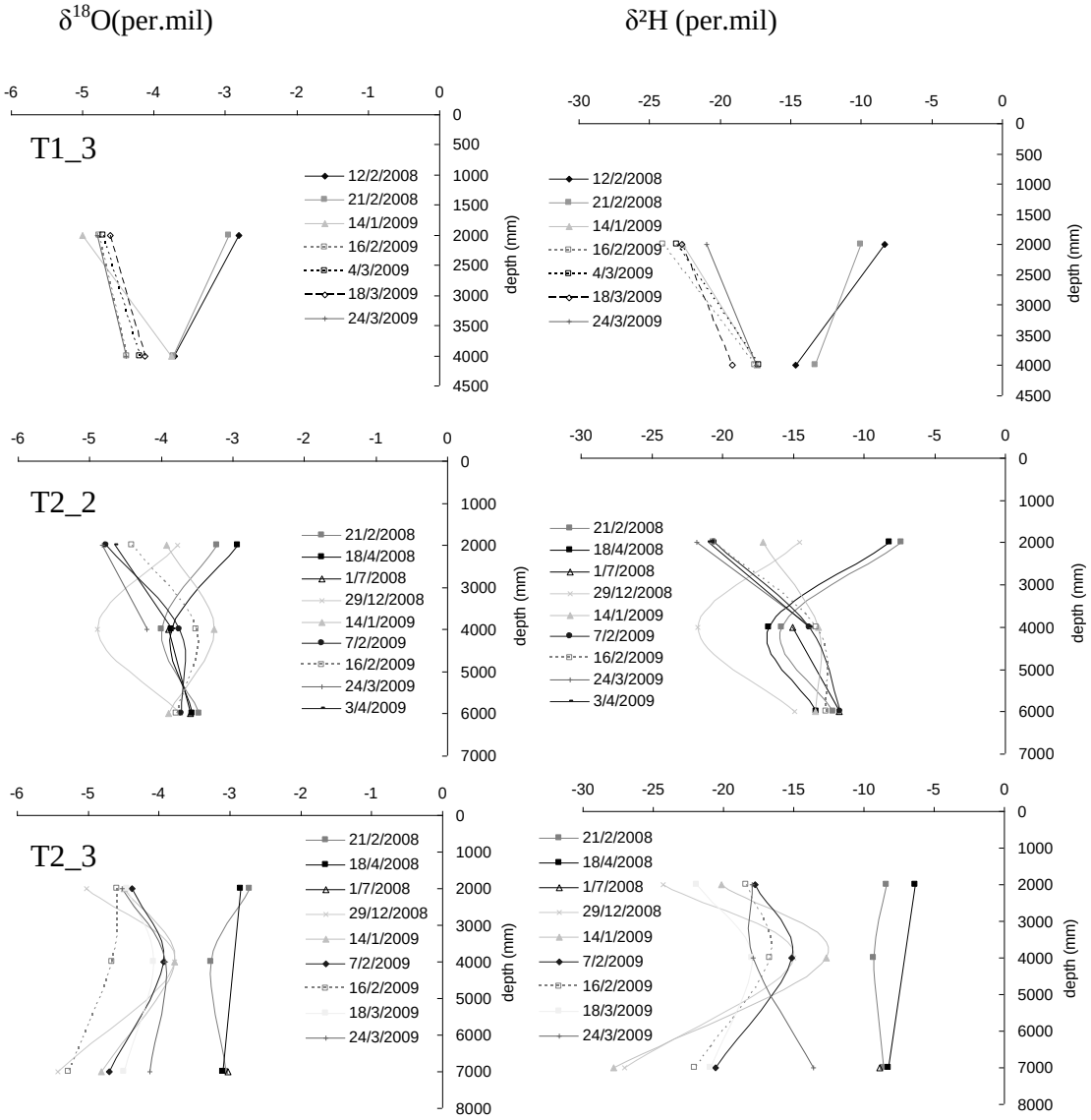

Figure v.e: Stable Isotope ($\delta^{18}O/\delta^{2}H$) ratios in nested piezometers during 2008-2009.

The isotopic signatures of the piezometers depicted as depth profiles in Figure v.e show that deeper waters retain a relatively stable isotopic signature over time, particularly at T1_3 and T2_2, whereas the deeper water table (7000 mm) at T2_3 adjacent to the weir shows similar variability to the surface suggesting some contact with near surface waters. The shallow groundwaters of the Craigieburn-Manalana therefore emit the variable isotopic ratio of in-coming rainfall and evaporation cycles, whilst the deeper waters are stable suggesting possible contact with a more sustained source of water – but since the conductivity of the material at depth is so extremely low stability could also simply be a reflection of the high moisture retention (much less transient water) at depth.

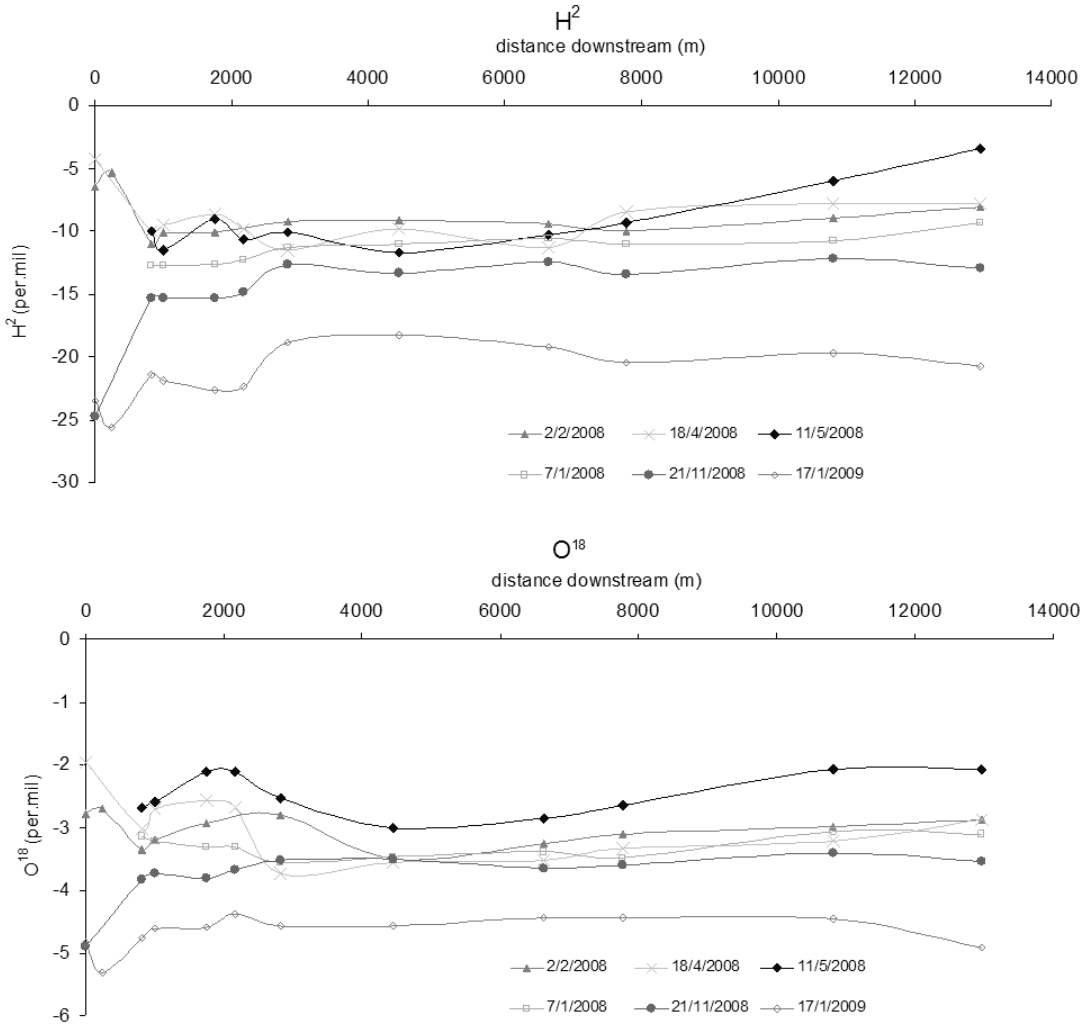

Figure v.f: Stable isotope ($\delta^{18}O/\delta^{2}H$) ratios at stream locations at specific distances downstream of the Craigieburn-Manalana wetland during 2008-2009.

Figure v.f shows the stable isotope ratios at locations downstream of the Craigieburn-Manalana. The first two points from the left are close to the installed buttress weir (first one upstream, second downstream), the third and fourth are downstream of the gabion dam, the fifth at a location just before the Manalana streams confluence with the Motlamogasane stream which then continues until the final sampling location (before the stream passes irrigated lands). Interesting is the marked difference between the two sampling locations close to the buttress weir which consistently show higher or lower concentrations of stable isotopes than compared with the rather stable ratio of the Motlamogasane mainstem. Whereas the third and fourth sampling locations show more similarity with downstream, whilst the remaining downstream samples show a generally stable isotope signature – suggesting that the gabion dam sits at a location that intersects the regional water table (possibly of the piedmonts of the Drakensberg escarpment), it is likely therefore that groundwater drives baseflow in these rivers and the upper most wetlands in these catchments are disconnected from the groundwater aquifers (NB. Recall discussion in Chapter 9).

APPENDIX vi – Groundwater flow estimate during aET determination

h1	h2				distance (D) between T1_3 and T2_2 (mm)	94100		
automated peizometer - GW level (mm)						i	Q	Q per day (mm)
Prg_T1_3, 1180, Hr	Prg_t2_2, 1500, Hr	TIMESTEP	K (mm/hr)			0.011126	0.000008	0.000182714
-166.39999	-1218.00000	28-Jan-09 02:00	T2_2	0.0000925		0.011175	0.000008	
-164.80000	-1211.80005	28-Jan-09 03:00	T1_3	0.0012618		0.011126	0.000008	
-166.39999	-1214.59998	28-Jan-09 04:00	average	0.0006772		0.011139	0.000008	
-168.00000	-1195.80005	28-Jan-09 05:00				0.010922	0.000007	
-168.00000	-1200.59998	28-Jan-09 06:00				0.010973	0.000007	
-168.00000	-1217.40002	28-Jan-09 07:00				0.011152	0.000008	
-168.00000	-1236.40002	28-Jan-09 08:00				0.011354	0.000008	
-168.00000	-1221.59998	28-Jan-09 09:00				0.011197	0.000008	
-157.20000	-1231.80005	28-Jan-09 10:00				0.011420	0.000008	
-147.60001	-1249.80005	28-Jan-09 11:00				0.011713	0.000008	
-146.00000	-1232.00000	28-Jan-09 12:00				0.011541	0.000008	
-146.00000	-1205.00000	28-Jan-09 13:00				0.011254	0.000008	
-142.80000	-1200.40002	28-Jan-09 14:00				0.011239	0.000008	
-142.00000	-1205.80005	28-Jan-09 15:00				0.011305	0.000008	
-142.00000	-1230.80005	28-Jan-09 16:00				0.011571	0.000008	
-142.00000	-1199.40002	28-Jan-09 17:00				0.011237	0.000008	
-142.00000	-1190.59998	28-Jan-09 18:00				0.011143	0.000008	
-143.60001	-1196.00000	28-Jan-09 19:00				0.011184	0.000008	
-145.20000	-1197.00000	28-Jan-09 20:00				0.011177	0.000008	
-143.60001	-1198.00000	28-Jan-09 21:00				0.011205	0.000008	
-146.00000	-1198.00000	28-Jan-09 22:00				0.011180	0.000008	
-143.60001	-1198.80005	28-Jan-09 23:00				0.011214	0.000008	
-142.00000	-1203.19995	29-Jan-09 00:00				0.011277	0.000008	
-137.00000	-1200.40002	29-Jan-09 01:00				0.011301	0.000008	0.000185035

The estimate determines the hydraulic gradient (i) between two piezometer groundwater levels and by multiplying by a saturated conductivity value (K – estimated using the Bouwer and Rice, 1976 Method described in Chapter 5) determines the hourly average discharge (Q) which is summed for the day (Q^d).

$$Q^d = \sum iK \qquad \text{Where} \qquad i = \frac{h1 - h2}{D}$$

APPENDIX vii - TDR Volumetric Water Content Responses

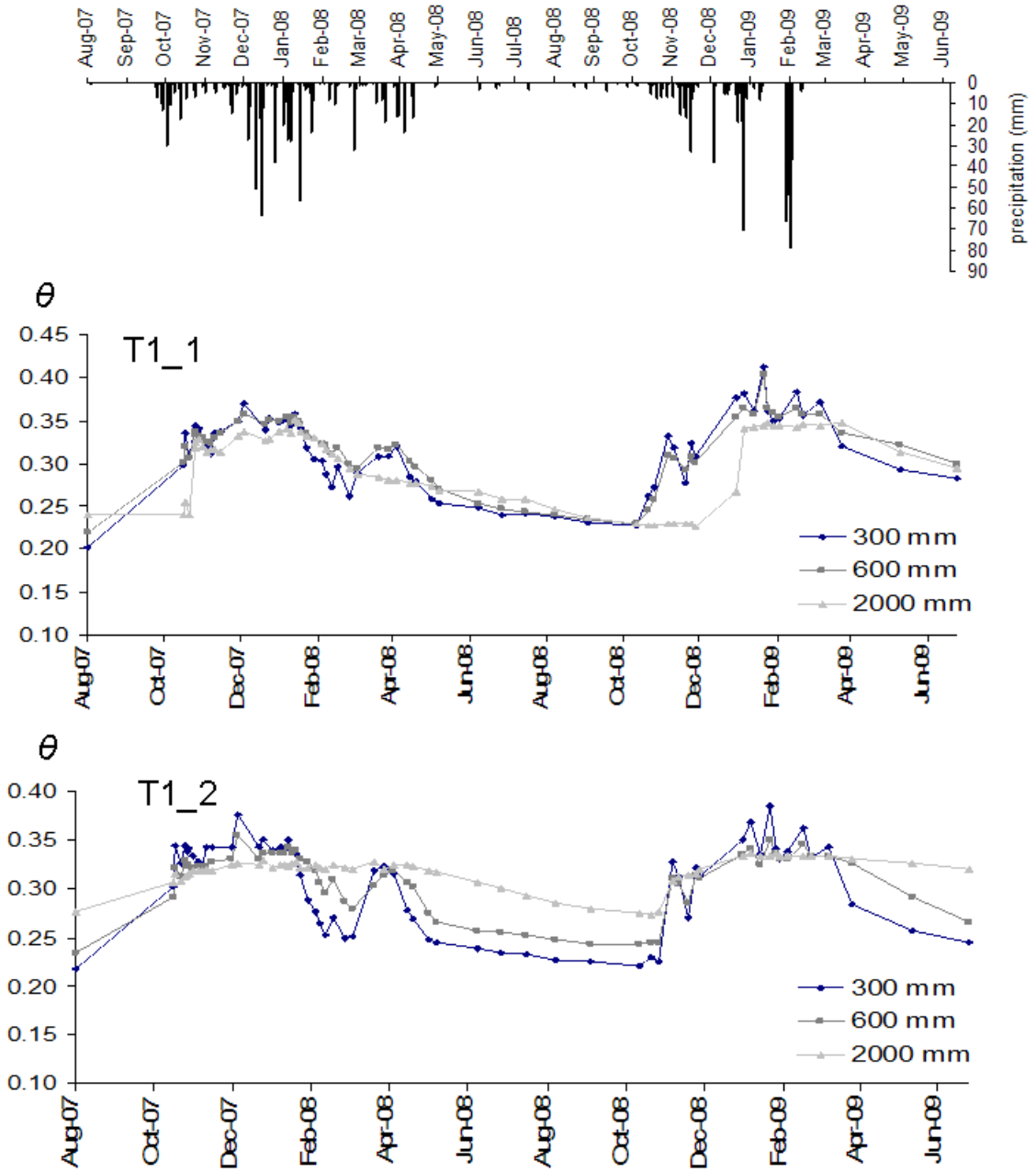

Figure vii.a: Volumetric Water Contents between 2007-2009 for sites T1_1 and T1_2 (NB high water contents of clay material at T1_2 2000 mm during dry periods)

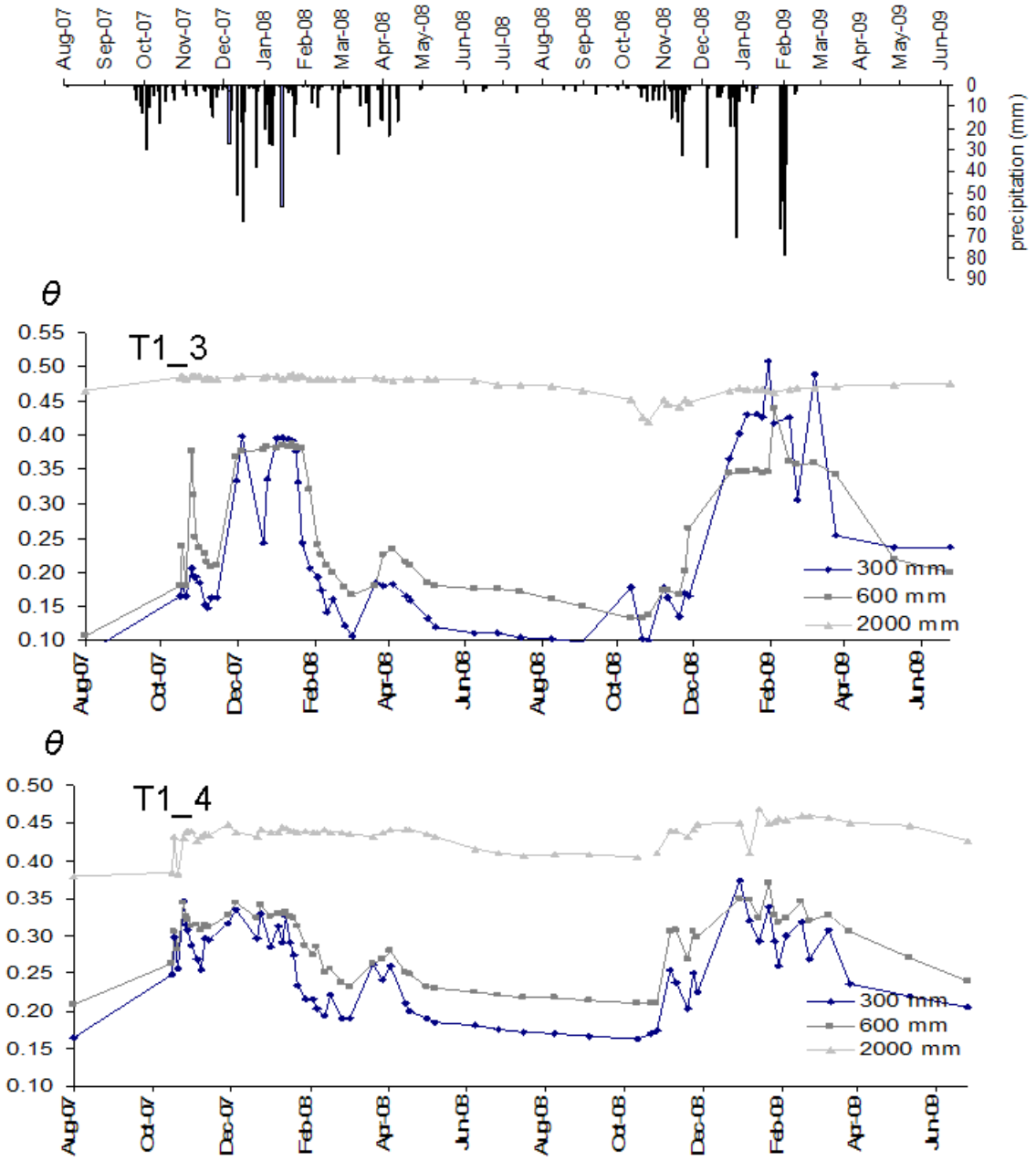

Figure vii.b: Volumetric Water Contents between 2007-2009 for sites T1_3 and T1_4 (NB high water contents of clay material at T1_4 2000 mm during dry periods, T1_3 remains wet at depth as this is the valley bottom wetland area)

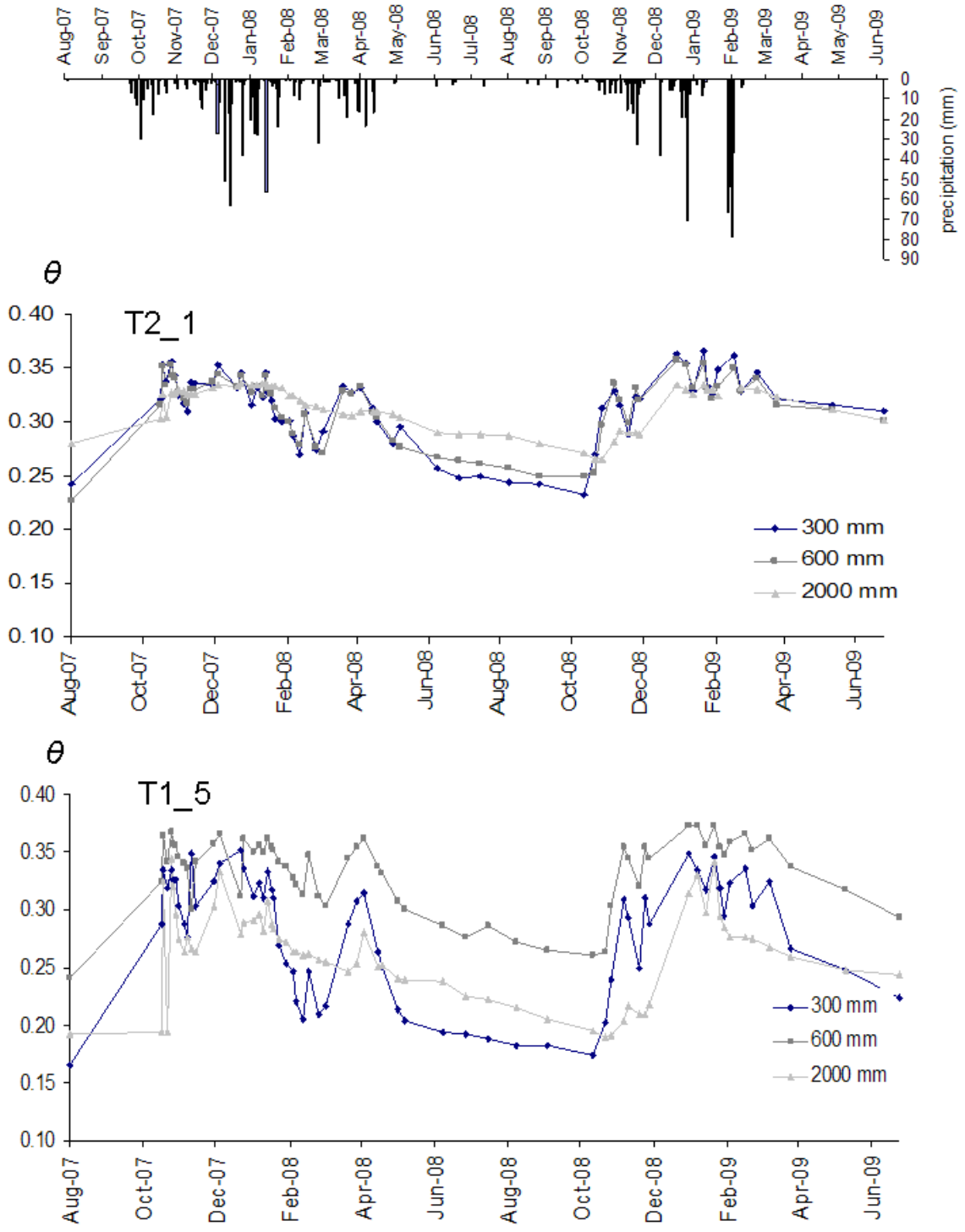

Figure vii.c: Volumetric Water Contents between 2007-2009 for sites T2_1 and T1_5

APPENDIX viii – Quantification of Actual Evapotranspiration

The following data comes from outsourced research by the Council for Scientific and Industrial Research (CSIR) who quantified actual evapo-transpiration in the Craigieburn-Manalana wetland *Phragmites* reedbed and *Parinari* dominated shrub uplands during winter (August) 2008 and summer (January-February) 2009 using energy balance techniques: Surface Layer Scintillometer (SLS), Surface Renewal (SR), Eddy-Covariance (EC) and estimated reference evapotranspiration (ETo).

Further data and analysis may be found in Everson, C., Clulow, A., Mengistu, M. (2009). Quantification of Evapotranspiration from a South African Rehabilitated Headwater Wetland. Water Research Commission, Pretoria. Project No. K8/826

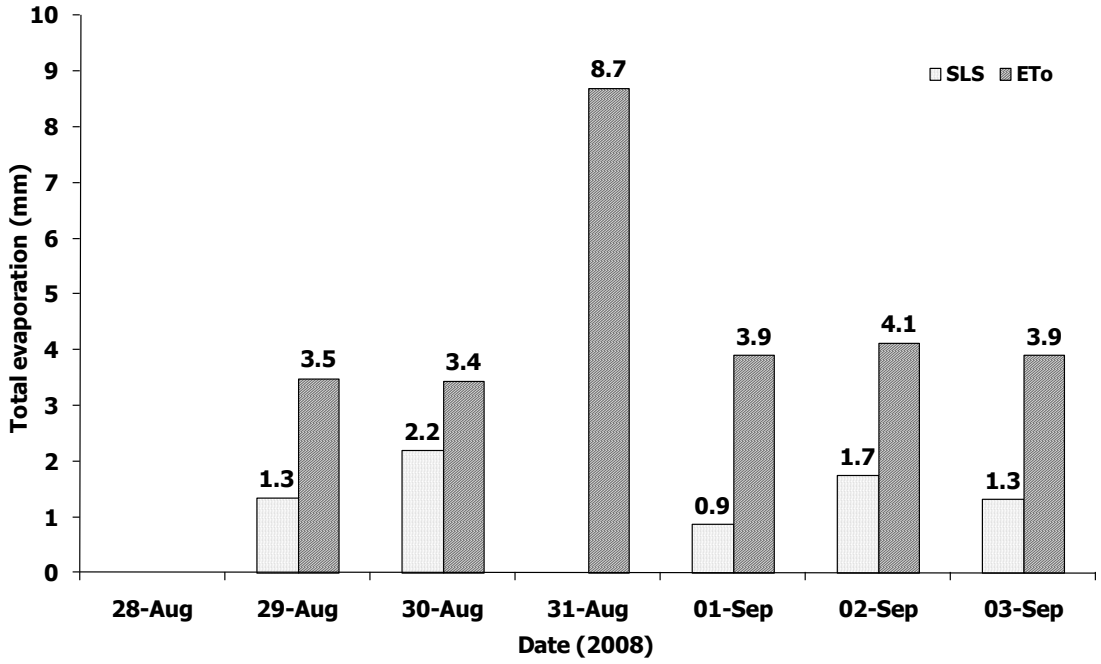

Figure viii.a: Quantified evapotranspiration losses for *Parinari* dominated upland shrub area in the Craigieburn-Manalana catchment for a winter period 2008.

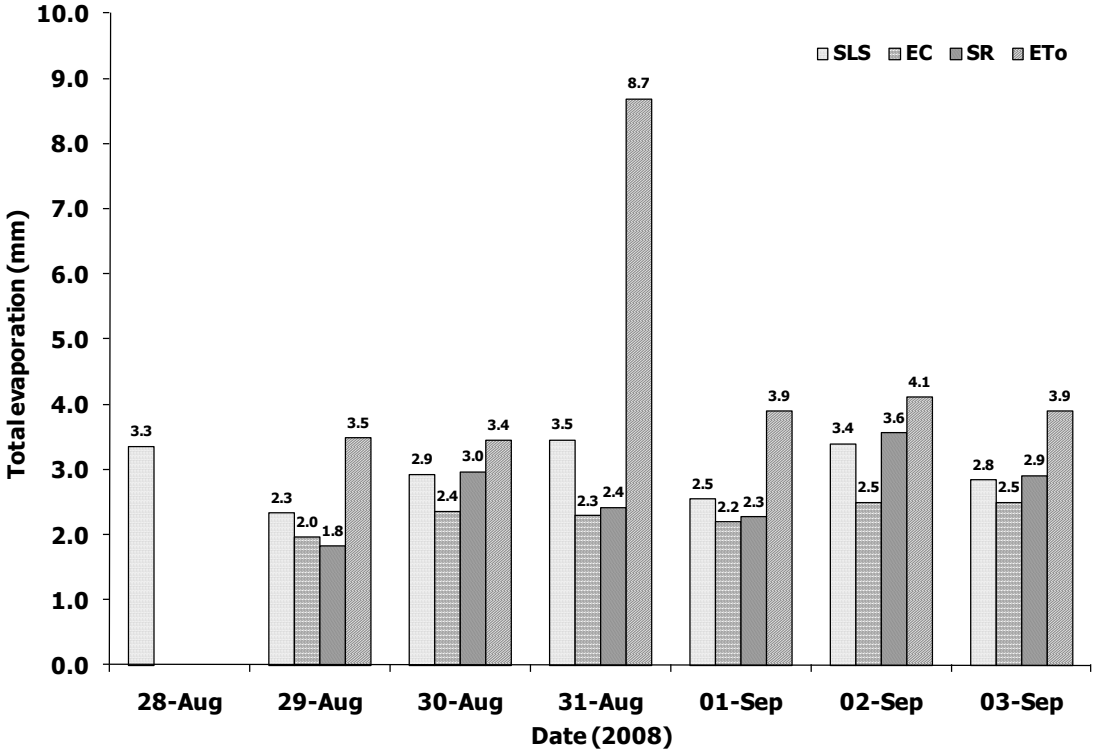

Figure viii.b: Quantified evapotranspiration losses for *Phragmites* dominated wetland area in the Craigieburn-Manalana catchment for a winter period 2008.

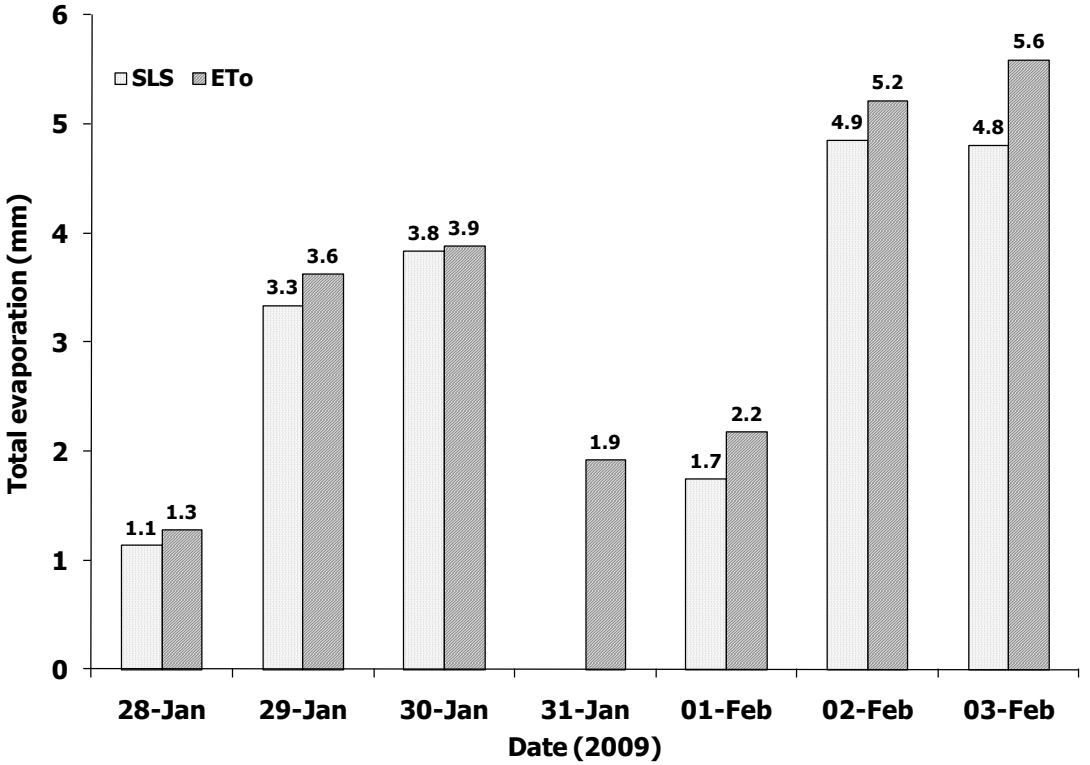

Figure viii.c: Quantified evapotranspiration losses for *Parinari* dominated upland shrub area in the Craigieburn-Manalana catchment for a summer period 2009.

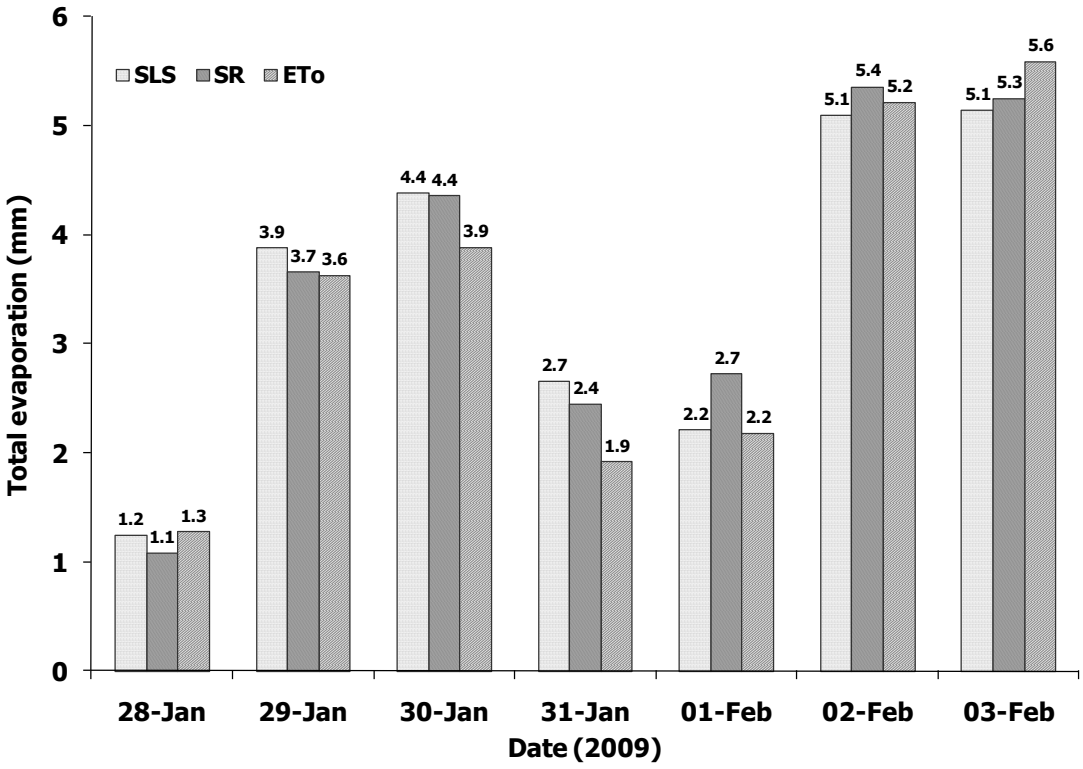

Figure viii.d: Quantified evapotranspiration losses for *Phragmites* dominated wetland area in the Craigieburn-Manalana catchment for a summer period 2009.

APPENDIX ix - Runoff plot time-series

Key:

CRGT1T2H – Mispah soil type (adjacent to site T1_5)
CRGT1T2M- Oakleaf soil type (adjacent to site T2_1)
CRGT1WST – Glenrosa soil type* Modelled in Chapter 4 (adjacent to site T1_2)
CRGT2STH – Oakleaf soil type (adjacent to site T2_4)

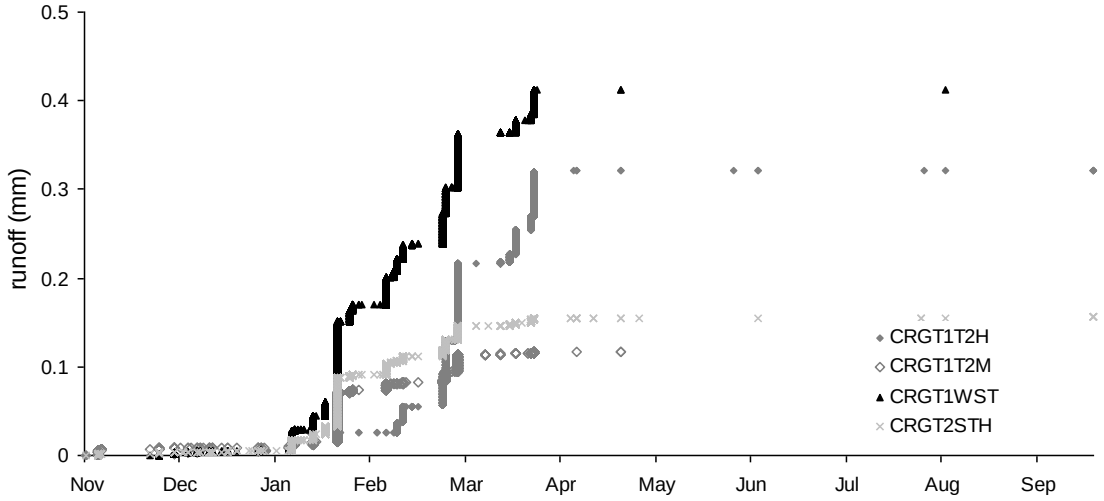

Figure ix.a: Cumulative runoff plot data for HY2005

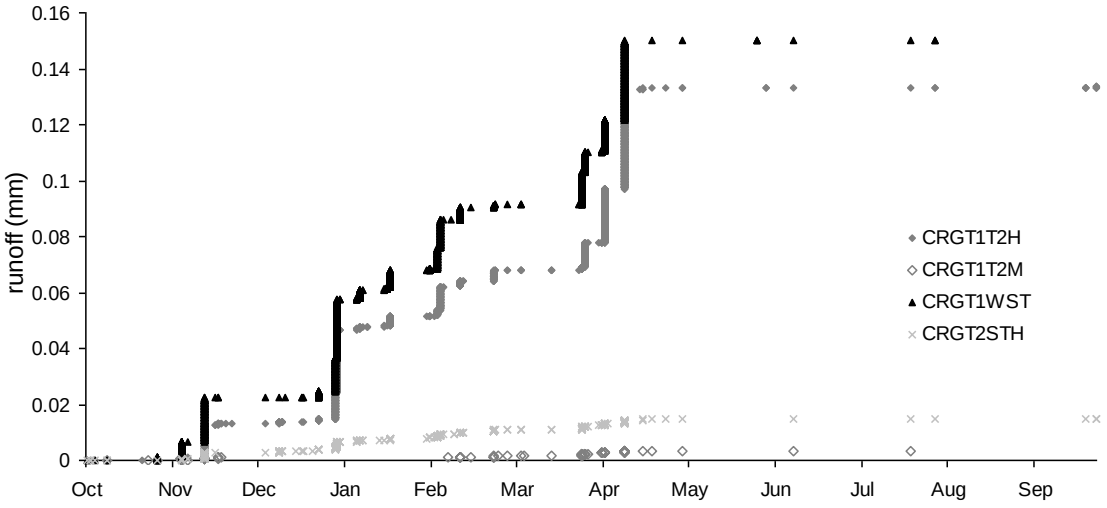

Figure ix.b: Cumulative runoff plot data for HY2006

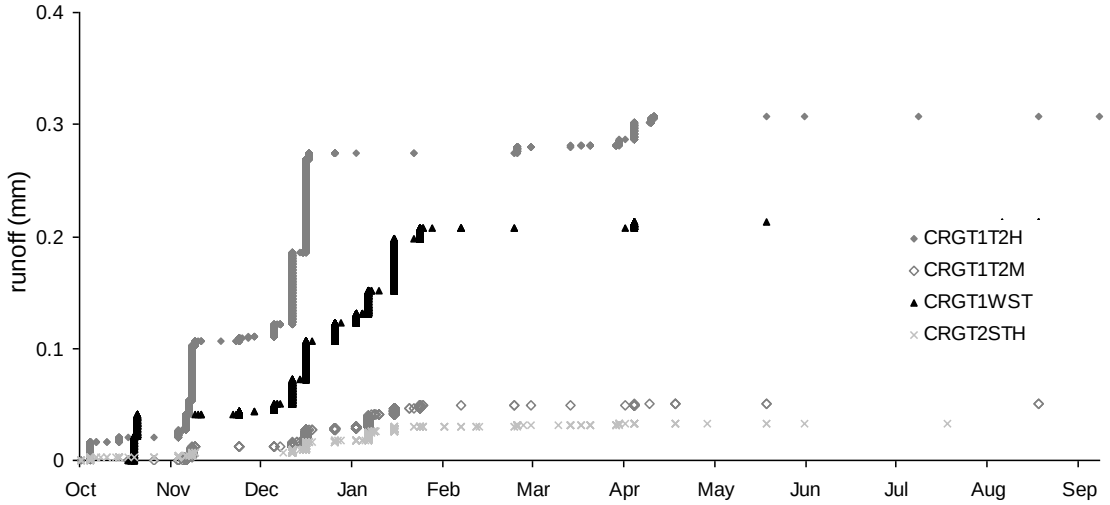

Figure ix.c: Cumulative runoff plot data for HY2007

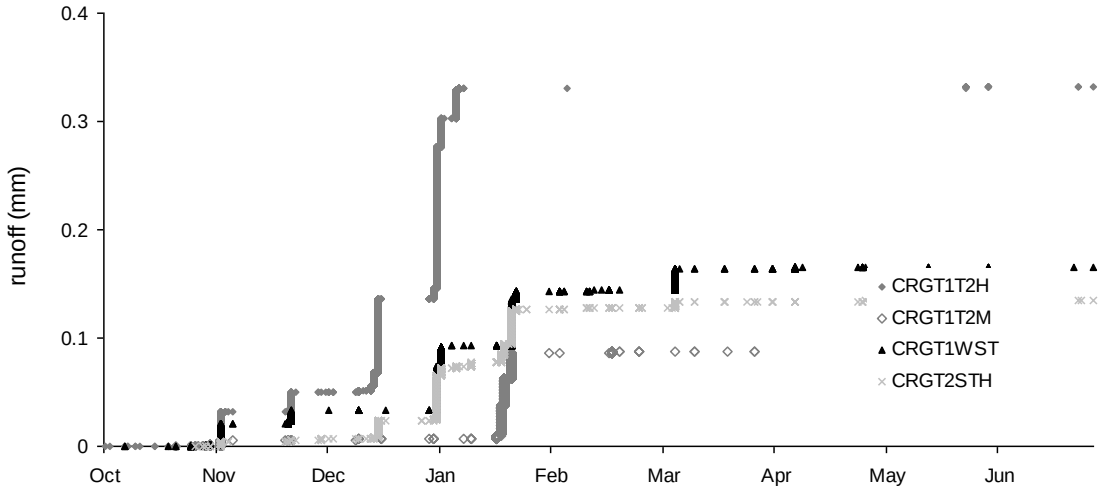

Figure ix.d: Cumulative runoff plot data for HY2008

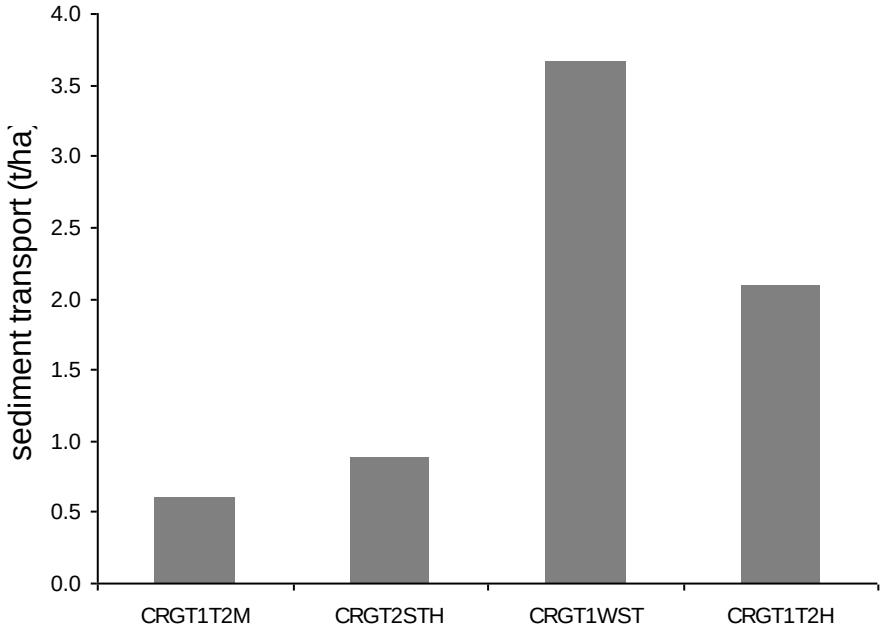

Figure ix.e: Total sediments collected in the runoff plots February-March 2006

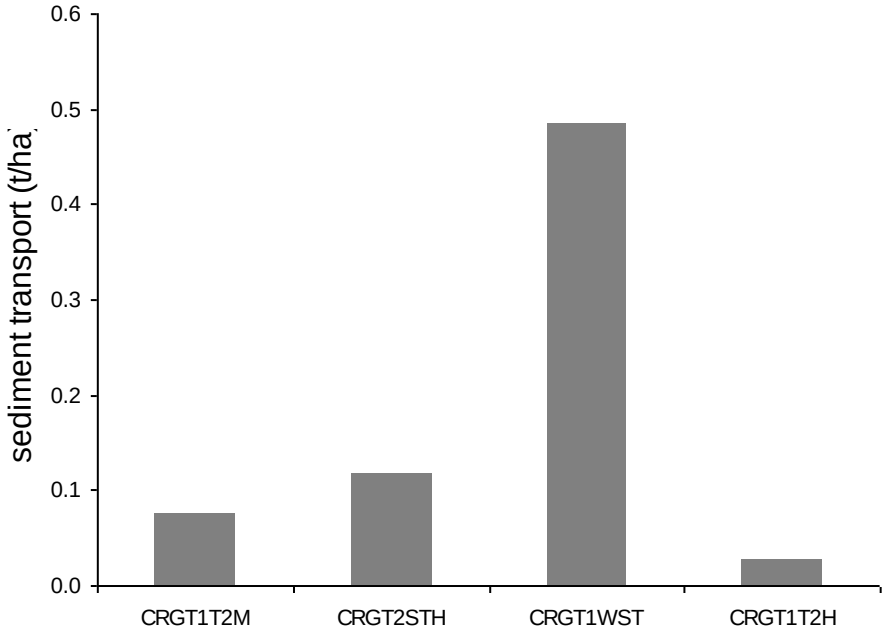

Figure ix.f: Total sediments collected in the runoff plots HY2006.

APPENDIX x – Wetland runoff gauging

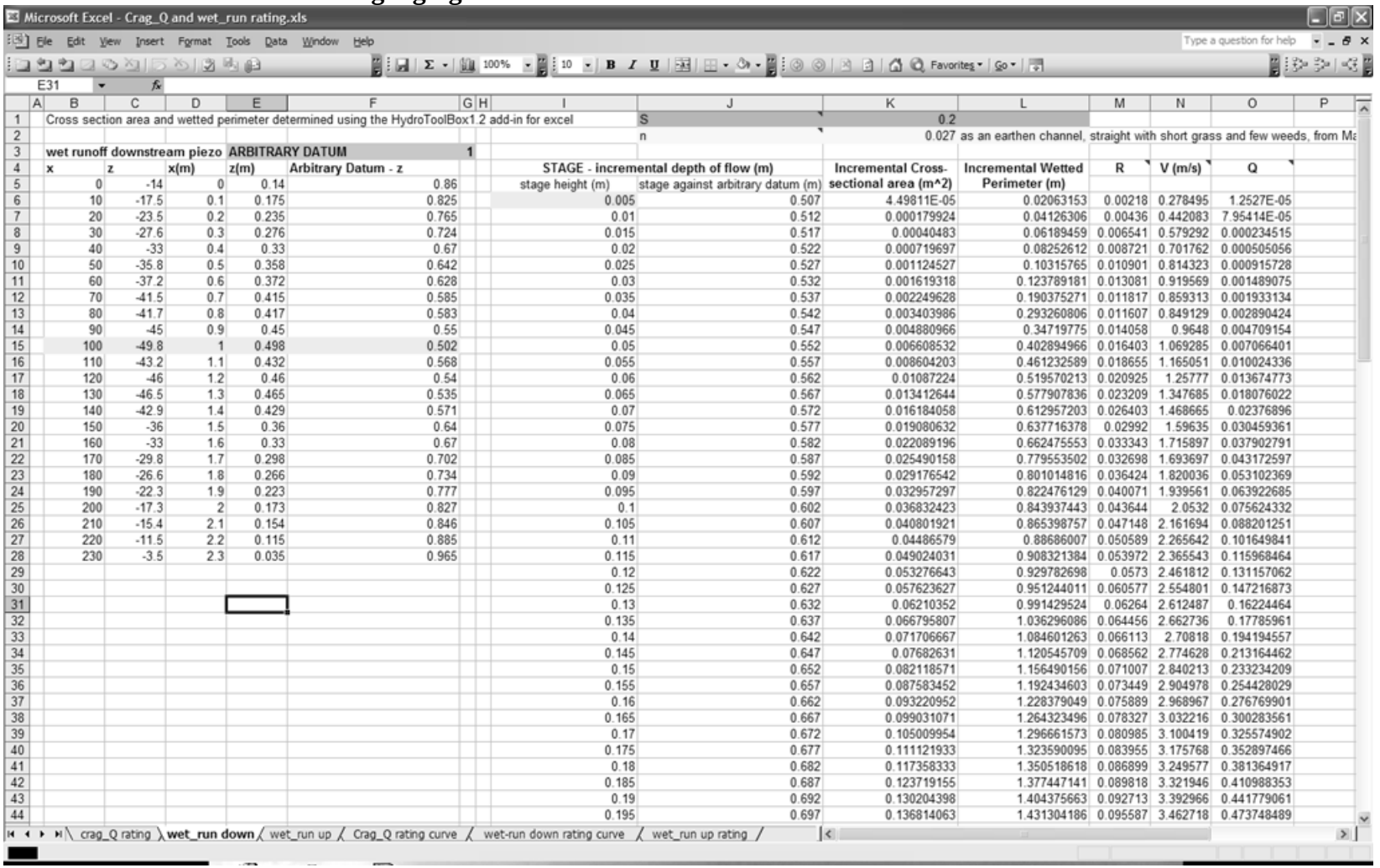

Microsoft Excel - Crag_Q and wet_run rating.xls

File Edit View Insert Format Tools Data Window Help

E31

	A	B	C	D	E	F	G	H	I	J	K	L	M	N	O	P
1		Cross section area and wetted perimeter determined using the HydroToolBox1.2 add-in for excel								S	0.2					
2										n	0.027	as an earthen channel, straight with short grass and few weeds, from Ma				
3		wet runoff downstream piezo			ARBITRARY DATUM		1									
4		x	z	x(m)	z(m)	Arbitrary Datum - z			STAGE - incremental depth of flow (m)		Incremental Cross-sectional area (m^2)	Incremental Wetted Perimeter (m)	R	V (m/s)	Q	
5		0	-14	0	0.14	0.86			stage height (m)	stage against arbitrary datum (m)						
6		10	-17.5	0.1	0.175	0.825			0.005	0.507	4.49811E-05	0.02063153	0.00218	0.278495	1.2527E-05	
7		20	-23.5	0.2	0.235	0.765			0.01	0.512	0.000179924	0.04126306	0.00436	0.442083	7.95414E-05	
8		30	-27.6	0.3	0.276	0.724			0.015	0.517	0.00040483	0.06189459	0.006541	0.579292	0.000234515	
9		40	-33	0.4	0.33	0.67			0.02	0.522	0.000719697	0.08252612	0.008721	0.701762	0.000505056	
10		50	-35.8	0.5	0.358	0.642			0.025	0.527	0.001124527	0.10315765	0.010901	0.814323	0.000915728	
11		60	-37.2	0.6	0.372	0.628			0.03	0.532	0.001619318	0.123789181	0.013081	0.919569	0.001489075	
12		70	-41.5	0.7	0.415	0.585			0.035	0.537	0.002249628	0.190375271	0.011817	0.859313	0.001933134	
13		80	-41.7	0.8	0.417	0.583			0.04	0.542	0.003403986	0.293260806	0.011607	0.849129	0.002890424	
14		90	-45	0.9	0.45	0.55			0.045	0.547	0.004880966	0.34719775	0.014058	0.9648	0.004709154	
15		100	-49.8	1	0.498	0.502			0.05	0.552	0.006608532	0.402894966	0.016403	1.069285	0.007066401	
16		110	-43.2	1.1	0.432	0.568			0.055	0.557	0.008604203	0.461232589	0.018655	1.165051	0.010024336	
17		120	-46	1.2	0.46	0.54			0.06	0.562	0.01087224	0.519570213	0.020925	1.25777	0.013674773	
18		130	-46.5	1.3	0.465	0.535			0.065	0.567	0.013412644	0.577907836	0.023209	1.347685	0.018076022	
19		140	-42.9	1.4	0.429	0.571			0.07	0.572	0.016184058	0.612957203	0.026403	1.468665	0.02376896	
20		150	-36	1.5	0.36	0.64			0.075	0.577	0.019080632	0.637716378	0.02992	1.59635	0.030459361	
21		160	-33	1.6	0.33	0.67			0.08	0.582	0.022089196	0.662475553	0.033343	1.715897	0.037902791	
22		170	-29.8	1.7	0.298	0.702			0.085	0.587	0.025490158	0.779553502	0.032698	1.693697	0.043172597	
23		180	-26.6	1.8	0.266	0.734			0.09	0.592	0.029176542	0.801014816	0.036424	1.820036	0.053102369	
24		190	-22.3	1.9	0.223	0.777			0.095	0.597	0.032957297	0.822476129	0.040071	1.939561	0.063922685	
25		200	-17.3	2	0.173	0.827			0.1	0.602	0.036832423	0.843937443	0.043644	2.0532	0.075624332	
26		210	-15.4	2.1	0.154	0.846			0.105	0.607	0.040801921	0.865398757	0.047148	2.161694	0.088201251	
27		220	-11.5	2.2	0.115	0.885			0.11	0.612	0.04486579	0.88686007	0.050589	2.265642	0.101649841	
28		230	-3.5	2.3	0.035	0.965			0.115	0.617	0.049024031	0.908321384	0.053972	2.365543	0.115968464	
29									0.12	0.622	0.053276643	0.929782698	0.0573	2.461812	0.131157062	
30									0.125	0.627	0.057623627	0.951244011	0.060577	2.554801	0.147216873	
31									0.13	0.632	0.06210352	0.991429524	0.06264	2.612487	0.16224464	
32									0.135	0.637	0.066795807	1.036296086	0.064456	2.662736	0.17785961	
33									0.14	0.642	0.071706667	1.084601263	0.066113	2.70818	0.194194557	
34									0.145	0.647	0.07682631	1.120545709	0.068562	2.774628	0.213164462	
35									0.15	0.652	0.082118571	1.156490156	0.071007	2.840213	0.233234209	
36									0.155	0.657	0.087583452	1.192434603	0.073449	2.904978	0.254428029	
37									0.16	0.662	0.093220952	1.228379049	0.075889	2.968967	0.276769901	
38									0.165	0.667	0.099031071	1.264323496	0.078327	3.032216	0.300283561	
39									0.17	0.672	0.105009954	1.296661573	0.080985	3.100419	0.325574902	
40									0.175	0.677	0.111121933	1.323590095	0.083955	3.175768	0.352897466	
41									0.18	0.682	0.117358333	1.350518618	0.086899	3.249577	0.381364917	
42									0.185	0.687	0.123719155	1.377447141	0.089818	3.321946	0.410988353	
43									0.19	0.692	0.130204398	1.404375663	0.092713	3.392966	0.441779061	
44									0.195	0.697	0.136814063	1.431304186	0.095587	3.462718	0.473748489	

crag_Q rating | wet_run down | wet_run up | Crag_Q rating curve | wet-run down rating curve | wet_run up rating

Figure x.a: Example calculation of streamflow discharge rating within a wetland drainage furrow using the slope-area method (Herschy, 1985)

Figure x.b: Adapted Google™ earth image with location of drainage furrow gauging piezometer nest and buttress weir.

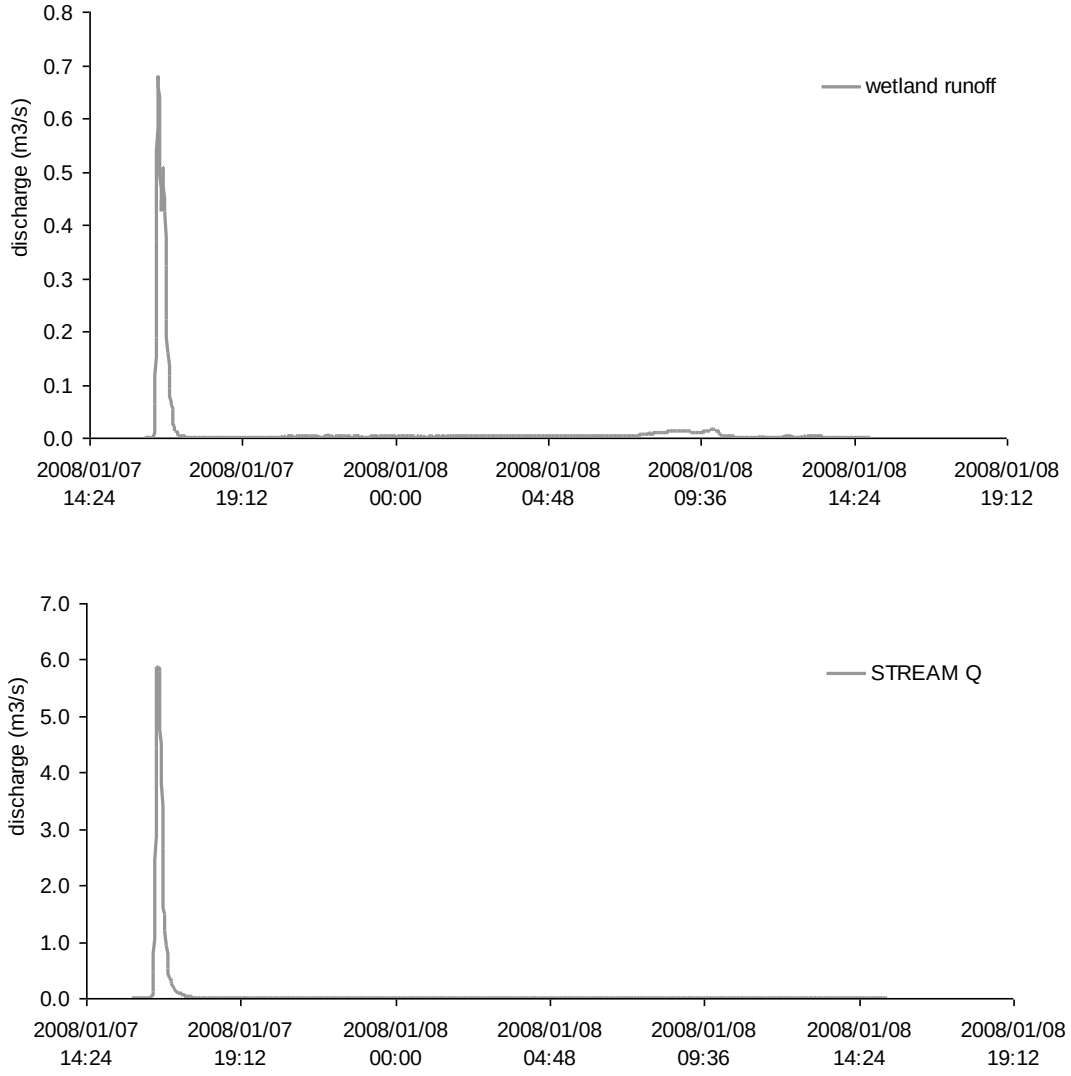

Figure x.c: determination of discharge in drainage furrow (above) for a rainfall event of 26 mm (between 16:19-16:37 hours on the 01/07/2008) compared the stream downstream of the buttress weir (below).

Unfortunately a good record of wetland throughflows (piezometer with pressure transducer placed within a drainage furrow) was not possible due to flooding and vandalism. However one event was successfully recorded and streamflow in the furrow was estimated using the slope-area method of Herschy (1985 – See Chapter 3). Whilst the buttress weir was also not functioning at the time due to erosion undermining of the structure, a piezometer system was also placed in the channel downstream. The calculation for stream discharge is shown by way of example for the drainage furrow in Figure ix.a. Meanwhile comparison of the two discharges is for the 86.7 mm/hr event of 01/07/2008 is shown in Figure ix.c. Here the estimated discharge from a drainage furrow contributes approximately 10% of the stream discharge.

APPENDIX xi - LIST OF SYMBOLS

These are defined in the text and are listed here for reference in the order that they appear in the text:

Chapter 1

V	is the volume of water storage in a wetland
t	is time
Pn	is gross precipitation
Si	surface inflows via streams or overland flow
Gi	groundwater inflows
ET	evapotranspiration
So	surface outflows
Go	groundwater outflows
Si	surface inflow
P_{catch}	catchment precipitation;
ET_{catch}	actual catchment evapotranspiration
$\triangle Ss$	change in soil moisture storage in the catchment
$\triangle Sg$	change in groundwater storage in the catchment.

Chapter 3

Q	discharge or stormflow depth (mm)
S	potential maximum soil water retention (mm), ≡ index of the wetness of the catchment's soil prior to a rainfall event
I_a	initial losses (abstractions) prior to the commencement of stormflow
CN	curve number
Δq_p	peak discharge of incremental unit hydrograph (m^3/s)
A	catchment area (km^2)
ΔQ	incremental stormflow depth (mm)
ΔD	unit duration of time, used with the distribution of daily rainfall
L	catchment lag time (h)
l	hydraulic length of catchment along the main channel (m)
y	average catchment slope (%)
Φ_T	total soil water potential
Φ_m	matric potential
Φ_z	gravitational potential
Φ_o	osmotic potential
ψ_g	gauged pressure
ψ_h	soil water/capillary pressure head (mm)
T	temperature (°C)
ε_b	the soil bulk dielectric constant
c	speed of light

v wave propogation velocity
t travel time for the pulse or wave to traverse down and back along TDR probe
L_p length of TDR probe
Q discharge in m^3/s
n Manning's roughness coefficient
R ratio of the channels cross-sectional area to wetted perimeter
S channel bed slope taken as the difference in elevation between two or more points
ET_o reference evapotranspiration (mm/d)
R_n net radiation at the vegetation surface ($MJ/m^2/d$)
G soil heat flux density
T mean air temperature at 2m height (°C)
u_2 average wind speed at 2m height (m/s)
e_s mean saturation vapour pressure (kPa)
e_a mean actual vapour pressure (kPa)
$e°$ hourly saturation vapour pressure at air temperature
e_s-e_a saturation pressure deficit (kPa)
Δ slope of the vapour pressure curve (kPa/°C)
y psychometric constant (kPa/°C)

Chapter 4

θ volumetric water content
ψ pressure head
z gravitational head
θ_r residual water content
θ_s saturated water content
α is the air entry value $[L^{-1}]$
S_e effective water content
m,n,l fitting parameters
K_r relative hydraulic conductivity $[L\ T^{-1}]$
K_k predicted hydraulic conductivity close to but less than K_s where dual-porosity is enabled
h_k predicted head corresponding to K_k [L]
θ_m fictitious/extrapolated parameter slightly larger than θ_s
θ_i initial water content $[L^3L^{-3}]$
i rainfall intensity (mm/hr)
h pressure head at the Green-Ampt wetting front
i_p rainfall intensity at ponding time
λ dimensionless pore size distribution index
h_b inverse air-entry pressure head $[L^{-1}]$
i_e rainfall excess (taken as the difference between rainfall intensity i and infiltration f)
A_e surface area of the flow element
Δt time increment (1-minute)
Δx_e space increment (22 m)
s slope (%)

w width of the surface element

Chapter 5

L height of the open screen portion of the piezometer at its interface with the wetland matrix,

y vertical distance between water level in the piezometer at any time

R_e effective radius over which y is dissipated

r_w horizontal radius between the centre of the piezometer and the aquifer (plus piezometer casing and screening material)

r_c inside radius of each of the piezometer casings

Chapter 6

k geometric factor

R resistance (ohms)

V voltage

I current

V_0 voltage at time (t) 0

Chapter 7

$\delta(t)$ the excitation function

$g(t)$ unit response function

q_{out} runoff response

D dispersion coefficient, describing the spread of travel times

τ response time

θ_{PAW} plant available water

θ_{WP} wilting point

θ_{FC} field capacity

d soil horizon depth

R^2 coefficient of determination

NS Nash-Sutcliffe efficiency

W Willmott efficiency

Chapter 8

Q_E total contribution of event (rainfall) water to stream discharge

Q_T total volume of discharge

c_T total isotopic composition of discharge water

c_P isotopic composition of pre-event water

c_E isotopic composition of event water

^{18}O stable isotope Oxygen-18

^{2}H stable isotope deuterium